

**FUNCTION ORIENTED SYNTHESIS OF BIOACTIVE MARINE NATURAL  
PRODUCTS AND THEIR PHARMACOPHORE ANALOGUES**

by

Labros G. Meimetis

B.Sc., Simon Fraser University, 2006

A THESIS SUBMITTED IN PARTIAL FULFILLMENT OF  
THE REQUIREMENTS FOR THE DEGREE OF

Doctor of Philosophy

in

THE FACULTY OF GRADUATE STUDIES

(Chemistry)

THE UNIVERSITY OF BRITISH COLUMBIA

(Vancouver)

July 2012

© Labros G. Meimetis, 2012

## Abstract

Natural products play a central role in drug discovery. The Andersen lab focuses its efforts on the isolation and structure elucidation of compounds from the marine environment. Many of these compounds possess biological activity, and often their total synthesis is undertaken, to provide structure-activity relationship (SAR) studies for new pharmacophores, and to provide material to probe *in vivo* biological effects. When possible, small molecule probes are designed based on the structure of the natural product, to provide insight into the mechanism of interaction between the active compound and its biological target. Several projects probing the biological activities of natural products and their analogues by synthesis are detailed in this thesis

The second chapter describes the construction of water-soluble activators of SHIP1, a phosphatase that is a negative regulator of the PI3K signal transduction pathway in hematopoietic cells. The structure of a known SHIP1 activator (**2.18**) was used to develop the water-soluble analogues **2.20** and **2.42** in order to enhance the drug-like properties of **2.18**.

The third chapter describes the total synthesis of two novel marine natural products, (*S*)-niphatenone A (**3.23**) and B (**3.35**). Both compounds inhibit transcriptional activity in prostate cancer cells. Their total synthesis was completed to verify their proposed structures and to supply material for biological testing. Several analogues of (*R*)-niphatenone B (**3.31**) were constructed providing a clear SAR for the natural product.

The fourth chapter describes a terpenoid natural product **4.1**, which was found to be an antagonist of the androgen receptor. Using lead compound **4.1**, a semisynthetic SAR study was completed and it was determined that analogue **4.4** has enhanced potency relative to **4.1**. Synthetic attempts to construct **4.4** analogues by an epoxide-initiated cascade are described.

The fifth chapter describes synthetic efforts towards the novel peptide-aldehyde natural product lichostatinal (**5.4**). Lichostatinal (**5.4**) is a potent cathepsin K inhibitor. Its total synthesis would provide material to support structure elucidation efforts and biological testing.

## Preface

Chapter 2 is based on work done at UBC, the BC Cancer Agency, and Aquinox Pharmaceuticals Inc. The author is responsible for the synthesis and characterization of all **2.18** analogues. In addition to the author, Dr. Matt Nodwell and Dr. Chelsea Wang constructed **2.20/2.34/2.42/2.43** for biological testing. Single crystal X-ray diffraction analysis was carried out by Dr. Brian O. Patrick. STDD NOE NMR experiments were run by Dr. David Williams. The SHIP1 phosphatase assay screening was done by Andrew Ming-Lum under the guidance of Dr. Alice-F. Mui at the BC Cancer Agency. The solubility of **2.18** analogues, the AKT phosphorylation inhibition assay, some measurements of SHIP1 enzymatic assay, and the *in vivo* PCA model was completed by Aquinox Pharmaceuticals Inc.

The work in chapter 3 has been published: Meimetis, Labros G.; Williams David E.; Mawji, Nasrin R.; Banuelos, Adriana.; Lal, Aaron A.; Park, Jacob J.; de Voogdt, Nicole J.; Fernandez J.C.; Sadar, Marianne D.; and Andersen, Raymond J. Niphatenones A and B, glycerol ethers from the sponge *Niphates Digitalis* block androgen receptor transcriptional activity in prostate cancer cells: structure elucidation, synthesis, and biological activity. *J. Med. Chem.* (2012), 55(1), 503-514. Copyright 2012 American Chemical Society. <http://pubs.acs.org/doi/pdf/10.1021/jm2014056>. The author was responsible for writing the experimental section as it relates to all synthetic compounds. The author is responsible for the construction and characterization of all synthetic compounds. Dr. David Williams is responsible for the isolation and structure determination of niphatenones A (**3.8**) and B (**3.9**). Nasrin R. Mawji, Adriana Banuelos, Aaron A. Lal, and Jacob J. Park under the leadership of Dr. Marianne D. Sadar at the BC Cancer Agency were responsible for generating all of the

biological data and “click” chemistry experimental data, in addition to Dr. Javier Garcia who provided insight for the “click” chemistry experiments. The potential fluorescent probe **3.78** was completed as a collaboration between Dr. Javier Garcia and the author.

Chapter 4 is work done at UBC, and the BC Cancer Agency. The lead compound (**4.1**) along with its subsequent hydrogenation product (**4.2**) was isolated and characterized by Dr. Gavin Carr. All other semisynthetic analogues, in addition to the synthetic study towards analogues of the natural product **4.4** was completed by the author. All biological data was acquired by Kevin Yang under the leadership of Dr. Marianne Sadar at the BC Cancer Agency.

Chapter 5 is work done at UBC. The isolation of lichostatinal (**5.4**) was completed by Vincent Paul Lavalee under the supervision of Dr. Dieter Bromme, using an *actinomycete* culture extract provided by the laboratory of Dr. Julian Davies. All synthetic compounds were constructed and characterized by the author.

## Table of Contents

<b>Abstract</b> .....	<b>ii</b>
<b>Preface</b> .....	<b>iv</b>
<b>Table of Contents</b> .....	<b>vi</b>
<b>List of Tables</b> .....	<b>ix</b>
<b>List of Figures</b> .....	<b>x</b>
<b>List of Schemes</b> .....	<b>xx</b>
<b>List of Symbols and Abbreviations</b> .....	<b>xxiii</b>
<b>Acknowledgements</b> .....	<b>xxvii</b>
<b>Dedication</b> .....	<b>xxviii</b>
<b>Chapter 1: Marine Natural Products From Benchtop to Bedside</b> .....	<b>1</b>
1.1 Nature as a Source of Medicine .....	1
1.2 Synthesis as an Aid to Structure Elucidation .....	6
1.3 Translating a Drug-Lead Into a Drug by Structure Activity Relationship (SAR) Studies .....	10
1.4 Bioactive Marine Natural Products Reveal Novel Mechanism of Action .....	13
1.5 Scope of Thesis .....	14
<b>Chapter 2: Synthesis and Biological Evaluation of SHIP1 Activators</b> .....	<b>16</b>
2.1 Inhibition of PI3K Signaling by Activation of SHIP1 .....	16
2.2 First Generation SHIP1 Agonist Pelorol and Analogues .....	18
2.3 Synthesis of SHIP1 Activators Using a Polyene-Initiated Cationic Cascade .....	21
2.4 Synthesis of Water Soluble Analogues to Facilitate Drug Administration .....	25
2.5 Saturation Transfer Difference (STD) Spectroscopy NMR .....	38

2.6	Synthesis of a Benzophenone Photoaffinity Probe .....	43
2.7	Biological Results .....	51
2.8	Conclusion .....	57
2.9	Experimental .....	60
<b>Chapter 3: Glycerol Ethers from the Sponge <i>Niphates digitalis</i> that Block Androgen</b>		
<b>Receptor Transcriptional Activity in Prostate Cancer Cells .....</b>		<b>101</b>
3.1	Castration Recurrent Prostate Cancer (CRPC) .....	101
3.2	The AR NTD as a Novel Therapeutic Target for Treating CRPC.....	103
3.3	Synthetic Analogues of ( <i>R</i> )-Niphatenone B ( <b>3.31</b> ).....	111
3.4	Synthesis of a Click Chemistry Probe and Fluorescent Probe.....	117
3.5	Biological Results .....	122
3.6	Conclusion .....	126
3.7	Experimental .....	128
<b>Chapter 4: Synthetic Efforts Towards a Novel AR Antagonist (4.1) .....</b>		<b>203</b>
4.1	Terpene AR Antagonist ( <b>4.1</b> ).....	203
4.2	Epoxide-Initiated Cationic Cascade Towards AR Antagonist <b>4.6</b> .....	207
4.3	Furan Blocking Group as a Strategy to Construct Desired Regioisomer <b>4.24</b> .....	211
4.4	Biological Results .....	217
4.5	Conclusion .....	220
4.6	Experimental .....	222
<b>Chapter 5: Synthetic Efforts Towards Lichostatinal (5.4): A Potent Cathepsin K</b>		
<b>Inhibitor .....</b>		<b>249</b>
5.1	Cysteine Protease Inhibitors .....	249

5.2	Lichostatinal ( <b>5.4</b> ) a Novel Peptide-Aldehyde Inhibitor of Cathepsin K .....	252
5.3	Conclusion .....	262
5.4	Experimental .....	264
<b>Chapter 6: Conclusion.....</b>		<b>301</b>
6.1	Biological and Pharmacokinetic Evaluation for Water Soluble SHIP1 Activators .....	301
6.2	Additional Biological Evaluations of the Niphatenones and their Analogues .....	302
6.3	Future Synthetic Strategies Towards Terpene <b>4.4</b> : An LBD AR Antagonist .....	303
6.4	Alternative Synthetic Strategy Towards Lichostatinal ( <b>5.4</b> ).....	307
<b>References .....</b>		<b>309</b>
<b>Appendix A: X-Ray Structure Reports.....</b>		<b>326</b>
A.1	Compound <b>2.30</b> .....	326
A.2	Compound <b>2.32</b> .....	330
A.3	Compound <b>2.42</b> .....	334

## List of Tables

Table 1.1 The properties of natural products compared with drugs, and synthetics. ....	3
Table 2.1 Solubilities of pelorol ( <b>2.1</b> ) analogues.....	53
Table 2.2 AKT phosphorylation inhibition of racemic amine mixture <b>2.20/2.42</b> . ....	53
Table 2.3 Activation of SHIP1 enzyme. ....	54
Table 4.1 EC <sub>50</sub> values for tested compounds in an AR competitor <i>in vitro</i> assay.....	219
Table 5.1 Results of arginol ( <b>5.24</b> ) oxidation model study.....	258
Table 5.2 Results of an O-benzyl deprotection model study of intermediate <b>5.15</b> .....	260

## List of Figures

Figure 1.1 Bioactive compounds of plants commonly used throughout human history. ....	1
Figure 1.2 Inhibitors of the 20S proteasome salinosporamide A ( <b>1.5</b> ) and omuralide ( <b>1.6</b> ). ...	4
Figure 1.3 Salinosporamide A ( <b>1.5</b> ) mechanism of action. ....	4
Figure 1.4 Marine natural product identification at the nM scale.....	7
Figure 1.5 Determination of the absolute configuration of muironolide A ( <b>1.11</b> ) using chemical degradation. ....	8
Figure 1.6 Family of imidazole marine natural products.....	9
Figure 1.7 Barans retrosynthesis of ( $\pm$ )-palau'amine ( <b>1.22</b> ).....	10
Figure 1.8 The antimitotic marine natural product (+)-spongistatin 1 ( <b>1.27</b> ).....	11
Figure 1.9 A pharmacophore analogue ( <b>1.28</b> ) of (+)-spongistatin 1 ( <b>1.27</b> ).....	12
Figure 1.10 A marine peptide with novel biological activity. ....	13
Figure 2.1 The PI3K pathway.....	16
Figure 2.2 The first selective SHIP1 activator marine natural product pelorol ( <b>2.1</b> ). ....	18
Figure 2.3 Pelorol ( <b>2.1</b> ) analogue <b>2.2</b> . ....	19
Figure 2.4 Chemical and enzymatic oxidation of catechol and subsequent 1,6-addition.....	20
Figure 2.5 Analogue <b>2.3</b> without the catechol functionality.....	20
Figure 2.6 Natural products made by biomimetically-inspired syntheses.....	22
Figure 2.7 Carbocation generation.....	22
Figure 2.8 Typical propagation and termination of a polyene cascade. ....	23
Figure 2.9 Water soluble prodrug analogues of <b>2.3</b> .....	26
Figure 2.10 Analogue <b>2.18</b> .....	27
Figure 2.11 Water soluble analogue design.....	27

Figure 2.12 CLogP values of <b>2.18</b> and related analogues.....	28
Figure 2.13 ORTEP diagram of Mosher ester <b>2.32</b> . .....	33
Figure 2.14 ORTEP diagram of alcohol <b>2.30</b> . .....	33
Figure 2.15 Analogues <b>2.42</b> and <b>2.43</b> constructed using a D-fructose derived Shi catalyst. ..	35
Figure 2.16 ORTEP diagram of racemic amine mixture <b>2.20/2.42</b> . .....	36
Figure 2.17 STD NMR. ....	39
Figure 2.18 STDD NMR sample preparation. ....	41
Figure 2.19 STDD NOE NMR of <b>2.42</b> . ....	42
Figure 2.20 Components of a photoaffinity probe.....	43
Figure 2.21 Examples of photoreactive groups. ....	44
Figure 2.22 Commonly used tags. ....	45
Figure 2.23 Examples of photoaffinity probes. ....	46
Figure 2.24 Principle of <b>2.3</b> based photoaffinity probe ( <b>2.53</b> ).....	47
Figure 2.25 SHIP1 phosphatase assay. ....	52
Figure 2.26 Efficacy of <b>2.20/2.42</b> versus cyproheptadine (Cyp, 1 mg/kg) in a mouse (PCA) model.....	56
Figure 2.27 <sup>1</sup> H and <sup>13</sup> C NMR spectra of <b>2.12</b> recorded in CDCl <sub>3</sub> at 400 MHz and 100 MHz respectively. ....	62
Figure 2.28 <sup>1</sup> H and <sup>13</sup> C NMR spectra of <b>2.28</b> recorded in CDCl <sub>3</sub> at 400 MHz and 100 MHz respectively. ....	65
Figure 2.29 <sup>1</sup> H and <sup>13</sup> C NMR spectra of <b>2.26</b> recorded in CDCl <sub>3</sub> at 400 MHz and 100 MHz respectively. ....	68

Figure 2.30 $^1\text{H}$ and $^{13}\text{C}$ NMR spectra of <b>2.30</b> recorded in $\text{CDCl}_3$ at 400 MHz and 100 MHz respectively. ....	70
Figure 2.31 $^1\text{H}$ and $^{13}\text{C}$ NMR spectra of <b>2.31</b> recorded in $\text{CDCl}_3$ at 400 MHz and 100 MHz respectively. ....	73
Figure 2.32 $^1\text{H}$ and $^{13}\text{C}$ NMR spectra of <b>2.32</b> recorded in $\text{CDCl}_3$ at 400 MHz and 100 MHz respectively. ....	75
Figure 2.33 $^1\text{H}$ and $^{13}\text{C}$ NMR spectra of <b>2.33</b> recorded in $\text{CDCl}_3$ at 400 MHz and 100 MHz respectively. ....	77
Figure 2.34 $^1\text{H}$ and $^{13}\text{C}$ NMR spectra of <b>2.19</b> recorded in $(\text{CD}_3)_2\text{CO}$ at 400 MHz and 100 MHz respectively. ....	79
Figure 2.35 $^1\text{H}$ and $^{13}\text{C}$ NMR spectra of <b>2.20</b> recorded in $\text{CD}_3\text{OD}$ at 600 MHz and 150 MHz respectively. ....	82
Figure 2.36 $^1\text{H}$ and $^{13}\text{C}$ NMR spectra of <b>2.34</b> recorded in $\text{CD}_3\text{OD}$ at 600 MHz and 150 MHz respectively. ....	83
Figure 2.37 $^1\text{H}$ and $^{13}\text{C}$ NMR spectra of <b>2.40</b> recorded in $(\text{CD}_3)_2\text{CO}$ at 400 MHz and 100 MHz respectively. ....	86
Figure 2.38 $^1\text{H}$ and $^{13}\text{C}$ NMR spectra of <b>2.44</b> recorded in $\text{CD}_3\text{OD}$ at 400 MHz and 100 MHz respectively. ....	88
Figure 2.39 $^1\text{H}$ and $^{13}\text{C}$ NMR spectra of <b>2.45</b> recorded in $\text{CD}_3\text{OD}$ at 600 MHz and 150 MHz respectively. ....	90
Figure 2.40 $^1\text{H}$ and $^{13}\text{C}$ NMR spectra of <b>2.61</b> recorded in $\text{CDCl}_3$ at 400 MHz and 100 MHz respectively. ....	94

Figure 2.41 $^1\text{H}$ and $^{13}\text{C}$ NMR spectra of <b>2.53</b> recorded in $\text{CDCl}_3$ at 400 MHz and 100 MHz respectively. ....	96
Figure 2.42 NOESY spectrum of <b>2.53</b> in $\text{CDCl}_3$ at 400 MHz. ....	97
Figure 3.1 Endogenous androgens found in humans. ....	101
Figure 3.2 Examples of antiandrogens. ....	103
Figure 3.3 Androgen receptor structure. ....	104
Figure 3.4 Small molecule antagonists of the AR NTD. ....	105
Figure 3.5 Niphatenones A ( <b>3.8</b> ) and B ( <b>3.9</b> ). ....	105
Figure 3.6 Ceratodictyol A ( <b>3.36</b> ) and B ( <b>3.37</b> ). ....	111
Figure 3.7 Proposed SAR of ( <i>R</i> )-niphatenone B ( <b>3.31</b> ). ....	111
Figure 3.8 Fluorescent probe mode of action. ....	118
Figure 3.9 Non-targeting and targeting fluorescent probes. ....	119
Figure 3.10 Cellular imaging agent of glutathione. ....	121
Figure 3.11 AR transcriptional activity assay of the niphatenones and their analogues. ....	123
Figure 3.12 Androgen induced proliferation assay. ....	125
Figure 3.13 Binding between alkyne probe <b>3.67</b> and the NTD AF1 region of the AR. ....	126
Figure 3.14 $^1\text{H}$ and $^{13}\text{C}$ NMR spectra of <b>3.16</b> recorded in $\text{CDCl}_3$ at 400 MHz and 100 MHz respectively. ....	130
Figure 3.15 $^1\text{H}$ and $^{13}\text{C}$ NMR spectra of <b>3.17</b> recorded in $\text{CDCl}_3$ at 400 MHz and 100 MHz respectively. ....	132
Figure 3.16 $^1\text{H}$ and $^{13}\text{C}$ NMR spectra of <b>3.18</b> recorded in $\text{CDCl}_3$ at 400 MHz and 100 MHz respectively. ....	134

Figure 3.17 $^1\text{H}$ and $^{13}\text{C}$ NMR spectra of <b>3.20</b> recorded in $\text{CDCl}_3$ at 400 MHz and 100 MHz respectively. ....	137
Figure 3.18 $^1\text{H}$ and $^{13}\text{C}$ NMR spectra of <b>3.21</b> recorded in $\text{C}_6\text{D}_6$ at 600 MHz and 150 MHz respectively. ....	139
Figure 3.19 $^1\text{H}$ and $^{13}\text{C}$ NMR spectra of <b>3.27</b> recorded in $\text{CDCl}_3$ at 400 MHz and 100 MHz respectively. ....	142
Figure 3.20 $^1\text{H}$ and $^{13}\text{C}$ NMR spectra of <b>3.28</b> recorded in $\text{CDCl}_3$ at 400 MHz and 100 MHz respectively. ....	144
Figure 3.21 $^1\text{H}$ and $^{13}\text{C}$ NMR spectra of <b>3.29</b> recorded in $\text{CDCl}_3$ at 400 MHz and 100 MHz respectively. ....	146
Figure 3.22 $^1\text{H}$ and $^{13}\text{C}$ NMR spectra of <b>3.30</b> recorded in $\text{C}_6\text{D}_6$ at 400 MHz and 100 MHz respectively. ....	148
Figure 3.23 $^1\text{H}$ and $^{13}\text{C}$ NMR spectra of <b>3.31</b> recorded in $\text{C}_6\text{D}_6$ at 600 MHz and 150 MHz respectively. ....	150
Figure 3.24 $^1\text{H}$ and $^{13}\text{C}$ NMR spectra of <b>3.33</b> recorded in $\text{CDCl}_3$ at 400 MHz and 100 MHz respectively. ....	152
Figure 3.25 $^1\text{H}$ and $^{13}\text{C}$ NMR spectra of <b>3.34</b> recorded in $\text{CDCl}_3$ at 300 MHz and 75 MHz respectively. ....	154
Figure 3.26 $^1\text{H}$ and $^{13}\text{C}$ NMR spectra of <b>3.25</b> recorded in $\text{CDCl}_3$ at 400 MHz and 100 MHz respectively. ....	156
Figure 3.27 $^1\text{H}$ and $^{13}\text{C}$ NMR spectra of <b>3.62</b> recorded in $\text{CDCl}_3$ at 400 MHz and 100 MHz respectively. ....	158

Figure 3.28 $^1\text{H}$ and $^{13}\text{C}$ NMR spectra of <b>3.63</b> recorded in $\text{C}_6\text{D}_6$ at 400 MHz and 75 MHz respectively. ....	160
Figure 3.29 $^1\text{H}$ and $^{13}\text{C}$ NMR spectra of <b>3.41</b> recorded in $\text{CDCl}_3$ at 400 MHz and 100 MHz respectively. ....	162
Figure 3.30 $^1\text{H}$ and $^{13}\text{C}$ NMR spectra of <b>3.42</b> recorded in $\text{CDCl}_3$ at 400 MHz and 100 MHz respectively. ....	164
Figure 3.31 $^1\text{H}$ and $^{13}\text{C}$ NMR spectra of <b>3.43</b> recorded in $\text{CD}_2\text{Cl}_2$ at 600 MHz and 150 MHz respectively. ....	166
Figure 3.32 $^1\text{H}$ and $^{13}\text{C}$ NMR spectra of <b>3.45</b> recorded in $\text{CDCl}_3$ at 400 MHz and 100 MHz respectively. ....	168
Figure 3.33 $^1\text{H}$ and $^{13}\text{C}$ NMR spectra of <b>3.46</b> recorded in $\text{C}_6\text{D}_6$ at 600 MHz and 150 MHz respectively. ....	170
Figure 3.34 $^1\text{H}$ and $^{13}\text{C}$ NMR spectra of <b>3.48</b> recorded in $\text{CDCl}_3$ at 400 MHz and 100 MHz respectively. ....	172
Figure 3.35 $^1\text{H}$ and $^{13}\text{C}$ NMR spectra of <b>3.49</b> recorded in $\text{CDCl}_3$ at 400 MHz and 100 MHz respectively. ....	174
Figure 3.36 $^1\text{H}$ and $^{13}\text{C}$ NMR spectra of <b>3.50</b> recorded in $\text{CDCl}_3$ at 400 MHz and 100 MHz respectively. ....	177
Figure 3.37 $^1\text{H}$ and $^{13}\text{C}$ NMR spectra of <b>3.52</b> recorded in $\text{C}_6\text{D}_6$ at 400 MHz and 100 MHz respectively. ....	179
Figure 3.38 $^1\text{H}$ and $^{13}\text{C}$ NMR spectra of <b>3.53</b> recorded in $\text{CDCl}_3$ at 400 MHz and 100 MHz respectively. ....	181

Figure 3.39 $^1\text{H}$ and $^{13}\text{C}$ NMR spectra of <b>3.54</b> recorded in $\text{CD}_2\text{Cl}_2$ at 600 MHz and 150 MHz respectively. ....	183
Figure 3.40 $^1\text{H}$ and $^{13}\text{C}$ NMR spectra of <b>3.57</b> recorded in $\text{CDCl}_3$ at 400 MHz and 100 MHz respectively. ....	186
Figure 3.41 $^1\text{H}$ and $^{13}\text{C}$ NMR spectra of <b>3.58</b> recorded in $\text{CDCl}_3$ at 400 MHz and 150 MHz respectively. ....	188
Figure 3.42 $^1\text{H}$ and $^{13}\text{C}$ NMR spectra of <b>3.59</b> recorded in $\text{CDCl}_3$ at 600 MHz and 150 MHz respectively. ....	190
Figure 3.43 $^1\text{H}$ and $^{13}\text{C}$ NMR spectra of <b>3.60</b> recorded in $\text{CDCl}_3$ at 600 MHz and 150 MHz respectively. ....	192
Figure 3.44 $^1\text{H}$ and $^{13}\text{C}$ NMR spectra of <b>3.61</b> recorded in $\text{CDCl}_3$ at 600 MHz and 150 MHz respectively. ....	194
Figure 3.45 $^1\text{H}$ and $^{13}\text{C}$ NMR spectra of <b>3.67</b> recorded in $\text{CDCl}_3$ at 600 MHz and 150 MHz respectively. ....	196
Figure 3.46 $^1\text{H}$ and $^{13}\text{C}$ NMR spectra of <b>3.77</b> recorded in $\text{CDCl}_3$ at 400 MHz and 100 MHz respectively. ....	198
Figure 3.47 $^1\text{H}$ and $^{13}\text{C}$ NMR spectra of <b>3.78</b> recorded in $\text{CD}_2\text{Cl}_2$ at 600 MHz and 150 MHz respectively. ....	200
Figure 4.1 AR antagonist lead compound <b>4.1</b> .....	203
Figure 4.2 Structural similarity between <b>4.1</b> and a steroid carbon skeleton. ....	204
Figure 4.3 Delocalization of charge in a furan ring system. ....	207
Figure 4.4 Favored and disfavored regioisomers. ....	211
Figure 4.5 Blocking group to construct A-ring analogues of <b>4.4</b> . ....	211

Figure 4.6 AR competitor <i>in vitro</i> assay.....	218
Figure 4.7 $^1\text{H}$ and $^{13}\text{C}$ NMR spectra of <b>4.16</b> recorded in $\text{CDCl}_3$ at 400 MHz and 100 MHz respectively. ....	224
Figure 4.8 $^1\text{H}$ and $^{13}\text{C}$ NMR spectra of <b>4.18</b> recorded in $\text{CDCl}_3$ at 400 MHz and 100 MHz respectively. ....	226
Figure 4.9 $^1\text{H}$ and $^{13}\text{C}$ NMR spectra of <b>4.19</b> recorded in $\text{CDCl}_3$ at 300 MHz and 75 MHz respectively. ....	228
Figure 4.10 $^1\text{H}$ and $^{13}\text{C}$ NMR spectra of <b>4.20</b> recorded in $\text{CDCl}_3$ at 300 MHz and 75 MHz respectively. ....	230
Figure 4.11 $^1\text{H}$ and $^{13}\text{C}$ NMR spectra of <b>4.21</b> recorded in $\text{CDCl}_3$ at 400 MHz and 100 MHz respectively. ....	232
Figure 4.12 $^1\text{H}$ and $^{13}\text{C}$ NMR spectra of <b>4.22</b> recorded in $\text{CDCl}_3$ at 400 MHz and 100 MHz respectively. ....	234
Figure 4.13 $^1\text{H}$ and $^{13}\text{C}$ NMR spectra of <b>4.23</b> recorded in $\text{CDCl}_3$ at 400 MHz and 100 MHz respectively. ....	236
Figure 4.14 $^1\text{H}$ spectrum of <b>4.24</b> recorded in $\text{CDCl}_3$ at 400 MHz.....	238
Figure 4.15 $^1\text{H}$ and $^{13}\text{C}$ NMR spectra of <b>4.40</b> recorded in $\text{CDCl}_3$ at 400 MHz and 100 MHz respectively. ....	240
Figure 4.16 $^1\text{H}$ and $^{13}\text{C}$ NMR spectra of <b>4.42</b> recorded in $\text{CD}_2\text{Cl}_2$ at 400 MHz and 100 MHz respectively. ....	243
Figure 4.17 $^1\text{H}$ and $^{13}\text{C}$ NMR spectra of <b>4.43</b> recorded in $\text{CDCl}_3$ at 400 MHz and 100 MHz respectively. ....	245

Figure 4.18 $^1\text{H}$ and $^{13}\text{C}$ NMR spectra of <b>4.44</b> recorded in $\text{CDCl}_3$ at 600 MHz and 150 MHz respectively. ....	247
Figure 5.1 Hydrolysis of a peptide by a cysteine protease. ....	249
Figure 5.2 Peptide-aldehyde inhibitors of cysteine proteases.....	251
Figure 5.3 Covalent binding mechanism between a peptide-aldehyde natural product and a cysteine protease. ....	252
Figure 5.4 Novel peptide-aldehyde lichostatinal ( <b>5.4</b> ).....	253
Figure 5.5 $^1\text{H}$ and $^{13}\text{C}$ NMR spectra of <b>5.12</b> recorded in $(\text{CD}_3)_2\text{SO}$ at 400 MHz and 100 MHz respectively. ....	266
Figure 5.6 $^1\text{H}$ and $^{13}\text{C}$ NMR spectra of <b>5.13</b> recorded in $\text{D}_2\text{O}$ at 400 MHz and 100 MHz respectively. ....	268
Figure 5.7 $^1\text{H}$ and $^{13}\text{C}$ NMR spectra of <b>5.15</b> recorded in $(\text{CD}_3)_2\text{SO}$ at 600 MHz and $\text{CD}_2\text{Cl}_2$ at 150 MHz respectively. ....	270
Figure 5.8 $^1\text{H}$ and $^{13}\text{C}$ NMR spectra of <b>5.16</b> recorded in $(\text{CD}_3)_2\text{SO}$ at 600 MHz and 150 MHz respectively. ....	272
Figure 5.9 $^1\text{H}$ and $^{13}\text{C}$ NMR spectra of <b>5.18</b> recorded in $(\text{CD}_3)_2\text{SO}$ at 600 MHz and 150 MHz respectively. ....	275
Figure 5.10 $^1\text{H}$ and $^{13}\text{C}$ NMR spectra of <b>5.20</b> recorded in $(\text{CD}_3)_2\text{SO}$ at 600 MHz and 150 MHz respectively.....	278
Figure 5.11 $^1\text{H}$ and $^{13}\text{C}$ NMR spectra of <b>5.24</b> recorded in $(\text{CD}_3)_2\text{SO}$ at 600 MHz and 150 MHz respectively.....	280
Figure 5.12 $^1\text{H}$ and $^{13}\text{C}$ NMR spectra of <b>5.29</b> recorded in $\text{CD}_2\text{Cl}_2$ at 600 MHz and 100 MHz respectively. ....	282

Figure 5.13 $^1\text{H}$ and $^{13}\text{C}$ NMR spectra of <b>5.30</b> recorded in $(\text{CD}_3)_2\text{SO}$ at 600 MHz and 150 MHz respectively. ....	284
Figure 5.14 $^1\text{H}$ and $^{13}\text{C}$ NMR spectra of <b>5.32</b> recorded in $(\text{CD}_3)_2\text{SO}$ at 600 MHz and 150 MHz respectively. ....	286
Figure 5.15 $^1\text{H}$ and $^{13}\text{C}$ NMR spectra of <b>5.33</b> recorded in $\text{D}_2\text{O}$ and $(\text{CD}_3)_2\text{SO}$ at 400 MHz and 100 MHz respectively. ....	288
Figure 5.16 $^1\text{H}$ and $^{13}\text{C}$ NMR spectra of <b>5.35</b> recorded in $\text{CD}_3\text{OD}$ at 400 MHz and $(\text{CD}_3)_2\text{SO}$ at 150 MHz respectively. ....	290
Figure 5.17 $^1\text{H}$ and $^{13}\text{C}$ NMR spectra of <b>5.36</b> recorded in $\text{CD}_3\text{OD}$ at 600 MHz and 150 MHz respectively. ....	292
Figure 5.18 $^1\text{H}$ and $^{13}\text{C}$ NMR spectra of <b>5.37</b> recorded in $\text{CD}_3\text{OD}$ at 600 MHz and 150 MHz respectively. ....	294
Figure 5.19 $^1\text{H}$ and $^{13}\text{C}$ NMR spectra of <b>5.38</b> recorded in $(\text{CD}_3)_2\text{SO}$ at 600 MHz and 150 MHz respectively. ....	296
Figure 5.20 $^1\text{H}$ and $^{13}\text{C}$ NMR spectra of <b>5.39</b> recorded in $\text{CD}_3\text{OD}$ at 600 MHz and 150 MHz respectively. ....	298
Figure 5.21 $^1\text{H}$ and $^{13}\text{C}$ NMR spectra of <b>5.40</b> recorded in $(\text{CD}_3)_2\text{SO}$ at 600 MHz and 150 MHz respectively. ....	300
Figure 6.1 Alternative route to lichostatinal ( <b>5.4</b> ).....	308

## List of Schemes

Scheme 2.1 Synthetic route to drug lead <b>2.3</b> . .....	21
Scheme 2.2 Retrosynthetic analysis of <b>2.3</b> . .....	24
Scheme 2.3 Synthesis of ( $\pm$ )- <b>2.3</b> . .....	24
Scheme 2.4 Elimination side products of chlorosulfonic acid cyclization. ....	25
Scheme 2.5 Inspiration for biomimetic synthesis: steroid biosynthesis from squalene ( <b>2.21</b> ). .....	29
Scheme 2.6 Retrosynthetic analysis of <b>2.20</b> . .....	30
Scheme 2.7 Synthesis of amine analogues <b>2.20</b> and <b>2.34</b> . .....	31
Scheme 2.8 Examples of indium tribromide promoted annulation methodology .....	32
Scheme 2.9 Alternative amination strategies towards <b>2.20</b> and <b>2.34</b> . .....	34
Scheme 2.10 Racemic synthesis of ( $\pm$ )- <b>2.20</b> using <i>m</i> CPBA. ....	36
Scheme 2.11 Polar analogues of <b>2.18</b> . .....	37
Scheme 2.12 Synthesis of the <b>2.18</b> enantiomer ( <b>2.48</b> ). .....	38
Scheme 2.13 Retrosynthetic analysis of <b>2.53</b> . .....	48
Scheme 2.14 Benzophenone photoaffinity probe ( <b>2.53</b> ) synthesis. ....	49
Scheme 2.15 Fries rearrangement and NOE observance in <b>2.53</b> . .....	50
Scheme 2.16 Rational drug design from a marine natural product ( <b>2.1</b> ) to drug lead ( <b>2.20/2.42</b> ). .....	60
Scheme 3.1 Retrosynthetic analysis of niphatenone A ( <b>3.8</b> ). .....	106
Scheme 3.2 Synthesis of ( <i>R</i> )-niphatenone A ( <b>3.21</b> ). .....	107
Scheme 3.3 Synthesis of ( <i>S</i> )-niphatenone A ( <b>3.23</b> ). .....	108
Scheme 3.4 Retrosynthesis of niphatenone B ( <b>3.9</b> ). .....	108

Scheme 3.5 Synthesis of ( <i>R</i> )-niphatenone B ( <b>3.31</b> ).....	109
Scheme 3.6 Synthesis of ( <i>S</i> )-niphatenone B ( <b>3.35</b> ). .....	110
Scheme 3.7 Synthesis of a long chain ( <i>R</i> )-niphatenone B ( <b>3.31</b> ) analogue <b>3.43</b> .....	112
Scheme 3.8 Synthesis of a short chain ( <i>R</i> )-niphatenone B ( <b>3.31</b> ) analogue <b>3.46</b> .....	113
Scheme 3.9 ( <i>R</i> )-Niphatenone B ( <b>3.31</b> ) glycerol analogues.....	114
Scheme 3.10 All carbon backbone ( <i>R</i> )-niphatenone B ( <b>3.31</b> ) analogue <b>3.61</b> .....	115
Scheme 3.11 Dihydro ( <i>R</i> )-niphatenone B ( <b>3.31</b> ) analogue <b>3.63</b> .....	116
Scheme 3.12 Propargyl ether analogue <b>3.67</b> .....	119
Scheme 3.13 Click chemistry of probe 3.67 and fluorophore <b>3.69</b> . .....	120
Scheme 3.14 Synthesis of a potential AR NTD fluorescent probe ( <b>3.78</b> ). .....	122
Scheme 4.1 Semisynthesis of <b>4.1</b> analogues.....	205
Scheme 4.2 Zoretic's synthesis of an A-ring <b>4.4</b> analogue ( <b>4.6</b> ). .....	206
Scheme 4.3 Retrosynthesis of a <b>4.4</b> A-ring analogue <b>4.6</b> . .....	206
Scheme 4.4 Synthesis of furanyl isoprene <b>4.13</b> . .....	208
Scheme 4.5 Synthesis of regioisomer <b>4.24</b> . .....	209
Scheme 4.6 Goldsmiths furan C-2 silylation strategy. ....	212
Scheme 4.7 Failed selective TMS deprotection.....	212
Scheme 4.8 Synthetic attempt towards C-2 silylated intermediate <b>4.35</b> .....	213
Scheme 4.9 Attempt at constructing thiolated analogue <b>4.38</b> .....	214
Scheme 4.10 Mono-thiolated analogues of <b>4.12</b> .....	215
Scheme 4.11 Di-thiolated analogues of <b>4.12</b> . .....	215
Scheme 4.12 Epoxide-initiated cationic cascade using a thiol blocking group.....	216
Scheme 5.1 Retrosynthetic analysis of lichostatinal ( <b>5.4</b> ). .....	254

Scheme 5.2 Synthesis toward lichostatinal ( <b>5.4</b> ).....	255
Scheme 5.3 Ito's reduction of Cbz protected arginine <b>5.22</b> .....	257
Scheme 5.4 Oxidation of Arginol ( <b>5.24</b> ). ....	258
Scheme 5.5 Synthesis towards lichostatinal ( <b>5.4</b> ).....	259
Scheme 5.6 Alternative route to lichostatinal ( <b>5.4</b> ). ....	261
Scheme 6.1 Syntheses towards polar analogues of <b>4.4</b> .....	304
Scheme 6.2 Lithiation strategy to construct A-ring analogues of <b>4.4</b> .....	305
Scheme 6.3 Deprotection of regioisomer <b>4.24</b> . ....	306
Scheme 6.4 Alternative synthesis of regioisomer ( $\pm$ )- <b>6.9</b> .....	307

## List of Symbols and Abbreviations

°	- degree(s)
%	- percent
(±)	- racemic
AcOH	- acetic acid
AF1	- activation function 1
AIBN	- azobisisobutyronitrile
AKT	- protein kinase B
Ala	- alanine
AR	- androgen receptor
Asp	- aspartic acid
br	- broad
Bn	- benzyl
Boc	- <i>t</i> -butoxycarbonyl
BRSM	- based on recovered starting material
Bu	- butyl
<i>n</i> -BuLi	- <i>n</i> -butyllithium
<i>t</i> -BuLi	- <i>t</i> -butyllithium
°C	- degrees Celsius
15C-5	- 1,4,7,10,13-pentaoxacyclopentadecane
18C-6	- 1,4,7,10,13,16-hexaoxacyclooctadecane
CA	- California
calcd	- calculated
Cbz	- carboxybenzyl
CDI	- carbonyldiimidazole
CLogP	- calculated octanol/water partition coefficient
COSY	- two-dimensional correlation spectroscopy
CRPC	- castrate recurrent prostate cancer
Cyp	- cyproheptadine
Cys	- cysteine
δ	- chemical shift in parts per million
d	- doublet
DBU	- 1,8-diazabicyclo[5.4.0]undec-7-ene
DCM	- dichloromethane
dd	- doublet of doublets
DHEA	- dehydroepiandrosterone
DIBAL-H	- diisobutylaluminium hydride
DIEA	- <i>N,N</i> -diisopropylethylamine
DIPT	- diisopropyl tartrate
DMAP	- 4-dimethylaminopyridine
DMF	- <i>N,N</i> -dimethylformamide
DMP	- Dess–Martin periodinane
DMS	- dimethyl sulfide
DMSO	- dimethyl sulfoxide
DNA	- deoxyribonucleic acid

DNP	- dinitrophenyl
DOM	- directed ortho metalation
DPBS	- Dulbecco's phosphate buffered saline
dppp	- 1,3-bis(diphenylphosphino)propane
dt	- doublet of triplets
DTT	- dithiothreitol
ED <sub>50</sub>	- effective dose
equiv.	- equivalent(s)
EIMS	- electron impact mass spectrometry
ESIMS	- electrospray ionization mass spectrometry
Et	- ethyl
EtOAc	- ethyl acetate
EtOH	- ethanol
FBS	- fetal bovine serum
Fmoc	- fluorenylmethoxycarbonyl
g	- gram(s)
Gly	- glycine
GSH	- glutathione
h	- hour(s)
HATU	- (2-(7-aza-1H-benzotriazole-1-yl)-1,1,3,3-tetramethyluronium hexafluorophosphate)
HCT-116	- human carcinoma cell line
HPLC	- high-performance liquid chromatography
HRESIMS	- high resolution electrospray mass spectrometry
HRP	- horseradish peroxidase
HSA	- human serum albumin
HTS	- high throughput screening
HWE	- Horner–Wadsworth–Emmons
Hz	- hertz
IBX	- 2-iodoxybenzoic acid
IC <sub>50</sub>	- median inhibitory concentration
IgE	- immunoglobulin E
IgG	- immunoglobulin G
IL-1	- interleukin-1
IL-6	- interleukin-6
J	- coupling constant in hertz
Kb	- kilo-base pair
Kg	- kilogram
KHMDS	- potassium bis(trimethylsilyl)amide
L	- levorotatory
lb.	- pound
LBD	- ligand binding domain
LCMS	- liquid-chromatography mass spectrometry
LDA	- lithium diisopropyl amine
Leu	- leucine
LPS	- lipopolysaccharide

Lys	- lysine
m	- multiplet
M	- molar concentration
<i>m</i> CPBA	- <i>meta</i> -chloroperbenzoic acid
Me	- methyl
MeCN	- acetonitrile
MeOH	- methanol
Met	- methionine
mg	- milligram(s)
MHz	- megahertz
min	- minute
mL	- milliliter(s)
mm	- millimeter(s)
mM	- millimolar
MM	- multiple myeloma
mmol	- millimol(s)
μl	- microliter
μM	- micromolar
mRNA	- messenger ribonucleic acid
MS	- mass spectrometry
MTPA	- $\alpha$ -methoxy- $\alpha$ -trifluoromethylphenylacetic acid
nM	- nanomolar
NCS	- <i>N</i> -chlorosuccinimide
ng	- nanogram
nm	- nanometers
NMR	- nuclear magnetic resonance
NOE	- nuclear overhauser enhancement
NOESY	- nuclear overhauser effect spectroscopy
NTD	- n-terminal domain
OSC	- oxidosqualene cyclase
PCC	- pyridinium chlorochromate
PCR	- polymerase chain reaction
PBS	- phosphate buffered saline
PEG	- poly(ethylene)glycol
pH	- $-\log_{10}[\text{H}^+]$
Ph	- phenyl
PIP <sub>3</sub>	- phosphatidylinositol-3,4,5-triphosphate
PIP <sub>2</sub>	- phosphatidylinositol-4,5-biphosphate
PI3K	- phosphatidylinositol-3-kinase
ppm	- parts per million
<i>i</i> -Pr	- isopropyl group
PSA	- prostate specific antigen
PtdIns(4,5)P <sub>2</sub>	- phosphatidylinositol-4,5-biphosphate
PtdIns(3,4,5)P <sub>3</sub>	- phosphatidylinositol-3,4,5-triphosphate
PtdIns(3,4)P <sub>2</sub>	- phosphatidylinositol-3,4-biphosphate
PTEN	- phosphatase and tensin homologue

Pyr	- pyridine
q	- quartet
RF	- radio frequency
rpm	- revolutions per minute
rt	- room temperature
s	- singlet
SAR	- structure-activity relationship
SCUBA	- self-contained underwater breathing apparatus
SDS-PAGE	- sodium dodecyl sulfate polyacrylamide gel electrophoresis
SE	- squalene epoxidase
Ser	- serine
SHC	- squalene hopene cyclase
SHIP	- src homology 2-containing Inositol 5'-phosphatase
sSHIP	- stem cell src homology 2-containing Inositol 5'-phosphatase
S <sub>N</sub> Ar	- addition-elimination
sp.	- species
STD	- saturation transfer difference
STDD	- saturation transfer double difference
t	- triplet
TBA	- tetrabutylammonium
TBDPSCI	- <i>tert</i> -butylchlorodiphenylsilane
TDPQ	- 1,2,3,4-tetrahydro-2,2-dimethyl-6-(trifluoromethyl)-8-pyridono[5,6-g]quinoline
TEA	- triethylamine
TEMPO	- (2,2,6,6-tetramethylpiperidin-1-yl)oxyl
TFA	- trifluoroacetic acid
TFAA	- trifluoroacetic anhydride
THF	- tetrahydrofuran
Thr	- threonine
TIPS	- triisopropylsilyl
TLC	- thin-layer chromatography
TMS	- trimethylsilyl
TNF	- tumor necrosis factor
TOCSY	- total correlation spectroscopy
tol	- toluene
Tyr	- tyrosine
ug	- microgram
U.S.A.	- United States of America
VCAM	- vascular cell adhesion molecule
v/v	- volume to volume

## Acknowledgements

What a trip. First, I must thank the ones closest to me, for without them none of this would be possible. I thank my beautiful wife Eszter for supporting my crazy and for being the 50-foot tall woman in a 5'8" package. You Rock! Tentacles! Keep building that death star! My parents for seeing me at my worst and still deciding to keep me instead of putting me up for adoption. Thank you. I also thank all of my family in Greece, and the country itself. Haters gonna hate!

I thank my supervisor Dr. Raymond Andersen for his guidance and support over the years. The diversity of chemistry that I had the privilege to work on was amazing, and the discoveries I made were thrilling. There is no challenge I cannot conquer and I have Raymond to thank for that.

I thank Dr. David Williams who has played a role in all my projects, and to whom I owe countless bags of chips. I thank Dr. Javier Garcia Fernandez for helping me make sense of it all and for all the laughs. Chamon MoFo! I thank all of my biological collaborators at UBC and the BC Cancer Agency. Dr. Glenn Sammis and Dr. Gregory Dake get thanks for their helpful discussions over the years. A thank you goes to everybody that gathered data for me in the NMR, MS, and X-ray labs, especially Maria Ezhova in the NMR lab. To all current and past Andersen group members we laughed, we cried, we had a good time. Mike I promise to take my silica over to the Chem department this time...let me just run this column.

I have many people to thank at SFU for many reasons. Thanks goes to Dr. Robert Britton for continuously supporting me from the time of broken glassware and chemical spill cover-ups. To Matt, Jeff, and Pat. As I am writing this, I want to grab a few pints with you guys. The sign of true friendship. You are all kings amongst men. Finally, in random order (not really I hate you Bart) the pets...Bubbles, Hammy, Fermi, Kosta, Jammy, Julia, Puppy, Smokey...Bart.

Lastly, I thank myself for all of my efforts.

‘Buy the ticket, take the ride...’

-Hunter S. Thompson

## Dedication

To my parents George and Martha,  
for all the car rides and sandwiches.

It's Friday.

# Chapter 1: Marine Natural Products From Benchtop to Bedside

## 1.1 Nature as a Source of Medicine

Mankind's ability to harness nature as a source of medicine was a key step in the evolutionary success of our species. In the early stages of human history, plants were the main source of medicine. Phyta of different varieties were used for many purposes including seduction, probing the boundaries of consciousness, pain relief, and even suicide.<sup>1,2,3,4</sup>

The 20<sup>th</sup> century brought about a new era of scientific enlightenment, allowing us to probe the structure of these once esoteric biologically active molecules. No longer would myth and folklore surround plants such as mint, peyote, willow, and hemlock, instead the active components could now be isolated and identified (Figure 1.1). Furthermore, new chemical entities could be classified as terpenes,<sup>5</sup> alkaloids,<sup>6</sup> polyketides,<sup>7</sup> and nonribosomal peptides<sup>8</sup> based on their common structural motifs and putative biogenetic origins.

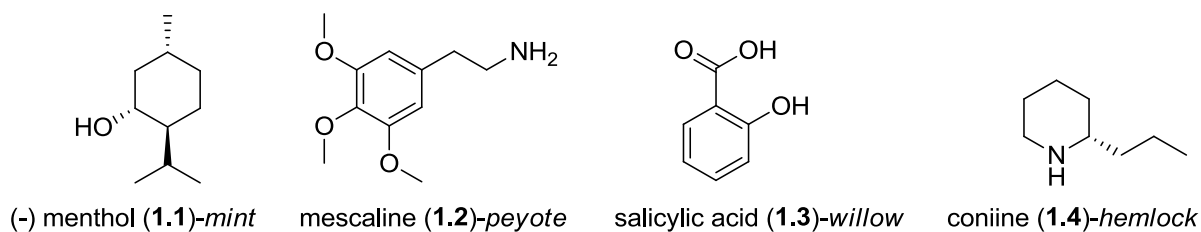


**Figure 1.1** Bioactive compounds of plants commonly used throughout human history.

With the commercialization of SCUBA in the 1950's, the shallow marine environment could be routinely explored. This catalyzed a renaissance in the field of natural products. It was realized that if bioactive compounds could be discovered from terrestrial sources, then the marine environment should provide a plethora of novel compounds as well.

While this has held true over the years, translating bioactive marine drug leads from benchtop to bedside has been an uphill battle. Over the past 25 years, the advent of high-throughput screening<sup>9</sup> (HTS) facilitated rapid large-scale analysis of synthetic compounds in a number of different assays. The most efficient automation systems currently employed test up to 100,000 compounds a day,<sup>10</sup> with the most current research in HTS suggesting the screening of 100 million reaction products in ten hours.<sup>11</sup> This development of HTS in the last couple of decades resulted in compound supply lagging behind testing capabilities. This stimulated the birth of combinatorial chemistry.<sup>12,13</sup> Combinatorial chemistry allows for the rapid syntheses of different analogues with structural similarity. HTS proved too alluring for many pharmaceutical companies in the 90's, leading giants such as GlaxoSmithKline and Pfizer to phase out screening of their natural product libraries. However, at the height of HTS in 2001, there was a twenty year low<sup>14</sup> in the number of new chemical entities reaching the market. As of 2012, the promise of HTS and combinatorial chemistry has yet to be realized.

The Achilles heel for combinatorial chemistry is its dependence on functional group interconversion. This results in libraries of oligomers and peptides that, compared to natural products, have limited chemical diversity. Roche<sup>15</sup> conducted a study in which trade drugs (compounds with a trade name associated with them), were compared to a natural product library and a purely synthetic compound library with no biological lineage (Table 1.1). Approximately 10 % of drugs violated two or more of the Lipinski<sup>16</sup> “drug-like” guidelines (Chapter 2, Section 2.4) compared to 12 % for natural products; in essence little difference. Additionally, synthetics relied more on nitrogen, sulfur, and halogens, whereas natural products contained more oxygen functional groups.

**Table 1.1** The properties of natural products compared with drugs, and synthetics.

	Natural Products	Drugs	Synthetics
Molecular weight	360-414	340-356	393
LogP	2.4-2.9	2.1-2.2	4.3
Number of chiral centers	3.2-6.2	1.2-2.3	0.1-0.4
Number of N atoms	0.84	1.64	2.69
Number of O atoms	5.9	4.03	2.77
% of rings that are aromatic	31 %	55 %	80 %

A significant difference<sup>17</sup> between natural products and synthetic compounds is that natural products have more steric complexity and rigidity due to a large number of rings, chiral centers, and bridgeheads. The origin of this spatial complexity is that natural products have evolved to bind biological targets, which have a defined spatial orientation. Furthermore, natural product building blocks are limited in variety and for an organism to compete in the environment nature has utilized space effectively resulting in complex three-dimensional shapes.

A great example illustrating how nature's palette has created a bioactive compound well-suited for human physiology is salinosporamide A (**1.5**). Salinosporamide A (**1.5**) is a hybrid polyketide/nonribosomal peptide isolated from the deep-sea actinomycete *Salinispora tropica*.<sup>18</sup> Initial testing showed *in vitro* cytotoxic activity with an IC<sub>50</sub> of 11 ng/mL towards HCT-116, a human colon carcinoma cell line. Structural similarity of **1.5** to omuralide (**1.6**) prompted its testing as a 20S proteasome inhibitor.<sup>19</sup> 20S proteasome is a multicatalytic, proteolytic complex involved in intracellular processes such as cell cycle regulation and cytokine stimulated signal transduction cascades. It plays an important role in

neurodegenerative diseases such as Parkinson's and Alzheimer's disease. Salinosporamide A (**1.5**) was found to be 35 times more potent than omuralide (**1.6**).

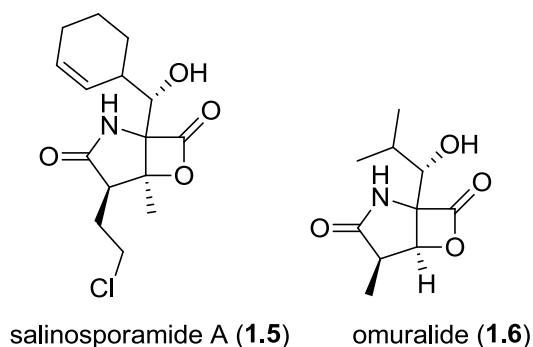


**Figure 1.2** Inhibitors of the 20S proteasome salinosporamide A (**1.5**) and omuralide (**1.6**).

Investigation of the substantial difference in activity between these two compounds revealed the mode of action between salinosporamide A (**1.5**) and 20S proteasome.<sup>20</sup> By obtaining a crystal structure of the ligand-enzyme complex, it was shown that the interaction between the ligand and the peptide was covalent (Figure 1.3).

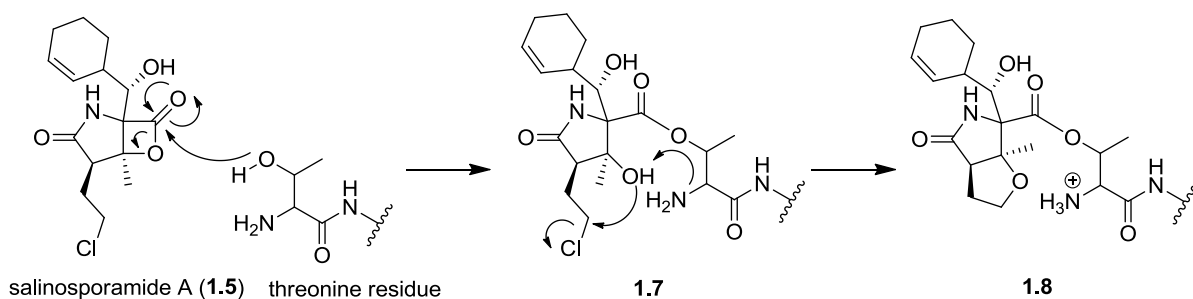


**Figure 1.3** Salinosporamide A (**1.5**) mechanism of action.

The proposed mechanism involves attack of the lactone carbonyl by a threonine residue forming a covalent bond in ester **1.7** (Figure 1.3). The amine moiety of threonine then

deprotonates the secondary alcohol of intermediate **1.7**, followed by an intramolecular annulation to form a tetrahydrofuran ring in **1.8** (Figure 1.3). The covalent nature of this interaction is necessary for the activity of salinosporamide A (**1.5**), however, it is the presence of the chloro-ethyl functionality which gives **1.5** enhanced potency relative to omuralide (**1.6**). The tetrahydrofuran ring in **1.8** was found to provide a barrier to water molecules, which would otherwise hydrolyze the ligand-enzyme complex **1.8**. Additionally, the protonated threonine amine in **1.8** is now deactivated as the protonated amine, which under normal circumstances would catalyze hydrolysis (as in the case with omuralide (**1.6**)). The hydrogen bonding interaction between the protonated amine and the tetrahydrofuran ring tightens the ligand-enzyme complex providing an additional barrier to water.

An understanding of chemical complexity as it relates to drug-enzyme interactions has provided natural products with a second wind. Considering that the majority of current natural product based therapeutics are terrestrial in origin, the question that needs to be asked is: “why look to the marine environment for drug development?”

There is promising news regarding the molecular complexity of marine natural products as shown in a recent review.<sup>21</sup> Approximately 71 % of marine molecular frameworks are used exclusively by marine organisms, with approximately 50 % having a one-time occurrence.

Marine natural products also show a higher occurrence of bioactivity when compared with terrestrial natural products.<sup>22</sup> In a preclinical cytotoxicity screen completed by the National Cancer Institute, it was shown that approximately 1 % of crude marine natural product extracts showed anti-tumor activity compared to 0.1 % of crude terrestrial natural

product extracts. The last couple years has seen an increase to approximately 1000 new marine natural products with varying biological profiles being isolated per annum.<sup>22</sup>

This diversity in marine natural products may provide future drug candidates. However, for any compound to achieve drug status<sup>23</sup> several major hurdles have to be overcome. It can be shown that synthetic organic chemistry plays a major role in each stage of development, from benchtop to bedside.

## 1.2 Synthesis as an Aid to Structure Elucidation

The compounds first identified by marine natural product chemists were “low hanging fruit” that were present in large quantities in the source organisms, and were easily separable from other constituents in the extracts. This was a direct result of limited separation and spectroscopic technologies available in the early days of marine natural product discovery. As techniques for chemical identification became more sophisticated, smaller amounts of material could provide the necessary data needed to elucidate a chemical structure.

A modern example is the macrolide phorboxazole A (**1.9**) that was isolated<sup>24</sup> from the marine sponge *Phorbas sp.* collected in Western Australia (Figure 1.4). Phorboxazole A (**1.9**) (95.1 mg) was isolated in the mid 1990’s at masses sufficient for characterization. A number of smaller peaks in the HPLC trace (0.78-3.0 mg) of the major metabolite (**1.9**) alluded to additional compounds. However, the NMR technology at the time was too insensitive for characterization of these minor components. Fifteen years would pass before phorbaside A<sup>25</sup> (**1.10**) and muironolide A<sup>26</sup> (**1.11**) were characterized (Figure 1.4).

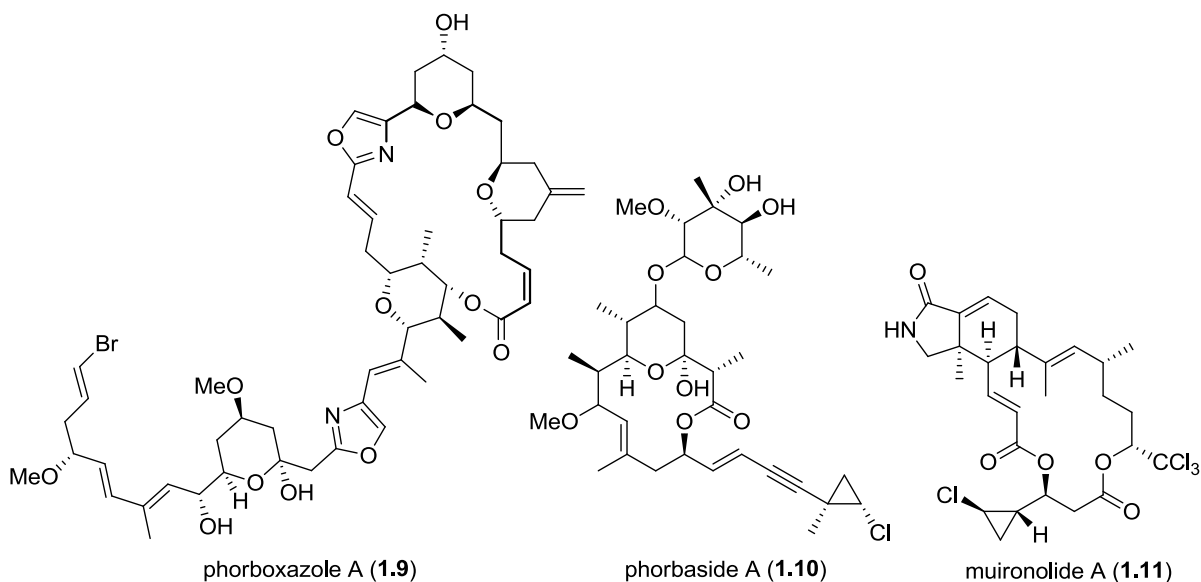


**Figure 1.4** Marine natural product identification at the nM scale

Muironolide A (**1.11**) is an example of how synthesis can help in the structure determination of novel marine natural products. Only 90.0  $\mu\text{g}$  of pure muironolide A (**1.11**) was obtained and a 1.7 mm NMR CryoProbe<sup>TM</sup> (600 MHz) was used for its structure elucidation. Unfortunately, the relative configuration of the chloro-cyclopropane ring moiety could not be assigned, since NOESY correlations could not be made to any of the macrolide ring stereocenters. However, synthesis was used to determine the absolute configuration of the chloro-cyclopropane functionality. Muironolide A (**1.11**) was degraded and its chemical degradation product was compared with known compounds in the literature in order to assign the absolute configuration of the chloro-cyclopropane ring moiety (Figure 1.5).

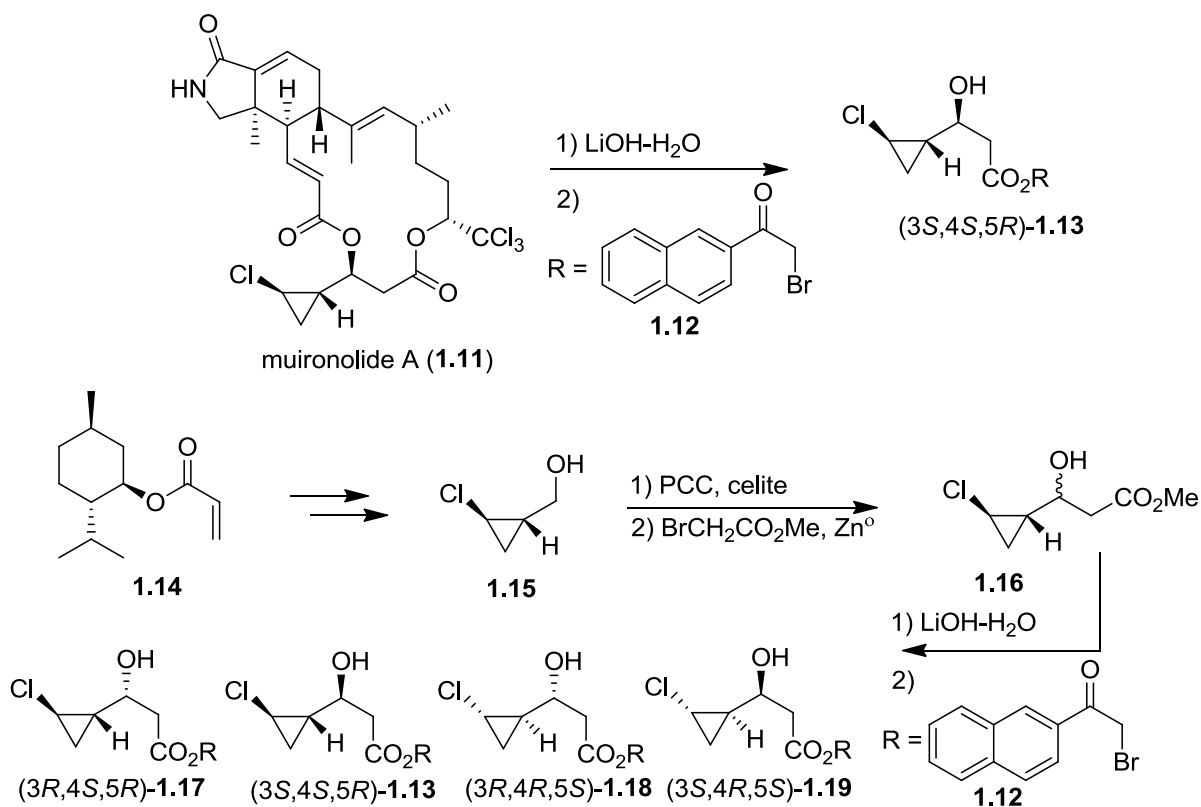


**Figure 1.5** Determination of the absolute configuration of muironolide A (**1.11**) using chemical degradation.

Muironolide A (**1.11**) was saponified and then esterified with  $\alpha$ -bromo-ketone **1.12** to yield degradation fragment **1.13** (Figure 1.5). A set of standards with known configuration was prepared starting from menthol-methyl methacrylate **1.14**. These standards were compared with the muironolide degradation product **1.13**. Chiral LCMS was used to show that the muironolide A (**1.11**) degradation product and synthetic standard **1.13** were identical, assigning the (3*S*,4*S*,5*R*) configuration to the natural product (Figure 1.5).

Another example of how synthesis can assist structural elucidation efforts is the imidazole alkaloid (–)-palau’amine (**1.22**). (–)-Palau’amine (**1.22**) is an alkaloid produced by the marine sponge *Stylotella agminata*. It was isolated in 1993<sup>27</sup> and represents the pinnacle of structural complexity in a family of imidazole containing natural products including (–)-

sceptrin<sup>28</sup> (**1.20**), and (-)-ageliferin<sup>29</sup> (**1.21**) (Figure 1.6). The key structural features of (-)-palau'amine (**1.22**) are eight contiguous stereocenters, six rings, and nine nitrogen's. The originally assigned relative configuration of (-)-palau'amine had a *cis* relationship between the protons in the pyrrolidine core, but this assignment was revised<sup>30</sup> to a *trans* relationship almost fifteen years later (Figure 1.6).

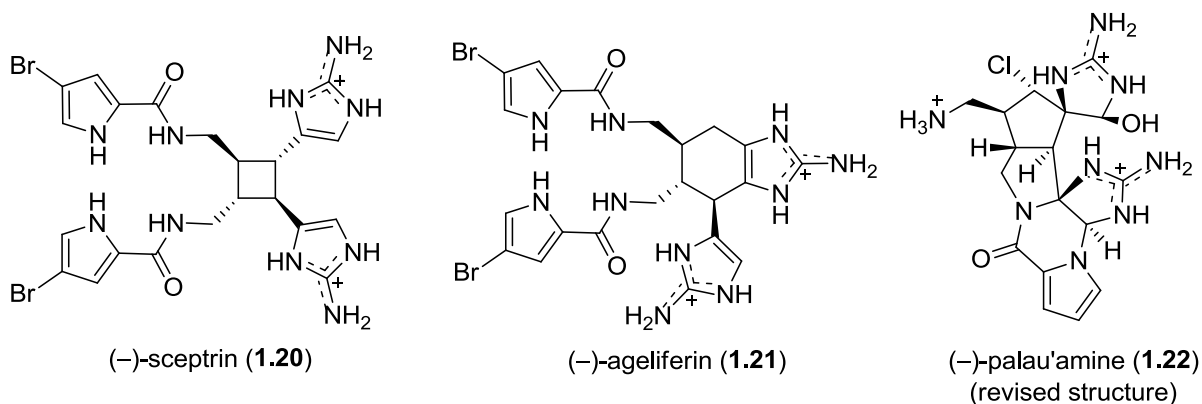


**Figure 1.6** Family of imidazole marine natural products.

The bioactivity of (-)-palau'amine (**1.22**) suggested, antifungal, antitumor, and immunosuppressive properties. Having an intricate structure that had been debated, in addition to its potential therapeutic effects made it an appealing target among synthetic organic chemists. Several manuscripts reporting studies towards the synthesis of (-)-palau'amine (**1.22**) were published subsequent to its isolation and structural revision. In 2010, Baran<sup>31</sup> and co-workers published the first synthesis of (±)-palau'amine (**1.22**) (Figure 1.7).

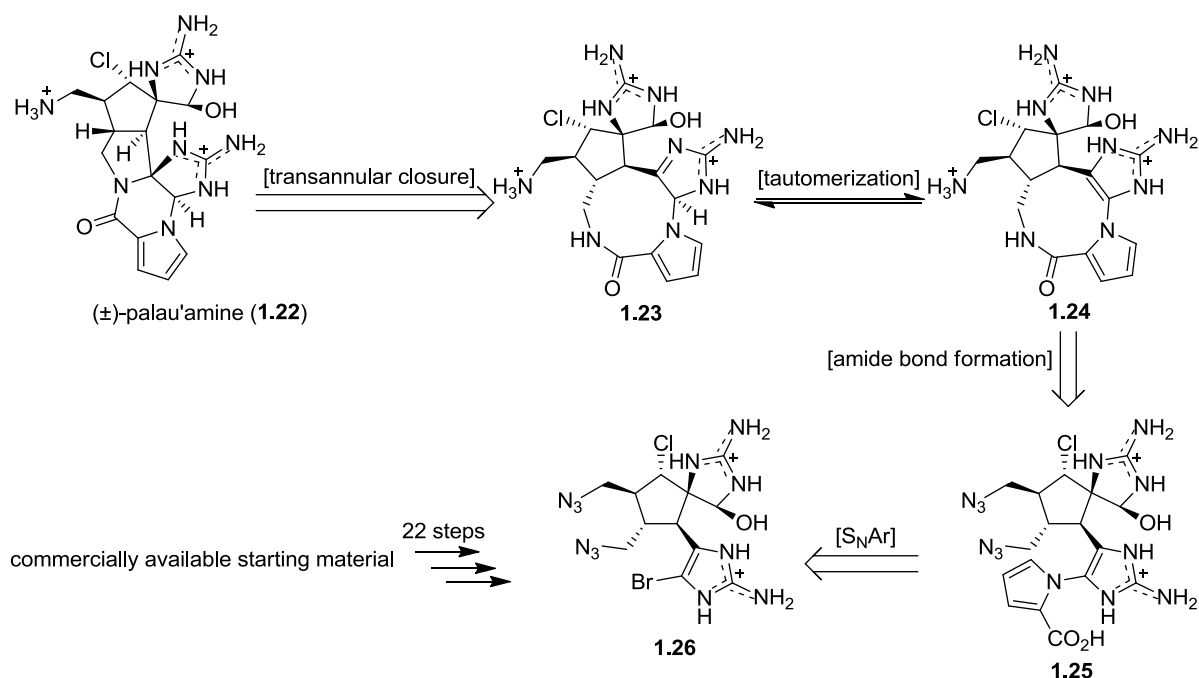


**Figure 1.7** Barans retrosynthesis of  $(\pm)$ -palau'amine (1.22).

The synthesis, which proceeded in 25 steps from commercially available starting material, was a six-year endeavor. The total synthesis of  $(\pm)$ -palau'amine (1.22) confirmed the revised structure. Furthermore, it was a testament to how the structural complexity that is offered by marine natural products forces synthetic organic chemistry to evolve.<sup>32</sup>

### 1.3 Translating a Drug-Lead Into a Drug by Structure Activity Relationship (SAR)

#### Studies

Constructing bioactive marine natural products can be a synthetic challenge. Often, the complexity of the target compound is such that producing the quantities necessary for clinical trials, let alone clinical use, is not feasible. SAR studies are used in an attempt to simplify the structure, yet maintain the biological activity of the lead compound. The

polyketide (+)-spongistatin 1 (**1.27**) isolated<sup>33</sup> from the marine sponge *Hyrtius erecta* is a good example of how SAR can produce a simplified analogue of the natural product, while still maintaining much of the activity (Figure 1.8).

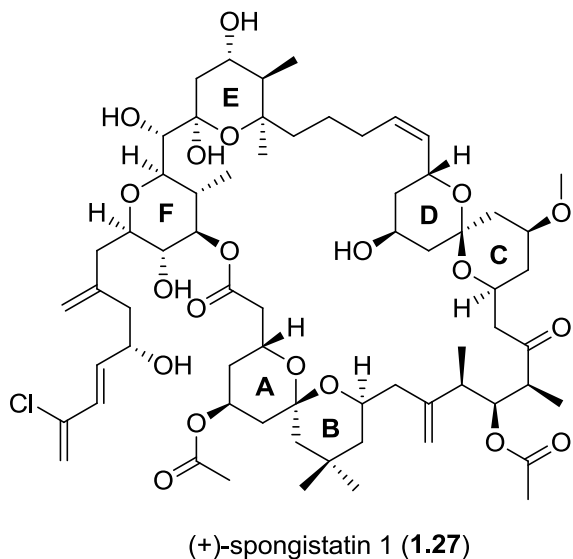


**Figure 1.8** The antimitotic marine natural product (+)-spongistatin 1 (**1.27**).

The macrolactone (+)-spongistatin 1 (**1.27**) is one of the most cytotoxic agents known, with an average  $IC_{50}$  of 0.12 nM tested against sixty human cancer cell lines.<sup>34</sup> Preliminary *in vivo* data showed an inhibition of mitosis and microtubule assembly. Despite the alluring biological data, all known syntheses of (+)-spongistatin 1 (**1.27**) are in excess of 100 steps,<sup>35,36</sup> which is too lengthy for clinical appeal.

To address this issue, SAR studies were undertaken to identify the structural components that are responsible for the sub nM activity. Inspired by the marine natural product derived drug Halaven<sup>®</sup> (an analogue of the polyketide halichondrin B<sup>37</sup>) the potential pharmacophore of the compound was identified. Through computational calculations<sup>38</sup> the

four lowest energy solution conformations of (+)-spongistatin 1 (**1.27**) were determined. The results suggest that the western hemisphere including the ABEF rings have a common conformation that does not change between the four lowest energy states (Figure 1.9). The eastern hemisphere including the DC rings have structurally significant differences in conformations between the four lowest energy states. This data suggested that the western hemisphere is rigid, while the eastern hemisphere is more flexible. It was hypothesized that the binding domain was located within the conformationally rigid portion of the molecule. Subsequently, analogues of (+)-spongistatin 1 (**1.27**) were constructed, which maintained the western hemisphere and ABEF rings, but had a simplified eastern hemisphere (Figure 1.9).

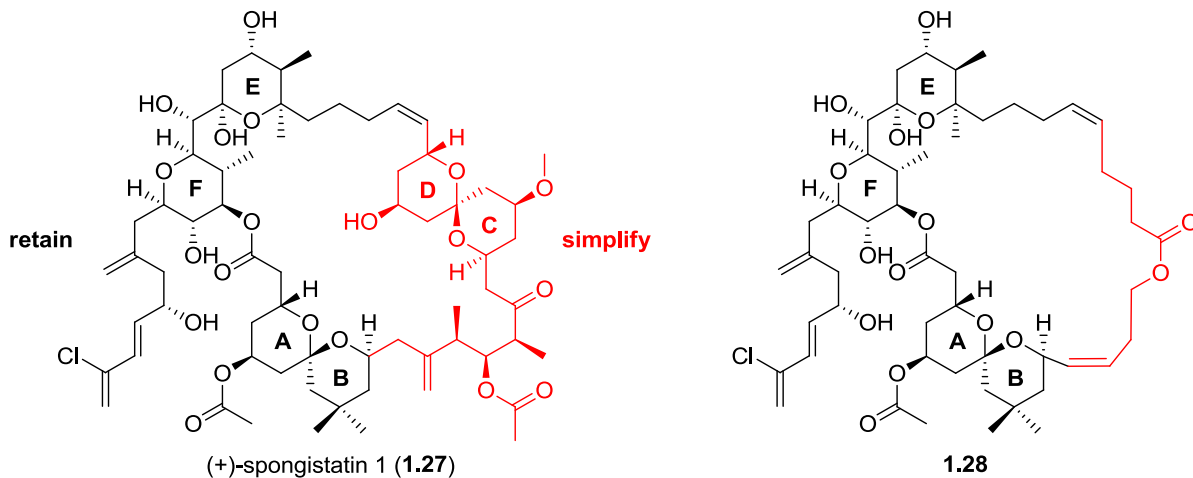


**Figure 1.9** A pharmacophore analogue (**1.28**) of (+)-spongistatin 1 (**1.27**).

Compound **1.28** represents a thirty-step decrease in its construction when compared to the natural product (**1.27**), and maintained nM activity with an  $IC_{50}$  of 60.5 nM in a U937 lymphoma cell line (**1.27** displayed an  $IC_{50}$  of 0.06 nM). SAR compliments total synthesis

allowing for construction of simplified pharmacophore analogues derived from complex marine natural products.<sup>39</sup>

#### 1.4 Bioactive Marine Natural Products Reveal Novel Mechanism of Action

The large chemical diversity associated with marine natural products often results in the identification of novel therapeutic targets. Ziconotide<sup>40</sup> (**1.29**) (PRIALT<sup>®</sup>) is an analgesic, and the first marine natural product peptide to be approved for use in the clinic. Its potency is 1000 times greater than morphine, and it does not elicit tolerance as with opiate-based therapies.

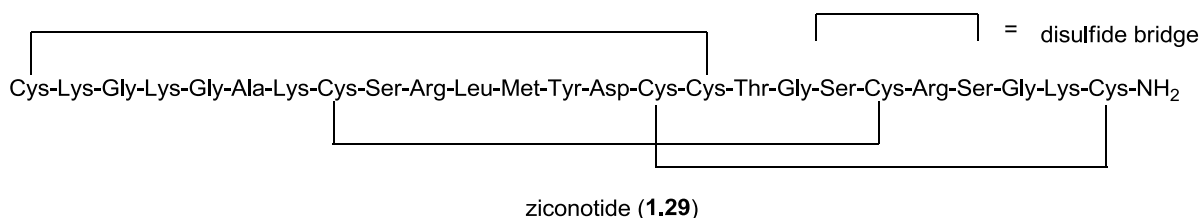


**Figure 1.10** A marine peptide with novel biological activity.

This twenty-five amino acid peptide is the synthetic counterpart of  $\omega$ -conotoxin, a secondary metabolite found in the venom of the marine snail *Conus magus*. Ziconotide (**1.29**) has an unprecedented mechanism of action. By blocking *N*-type voltage sensitive calcium channels, a subset of neurons including primary nociceptors is inhibited, which is responsible for sending signals to the spinal cord and brain in response to pain.

This unique mode of action<sup>41</sup> for ziconotide (**1.29**) provides a new avenue for treatment of severe chronic pain. In effect, the discovery of bioactive marine natural products

such as ziconotide (**1.29**) broadens our understanding of human biology and allows drug development to move forward.

## 1.5 Scope of Thesis

The body of work presented in this thesis details the use of synthetic organic chemistry to facilitate drug discovery through structure verification, SAR, and probe development.

Chapter 2 describes the construction of water-soluble SHIP1 activators in an attempt to develop compounds with enhanced drug-like properties. Small molecule activators of SHIP1 may be used as novel therapies for hematopoietic malignancies as well as inflammatory disorders and they could be an alternative to PI3K inhibition. Biological studies on the constructed SHIP1 activators were conducted and include enzymatic, *in vitro*, and *in vivo* assays.

Chapter 3 describes the total syntheses of two novel glycerol ether marine natural products to aid in structural elucidation efforts and to provide synthetic material for biological testing. The natural products are AR-NTD antagonists and represent a novel pharmacophore. SAR of the natural products was conducted to observe the biological effects that structural modification may have. A probe based on one of the natural products was used to show that the binding mechanism between the ligand and the drug target was covalent in nature. *In vitro* biological studies were conducted on the natural products and their SAR analogues to probe the biological effects of these novel AR-NTD pharmacophores.

Chapter 4 describes a known marine natural product that was shown to be an AR-LBD antagonist. Semisynthesis using the lead compound produced an analogue of enhanced

potency, and the synthetic efforts towards constructing analogues of this novel AR-LBD antagonist are detailed.

Chapter 5 describes the synthetic efforts toward a novel peptide-aldehyde terrestrial natural product, which was found to be a potent inhibitor of cathepsin K. The purpose of the synthesis was to aid in structure elucidation efforts, and to provide additional material for biological testing.

## Chapter 2: Synthesis and Biological Evaluation of SHIP1 Activators

### 2.1 Inhibition of PI3K Signaling by Activation of SHIP1

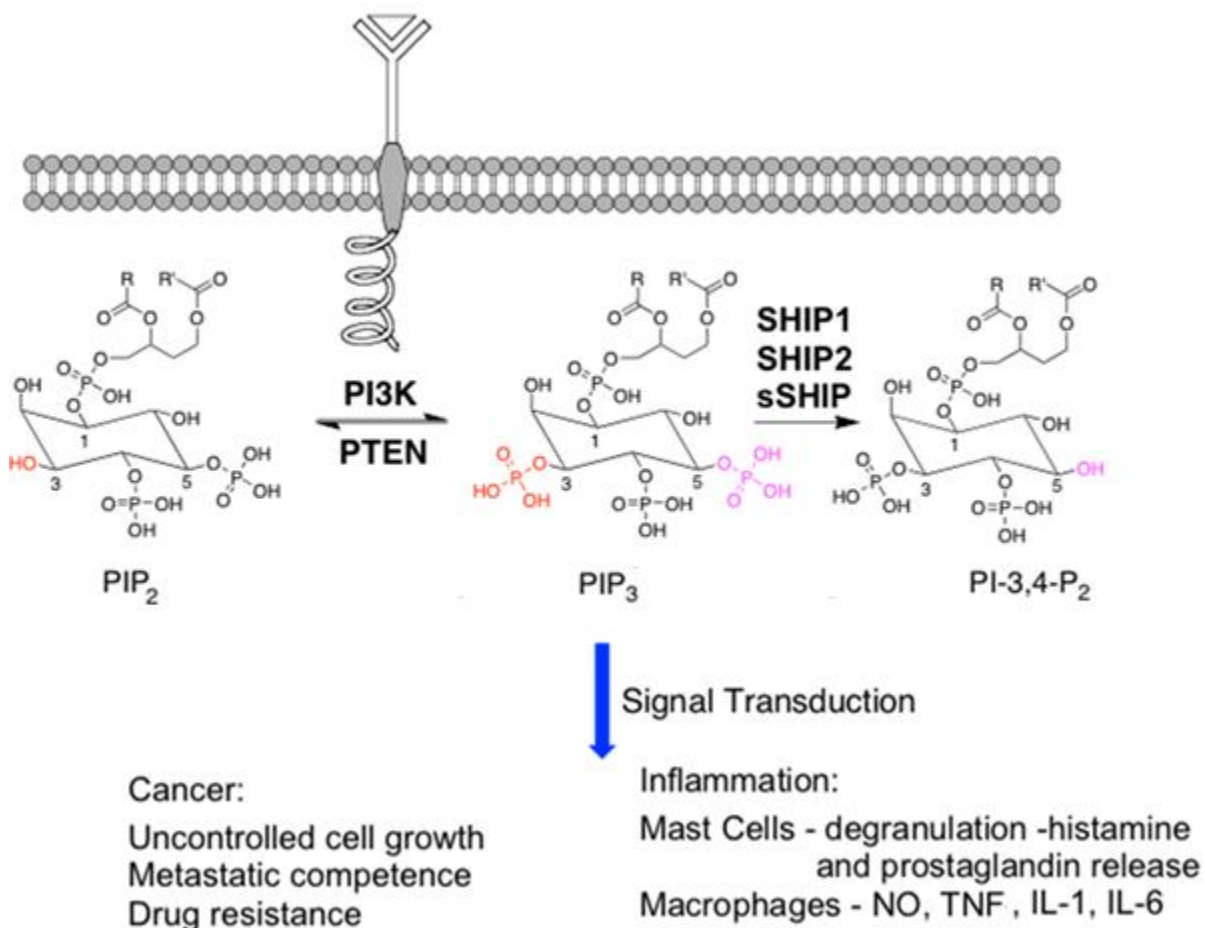


**Figure 2.1** The PI3K pathway.

The Phosphoinositide 3-kinase (PI3K) signal transduction pathway (Figure 2.1) regulates many cellular processes such as cell proliferation, activation, and growth.<sup>42,43,44,45</sup>

Specific binding between extracellular ligands and receptors on the cell surface activate the PI3K pathway, which leads to phosphorylation of phosphatidylinositol-4,5-bisphosphate (PI-

4,5-P<sub>2</sub>, or PIP<sub>2</sub>). This generates an important second messenger phosphatidylinositol-3,4,5-trisphosphate (PI-3,4,5-P<sub>3</sub>, or PIP<sub>3</sub>) in the plasma membrane.

The levels of PIP<sub>3</sub> in unstimulated cells are very low. However, PIP<sub>3</sub> is rapidly synthesized from PIP<sub>2</sub> in response to extracellular stimuli. PIP<sub>3</sub> concentrations are controlled by the tumor suppressor phosphatase and tensin homolog (PTEN). PTEN hydrolyzes PIP<sub>3</sub> back to PIP<sub>2</sub>, and the Src homology 2-containing inositol 5-phosphatases<sup>46</sup> (SHIP1, sSHIP, and SHIP2), which hydrolyze PIP<sub>3</sub> to phosphatidylinositol-3,4-bisphosphate (PI-3,4-P<sub>2</sub>). Both of these events dampen the signal. Elevated PIP<sub>3</sub> concentrations result in amplification of the signal transduction cascade leading to human diseases such as cancer and inflammation.<sup>42,43,44,45</sup> Consequently, a number of drugs targeting the PI3K signaling pathway are being developed.<sup>47</sup> Most of these therapeutics are designed to prevent formation of the second messenger PIP<sub>3</sub> by inhibiting PI3K, or to inhibit downstream targets in the signal transduction cascade. An alternative method of down-regulating PIP<sub>3</sub> production is to activate PTEN. However, PTEN mutation or silencing occurs in many human malignancies<sup>48</sup> therefore suitable treatment utilizing this pathway remains elusive.

Unlike PTEN, SHIP1 has not been found to mutate during human malignancies. Activation of the phosphatase SHIP1<sup>49</sup> is an attractive alternative to current therapies since its expression is restricted to hematopoietic cells, which should minimize off-target tissue effects.

## 2.2 First Generation SHIP1 Agonist Pelorol and Analogues

The discovery of the SHIP enzyme by Dr. Gerald Krystal,<sup>50</sup> led to a collaboration in which the Andersen natural product library of extracts was screened by Dr. Alice Mui in an effort to discover small molecule activators of SHIP1. A methanol extract of the sponge *Dactylospongia elegans* collected in Papua New Guinea exhibited promising activity in the screening assay. Bioassay-guided fractionation of the extract led to the identification of the meroterpenoid pelorol (**2.1**) as a selective SHIP1 activator (Figure 2.2).<sup>51</sup>

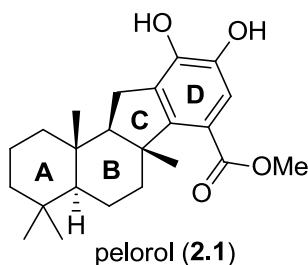


**Figure 2.2** The first selective SHIP1 activator marine natural product pelorol (**2.1**).

While biological evaluation of pelorol (**2.1**) was underway in the Mui and Andersen labs, pelorol (**2.1**) was isolated by the König<sup>52</sup> and Schmitz<sup>53</sup> groups from the sponges *Dactylospongia elegans*, and *Petrosaspongia metachromia* collected at the Great Barrier Reef and Yap in the Federated States of Micronesia, respectively. In order to fully explore the potential biological impact of this drug lead, the total synthesis of pelorol (**2.1**) was completed by Lu Yang in the Andersen group,<sup>51</sup> along with a preliminary SAR study which generated a small number of analogues.

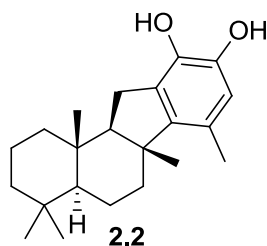


**Figure 2.3** Pelorol (**2.1**) analogue **2.2**.

It was revealed that analogue **2.2** (Figure 2.3), was more potent than the natural product and more readily synthesized. With a scalable synthesis to the potent SHIP1 agonist **2.2** in hand, enough material was produced to allow for both *in vitro* and *in vivo* evaluation. *In vitro* data suggested that **2.2** and pelorol (**2.1**) suppressed mast cell degranulation and subsequent TNF release in cells expressing SHIP1. The same effect was not observed in cells lacking SHIP1 providing evidence for the selective targeting of SHIP1. This suggested that pelorol (**2.1**) and **2.2** were promising lead structures for developing a drug candidate.

Pelorol (**2.1**) and analogue **2.2** provided preliminary proof of principle for the biological activity resulting from small molecule activation of SHIP1, however, an inherent structural lability present in the structures needed to be addressed. Catechol functionalities can be oxidized to ortho-quinones (Figure 2.4), making the molecule susceptible to 1,6-addition resulting in potential off-target effects, which may have carcinogenic consequences.<sup>54</sup>

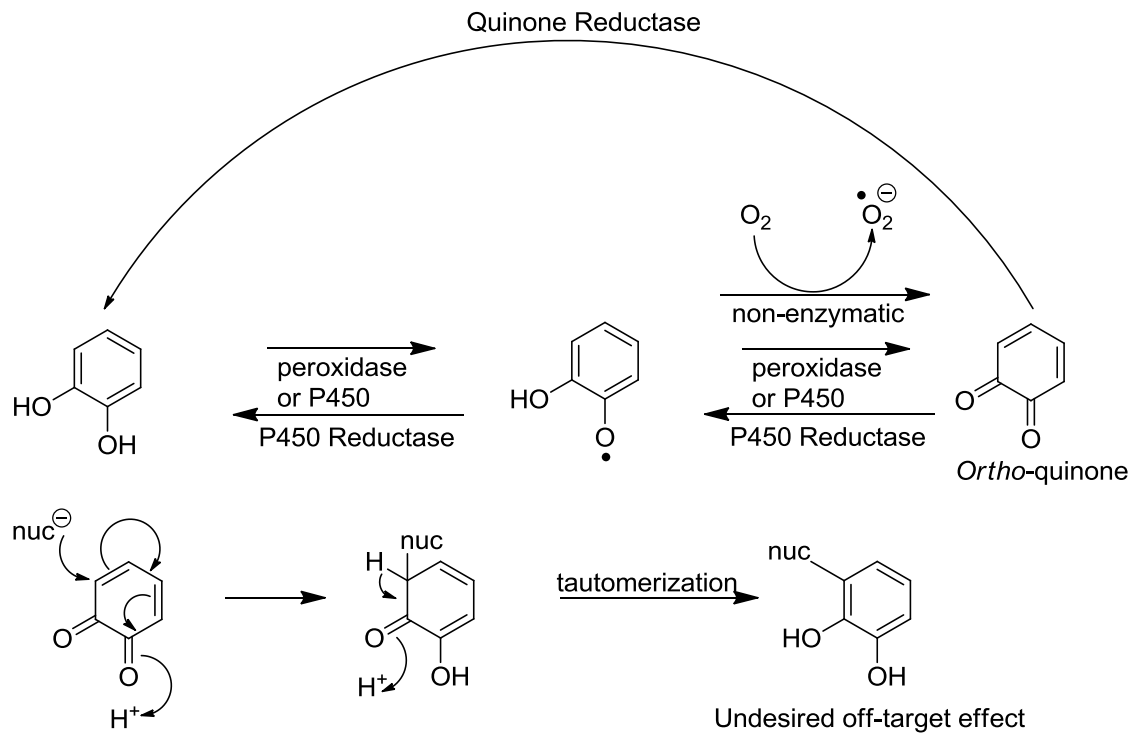


**Figure 2.4** Chemical and enzymatic oxidation of catechol and subsequent 1,6-addition.

A more in-depth SAR study based on analogue **2.2** was completed to overcome these unwanted effects. The majority of these new analogues proved to be active in the SHIP1 assay. Compound **2.3** (Figure 2.5), prepared by Matt Nodwell in the Andersen lab, lacked the labile catechol functionality and had enhanced potency relative to pelorol (**2.1**).

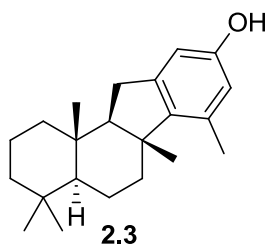
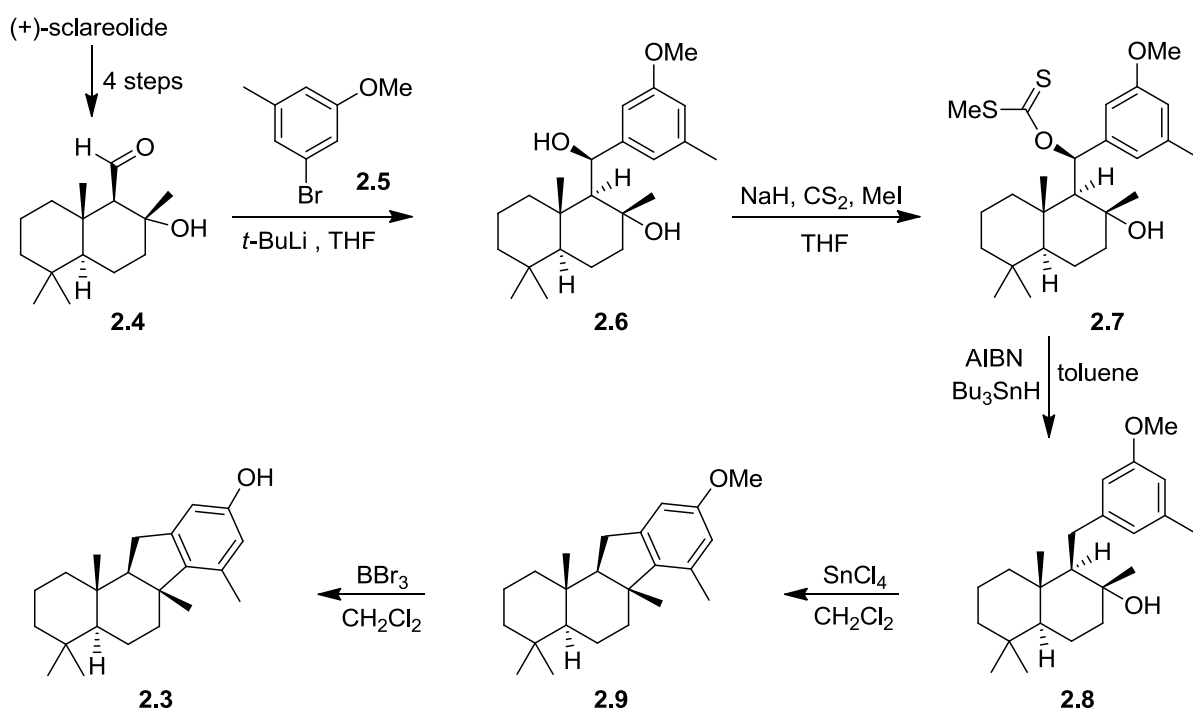


**Figure 2.5** Analogue **2.3** without the catechol functionality.

## 2.3 Synthesis of SHIP1 Activators Using a Polyene-Initiated Cationic Cascade

With the promising new drug lead **2.3** identified, it was necessary to provide enough material to fully explore its biological activities. The synthesis of **2.3** used (+)-sclareolide (Scheme 2.1) as the starting material and followed a reaction sequence similar to that used for the chiral synthesis of pelorol (**2.1**).



**Scheme 2.1** Synthetic route to drug lead **2.3**.

Since larger amounts of **2.3** were needed for further testing, a more concise synthesis was required. A biomimetically-inspired synthesis utilizing a polyene-initiated cationic cascade was devised. The concept of polyene cyclizations is not a recent one.<sup>55</sup> It has been

used in many biomimetically-inspired syntheses of terpenes and steroids such as germanicol (2.10) and progesterone (2.11) shown in Figure 2.6.<sup>56,57</sup>

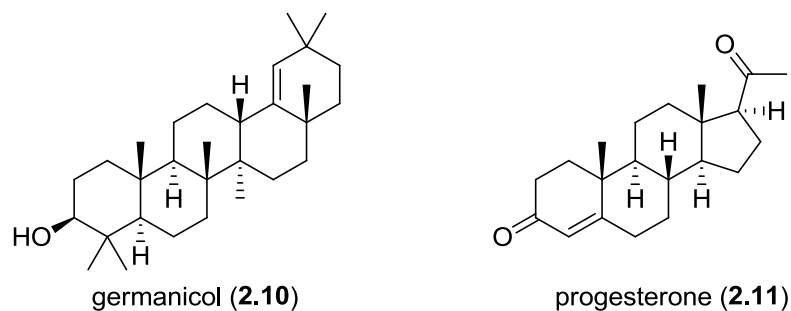


**Figure 2.6** Natural products made by biomimetically-inspired syntheses.

Many variations of polyene cyclizations exist. However, a few themes occur in the course of all these annulations. Cyclization initiation begins with the generation of a carbocation. Various functional groups are used to generate a carbocation, such as sulfonate esters,<sup>58</sup> acetals,<sup>59</sup> allylic alcohols,<sup>60</sup> epoxides,<sup>56</sup> and *N*-acyl iminiums.<sup>61</sup>

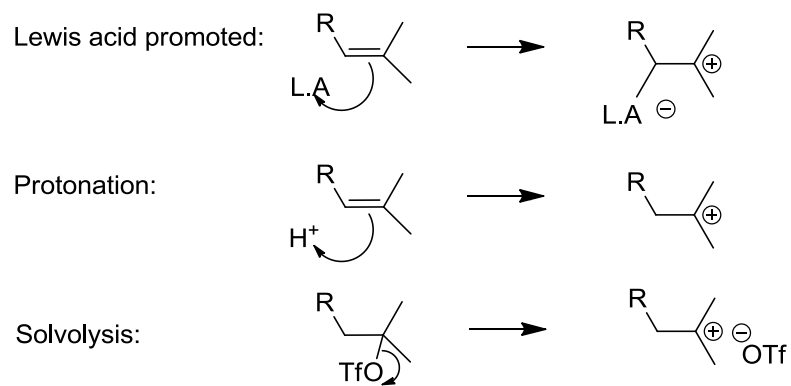


**Figure 2.7** Carbocation generation.

The methods of carbocation generation include protonation, solvolysis, or the presence of a Lewis acid (Figure 2.7). Once the cation is generated, it undergoes an

intramolecular attack by a nucleophile. Different nucleophiles such as vinylic,<sup>62</sup> acetylenic,<sup>63</sup> aromatic,<sup>64</sup> and heterocyclic<sup>65</sup> functionalities exist (Figure 2.8). Finally, termination occurs by the elimination of a proton.

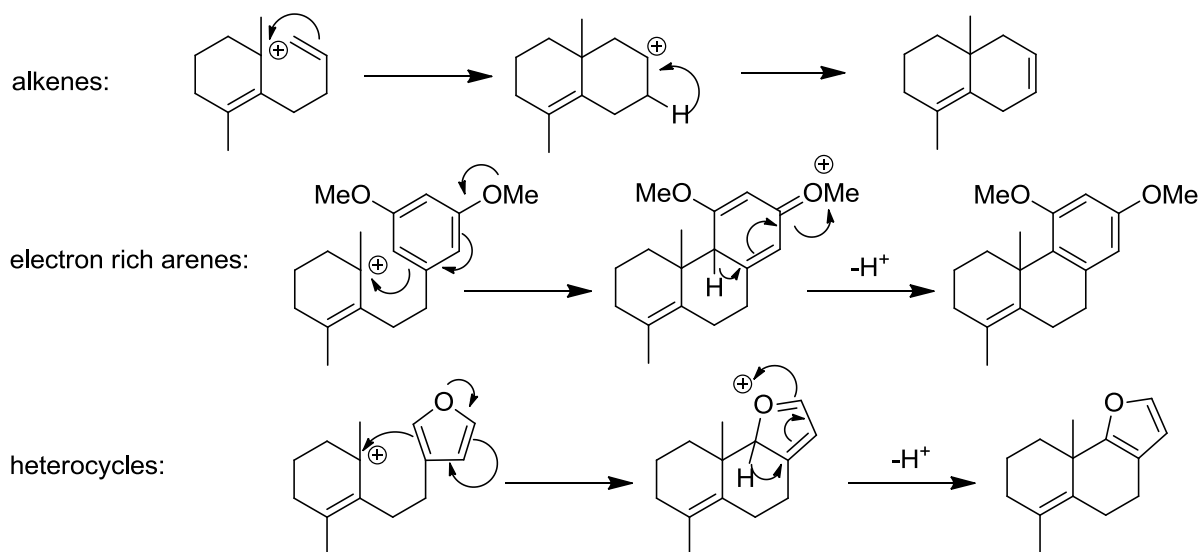
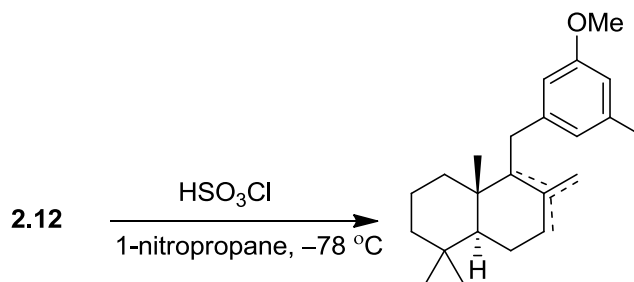


**Figure 2.8** Typical propagation and termination of a polyene cascade.

A retrosynthetic analysis of **2.3** (Scheme 2.2) reveals the polyene needed to undergo the cascade. With this in mind, construction of polyene **2.12** began. Aryl bromide **2.5** underwent halogen-metal exchange followed by cuprate formation *in situ*. The cuprate was coupled to trans,trans-farnesyl bromide (**2.13**) to give polyene **2.12** in 45 % yield (Scheme 2.3).





**Scheme 2.4** Elimination side products of chlorosulfonic acid cyclization.

This method allows the synthesis of racemic **2.3** in three linear steps as opposed to nine from (+)-sclareolide in the chiral synthesis of **2.3** (Scheme 2.1). Furthermore, the racemic synthesis produced the antipodal configuration of the lead compound pelorol (**2.1**) in analogue **2.14**, which had not been constructed up to that point.

## 2.4 Synthesis of Water Soluble Analogues to Facilitate Drug Administration

CLogP is the partition coefficient of a compound between water and octanol. It is a good predictor of oral bioavailability,<sup>67</sup> which is an important pharmacokinetic property. Having a CLogP of less than five is in agreement with the Lipinski rules of five.<sup>16</sup> These guidelines were devised by Christopher A. Lipinski, a chemist at Pfizer, after the observations he made on the pharmacokinetic properties of the current drugs on the market. The guidelines are meant to predict the drug-likeness of a molecule but not pharmacological activity. In addition to having a CLogP of less than five, an orally active drug should have no more than five hydrogen bond donors, ten hydrogen bond acceptors, and a molecular mass of less than 500 daltons.

Pelorol (**2.1**) has a CLogP of 5.74, well outside of the Lipinski range. Similarly, synthetic analogues **2.2** (CLogP = 5.56), and **2.3** (CLogP = 6.16) are too lipophilic to be

considered drug-like. To address the issue of water solubility, prodrugs based on **2.3** were constructed by Matt Nodwell in the Andersen group (Figure 2.9).

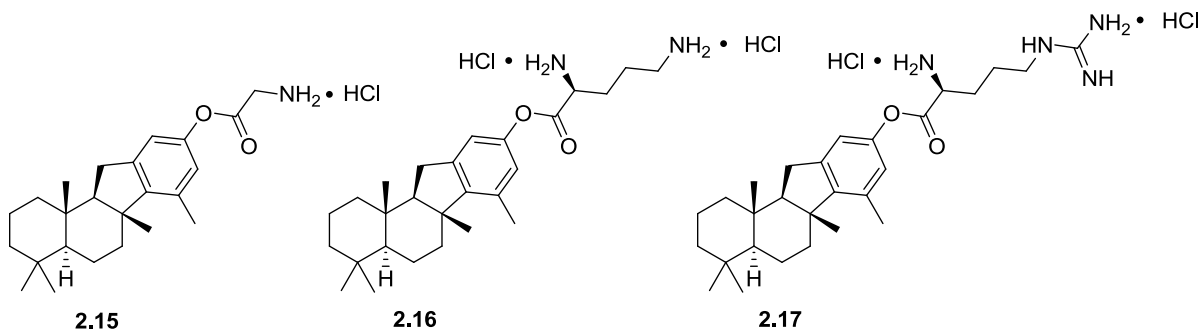


**Figure 2.9** Water soluble prodrug analogues of **2.3**.

The purpose of a prodrug is to aid in the delivery of an active compound to the cellular environment. Upon entering the cell, the prodrug is metabolically transformed into the active compound.<sup>68</sup> In the case of prodrugs **2.15**, **2.16**, and **2.17**, the ester functionality would be cleaved *in vitro* to release a biological promoiety and the parent compound (**2.3**).

An enzymatic SHIP1 assay was used to evaluate prodrugs **2.15**, **2.16**, and **2.17**, and it was shown that none successfully activated SHIP1. This was not surprising since cleavage of the prodrug was not expected in the enzymatic assay. The data was consistent with the hypothesis that the aryl moiety is an important part of the pharmacophore of **2.3**. Prodrug **2.15** was tested *in vitro* and found to inhibit the release of TNF to the same extent as **2.3**. Prodrug **2.15** was further evaluated by dissolving it in a pH 7.4 buffer solution to mimic cellular conditions. It was determined that cleavage of the prodrug did occur. However, the parent compound (**2.3**) precipitated in the aqueous medium, not solving the problem of solubility of the active form (**2.3**) in plasma.

As this issue of water solubility in **2.3** was being investigated, a new analogue (**2.18**) was constructed and determined to be a more effective SHIP1 activator than **2.3** (Figure 2.10). Analogue **2.18** has a CLogP of 4.99 just under the Lipinski rule of five. However, this CLogP value is not ideal and an alternative approach was needed to develop a water-soluble analogue.

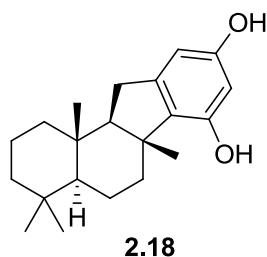


**Figure 2.10** Analogue **2.18**.

We decided to construct compounds with polar functionality incorporated into the A-ring far from the putative pharmacophore (Figure 2.11) to develop analogues of **2.18** with acceptable CLogP values and at the same time robust enough to construct the quantities required for animal testing. By comparing CLogP values of potential A-ring analogues, it became clear they might have potential for enhanced water solubility (Figure 2.12).

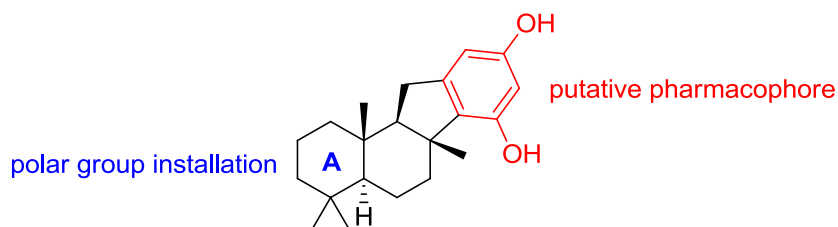


**Figure 2.11** Water soluble analogue design.

The C-3 ketone analogue **2.19** has a CLogP of 3.23, and the corresponding C-3 neutral amino derivative **2.20** has a CLogP of 3.58 (Figure 2.12). The amino derivative **2.20** was of particular interest because the amino group should be protonated at physiological pH. The resulting ammonium ion salt would be expected to have increased water solubility.

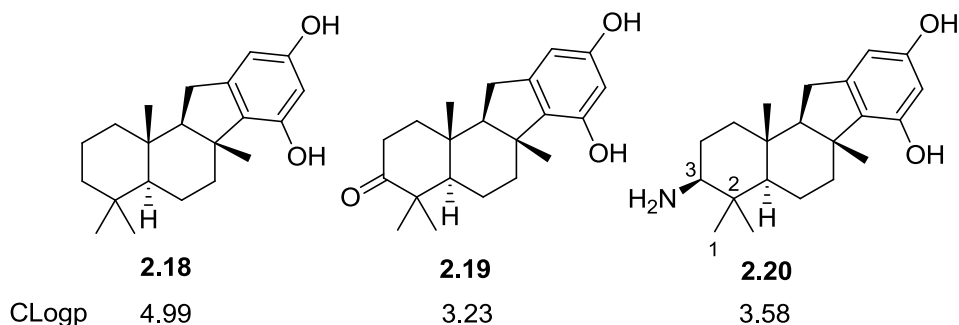
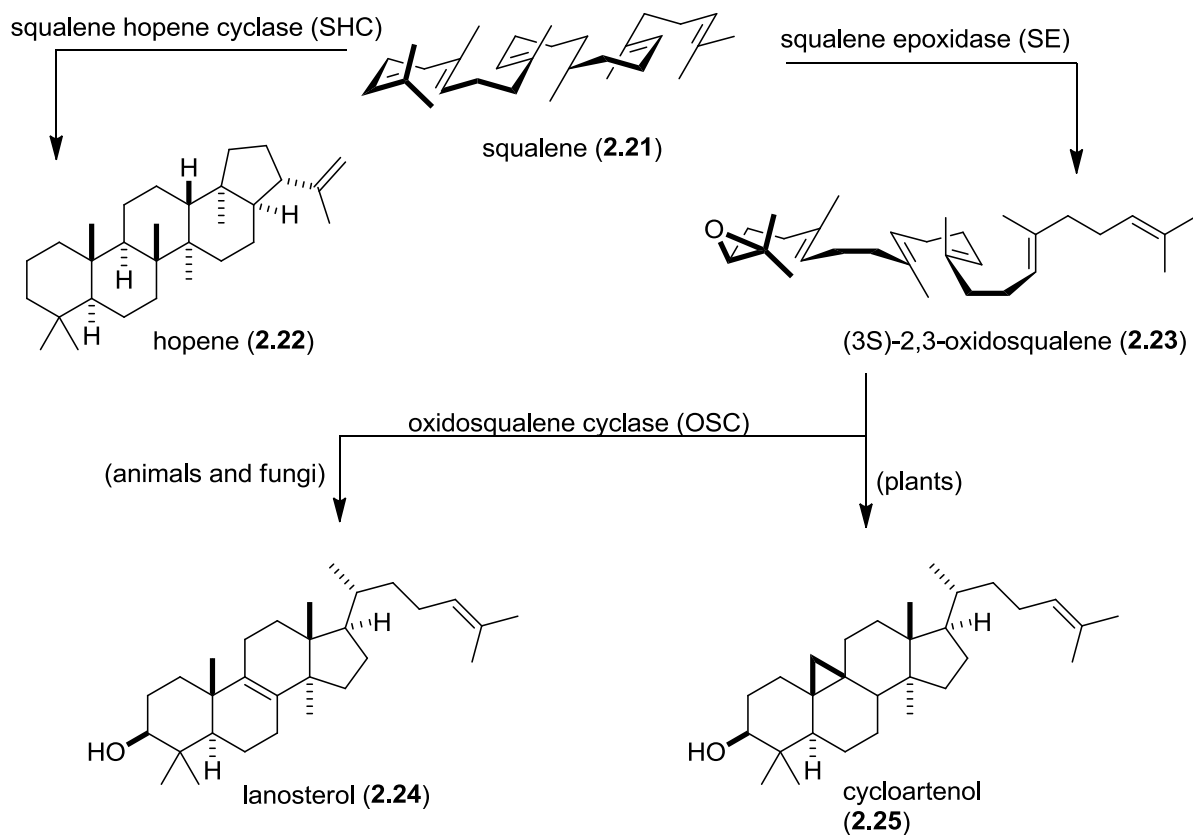


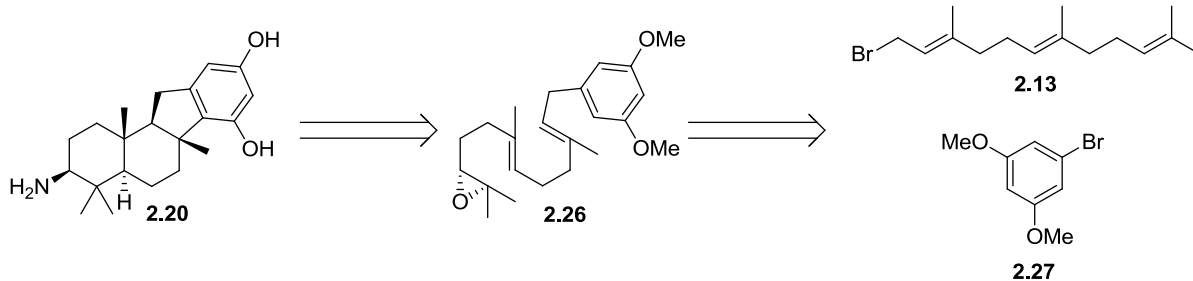
**Figure 2.12** CLogP values of **2.18** and related analogues.

To access these compounds an epoxide-initiated cationic cascade was proposed. Epoxide-initiated cascades, similar to the aforementioned polyene-initiated cascade, are utilized by nature. A well-known example from nature is the biosynthesis of steroids from squalene (**2.21**) (Scheme 2.5).<sup>69</sup>



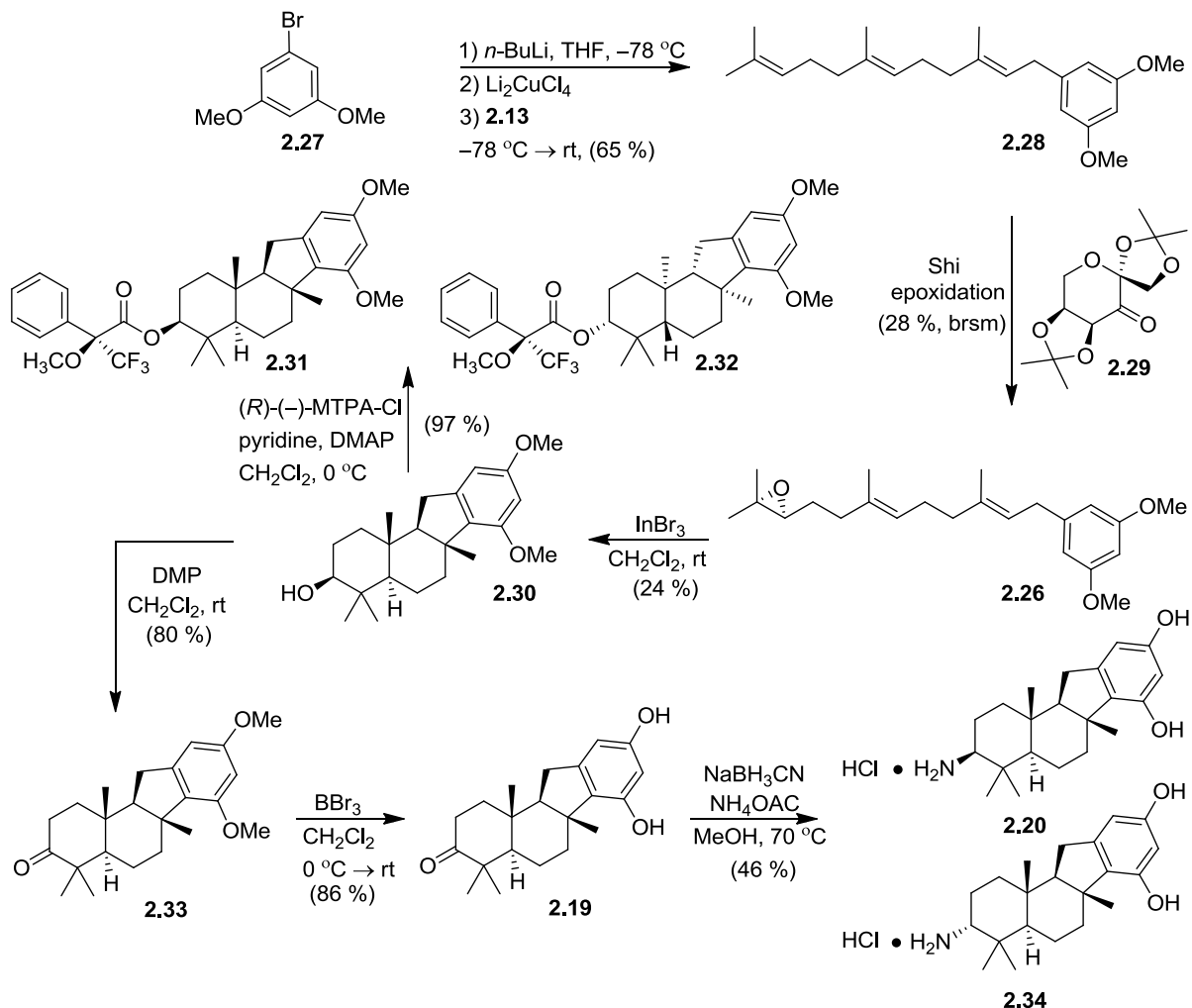
**Scheme 2.5** Inspiration for biomimetic synthesis: steroid biosynthesis from squalene (2.21).

In this biosynthetic pathway, squalene (2.21) is converted to hopene (2.22) by squalene hopene cyclase (SHC) via a polyene-initiated cascade in an enantioselective and diastereoselective fashion. Similarly, (3S)-2,3-oxidosqualene (2.23) undergoes an epoxide-initiated cationic cascade in the presence of oxidosqualene cyclase (OSC) to give lanosterol (2.24), or cycloartenol (2.25), depending on which OSC is used. It is biosynthetic pathways such as these that have inspired biomimetic syntheses. Many examples exist,<sup>70,71</sup> which utilize epoxide-initiated cascades. Having specific analogues in mind (Figure 2.12), the retrosynthetic analysis shown in Scheme 2.6 reveals the terminal epoxide required (2.26) to construct polar analogues of 2.18 using an epoxide-initiated cascade.



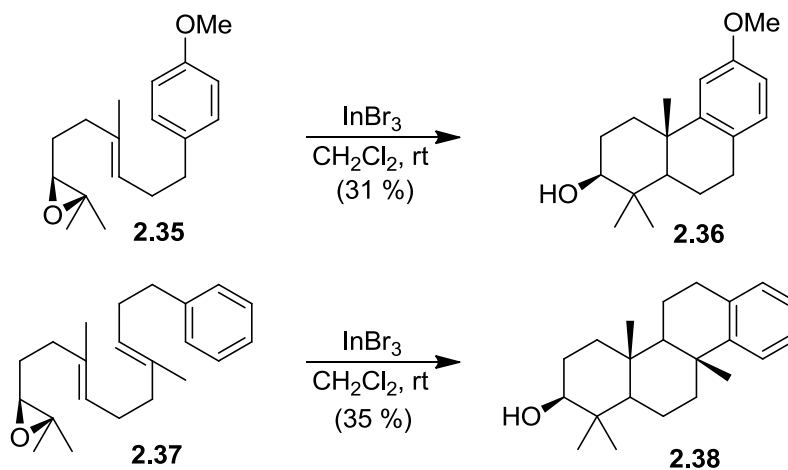
**Scheme 2.6** Retrosynthetic analysis of **2.20**.

The synthetic route to amine **2.20** begins with the construction of polyene **2.26**, which was accomplished by lithiation of aryl bromide **2.27** followed by alkylation with trans,trans-farnesyl bromide **2.13** (Scheme 2.7).<sup>72</sup> With the original, as well as the antipodal configuration of pelorol (**2.1**) in mind, we designed a chiral synthesis. For this, we needed to construct the terminal epoxide enantioselectively. Several asymmetric epoxidation methods have been developed<sup>73</sup> for alkyl-substituted olefins and we felt the Shi<sup>74</sup> epoxidation would suit our needs. Using Shi catalyst **2.29**, which is derived from L-fructose, we were able to obtain (*S*) terminal epoxide **2.26** in 28 % yield.



**Scheme 2.7** Synthesis of amine analogues **2.20** and **2.34**.

The key step of the synthesis was next, which is the epoxide-initiated cyclization cascade. A number of Lewis acids are effective at opening epoxides to initiate a cascade, such as tin(IV) chloride,<sup>75</sup> methylaluminum dichloride,<sup>76</sup> and scandium triflate.<sup>77</sup> However, during this project new methodology utilizing indium tribromide to promote arene-terminated epoxide opening cyclizations was published by Zhao *et al.* which used similar substrates as **2.26** (Scheme 2.8).<sup>78</sup>



**Scheme 2.8** Examples of indium tribromide promoted annulation methodology

Enantio-enriched epoxide **2.26** was exposed to two equivalents of indium tribromide in methylene chloride to give a bright orange solution. After the workup step, secondary alcohol **2.30** was found to be present as part of a complex product mixture. A small quantity of secondary alcohol **2.30**, which was devoid of any side products that was obtained from flash column chromatography, was reacted with (*R*)-MTPA-Cl to give Mosher esters<sup>79</sup> **2.31** and **2.32** in 95 % and 2.0 %, yield, respectively. Analysis of the Mosher's esters **2.31** and **2.32** via NMR allowed us to determine the combined enantiomeric excess of the Shi epoxidation and the epoxide-initiated cascade, which was 94 % ee. In addition, single crystal X-ray diffraction analysis of Mosher ester **2.32** confirmed its absolute and relative configuration (Figure 2.13).

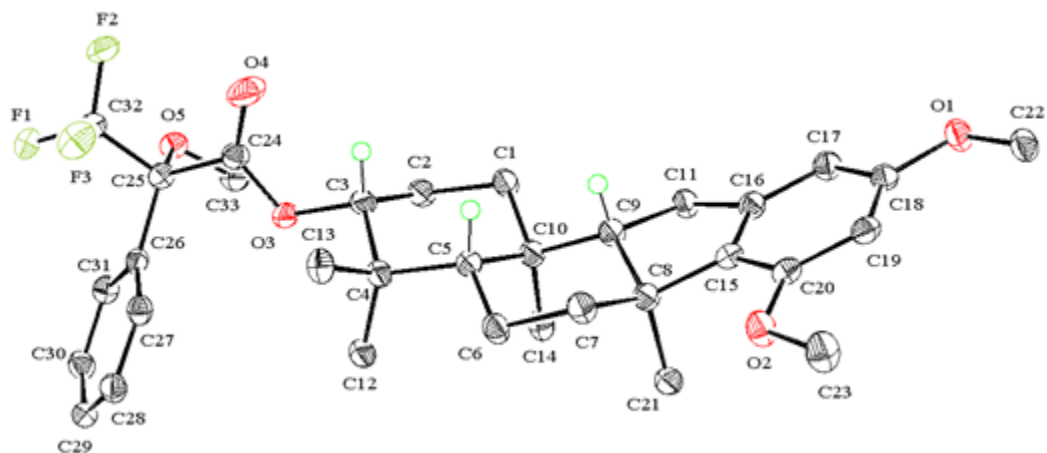


**Figure 2.13** ORTEP diagram of Mosher ester **2.32**.

Since larger quantities were required for *in vivo* testing, another purification method for **2.30** was necessary. Single recrystallization from boiling hexanes:ethyl acetate of the crude product mixture after cyclization gave > 99.5 % of the single enantiomer in alcohol **2.30** (Figure 2.14).

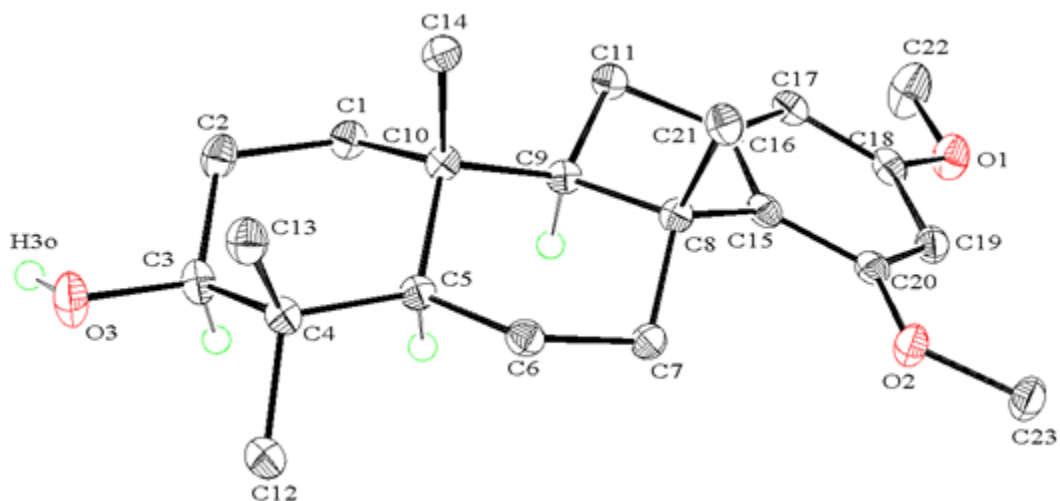
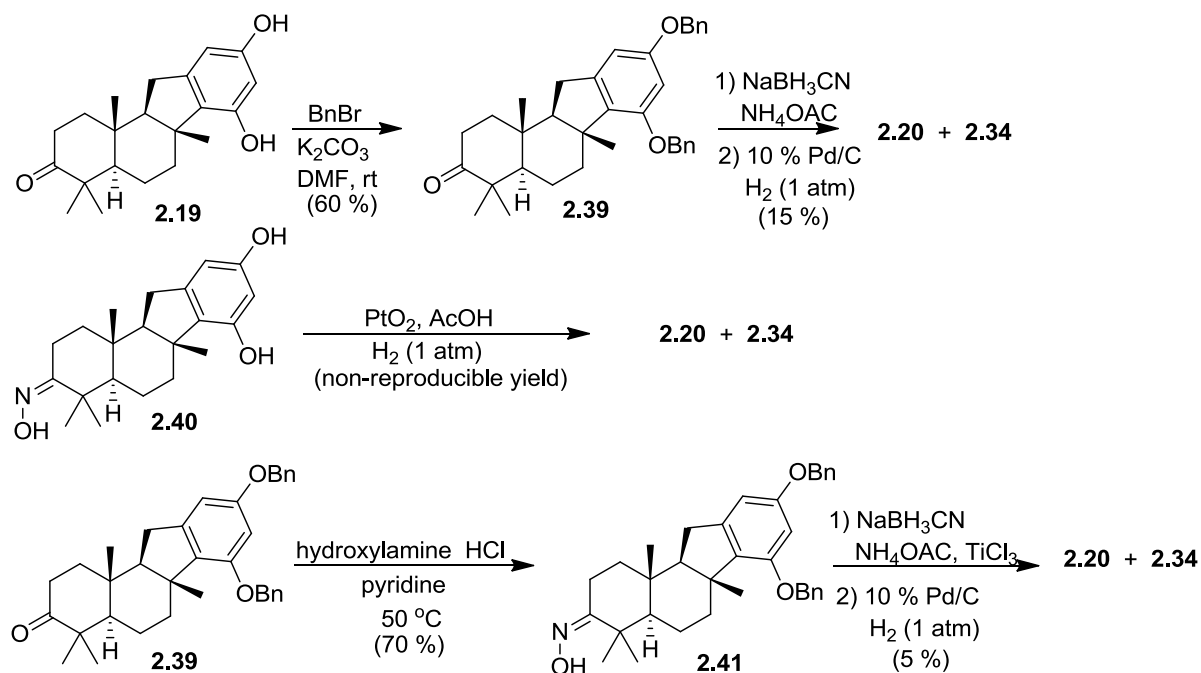


**Figure 2.14** ORTEP diagram of alcohol **2.30**.

The enantiomeric excess of **2.30** after recrystallization was determined by esterifying the crystalline material with (*R*)-MTPA-Cl and observing only the single diastereomer **2.31** by NMR. Next, Dess–Martin periodinane (DMP) oxidation of the secondary alcohol **2.30** gave the ketone **2.33** (Scheme 2.7). Removal of the methyl ether protecting groups of **2.33** with  $\text{BBr}_3$  gave the resorcinol intermediate **2.19**.



**Scheme 2.9** Alternative amination strategies towards **2.20** and **2.34**.

With the deprotected ketone **2.19** in hand, the remaining step was a reductive amination. Several routes were explored<sup>80,81</sup> to address the overall yield for the amination, and to discover which method gave the highest diastereoselectivity (Scheme 2.9). Reductive amination of the bis-benzyl protected ketone **2.39**, followed by deprotection of the benzyl groups gave unsatisfactory yields. Platinum oxide catalyzed hydrogenation of oxime **2.40**, was promising, but the yields were too irreproducible.

Reductive amination of oxime **2.41** gave unsatisfactory yields. It was found that reductive amination<sup>82</sup> with sodium cyanoborohydride and ammonium acetate, followed by acidification, extraction, and subsequent purification using a C<sub>18</sub> solid phase cartridge gave the amine analogues **2.20** and **2.34** as the hydrochloride salts in a 20:3 ratio and 46 % yield (Scheme 2.7). Repeating the synthesis with the Shi catalyst that is the optical antipode of **2.29** prepared from D-fructose using literature methods<sup>83</sup> gave the amine analogues **2.42** and **2.43** (Figure 2.15). This was to determine whether the absolute configuration would play a role in the activity of these analogues. The  $\beta$ -amines **2.20/2.42** were chosen as the lead compounds since they were formed in much higher yields compared to their  $\alpha$ -amine epimers **2.34/2.43**.

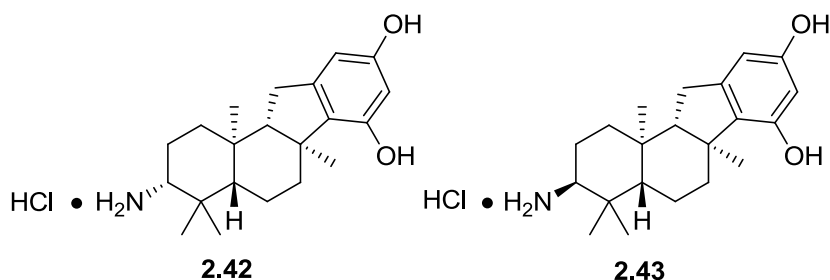
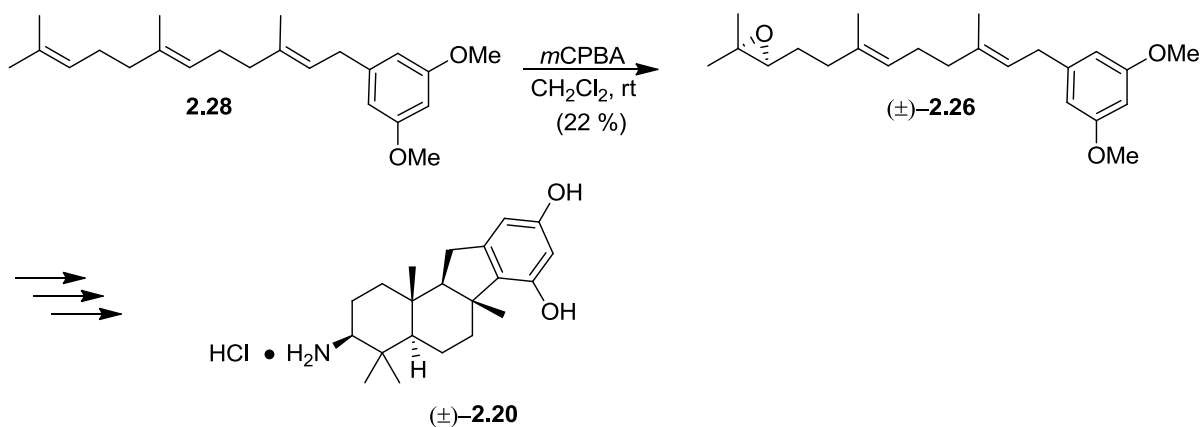


**Figure 2.15** Analogues **2.42** and **2.43** constructed using a D-fructose derived Shi catalyst.

The synthesis was also completed using *m*CPBA<sup>84</sup> as an oxidant (Scheme 2.10). This yielded racemic epoxide ( $\pm$ ) **2.26** which was carried through the already established synthetic route (Scheme 2.7) to give **2.20** and **2.42** as a racemic mixture (Scheme 2.10). Single crystal X-ray diffraction analysis of the racemic mixture **2.20/2.42** confirmed the relative configuration (Figure 2.16).



**Scheme 2.10** Racemic synthesis of (±)-2.20 using *m*CPBA.

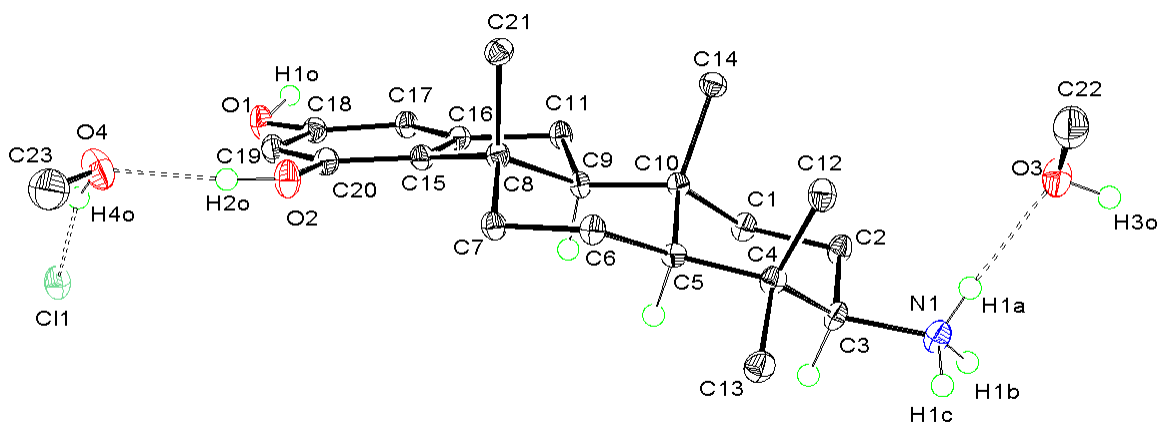
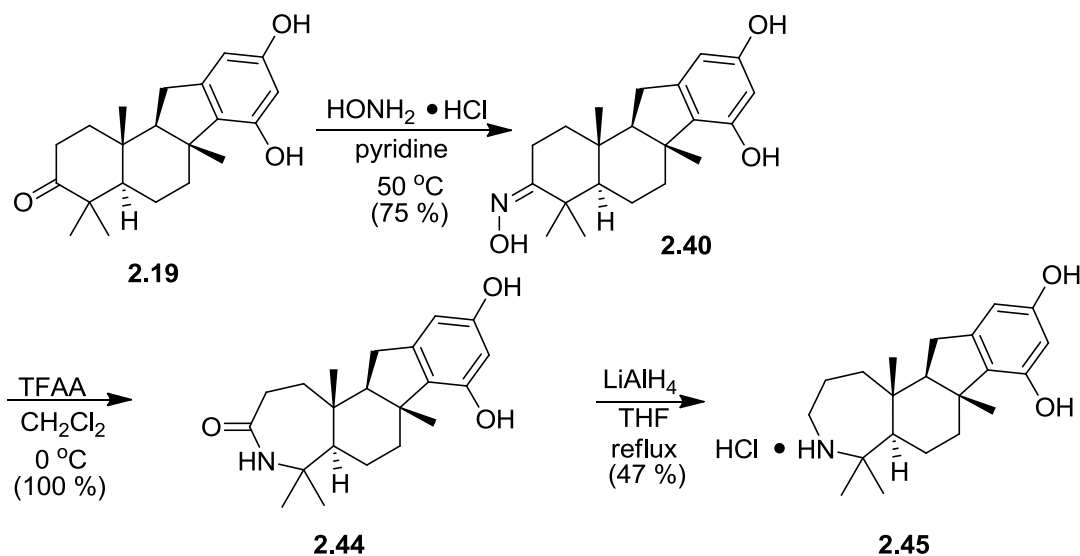


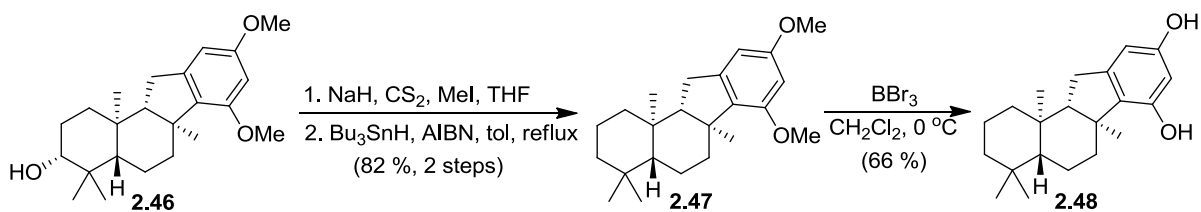
**Figure 2.16** ORTEP diagram of racemic amine mixture 2.20/2.42.

While primary amines **2.20** and **2.42** were chosen as the lead compounds for biological testing, a variety of polar analogues were constructed to further probe the SAR (Scheme 2.11). Intermediate **2.19**, was exposed to hydroxylamine hydrochloride under basic conditions to give oxime **2.40**<sup>85</sup> (Scheme 2.11).



**Scheme 2.11** Polar analogues of **2.18**.

Oxime **2.40** underwent a Beckmann rearrangement in the presence of trifluoroacetic anhydride to give lactam **2.44** in quantitative yield.<sup>86</sup> Lactam **2.44** was reduced with LAH in refluxing tetrahydrofuran, followed by an acidic workup and  $\text{C}_{18}$  solid phase purification to give secondary amine hydrochloride salt **2.45**.<sup>87</sup> These analogues utilize various nitrogen functional groups for enhanced polarity, and have CLogP values of 3.48, 2.68, and 3.84 for the oxime (**2.40**), lactam (**2.44**), and secondary amine (**2.45**), respectively.



**Scheme 2.12** Synthesis of the **2.18** enantiomer (**2.48**).

Along with these new polar analogues, we were able to access the antipodal configuration of **2.18**, which had not been constructed up to this point (Scheme 2.12). This would provide insight as to whether or not configuration played a role in the activity of **2.18**. The optical antipode of Shi catalyst **2.29** was used to construct secondary alcohol intermediate **2.46**, which was deprotonated with NaH followed by quenching with CS<sub>2</sub> and MeI. The crude mixture was subjected to Barton-McCombie deoxygenation conditions<sup>88</sup> followed by deprotection of the aryl methyl ethers by boron tribromide to give resorcinol analogue **2.48**. This three step reaction sequence gave a 54 % overall yield.

## 2.5 Saturation Transfer Difference (STD) Spectroscopy NMR

Having constructed polar analogues of **2.18**, we wanted to show that these compounds interact with the SHIP1 enzyme. Furthermore, we wanted to prove that the aryl moiety is an essential part of the pharmacophore of not only **2.18**, but of all analogues of pelorol (**2.1**) that had only been alluded to through synthesis thus far. A classical method of observing ligand-enzyme interactions is X-ray analysis of co-crystallized ligand-enzyme complexes.<sup>89,90,91</sup> However, growing a crystal of this type is often challenging.

Therefore, we turned our attention to saturation transfer difference NMR spectroscopy (STD NMR) to answer the key questions about which moiety of the ligand

interacts with SHIP1 and if there is a preference for a specific configuration. STD NMR was developed by Mayer and Meyer<sup>92</sup> to observe binding interactions between an enzyme and potential ligands. Various NMR experiments had previously been developed to study binding processes such as competitive binding spectroscopy,<sup>93</sup> SAR by NMR<sup>94</sup> transferred nuclear Overhauser effect,<sup>95</sup> and NOE pumping.<sup>96</sup> However, these methods do not have the high sensitivity that STD NMR has, or the ability to observe enzyme-ligand interactions *in vitro*.<sup>97</sup>

STD NMR measures the transfer of magnetization from an enzyme to a ligand. Only ligands that are bound to the enzyme show an STD effect. Thus, STD NMR lends itself to a number of experiments, providing structural insight to the binding regions of the ligand, the peptide, or both. STD versions of TOCSY, COSY, NOESY, and 1D NOE experiments all exist.<sup>92</sup>

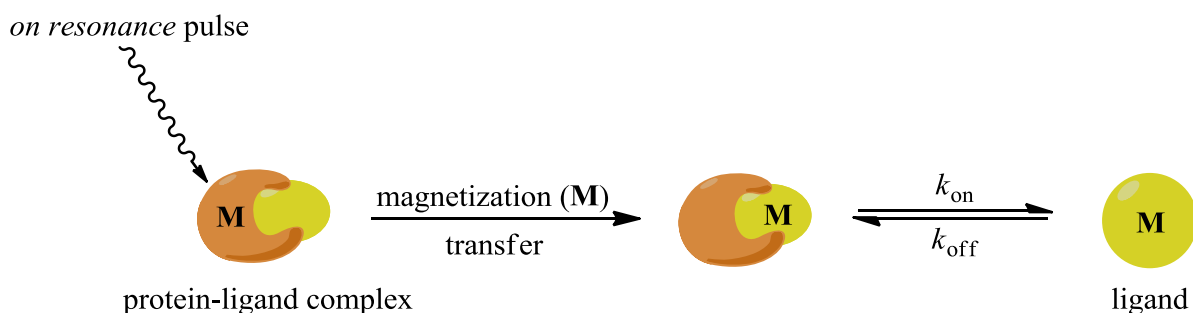


**Figure 2.17** STD NMR.

The focus of our efforts was a STD 1D NOE experiment. In order to achieve this effect, the experiment is performed by first magnetizing the peptide (Figure 2.17). This is accomplished by irradiating the peptide, or “saturating” the peptide with magnetization, at a radio frequency (RF) that only contains the protein envelope resonances (*on-resonance irradiation*).<sup>98</sup> Under these irradiation conditions, the protein transfers some magnetization to

the surrounding locality as it begins to relax. The protein also transfers some of its magnetization to any bound ligand through spin diffusion. A series of RF irradiations at a resonance that does not contain the protein envelope or ligand resonances (*off-resonance* irradiation) is then carried out. Subtraction of the spectrum without peptide magnetization (*off-resonance* irradiation) from the spectrum with peptide magnetization (*on-resonance* irradiation) gives the final STD NOE NMR. This only shows resonances for hydrogen atoms of the ligand that have NOE's due to their close contact with the peptide in the bound state.

A further refinement of this technique by Meyers and co-workers<sup>92</sup> is known as saturated transfer double difference (STDD). This technique was developed to overcome the poor signal to noise ratios due to biological components typically found in these experiments, such as buffers, glucose, and host cells. These undesired components produce regions of extreme overlap making detection of ligand resonances difficult. The technique of STDD is complementary to that of STD. Along with a sample containing the biological component and ligand there is a second sample that contains the biological components and no ligand. The former provides an STD NOE spectrum of the signals arising from ligand-peptide interaction along with background noise. The latter provides a STD NOE NMR of just background noise. A subtraction of these two spectra yields the STDD NOE spectrum, which shows the resonances of the ligand that have received NOE enhancement from binding to the peptide (Figure 2.18). The main advantage of the STDD experiment is a better signal to noise ratio.

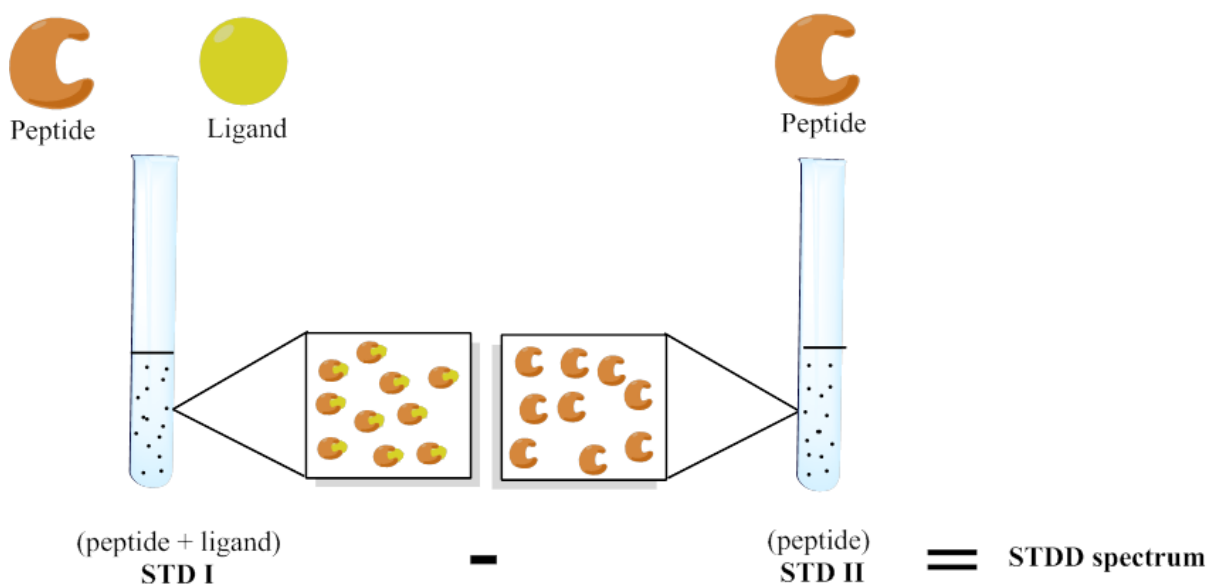


**Figure 2.18** STDD NMR sample preparation.

Having constructed a water-soluble analogue in **2.20** along with its enantiomer **2.42**, we wished to use the method of STDD NOE NMR to observe binding interactions with a fragment of SHIP1, that still contains phosphatase activity and is subject to allosteric regulation. This fragment was previously found to be activated by **2.3**,<sup>99</sup> and we hoped that amine analogues **2.20** and **2.42** would have a similar binding interaction. Due to the small quantities of the SHIP1 fragment available for the experiment, we decided to test both analogues sequentially in the same NMR tube. The author was responsible for sample preparation and David Williams ran the STDD experiments.

First, we combined the peptide and **2.42** at a 200:1 ligand to peptide ratio<sup>100</sup> and subtracted an STD NOE NMR spectrum of the peptide by itself from the resultant STD NOE NMR spectrum of the peptide and **2.42** to give an STDD NOE spectrum of **2.42**. Next, to the **2.42**/peptide sample was added **2.20** giving a 100:1 ligand to peptide ratio<sup>97</sup> and an STD NOE NMR was generated. From this was subtracted an STD NOE NMR spectrum of the

peptide by itself and the STDD NOE NMR spectrum of **2.42**, in order to observe STD NOE effects for **2.20** alone. This generated an STDD NOE spectrum of **2.20**. The STDD NOE NMR spectrum of **2.20** showed the absence of any ligand resonances, suggesting that there was little to no binding to the peptide. The STDD NOE NMR spectrum of **2.42**, however, showed ligand resonances suggesting binding to the peptide (Figure 2.19).

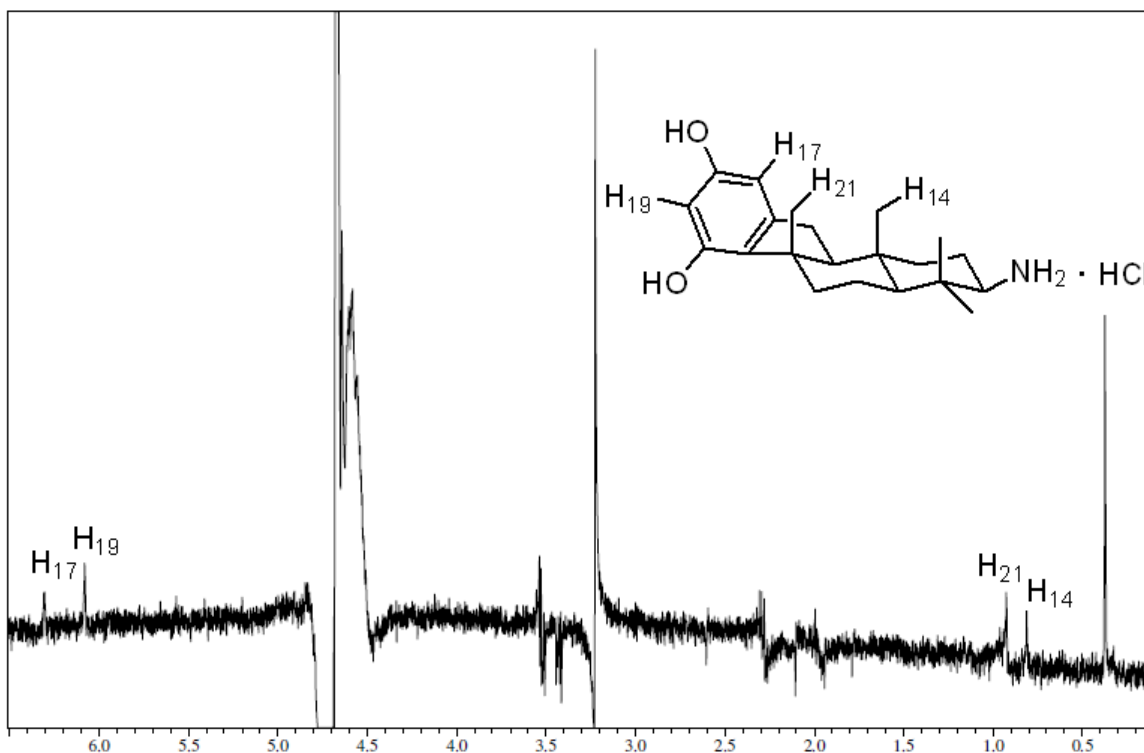


**Figure 2.19** STDD NOE NMR of **2.42**.

This data provided evidence supporting the hypothesis that the pharmacophore of pelorol (**2.1**) and all subsequent analogues includes the aryl moiety, due to STD NOE signals for H<sub>19</sub> and H<sub>17</sub>. Furthermore, the data indicates that the methyl groups Me<sub>21</sub> and Me<sub>14</sub> also play a role in SHIP1 binding. Since Me<sub>21</sub> and Me<sub>14</sub> have a *cis* relationship, and no other

STDD effects are observed for proton resonances on the ABC ring system, this suggests that there is a potential facial selectivity in the binding of **2.42** to SHIP1.

A surprising outcome of this experiment is that the antipodal configuration of pelorol (**2.1**) in analogue **2.42** was found to bind. However, the analogue **2.20** having the absolute configuration of the natural product pelorol (**2.1**) was found not to bind. This suggests that a positive charge on the A-ring moiety of analogue **2.42** may play a role in binding to SHIP1. Additional experiments are necessary for further evidence to support this hypothesis.

## 2.6 Synthesis of a Benzophenone Photoaffinity Probe

Photoaffinity probes are a powerful tool for obtaining structural information about the binding site of a ligand, to facilitate crystallization of an enzyme-ligand complex, and in the identification of previously unknown biological targets.<sup>101</sup> With the STDD NOE NMR evidence for binding to SHIP1 of **2.42** in hand, we decided to construct a photoaffinity probe (photoprobe). The goal was to provide proof of interaction between a ligand and SHIP1 in cells and structural information about the protein-binding site, which had not been characterized thus far. To construct a successful photoaffinity probe several structural motifs are typically present (Figure 2.20).

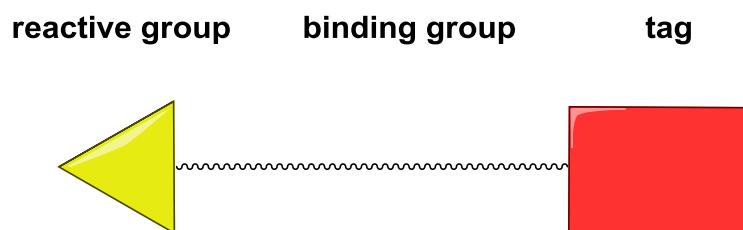


**Figure 2.20** Components of a photoaffinity probe.

The first is a reactive group, which is an electrophilic or a photoreactive moiety, that covalently binds to the enzyme. Common electrophilic groups are electrophilic phosphonates<sup>102,103</sup> and  $\alpha$ -halomethyl ketones.<sup>104</sup> Often fine-tuning of the electrophilic group incorporated into the probe is necessary for successful reactivity towards a residue in the enzyme-binding pocket. Photoreactive substructures are another type of reactive group that bind covalently to a residue in an enzyme active site only after UV irradiation. Various photoreactive groups have been utilized, including diazirine<sup>105</sup> and benzophenone<sup>106</sup> photophores (Figure 2.21).

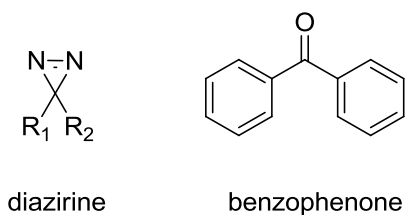


**Figure 2.21** Examples of photoreactive groups.

The second required element in a photoaffinity probe is the tag or reporter group. It is responsible for target identification and its identity dictates the type of analysis used later on. Examples include fluorophores<sup>107</sup> and biotin,<sup>108</sup> along with chemical handles such as azides,<sup>109</sup> or alkynes,<sup>110</sup> which can be modified by copper catalyzed Huisgen cycloaddition<sup>111</sup> (click chemistry) to allow for visualization of targets post labeling (Figure 2.22).

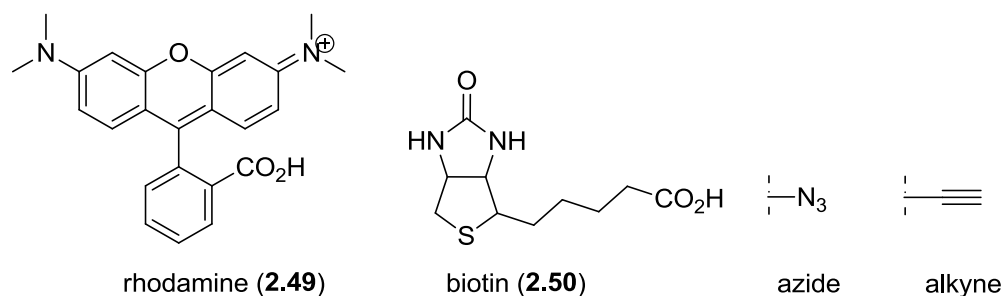


**Figure 2.22** Commonly used tags.

The third and last required component is a binding group, which is the component that has an affinity for a biological target. The most important characteristic of a photoaffinity probe is that it must maintain biological activity. Compound **2.51** is a photoaffinity probe analogue of HUN-7293, a fungal cyclodepsipeptide that was first identified as an inhibitor of vascular cell adhesion molecule (VCAM) expression<sup>107</sup> (Figure 2.23). In this case, the photoprobe incorporates a diazirine photophore and an alkyne tag. Another example is **2.52**, the photoprobe version of SecinPP, the first example of a cytoplasmic regulatory protein inhibitor. Its structure incorporates a benzophenone photoprobe along with a biotin tag (Figure 2.23).<sup>112</sup>

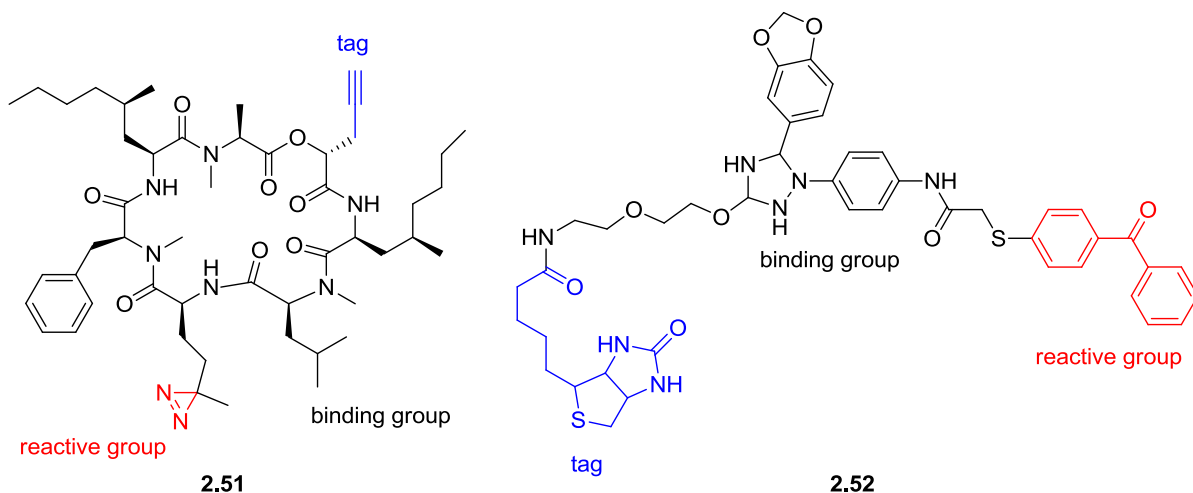


**Figure 2.23** Examples of photoaffinity probes.

In our own efforts to design a photoaffinity probe of pelorol (**2.1**), we took all previous considerations into account. There were several analogues of pelorol (**2.1**) to choose from, with pelorol (**2.1**) not being a satisfactory candidate, since it contained a labile catechol functionality that could potentially bind off-target (Figure 2.4). Amine **2.42** had proved successful in generating STDD NOE data showing binding to SHIP1, however, the lack of biological data (at the time) did not make it an appealing candidate. Analogue **2.3** was designed at an earlier stage and had biological data showing it activates SHIP1.<sup>99</sup> Also, from a practical standpoint our laboratory possessed 1 kg of material from a previous contract synthesis. Therefore, **2.3** was chosen as the starting material for construction of a photoaffinity probe.

A benzophenone moiety was chosen as the photophore for several reasons. One is that this photophore is known to preferentially label to hydrophobic binding regions.<sup>113</sup> When considering the lipophilicity of pelorol (**2.1**) (CLogP = 5.74) it is likely that the region of SHIP1 responsible for binding is hydrophobic. Secondly, it was thought that one-half of the

benzophenone fragment can come from the aryl group already incorporated in **2.3**. This works well with the STDD NOE data suggesting the aryl moiety plays a role in binding to SHIP1. In order to incorporate the tag into the molecule an alkyne moiety was selected. This would provide a conservative modification in order to preserve the biological potency of **2.3**. One potential probe (**2.53**) along with its subsequent retrieval of the ligand-enzyme complex from the cellular environment is shown in Figure 2.24.

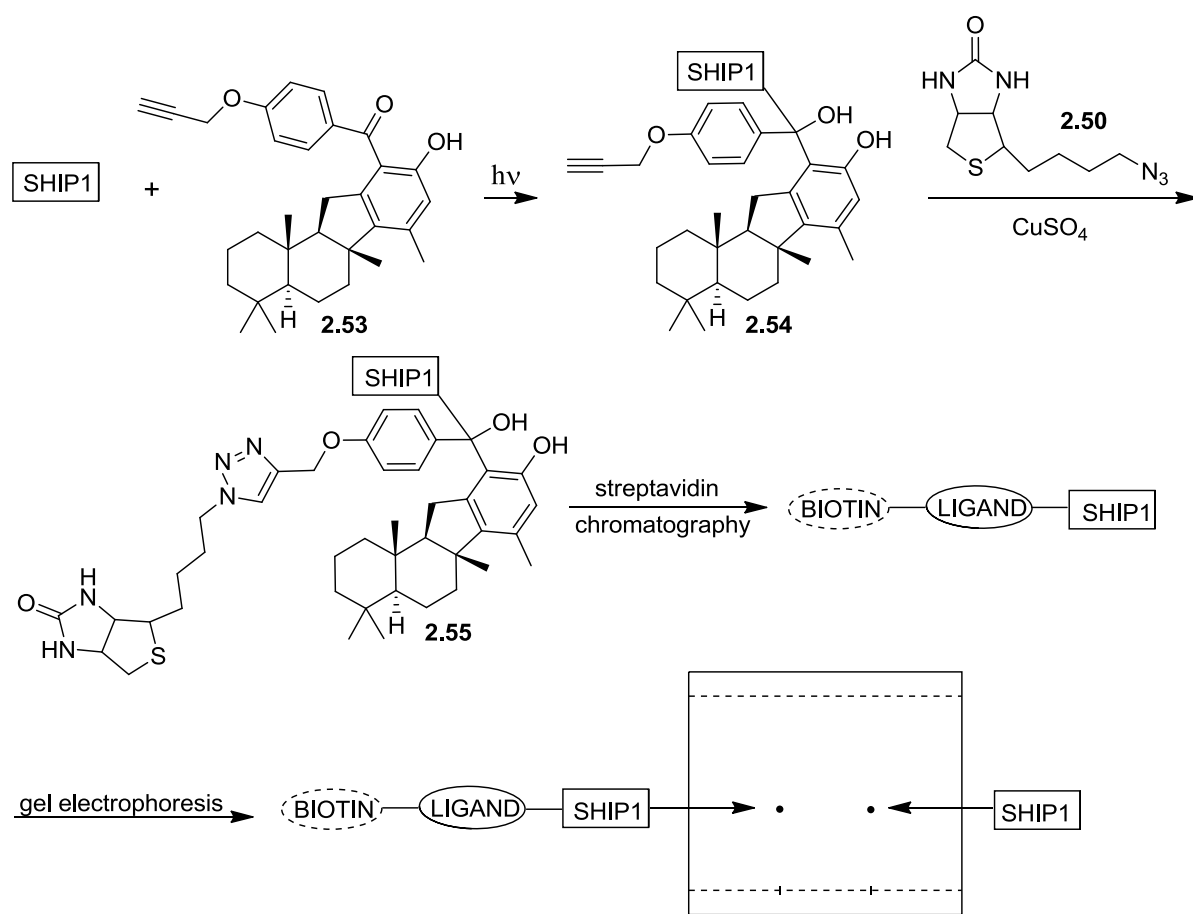
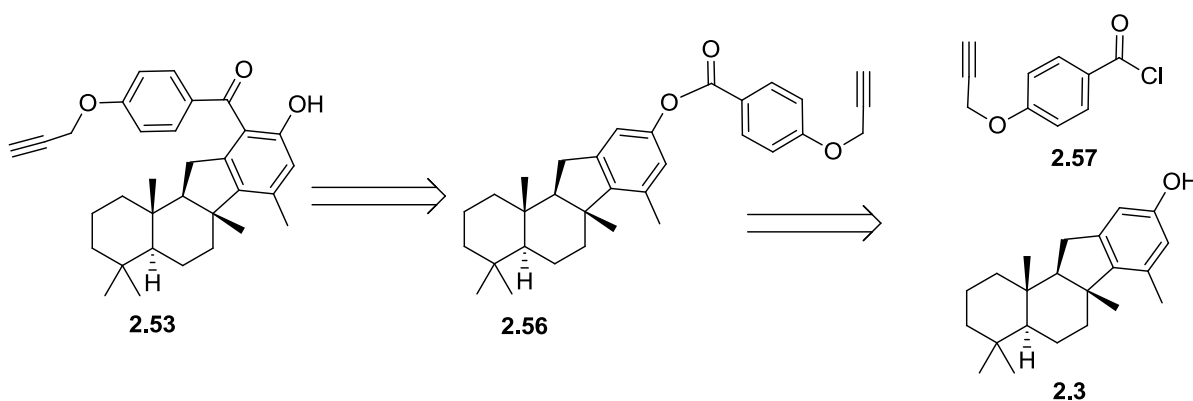


**Figure 2.24** Principle of **2.3** based photoaffinity probe (**2.53**).

For target identification, we desired to use the aforementioned click chemistry between the alkyne and an azide bound to biotin after covalent binding between the ligand

and peptide. The purpose of biotin is to retrieve the ligand-enzyme complex (Figure 2.24), and this can be accomplished by utilizing Streptavidin chromatography.<sup>114</sup> Streptavidin chromatography is used to separate the biotin-ligand-enzyme complex from all other cellular components due to the high affinity Streptavidin has for biotin.<sup>115</sup> Finally, polyacrylamide gel electrophoresis (PAGE) can be done on the purified complex and compared with the SHIP1 enzyme alone resulting in bands with similar retention<sup>116</sup> (Figure 2.24). Typically, the gel is exposed separately to a SHIP1 antibody and a biotin antibody with fluorescent markers. If the band of interest fluoresces with both antibodies, then the ligand-enzyme complex is present. This along with mass spectral data of the complex may provide concrete evidence of binding by the ligand to SHIP1.

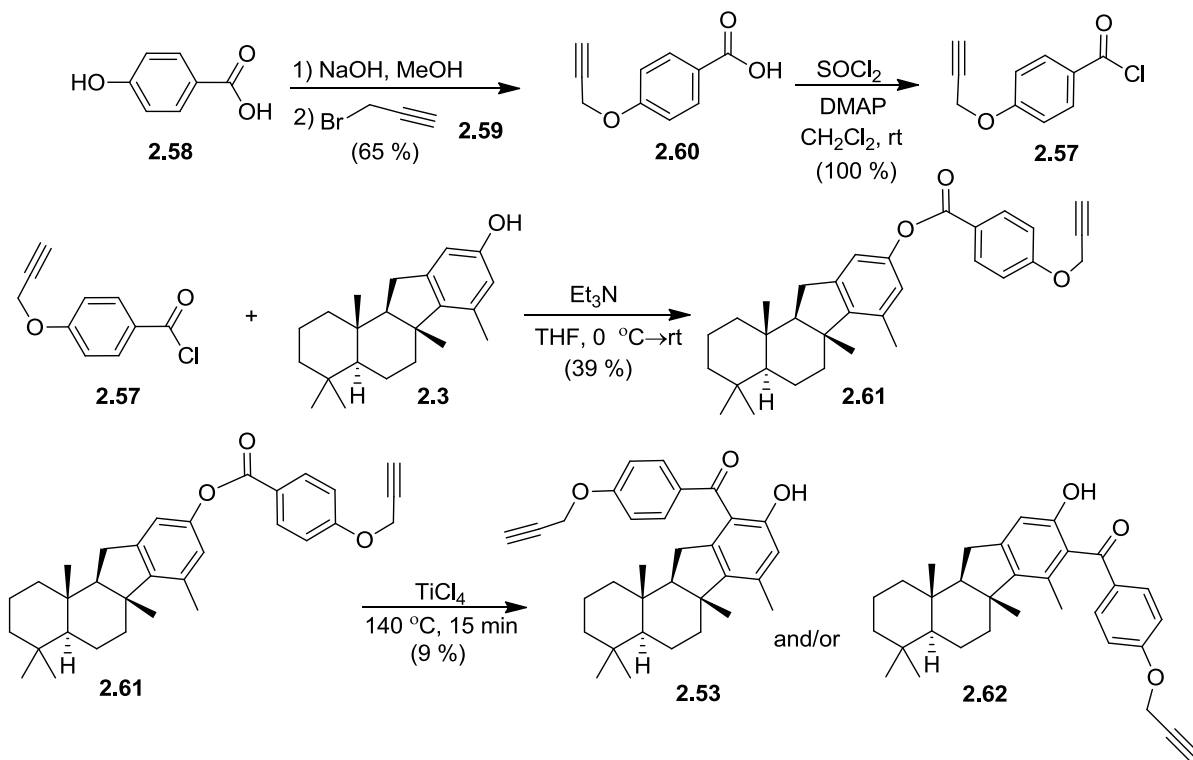
Retrosynthetic analysis of the desired photoprobe **2.53** reveals that it can come from ester **2.56** by a Fries rearrangement.<sup>117</sup> Ester **2.56** can come from acid chloride **2.57** and **2.3** (Scheme 2.13).



**Scheme 2.13** Retrosynthetic analysis of **2.53**.

The synthesis started with commercially available acid **2.58**. Etherification of **2.58** with propargyl bromide (**2.59**) gave **2.60** in 65 % yield (Scheme 2.14). Chlorination of **2.60**

with thionyl chloride gave acid chloride **2.57**, which under basic conditions and **2.3** gave the key ester intermediate **2.61**. This set up the key step of the synthesis, which is the Fries rearrangement.

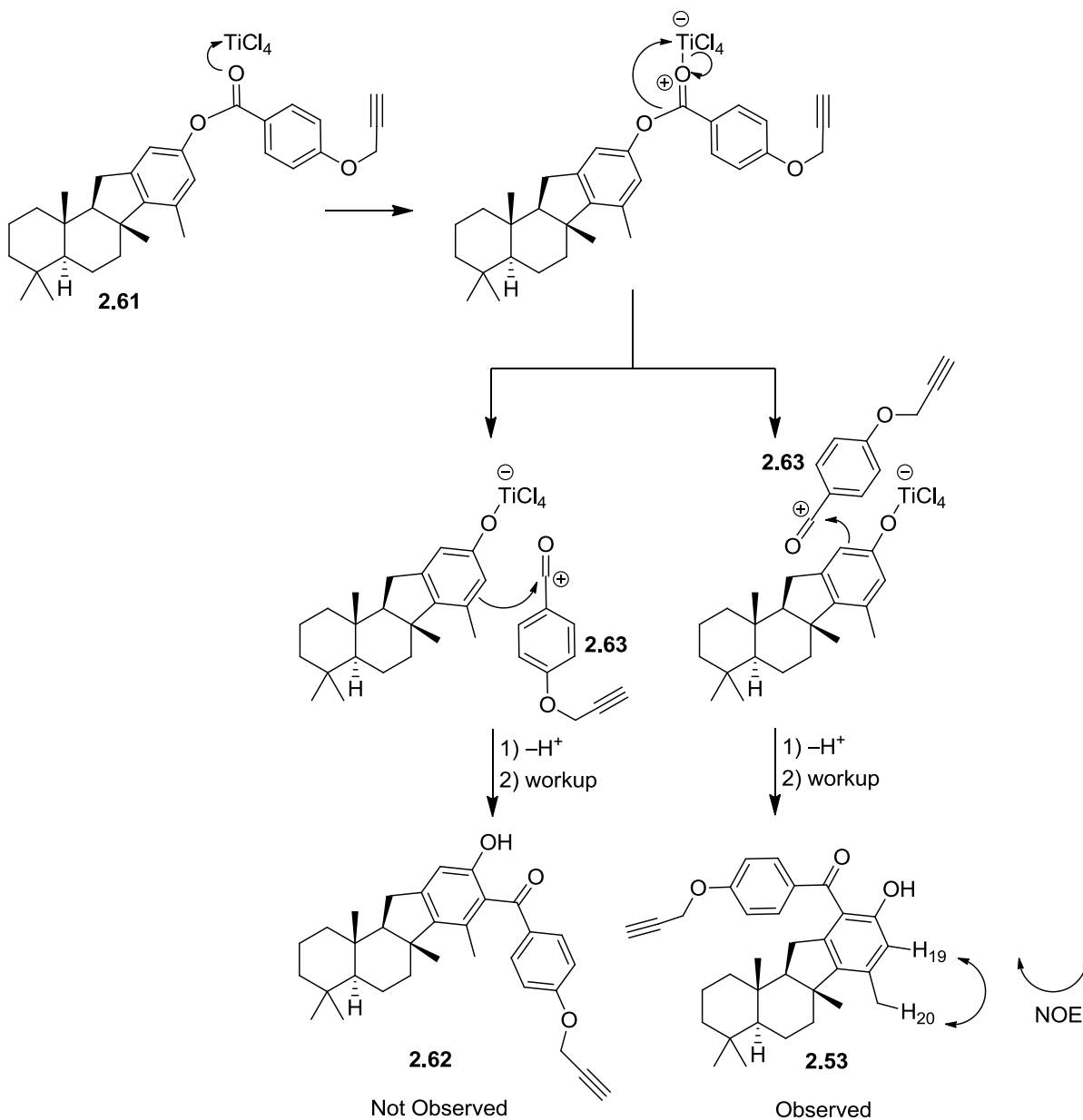


**Scheme 2.14** Benzophenone photoaffinity probe (**2.53**) synthesis.

Common acids used in the Fries rearrangement include HF,<sup>118</sup> AlCl<sub>3</sub>,<sup>119</sup> BF<sub>3</sub>,<sup>120</sup> TiCl<sub>4</sub><sup>121</sup> and SnCl<sub>4</sub>.<sup>122</sup> Aluminum trichloride gave no observable product. However, aryl ester **2.61** in the presence of titanium tetrachloride at 140 °C, gave a complex reaction mixture after a short reaction time. The crude mixture was purified and the major compound isolated.

To understand the potential product distribution for the final step of this synthesis, we had to look at the mechanism of the Fries rearrangement. The Fries rearrangement generates an acylium carbocation **2.63** (Scheme 2.15). This electrophilic intermediate can be attacked

by two possible aryl positions in a Friedel-Crafts type mechanism, resulting in two potential products **2.53** and **2.62** (Scheme 2.15).



**Scheme 2.15** Fries rearrangement and NOE observance in **2.53**.

These two regioisomers could not be definitively distinguished with 1D  $^1\text{H}$  NMR. Therefore, the major product of the reaction was analyzed by a NOESY experiment to determine the site of benzoyl attachment. An NOE was observed between the aryl proton  $\text{H}_{19}$  and  $\text{Me}_{20}$ , which is only possible in compound **2.53**, thus identifying the correct regioisomer. The ability of photoprobe **2.53** to bind covalently to SHIP1 upon irradiation is currently being investigated in the laboratory of Dr. Alice Mui at the BC Cancer Agency.

## 2.7 Biological Results

The biological activity of selected compounds was investigated by our collaborator Dr. Alice Mui at the BC Cancer Agency, Aquinox pharmaceuticals, and SignalChem. The first set of compounds that was analyzed included **2.48** and the corresponding racemate **2.48/2.18**. The goal was to gain insight about the role of the absolute configuration of these analogues in activating SHIP1. In addition, the benzophenone photoprobe **2.53** was tested for SHIP1 activity.

The SHIP1 activating properties of these compounds were evaluated using a chromogenic kinetic assay for SHIP1 phosphatase activity. In this assay, SHIP1 was incubated with compounds **2.3**, **2.53**, **2.48**, and **2.48/2.18** for 15 minutes before the addition of inositol-1,3,4,5-tetrakisphosphate. At this point SHIP1 dephosphorylates inositol-1,3,4,5-tetrakisphosphate, and a phosphate group is released into solution. At a particular time period, Malachite green along with molybdate are added, and together with free orthophosphate, they form a green complex that can be measured on a spectrophotometer at 650 nm. The magnitude of the reading on the spectrophotometer is directly related to the

amount of green complex formed, and correlates to the degree to which SHIP1 is activated. The results are shown in Figure 2.25.

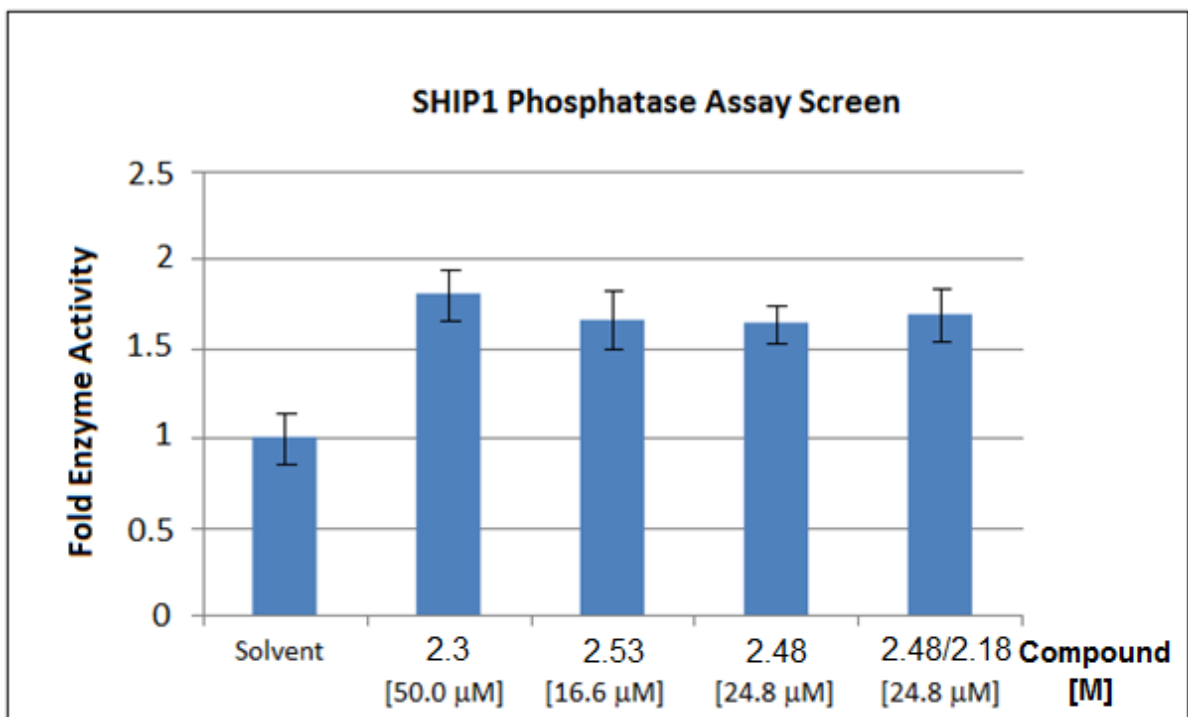


**Figure 2.25** SHIP1 phosphatase assay.

Interestingly, **2.48**, and **2.48/2.18** have almost the same activity, which indicates that the absolute configuration does not seem to play a major role in SHIP1 activation. Another important finding of this study is that photoprobe **2.53** activates SHIP1. This result is a requirement for it to be a successful photoaffinity probe.

Our attention then turned to the A-ring analogues of **2.18**. The first piece of information was to determine the solubility of amine **2.20** versus its less polar counterparts **2.3** and **2.18**. The method to determine solubility in water is as follows. A compound (**2.3**, **2.18**, or **2.20**) of known mass was dissolved in water to a predetermined concentration.

This sample was stirred at room temperature for a specific time period after which the sample was filtered, and then centrifuged. The supernatant was then analyzed by HPLC using a standard of known concentration.

**Table 2.1** Solubilities of pelorol (**2.1**) analogues.

Compound	Solubility in Water ( $\mu\text{g/mL}$ )	Solubility in Tris Buffer ( $\mu\text{g/mL}$ )
<b>2.3</b>	-	0.003
<b>2.18</b>	-	0.92
<b>2.20</b>	1,400	-

Data are summarized in table 2.1. There is an approximate 500,000 fold increase in solubility going from **2.3** to **2.20** and an approximate 1500 fold increase going from **2.18** to **2.20**. This demonstrated that we had achieved our goal of constructing an analogue with enhanced solubility in water. The next goal was to ensure that the racemic mixture **2.20/2.42** activated SHIP1 in cells. *In vitro* evidence for inhibition of AKT phosphorylation was obtained by incubating **2.20/2.42** with MOLT-4 (SHIP1+) cells and Jurkat (SHIP1-) cells stimulated with LPS. It was found that AKT phosphorylation was inhibited only in the MOLT-4 cells that express the SHIP1 enzyme, whereas there was no AKT phosphorylation inhibition in the Jurkat cells missing SHIP1 (Table 2.2). This is evidence that the inhibition of AKT phosphorylation by **2.20/2.42** is SHIP1 dependent.

**Table 2.2** AKT phosphorylation inhibition of racemic amine mixture **2.20/2.42**.

Compound	MOLT-4 (SHIP1+)	JURKAT (SHIP1-)
<b>2.20/2.42</b>	Inhibition	No Effect

Next, a SHIP1 chromogenic kinetic assay was carried out to test the less polar analogues **2.3** and **2.18** alongside polar analogues **2.19**, **2.20/2.42**, **2.34/2.43**, **2.20**, and **2.42** and the results are presented in Table 2.3. Percent (%) activation of SHIP1 is expressed as a percentage increase relative to background. Scoring is expressed as follows: + (< 25 %); ++ ( $\geq 25$  % but < 50 %); +++ ( $\geq 50$  %).

**Table 2.3** Activation of SHIP1 enzyme.

Compound	Scoring
<b>2.3</b>	++
<b>2.18</b>	+++
<b>2.19</b>	+++
<b>2.20/2.42</b>	++
<b>2.34/2.43</b>	++
<b>2.20</b>	+
<b>2.42</b>	++

Several conclusions can be made from these enzymatic assay results. Analogue **2.18**, which is missing A-ring derivatization, along with its A-ring ketone counterpart **2.19**, both activate SHIP1 the most effectively. None of the amines activated SHIP1 as much as **2.18** or **2.19**. Interestingly, the antipodal configuration to pelorol (**2.1**) in amine **2.42** was more active than amine **2.20**, which retained the natural product configuration and yet was almost inactive. This is in contrast to the difference in activity between **2.48** and **2.48/2.18** (Figure 2.25), which was negligible. This is encouraging evidence as it was shown in the STDD NOE NMR of **2.20**, and **2.42**, that only **2.42** had observable binding to SHIP1, an outcome also verified by this enzymatic study. This leads us to believe that having a positive charge on the A-ring must affect the binding in a manner yet to be determined. Another outcome is that the

minor  $\alpha$ -amine epimers **2.34/2.43** showed no difference in activity compared to the  $\beta$ -amine epimers **2.20/2.42**.

Racemic amine mixture **2.20/2.42** was then evaluated in a standard mouse passive cutaneous anaphylaxis (PCA) ear model of inflammation.<sup>123</sup> The right ear of the mouse is inoculated with anti-DNP-IgE, which is an antigen that binds to mast cells in the local environment. After 24 hours, the compound (**2.20/2.42**) is administered by oral gavage, followed by an injection of Evans blue and DNP-HSA. DNP-HSA is an antigen that causes cross-linking of anti-DNP-IgE molecules bound on the mast cells. This cross-linking triggers the release of histamine and other small molecules from mast cell granules. Evans blue is injected to allow for visualization of increased vascular permeability and will stain the tissue blue where excess extravasation has occurred.

Ideally, the compound administered to the mouse before the DNP-HAS/Evans blue injection is taken up by the cells, and will prevent the anaphylactic response, thus the ear will stain minimally blue. Afterwards, the mice are sacrificed and a portion of the inoculated ear is taken, extracted into solution, and analyzed using a spectrophotometer at 620 nm. A smaller reading suggests that less Evans blue was retained in the tissue indicating the effectiveness of the compound at preventing anaphylaxis.

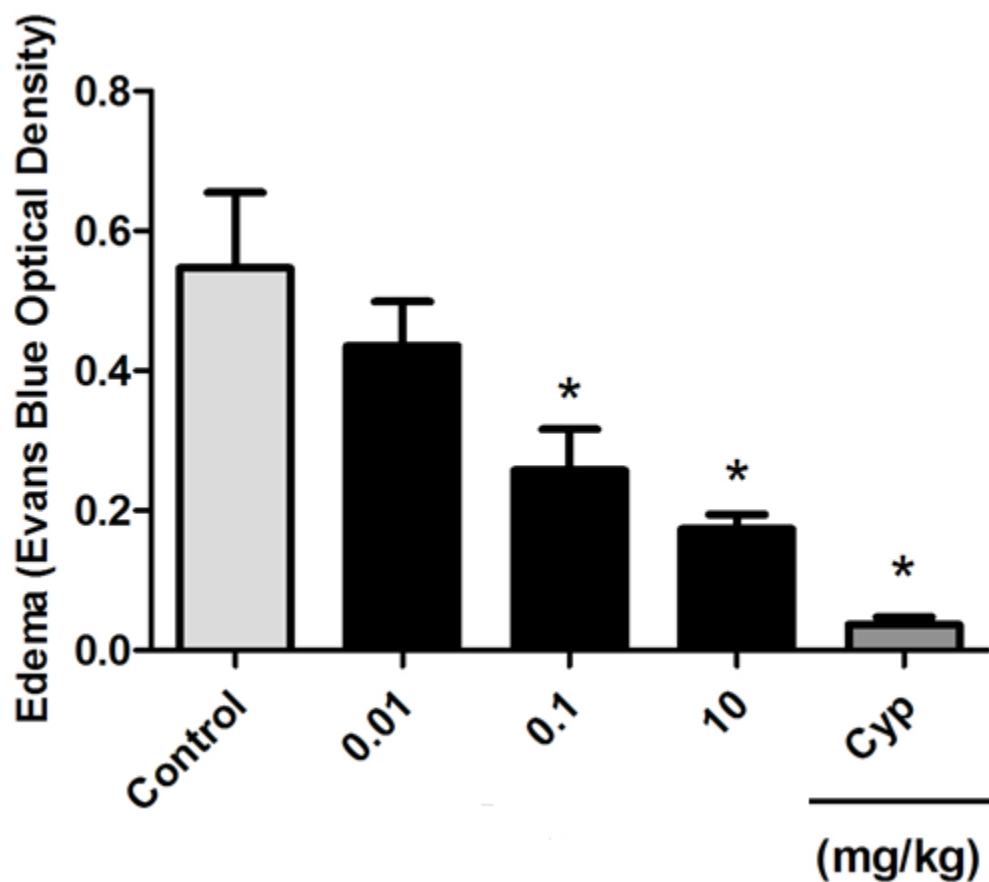


**Figure 2.26** Efficacy of **2.20/2.42** versus cyproheptadine (Cyp, 1 mg/kg) in a mouse (PCA) model.

When administered by oral gavage, racemate **2.20/2.42** showed effective anti-inflammatory activity with a clear dose response and an  $ED_{50}$  of approximately 0.1 mg/kg (Figure 2.26). This is a promising result since the desired biological effect is concentration dependent, a step in the right direction for constructing a compound with drug-like properties.

## 2.8 Conclusion

The activation of SHIP1 is a novel and selective method to modulate the PI3K cell-signaling pathway. It is an alternative to classic kinase therapeutic targets and may be useful for the development of drugs to treat hematopoietic diseases that involve PI3K signaling. The lead compound pelorol (**2.1**) was identified as the first SHIP1 activator, and provided a proof of principle test for our target hypothesis. Pelorol (**2.1**) was synthesized to confirm its absolute configuration, and a number of analogues were constructed by Lu Yang to further probe the SAR. Analogue **2.2** was found to have increased potency relative to pelorol (**2.1**) and was easier to construct. However, the labile catechol functionality prevented it from being a viable drug lead.

An SAR study was done by Matt Nodwell to construct analogues, which maintained the biological activity of **2.2** but without the labile catechol functionality. This culminated in analogue **2.3**. However, its low solubility (CLogP = 6.16) in water posed a problem for drug administration. Analogue **2.18** with resorcinol functionality was constructed in order to enhance water solubility and retain its SHIP1 activation property. Resorcinol **2.18** was found to have enhanced activity relative to **2.3** and while its CLogP (4.99) did benefit from an extra aryl alcohol, it still fell short of ideal.

The focus of this chapter is a third generation of SAR based on analogue **2.18** in order to construct water-soluble compounds that activate SHIP1. All of the SAR completed by Lu Yang and Matt Nodwell was devoted to the aryl moiety of pelorol (**2.1**) because this was considered as the putative pharmacophore. With this in mind, the author constructed analogues of **2.18** that had synthetic modifications to the A-ring, far from the putative

pharmacophore. Amines **2.20** and **2.42** were chosen as the main synthetic targets with a CLogP value of 3.58, below the Lipinski rule of five.

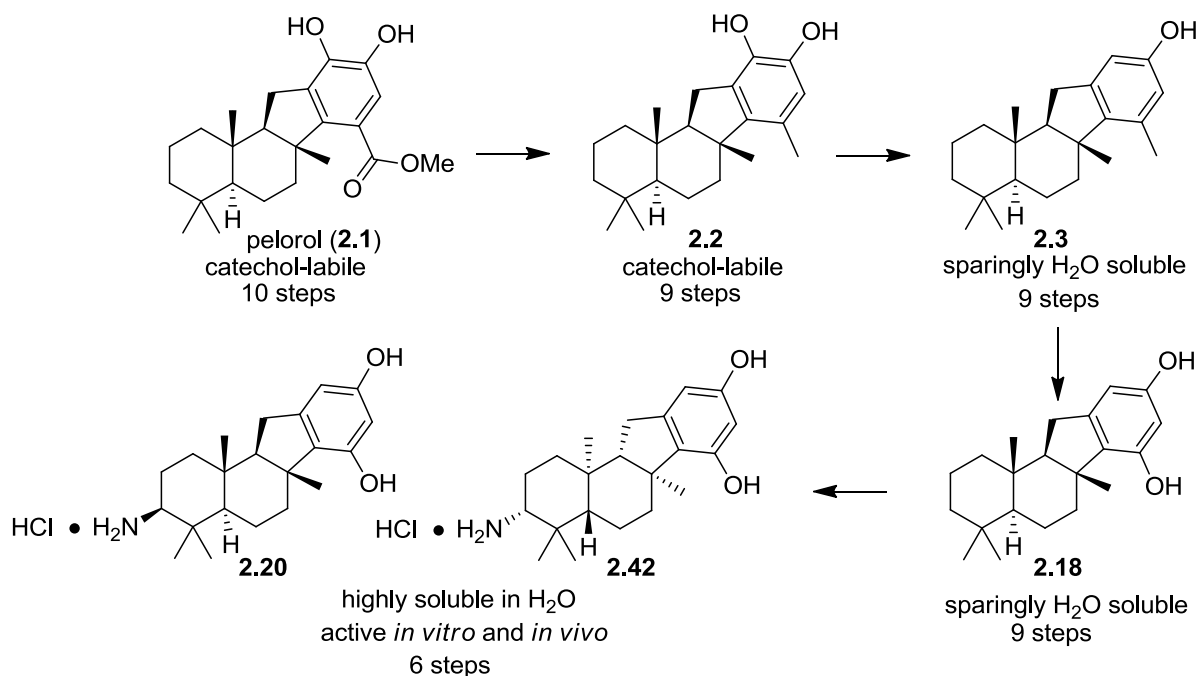
We used an epoxide-initiated cationic cascade to construct these analogues, and we utilized an asymmetric Shi epoxidation to affect a chiral synthesis. The syntheses of amines **2.20** and **2.42** are more concise than any of the previous syntheses used to construct SHIP1 activators, such as pelorol (**2.1**) and **2.3**, which require ten and nine steps respectively. In contrast, the syntheses of **2.20** and **2.42** proceed in six steps starting from achiral commercially available starting material. This allows rapid access to enantiopure SHIP1 activators that are highly soluble in water, and active *in vitro* and *in vivo*. The solubility of the racemic amine mixture **2.20/2.42** in water was determined and compared to **2.3** and **2.18**. There was an approximate 500,000, and 1500 fold increase in water solubility respectively. This result validated our hypothesis of enhanced water solubility of amine analogues **2.20** and **2.42**.

Next, the racemic amine mixture **2.20/2.42** was tested in an *in vitro* AKT phosphorylation inhibition assay to determine if the SHIP1 enzyme was activated by these analogues. It was found that SHIP1 was being selectively activated, making **2.20/2.42** suitable candidates for additional biological testing.

The amine analogues **2.20** and **2.42** were tested in a chromogenic kinetic assay against their less polar counterpart **2.18** to determine their effectiveness as SHIP1 activators. It was found that neither amine activated SHIP1 to the extent of **2.18**. However, these polar analogues did activate SHIP1 to the same degree as **2.3** which has precedent in SHIP1 activation.<sup>99</sup> Further validation of the amine analogues **2.20** and **2.42** as potential drug candidates included *in vivo* testing of the corresponding racemic mixture **2.20/2.42** in a PCA

mouse model. The compounds were effective in diminishing the anaphylactic response caused by administered antigens. There was a clear dose response, with an ED<sub>50</sub> of approximately 0.1 mg/kg. Making these analogues viable drug candidates for further testing.

One of the interesting outcomes of the biological testing was that amine **2.20**, which has the same configuration as pelorol (**2.1**), was less active than **2.42**, which has the opposite configuration. We used the method of STDD NOE NMR to determine which moieties in **2.42** and **2.20** were binding to SHIP1 in order to gain information about to the pharmacophore of these analogues. It was shown that the aryl group had binding interactions with the enzyme, validating the putative pharmacophore of pelorol (**2.1**) and all subsequent analogues. Furthermore, both *cis* methyl groups on the B/C ring junctions showed binding interactions, suggesting facial selectivity in binding to SHIP1. The work done in this chapter represents the continuation of a rational marine product based drug design starting from an initial lead in pelorol (**2.1**) and evolving to an analogue with enhanced drug-like properties in **2.42** and **2.20** with promising *in vitro* and *in vivo* activity (Scheme 2.16).



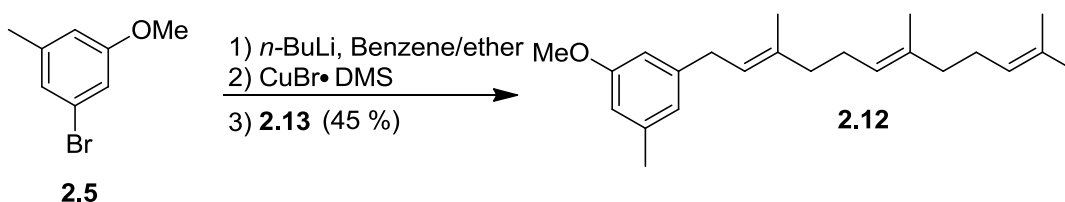
**Scheme 2.16** Rational drug design from a marine natural product (**2.1**) to drug lead (**2.20/2.42**).

## 2.9 Experimental

**General Methods:** All non-aqueous reactions were carried out in flame-dried glassware and under an Ar or N<sub>2</sub> atmosphere unless otherwise noted. Air and moisture sensitive liquid reagents were manipulated via a dry syringe. All solvents and reagents were used as obtained from commercial sources without further purification. <sup>1</sup>H and <sup>13</sup>C NMR spectra were obtained on Bruker Avance 400 direct, 300 direct, or Bruker Avance 600 CryoProbe spectrometers at room temperature. Flash column chromatography was performed using Silicycle Ultra-Pure silica gel (230-400 mesh). Analytical thin-layer chromatography (TLC) plates were aluminum-backed ultrapure silica gel 250 μm. Electrospray ionization mass spectrometry (ESI-MS) spectra were recorded on a Micromass LCT instrument. Optical

rotations were measured with a JASCO P-1010 polarimeter at 24 °C and 589 nm (sodium D line) in methanol (g/100 mL).

### Preparation of **2.12**:



To a mixture of benzene (7 mL) and ether (3.5 mL) was added bromide **2.5** (180 mg, 0.895 mmol) followed by the dropwise addition of *n*-BuLi (0.69 mL, 0.98 mmol) at room temperature. Halogen metal exchange was monitored using thin layer chromatography, after which CuBr · DMS (92 mg, 0.45 mmol) was added and the reaction mixture was allowed to stir for 1 hr. Trans,trans-farnesyl bromide (**2.13**) was then added neat and allowed to stir overnight. The reaction mixture was quenched with saturated NH<sub>4</sub>Cl<sub>(aq)</sub> (25 mL), and the aqueous layer was extracted with ethyl acetate (100 mL). The combined organic extracts were washed with 10 % NH<sub>4</sub>OH followed by brine, dried with MgSO<sub>4</sub> and concentrated using a rotary evaporator. Purification by flash column chromatography (hexane:methylene chloride 9:2) yielded polyene **2.12** as a light yellow oil (131.5 mg, 0.40 mmol, 45 %). <sup>1</sup>H NMR (400 MHz, CDCl<sub>3</sub>) δ 6.64 (s, 1H), 6.58 (s, 2H), 5.36 (t, J = 7.3 Hz, 1H), 5.14 (m, 2H), 3.81 (s, 3H), 3.34 (d, J = 7.3 Hz, 2H), 2.33 (s, 3H), 2.15-1.95 (m, 8H), 1.75 (s, 3H), 1.71 (s, 3H), 1.63 (s, 6H); <sup>13</sup>C NMR (100 MHz, CDCl<sub>3</sub>) δ 159.7, 143.2, 139.2, 136.1, 135.0, 131.2, 124.4, 124.1, 122.9, 121.6, 111.8, 111.1, 55.1, 39.7, 39.7, 34.2, 26.7, 26.6, 25.7, 21.5, 17.7, 16.2, 16.0. HRESIMS [M+Na]<sup>+</sup> calcd for C<sub>23</sub>H<sub>34</sub>ONa 349.2507, found 349.2502.

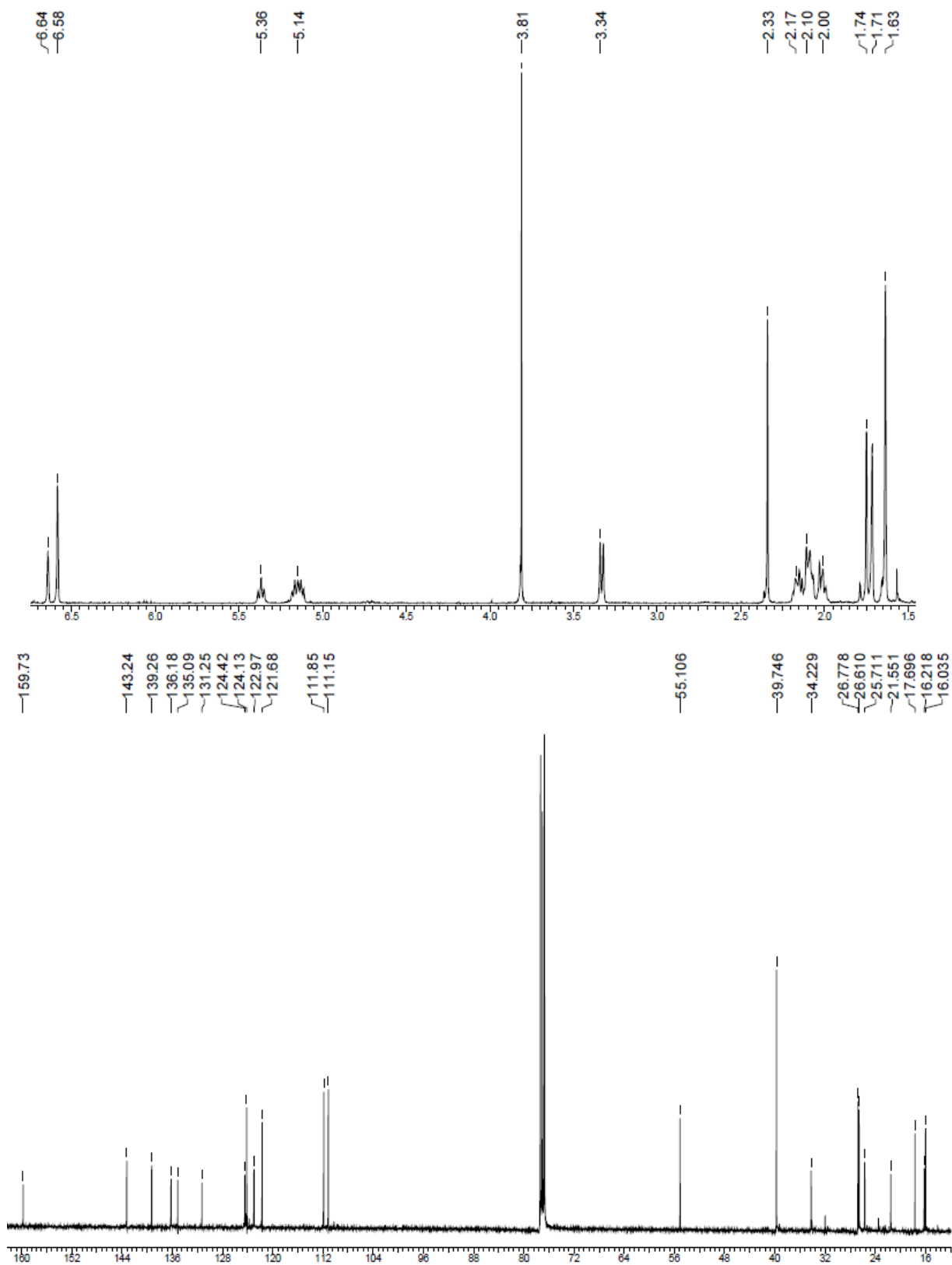
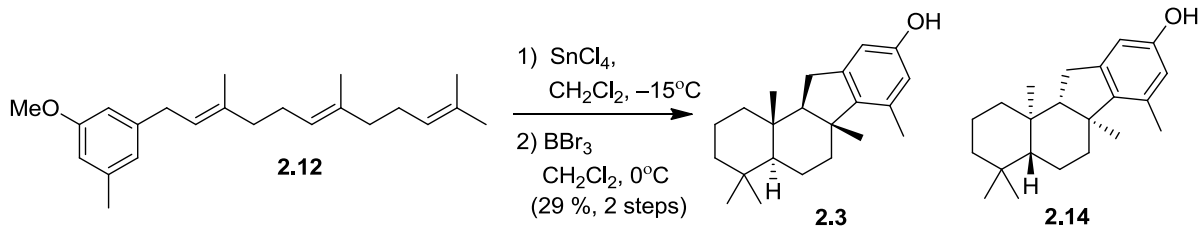


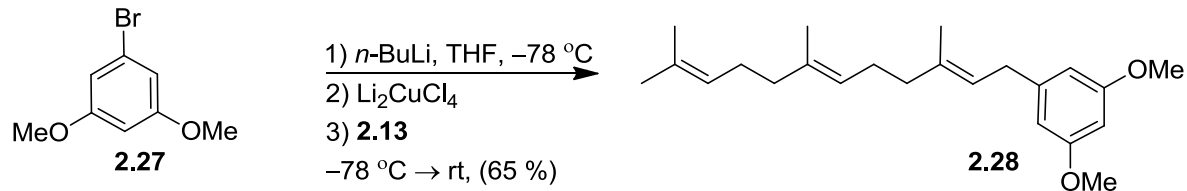
**Figure 2.27**  $^1\text{H}$  and  $^{13}\text{C}$  NMR spectra of **2.12** recorded in  $\text{CDCl}_3$  at 400 MHz and 100 MHz respectively.

### Preparation of 2.3/2.14:



To a solution of **2.12** (40 mg, 0.12 mmol) in methylene chloride at  $-15^\circ\text{C}$  was added  $\text{SnCl}_4$  (127.7 mg, 0.49 mmol) dropwise and allowed to stir for 2 hours. The mixture was quenched with 1 mL of methanol, and then saturated  $\text{NH}_4\text{Cl}$  (aq) (25 mL) was added. The aqueous layer was extracted with ethyl acetate (100 mL) and the combined organic extracts were washed with brine, dried with  $\text{MgSO}_4$ , and concentrated using a rotary evaporator. The crude was then deprotected in a similar fashion as **2.47**, and purified using flash column chromatography (hexane:ethyl acetate 7:1) to yield a mixture of diastereomers and regioisomers. This mixture was further purified with reversed phase HPLC to give racemic **2.3/2.14** (11.1 mg, 0.035 mmol, 29 % over two steps).  $^1\text{H}$  and  $^{13}\text{C}$  NMR spectra are identical to previously reported (Matt Nodwell). HRESIMS  $[\text{M} + \text{H}]^+$  calcd for  $\text{C}_{22}\text{H}_{33}\text{O}$  313.2531, found 313.2526.

### Preparation of **2.28**:



Bromide **2.27** (1.0 g, 4.60 mmol) was dissolved in 23 mL of tetrahydrofuran and brought to  $-78\text{ }^{\circ}\text{C}$ , to which 3.45 mL of 1.6 M *n*-BuLi in hexanes (5.52 mmol) was added dropwise, and allowed to stir for 15 minutes. To this solution was added 1.38 mL of 0.1 M  $\text{Li}_2\text{CuCl}_4$  in tetrahydrofuran (0.13 mmol) and allowed to stir for 10 minutes at  $-78\text{ }^{\circ}\text{C}$ , finally trans,trans-farnesyl bromide **2.13** (1.64 g, 5.75 mmol) dissolved in 20 mL of tetrahydrofuran was added dropwise and allowed to warm with stirring from  $-78\text{ }^{\circ}\text{C}$  to room temperature overnight. The reaction was quenched with saturated  $\text{NH}_4\text{Cl}_{(\text{aq})}$  (50 mL), and the aqueous phase was extracted three times with methylene chloride (200 mL). The organic extracts were dried with  $\text{MgSO}_4$ , and concentrated using a rotary evaporator. The crude mixture was purified using flash column chromatography (hexanes:ethyl acetate 30:1), to give **2.28** as a clear oil (1.02 g, 2.99 mmol, 65 %).  $^1\text{H}$  NMR (400 MHz,  $\text{CDCl}_3$ )  $\delta$  6.36 (d,  $J = 2.3$  Hz, 2H), 6.30 (t,  $J = 2.7$  Hz, 1H), 5.34 (t,  $J = 7.3$  Hz, 1H), 5.15-5.08 (m, 2H), 3.78 (s, 6H), 3.31 (d, 2H), 2.16-1.96 (m, 8H), 1.71 (s, 3H), 1.69 (s, 3H), 1.60 (s, 6H);  $^{13}\text{C}$  NMR (100 MHz,  $\text{CDCl}_3$ )  $\delta$  160.8, 160.8, 144.2, 136.5, 135.1, 131.2, 124.4, 124.1, 122.6, 106.4, 106.4, 97.6, 55.2, 55.2, 39.7, 39.7, 34.4, 26.7, 26.6, 25.7, 17.6, 16.2, 16.0. HRESIMS  $[\text{M}+\text{Na}]^+$  calcd for  $\text{C}_{23}\text{H}_{35}\text{O}_2$  343.2637, found 343.2628.

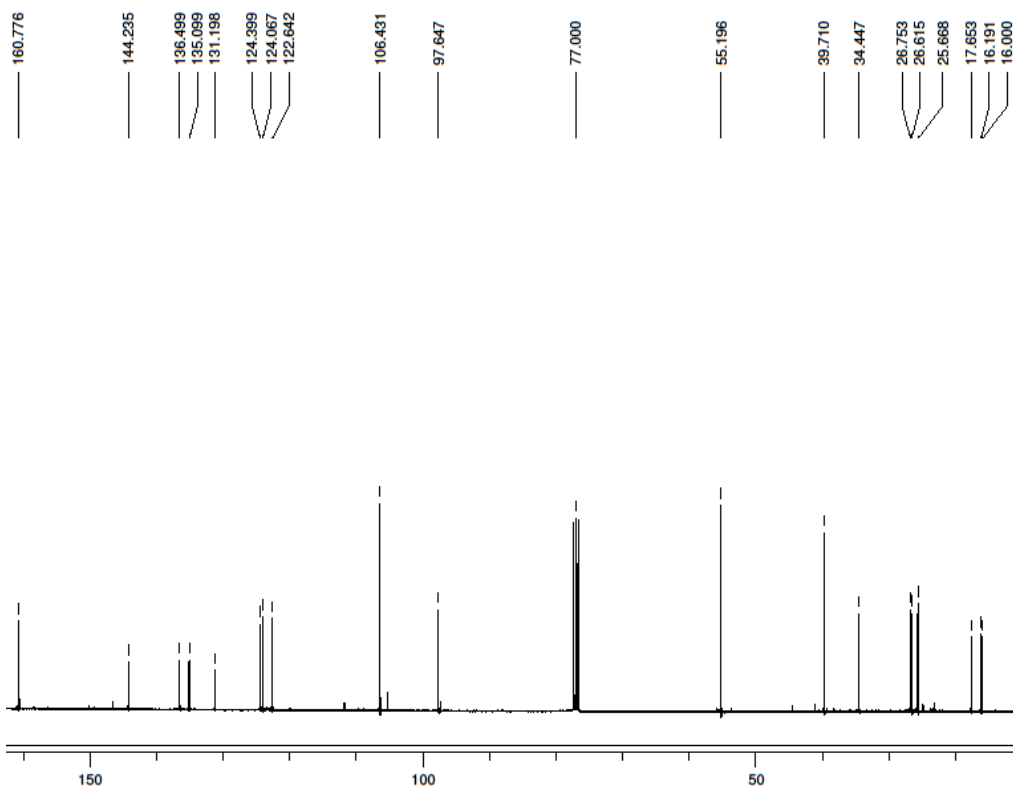
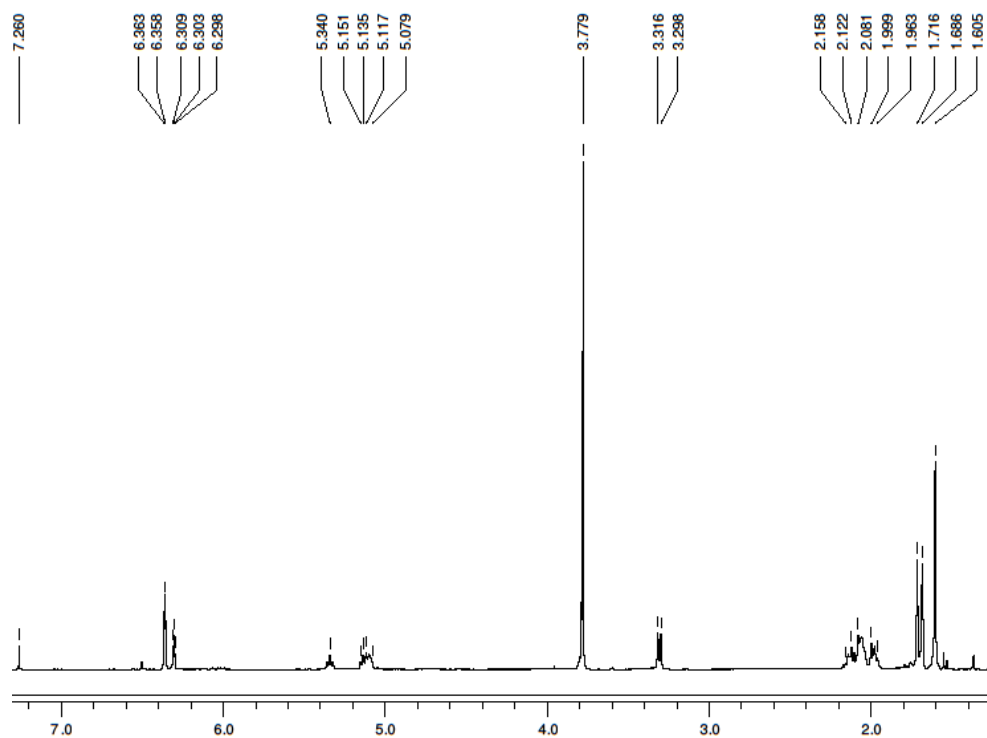
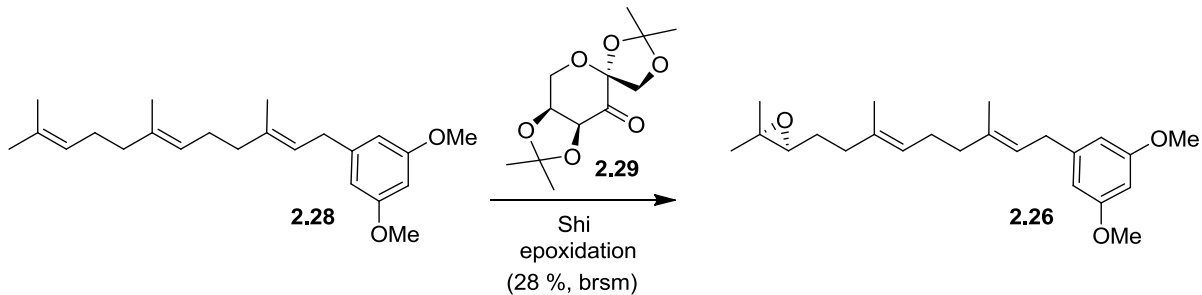


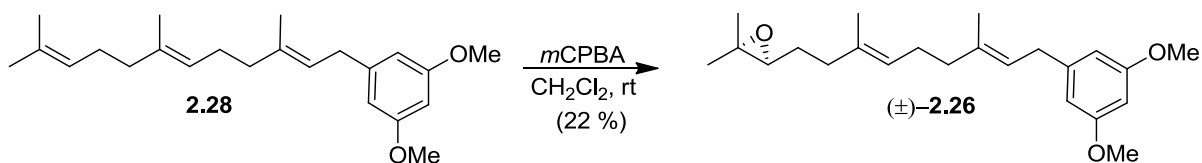
**Figure 2.28**  $^1\text{H}$  and  $^{13}\text{C}$  NMR spectra of **2.28** recorded in  $\text{CDCl}_3$  at 400 MHz and 100 MHz respectively.

### Preparation of **2.26**:



Epoxide **2.26** was prepared according to literature procedures<sup>74</sup> using the ent-Shi catalyst **2.29**. Polyene **2.28** (1 g, 2.90 mmol) was oxidized to **2.26** (113.0 mg, 0.315 mmol, 11 %), which was purified by flash column chromatography (hexanes:ethyl acetate 12:1). Based on recovered starting material **2.28** (622.5 mg, 1.82 mmol), the yield of **2.26** was 28 %. <sup>1</sup>H NMR (400 MHz, CDCl<sub>3</sub>) δ 6.34 (d, J = 2.2 Hz, 2H), 6.29 (t, J = 2.2 Hz, 1H), 5.33 (t, J = 6.1 Hz, 1H), 5.18 (t, J = 5.7 Hz, 1H), 3.76 (s, 6H), 3.29 (d, J = 7.2 Hz, 2H), 2.68 (t, J = 6.2 Hz, 1H), 2.11-2.14 (m, 4H), 2.04-2.08 (m, 4H), 1.71 (s, 3H), 1.62 (s, 3H), 1.29 (s, 3H), 1.25 (s, 3H); <sup>13</sup>C NMR (100 MHz, CDCl<sub>3</sub>) δ 160.6, 143.9, 136.1, 134.0, 124.6, 122.7, 106.3, 97.4, 63.9, 58.0, 55.0, 39.5, 36.1, 34.3, 27.3, 26.4, 24.7, 18.6, 16.0, 15.9. HRESIMS [M + Na]<sup>+</sup> calcd for C<sub>23</sub>H<sub>34</sub>O<sub>3</sub>Na 381.2406, found 381.2415.

### Preparation of (±)-2.26:



To polyene **2.28** (9.62 g, 27.9 mmol) dissolved in 100 mL of methylene chloride was added a solution of *m*CPBA (5.06 g, 29.3 mmol) in 100 mL of methylene chloride. The reaction was allowed to stir at room temperature for 3.5 h, after which it was quenched with saturated NaHCO<sub>3</sub>, and extracted three times with methylene chloride. The organic extracts were combined, dried with MgSO<sub>4</sub>, and concentrated using a rotary evaporator. The crude mixture was purified using flash column chromatography to give (±)-**2.26** (2.24 g, 6.24 mmol, 22 %). <sup>1</sup>H, <sup>13</sup>C, and mass spectrometry data matched that of **2.26** (page 66).

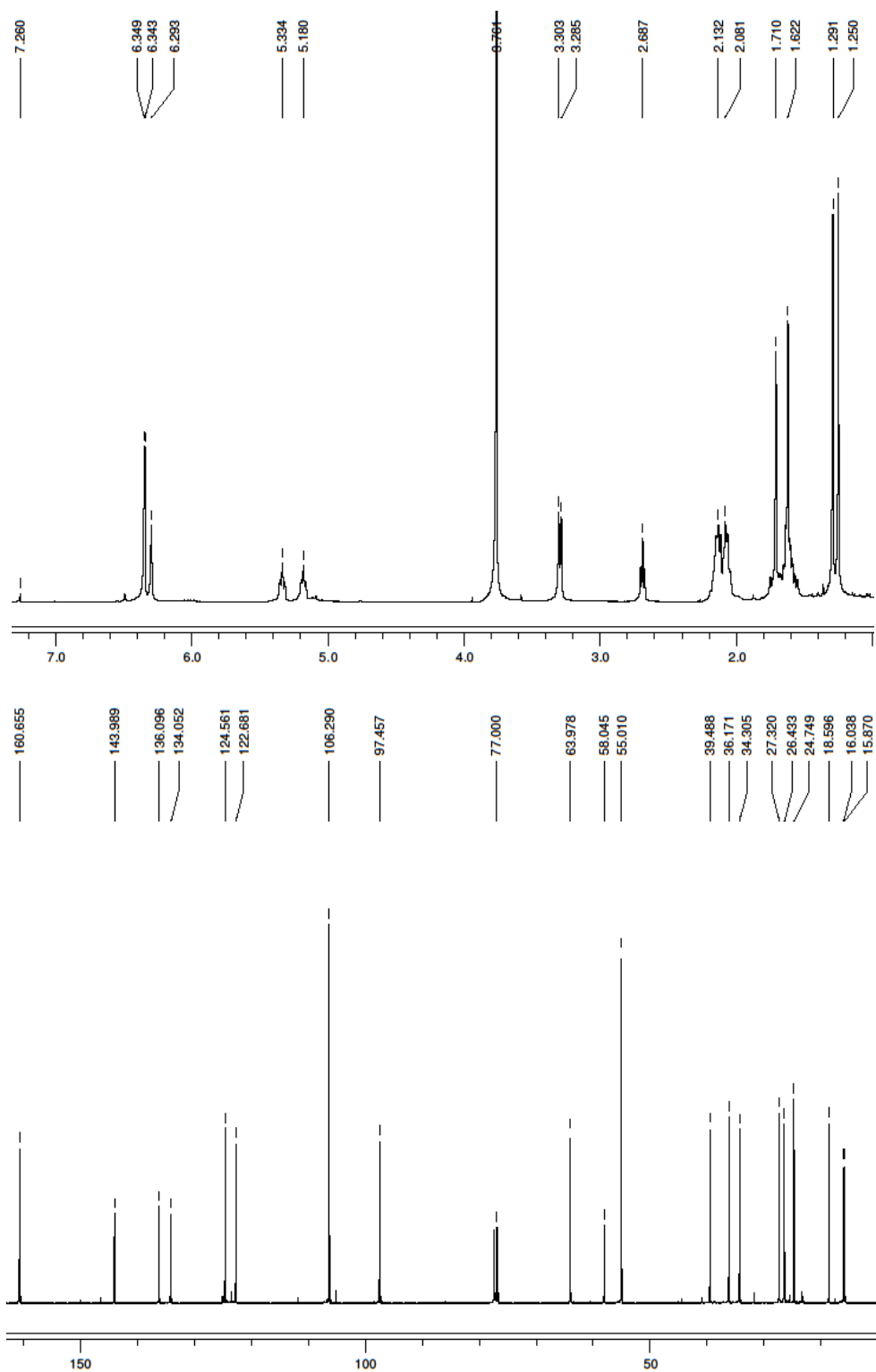
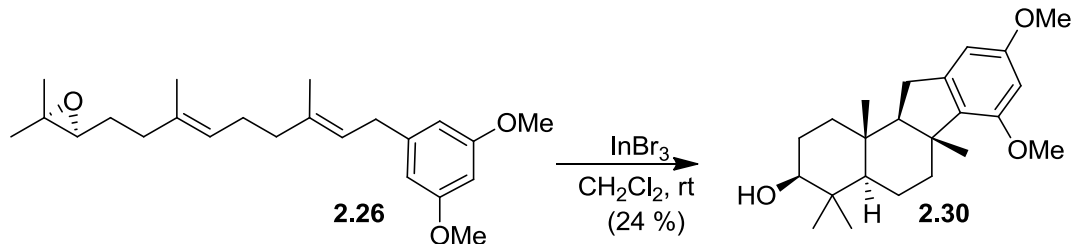


**Figure 2.29**  $^1\text{H}$  and  $^{13}\text{C}$  NMR spectra of **2.26** recorded in  $\text{CDCl}_3$  at 400 MHz and 100 MHz respectively.

### Preparation of **2.30**:



To epoxide **2.26** (3.53 g, 9.86 mmol) dissolved in 105 mL of methylene chloride was added  $\text{InBr}_3$  (6.99 g, 19.7 mmol), and allowed to stir for 1 hour at room temperature. The reaction mixture was then quenched with saturated  $\text{NaHCO}_3$  (100 mL) and the aqueous layer was extracted three times with methylene chloride (500 mL). The organic extracts were combined and dried with  $\text{MgSO}_4$ , then concentrated using a rotary evaporator. The crude reaction mixture was purified using flash column chromatography (hexanes:ethyl acetate 3:1), to give a mixture of **2.30** and various uncyclized products. The product mixture was then crystallized using boiling solvent (hexanes:ethyl acetate 15:1), to give **2.30** (860.3 mg, 2.39 mmol, 24 %).  $^1\text{H}$  NMR (400 MHz,  $\text{CDCl}_3$ )  $\delta$  6.40 (d,  $J = 1.8$  Hz, 1H), 6.26 (d,  $J = 2$  Hz, 1H), 3.77 (s, 3H), 3.75 (s, 3H), 3.22 (m, 1H), 2.62 (m, 1H), 2.50 (dd,  $J = 14.4, 6.2$  Hz, 1H), 2.45 (dd,  $J = 9.5, 3.2$  Hz, 1H), 1.74-1.55 (m, 7H), 1.18-1.11 (m, 1H), 1.08 (s, 3H), 1.03 (s, 3H), 0.99 (s, 3H), 0.91 (m, 1H), 0.84 (s, 3H);  $^{13}\text{C}$  NMR (100 MHz,  $\text{CDCl}_3$ )  $\delta$  159.3, 155.8, 144.8, 133.4, 101.9, 96.8, 79.1, 64.4, 56.1, 55.4, 55.0, 46.0, 38.8, 38.5, 38.2, 36.6, 29.5, 27.9, 27.1, 20.3, 19.2, 16.2, 15.1. HRESIMS  $[\text{M}+\text{Na}]^+$  calcd for  $\text{C}_{23}\text{H}_{34}\text{O}_3\text{Na}$  381.2406, found 381.2415;  $[\alpha]_{\text{D}}^{24} = +18.86^\circ$  ( $c$  0.16).

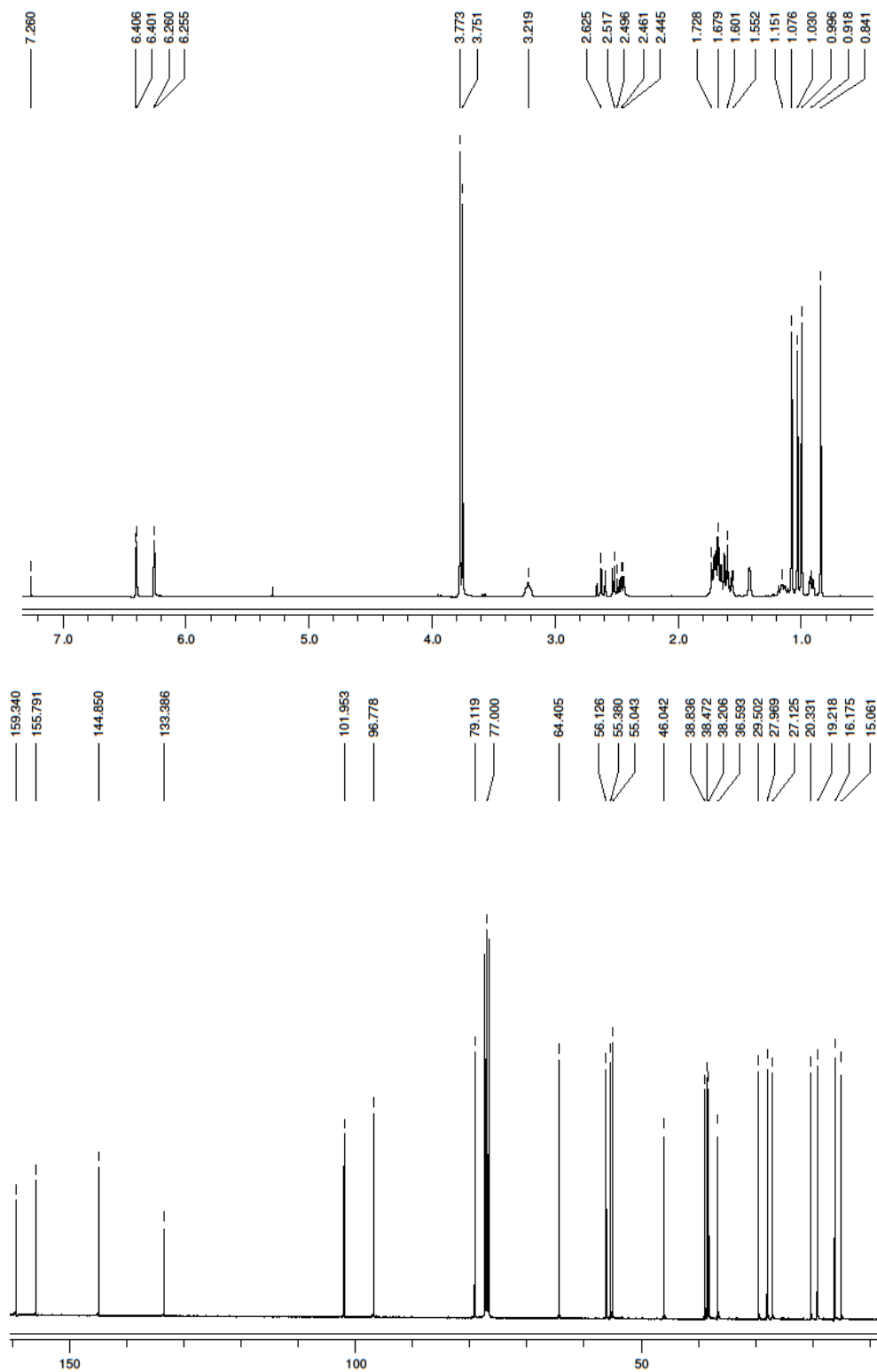
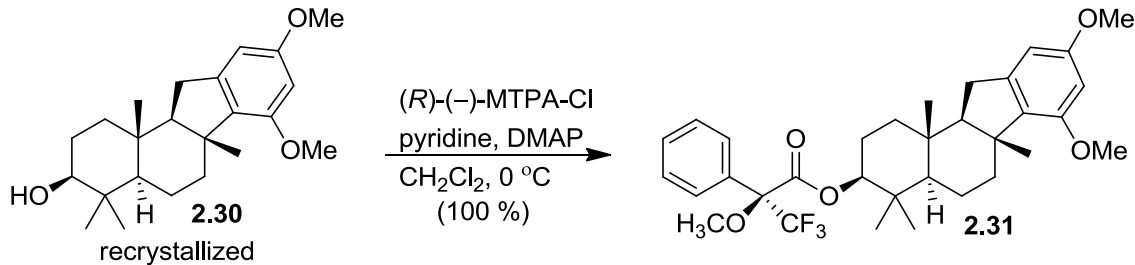


**Figure 2.30**  $^1\text{H}$  and  $^{13}\text{C}$  NMR spectra of **2.30** recorded in  $\text{CDCl}_3$  at 400 MHz and 100 MHz respectively.

### Preparation of **2.31**:



Alcohol **2.30** (219.4 mg, 0.61 mmol, after recrystallization), dissolved in 4 mL of methylene chloride and to this mixture was added pyridine (0.074 mL, 0.92 mmol), and DMAP (7.4 mg, 0.061 mmol) then cooled to  $0\text{ }^\circ\text{C}$ . To the reaction was added  $(R)$ -(-)-MTPA-Cl (169.5 mg, 0.671 mmol) and allowed to warm to room temperature overnight. The reaction was quenched with saturated  $\text{NH}_4\text{Cl}$  (aq) (25 mL) and the aqueous layer was extracted three times with methylene chloride (100 mL). The organic extracts were combined and dried with  $\text{MgSO}_4$  and concentrated using a rotary evaporator. A  $^1\text{H}$  spectrum of the crude mixture showed the absence of diastereomers, meaning that alcohol **2.30** was enantiopure (at least  $> 99.5\%$ ) after crystallization. The product mixture was then purified using flash column chromatography (hexanes:ethyl acetate 12:1), to give **2.31** quantitatively.  $^1\text{H}$  NMR (400 MHz,  $\text{CDCl}_3$ )  $\delta$  7.54 (m, 2H), 7.41 (m, 3H), 6.40 (d,  $J = 1.9$  Hz, 1H), 6.26 (d,  $J = 1.9$  Hz, 1H), 4.72 (dd,  $J = 11.5, 4.9$  Hz, 1H), 3.77 (s, 3H), 3.75 (s, 3H), 3.54 (s, 3H), 2.62 (m, 1H), 2.51 (dd,  $J = 14.5, 6.1$  Hz, 1H), 2.46 (dd,  $J = 8.4, 2.9$  Hz, 1H), 1.85-1.76 (m, 1H), 1.74-1.67 (m, 3H), 1.65-1.57 (m, 3H), 1.23 (td,  $J = 13.5, 4.2$  Hz, 1H), 1.07 (s, 3H), 1.04 (s, 3H), 1.04 (m, 1H), 0.92 (s, 3H), 0.87 (s, 3H);  $^{13}\text{C}$  NMR (100 MHz,  $\text{CDCl}_3$ )  $\delta$  166.3, 159.5, 155.8, 144.7, 133.2, 132.3, 129.5, 128.3, 128.3, 127.6, 127.6, 124.9, 122.0, 101.9, 96.9, 84.5, 64.2, 56.2, 55.4, 55.3, 55.1, 46.1, 38.1, 38.0, 37.9, 36.5, 29.5, 28.1, 23.0, 20.3, 19.0, 16.2,

16.1. HRESIMS  $[M+Na]^+$  calcd for  $C_{33}H_{41}O_5F_3Na$  597.2804, found 597.2814;  $[\alpha]_D^{24} = -31.76^\circ$  (*c* 0.65).

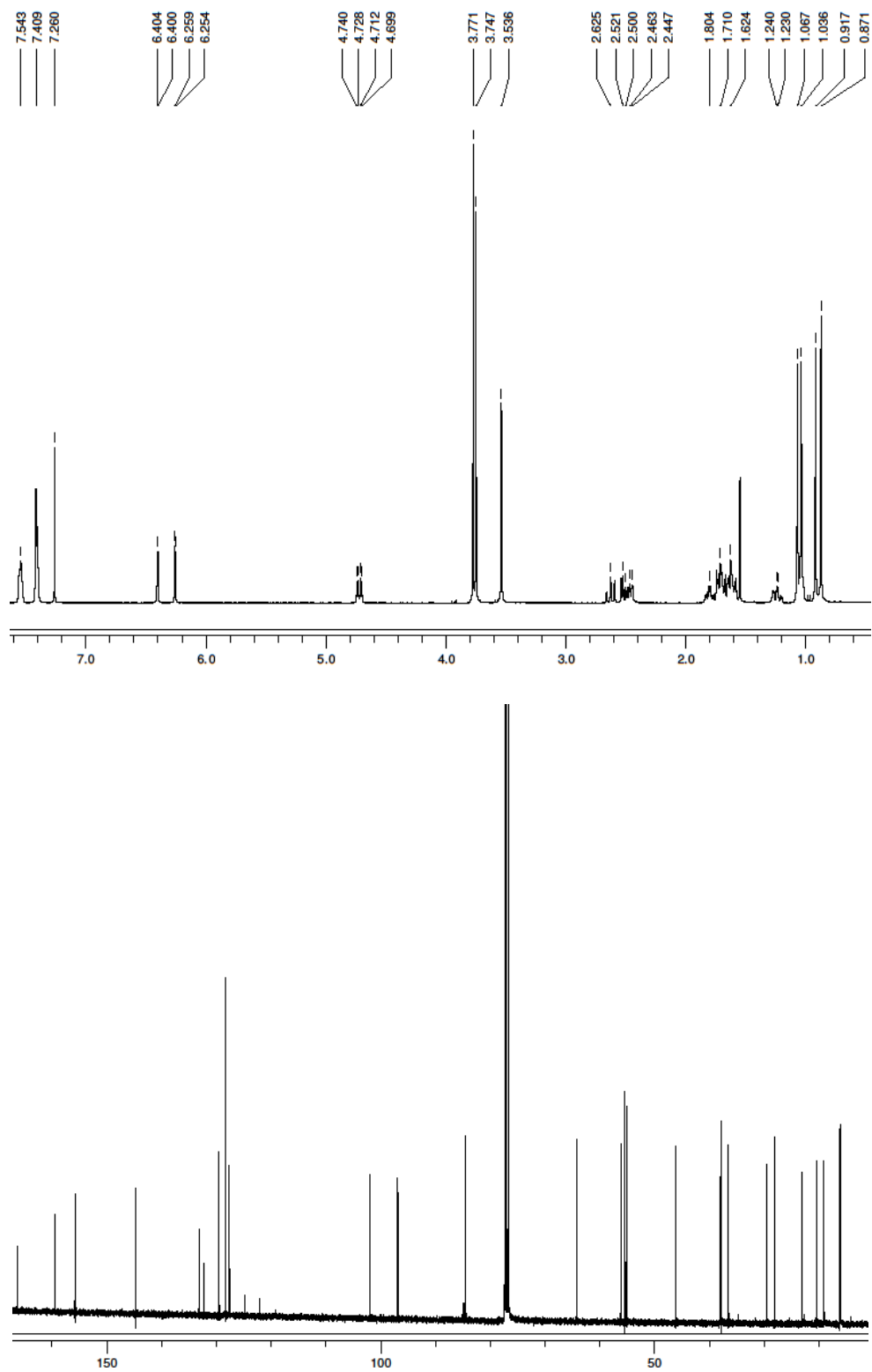
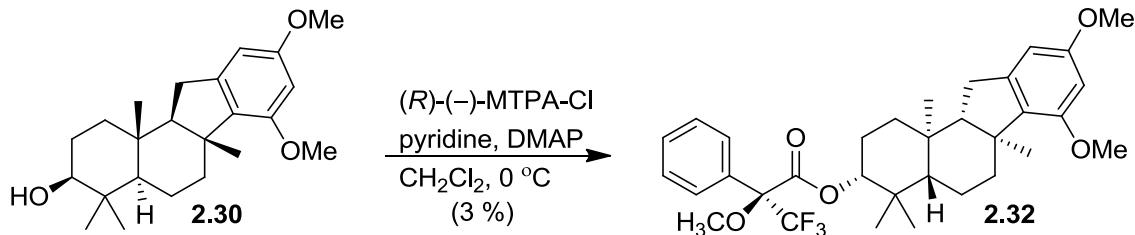


**Figure 2.31**  $^1\text{H}$  and  $^{13}\text{C}$  NMR spectra of **2.31** recorded in  $\text{CDCl}_3$  at 400 MHz and 100 MHz respectively.

### Preparation of 2.32



The preparation is identical to **2.31**, with the exception that alcohol **2.30** was used without crystallization. Integration of diastereomers in the  $^1\text{H}$  crude gave a diastereomeric ratio of 97:3 (**2.31**:**2.32**) meaning that the epoxidation proceeded in 94 % ee. Recrystallization from boiling solvents (hexanes:ethyl acetate 30:1) gave crystals from which a crystal structure was obtained.  $^1\text{H}$  NMR (400 MHz,  $\text{CDCl}_3$ )  $\delta$  7.57 (m, 2H), 7.41 (t, 3H), 6.41 (s, 1H), 6.26 (d,  $J = 1.5$  Hz, 1H), 4.75 (dd,  $J = 10.4, 5.9$  Hz, 1H), 3.77 (s, 3H), 3.75 (s, 3H), 3.58 (s, 3H), 2.64 (t,  $J = 13.8$  Hz, 1H), 2.52 (dd,  $J = 14.3, 6.1$  Hz, 1H), 2.46 (m, 1H), 1.91-1.79 (m, 2H), 1.75-1.70 (m, 2H), 1.66-1.62 (m, 4H), 1.25 (td,  $J = 12.5, 4.9$  Hz, 1H), 1.08 (s, 3H), 1.07 (s, 3H), 0.86 (s, 3H), 0.83 (s, 3H);  $^{13}\text{C}$  NMR (100 MHz,  $\text{CDCl}_3$ )  $\delta$  166.1, 159.5, 155.8, 144.7, 133.2, 132.7, 129.5, 128.3, 127.3, 124.9, 122.1, 101.9, 96.9, 84.3, 64.2, 56.2, 55.42, 55.39, 55.1, 46.1, 38.1, 38.0, 37.9, 36.5, 29.5, 27.7, 23.4, 20.3, 19.0, 16.2, 15.9. HRESIMS  $[\text{M}+\text{Na}]^+$  calcd for  $\text{C}_{33}\text{H}_{41}\text{O}_5\text{F}_3\text{Na}$  597.2804, found 597.2814;  $[\alpha]_{\text{D}}^{24} = -22.87^\circ$  ( $c$  1.20).

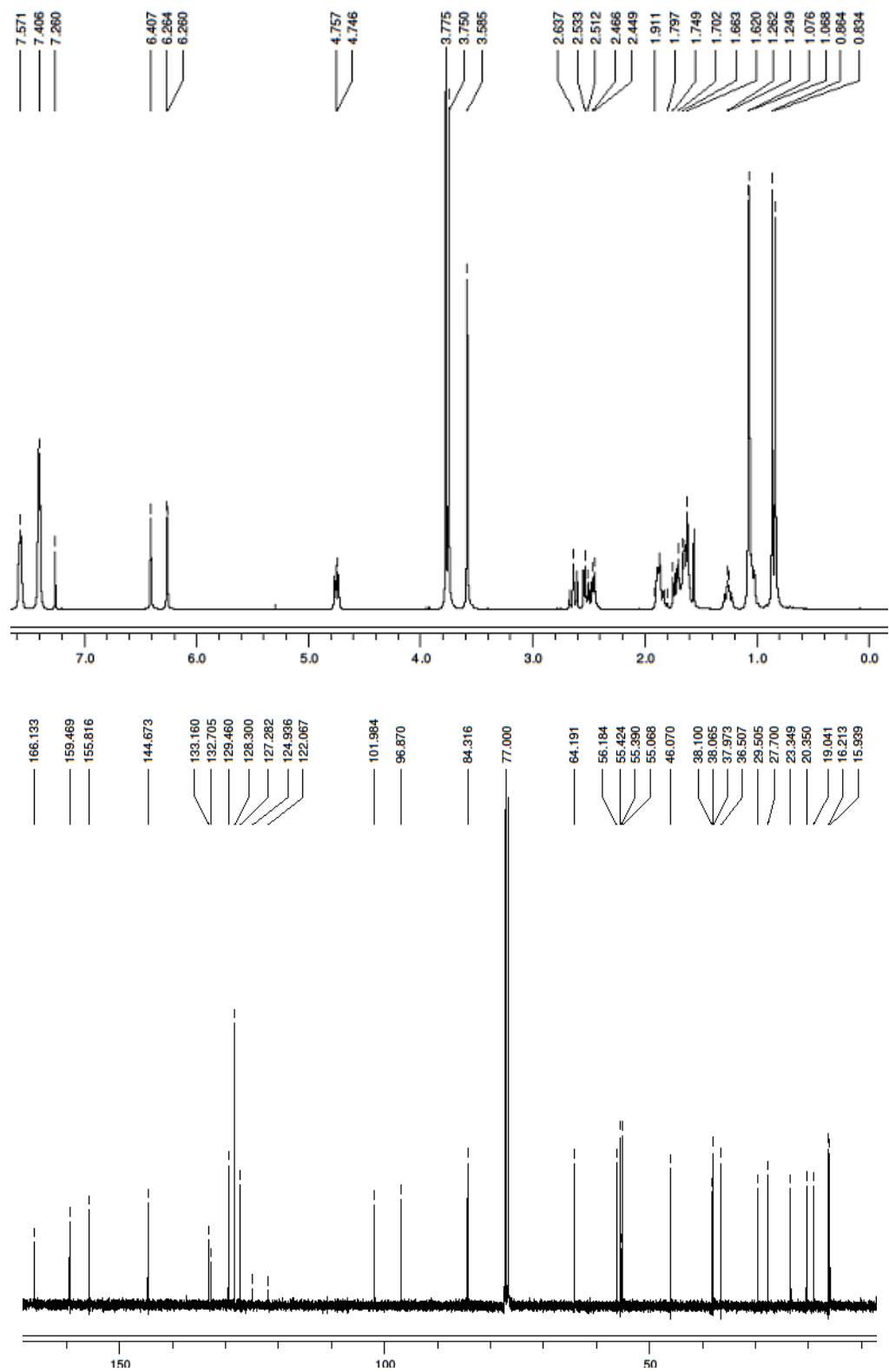
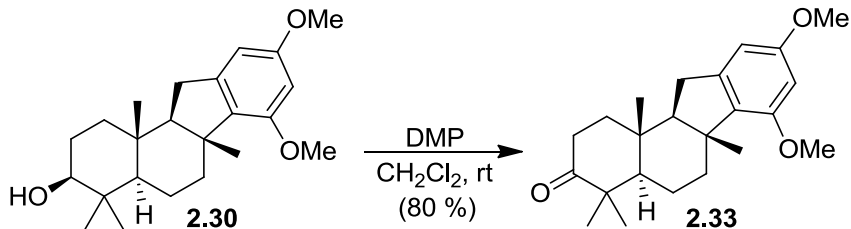


**Figure 2.32**  $^1\text{H}$  and  $^{13}\text{C}$  NMR spectra of **2.32** recorded in  $\text{CDCl}_3$  at 400 MHz and 100 MHz respectively.

### Preparation of 2.33:



To alcohol **2.30** (600.0 mg, 1.67 mmol) dissolved in 85 mL of methylene chloride was added Dess–Martin periodinane (1.41 g, 3.34 mmol), and the mixture was allowed to stir at room temperature for 1.5 hours. Upon completion, saturated NaHCO<sub>3</sub> (100 mL) was added and the aqueous phase was extracted three times with methylene chloride (250 mL). The organic extracts were combined, then dried with MgSO<sub>4</sub>, and concentrated using a rotary evaporator. The crude mixture was purified using flash column chromatography (hexanes:ethyl acetate 7:1), to give **2.33** (476 mg, 1.34 mmol, 80 %) as a white crystalline solid. <sup>1</sup>H NMR (400 MHz, CDCl<sub>3</sub>) δ 6.41 (s, 1H), 6.27 (s, 1H), 3.77 (s, 3H), 3.75 (s, 3H), 2.71-2.65 (m, 1H), 2.64-2.56 (m, 2H), 2.54-2.41 (m, 2H), 1.87-1.81 (m, 1H), 1.78-1.73 (m, 2H), 1.71-1.48 (m, 4H), 1.13 (s, 3H), 1.11 (s, 6H), 1.09 (s, 3H); <sup>13</sup>C NMR (100 MHz, CDCl<sub>3</sub>) δ 217.2, 159.5, 155.8, 144.4, 132.9, 101.9, 96.8, 63.4, 55.4, 55.3, 54.9, 47.5, 45.8, 38.8, 37.4, 36.2, 33.9, 29.5, 26.5, 20.7, 20.5, 19.8, 15.5. HRESIMS [M+Na]<sup>+</sup> calcd for C<sub>23</sub>H<sub>32</sub>O<sub>3</sub>Na 379.2249, found 379.2243; [α]<sub>D</sub><sup>24</sup> = +26.78° (c 0.083).

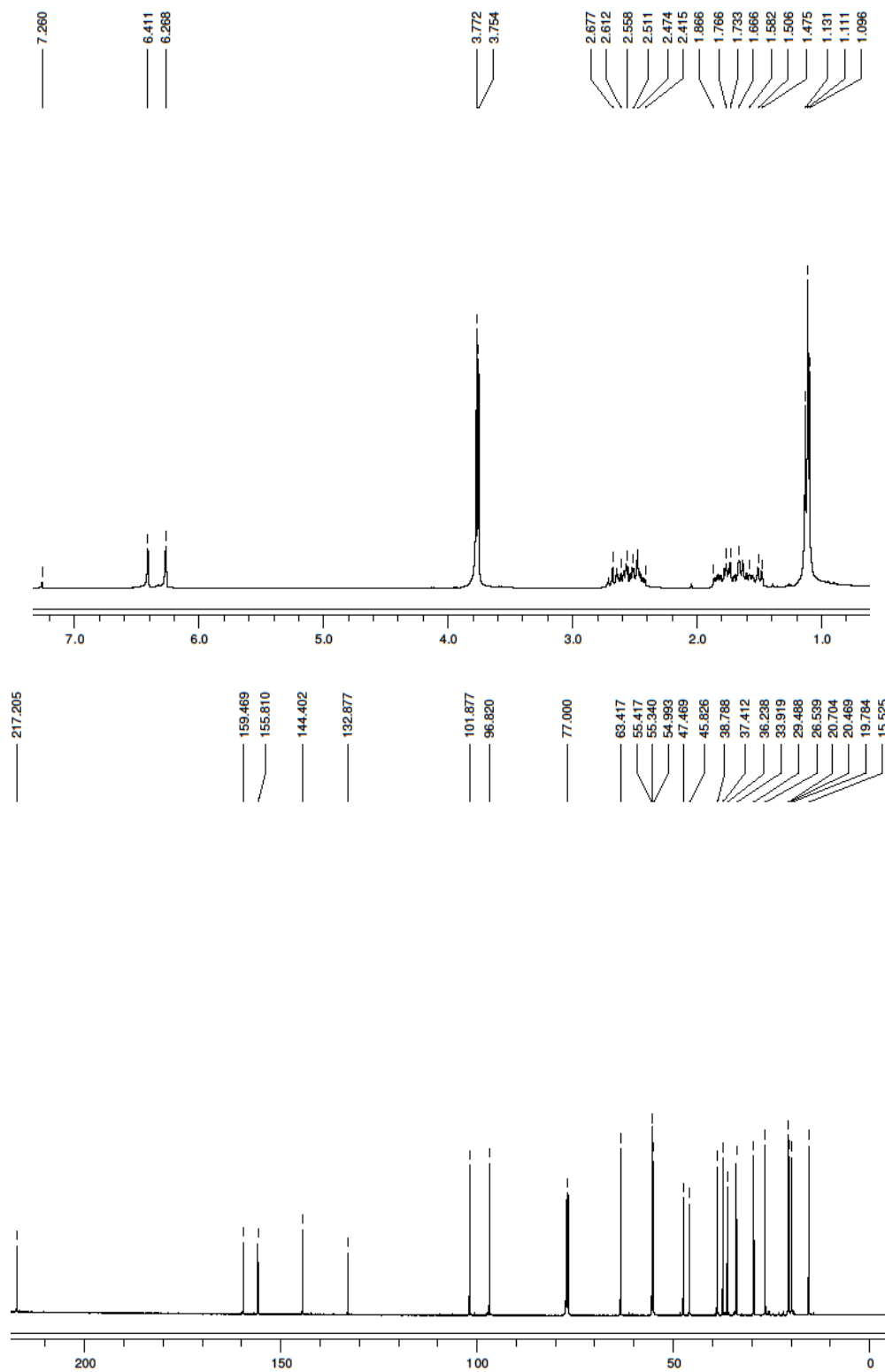
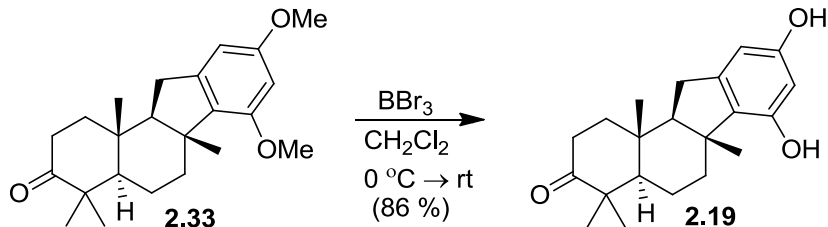


**Figure 2.33**  $^1\text{H}$  and  $^{13}\text{C}$  NMR spectra of **2.33** recorded in  $\text{CDCl}_3$  at 400 MHz and 100 MHz respectively.

### Preparation of 2.19:



To ketone **2.33** (240 mg, 0.67 mmol), dissolved in 20 mL of methylene chloride stirring at  $0\text{ }^\circ\text{C}$  was added 2.7 mL of  $\text{BBr}_3$  (1.0 M in methylene chloride, 2.69 mmol). After stirring for one hour at  $0\text{ }^\circ\text{C}$ , **2.33** was still present, and the reaction was allowed to reach room temperature over the next two hours. The reaction was quenched with 1 mL of methanol and 50 mL of water was added to the mixture. The aqueous phase was extracted three times with methylene chloride (150 mL). The combined organic extracts were dried with  $\text{MgSO}_4$  and concentrated using a rotary evaporator. The crude mixture was purified using flash column chromatography to give **2.19** (190 mg, 0.58 mmol, 86 %) as a white crystalline solid.  $^1\text{H}$  NMR (400 MHz,  $(\text{CD}_3)_2\text{CO}$ )  $\delta$  7.76 (s, 1H), 7.73 (s, 1H), 6.24 (t,  $J = 1.0$  Hz, 1H), 6.13 (d,  $J = 1.6$  Hz), 2.66-2.61 (m, 1H), 2.59-2.52 (m, 2H), 2.49-2.46 (m, 1H), 2.44-2.37 (m, 1H), 1.86-1.82 (m, 1H), 1.81-1.77 (m, 1H), 1.76-1.71 (m, 1H), 1.67-1.55 (m, 4H), 1.15 (s, 3H), 1.13 (s, 3H), 1.07 (s, 3H), 1.09 (s, 3H);  $^{13}\text{C}$  NMR (100 MHz,  $(\text{CD}_3)_2\text{CO}$ )  $\delta$  216.9, 158.5, 154.8, 146.7, 131.9, 105.8, 102.8, 65.4, 57.2, 48.9, 47.3, 40.5, 39.6, 38.0, 35.4, 30.9, 27.9, 22.2, 22.1, 21.3, 16.9. HRESIMS  $[\text{M}+\text{Na}]^+$  calcd for  $\text{C}_{21}\text{H}_{28}\text{O}_3\text{Na}$  351.1936, found 351.1929;  $[\alpha]_{\text{D}}^{24} = +24.07^\circ$  ( $c$  0.81).

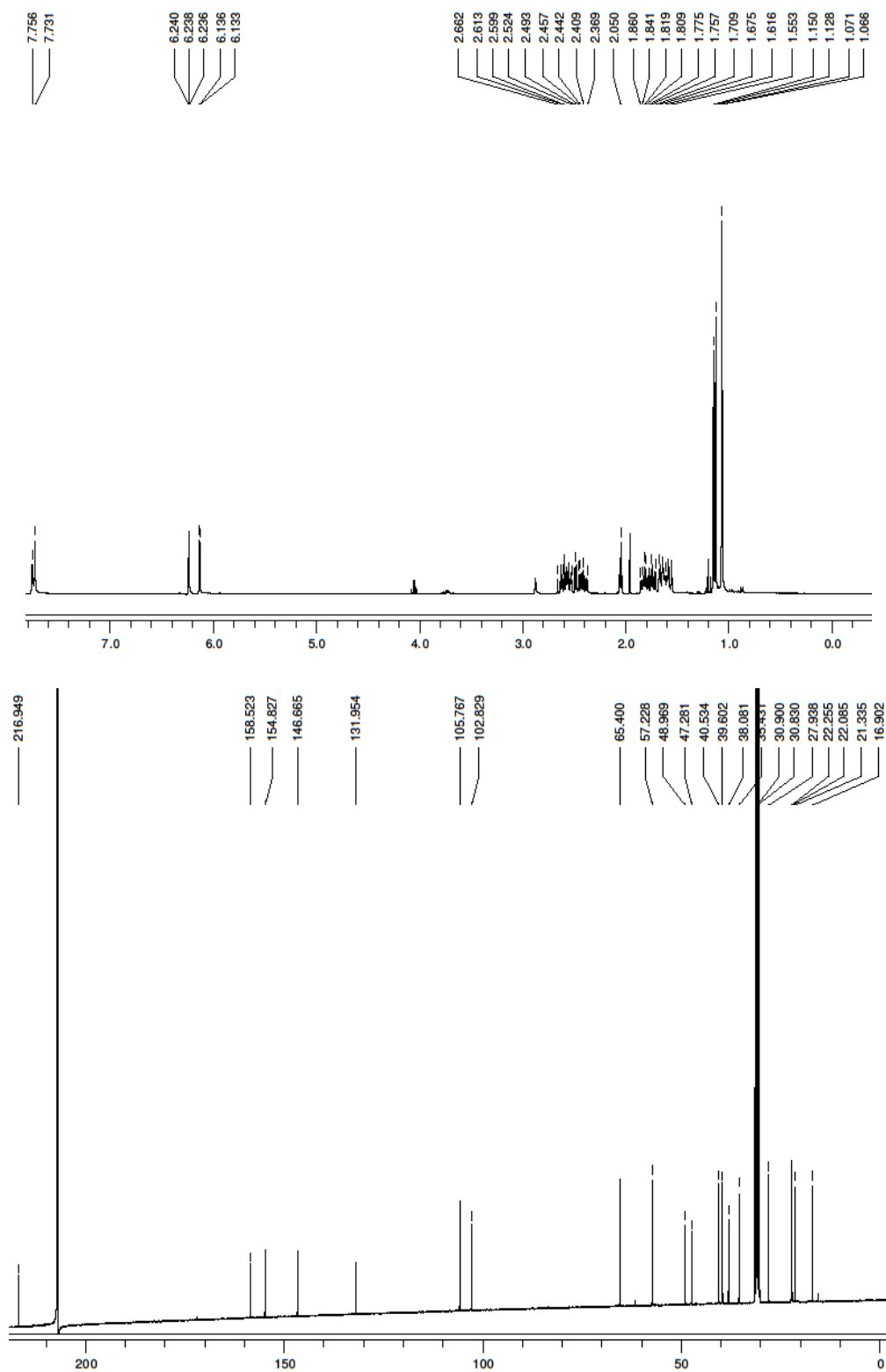
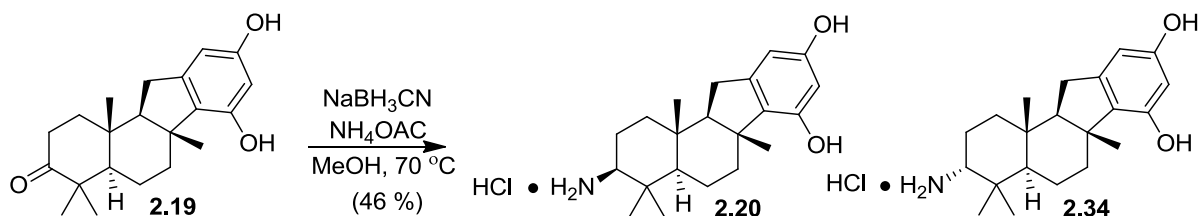


**Figure 2.34**  $^1\text{H}$  and  $^{13}\text{C}$  NMR spectra of **2.19** recorded in  $(\text{CD}_3)_2\text{CO}$  at 400 MHz and 100 MHz respectively.

### Preparation of **2.20** and **2.34**



To a suspension of ketone **2.19** (250 mg, 0.76 mmol) in 50 mL of methanol was added  $\text{NaBH}_3\text{CN}$  (71.7 mg, 1.14 mmol) and  $\text{NH}_4\text{OAc}$  (586.5 mg, 7.61 mmol). The reaction was heated to  $70\text{ }^\circ\text{C}$  overnight. Upon the disappearance of starting material, the reaction was cooled to rt, then concentrated using a rotary evaporator. The crude material was partitioned between water (200 mL) and methylene chloride (100 mL) and acidified to pH 5 with 6 M HCl. The aqueous phase was then extracted five times with methylene chloride (400 mL). The resultant aqueous phase was frozen and lyophilized overnight, which gave a white amorphous solid. To this solid was added 10 mL of water and sonicated to give a heterogeneous mixture, which was loaded on to a 10 g reversed phase sep-pak (which was washed with 100 mL of methanol followed by 100 mL of water). Once loaded the column was flushed with water (100 mL), 60:40 water:methanol (100 mL, 3x), and methanol. The fractions of interest were the first 60:40 water:methanol fraction containing 78.2 mg of **2.20** pure, and the second and third fraction contained 50.7 mg of a 2:1 mixture of **2.20** and **2.34** as the HCl salt and the freebase, which was acidified and subsequently purified using the same method. When fully purified the result was **2.20** (112 mg, 0.31 mmol, 40 %), and **2.34** (16.9 mg, 0.046 mmol, 6 %), with a diastereomeric ratio between the two epimers of 20:3.

Compound **2.20**:  $^1\text{H}$  NMR (600 MHz,  $\text{CD}_3\text{OD}$ )  $\delta$  6.16 (s, 1H), 6.02, (d,  $J = 1.5$  Hz, 1H), 2.93 (dd,  $J = 12.5, 4.3$  Hz, 1H), 2.57 (t,  $J = 13.6$  Hz, 1H), 2.51 (dt,  $J = 12.5, 3.0$  Hz, 1H), 2.42 (dd,  $J = 14.2, 6.0$  Hz, 1H), 1.85 (qd,  $J = 13.1, 3.4$  Hz, 1H), 1.79-1.73 (m, 2H), 1.71-1.67 (m, 3H), 1.63 (td,  $J = 12.2, 3.4$  Hz, 1H), 1.27 (td,  $J = 13.3, 3.3$  Hz, 1H), 1.11 (dd,  $J = 11.3, 2.3$  Hz, 1H), 1.085 (s, 3H), 1.081 (s, 3H), 1.076 (s, 3H), 0.94 (s, 3H);  $^{13}\text{C}$  NMR (150 MHz,  $\text{CD}_3\text{OD}$ )  $\delta$  157.5, 154.2, 145.9, 131.7, 104.7, 101.9, 65.6, 61.7, 57.6, 46.8, 39.6, 39.2, 37.8, 37.7, 30.1, 28.2, 24.3, 20.8, 20.2, 16.4, 15.9. HRESIMS  $[\text{M}+\text{H}]^+$  calcd for  $\text{C}_{21}\text{H}_{32}\text{NO}_2$  330.2433, found 330.2440;  $[\alpha]_{\text{D}}^{24} = -8.27^\circ$  ( $c$  3.68).

Compound **2.34**:  $^1\text{H}$  NMR (600 MHz,  $\text{CD}_3\text{OD}$ )  $\delta$  6.16 (s, 1H), 6.02 (d,  $J = 1.2$  Hz, 1H), 3.09 (m, 1H), 2.58 (t,  $J = 13.7$  Hz, 1H), 2.51 (m, 1H), 2.44 (dd,  $J = 14.2, 6.0$  Hz, 1H), 2.29 (tt,  $J = 14.8, 3.3$  Hz, 1H), 1.83 (dd,  $J = 12.9, 6.1$  Hz, 1H), 1.71-1.69 (m, 1H), 1.68-1.66 (m, 1H), 1.64-1.59 (m, 1H), 1.49 (dt,  $J = 11.4, 2.1$  Hz, 1H) 1.39 (d,  $J = 8.5$  Hz, 1H), 1.34-1.27 (m, 2H), 1.11 (s, 3H), 1.09 (s, 3H), 1.07 (s, 3H), 1.01 (s, 3H);  $^{13}\text{C}$  NMR (150 MHz,  $\text{CD}_3\text{OD}$ )  $\delta$  157.5, 154.2, 146.0, 131.8, 104.7, 101.9, 65.1, 59.5, 51.4, 47.1, 39.6, 37.9, 36.6, 34.1, 30.1, 28.4, 22.9, 22.7, 20.9, 20.2, 16.5. HRESIMS  $[\text{M}+\text{H}]^+$  calcd for  $\text{C}_{21}\text{H}_{32}\text{NO}_2$  330.2433, found 330.2441;  $[\alpha]_{\text{D}}^{24} = +6.98^\circ$  ( $c$  1.80).

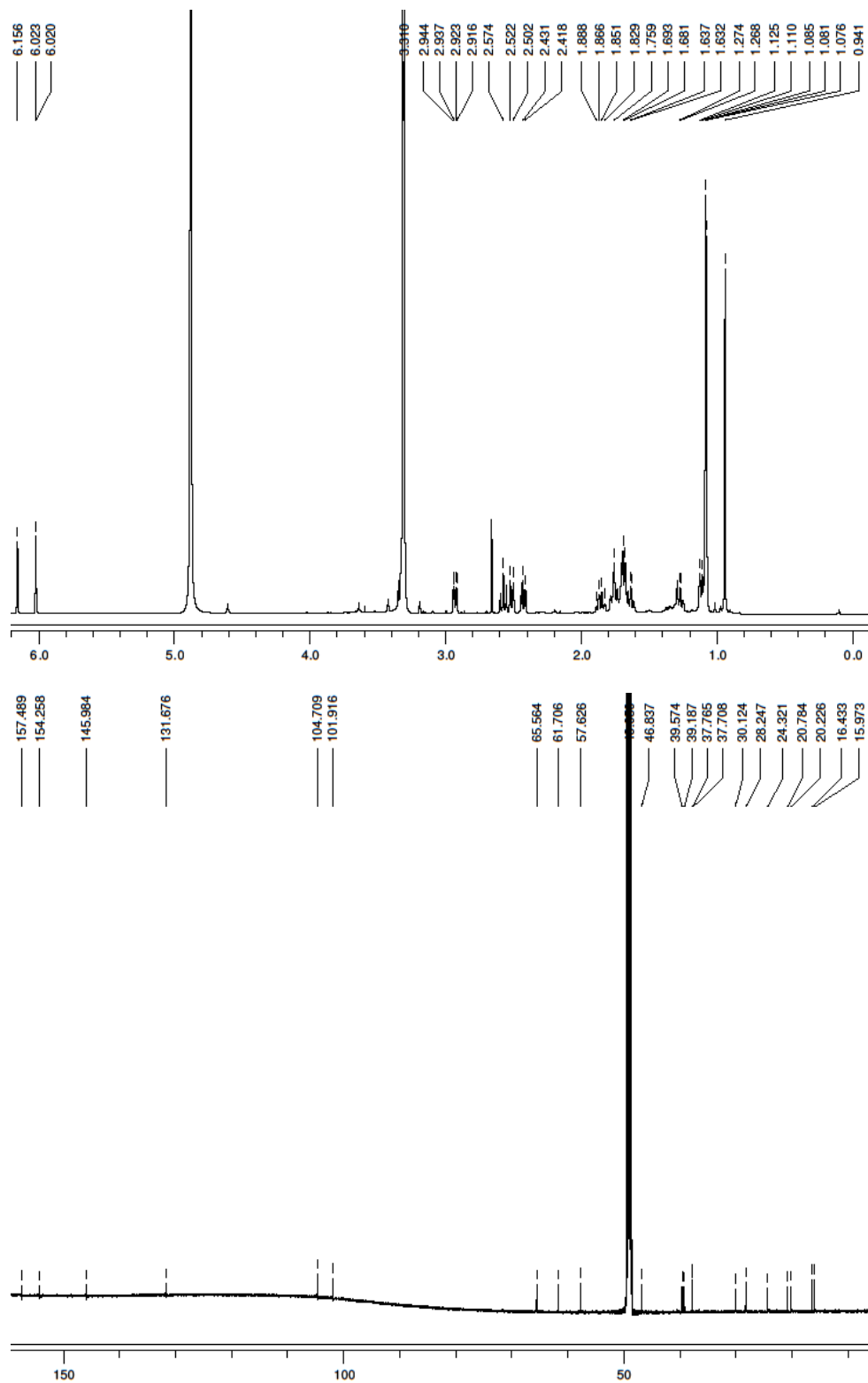


**Figure 2.35**  $^1\text{H}$  and  $^{13}\text{C}$  NMR spectra of **2.20** recorded in  $\text{CD}_3\text{OD}$  at 600 MHz and 150 MHz respectively.

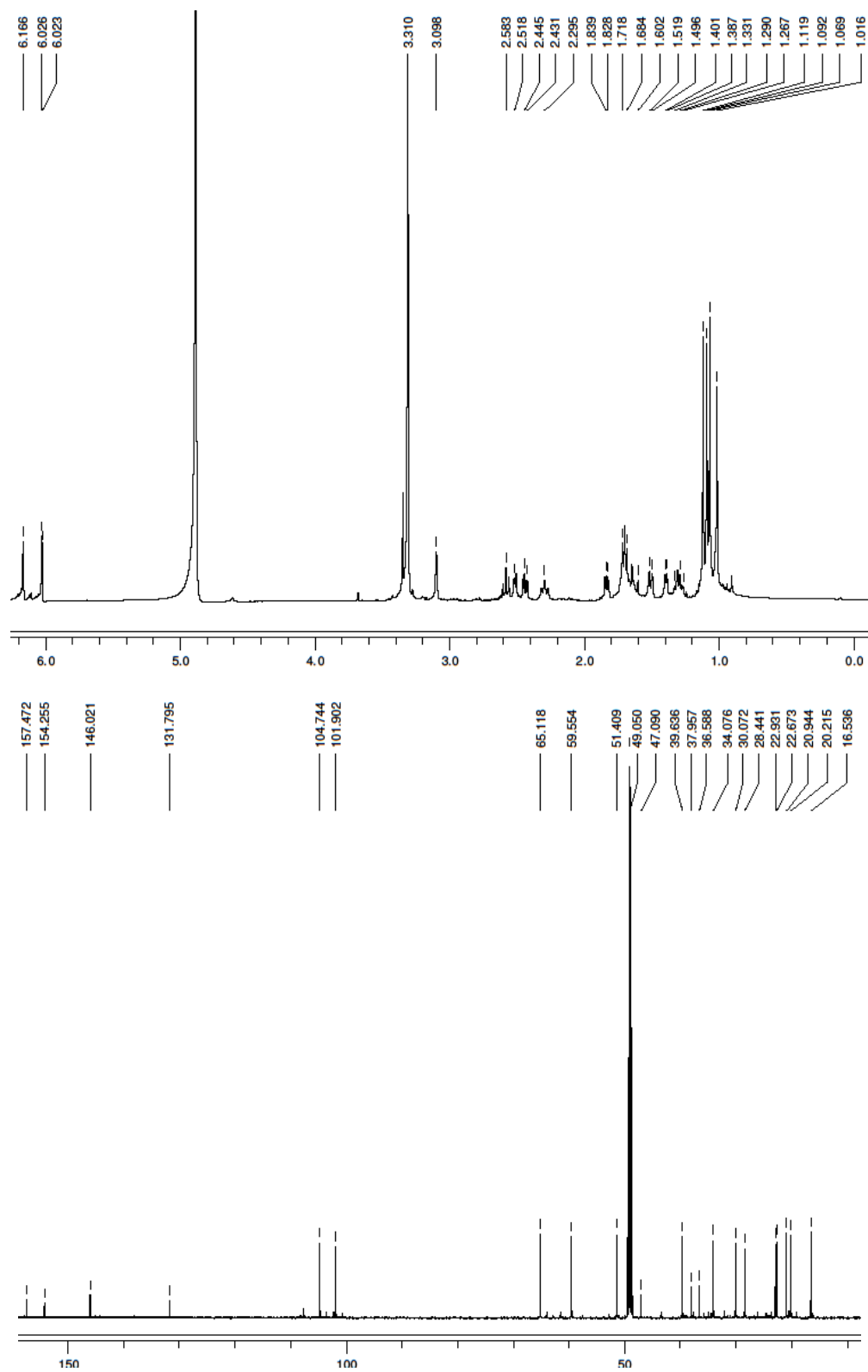
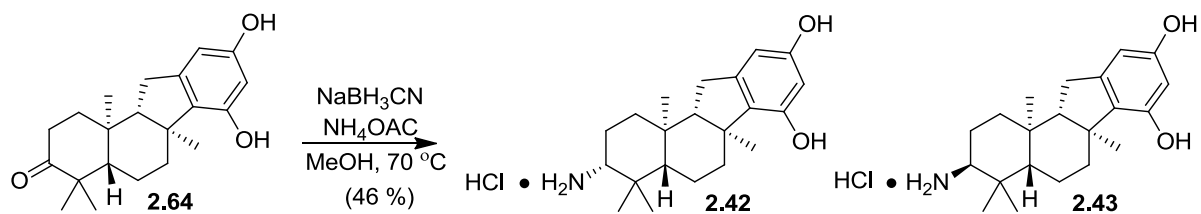


**Figure 2.36**  $^1\text{H}$  and  $^{13}\text{C}$  NMR spectra of **2.34** recorded in  $\text{CD}_3\text{OD}$  at 600 MHz and 150 MHz respectively.

**Preparation of 2.42 and 2.43:**

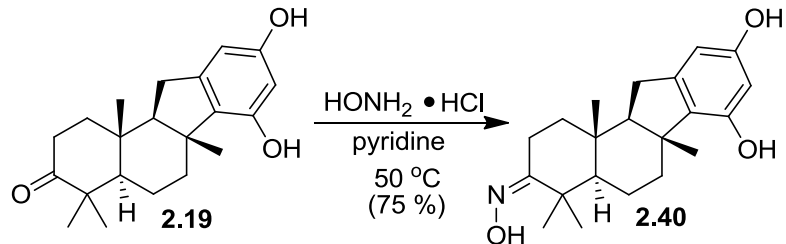


Identical to **2.20** and **2.34**.

For **2.42** HRESIMS  $[\text{M}+\text{H}]^+$  calcd for  $\text{C}_{21}\text{H}_{32}\text{NO}_2$  330.2433, found 330.2440;  $[\alpha]_{\text{D}}^{24} = +8.3^\circ$  (*c* 3.21).

For **2.43** HRESIMS  $[\text{M}+\text{H}]^+$  calcd for  $\text{C}_{21}\text{H}_{32}\text{NO}_2$  330.2433, found 330.2440;  $[\alpha]_{\text{D}}^{24} = -5.7^\circ$  (*c* 1.47).

### Preparation of 2.40:



To **2.19** (20 mg, 0.060 mmol) dissolved in 1 mL of pyridine was added hydroxylamine hydrochloride (33.8 mg, 0.49 mmol), and heated at  $50\text{ }^\circ\text{C}$ . After three and a half hours the reaction mixture was cooled to room temperature, saturated  $\text{NH}_4\text{Cl}_{(\text{aq})}$  solution was added (20 mL), and the aqueous phase was extracted three times with methylene chloride (100 mL). The organic extracts were combined and dried with  $\text{MgSO}_4$ , and concentrated using a rotary evaporator. The crude was purified using flash column chromatography (hexanes:ethyl acetate 1:1) to give **2.40** as a white solid (15.5 mg, 0.045 mmol, 75 %).  $^1\text{H}$  NMR (400 MHz,  $(\text{CD}_3)_2\text{CO}$ )  $\delta$  6.22 (s, 1H), 6.12 (s, 1H), 3.06 (ddd,  $J = 15.9, 3.2, 2.7$  Hz, 1H), 2.59 (t,  $J = 14.1$  Hz, 1H), 2.53 (dt,  $J = 12.1, 3.1$  Hz, 1H), 2.44 (dd,  $J = 14.4, 6.1$  Hz, 1H), 2.29 (ddd,  $J = 18.5, 6.4, 5.8$  Hz, 1H), 1.75-1.72 (m, 1H), 1.71-1.69 (m, 2H), 1.68-1.66 (m, 1H), 1.65-1.61 (m, 1H), 1.29-1.23 (m, 2H), 1.15 (s, 3H), 1.14 (s, 3H), 1.11 (s, 3H), 1.08 (s, 3H);  $^{13}\text{C}$  NMR (100 MHz,  $(\text{CD}_3)_2\text{CO}$ )  $\delta$  171.9, 165.8, 158.5, 154.8, 146.8, 132.1, 105.8, 102.8, 65.9, 61.5, 58.3, 47.4, 41.7, 40.0, 38.4, 29.2, 24.3, 21.7, 18.1, 16.8, 15.5. HRESIMS  $[\text{M}+\text{H}]^+$  calcd for  $\text{C}_{21}\text{H}_{30}\text{O}_3\text{N}$  344.2226, found 344.2230;  $[\alpha]_{\text{D}}^{24} = -14.94^\circ$  ( $c$  0.02).

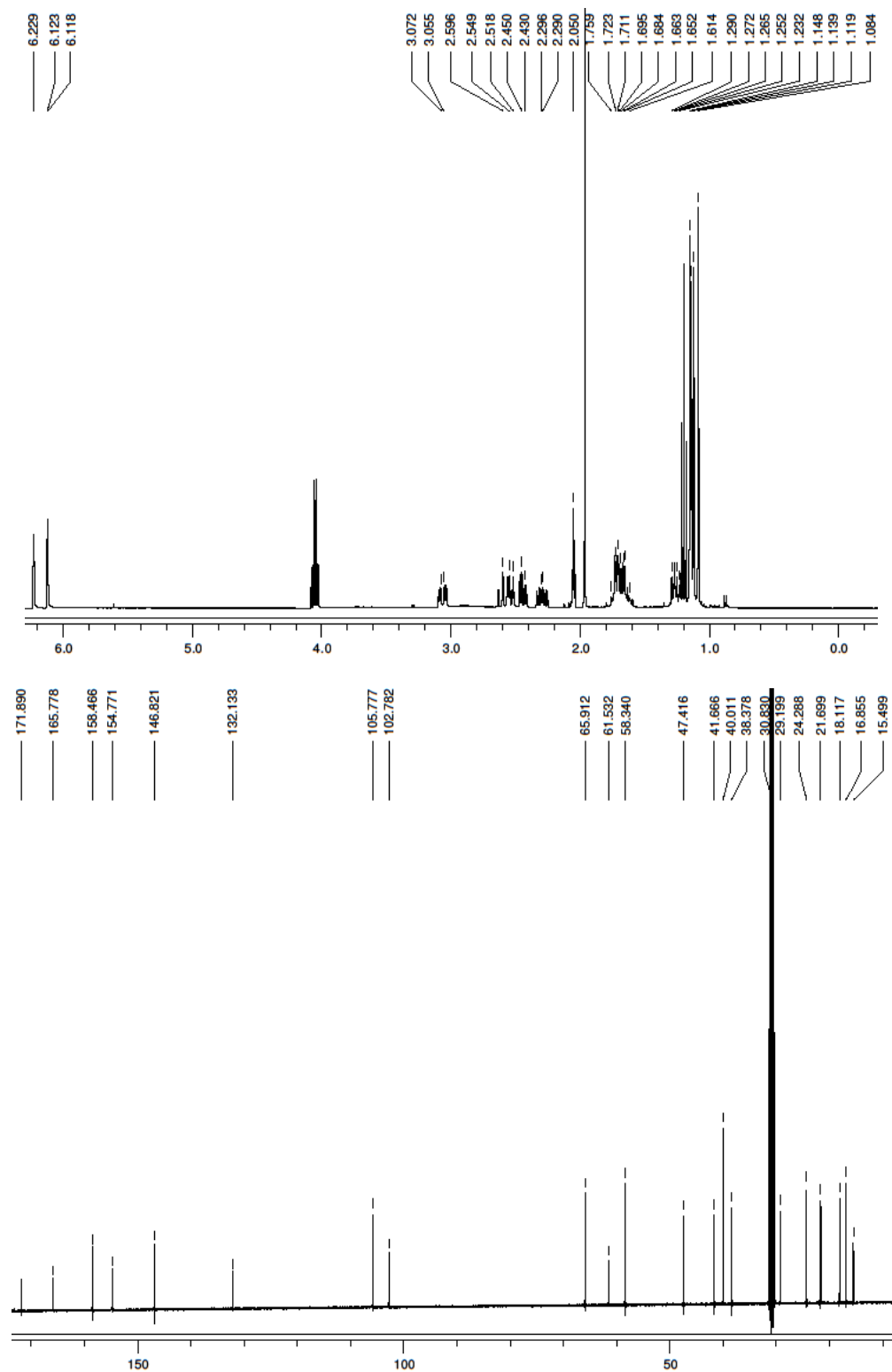
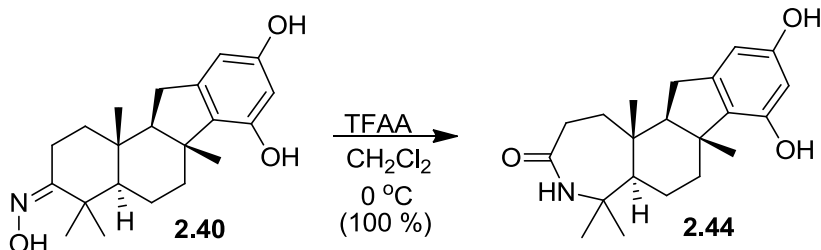


**Figure 2.37**  $^1\text{H}$  and  $^{13}\text{C}$  NMR spectra of **2.40** recorded in  $(\text{CD}_3)_2\text{CO}$  at 400 MHz and 100 MHz respectively.

### Preparation of **2.44**:



To **2.40** (10.3 mg, 0.029 mmol) dissolved in 1 mL of methylene chloride at 0 °C was added trifluoroacetic anhydride (0.11 mL, 0.79 mmol) and allowed to stir for 1 hour. The reaction was quenched with 0.1 mL of water and the reaction mixture was concentrated under a stream of nitrogen. The crude was purified using flash column chromatography (methylene chloride:methanol 12:1) to give **2.44** (10.0 mg, 0.029 mmol, 100 %) as a white solid. <sup>1</sup>H NMR (400 MHz, CD<sub>3</sub>OD) δ 6.17 (d, J = 1.7 Hz, 1H), 6.02 (d, J = 1.9 Hz, 1H), 3.45 (s, 1H), 2.65-2.56 (m, 2H), 2.51-2.43 (m, 3H), 1.83-1.70 (m, 4H), 1.69-1.61 (m, 2H), 1.59-1.52 (m, 1H), 1.33 (s, 3H), 1.32 (s, 3H), 1.22 (s, 3H), 1.11 (s, 3H); <sup>13</sup>C NMR (100 MHz, CD<sub>3</sub>OD) δ 179.3, 157.5, 154.3, 145.8, 131.6, 104.6, 101.9, 65.5, 57.8, 56.9, 46.6, 41.2, 39.3, 39.0, 33.7, 32.6, 30.6, 26.4, 24.3, 20.3, 17.5. HRESIMS [M+Na]<sup>+</sup> calcd for C<sub>21</sub>H<sub>29</sub>NO<sub>3</sub>Na 366.2045, found 366.2035; [α]<sub>D</sub><sup>24</sup> = +122.1° (c 0.07).

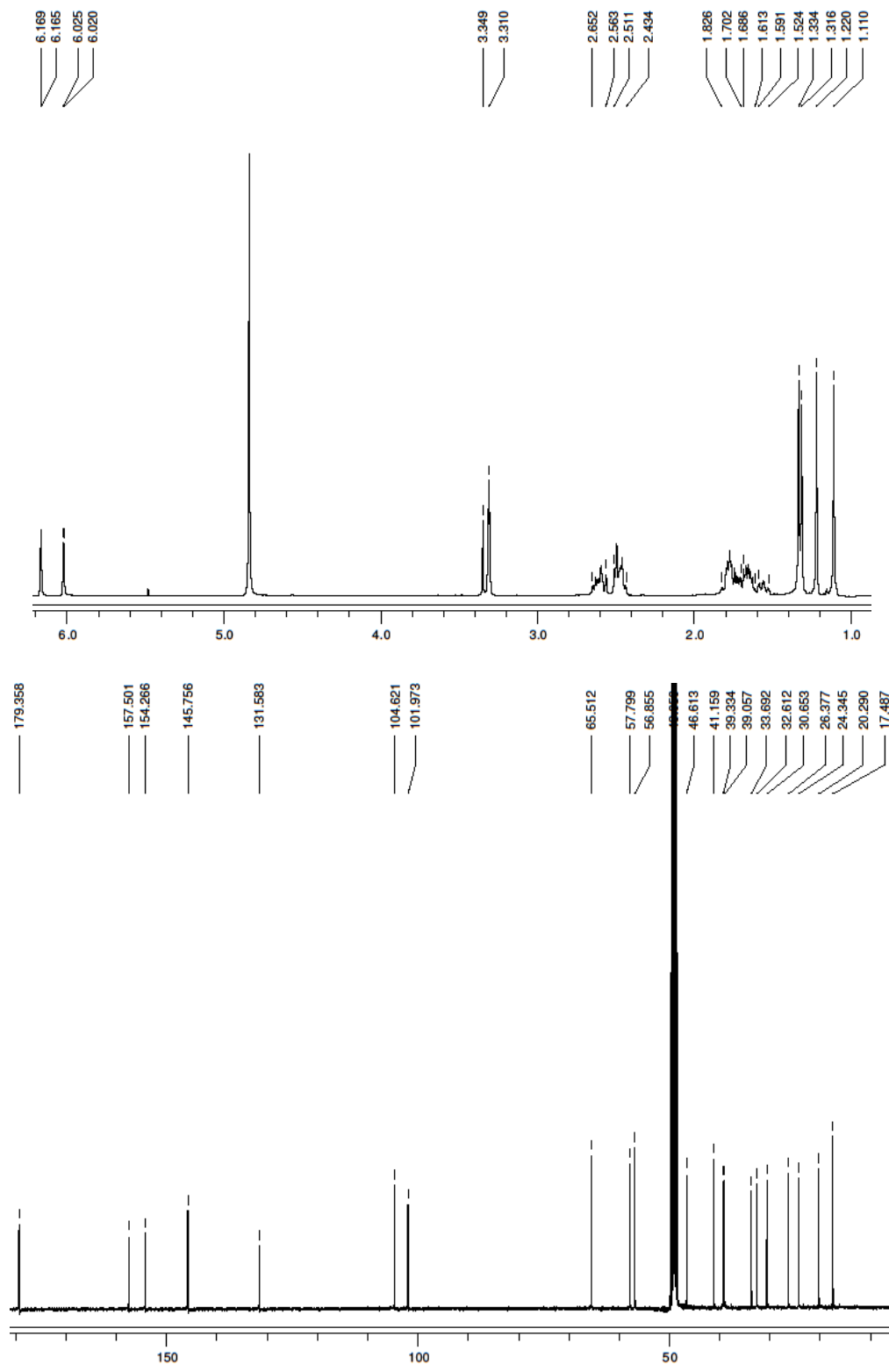
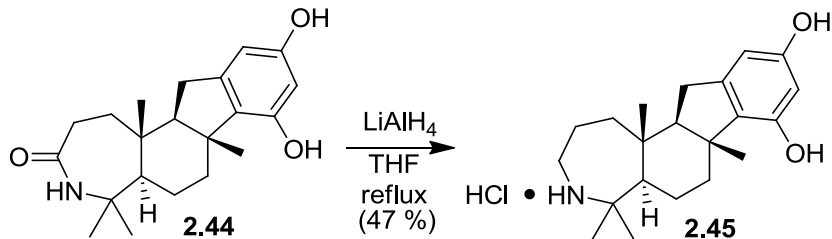


**Figure 2.38**  $^1\text{H}$  and  $^{13}\text{C}$  NMR spectra of **2.44** recorded in  $\text{CD}_3\text{OD}$  at 400 MHz and 100 MHz respectively.

### Preparation of 2.45:



To **2.44** (8.0 mg, 0.023 mmol) dissolved in 4 mL of tetrahydrofuran was added LiAlH<sub>4</sub> (0.072 mL, 2.0 M in tetrahydrofuran, 0.14 mmol) and heated to reflux overnight. Upon completion, the reaction was quenched with 0.1 mL methanol, and 0.1 mL of 6 M HCl added. The mixture was concentrated using a rotary evaporator, then lyophilized and purified using a 2 g reversed phase sep-pak (which was washed with 10 mL of methanol followed by 10 mL of water). Once loaded the column was flushed with water (20 mL), 60:40 water:methanol (50 mL), and methanol (50 mL). The water:methanol fraction after concentration and lyophilization contained **2.45** (4 mg, 0.011 mmol, 47 %) as a white solid. <sup>1</sup>H NMR (600 MHz, CD<sub>3</sub>OD)  $\delta$  6.16 (s, 1H), 6.03 (d, J = 1.5 Hz, 1H), 3.23-3.15 (m, 2H), 2.62 (t, J = 13.9 Hz, 1H), 2.57 (dd, J = 8.2 Hz, 1H), 2.52 (dt, J = 12.9, 2.9 Hz, 1H), 2.00-1.96 (m, 1H), 1.94-1.87 (m, 3H), 1.75-1.72 (m, 2H), 1.70-1.66 (m, 1H), 1.64-1.58 (m, 1H), 1.48 (s, 3H), 1.42 (s, 3H), 1.39 (m, 1H), 1.22 (s, 3H), 1.13 (s, 3H); <sup>13</sup>C NMR (150 MHz, CD<sub>3</sub>OD)  $\delta$  157.7, 154.3, 145.2, 131.2, 104.4, 101.9, 64.6, 63.6, 54.7, 46.2, 43.9, 42.6, 42.2, 38.3, 31.2, 27.9, 24.9, 24.3, 24.0, 19.5, 14.9. HREIMS [M]<sup>+</sup> calcd for C<sub>21</sub>H<sub>31</sub>NO<sub>2</sub> 329.23548, found 329.23569; [ $\alpha$ ]<sub>D</sub><sup>24</sup> = +20.50° (c 0.02).

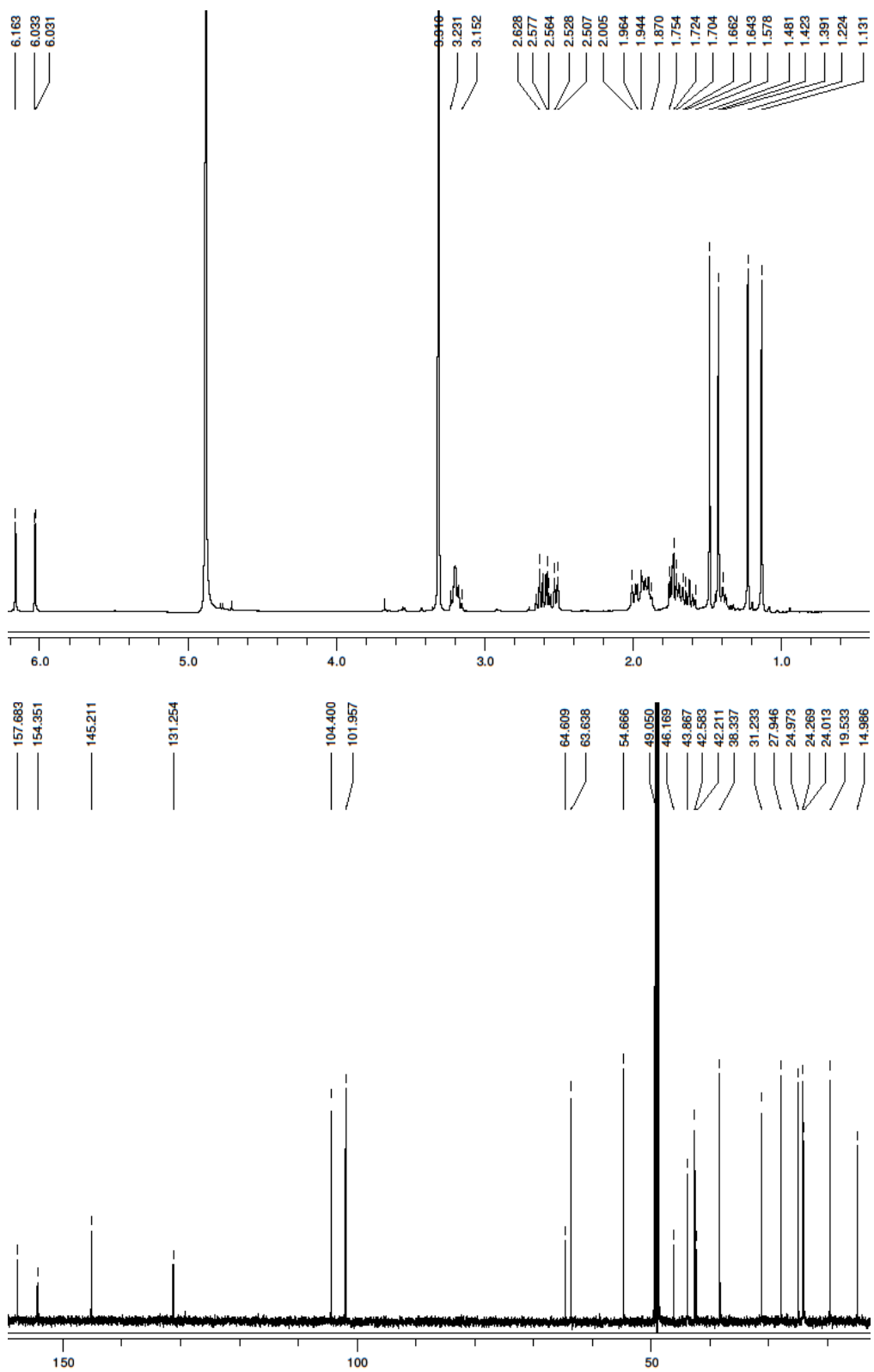
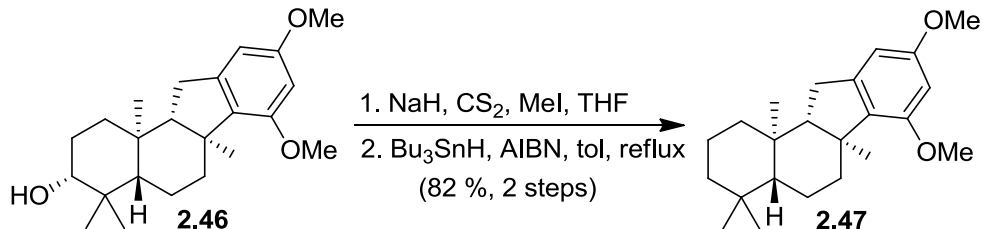


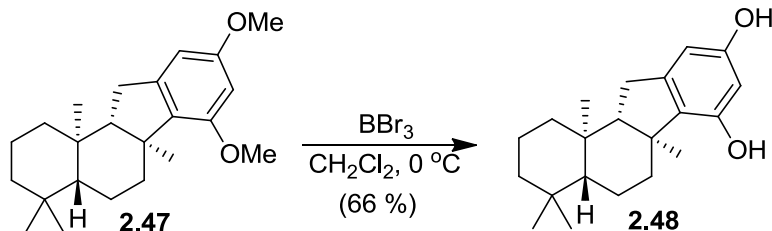
Figure 2.39  $^1\text{H}$  and  $^{13}\text{C}$  NMR spectra of **2.45** recorded in  $\text{CD}_3\text{OD}$  at 600 MHz and 150 MHz respectively.

### Preparation of **2.47**:



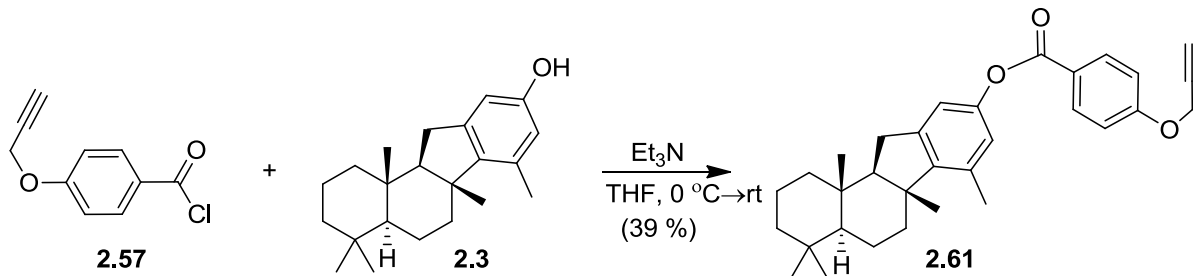
To sodium hydride (8.0 mg, 60 % in mineral oil, 0.20 mmol) washed two times with hexanes was added 0.5 mL of tetrahydrofuran. To this heterogeneous mixture was added **2.46** (24.3 mg, 0.067 mmol) dissolved in 2.0 mL of tetrahydrofuran and allowed to stir for 10 minutes. To this mixture was added carbon disulfide (0.024 mL, 0.402 mmol), and allowed to stir for thirty minutes. Then methyl iodide (0.037 mL, 0.60 mmol) was added neat and the mixture allowed to stir overnight at room temperature. The mixture was quenched with 0.1 mL of methanol, concentrated under a stream of nitrogen and filter through a plug of silica with 20 mL of hexanes:ethyl acetate (3:1), and concentrated using a rotary evaporator. The crude mixture was used in the following step without further purification. The mixture was dissolved in 3 mL of toluene to which was added tributyltin hydride (87.5 mg, 0.30 mmol) and AIBN (0.06 mL, 0.012 mmol), and the reaction mixture heated to 120 °C for thirty minutes. The reaction was then allowed to cool down to room temperature, and concentrated under a stream of nitrogen. The crude mixture was purified using flash column chromatography (hexanes:ethyl acetate 15:1), to give **2.47** (18.8 mg, 0.054 mmol, 82 % over two steps). The <sup>1</sup>H and <sup>13</sup>C NMR spectra were identical to previously reported data (Matt Nodwell). HRESIMS [M+H]<sup>+</sup> calcd for C<sub>23</sub>H<sub>35</sub>O<sub>2</sub> 343.2637, found 343.2640; [α]<sub>D</sub><sup>24</sup> = -4.25° (c 0.07).

### Preparation of **2.48**:



To **2.47** (20 mg, 0.058 mmol) dissolved in 20 mL methylene chloride was added boron tribromide (0.17 mL, 0.175 mmol, 1.0 M solution in methylene chloride). After stirring for ninety minutes the reaction was quenched with the addition of 0.1 mL of methanol, and concentrated under a stream of nitrogen. The crude mixture was then purified using flash column chromatography to give **2.48** (12.1 mg, 0.038 mmol, 66 %). The  $^1\text{H}$  and  $^{13}\text{C}$  NMR spectra were identical to **2.18** (Matt Nodwell). HRESIMS  $[\text{M}+\text{H}]^+$  calcd for  $\text{C}_{21}\text{H}_{29}\text{O}_2$  313.2176, found 313.2168;  $[\alpha]_{\text{D}}^{24} = -18.1^\circ$  (*c* 0.05).

### Preparation of **2.61**:



To acid chloride **2.57** (28.7 mg, 0.163 mmol) dissolved in 2 mL of tetrahydrofuran was added **2.3** (56.0 mg, 0.179 mmol) and triethylamine (0.22 mL, 1.57 mmol) at  $0\text{ }^\circ\text{C}$ , and the reaction mixture allowed to warm to room temperature overnight. The crude reaction mixture was concentrated under a stream of nitrogen, and purified using flash column chromatography (hexanes:ethyl acetate 12:1) to give **2.61** (30.0 mg, 0.063 mmol, 38.6 %).  $^1\text{H}$  NMR (400 MHz,  $\text{CDCl}_3$ )  $\delta$  8.17 (d,  $J = 8.8$  Hz, 2H), 7.07 (d,  $J = 8.8$  Hz, 2H), 6.91 (s, 1H), 6.73 (s, 1H), 4.77 (s, 2H), 2.7 (m, 1H), 2.60-2.55 (m, 2H), 2.40 (dt,  $J = 12.0, 3.2$  Hz, 1H), 2.35 (s, 3H), 1.85-1.44 (m, 8H), 1.24 (td,  $J = 14.4, 4.8$  Hz, 1H), 1.14 (s, 3H), 1.08 (s, 3H), 1.04 (m, 1H), 1.01 (m, 1H), 0.92 (s, 6H);  $^{13}\text{C}$  NMR (100 MHz,  $\text{CDCl}_3$ )  $\delta$  165.2, 161.7, 149.3, 148.9, 144.5, 133.2, 132.3, 123.2, 121.6, 116.2, 114.8, 78.0, 76.4, 64.5, 57.2, 56.0, 47.6, 42.7, 40.2, 38.8, 37.2, 33.5, 33.2, 29.1, 21.3, 20.4, 19.7, 19.1, 18.5, 16.3. HRESIMS  $[\text{M}+\text{H}]^+$  calcd for  $\text{C}_{32}\text{H}_{39}\text{O}_3$  471.2899, found 471.2829;  $[\alpha]_D^{24} = +12.63^\circ$  ( $c$  2.2).

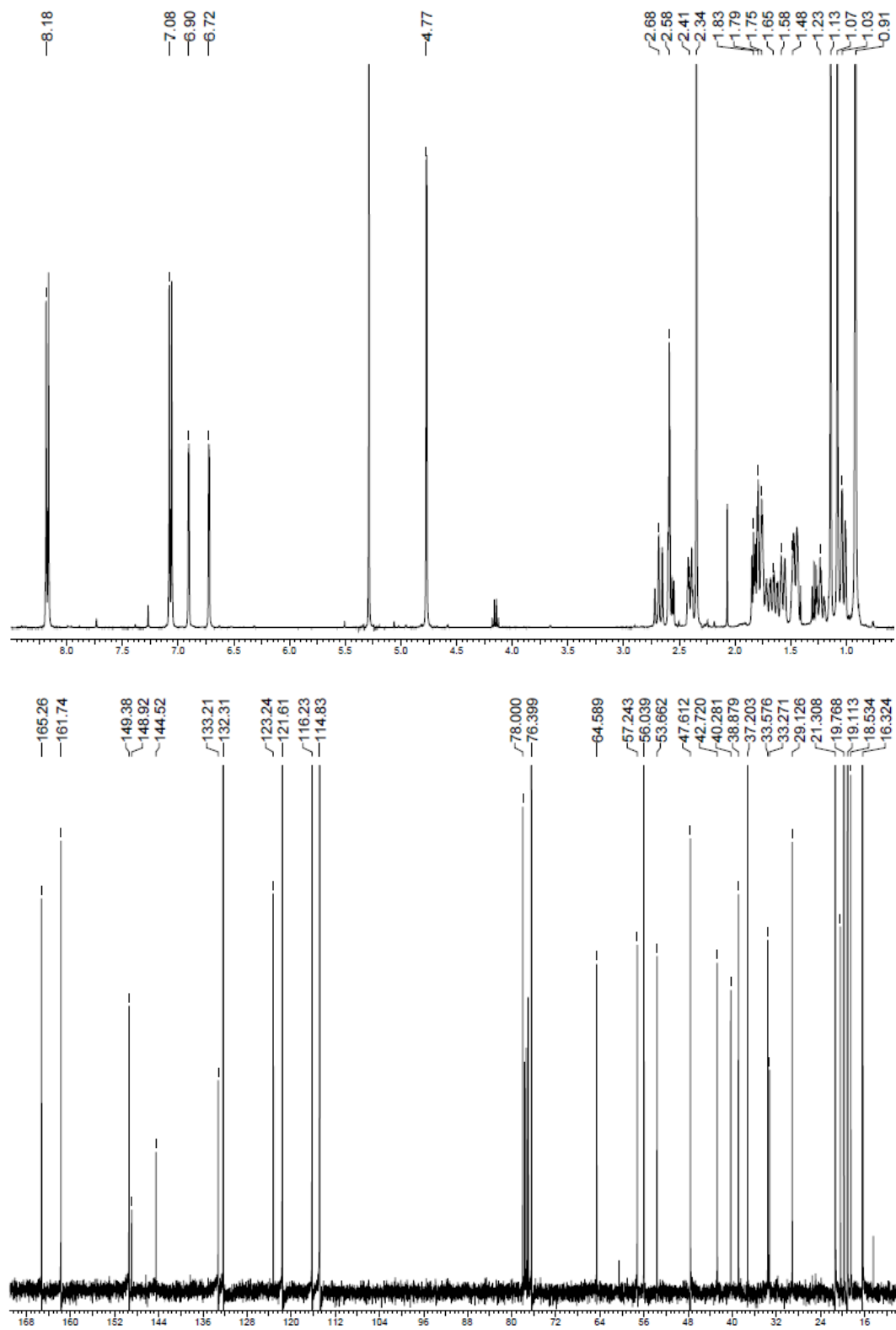
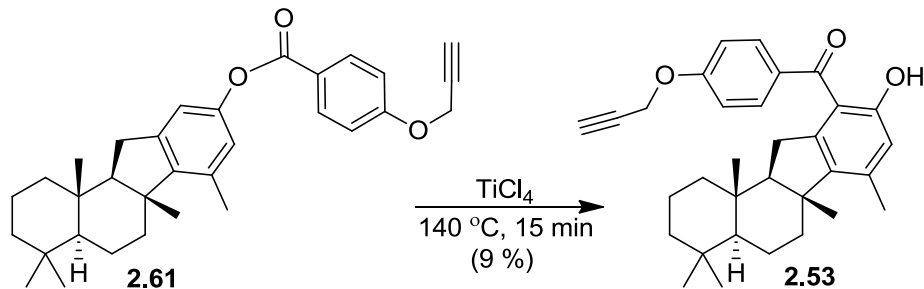


**Figure 2.40**  $^1\text{H}$  and  $^{13}\text{C}$  NMR spectra of **2.61** recorded in  $\text{CDCl}_3$  at 400 MHz and 100 MHz respectively.

### Preparation of **2.53**:



To **2.61** (754 mg, 1.60 mmol) was added titanium tetrachloride (0.35 mL, 3.20 mmol) and the mixture exposed to an oil bath at  $140\text{ }^\circ\text{C}$  for fifteen minutes. The black mixture was then quenched with 50 mL of 0.1 N HCl and extracted three times with methylene chloride (250 mL). The organic extracts were combined, concentrated using a rotary evaporator, and purified using flash column chromatography (hexanes:ethyl acetate 7:1) to give **2.53** (69.3 mg, 0.147 mmol, 9.1 %).  $^1\text{H}$  NMR (400 MHz,  $\text{CDCl}_3$ )  $\delta$  9.97 (s, 1H), 7.63 (d,  $J = 9.2$  Hz, 2H), 7.03 (d,  $J = 8.8$  Hz, 2H), 6.60 (s, 1H), 4.79 (s, 2H), 2.56 (t,  $J = 2.4$  Hz, 1H), 2.33 (s, 3H), 2.26-2.19 (m, 1H), 1.98 (dd,  $J = 15.2, 6.0$  Hz, 1H), 1.71-1.16 (m, 9H), 1.13 (s, 3H), 1.07-0.98 (m, 1H), 0.90 (s, 3H), 0.87 (m, 1H), 0.84 (s, 3H), 0.82 (s, 3H), 0.77 (td,  $J = 12, 4$  Hz, 1H);  $^{13}\text{C}$  NMR (100 MHz,  $\text{CDCl}_3$ )  $\delta$  200.0, 161.0, 158.2, 144.5, 144.5, 140.1, 133.7, 131.2, 117.9, 117.5, 114.7, 77.4, 76.2, 64.3, 57.0, 56.0, 46.7, 42.5, 39.8, 38.9, 36.9, 33.4, 33.1, 31.4, 21.2, 20.4, 19.7, 19.6, 18.2, 16.0. HRESIMS  $[\text{M}+\text{Na}]^+$  calcd for  $\text{C}_{32}\text{H}_{38}\text{O}_3\text{Na}$  493.2719, found 493.2726;  $[\alpha]_D^{24} = +59.49^\circ$  ( $c$  3.46).

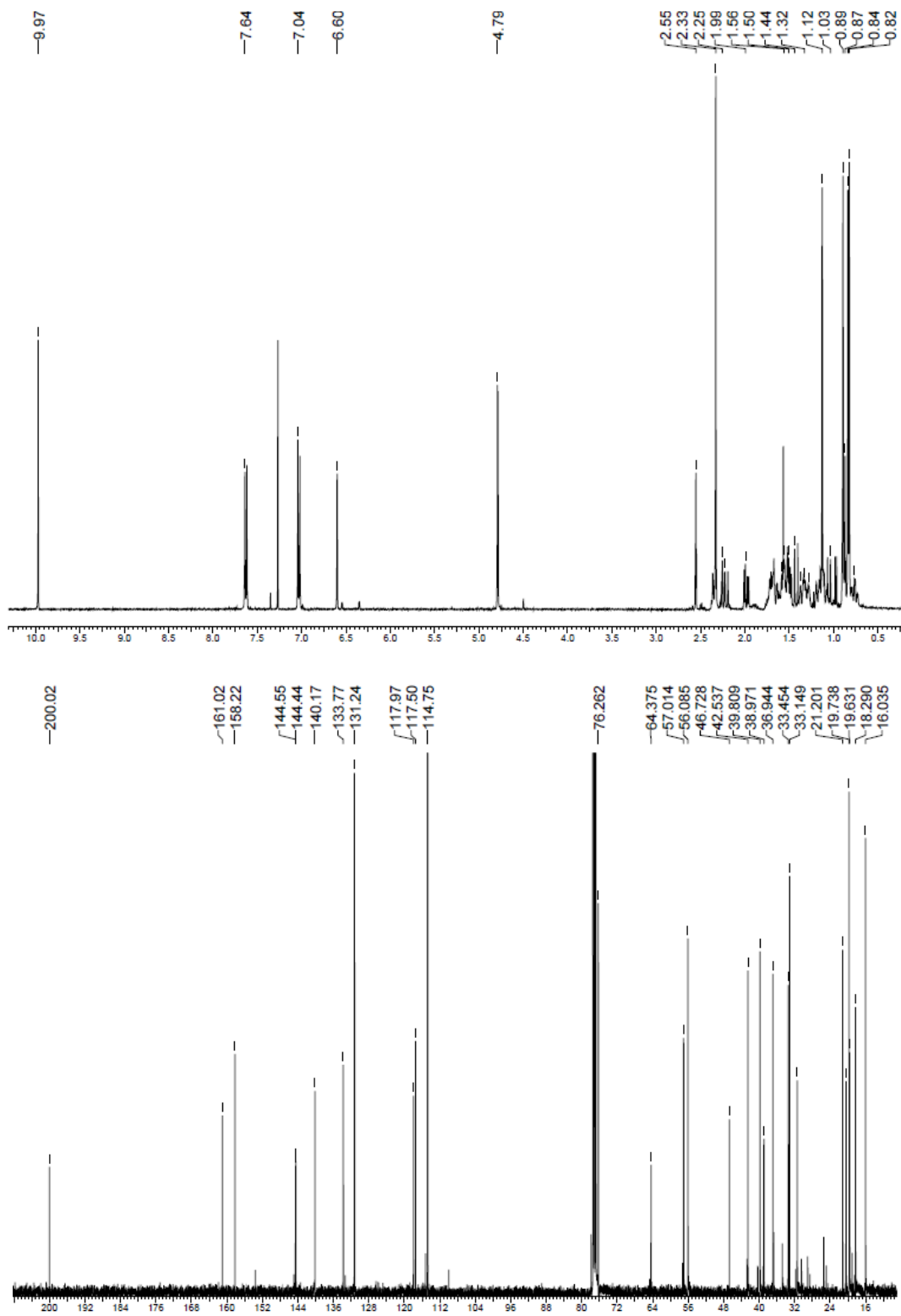


**Figure 2.41**  $^1\text{H}$  and  $^{13}\text{C}$  NMR spectra of **2.53** recorded in  $\text{CDCl}_3$  at 400 MHz and 100 MHz respectively.

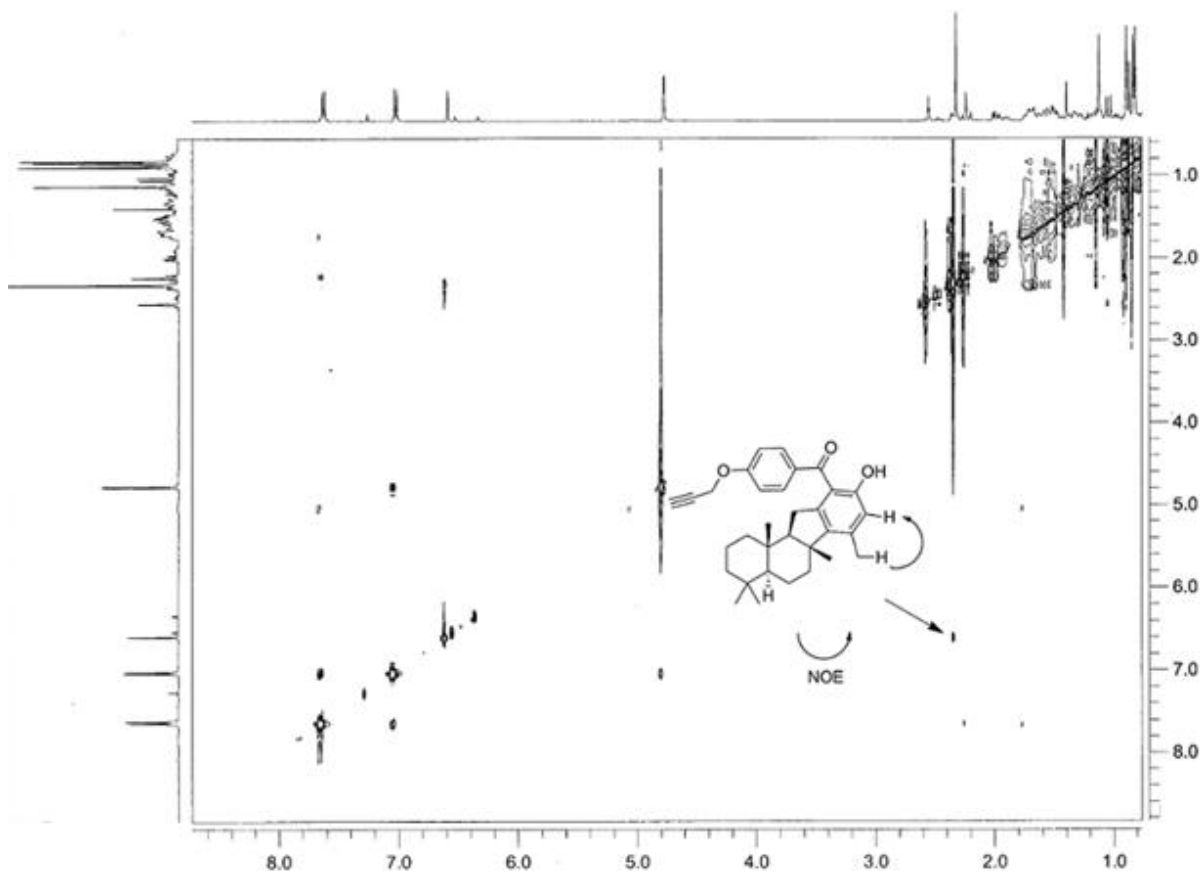


**Figure 2.42** NOESY spectrum of **2.53** in CDCl<sub>3</sub> at 400 MHz.

**His-hSHIP1 Enzyme Assay:** His-hSHIP1 enzyme assay was performed in 96-well microtiter plates with 2.5 to 10 ng enzyme/well and 50 ng/well, respectively, in a total volume of 25  $\mu$ L of SHIP1 assay buffer (20 mM Tris HCl (pH 7.5), 10 mM MgCl<sub>2</sub> and 0.02 % Tween-20). Recombinant His-hSHIP1 enzyme was incubated with test articles or vehicle (2 % ethanol) and 50  $\mu$ M inositol-1,3,4,5-tetrakisphosphate (IP<sub>4</sub>) for 15 min at 37 °C in a shaking incubator. After 15 min at 37 °C, the amount of inorganic phosphate released was assessed by the addition of BIOMOL GREEN™ reagent and incubation for 20 min at room temperature before measuring the absorbance at 650 nm.

**Akt Activation Assay:** MOLT-4 and Jurkat T-ALL cells were cultured in RPMI 1640 containing 10 % FBS and 1 % penicillin/streptomycin at 37 °C in a water-jacketed CO<sub>2</sub> (5 %) incubator. Cells were seeded at 0.2-0.3 x 10<sup>6</sup> cells/mL and grown for 2 to 3 days before passaging. Cells that exceeded 25 passages were not used for studies and were discarded.

**Akt Phosphorylation Assay:** Cells were cultured in serum free RPMI at 1 x 10<sup>6</sup> cells/mL. After overnight culture, 2-3 x 10<sup>6</sup> cells were treated in a 15 mL conical tube with test article for 30 min followed by IGF-1 stimulation at 0.1 µg/ml for 60 min. The final concentration of the drug vehicle (dimethyl sulfoxide) was 0.1 %. After treatment, cells were washed once with ice cold DPBS and lysed with lysis buffer (20 mM Tris-HCl, pH 7.5, 140 mM NaCl, 1 % NP-40, Complete Mini Protease Inhibitor Cocktail, 10 mM NaF, 1 mM Na<sub>3</sub>VO<sub>4</sub>, and 1 mM β-glycerol phosphate) on ice for 30 min with vortexing every 10 min. Samples were then centrifuged at 14,000 rpm for 20 min, and supernatants were collected as total cell lysates. Akt phosphorylation at S473 in each sample was determined by western blotting.

**Western Blotting:** Protein concentration in each sample was determined colorimetrically using bicinchoninic acid (BCA) assay. Approximately 15-20 µg of total protein from each sample was mixed with 6 x sample loading buffer (250 mM Tris-HCl, pH 6.8, 30 % glycerol, 10 % SDS, 0.012 % bromophenol blue and 0.6 M DTT) and boiled for 5 min before loading onto a polyacrylamide gel for SDS-PAGE. Proteins from each sample were separated on a 4-12 % Tris-Glycine gel for 1.5 h with a constant voltage of 125 Volts. After electrophoresis, proteins were transferred to a nitrocellulose membrane using the iBlot

Dry Transfer system (Life Technologies, Carlsbad, CA, USA). The membrane was then blocked in 5 % BSA in PBS containing 0.1 % Tween-20 (PBS-T) for 1 h at room temperature before probing with primary antibodies overnight at 4 °C. The following antibodies were used: mouse anti-SHIP1 (1:500; v/v), rabbit anti-pAkt (S473) (1:1000; v/v), rabbit anti-Akt (1:2000), and rabbit anti- $\beta$ -actin (1:2000; v/v). The membrane was then incubated with goat anti-rabbit IgG HRP-linked or goat anti-mouse IgG HRP-linked secondary antibodies (1:3000; v/v) for 1 h at room temperature. Target proteins on the membrane were detected with ECL solution and exposed on a film.

**Mouse Passive Cutaneous Anaphylaxis Model:** The *in vivo* animal study protocols were approved by the local ethics committee. Forty BALB/c male mice (8 weeks old) were obtained from Charles River Laboratories (Hollister, CA, USA). Animals were acclimated for a minimum of five days prior to the start of the study. They were housed five animals per cage in polypropylene cages, and were allowed free access to food and water. A 12 h light/dark cycle was maintained. Each animal was injected intradermally in the right ear with 25 ng of anti-DNP-IgE in 20  $\mu$ L PBS. The left ears were not injected and served as a negative control. 24 h post-injection, **2.20/2.42** was administered once by oral gavage in saline (0.01, 0.1, or 10 mg/kg; 10.0 ml/kg dose volume) in a model of IgE-mediated passive cutaneous anaphylaxis. Sixty minutes after dosing, each animal was given a tail vein injection of 2 % Evans' blue (0.22  $\mu$ m filtered, in 200  $\mu$ L saline) followed by a second tail intravenous injection of 100  $\mu$ g DNP-HSA (in 200  $\mu$ L PBS) (Sigma). Sixty minutes following the DNP-HSA injection, mice were euthanized using CO<sub>2</sub> inhalation. Ear biopsies were performed with four-millimeter punches from both ears placed into 100  $\mu$ L formamide in 96 well PCR

plates to elute the Evans' Blue dye. To minimize evaporation, plates were then sealed during incubation in a 70 °C water bath overnight. Eighty µL of eluents were transferred to flat-bottom 96-well plates and read using a SpectraMax M5 spectrophotometer (Molecular Devices, Sunnyvale, CA, USA) at 620 nm. Background readings from all samples were taken at 740 nm and subtracted from the 620 nm readings. A blank reading was made on a sample of formamide and subtracted from all readings. Data are reported as optical density.

**Water Solubility of Pelorol Analogues:** Samples were weighed accurately in duplicate (~3 mg each) in 4 mL glass vials. The appropriate amount of deionized water was added to obtain a final concentration of 6 mg/mL. A stir bar was placed in the vial and the two mixtures were stirred for 24 h, after which the samples were filtered using a glass filter membrane. The resulting filtrate was centrifuged in a glass conical tube for 10 min at 10,000 rpm to sediment any precipitate that may have passed through the glass membrane. The supernatant was sampled for HPLC analysis. The concentration of the test compound was determined by HPLC using a six-point standard curve of the compound prepared in methanol.

## Chapter 3: Glycerol Ethers from the Sponge *Niphates digitalis* that Block Androgen Receptor Transcriptional Activity in Prostate Cancer Cells

### 3.1 Castration Recurrent Prostate Cancer (CRPC)

Prostate cancer ranks second among most often diagnosed cancers in Canadian men. It ranks third as a cause of cancer death in Canadian men aged 65 and over. A key nuclear receptor associated with the prostate is the androgen receptor (AR). Endogenous androgens such as testosterone (**3.1**) and dihydrotestosterone (**3.2**) mediate their biological effects through the AR (Figure 3.1).<sup>124</sup>

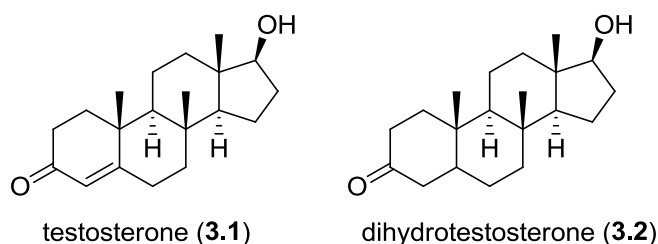


**Figure 3.1** Endogenous androgens found in humans.

The rate of prostate tissue growth is dependent on the levels of endogenous androgens in the body.<sup>125</sup> This is typified during puberty when increased androgen production causes growth of the prostate. Conversely, there is a decrease in prostate volume when androgen levels diminish.<sup>126</sup> The dependence on androgens by the prostate for mitogenic stimulus is currently used as a means to treat prostate cancer.

The first line treatment for low grade tumors<sup>127</sup> is prostatectomy (prostate removal) and localized radiation therapy. Unfortunately, tumour recurrence occurs in approximately

20-40 % of patients treated with first line therapies, at which point androgen ablation therapy is used. Androgen ablation therapy is achieved either by surgical castration (testes removal), or by chemical castration. The goal of these therapeutic treatments is to diminish the levels of androgens in the body in order to decrease prostate tumour size. There are two ways of achieving chemical castration. The first is the use of small molecules, which inhibit the production of androgens. Abiraterone (**3.3**) is a good example (Figure 3.2).<sup>128</sup> Abiraterone (**3.3**) inhibits 17  $\alpha$ -hydroxylase/C17,20-lyase<sup>129</sup> (CYP17A1), an enzyme that is expressed in testicular, adrenal, and prostatic tumor tissues. The enzyme CYP17A1 is responsible for the production of dehydroepiandrosterone and androstenedione, both of which are endogenous androgens and precursors to testosterone (**3.1**). By decreasing the level of dehydroepiandrosterone in the body, abiraterone (**3.3**) decreases the level of testosterone (**3.1**) resulting in a decrease in prostate tissue volume.

The second method of achieving chemical castration is by using androgen receptor antagonists.<sup>130</sup> Antagonists are ligands which have binding affinity to a biological target but do not trigger the biological response of the target upon binding. Instead they block androgen binding and, therefore, prevent the agonist (androgens) mediated response. Examples include bicalutamide (**3.3**)<sup>131</sup> and MDV3100 (**3.5**)<sup>132</sup> (phase III clinical trials) (Figure 3.2).

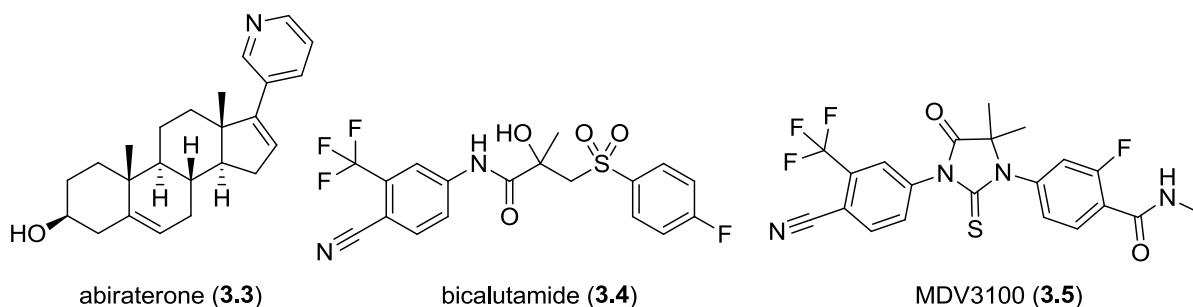


**Figure 3.2** Examples of antiandrogens.

Chemical methods of decreasing the level of androgens are only effective for a short period of time. Eventually, the malignancy will begin to grow in the absence of androgens to form castration recurrent prostate cancer<sup>133</sup> (CRPC). Once CRPC has been established, alternative treatments are employed which do not specifically target the AR (docetaxel or sipuleucel-T), however, they only result in an increased life expectancy of two to four months. There is currently no successful treatment of CRPC.

### 3.2 The AR NTD as a Novel Therapeutic Target for Treating CRPC

The AR comprises a C-terminal ligand binding domain (LBD), a DNA binding domain (DBD), a hinge region, and an N-terminus domain (NTD), containing the activation function-1 (AF1) region (Figure 3.3).<sup>127</sup> Current therapies for treating prostate cancer involve targeting the LBD of the AR. Although these therapies are effective initially, these approaches eventually fail.<sup>134</sup> Evidence supporting several mechanisms for the failure of antiandrogens exist and include overexpression of the AR,<sup>135</sup> mutations allowing for the activation of the AR by androgens or antiandrogens,<sup>136</sup> AR activation by non-ligands,<sup>137</sup> and

expression of splice variants of the AR which lack the LBD altogether.<sup>138</sup> These factors result in the failure of treating CRPC by small molecule antagonists of the LBD of the AR.

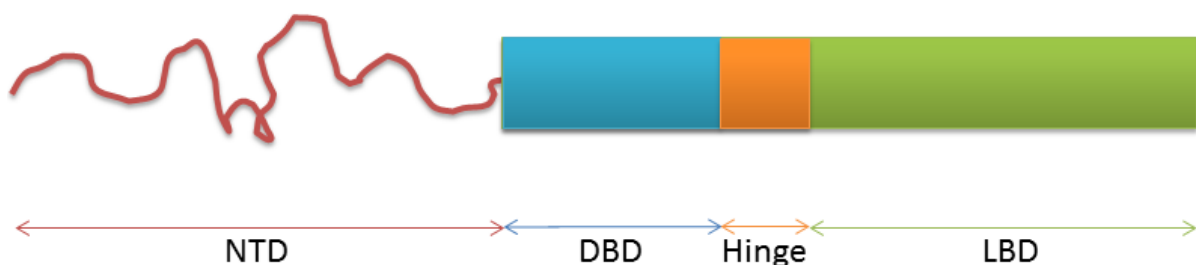


**Figure 3.3** Androgen receptor structure.

Targeting the AR through the DBD is an alternative method, since it has been crystallized,<sup>139</sup> and so could potentially allow for rational drug design. However, the high degree of homology found in the DBD to other steroid receptors sites prevents it from being a promising biological target in the development of a therapeutic candidate.

An important component of the AR is the NTD, a disordered region of the protein. The NTD plays a critical role in transcriptional activity of the AR in the absence of androgens, resulting in androgen-independent proliferation of prostate cancer cells. No AR transcriptional activity is possible without a functioning NTD AF1 region. This has made targeting of the NTD by small molecules an appealing avenue of exploration for treating CRPC. A novel cell-based assay developed by Sadar<sup>140</sup> *et al.* has provided a method to screen extract libraries for compounds that are NTD antagonists. Use of this assay led to the isolation and structural elucidation of the AR NTD antagonists sintokamide A (**3.6**)<sup>140</sup> and EPI-001 (**3.7**)<sup>141</sup> (Figure 3.4).

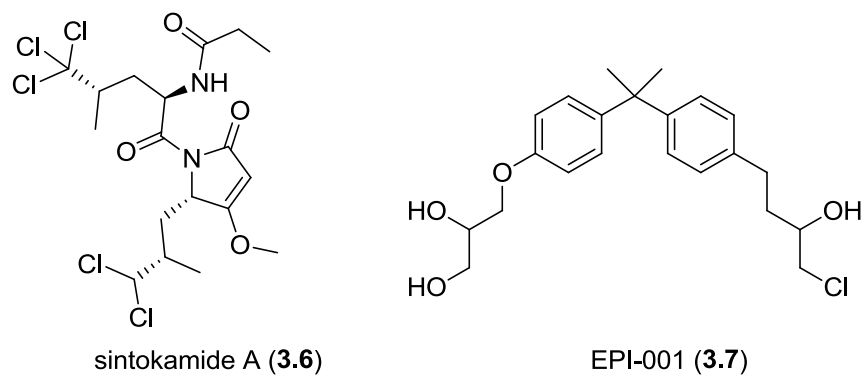


**Figure 3.4** Small molecule antagonists of the AR NTD.

Continued efforts to discover new AR NTD antagonists led to further screening of the Andersen natural product library. The crude methanol extracts of the marine sponge *Niphates digitalis* collected in Dominica showed strong activity in the screening assay. Bioactivity-guided fractionation of the extracts led to the isolation of the glycerol ethers niphatenone A (3.8) and B (3.9) as the active compounds by David Williams (Figure 3.5).

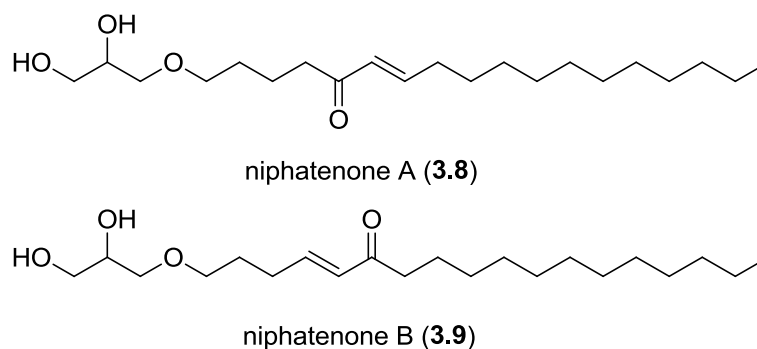
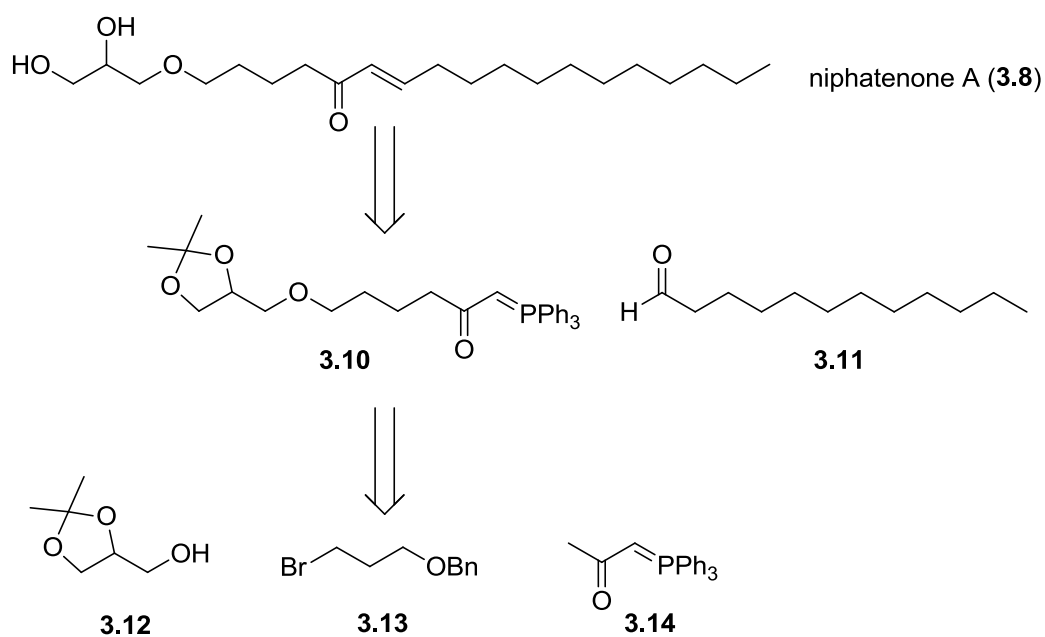


**Figure 3.5** Niphatenones A (3.8) and B (3.9).

The small quantity of niphatenone A (3.8) (0.1 mg) and B (3.9) (0.1 mg) available from the *Niphates digitalis* extract made it impossible to determine the absolute configuration

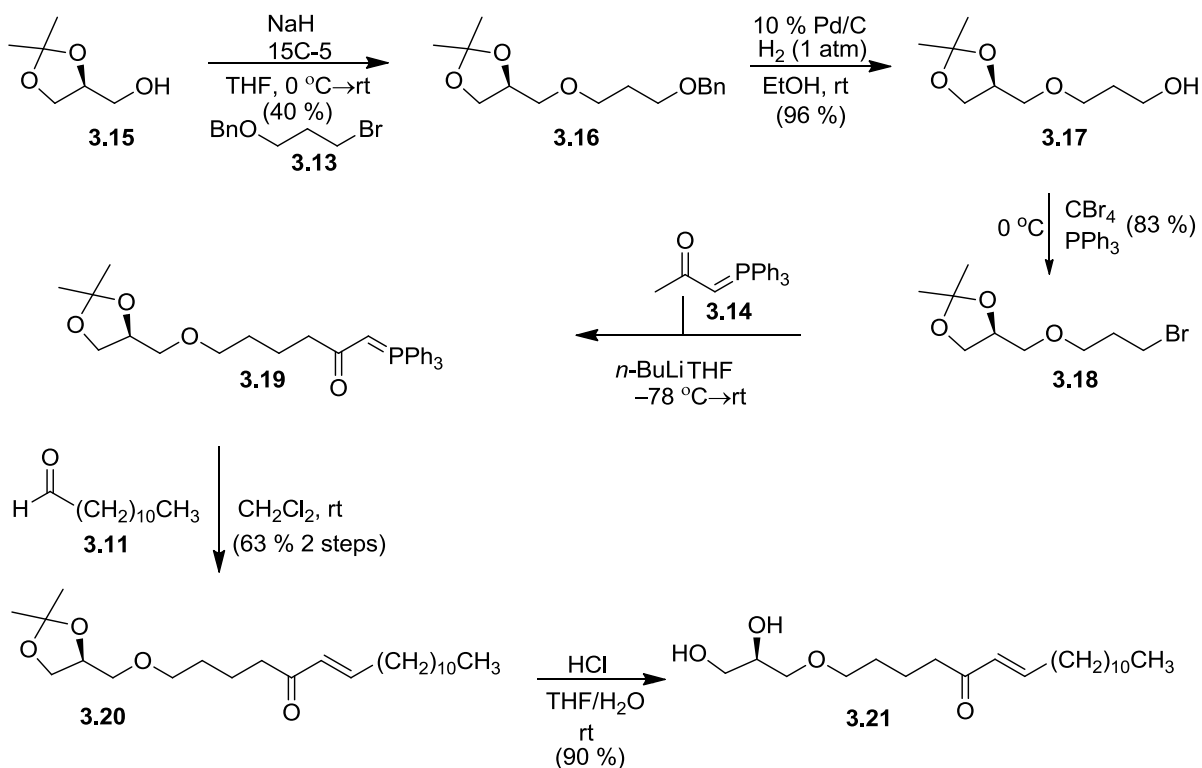
of the natural products, or carry out further evaluation of their biological activities. Hence, a total synthesis of (*S*) and (*R*)-niphatenone A (**3.8**) and (*S*) and (*R*)-niphatenone B (**3.9**) was undertaken. Niphatenone A (**3.8**) was the first of the two natural products to be constructed. Retrosynthetic analysis indicated that the *E*-enone of the natural product may come from phosphorane **3.10** and aldehyde **3.11**. Phosphorane **3.10** can be constructed from glycerol **3.12**, alkyl bromide **3.13**, and phosphorane **3.14** (Scheme 3.1).



**Scheme 3.1** Retrosynthetic analysis of niphatenone A (**3.8**).

The configuration of the natural product was unknown, therefore both stereoisomers needed to be constructed and compared with the natural material. The synthesis of (*R*)-niphatenone A (**3.21**) began with commercially available (*S*)-dioxolane (**3.15**). This would provide the only stereocenter of the natural product (Scheme 3.2). Deprotonation of **3.15** with sodium hydride in the presence of 15C-5 followed by treatment with alkyl bromide **3.13** gave

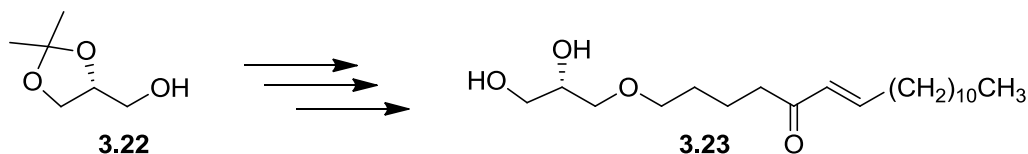
the benzyl protected glycerol ether **3.16**.<sup>142</sup> Hydrogenolysis of **3.16** with 10 % palladium/charcoal under hydrogen (1 atm) gave the primary alcohol **3.17**. Intermediate **3.17** was converted to bromide **3.18** by the Appel reaction.<sup>143</sup> Deprotonation of commercially available phosphorane<sup>144</sup> **3.14** with *n*-BuLi, followed by alkylation with bromide **3.18**, provided the Wittig reagent **3.19** (Scheme 3.2).



**Scheme 3.2** Synthesis of (*R*)-niphatenone A (**3.21**).

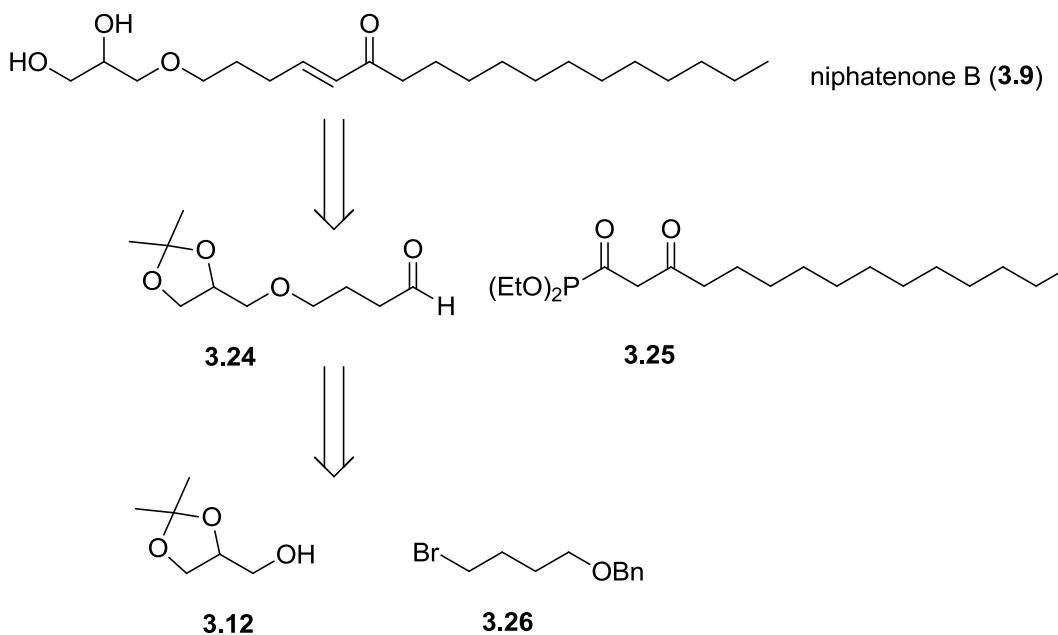
Without any further purification, intermediate **3.19** was used in the subsequent olefination with commercially available aldehyde **3.11** to give enone **3.20** in a 63 % yield over two steps. Attempts to remove the acetonide protecting group of **3.20** with *p*-toluenesulfonic acid in methanol gave poor yields (17 %). However, HCl in a mixture of

tetrahydrofuran and water<sup>145</sup> gave (*R*)-niphatenone (**3.21**) in high yield (Scheme 3.2). Repeating the synthesis using (*R*)-dioxolane (**3.22**) as the starting material gave (*S*)-niphatenone A (**3.23**) (Scheme 3.3).



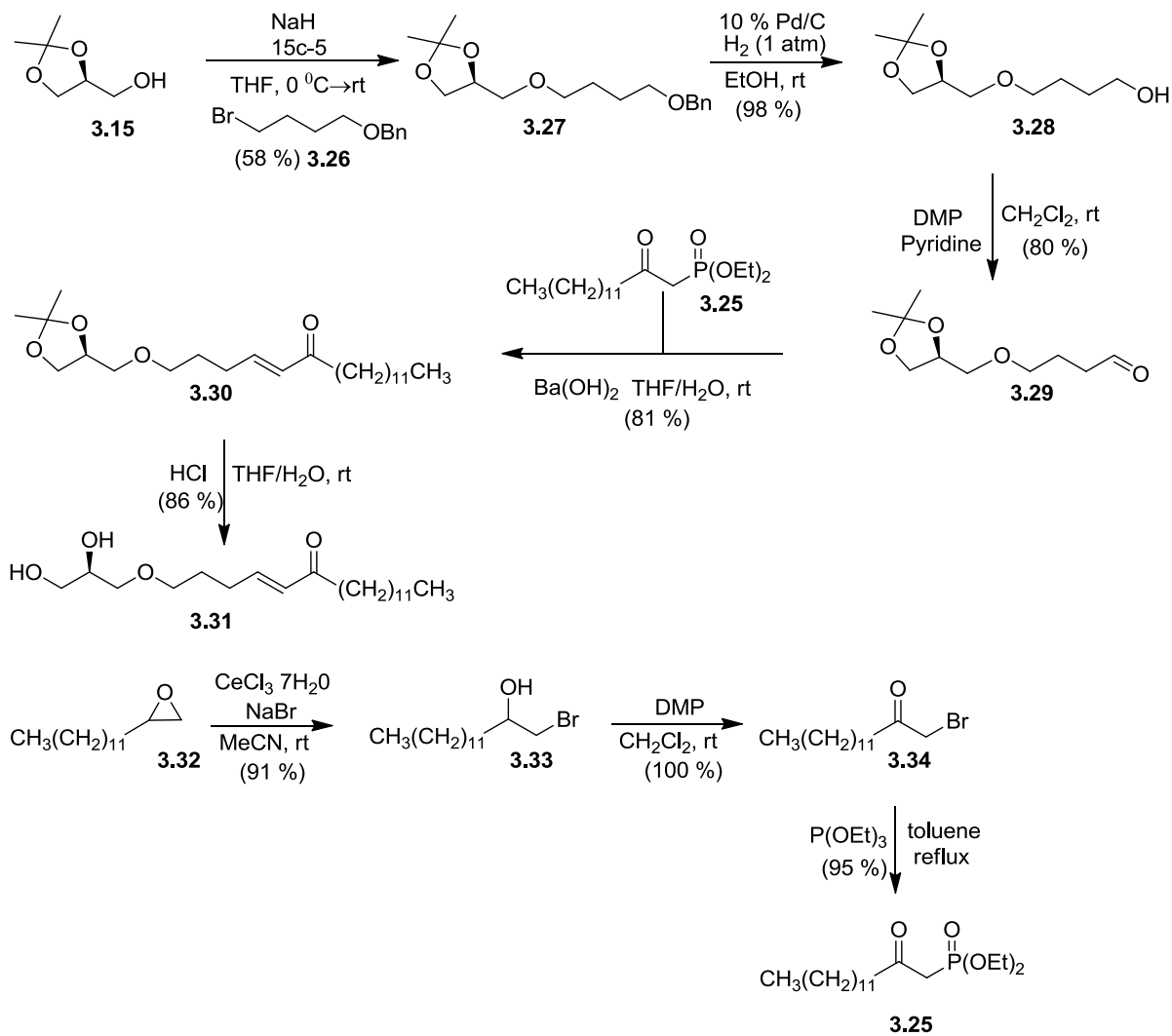
**Scheme 3.3** Synthesis of (*S*)-niphatenone A (**3.23**).

Next, we wanted to construct niphatenone B (**3.9**). Using retrosynthetic analysis, we see that the *E*-enone in **3.9** can come from a Horner–Wadsworth–Emmons<sup>146</sup> (HWE) olefination between aldehyde **3.24** and phosphonate **3.25**. Aldehyde **3.24** can be furnished from coupling glycerol **3.12** and bromide **3.26** (Scheme 3.4).



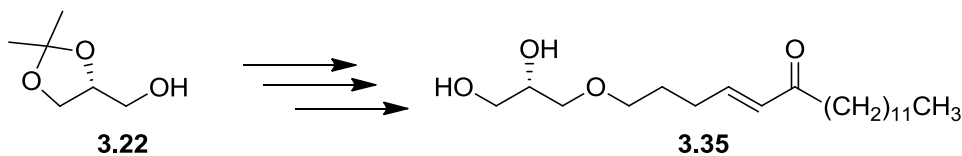
**Scheme 3.4** Retrosynthesis of niphatenone B (**3.9**).

The synthesis of (*R*)-niphatenone B (**3.31**) started with the deprotonation of (*S*)-dioxolane (**3.15**) with sodium hydride followed by alkylation with bromide **3.26** to give ether **3.27** (Scheme 3.5). Deprotection of the benzyl protecting group of **3.27**, followed by Dess–Martin periodinane oxidation<sup>147</sup> under basic conditions gave aldehyde **3.29**.



Scheme 3.5 Synthesis of (*R*)-niphatenone B (**3.31**).

For the HWE olefination, phosphonate **3.25** was required (Scheme 3.5). Treatment of commercially available epoxide **3.32** with cerous chloride<sup>148</sup> and sodium bromide gave bromohydrin **3.33**. Intermediate **3.33** was then oxidized with DMP to afford  $\alpha$ -bromo-ketone **3.34**. Refluxing **3.34** in the presence of triethylphosphite gave phosphonate **3.25**<sup>149</sup> in high yield. Sodium hydride was initially used as the base for the HWE step. However, it provided poor yields (< 40 %). It was found that barium hydroxide<sup>150</sup> in a mixture of tetrahydrofuran and water gave **3.30** in a good yield. Finally, deprotection of acetonide **3.30** provided (*R*)-niphatenone B (**3.31**) in an 86 % yield (Scheme 3.5). Repeating the synthesis using (*R*)-dioxolane (**3.22**) as the starting material gave (*S*)-niphatenone B (**3.35**) (Scheme 3.6).



**Scheme 3.6** Synthesis of (*S*)-niphatenone B (**3.35**).

Comparison of the <sup>1</sup>H NMR, <sup>13</sup>C NMR, and MS data of the natural product with the synthetic material confirmed the proposed structures of niphatenone A (**3.8**) and B (**3.9**). Furthermore, having constructed all four stereoisomers of niphatenone A (**3.8**) and B (**3.9**), it was possible to determine the absolute configuration of the natural product. The natural product was re-isolated from the sponge by the author, and chiral HPLC analysis completed by David Williams suggested that the natural product configuration for both niphatenones A (**3.8**) and B (**3.9**) was the (*S*) configuration.

This configuration was in agreement with ceratodictyol A (**3.36**) and B (**3.37**), that are homologs of (*S*)-niphatenone A (**3.23**) and B (**3.35**) (Figure 3.6). Ceratodictyol A (**3.36**)

and B (**3.37**) were isolated by Matsunaga<sup>151</sup> and coworkers from the red algae/sponge assembly *Ceratodictyon spongiosum/Haliclona cymaeformis*. The ceratodictyols were reported to have modest *in vitro* cytotoxicity against a human cervical cancer cell line (IC<sub>50</sub> = 67 μM).

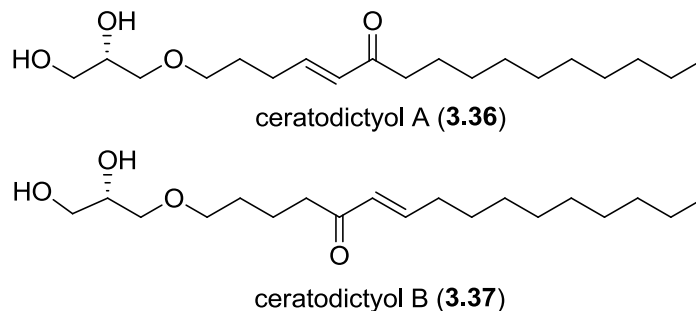


**Figure 3.6** Ceratodictyol A (**3.36**) and B (**3.37**).

### 3.3 Synthetic Analogues of (*R*)-Niphatenone B (**3.31**)

Having confirmed the structure and absolute configuration of both niphatenone A (**3.8**) and B (**3.9**), we wanted to probe the SAR of these novel AR antagonists. (*R*)-Niphatenone B (**3.31**) was chosen as the lead structure since preliminary biological data suggested it was the most potent of the four natural and synthetic compounds constructed (Section 3.5). We were interested in how modifications to the glycerol ether, double bond, and alkyl chain moieties would affect the activity of these compounds *in vitro* (Figure 3.7).

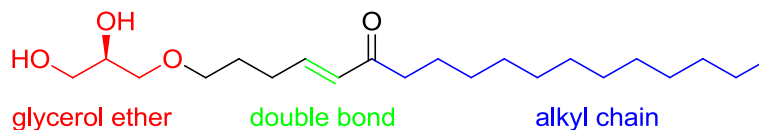
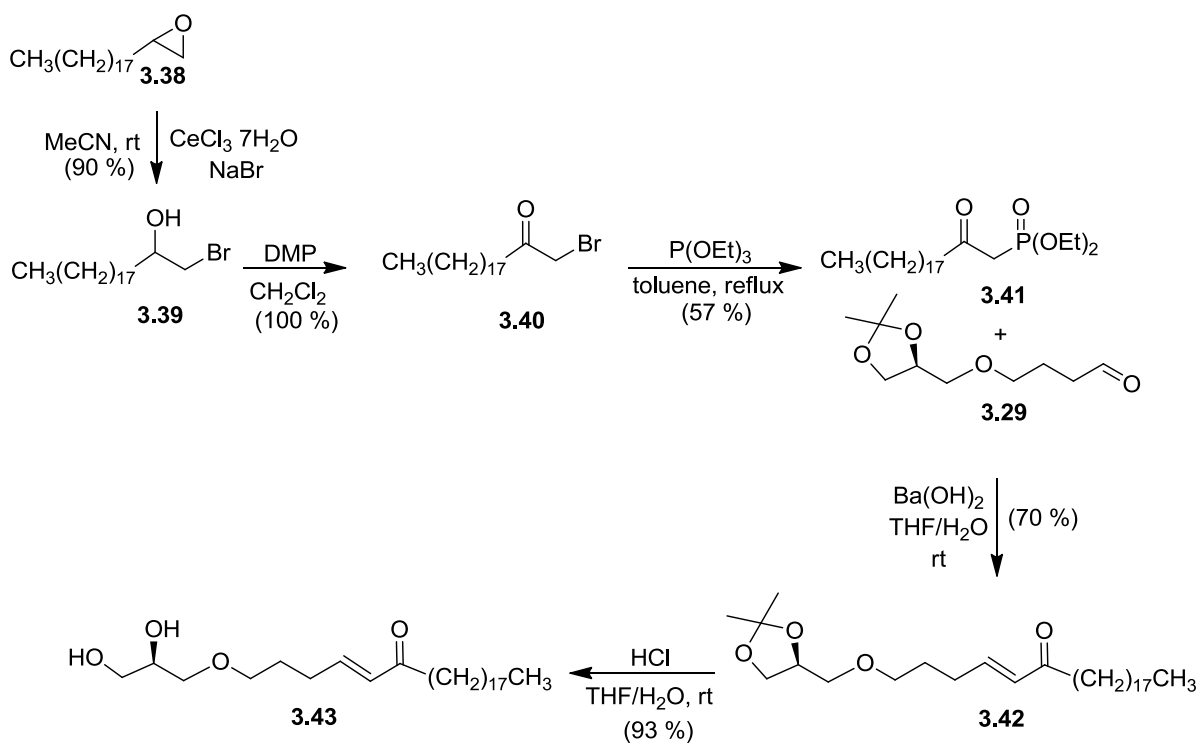


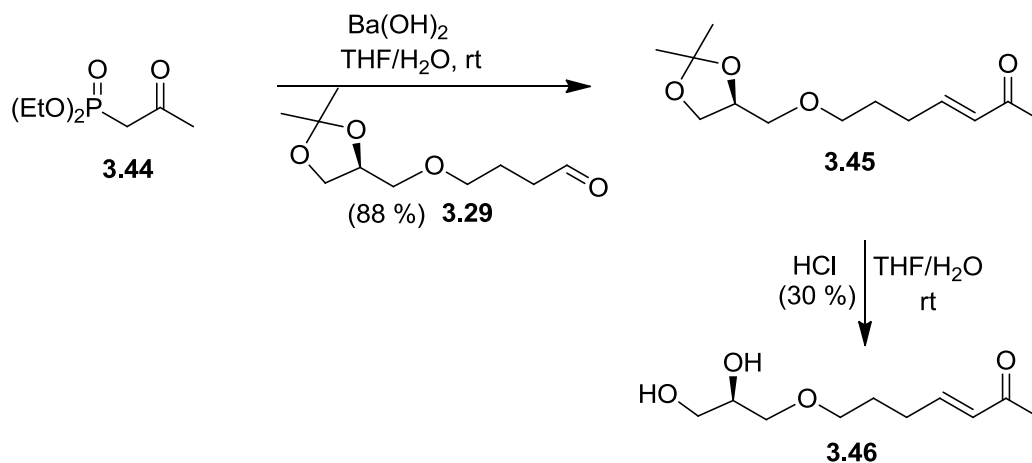
**Figure 3.7** Proposed SAR of (*R*)-niphatenone B (**3.31**).

The first goal was to examine the effect of chain length modification. An analogue of (*R*)-niphatenone B (**3.31**) was constructed with a chain length exceeding the natural product by six carbon units (**3.43**) (Scheme 3.7). The synthesis was analogous to that of (*R*)-niphatenone B (**3.31**) except for the structure of the phosphonate (**3.41**) required for the HWE olefination step.



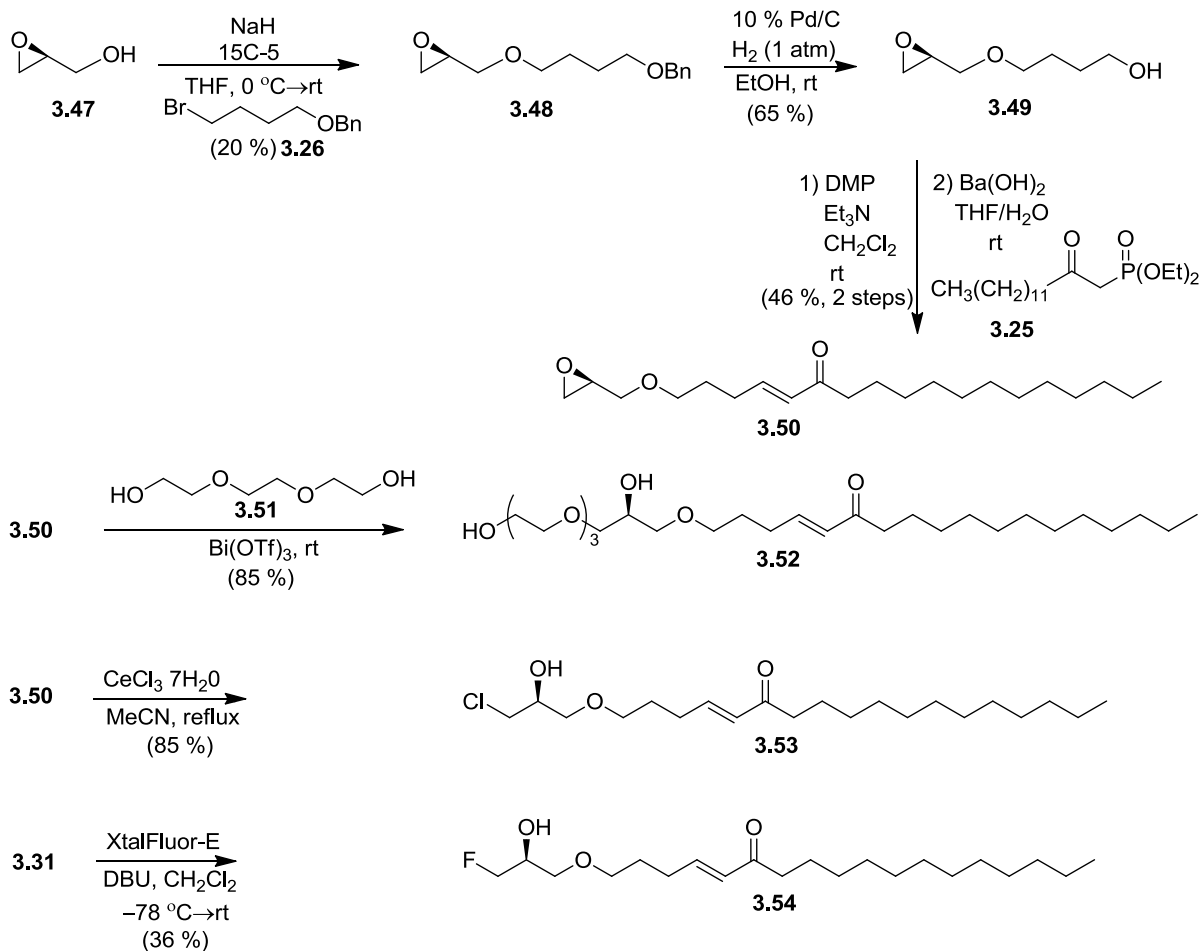
**Scheme 3.7** Synthesis of a long chain (*R*)-niphatenone B (**3.31**) analogue **3.43**.

Similarly, an analogue with ten carbon units less was constructed (Scheme 3.8). This synthesis utilized commercially available phosphonate **3.44** to provide the methyl ketone moiety in analogue **3.46**.



**Scheme 3.8** Synthesis of a short chain (*R*)-niphatenone B (**3.31**) analogue **3.46**.

Next, modifications to the glycerol ether portion of (*R*)-niphatenone B (**3.31**) were undertaken. An epoxide intermediate was designed to provide access to several different glycerol-modified analogues. The synthesis began with deprotonation of glycidol **3.47** (98 % ee) in the presence of 15C-5 and bromide **3.26** to yield benzyl-protected alcohol **3.48**. Deprotection of the benzyl group followed by DMP oxidation and HWE olefination with phosphonate **3.25** yielded the key epoxide intermediate **3.50** (Scheme 3.9).

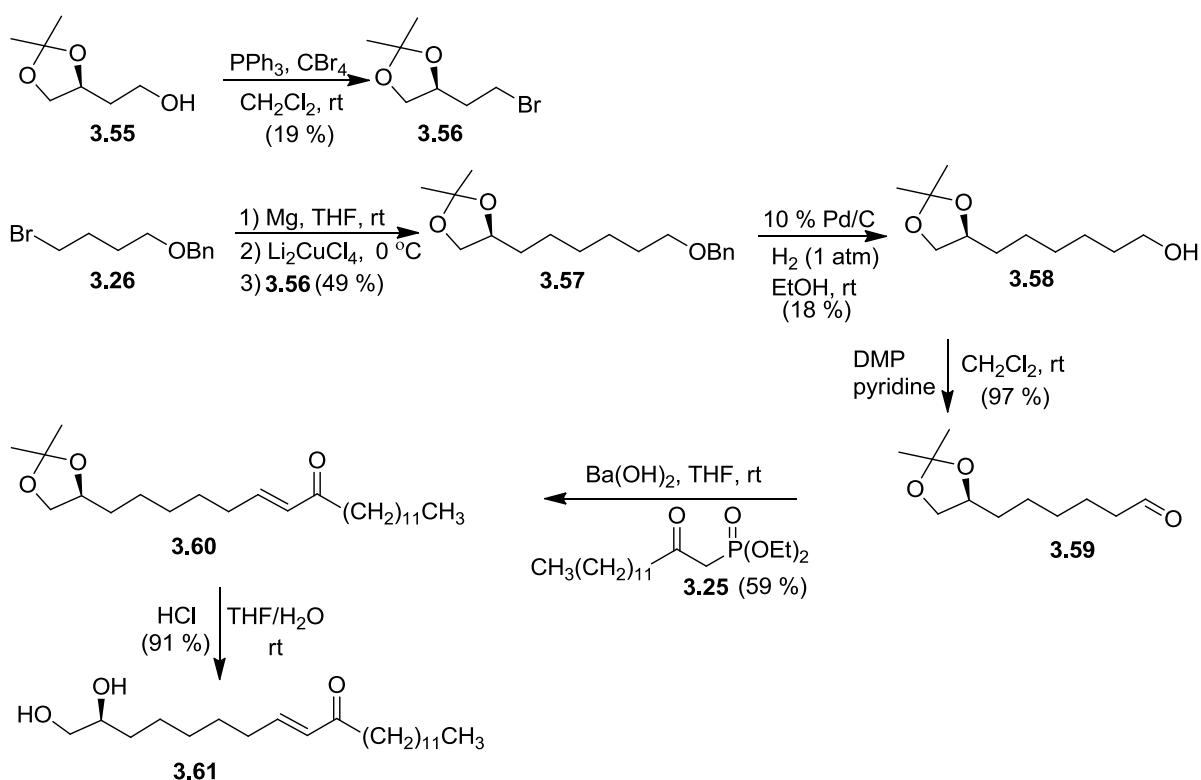


**Scheme 3.9** (*R*)-Niphatenone B (**3.31**) glycerol analogues.

In an effort to enhance the solubility of (*R*)-niphatenone B (**3.31**) (CLogP = 4.59) in water, a pegylated<sup>152</sup> version was constructed. Epoxide **3.50** in triethylene glycol (**3.51**) as the solvent in the presence of catalytic amounts of bismuth triflate gave the PEG analogue **3.52** (CLogP = 4.39). The glycerol fragment of the niphatenones is also found in EPI-001<sup>141</sup> (**3.6**) (Figure 3.4), a highly effective antagonist of the AR NTD. It was found that the chlorohydrin functionality of EPI-001 (**3.6**) is required for its AR NTD antagonist properties. Therefore, it was of interest to construct the chlorohydrin analogue of (*R*)-niphatenone B

(**3.31**). This was accomplished by opening the epoxide of **3.50** with cerous chloride to give chlorohydrin **3.53** (Scheme 3.9).

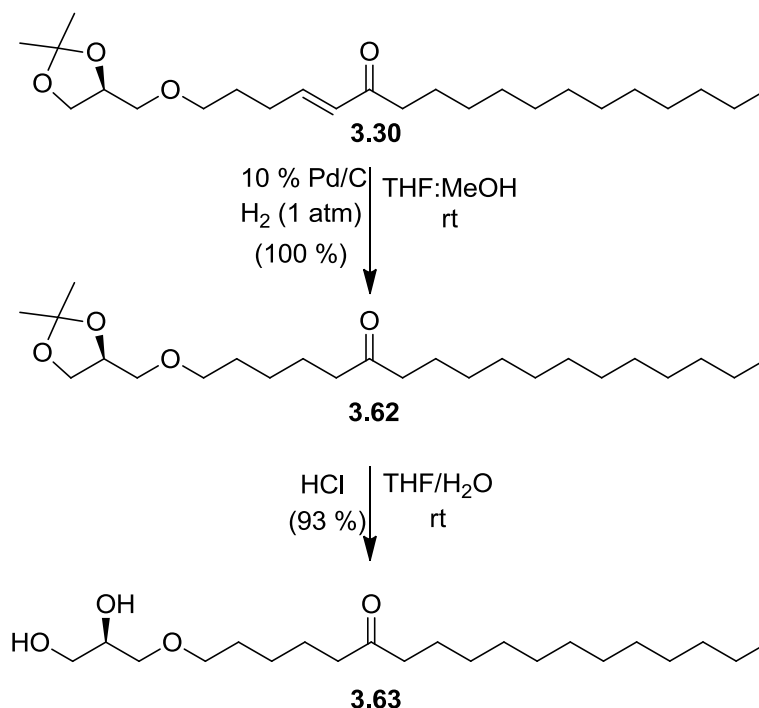
It has been shown that fluorine substitution in the context of small molecule drug development allows for enhanced physical chemical properties and metabolic stabilities.<sup>153</sup> With this in mind, fluorohydrin **3.54** was prepared from **3.31** using Xtal-FluorE<sup>®154</sup> (Scheme 3.9).



**Scheme 3.10** All carbon backbone (*R*)-niphatenone B (**3.31**) analogue **3.61**.

Next we constructed the all carbon backbone version of (*R*)-niphatenone B (**3.31**) (Scheme 3.10). The synthesis began by brominating primary alcohol **3.55** using the Appel reaction to provide bromide **3.56**. Next, bromide **3.26** was dissolved in tetrahydrofuran and in

the presence of magnesium metal formed the Grignard reagent *in situ*, followed by alkylation with bromide **3.56** to give benzyl protected acetonide **3.57** (Scheme 3.10). Deprotection of **3.57** with 10 % palladium/charcoal under H<sub>2</sub> (1 atm) followed by DMP oxidation afforded aldehyde **3.59**. Subsequent HWE olefination between aldehyde **3.59** and phosphonate **3.25** gave intermediate **3.60**. Acetonide deprotection of enone **3.60** gave the all carbon backbone analogue **3.61** (Scheme 3.10). In addition to the alkyl and glycerol moieties, the niphatenones also contain an enone functionality, which may be a potential Michael acceptor to the biological target. In order to determine if there is a covalent binding mechanism between the niphatenones, and the AR by a Michael addition, a reduced version of (*R*)-niphatenone B (**3.31**) was constructed in analogue **3.63** (Scheme 3.11).



**Scheme 3.11** Dihydro (*R*)-niphatenone B (**3.31**) analogue **3.63**.

Acetonide **3.30** was hydrogenated in the presence of 10 % palladium/charcoal and H<sub>2</sub> (1 atm) to give **3.62**. Compound **3.62** was deprotected with HCl in a mixture of tetrahydrofuran and water to give analogue **3.63** (Scheme 3.11). Biological testing of **3.63** (Section 3.5) showed attenuated activity relative to (*R*)-niphatenone B (**3.31**), which indicated a potential covalent interaction between the natural products and the NTD of the AR.

#### **3.4 Synthesis of a Click Chemistry Probe and Fluorescent Probe**

The decreased biological activity that was obtained from the reduced enone analogue **3.63** suggested covalent binding between the natural product and the NTD of the AR. To test our hypothesis, a chemical probe (Chapter 2, Section 2.5) based on (*R*)-niphatenone B (**3.31**) was constructed. The probe needed to incorporate functionality that would allow for the attachment of a fluorophore for visualization of the probe-ligand complex after covalent binding had occurred (Figure 3.8).

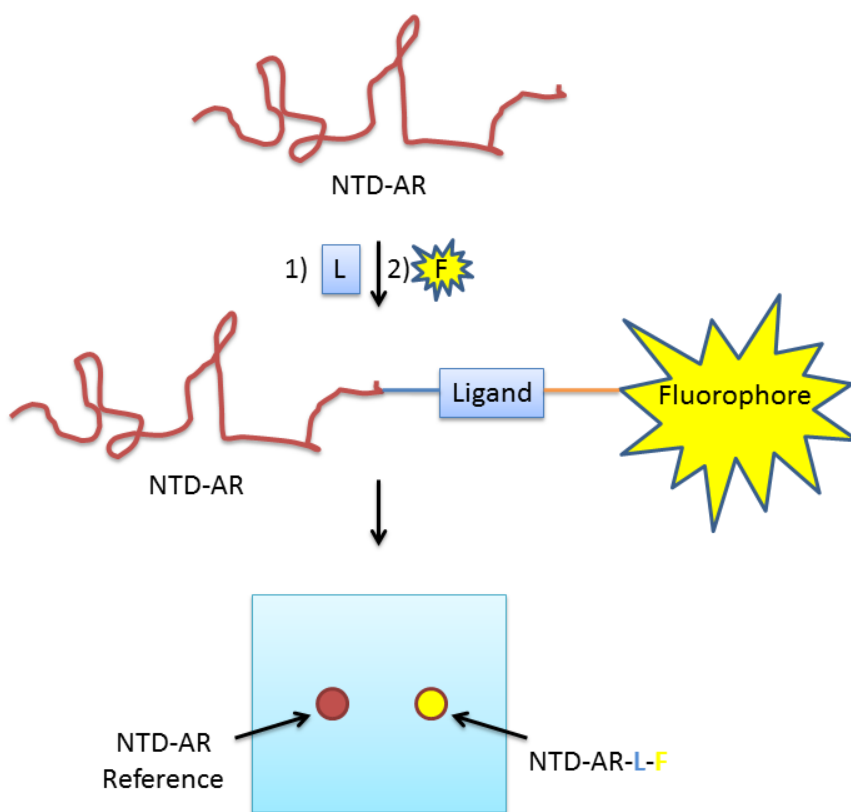


**Figure 3.8** Fluorescent probe mode of action.

Fluorescent probes have been developed for *in vitro* and *in vivo* imaging of different biological targets.<sup>155</sup> There are two main types of fluorescent imaging probes (Figure 3.9). Non-targeting probes do not have affinity for a specific biological target, and are typically used to observe a biological process. An example is indocyanine green (**3.64**),<sup>156</sup> which is in current clinical use for evaluating blood flow and clearance (Figure 3.9).

The second type of fluorescent imaging probe is a targeting probe in which a fluorophore is bound to a ligand that has a high affinity for a biological target. Accumulation of the fluorophore at the target site allows for visualization of the desired tissue. An example

of an active probe is the quinoline derivative TDPQ (**3.65**),<sup>157</sup> which is a selective non-steroidal AR antagonist, with fluorescent properties (Figure 3.9).

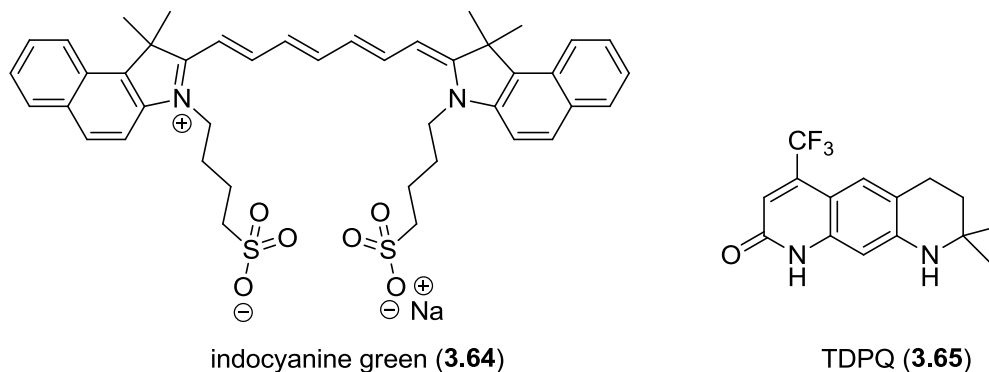
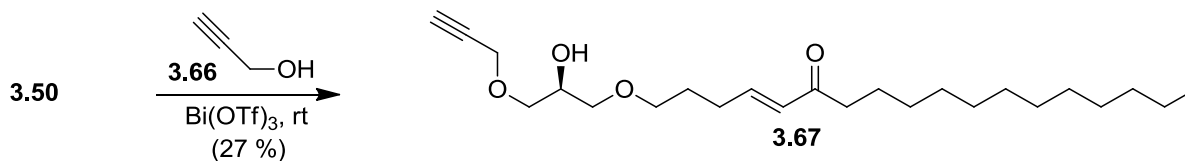


**Figure 3.9** Non-targeting and targeting fluorescent probes.

We chose click chemistry<sup>111</sup> to attach the fluorophore to the probe-ligand complex. This led to the construction of the propargyl ether probe **3.67**. The synthesis started with epoxide analogue **3.50** and ring opening with propargyl alcohol (**3.66**) in the presence of catalytic amounts of bismuth triflate gave the propargyl ether analogue **3.67** (Scheme 3.12).

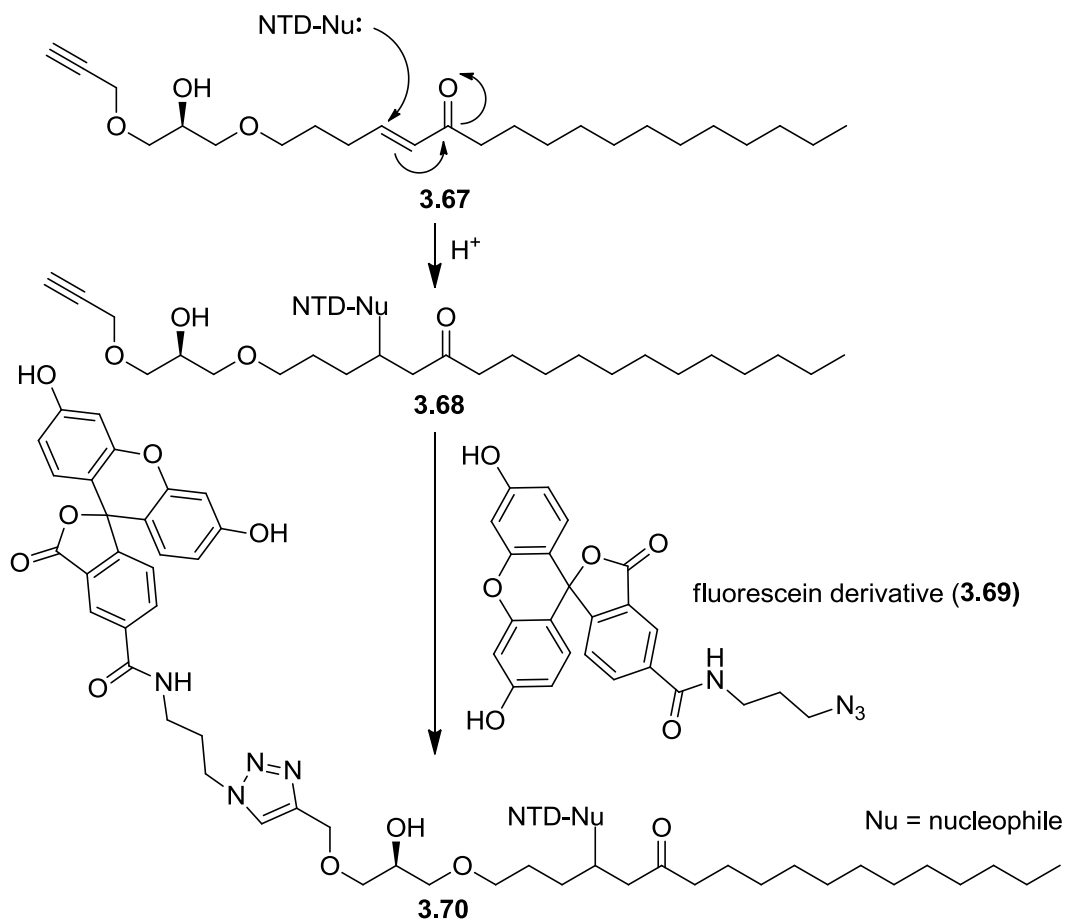


**Scheme 3.12** Propargyl ether analogue **3.67**.

The fluorescent tag chosen was a fluorescein derivative (**3.69**) carrying an azide<sup>158</sup> moiety, which allows for attachment using click chemistry. Scheme 3.13 illustrates a

potential mechanism for the covalent binding between probe **3.67** and the NTD of the AR.

The results are described in Section 3.5.



**Scheme 3.13** Click chemistry of probe **3.67** and fluorophore **3.69**.

An alternative fluorescent probe for the NTD of the AR was also designed based on (*S*)-niphatenone B (**3.35**). Instead of using a tagged approach as in probe **3.67**, the enone functionality was incorporated into the fluorophore, similar to a fluorescent imaging agent developed to detect cellular glutathione by Kim *et al.* (Figure 3.10).<sup>159</sup> The basis of the design is that the unreacted form in **3.71** emits a green fluorescence, however, when the

conjugation is disrupted by the nucleophilic attack of GSH to give **3.72** a blue shift in fluorescence emission occurs. This allowed for cellular imaging and detection of GSH *in vivo*. Since the coumarin-based fluorescent probe in **3.71** contained an enone functionality that was also found in the niphatenones, **3.71** was incorporated into the natural product, similar to some reported for fluorescent estrogen receptor ligands.<sup>160</sup>

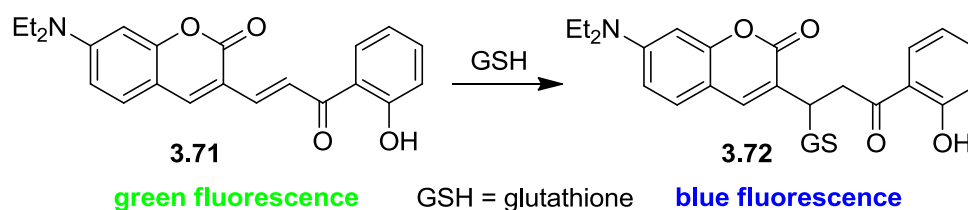
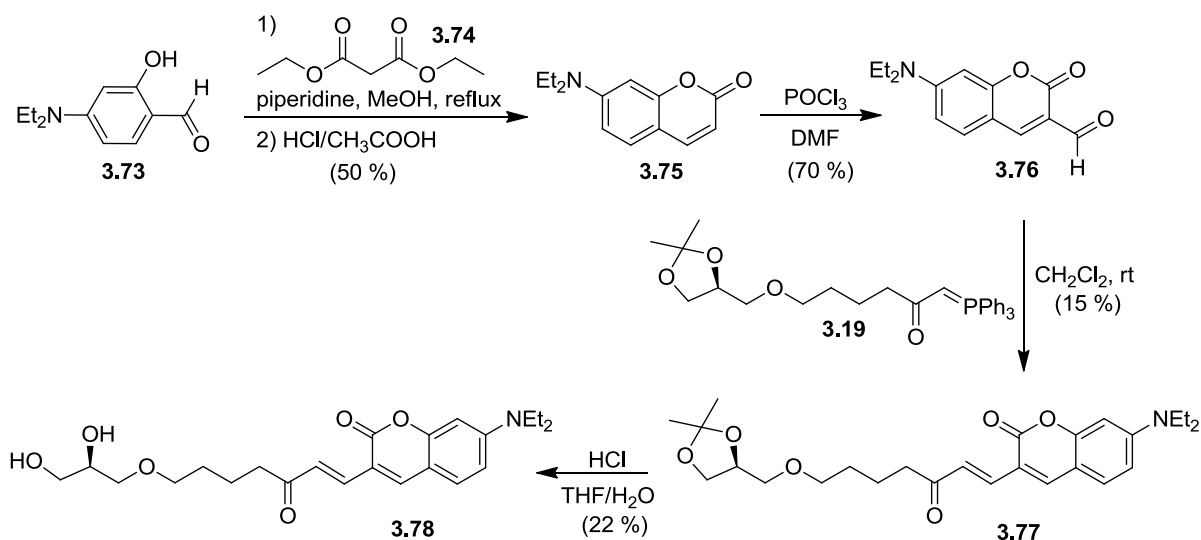


**Figure 3.10** Cellular imaging agent of glutathione.

The synthesis of a potential fluorescent probe for the NTD of the AR started with commercially available aldehyde **3.73** which was cyclized with diethyl malonate under basic conditions, followed by refluxing in acid to give coumarin **3.75** (Scheme 3.14). Intermediate **3.75** underwent the subsequent Vilsmeier-Haack reaction to give aldehyde **3.76** following known protocol.<sup>161</sup> Aldehyde **3.76** was then reacted with Wittig reagent **3.19** used in the synthesis of (*R*) (**3.31**) and (*S*)-niphatenone B (**3.35**) (Scheme 3.1), to give acetone **3.77**. Deprotection of **3.77** yielded coumarin analogue **3.78**, a potential fluorescent probe of the NTD AR (Scheme 3.14). Dr. Marianne Sadar at the BC Cancer Agency is currently investigating compound **3.78**.



**Scheme 3.14** Synthesis of a potential AR NTD fluorescent probe (**3.78**).

### 3.5 Biological Results

The biological activities of the natural product (*S*)-niphatenones A (**3.23**), and B (**3.35**), along with selected synthetic analogues were tested in an assay that measures AR transcriptional activity<sup>140</sup> (Figure 3.11). This assay consists of transfecting LNCaP human prostate cancer cells that express functional AR, with a luciferase reporter that is regulated by the AR in response to androgen. If a compound is an AR antagonist, the amount of light emission produced by luciferase when cells are stimulated with a synthetic androgen or forskolin is diminished.

All the compounds were tested at a concentration of 7  $\mu$ M with the exception of **3.43**, which was limited to 3.5  $\mu$ M due to poor solubility. (*S*)-Niphatenone B (**3.35**) shows approximately 50 % inhibition at the test concentration, while (*S*)-niphatenone A (**3.23**) shows weaker activity.

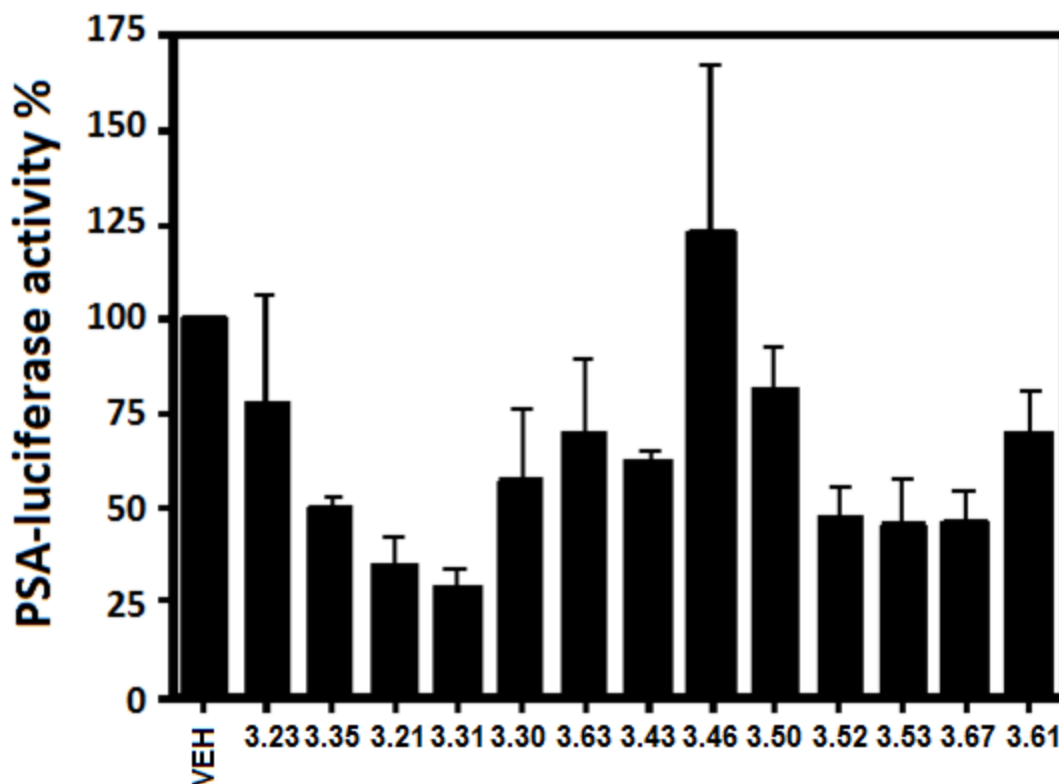


**Figure 3.11** AR transcriptional activity assay of the niphatenones and their analogues.

The synthetic unnatural enantiomers (*R*)-niphatenone A (**3.21**) and (*R*)-niphatenone B (**3.31**) are both more active than the corresponding natural (*S*) isomers **3.23** and **3.35**. (*R*)-niphatenone B (**3.31**) is the most active compound tested in this series. The reduced enone analogue (**3.63**) is less active than (*R*)-niphatenone B (**3.31**), but only slightly less active than (*S*)-niphatenone B (**3.35**). This indicates that the enone moiety plays a role in the activity of (*R*)-niphatenone B (**3.31**), and most likely plays a role for the other analogues. However, covalent binding is not required for activity in the assay. Lengthened alkyl chain analogue **3.43** is about half as active as (*R*)-niphatenone B (**3.31**) at half the concentration. Analogue **3.46** with a one-carbon alkyl substituent has essentially lost all activity. This indicates that

the alkyl substituent is necessary for activity and that there is most likely an ideal chain length.

Removing the glycerol ether oxygen atom from the linear skeleton of (*R*)-niphatenone B (**3.31**) to give the all carbon chain analogue **3.61** produced a compound with roughly half the activity of **3.31**. This indicates that the glycerol ether moiety plays a role in the activity, most likely through hydrogen bonding. Similarly, acetonide **3.30** and epoxide **3.50** are less active than **3.31**. PEG ether (**3.52**), chlorohydrin (**3.53**), and alkyne ether (**3.67**) analogues are all less active than (*R*)-niphatenone B (**3.31**) and comparable in activity to the natural product (*S*)-niphatenone B (**3.35**). The diminished activity observed for analogues **3.52**, **3.53**, and **3.67** can perhaps be attributed to the loss of the glycerol primary alcohol as it was also the case for acetonide **3.30**, and the epoxide **3.50**. While these modifications were successful for EPI-001 (**3.7**), they were unfruitful for the niphatenones and suggest a different binding mechanism.

Next, an *in vitro* assay was completed to observe whether the effects of the niphatenones are due to non-specific toxicity, or due to a specific interaction with the AR. This was accomplished by comparing the proliferation of LNCaP (AR<sup>-</sup>) cells versus PC3 (AR<sup>+</sup>) cells (Figure 3.12). The assay works by incubating LNCaP cells in the presence of a known androgen R1881 (metribolone), causing mitogenic effects, in addition to the test compound. If the compound inhibits the AR there should be little to no R1881 stimulated proliferation of LNCaP cells. The reference experiment is done with bicalutamide (**3.4**), a known AR antagonist resulting in no R1881 stimulated proliferation. When (*S*)-niphatenone B (**3.35**) and (*R*)-niphatenone B (**3.31**) were tested, they inhibited R1881-induced proliferation of LNCaP cells at comparable concentrations to bicalutamide (**3.4**). The same

concentration of either (*S*) or (*R*) niphatenone B (**3.35**) or (**3.31**) had no effect on the proliferation of PC3 cells that do not express functional AR. This suggests that the niphatenones are AR antagonists and that their activity is not due to non-specific toxicity (Figure 3.12).

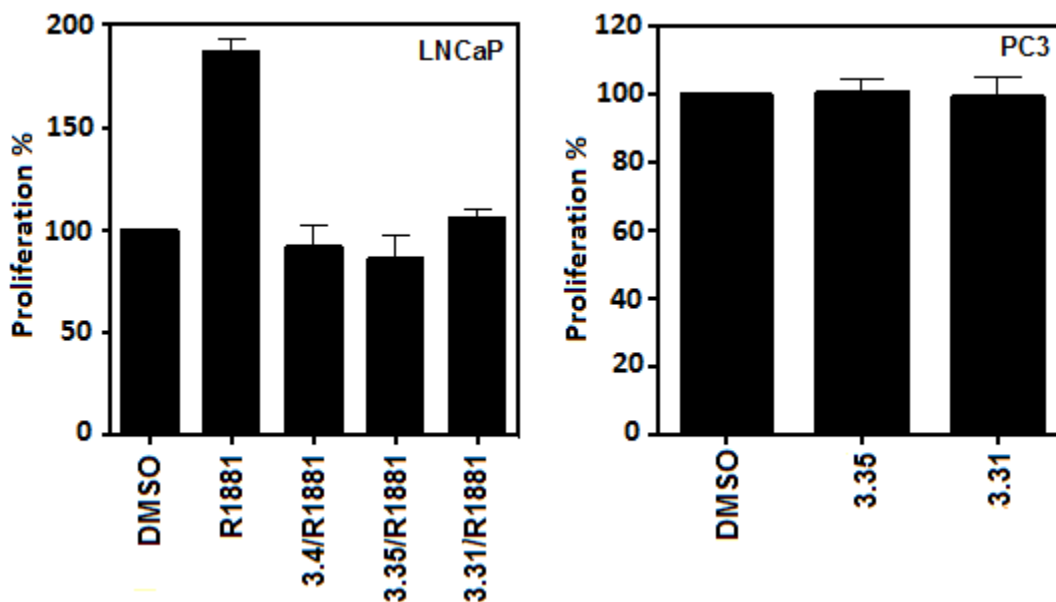


**Figure 3.12** Androgen induced proliferation assay.

To determine if (*R*)-niphatenone B (**3.31**) is an AR NTD antagonist, the click chemistry probe **3.67** was utilized. Since **3.67** was found to be active in the AR transcriptional activity assay (Figure 3.11) it was a viable click chemistry probe. The click chemistry experiment began by exposing analogue **3.67** to recombinant NTD AF1 protein. After 50 minutes of exposure at 0 °C, click chemistry was used to attach a fluorescein tag (**3.69**, Scheme 3.13) and the protein was analyzed using a SDS PAGE gel. Figure 3.13 shows that the band corresponding to the AF1 protein is labeled with the fluorescent tag,

demonstrating that the probe **3.67** binds covalently to the NTD AF1 protein. The niphatenones represent the first AR NTD antagonists that were shown to bind covalently.

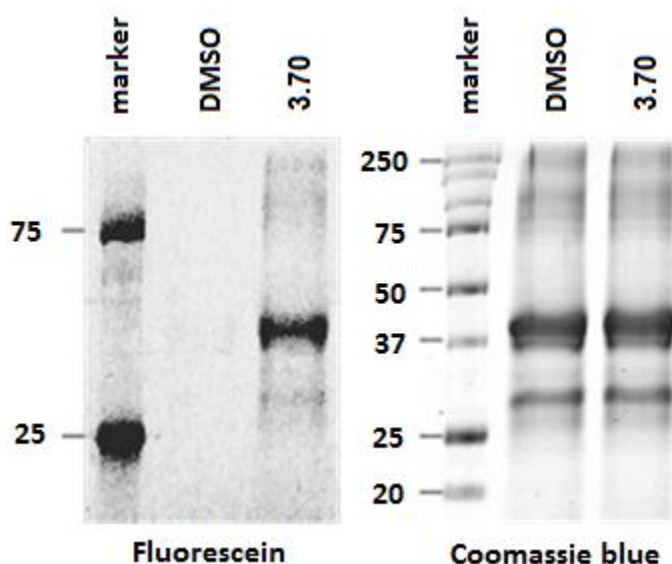


**Figure 3.13** Binding between alkyne probe **3.67** and the NTD AF1 region of the AR.

### 3.6 Conclusion

The NTD of the AR has been identified as a novel therapeutic target in the development of small molecules for combating CRPC, which is an advanced stage of prostate cancer. Current therapies are ineffective for the treatment of CRPC. In a continued effort to identify small molecule AR NTD antagonists isolated from the marine environment, the glycerol ethers niphatenone A (**3.8**) and B (**3.9**) were identified. These marine natural products represent a novel class of AR NTD antagonist pharmacophores. However, the small quantities isolated from the sponge prevented the assignment of the absolute configuration and any further biological testing.

Each natural product contains one stereocenter, and the synthesis of all four possible stereoisomers of the two natural products was completed. The synthesis of (*R*) (**3.21**) and (*S*)-niphatenone A (**3.23**) was completed in an 18 % overall yield. The synthesis of (*R*) (**3.31**) and (*S*)-niphatenone B (**3.35**) was completed in a 32 % overall yield. Chiral HPLC analysis using synthetic and natural material revealed that both natural products have the (*S*) configuration.

Having designed a robust synthesis for both natural products, further biological testing was possible. Both (*R*) (**3.31**) and (*S*)-niphatenone B (**3.35**) were found to inhibit androgen induced proliferation in an *in vitro* assay using LNCaP cells expressing the AR. Comparison of *in vitro* data with PC3 cells lacking the AR showed no inhibition. This suggested that these compounds are antagonists of the AR and that their activity was not due to cell toxicity. This result suggests target specificity, which is a key step towards developing therapeutic compounds.

To gain more insight into this novel pharmacophore, a number of analogues based on (*R*)-niphatenone B (**3.31**) were constructed and assayed. Several conclusions were drawn from this data: 1) the unnatural (*R*) configuration is more potent than the natural (*S*) configuration, 2) any modification to the glycerol moiety attenuates the activity, 3) there is an ideal chain length for enhanced activity, 4) the enone moiety plays a role in the activity but is not required. These results suggest a clear SAR and the potential to construct analogues that retain much of the activity without the undesirable enone functionality.

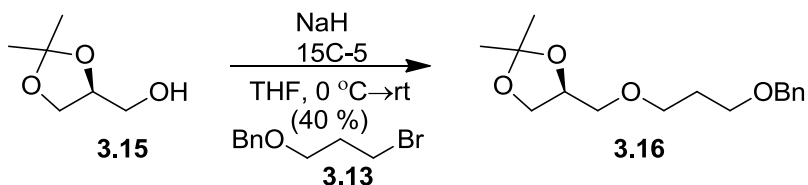
Finally, a propargyl ether analogue (**3.67**) was constructed for use as a click chemistry probe that was used to demonstrate that (*R*)-niphatenone B (**3.31**), binds covalently to the AF1 region of the NTD AR. (*R*)-niphatenone B (**3.31**) represents the first known NTD

AR antagonist with a binding mechanism elucidated using click chemistry. Having completed an SAR study along with determining the mode of interaction to the NTD AR, the niphatenones and their corresponding analogues represent potential lead compounds for the development of therapeutics for the treatment of CRPC.

### 3.7 Experimental

**General Methods:** All non-aqueous reactions were carried out in flame-dried glassware and under an Ar or N<sub>2</sub> atmosphere unless otherwise noted. Air and moisture sensitive liquid reagents were manipulated via a dry syringe. All solvents and reagents were used as obtained from commercial sources without further purification. <sup>1</sup>H and <sup>13</sup>C NMR spectra were obtained on Bruker Avance 400 direct, 300 direct, or Bruker Avance 600 CryoProbe spectrometers at room temperature. Flash column chromatography was performed using Silicycle Ultra-Pure silica gel (230-400 mesh). Analytical thin-layer chromatography (TLC) plates were aluminum-backed ultrapure silica gel 250 μm. Electrospray ionization mass spectrometry (ESI-MS) spectra were recorded on a Micromass LCT instrument. Optical rotations were measured with a JASCO P-1010 polarimeter at 24 °C and 589 nm (sodium D line) in ethyl acetate (g/mL).

### Preparation of 3.16:



Tetrahydrofuran (45 mL) was added to sodium hydride (436 mg, 10.9 mmol, 60 % suspension in oil) that was washed twice with hexanes (20.0 mL total) and the suspension was cooled to 0 °C. To this was added alcohol **3.15** (720 mg, 5.45 mmol) neat, along with 15C-5 (240 mg, 1.09 mmol). The mixture was then allowed to stir at room temperature for 1 h, after which bromide **3.13** (2.5 g, 10.9 mmol) was added dropwise. After 4.5 h the reaction mixture was cooled to 0 °C and quenched with the addition of 50 mL of water, and the aqueous phase was extracted three times with methylene chloride (250 mL). The organic extracts were dried with MgSO<sub>4</sub>, and concentrated using a rotary evaporator. The crude mixture was purified using flash column chromatography (hexanes:ethyl acetate 9:1) to give **3.16** as a clear oil (623 mg, 2.22 mmol, 40 %). <sup>1</sup>H NMR (400 MHz, CDCl<sub>3</sub>) δ 7.33 (m, 4H), 7.28 (m, 1H), 4.50 (s, 2H), 4.25 (quin, J = 5.8 Hz, 1H), 4.04 (dd, J = 6.5, 1.7 Hz, 1H), 3.71 (dd, J = 6.1, 2.1 Hz, 1H), 3.56 (m, 5H), 3.42 (dd, J = 5.5, 4.4 Hz, 1H), 1.90 (quin, J = 6.1 Hz, 2H), 1.42 (s, 3H), 1.37 (s, 3H); <sup>13</sup>C NMR (100 MHz, CDCl<sub>3</sub>) δ 138.7, 128.5, 127.8, 127.7, 109.5, 74.9, 73.1, 72.1, 68.8, 67.3, 66.9, 30.2, 26.9, 25.6. HRESIMS [M + H]<sup>+</sup> calcd for C<sub>16</sub>H<sub>25</sub>O<sub>4</sub> 281.1753, found 281.1747; [α]<sub>D</sub><sup>24</sup> = +13.6° (c 0.12).

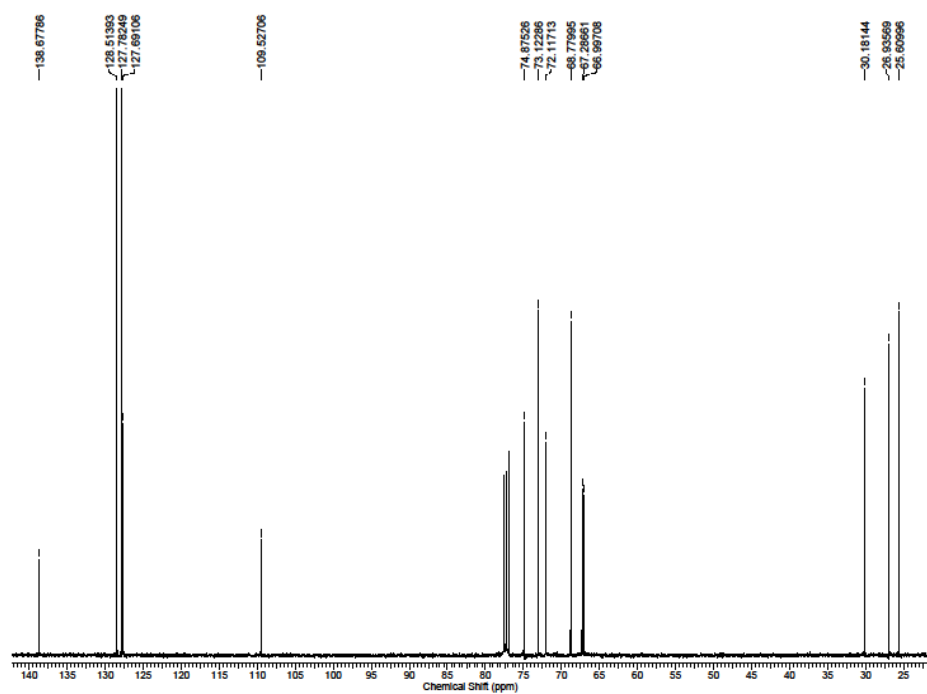
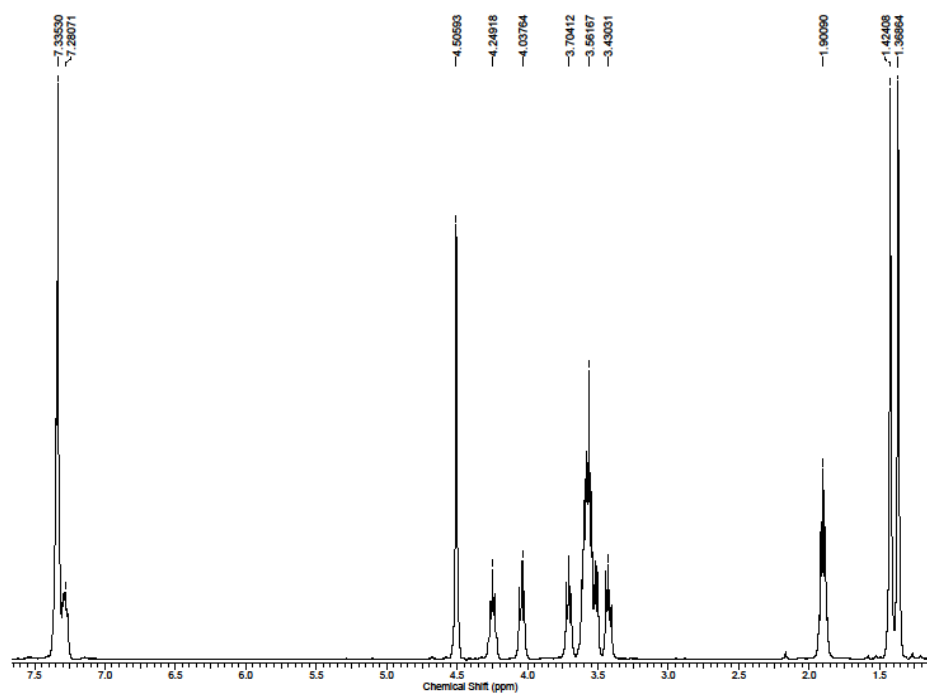
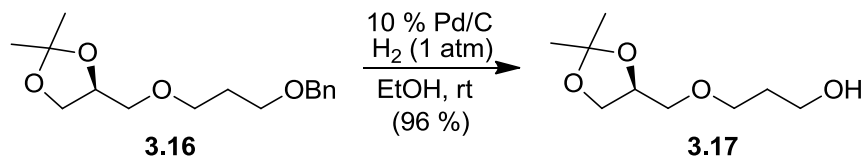


**Figure 3.14**  $^1\text{H}$  and  $^{13}\text{C}$  NMR spectra of **3.16** recorded in  $\text{CDCl}_3$  at 400 MHz and 100 MHz respectively.

### Preparation of 3.17:



To compound **3.16** (575 mg, 2.05 mmol) dissolved in 2.6 mL of ethanol was added 10 % Pd/C (133 mg), in a round bottom and the system flushed with H<sub>2</sub>. The reaction mixture was then exposed to 1 atm of H<sub>2</sub> (balloon) overnight. Upon completion, the heterogeneous mixture was filtered and the filtrate washed three times with ethanol (60 mL). The organic extracts were concentrated using a rotary evaporator, and the crude mixture was purified using flash column chromatography (hexanes:ethyl acetate 1:1), to give **3.17** as a clear oil (375 mg, 1.97 mmol, 96 %). <sup>1</sup>H NMR (400 MHz, CDCl<sub>3</sub>) δ 4.16 (quin, J = 5.8 Hz, 1H), 3.94 (dd, J = 8.2, 6.5 Hz, 1H), 3.62 (m, 3H), 3.54 (t, J = 6.0 Hz, 2H), 3.39 (m, 2H), 3.02 (s, 1H), 1.72 (quin, J = 6.0 Hz, 2H), 1.31 (s, 3H), 1.25 (s, 3H); <sup>13</sup>C NMR (100 MHz, CDCl<sub>3</sub>) δ 109.5, 74.7, 71.9, 69.9, 66.6, 60.6, 32.2, 26.7, 25.4. HRESIMS [M + Na]<sup>+</sup> calcd for C<sub>9</sub>H<sub>18</sub>O<sub>4</sub>Na 213.1103, found 213.1105; [α]<sub>D</sub><sup>24</sup> = +16.3° (c 0.12).

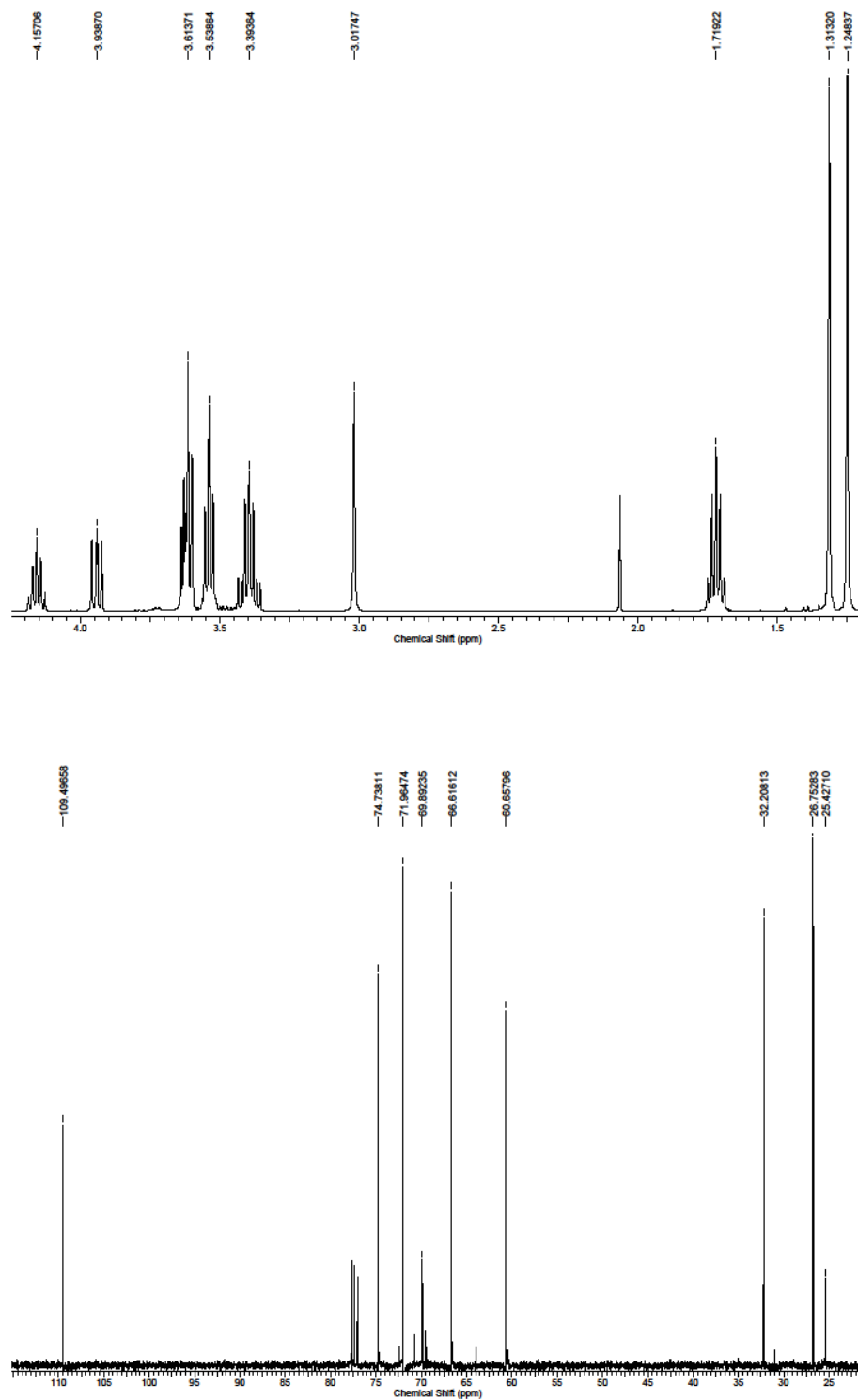
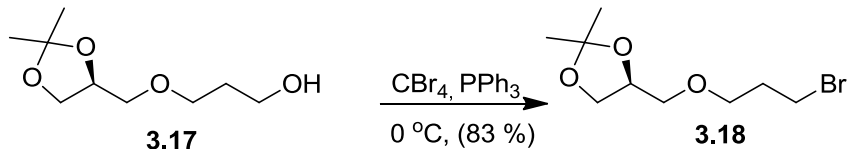


**Figure 3.15**  $^1\text{H}$  and  $^{13}\text{C}$  NMR spectra of **3.17** recorded in  $\text{CDCl}_3$  at 400 MHz and 100 MHz respectively.

### Preparation of 3.18:



To alcohol **3.17** (150 mg, 0.788 mmol) dissolved in 2 mL of methylene chloride was added  $\text{PPh}_3$  (248 mg, 0.946 mmol) and the solution was cooled to 0 °C.  $\text{CBr}_4$  was added to this solution and it was stirred for 1 h after which the mixture was concentrated under a stream of nitrogen. The crude mixture was purified using flash column chromatography (hexanes:ethyl acetate 12:1), to give **3.18** as a clear oil (166 mg, 0.657 mmol, 83 %).  $^1\text{H}$  NMR (400 MHz,  $\text{CDCl}_3$ )  $\delta$  4.19 (quin,  $J = 6.0$  Hz, 1H), 3.98 (dd,  $J = 6.5, 1.7$  Hz, 1H), 3.65 (dd,  $J = 6.5, 1.7$  Hz, 1H), 3.54 (td,  $J = 5.9, 2.6$  Hz, 2H), 3.43 (m, 4H), 2.04 (td,  $J = 6.2, 2.9$  Hz, 2H), 1.35 (s, 3H), 1.29 (s, 3H);  $^{13}\text{C}$  NMR (100 MHz,  $\text{CDCl}_3$ )  $\delta$  109.5, 74.7, 72.2, 69.0, 66.7, 32.8, 30.6, 26.9, 25.5. HRESIMS  $[\text{M} + \text{H}]^+$  calcd for  $\text{C}_9\text{H}_{18}\text{O}_3^{79}\text{Br}$  253.0439, found 253.0439.

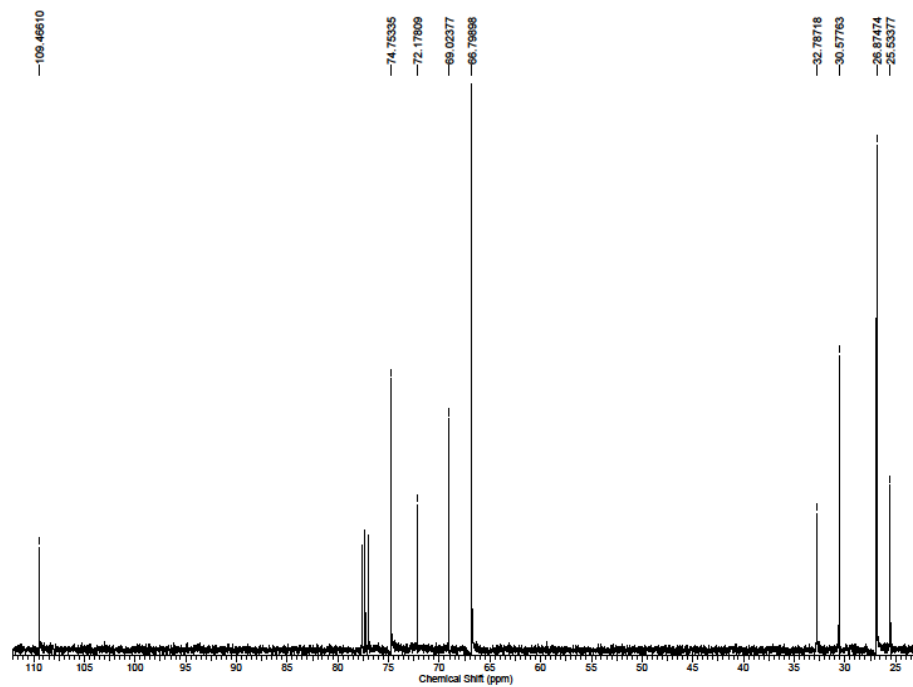
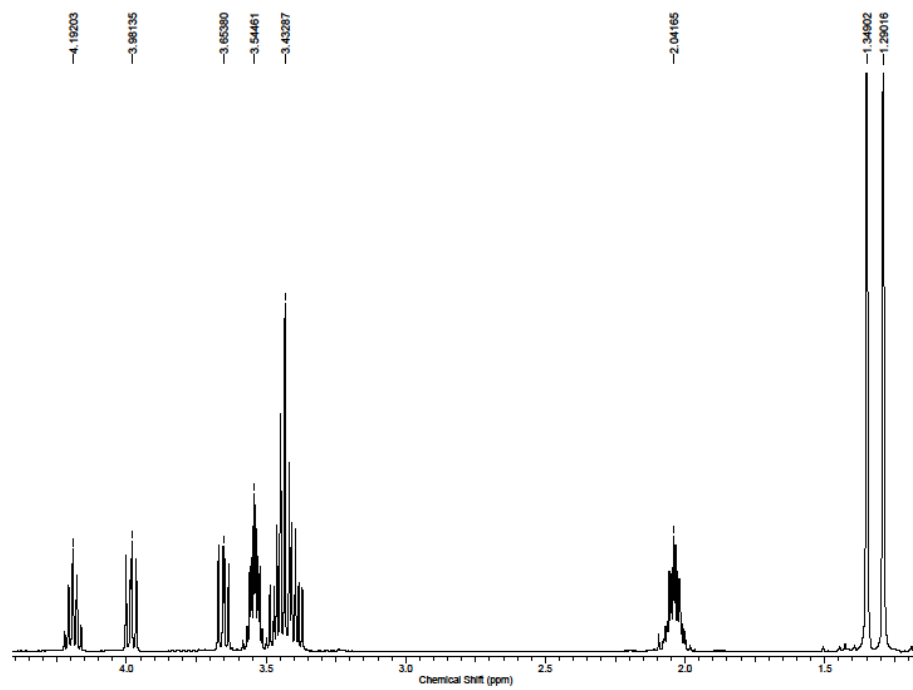
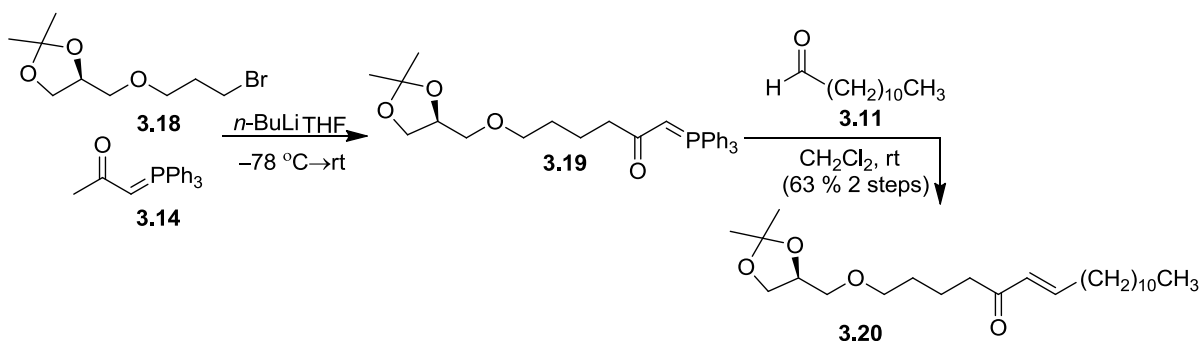


**Figure 3.16**  $^1\text{H}$  and  $^{13}\text{C}$  NMR spectra of **3.18** recorded in  $\text{CDCl}_3$  at 400 MHz and 100 MHz respectively.

### Preparation of 3.20:



Phosphorane **3.14** (248 mg, 0.78 mmol) was dissolved in 5 mL of tetrahydrofuran and the solution was cooled to  $-78\text{ }^{\circ}\text{C}$ . To this solution was added 1.6 M *n*-BuLi (0.53 mL, 0.86 mmol) and it was stirred for 20 min. To this solution, bromide **3.18** (166 mg, 0.66 mmol) dissolved in 0.5 mL methylene chloride was added dropwise, and the mixture was allowed to warm from  $0\text{ }^{\circ}\text{C}$  to room temperature overnight. The reaction mixture was then diluted with 50 mL of water and extracted three times with methylene chloride (250 mL). The organic extracts were dried with  $\text{MgSO}_4$  and concentrated using a rotary evaporator. The crude phosphorane (**3.19**) was then used immediately in the follow up Wittig reaction by dissolving it in 1 mL of methylene chloride and adding aldehyde **3.11** (121 mg, 0.657 mmol) before stirring at room temperature overnight. The reaction mixture was concentrated under a stream of  $\text{N}_2$ . The crude mixture was purified using flash column chromatography (hexanes:ethyl acetate 7:1), to give **3.20** as a clear oil (165 mg, 0.415 mmol, 63 % over 2 steps).  $^1\text{H}$  NMR (400 MHz,  $\text{CDCl}_3$ )  $\delta$  4.19 (dt,  $J = 16.0, 7.2$  Hz, 1H), 6.01 (d,  $J = 16.0$  Hz, 1H), 4.19 (quin,  $J = 6.1$  Hz, 1H), 3.99 (dd,  $J = 8.2, 6.5$  Hz, 1H), 3.66 (dd,  $J = 6.5, 1.7$  Hz, 1H), 3.42 (m, 4H), 2.50 (t,  $J = 7.2$  Hz, 2H), 2.15 (q,  $J = 6.8$  Hz, 2H), 1.57 (m, 4H), 1.40 (m, 1H), 1.35 (s, 3H), 1.30 (s, 3H), 1.21 (m, 17H), 0.82 (t,  $J = 6.8$  Hz, 3H);  $^{13}\text{C}$  NMR (100 MHz,  $\text{CDCl}_3$ )  $\delta$  200.4, 147.5, 130.3, 109.4, 74.8, 71.9, 71.5, 66.9, 39.7, 32.5, 32.0, 29.7, 29.7, 29.6,

29.5, 29.4, 29.3, 29.2, 28.2, 26.9, 25.5, 22.8, 20.9, 14.2. HRESIMS  $[M + H]^+$  calcd for  $C_{24}H_{45}O_4$  397.3318, found 397.3310;  $[\alpha]_D^{24} = +11.4^\circ$  (*c* 0.09).

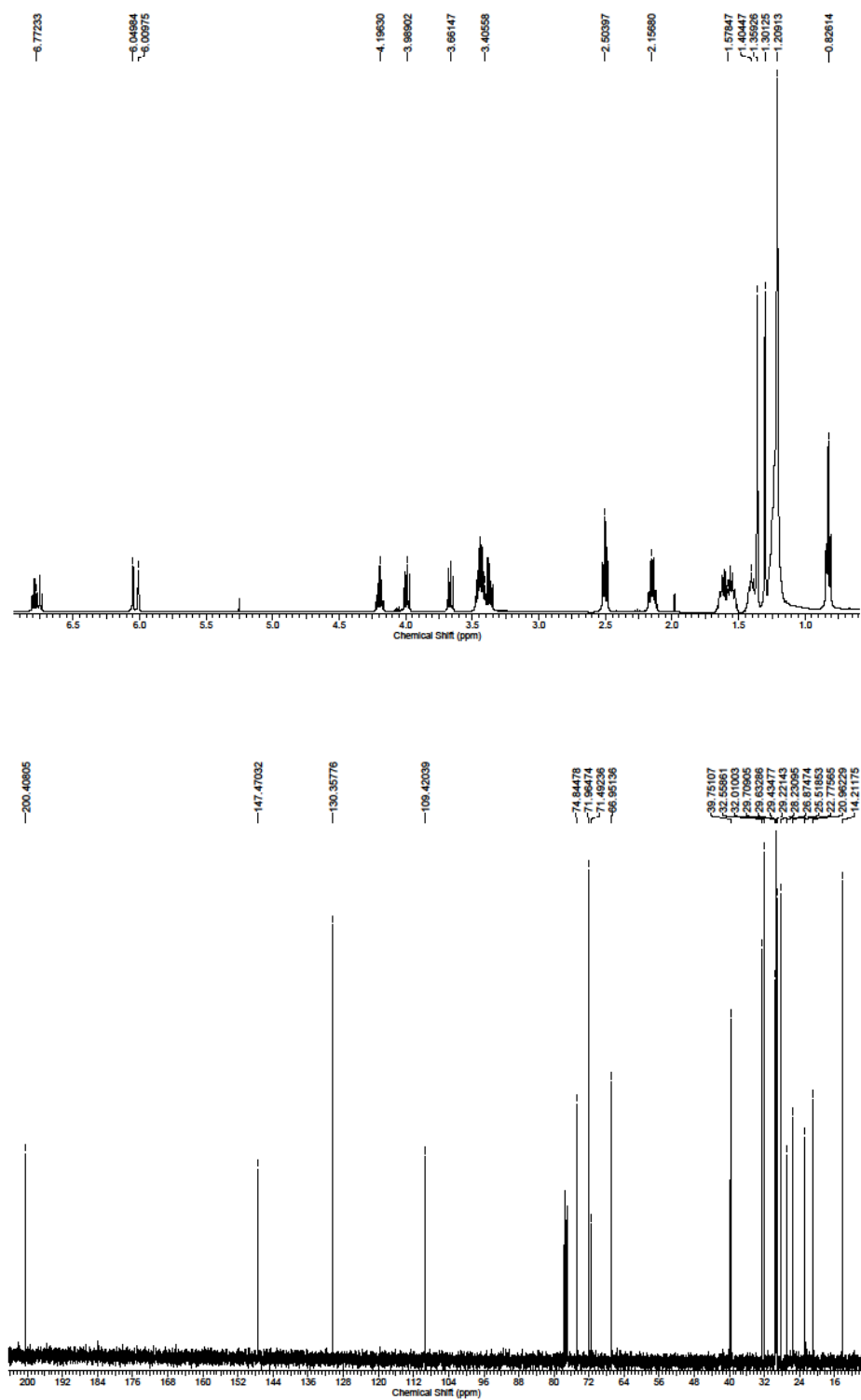
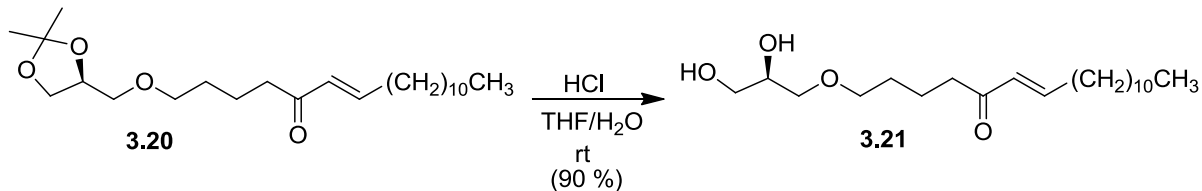


**Figure 3.17**  $^1\text{H}$  and  $^{13}\text{C}$  NMR spectra of **3.20** recorded in  $\text{CDCl}_3$  at 400 MHz and 100 MHz respectively.

### Preparation of 3.21:



To acetonide **3.20** (45 mg, 0.11 mmol), dissolved in 1.65 mL of a tetrahydrofuran:water mixture (5:1), was added 12.4 M HCl (0.045 mL, 0.56 mmol), and the solution was stirred at room temperature for 30 min. The reaction mixture was then quenched with the addition of saturated NaHCO<sub>3</sub> (50 mL) and the aqueous phase was extracted three times with methylene chloride (100 mL). The organic extracts were dried with MgSO<sub>4</sub> and concentrated using a rotary evaporator. The crude mixture was purified using flash column chromatography (hexanes:ethyl acetate 1:4) to give **3.21** as a white solid (35 mg, 0.099 mmol, 90 %). <sup>1</sup>H NMR (600MHz, C<sub>6</sub>D<sub>6</sub>)  $\delta$  6.70 (dt, J = 15.6, 7.2 Hz, 1H), 6.03 (d, J = 15.6 Hz, 1H), 3.91 (bs, 1H), 3.81 (bs, 1H), 3.73 (m, 1H), 3.66 (m, 1H), 3.41 (m, 2H), 3.26 (m, 2H), 3.28 (bs, 1H), 2.29 (t, J = 7.2 Hz, 2H), 1.90 (q, J = 6.6 Hz, 2H), 1.67 (quin, J = 7.2 Hz, 2H), 1.48 (quin, J = 6.6 Hz, 2H), 1.28 (m, 18H), 0.91 (t, J = 4.8 Hz, 3H); <sup>13</sup>C NMR (150 MHz, C<sub>6</sub>D<sub>6</sub>)  $\delta$  199.2, 146.6, 130.6, 72.6, 71.3, 71.3, 64.4, 39.8, 32.5, 32.3, 30.0, 30.0, 29.9, 29.8, 29.8, 29.6, 29.4, 28.4, 23.1, 21.0, 14.3. HRESIMS [M + Na]<sup>+</sup> calcd for C<sub>21</sub>H<sub>40</sub>O<sub>4</sub>Na 379.2824, found 379.2814; [ $\alpha$ ]<sub>D</sub><sup>24</sup> = +2.8° (c 0.07).

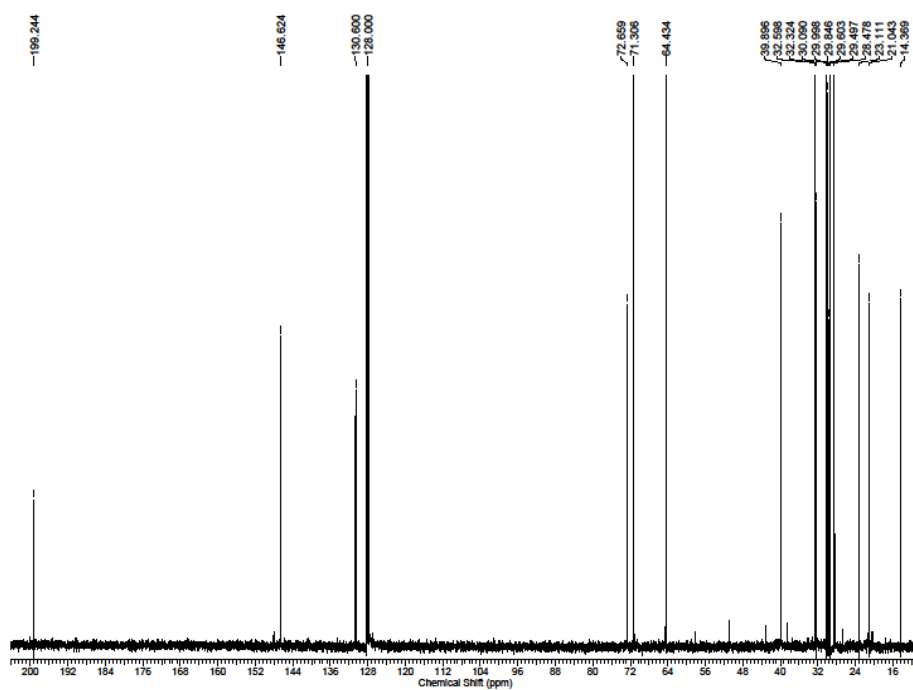
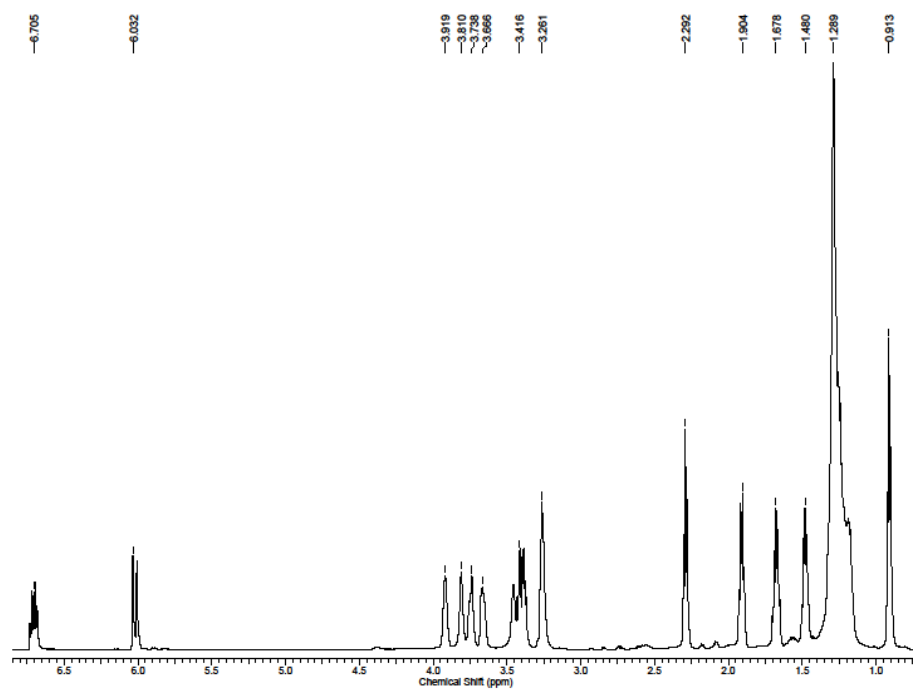
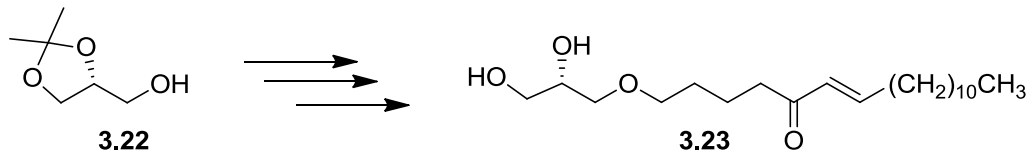


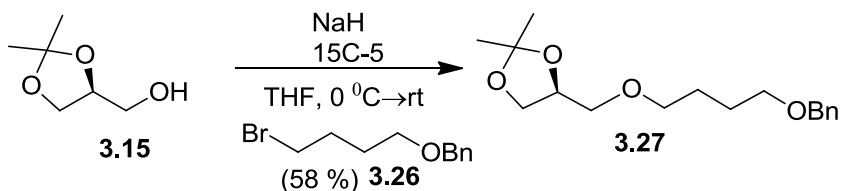
**Figure 3.18**  $^1\text{H}$  and  $^{13}\text{C}$  NMR spectra of **3.21** recorded in  $\text{C}_6\text{D}_6$  at 600 MHz and 150 MHz respectively.

**Preparation of 3.23:**



Procedures identical to those used to prepare **3.21**, only using (*R*)-4-hydroxymethyl-2,2-dimethyl-1,3-dioxolane (**3.22**) as the starting material. HRESIMS  $[M + Na]^+$  calcd for  $C_{21}H_{40}O_4Na$  379.2824, found 379.2813;  $[\alpha]_D^{24} = -2.5^\circ$  (*c* 0.08).

### Preparation of **3.27**:



NaH (330 mg, 8.2 mmol, 60 % suspension in oil) was washed twice with hexanes (20 mL total) and added to 4 mL of tetrahydrofuran to give a suspension that was cooled to 0 °C. To this suspension was added alcohol **3.15** (271 mg, 2.1 mmol) dissolved in 1 mL of tetrahydrofuran along with 15C-5 (90 mg, 0.41 mmol). The mixture was then allowed to stir at room temperature for 30 min. after which bromide **3.26** (1.0 g, 4.1 mmol) was added dropwise. After 4.5 h the reaction mixture was cooled to 0 °C and quenched with the addition of 100 mL of water, and the aqueous phase was extracted three times with methylene chloride (250 mL). The organic extracts were dried with MgSO<sub>4</sub> and concentrated using a rotary evaporator. The crude mixture was purified using flash column chromatography (hexanes:ethyl acetate 9:1), to give **3.27** as a clear oil (350 mg, 1.18 mmol, 58 %). <sup>1</sup>H NMR (400 MHz, CDCl<sub>3</sub>) δ 7.32 (m, 2H), 7.31 (m, 2H), 7.25 (m, 1H), 4.47 (s, 2H), 4.23 (quin, J = 6.0 Hz, 1H), 4.01 (dd, J = 8.2, 6.5 Hz, 1H), 3.70 (dd, J = 8.2, 6.5 Hz 1H), 3.45 (m, 5H), 3.39 (m, 1H), 1.66 (m, 4H), 1.41 (s, 3H), 1.34 (s, 3H); <sup>13</sup>C NMR (100 MHz, CDCl<sub>3</sub>) δ 138.7, 128.5, 127.7, 127.6, 109.4, 74.9, 72.9, 71.9, 71.6, 70.2, 67.0, 26.9, 26.9, 26.5, 26.5, 25.5. HRESIMS [M + Na]<sup>+</sup> calcd for C<sub>17</sub>H<sub>26</sub>O<sub>4</sub>Na 317.1729, found 317.1733; [α]<sub>D</sub><sup>24</sup> = +9.9° (c 0.35).

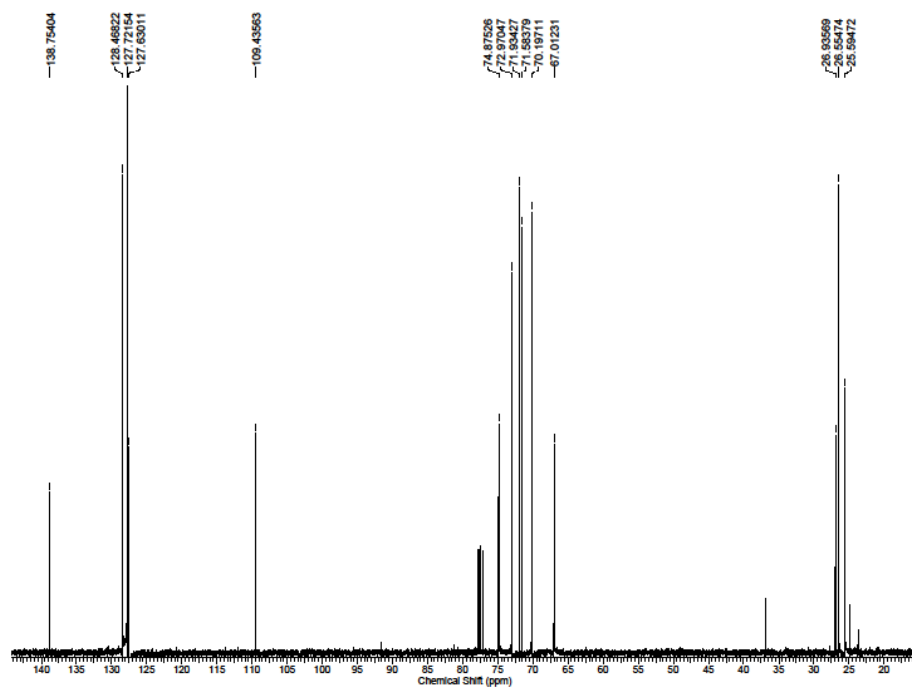
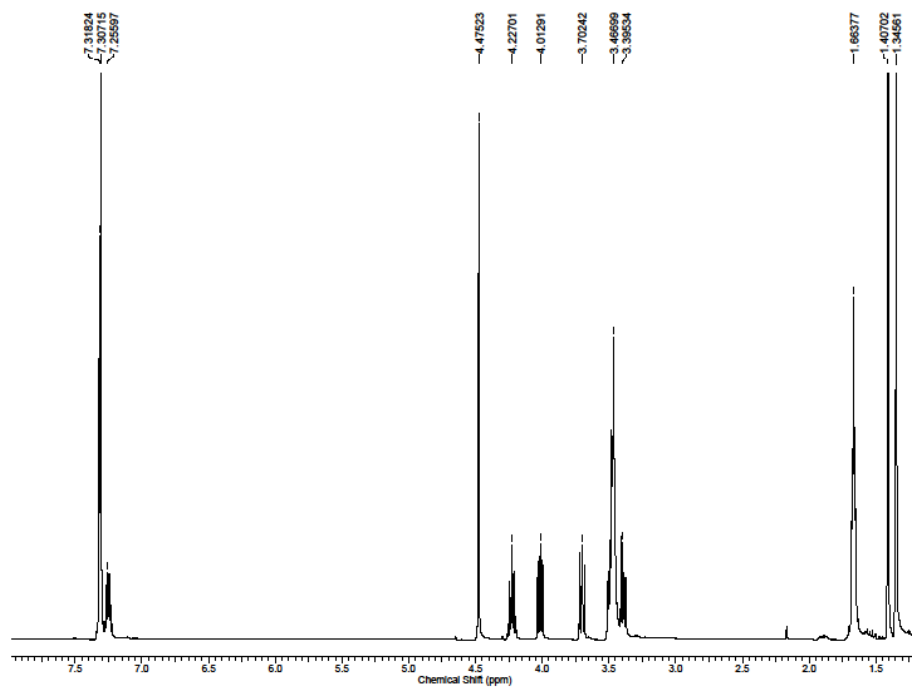
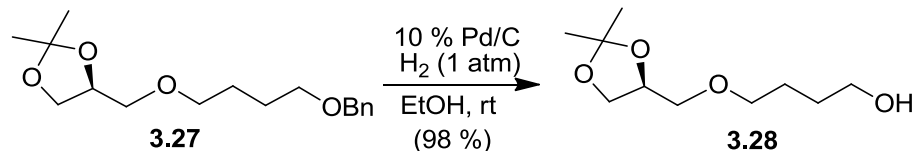


**Figure 3.19**  $^1\text{H}$  and  $^{13}\text{C}$  NMR spectra of **3.27** recorded in  $\text{CDCl}_3$  at 400 MHz and 100 MHz respectively.

### Preparation of 3.28:



To compound **3.27** (760 mg, 2.6 mmol) dissolved in 4 mL of ethanol in a round bottom flask was added 10 % Pd/C (200 mg) and the system was flushed with H<sub>2</sub>. The reaction mixture was then exposed to 1 atm of H<sub>2</sub> (balloon) overnight. Upon completion, the heterogeneous mixture was filtered and the filtrate washed three times with ethanol (60 mL). The organic extracts were concentrated using a rotary evaporator and the crude mixture was purified using flash column chromatography (hexanes:ethyl acetate 2:1), to give **3.28** as a clear oil (515 mg, 2.52 mmol, 98 %). <sup>1</sup>H NMR (400 MHz, CDCl<sub>3</sub>) δ 4.20 (quin, J = 5.8 Hz, 1H), 3.99 (dd, J = 8.2, 6.5 Hz, 1H), 3.66 (dd, J = 8.4, 6.3 Hz, 1H), 3.57 (t, J = 5.8 Hz, 2H), 3.46 (m, 3H), 3.39 (m, 1H), 2.59 (bs, 1H), 1.60 (m, 4H), 1.36 (s, 3H), 1.31 (m, 3H); <sup>13</sup>C NMR (100 MHz, CDCl<sub>3</sub>) δ 109.5, 74.7, 71.9, 71.7, 66.9, 62.5, 29.9, 26.8, 26.4, 25.5. HRESIMS [M + Na]<sup>+</sup> calcd for C<sub>10</sub>H<sub>20</sub>O<sub>4</sub>Na 227.1259, found 227.1265; [α]<sub>D</sub><sup>24</sup> = +12° (c 0.09).

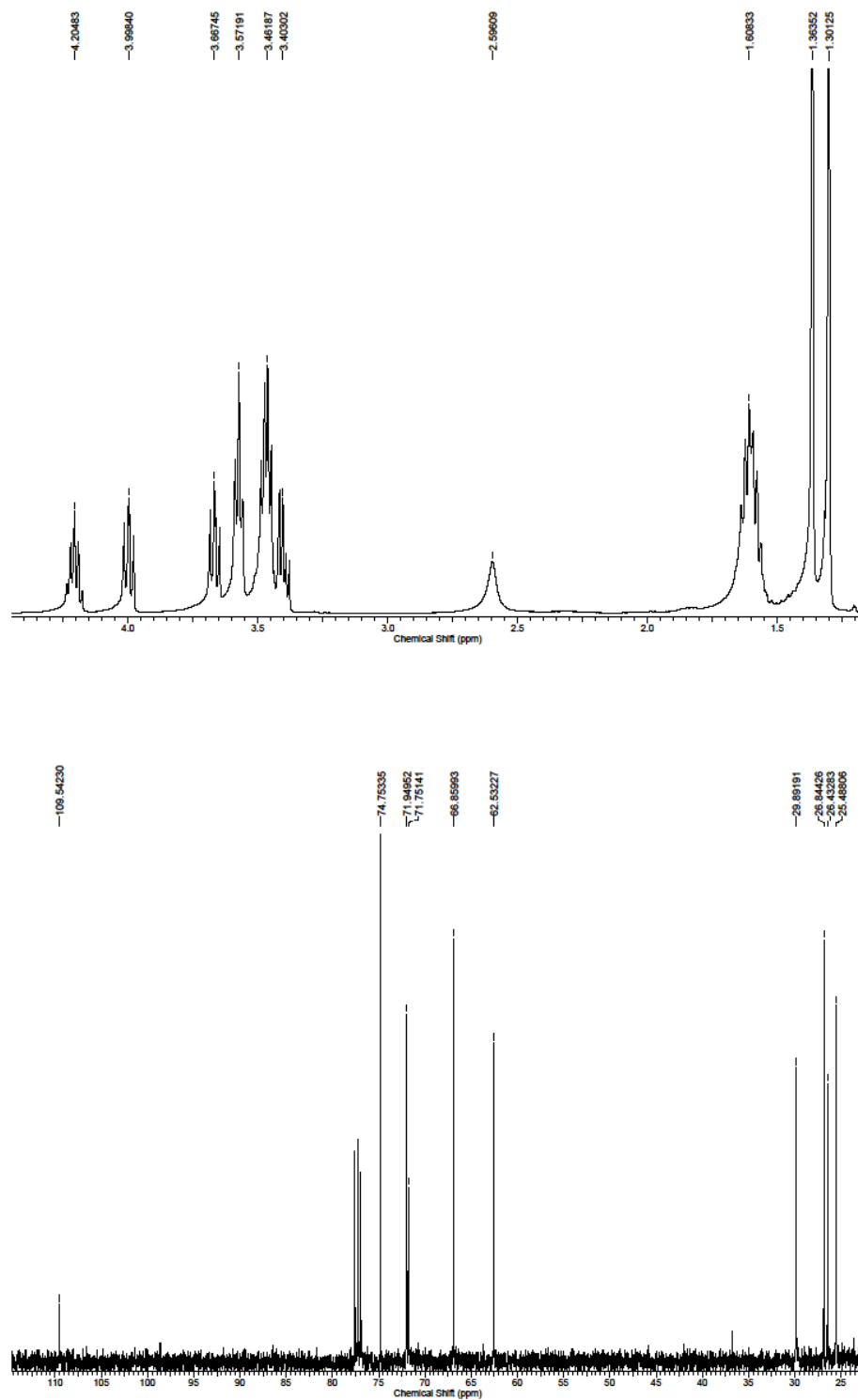
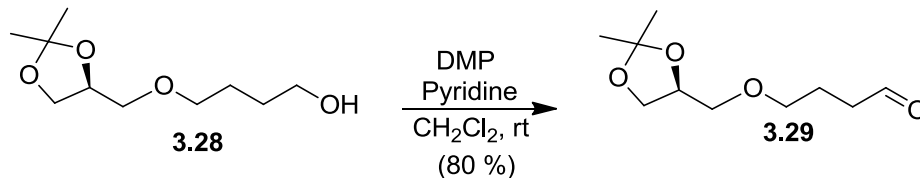


**Figure 3.20**  $^1\text{H}$  and  $^{13}\text{C}$  NMR spectra of **3.28** recorded in  $\text{CDCl}_3$  at 400 MHz and 100 MHz respectively.

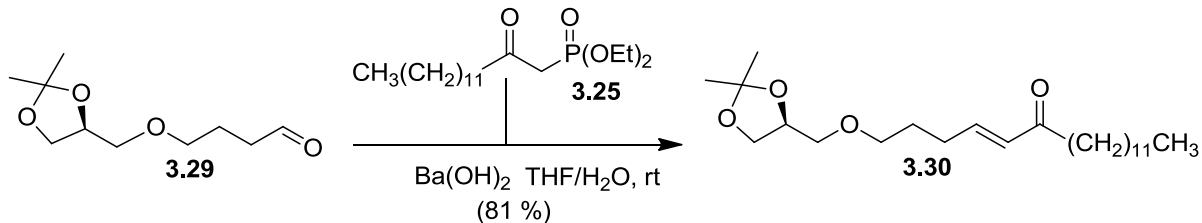
### Preparation of **3.29**:



To Dess–Martin periodinane (622 mg, 1.46 mmol) was added 9 mL of methylene chloride, followed by pyridine (387 mg, 4.9 mmol). To this mixture was added alcohol **3.28** (190 mg, 0.97 mmol) dissolved in 0.5 mL of methylene chloride, and the solution was stirred at room temperature for 30 min. The crude mixture was then concentrated using a rotary evaporator and purified using flash column chromatography (hexanes:ethyl acetate 2:1), to give **3.29** as a clear oil (150 mg, 0.74 mmol, 80 %). <sup>1</sup>H NMR (400 MHz, CDCl<sub>3</sub>) δ 9.75 (s, 1H), 4.21 (quin, J = 6.0 Hz, 1H), 4.02 (dd, J = 8.4, 6.7 Hz, 1H), 3.66 (dd, J = 8.2, 6.5 Hz, 1H), 3.48 (m, 3H), 3.39 (m, 1H), 2.49 (td, J = 7.2, 1.2 Hz, 2H), 1.89 (quin, J = 6.8 Hz, 2H), 1.39 (s, 3H), 1.33 (s, 3H); <sup>13</sup>C NMR (100 MHz, CDCl<sub>3</sub>) δ 202.3, 109.5, 74.8, 71.9, 70.6, 66.8, 40.9, 26.8, 25.5, 22.5. HRESIMS [M + Na]<sup>+</sup> calcd for C<sub>10</sub>H<sub>18</sub>O<sub>4</sub>Na 225.1103, found 225.1098; [α]<sub>D</sub><sup>24</sup> = +13° (c 0.03).



### Preparation of 3.30:



To phosphonate **3.25** (353 mg, 1.0 mmol) dissolved in 3.0 mL tetrahydrofuran was added  $\text{Ba}(\text{OH})_2$  (254 mg, 0.80 mmol) and the suspension was stirred at rt for 30 min. To the suspension was added aldehyde **3.29** (205 mg, 1.0 mmol), dissolved in 5.2 mL of a tetrahydrofuran:water mixture (40:1) and was stirred at room temperature for 1 h. The reaction mixture was then diluted with 100 mL of water and the aqueous phase was extracted three times with methylene chloride (250 mL). The organic extracts were dried with  $\text{MgSO}_4$  and concentrated using a rotary evaporator. The crude mixture was purified using flash column chromatography (hexanes:ethyl acetate 6:1) to give **3.30** as a clear oil (326 mg, 0.82 mmol, 81 %).  $^1\text{H}$  NMR (400 MHz,  $\text{C}_6\text{D}_6$ )  $\delta$  6.65 (dt,  $J = 15.6, 7.2$  Hz, 1H), 6.02 (d,  $J = 15.6$  Hz, 1H), 4.12 (quin,  $J = 5.2$  Hz, 1H), 3.83 (dd,  $J = 6.4, 1.6$  Hz, 1H), 3.67 (dd,  $J = 6.4, 2.0$  Hz, 1H), 3.32 (dd,  $J = 6.4, 4.8$  Hz, 1H), 3.19 (dd,  $J = 6.0, 3.6$  Hz, 1H), 3.11 (t,  $J = 6.8$  Hz, 2H), 2.27 (t,  $J = 7.3$  Hz, 2H), 1.96 (q,  $J = 7.6$  Hz, 2H), 1.66 (m, 2H), 1.42 (s, 3H), 1.38 (m, 2H), 1.30 (s, 3H), 1.28 (m, 18H), 0.90 (t,  $J = 6.8$  Hz, 3H);  $^{13}\text{C}$  NMR (100 MHz,  $\text{C}_6\text{D}_6$ )  $\delta$  198.5, 145.2, 130.8, 109.3, 75.1, 72.1, 70.5, 67.1, 40.4, 32.3, 30.0, 30.0, 29.9, 29.9, 29.7, 29.7, 29.7, 29.1, 28.5, 27.1, 25.6, 24.4, 23.0, 14.3. HRESIMS  $[\text{M} + \text{Na}]^+$  calcd for  $\text{C}_{24}\text{H}_{44}\text{O}_4\text{Na}$  419.3124, found 419.3130;  $[\alpha]_D^{24} = +10^\circ$  (c 0.15).

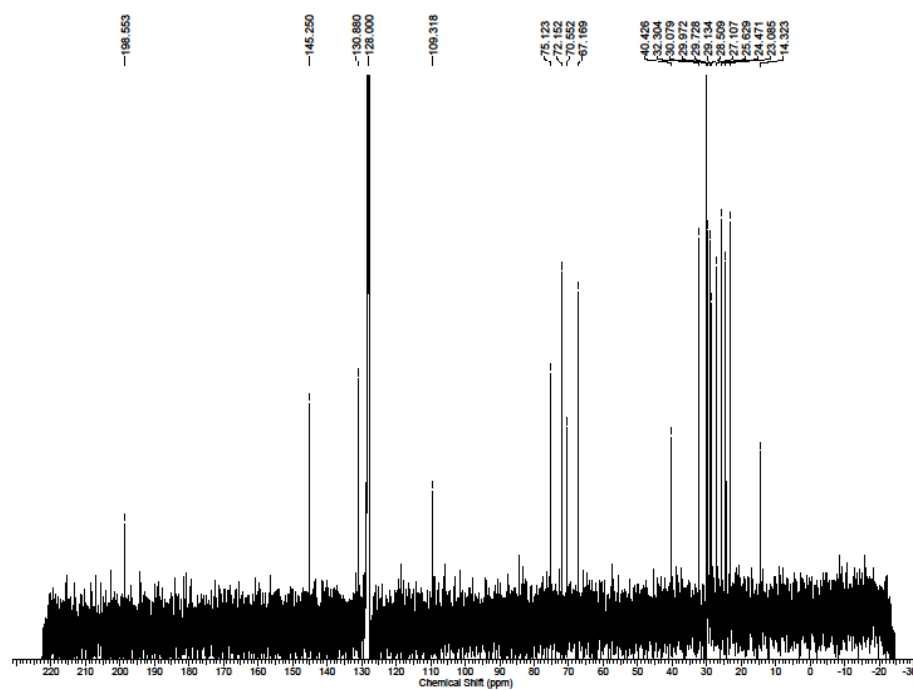
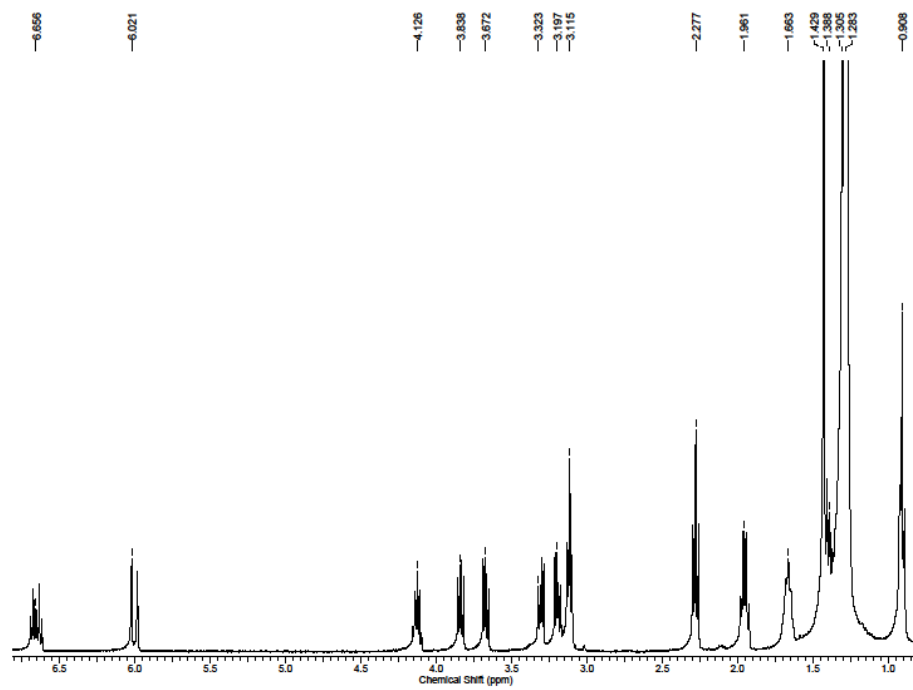
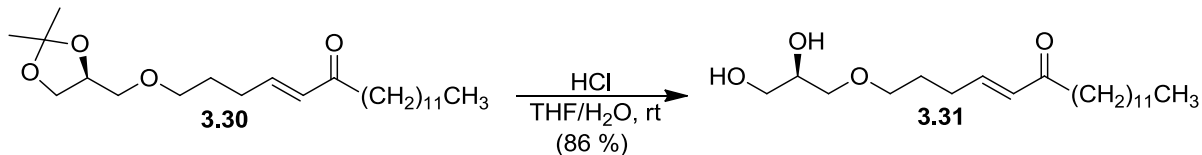


**Figure 3.22**  $^1\text{H}$  and  $^{13}\text{C}$  NMR spectra of **3.30** recorded in  $\text{C}_6\text{D}_6$  at 400 MHz and 100 MHz respectively.

### Preparation of 3.31:



To acetonide **3.30** (218 mg, 0.55 mmol) dissolved in 8 mL of a tetrahydrofuran:water mixture (5:1) was added 12.4 M HCl (0.22 mL, 2.7 mmol) and the solution was stirred at room temperature for 30 min. The reaction mixture was then quenched with the addition of saturated NaHCO<sub>3</sub> (50 mL) and the aqueous phase was extracted three times with methylene chloride (150 mL). The organic extracts were dried with MgSO<sub>4</sub> and concentrated using a rotary evaporator. The crude mixture was purified using flash column chromatography (ethyl acetate) to give **3.31** as a white solid (168 mg, 0.47 mmol, 86 %). <sup>1</sup>H NMR (600 MHz, C<sub>6</sub>D<sub>6</sub>) δ 6.69 (dt, J = 14.4, 7.2 Hz, 1H), 6.02 (d, J = 15.6 Hz, 1H), 3.87 (m, 1H), 3.70 (m, 1H), 3.63 (m, 2H), 3.33 (m, 3H), 3.16 (m, 2H), 2.31 (t, J = 6.6 Hz, 2H), 1.99 (q, J = 6.6 Hz, 2H), 1.65 (m, 2H), 1.45 (quin, J = 7.2 Hz, 2H), 1.28 (s, 18H), 0.91 (t, J = 7.2 Hz, 3H); <sup>13</sup>C NMR (150 MHz, C<sub>6</sub>D<sub>6</sub>) δ 199.3, 145.8, 130.7, 72.5, 71.2, 70.5, 64.3, 40.4, 32.3, 30.1, 30.1, 30.0, 30.0, 29.9, 29.8, 29.7, 29.2, 28.3, 24.4, 23.0, 14.3. HRESIMS [M + Na]<sup>+</sup> calcd for C<sub>21</sub>H<sub>40</sub>O<sub>4</sub>Na 379.2835, found 379.2830; [α]<sub>D</sub><sup>24</sup> = +2.9° (c 0.16).

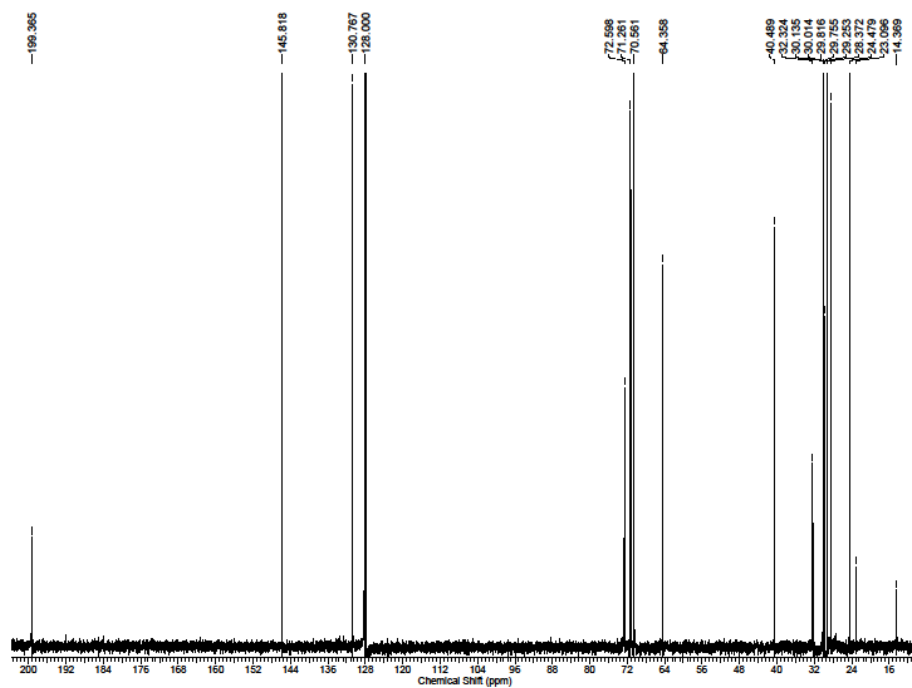
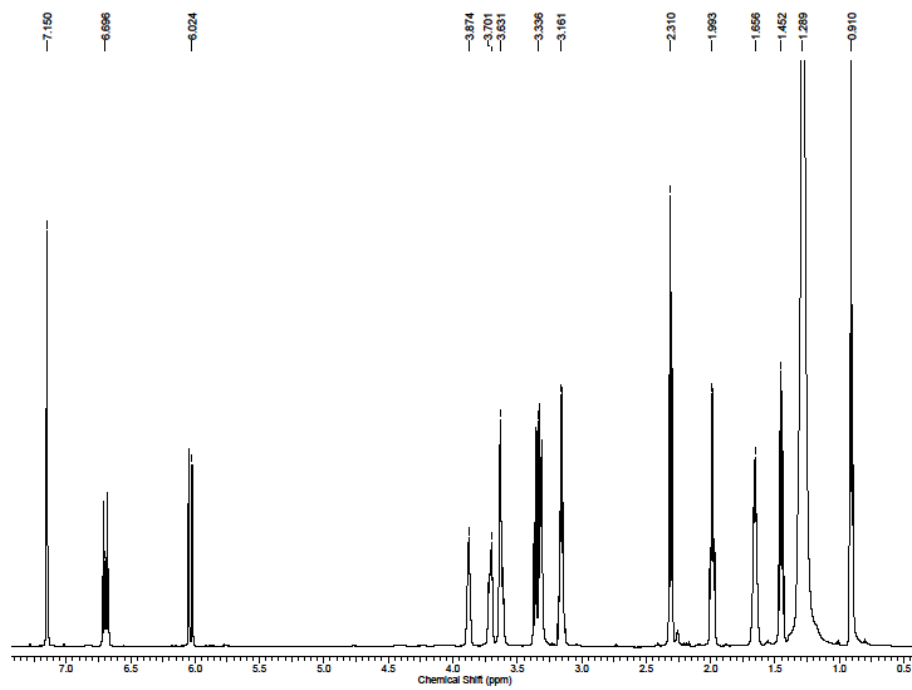
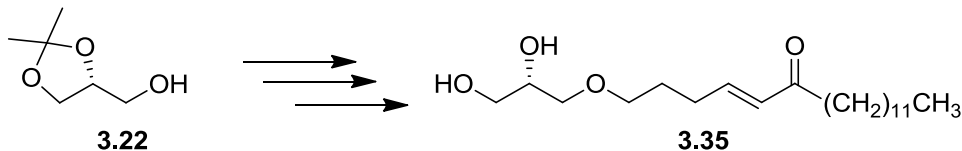


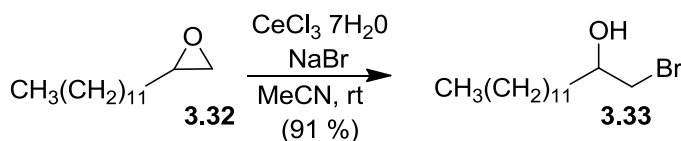
**Figure 3.23**  $^1\text{H}$  and  $^{13}\text{C}$  NMR spectra of **3.31** recorded in  $\text{C}_6\text{D}_6$  at 600 MHz and 150 MHz respectively.

### Preparation of 3.35:



Procedures identical to those used to prepare **3.31**, only using (*R*)-4-hydroxymethyl-2,2-dimethyl-1,3-dioxolane (**3.22**) as the starting material. HRESIMS  $[\text{M} + \text{Na}]^+$  calcd for  $\text{C}_{21}\text{H}_{40}\text{O}_4\text{Na}$  379.2824, found 379.2816;  $[\alpha]_D^{24} = -2.7^\circ$  (*c* 0.04).

### Preparation of 3.33:



To epoxide **3.32** (2.55 g, 11.9 mmol) dissolved in 150 mL of acetonitrile was added  $\text{NaBr}$  (1.45 g, 14.1 mmol) followed by cerium(III) chloride heptahydrate (5.26 g, 14.1 mmol) and the solution was stirred at room temperature for 24 h. The reaction mixture was then concentrated using a rotary evaporator and extracted three times with ethyl acetate (150 mL). The ethyl acetate fractions were combined, concentrated *in vacuo*, and purified using flash column chromatography (hexanes:ethyl acetate gradient 15:1, 10:1, 7:1) to give bromohydrin **3.33** as a white solid (3.19 g, 10.9 mmol, 91 %).  $^1\text{H}$  NMR (400 MHz,  $\text{CDCl}_3$ )  $\delta$  3.78 (bs, 1H), 3.53 (dd,  $J = 6.8, 3.2$  Hz, 1H), 3.38 (dd,  $J = 6.8, 3.2$  Hz, 1H), 2.26 (m, 1H), 1.53 (m, 2H), 1.26 (m, 20H), 0.88 (t,  $J = 7.2$  Hz, 3H);  $^{13}\text{C}$  NMR (100 MHz,  $\text{CDCl}_3$ )  $\delta$  71.2, 40.8, 35.3, 32.1, 29.83/29.80/29.72/29.67/29.52 (all four signals account for a total of 7C), 25.7, 22.8, 14.3; Elemental analysis calcd. (found) for  $\text{C}_{14}\text{H}_{29}\text{BrO}$ : Theoretical to be C, 57.33 (57.51); H, 9.97 (10.04).

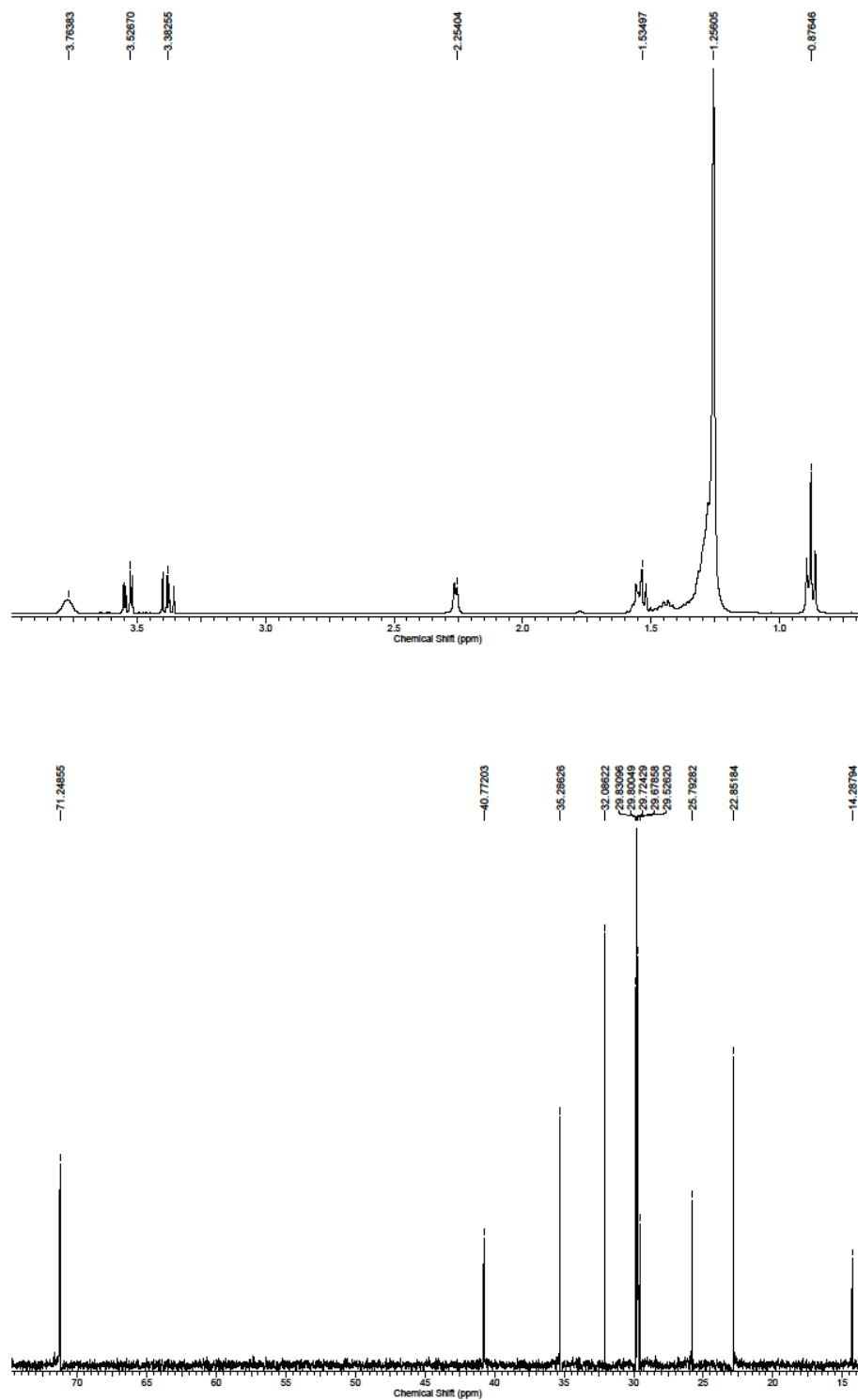
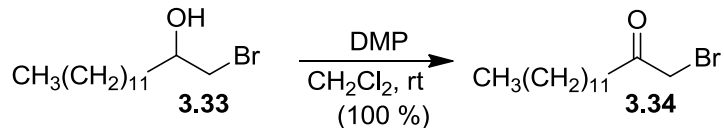


**Figure 3.24**  $^1\text{H}$  and  $^{13}\text{C}$  NMR spectra of **3.33** recorded in  $\text{CDCl}_3$  at 400 MHz and 100 MHz respectively.

### Preparation of 3.34:



To bromohydrin **3.33** (158 mg, 0.54 mmol) dissolved in 6 mL of methylene chloride at room temperature was added Dess–Martin periodinane (455 mg, 1.07 mmol) and the mixture was stirred for 1 h. The reaction mixture was then quenched with the addition of saturated  $\text{NaHCO}_3$  (50 mL) and the aqueous phase was extracted three times with methylene chloride (150 mL). The organic extracts were dried with  $\text{MgSO}_4$  and concentrated *in vacuo*. The crude mixture was purified using flash column chromatography (hexanes:ethyl acetate 30:1), to give **3.34** as a white solid (126 mg, 0.43 mmol, 100 %).  $^1\text{H}$  NMR (300 MHz,  $\text{CDCl}_3$ )  $\delta$  3.89 (s, 2H), 2.64 (t,  $J = 7.4$  Hz, 2H), 1.60 (m, 2H), 1.26 (m, 18H), 0.88 (t,  $J = 6.7$  Hz, 3H);  $^{13}\text{C}$  NMR (75 MHz,  $\text{CDCl}_3$ )  $\delta$  202.2, 39.9, 34.4, 32.0, 31.7, 29.8, 29.7, 29.6, 29.6, 29.5, 29.2, 24.0, 22.9, 14.2. HRESIMS  $[\text{M} + \text{Na}]^+$  calcd for  $\text{C}_{14}\text{H}_{27}\text{ONa}^{79}\text{Br}$  313.1143, found 313.1136.

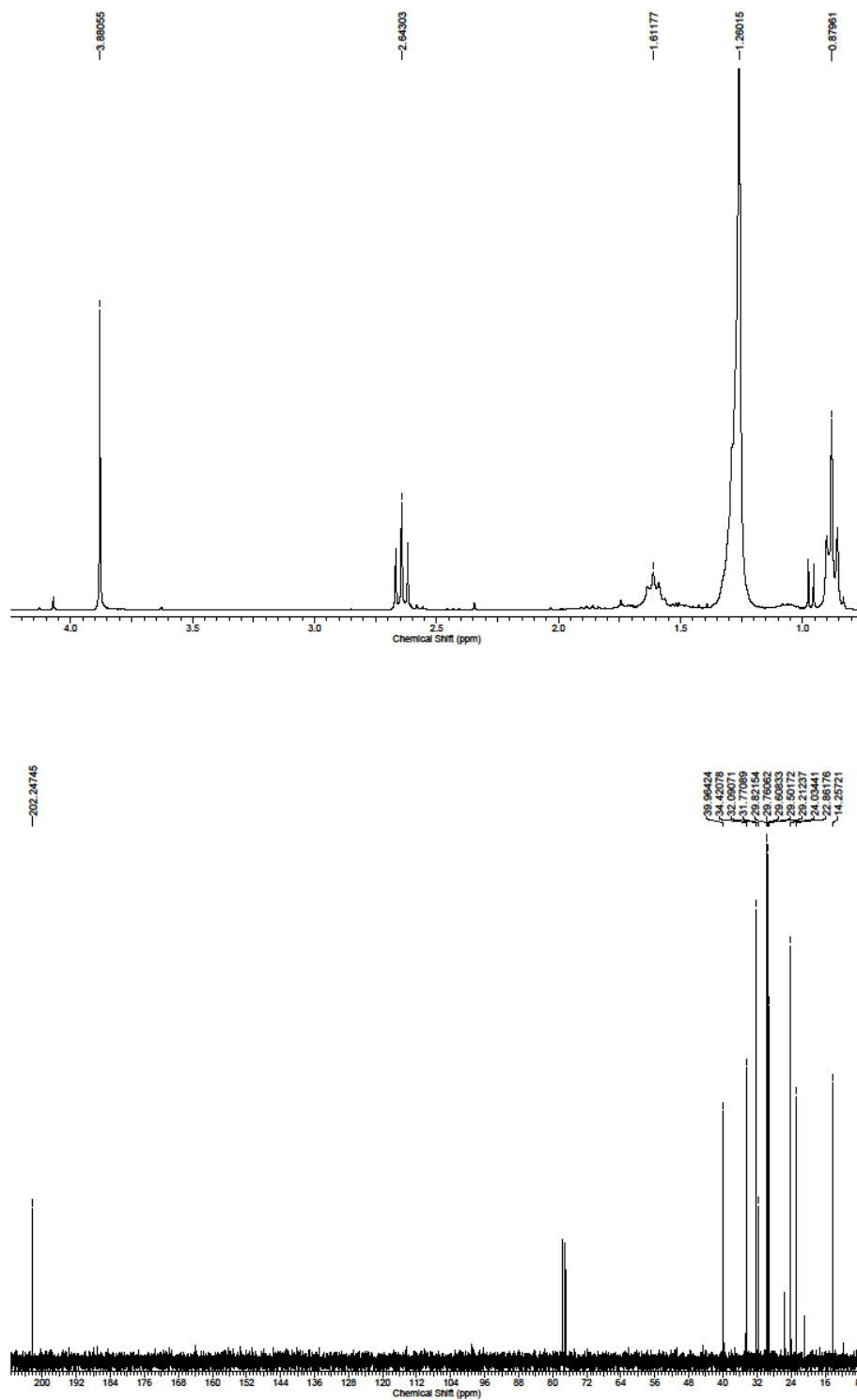
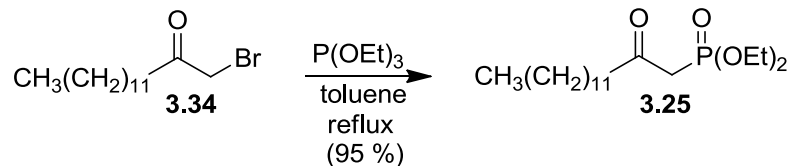


**Figure 3.25**  $^1\text{H}$  and  $^{13}\text{C}$  NMR spectra of **3.34** recorded in  $\text{CDCl}_3$  at 300 MHz and 75 MHz respectively.

### Preparation of 3.25:



To bromide **3.34** (80 mg, 0.27 mmol) dissolved in 1 mL of toluene was added triethylphosphite (228 mg, 1.4 mmol). The reaction mixture was heated to reflux for 24 h, after which it was cooled to room temperature and concentrated under a stream of N<sub>2</sub>. The crude mixture was purified using flash column chromatography (hexanes:ethyl acetate 1:1), to give **3.25** as a clear oil (89 mg, 0.25 mmol, 95 %). <sup>1</sup>H NMR (400 MHz, CDCl<sub>3</sub>) δ 4.09 (t, J = 7.2 Hz, 4H), 3.02 (m, 2H), 2.56 (t, J = 7.2 Hz, 2H), 1.53 (m, 2H), 1.28 (t, J = 7.0 Hz, 6H), 1.19 (m, 18H), 0.82 (t, J = 6.0 Hz, 3H); <sup>13</sup>C NMR (100 MHz, CDCl<sub>3</sub>) δ 202.3, 62.6, 44.2, 43.1, 41.8, 32.0, 29.7, 29.6(2C), 29.5, 29.48, 29.43, 29.1, 23.5, 22.8, 16.4, 16.3, 14.2. HRESIMS [M + Na]<sup>+</sup> calcd for C<sub>18</sub>H<sub>38</sub>O<sub>4</sub>P 349.2508, found 349.2517.

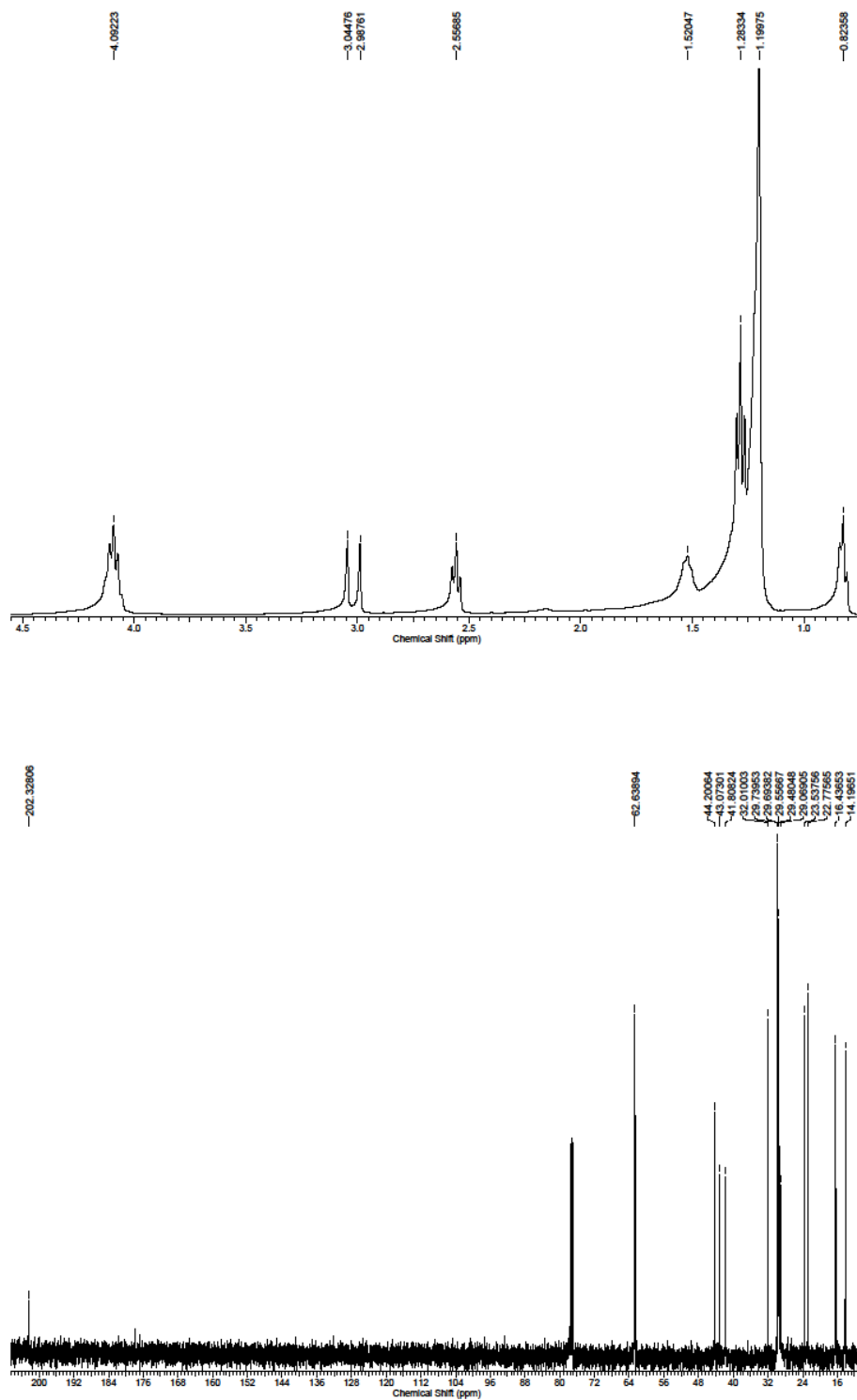
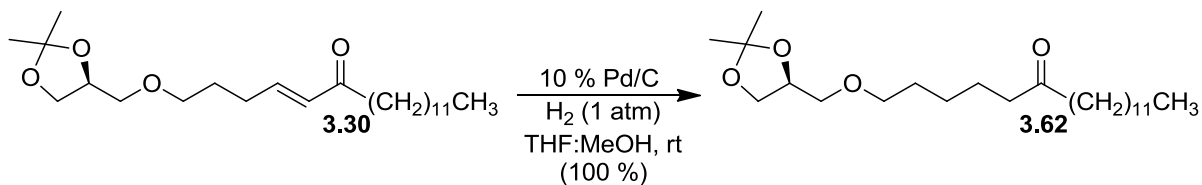


**Figure 3.26**  $^1\text{H}$  and  $^{13}\text{C}$  NMR spectra of **3.25** recorded in  $\text{CDCl}_3$  at 400 MHz and 100 MHz respectively.

### Preparation of 3.62:



To acetonide **3.30** (20 mg, 0.050 mmol) dissolved in 1 mL of tetrahydrofuran:methanol (1:1), was added 5 mg of 10 % Pd/C, and the system subjected to 1 atm of H<sub>2</sub> for 12 h. The reaction was then filtered using 20 mL of methanol, and evaporated under a stream of nitrogen. The crude mixture was purified using flash column chromatography (hexanes:ethyl acetate 6:1) to give **3.62** as a white solid (19.9 mg, 0.05 mmol, 100 %). <sup>1</sup>H NMR (400 MHz, CDCl<sub>3</sub>) δ 4.25 (quin, J = 5.5 Hz, 1H), 4.05 (dd, J = 6.1, 2.0 Hz, 1H), 3.71 (dd, J = 6.5, 1.7 Hz, 1H), 3.47 (m, 4H), 2.38 (q, J = 7.5 Hz, 4H), 1.58 (m, 7H), 1.42 (s, 3H), 1.36 (s, 3H), 1.31 (m, 1H), 1.25 (m, 19H), 0.88 (t, J = 6.8 Hz, 3H); <sup>13</sup>C NMR (100 MHz, CDCl<sub>3</sub>) δ 211.5, 109.5, 100.1, 74.9, 72.0, 71.7, 67.0, 43.0, 42.8, 32.0, 29.8, 29.7, 29.6, 29.5, 29.5, 29.4, 29.4, 26.9, 25.9, 25.6, 24.0, 23.7, 22.8, 14.2. HRESIMS [M+Na]<sup>+</sup> calcd for C<sub>24</sub>H<sub>46</sub>O<sub>4</sub>Na 421.3294, found 421.3283; [α]<sub>D</sub><sup>24</sup> = +18.10° (c 0.04).

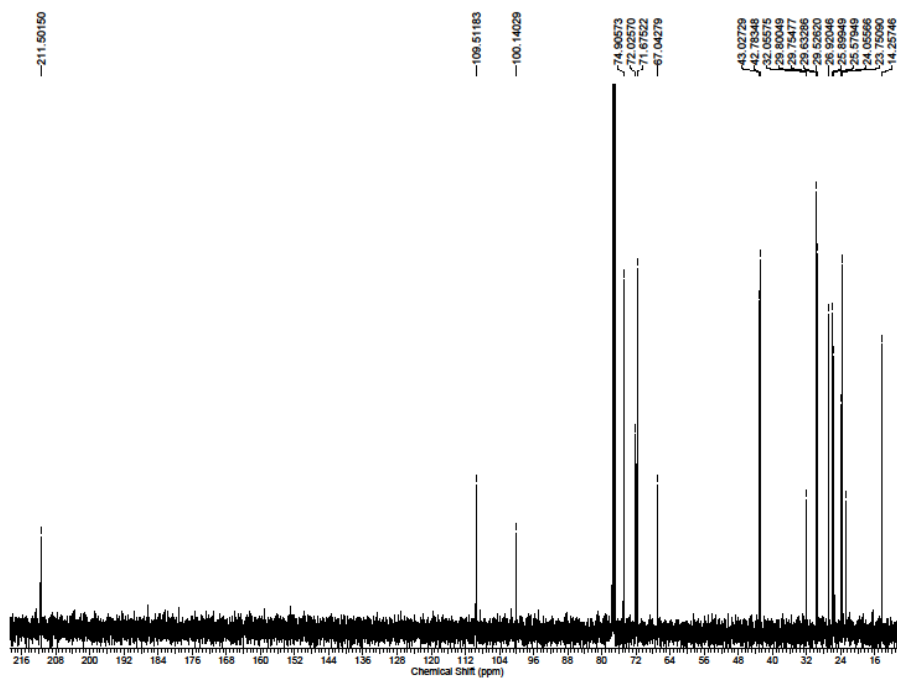
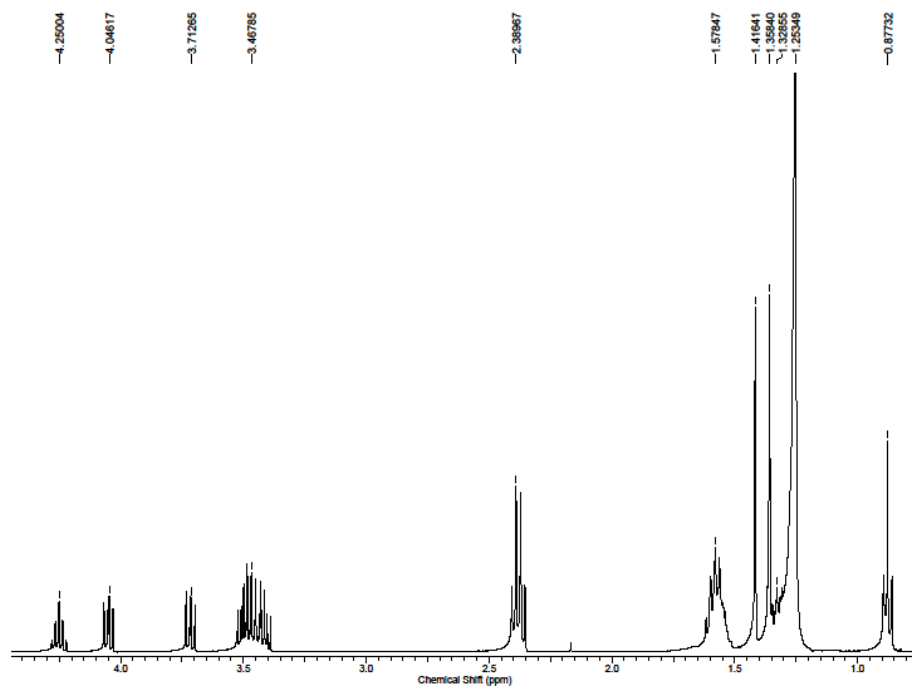
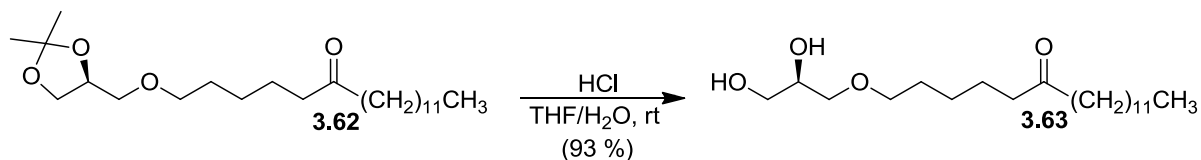


**Figure 3.27**  $^1\text{H}$  and  $^{13}\text{C}$  NMR spectra of **3.62** recorded in  $\text{CDCl}_3$  at 400 MHz and 100 MHz respectively.

### Preparation of 3.63:



To acetonide **3.62** (12 mg, 0.030 mmol), dissolved in 0.5 mL of a tetrahydrofuran:water mixture (5:1) was added 12.4 M HCl (0.012 mL, 0.14 mmol), and allowed to stir at room temperature for 30 min. The reaction mixture was then quenched with the addition of saturated NaHCO<sub>3</sub> (15 mL) and the aqueous phase was extracted three times with methylene chloride (50 mL). The organic extracts were dried with MgSO<sub>4</sub>, and concentrated using a rotary evaporator. The crude mixture was purified using flash column chromatography (hexanes:ethyl acetate 1:4) to give **3.63** as a white solid (10 mg, 0.027 mmol, 92.7 %). <sup>1</sup>H NMR (400 MHz, C<sub>6</sub>D<sub>6</sub>) δ 3.69 (quin, J = 4.8 Hz, 1H), 3.54 (dd, J = 10.9, 4.3 Hz, 1H), 3.46 (dd, J = 10.9, 5.2 Hz, 1H), 3.24 (m, 2H), 3.14 (m, 2H), 2.46 (bs, 1H), 2.00 (m, 4H), 1.85 (bs, 1H), 1.51 (m, 5H), 1.38 (m, 4H), 1.29 (m, 14H), 1.20 (m, 3H), 0.91 (t, J = 6.7 Hz, 3H); <sup>13</sup>C NMR (75 MHz, C<sub>6</sub>D<sub>6</sub>) δ 208.9, 72.7, 71.2, 70.7, 64.2, 42.7, 42.4, 32.2, 30.1, 30.1, 30.1, 30.0, 29.9, 29.9, 29.7, 29.6, 26.0, 24.1, 23.6, 23.0, 14.3. ESIMS [M+Na]<sup>+</sup> calcd for C<sub>21</sub>H<sub>42</sub>O<sub>4</sub>Na 381.2981, found 381.2968; [α]<sub>D</sub><sup>24</sup> = +6.90° (c 0.01).

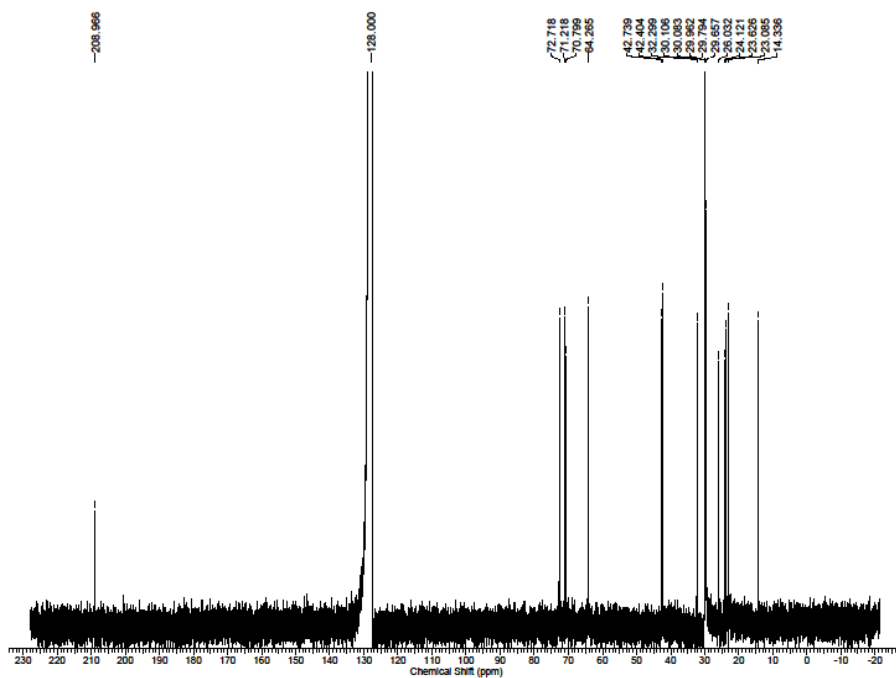
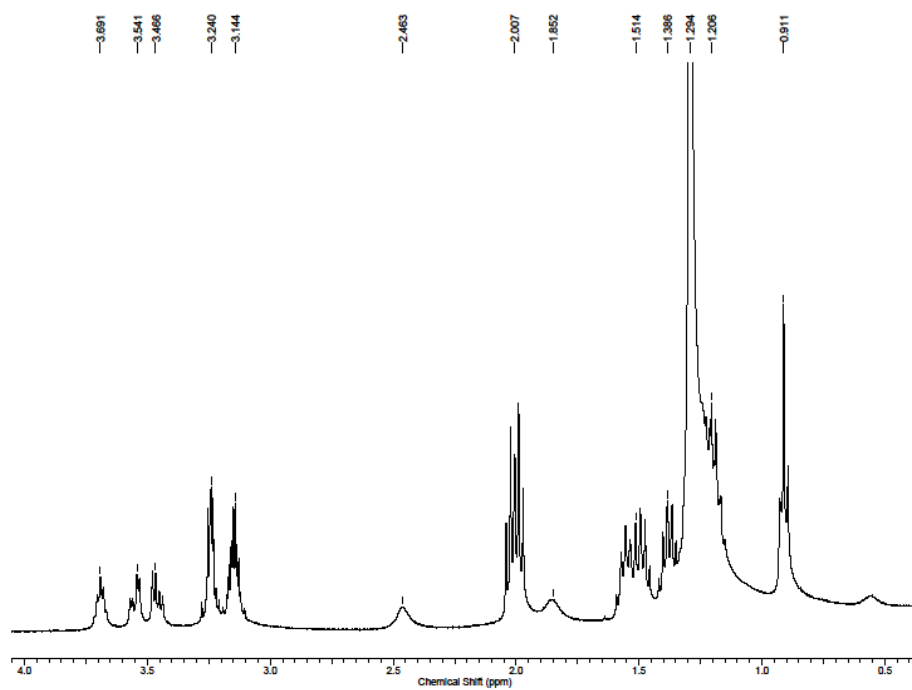
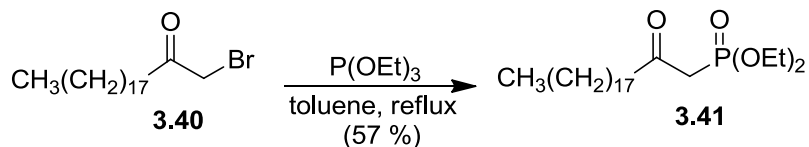


**Figure 3.28**  $^1\text{H}$  and  $^{13}\text{C}$  NMR spectra of **3.63** recorded in  $\text{C}_6\text{D}_6$  at 400 MHz and 75 MHz respectively.

### Preparation of 3.41:



To ketone **3.40** (546.5 mg, 1.45 mmol) was added 4 mL was added triethylphosphite (2.53 mL, 14.55 mmol). The reaction mixture was heated to reflux for 48 h, after which it was cooled to room temperature, and then concentrated under a stream of nitrogen. The crude mixture was then purified using flash column chromatography (hexanes:ethyl acetate 1:1), to give **3.41** as a clear oil (358.4 mg, 0.82 mmol, 57.1 %).  $^1\text{H}$  NMR (400 MHz,  $\text{CDCl}_3$ )  $\delta$  4.06 (m, 4H), 3.0 (m, 2H), 2.53 (t,  $J = 7.31$  Hz, 2H), 1.49 (m, 2H), 1.26 (t,  $J = 7.0$  Hz, 8H), 1.18 (m, 28H), 0.80 (t,  $J = 5.5$  Hz, 3H);  $^{13}\text{C}$  NMR (100 MHz,  $\text{CDCl}_3$ )  $\delta$  202.1(doublet), 62.6 (doublet), 44.1, 43.0, 47.7, 32.0, 29.8, 29.8, 29.8, 29.8, 29.8, 29.8, 29.8, 29.8, 29.8, 29.7, 29.6, 29.5, 29.4, 29.1, 23.5, 27.8, 16.4, 16.3, 14.2. HRESIMS  $[\text{M}+\text{H}]^+$  calcd for  $\text{C}_{24}\text{H}_{50}\text{O}_4\text{P}$  433.3447, found 433.3438.

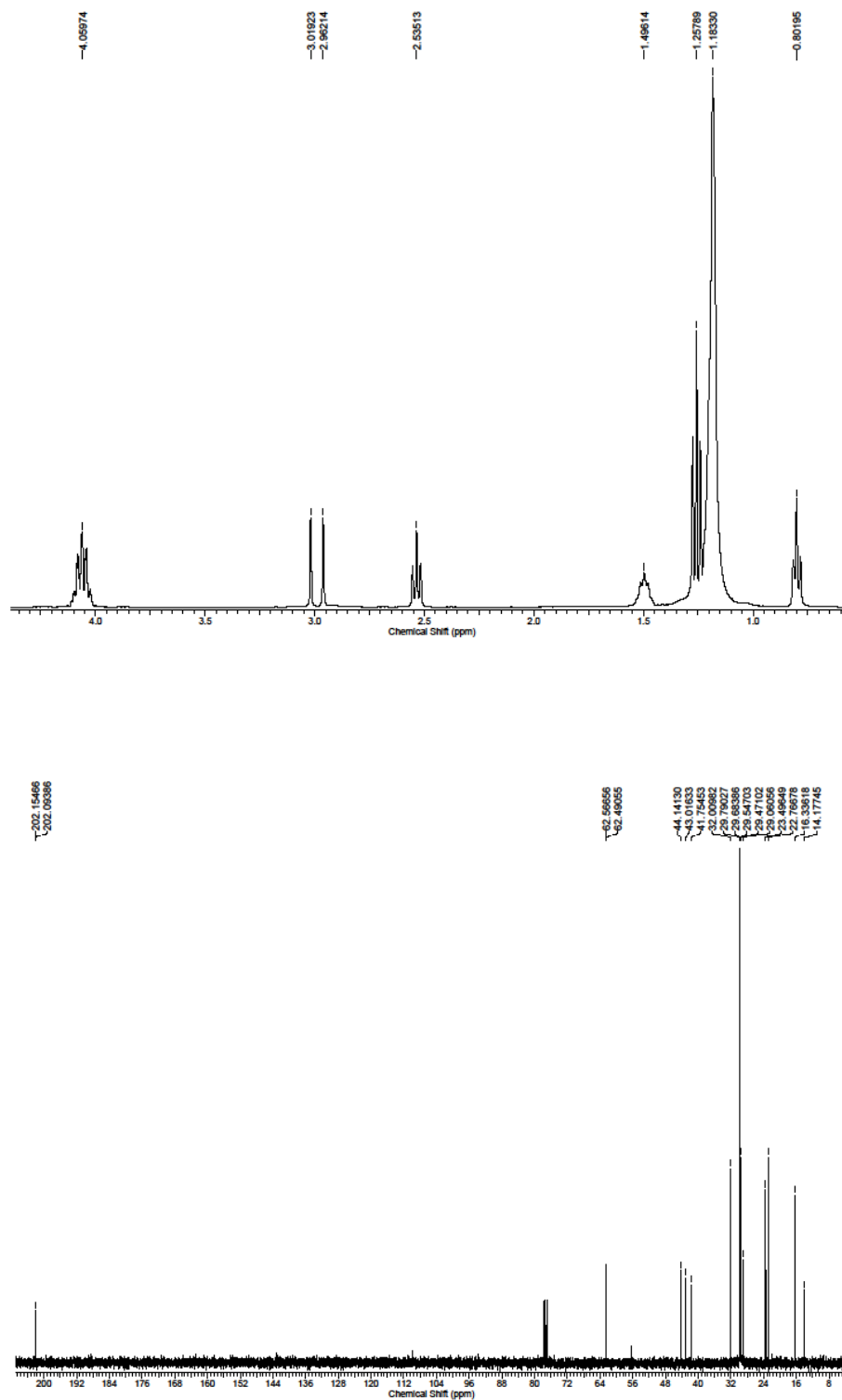
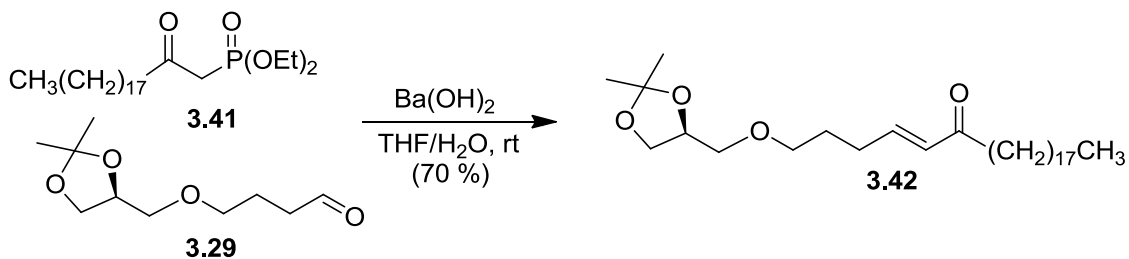


**Figure 3.29**  $^1\text{H}$  and  $^{13}\text{C}$  NMR spectra of **3.41** recorded in  $\text{CDCl}_3$  at 400 MHz and 100 MHz respectively.

### Preparation of 3.42:



To phosphonate **3.41** (57 mg, 0.131 mmol) dissolved in 1 mL tetrahydrofuran, was added Ba(OH)<sub>2</sub> (33.2 mg, 0.104 mmol), and allowed to stir at room temperature for 30 min. To the suspension was added aldehyde **3.29** (26.6 mg, 0.131 mmol), dissolved in 1.6 mL of a tetrahydrofuran:water mixture (40:1), and allowed to stir at room temperature for 1 h. The reaction mixture was then diluted with 50 mL of water and the aqueous phase was extracted three times with methylene chloride (100 mL). The organic extracts were dried with MgSO<sub>4</sub>, and concentrated using a rotary evaporator. The crude mixture was purified using flash column chromatography (hexanes:ethyl acetate 8:1) to give **3.42** as a white solid (44.4 mg, 0.092 mmol, 70.4 %). <sup>1</sup>H NMR (400 MHz, CDCl<sub>3</sub>) δ 6.84 (dt, J = 16.0, 6.8 Hz, 1H), 6.10 (d, J = 15.7 Hz, 1H), 4.25 (quin, J = 5.8 Hz, 1H), 4.05 (dd, J = 6.5, 1.7 Hz, 1H), 3.72 (dd, J = 6.5, 1.7 Hz, 1H), 3.47 (m, 4H), 2.51 (t, J = 7.5 Hz, 2H), 2.29 (q, J = 6.8 Hz, 2H), 1.75 (quin, J = 6.8 Hz, 2H), 1.59 (m, 2H), 1.42 (s, 3H), 1.36 (s, 3H), 1.25 (m, 30 H), 0.87 (t, J = 6.8 Hz, 3H); <sup>13</sup>C NMR (100 MHz, CDCl<sub>3</sub>) δ 200.9, 146.4, 130.7, 109.6, 100.1, 74.9, 72.1, 70.8, 66.9, 40.4, 32.1, 29.8, 29.8, 29.8, 29.7, 29.6, 29.6, 29.5, 29.2, 28.2, 26.9, 25.6, 24.4, 22.8, 14.3. HRESIMS [M+Na]<sup>+</sup> calcd for C<sub>30</sub>H<sub>56</sub>O<sub>4</sub>Na 503.4076, found 503.4089; [α]<sub>D</sub><sup>24</sup> = +7.02° (c 0.08).

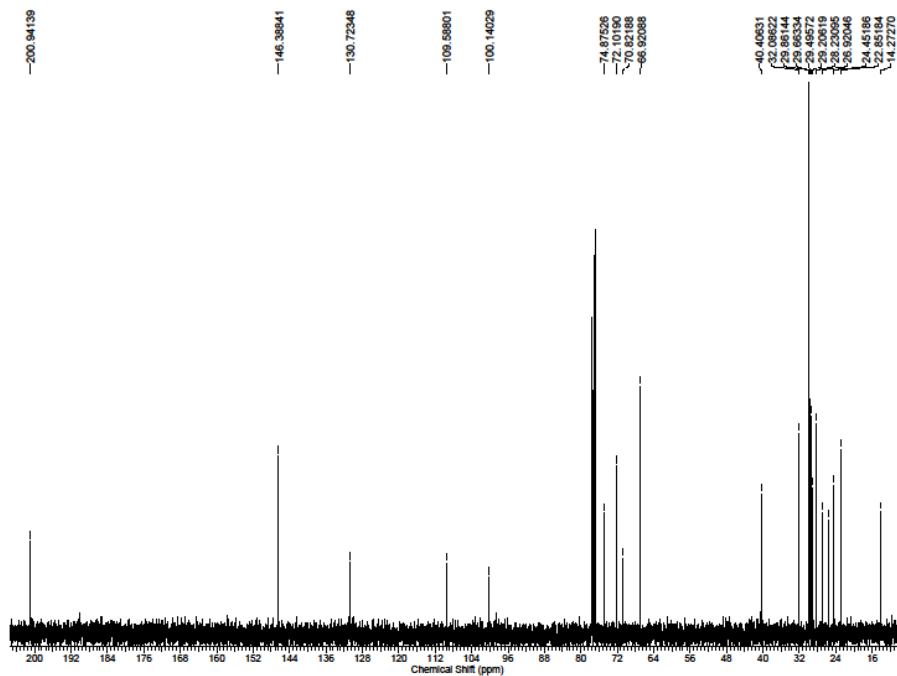
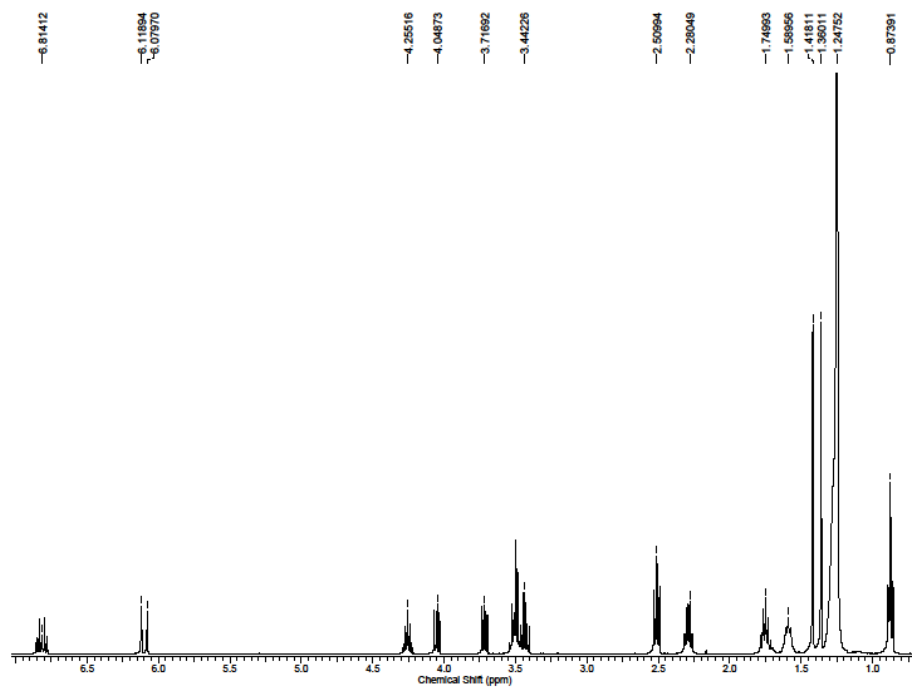
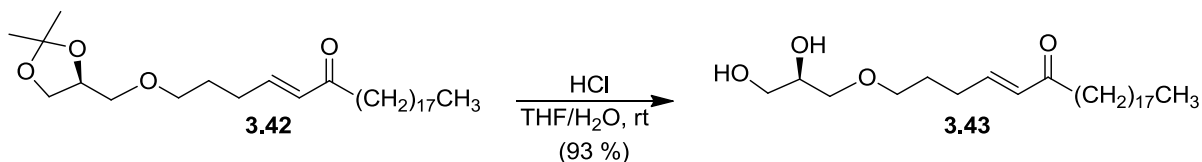


**Figure 3.30**  $^1\text{H}$  and  $^{13}\text{C}$  NMR spectra of **3.42** recorded in  $\text{CDCl}_3$  at 400 MHz and 100 MHz respectively.

### Preparation of 3.43:



To acetonide **3.42** (30 mg, 0.062 mmol), dissolved in 0.6 mL of a tetrahydrofuran:water mixture (5:1) was added 12.4 M HCl (0.025 mL, 0.31 mmol), and allowed to stir at room temperature for 30 min. The reaction mixture was then quenched with the addition of saturated NaHCO<sub>3</sub> (25 mL) and the aqueous phase was extracted three times with methylene chloride (100 mL). The organic extracts were dried with MgSO<sub>4</sub>, and concentrated using a rotary evaporator. The crude mixture was purified using flash column chromatography (ethyl acetate) to give **3.43** as a white solid (25.3 mg, 0.057 mmol, 92.6 %). <sup>1</sup>H NMR (600 MHz, CD<sub>2</sub>Cl<sub>2</sub>) δ 6.82 (dt, J = 15.9, 7.1 Hz, 1H), 6.11 (d, J = 15.9 Hz, 1H), 3.81 (m, 1H), 3.66 (dd, J = 11.3, 3.5 Hz, 1H), 3.58 (dd, J = 11.3, 5.6 Hz, 1H), 3.48 (m, 4H), 2.51 (t, J = 7.2 Hz, 2H), 2.42 (bs, 2H), 2.29 (q, J = 7.7 Hz, 2H), 1.75 (quin, J = 7.2 Hz, 2H), 1.57 (m, 2H), 1.27 (m, 30H), 0.89 (t, J = 7.2 Hz, 3H); <sup>13</sup>C NMR (150 MHz, CD<sub>2</sub>Cl<sub>2</sub>) δ 200.0, 145.6, 130.0, 71.9, 70.2, 70.1, 63.6, 39.7, 31.5, 29.2, 29.2, 29.2, 29.09, 29.03, 28.9, 28.8, 28.6, 27.7, 23.8, 22.2, 13.4. HRESIMS [M+Na]<sup>+</sup> calcd for C<sub>27</sub>H<sub>52</sub>O<sub>4</sub>Na 463.3763, found 463.3756; [α]<sub>D</sub><sup>24</sup> = +2.43° (c 0.08).

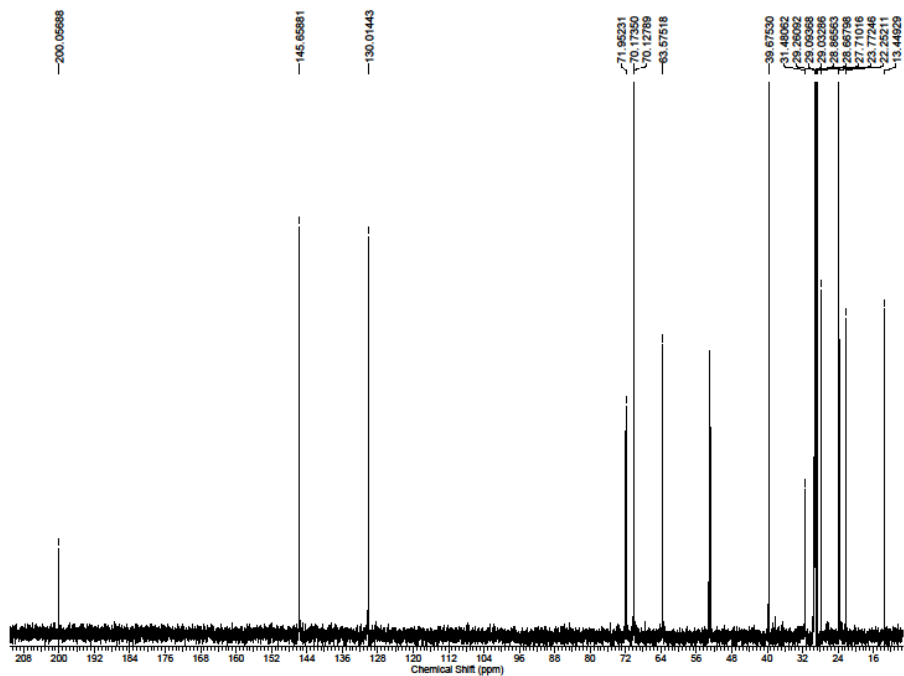
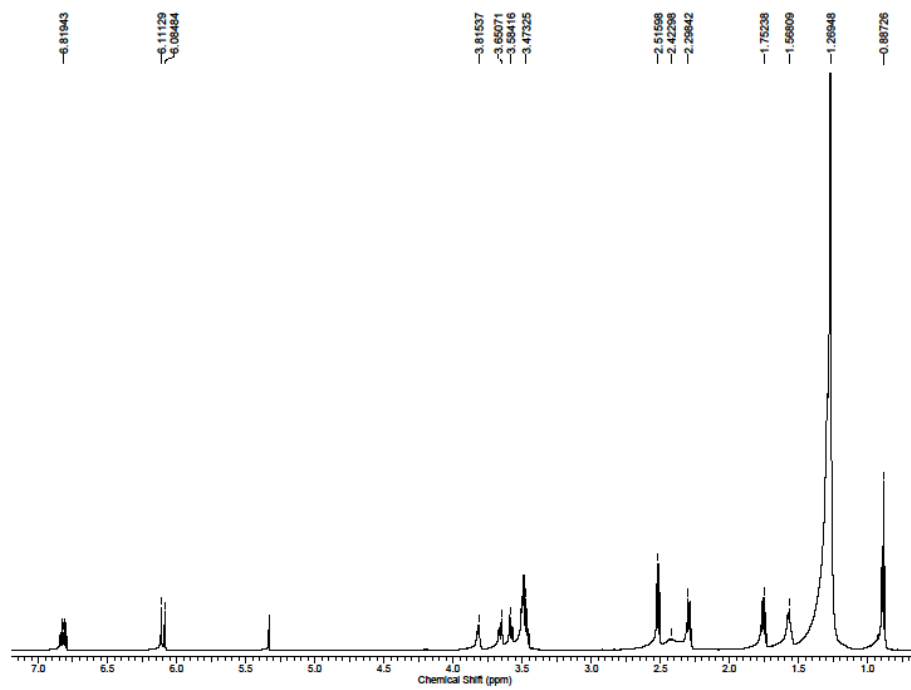
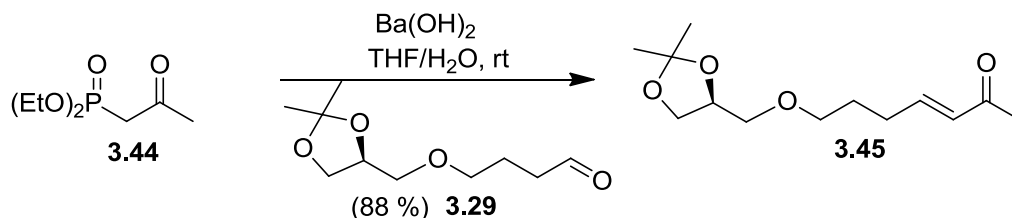
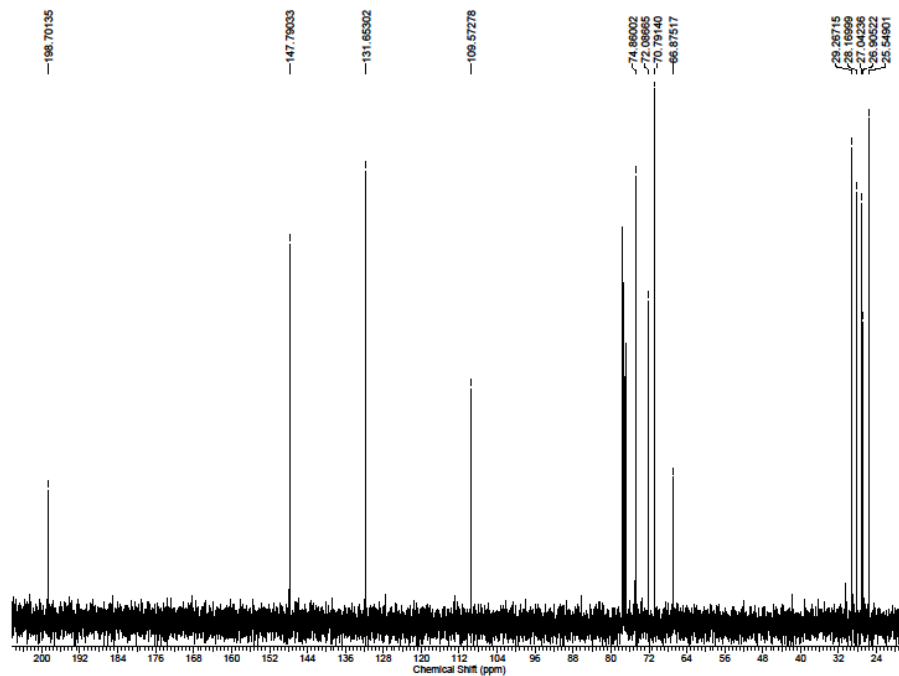
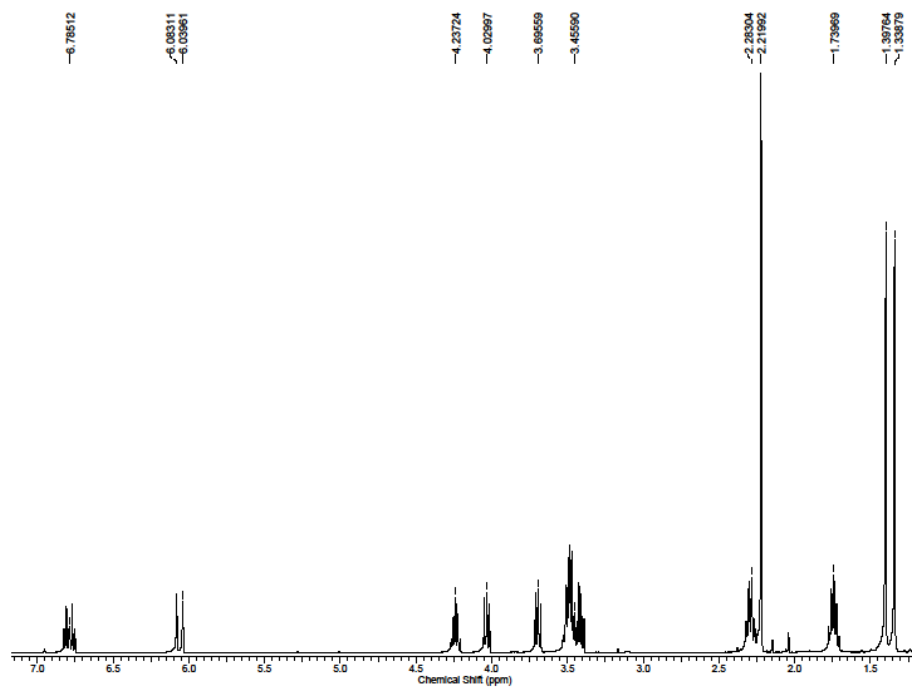


Figure 3.31  $^1\text{H}$  and  $^{13}\text{C}$  NMR spectra of **3.43** recorded in  $\text{CD}_2\text{Cl}_2$  at 600 MHz and 150 MHz respectively.

### Preparation of 3.45:

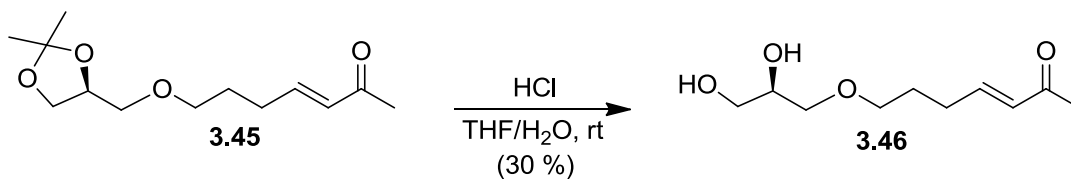


To phosphonate **3.44** (57.4 mg, 0.296 mmol) dissolved in 1 mL tetrahydrofuran, was added Ba(OH)<sub>2</sub> (75 mg, 0.237 mmol), and allowed to stir at room temperature for 30 min. To the suspension was added aldehyde **3.29** (60 mg, 0.296 mmol), dissolved in 1.6 mL of a tetrahydrofuran:water mixture (40:1), and allowed to stir at room temperature for 1 h. The reaction mixture was then diluted with 50 mL of water and the aqueous phase was extracted three times with methylene chloride (150 mL). The organic extracts were dried with MgSO<sub>4</sub>, and concentrated using a rotary evaporator. The crude mixture was purified using flash column chromatography (hexanes:ethyl acetate 2:1 ) to give **3.45** as a clear liquid (63.1 mg, 0.26 mmol, 87.9 %). <sup>1</sup>H NMR (400 MHz, CDCl<sub>3</sub>) δ 6.79 (dt, J = 16.0, 6.8 Hz, 1H), 6.06 (d, J = 16.0 Hz, 1H), 4.24 (quin, J = 5.8 Hz, 1H), 4.03 (dd, J = 6.5, 1.7 Hz, 1H), 3.69 (dd, J = 6.5, 1.7 Hz, 1H), 3.46 (m, 4H), 2.30 (q, J = 8 Hz, 2H), 2.22 (s, 3H), 1.74 (q, J = 6.8 Hz, 2H), 1.39 (s, 3H), 1.34 (s, 3H); <sup>13</sup>C NMR (100 MHz, CDCl<sub>3</sub>) δ 198.7, 147.8, 131.6, 109.6, 74.9, 72.1, 70.8, 66.9, 29.3, 28.2, 27.0, 26.9, 25.5. HRESIMS [M+Na]<sup>+</sup> calcd for C<sub>13</sub>H<sub>22</sub>O<sub>4</sub>Na 265.1416, found 265.1413; [α]<sub>D</sub><sup>24</sup> = +19.25° (c 0.12).



**Figure 3.32**  $^1\text{H}$  and  $^{13}\text{C}$  NMR spectra of **3.45** recorded in  $\text{CDCl}_3$  at 400 MHz and 100 MHz respectively.

### Preparation of 3.46:



To acetonide **3.45** (30 mg, 0.123 mmol), dissolved in 1.2 mL of a tetrahydrofuran:water mixture (5:1) was added 12.4 M HCl (0.05 mL, 0.62 mmol), and allowed to stir at room temperature for 30 min. The reaction mixture was then quenched with the addition of saturated NaHCO<sub>3</sub> (25 mL) and the aqueous phase was extracted three times with methylene chloride (100 mL). The organic extracts were dried with MgSO<sub>4</sub>, and concentrated using a rotary evaporator. The crude mixture was purified using a reversed phase sepak (water:methanol 6:4) to give **3.46** as a clear liquid (7.46 mg, 0.037 mmol, 30 %). <sup>1</sup>H NMR (600 MHz, C<sub>6</sub>D<sub>6</sub>) δ 6.43 (dt, J = 15.9, 6.6 Hz, 1H), 5.94 (d, J = 15.9 Hz, 1H), 3.75 (quin, J = 5.1 Hz, 1H), 3.59 (dd, J = 7.2, 4.1 Hz, 1H), 3.52 (dd, J = 11.3, 5.6 Hz, 1H), 3.24 (m, 2H), 3.05 (m, 2H), 2.93 (bs, 1H), 2.51 (bs, 1H), 1.87 (s, 3H), 1.85 (m, 2H), 1.33 (quin, J = 6.6 Hz, 2H); <sup>13</sup>C NMR (150 MHz, C<sub>6</sub>D<sub>6</sub>) δ 196.9, 146.6, 131.5, 72.5, 71.0, 70.4, 64.2, 29.1, 28.1, 26.7. HRESIMS [M+Na]<sup>+</sup> calcd for C<sub>10</sub>H<sub>18</sub>O<sub>4</sub>Na 225.1103, found 225.1100; [α]<sub>D</sub><sup>24</sup> = +5.35° (c 0.01).

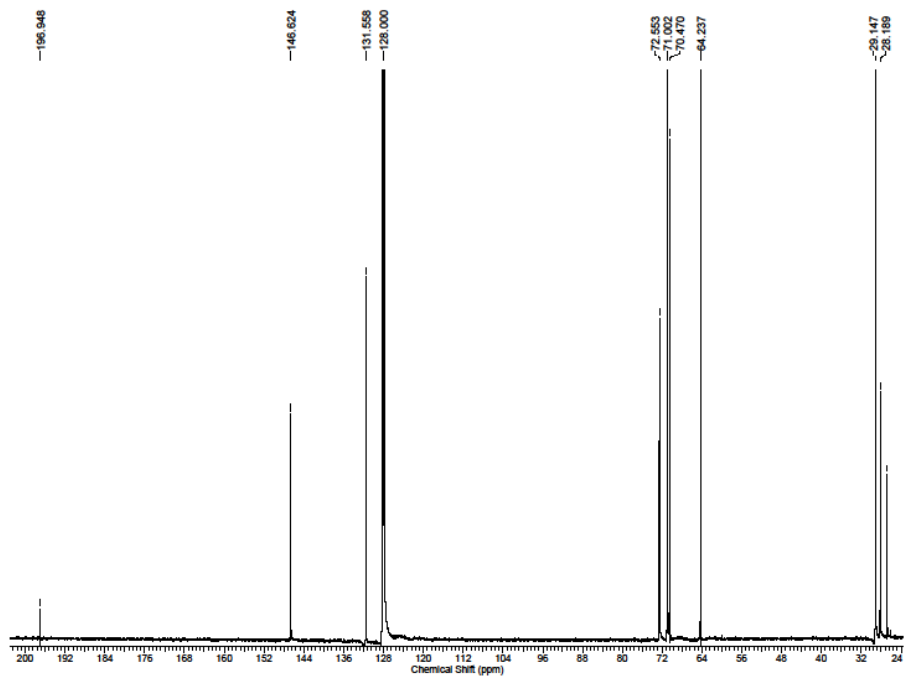
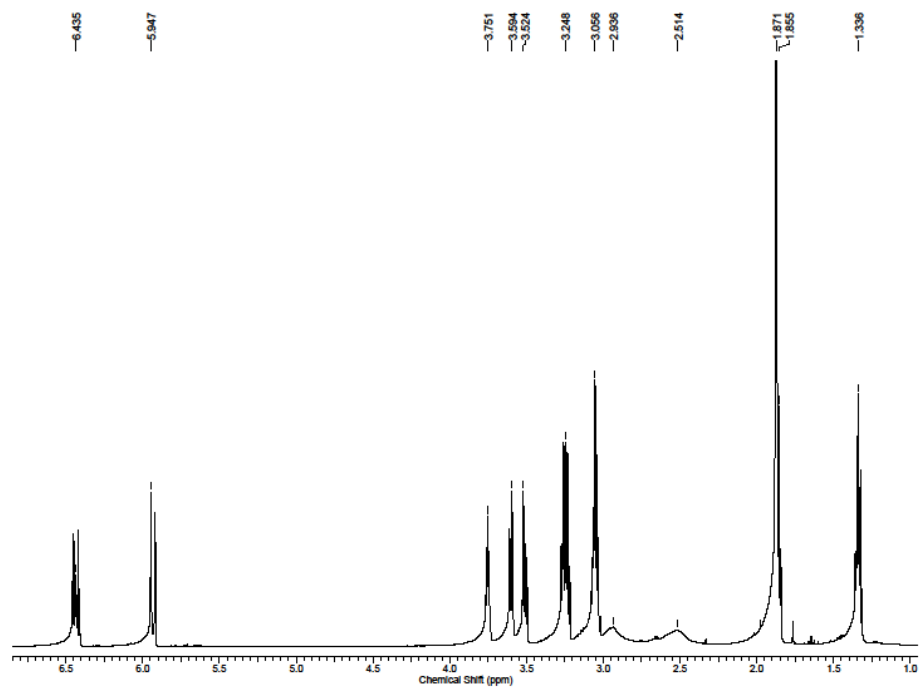
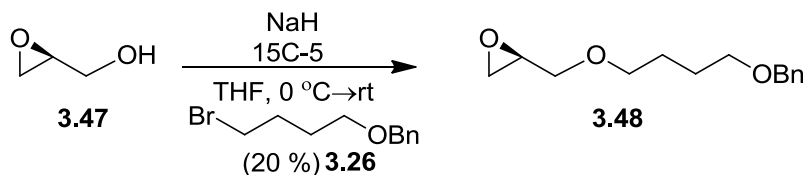


**Figure 3.33**  $^1\text{H}$  and  $^{13}\text{C}$  NMR spectra of **3.46** recorded in  $\text{C}_6\text{D}_6$  at 600 MHz and 150 MHz respectively.

### Preparation of 3.48:



Sodium hydride (2.46 g, 61.7 mmol, 60 % suspension in oil) was washed twice with hexanes (50.0 mL total), to which was added 260 mL of tetrahydrofuran, was cooled to 0 °C. To this suspension was added alcohol **3.47** (3.04 g, 41.1 mmol) neat, along with 15C-5 (1.81 g, 8.2 mmol). The mixture was then allowed to stir at room temperature for 1 h. after which bromine **3.26** (5.0 g, 20.5 mmol) was added dropwise, and the reaction mixture was allowed to warm to room temperature overnight. The reaction mixture was quenched with the addition of 100 mL of water, and the aqueous phase was extracted three times with methylene chloride (500 mL). The organic extracts were dried with MgSO<sub>4</sub>, and concentrated using a rotary evaporator. The crude mixture was purified using flash column chromatography (hexanes:ethyl acetate 4:1), to give **3.48** as a clear oil (996.0 mg, 4.21 mmol, 20.5 %). <sup>1</sup>H NMR (400 MHz, CDCl<sub>3</sub>) δ 7.34 (m, 3H), 7.29 (m, 1H), 4.51 (s, 2H), 3.70 (dd, J = 11.6, 3.2 Hz, 1H), 3.50 (m, 4H), 3.38 (dd, J = 11.6, 6 Hz, 1H), 3.14 (m, 1H), 2.79 (t, J = 4 Hz, 1H), 2.60 (dd, J = 5.2, 2.8 Hz, 1H), 1.69 (m, 4H); <sup>13</sup>C NMR (100 MHz, CDCl<sub>3</sub>) δ 138.8, 128.5, 128.5, 127.8, 127.8, 127.6, 73.0, 71.6, 71.5, 70.2, 51.0, 44.5, 26.6, 26.5. HRESIMS [M+H]<sup>+</sup> calcd for C<sub>14</sub>H<sub>21</sub>O<sub>3</sub> 237.1491, found 237.1494.

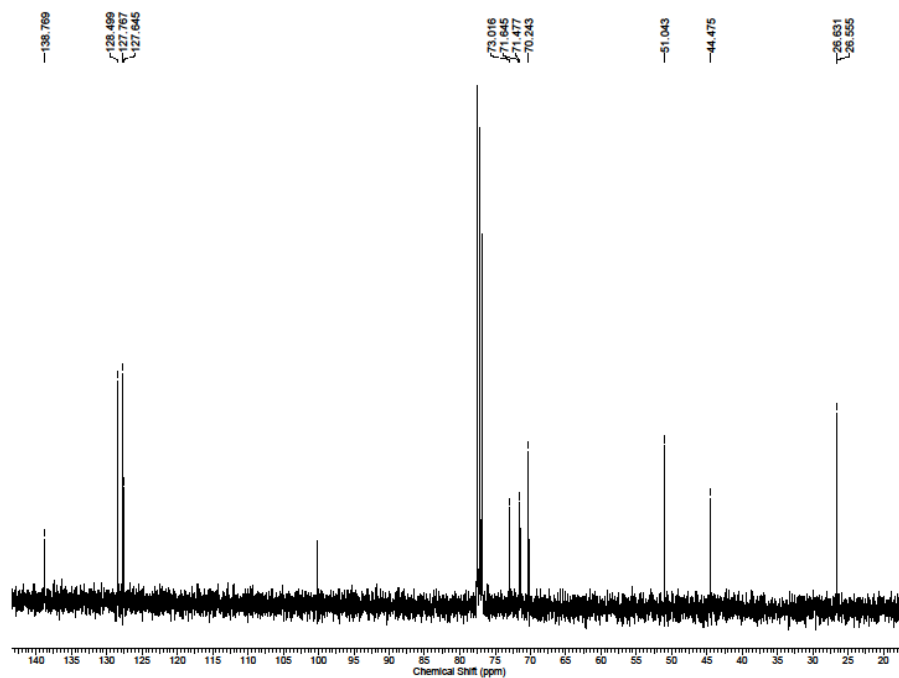
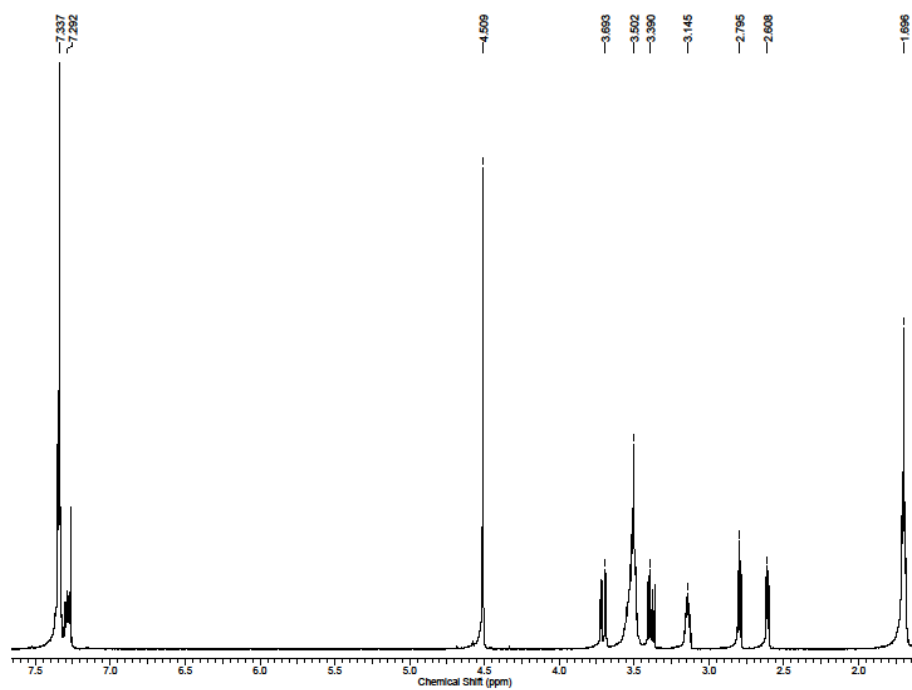
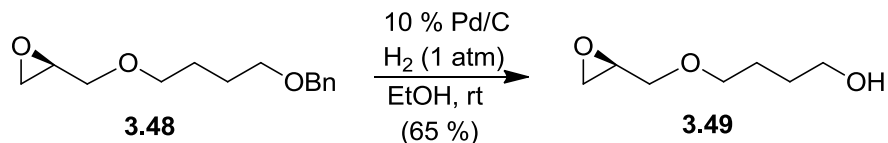


**Figure 3.34**  $^1\text{H}$  and  $^{13}\text{C}$  NMR spectra of **3.48** recorded in  $\text{CDCl}_3$  at 400 MHz and 100 MHz respectively.

### Preparation of 3.49:



To compound **3.48** (900 mg, 3.80 mmol) dissolved in 5 mL of ethanol was added 10 % Pd/C dry (200 mg), in a round bottom and the system flushed with H<sub>2</sub>. The reaction mixture was then exposed to 1 atm of H<sub>2</sub> (balloon) overnight. Upon completion the heterogeneous mixture was filtered and the filtrate washed three times with ethanol (60 mL). The organic extracts were concentrated using a rotary evaporator and the crude mixture was purified using flash column chromatography (hexanes:ethyl acetate 3:2), to give **3.49** as a volatile clear oil (360.5 mg, 2.46 mmol, 64.7 %). <sup>1</sup>H NMR (400 MHz, CDCl<sub>3</sub>) δ 3.70 (dd, J = 11.6, 2.8 Hz, 1H), 3.58 (m, 2H), 3.48 (m, 2H), 3.33 (dd, J = 11.6, 6.0 Hz, 1H), 3.1 (m, 1H), 2.75 (t, J = 4.0 Hz, 1H), 2.6 (bs, 1H), 2.56 (m, 1H), 1.62 (m, 4H); <sup>13</sup>C NMR (100 MHz, CDCl<sub>3</sub>) δ 71.6, 71.6, 62.6, 50.9, 44.4, 29.9, 26.5. HRESIMS [M+H]<sup>+</sup> calcd for C<sub>7</sub>H<sub>15</sub>O<sub>3</sub> 147.1021, found 147.1018.

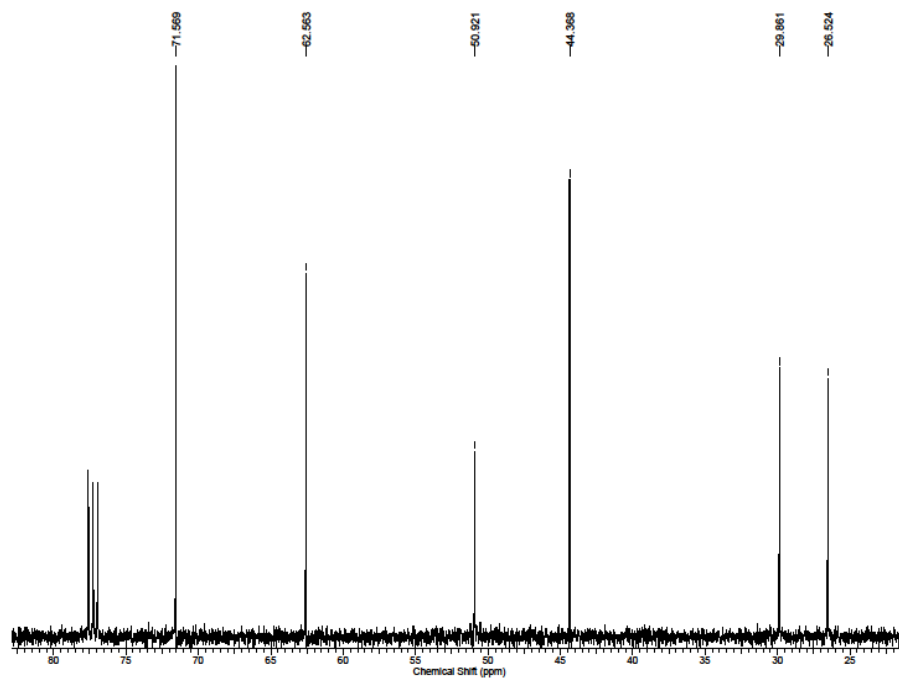
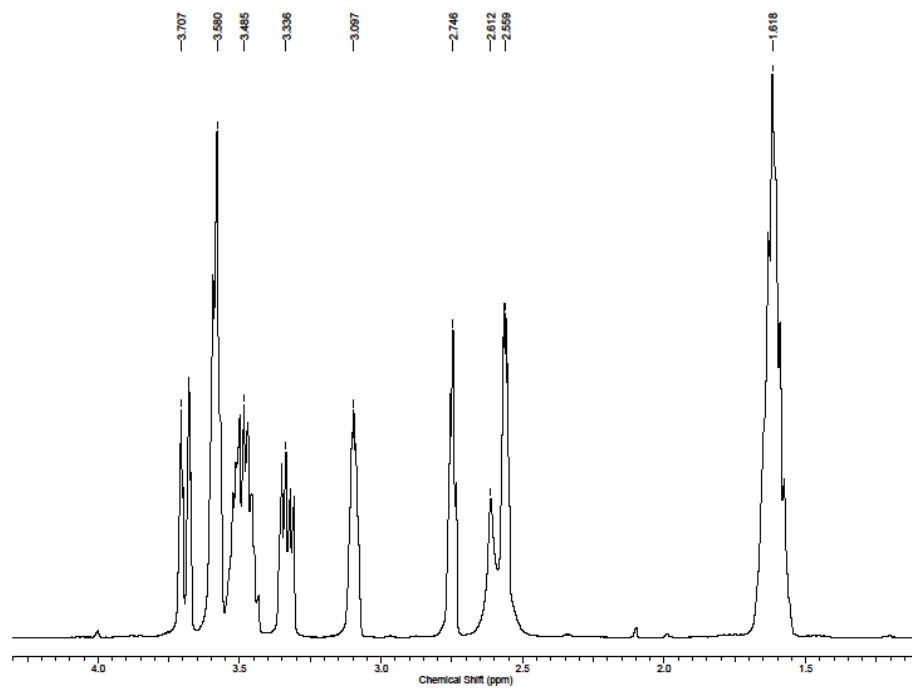
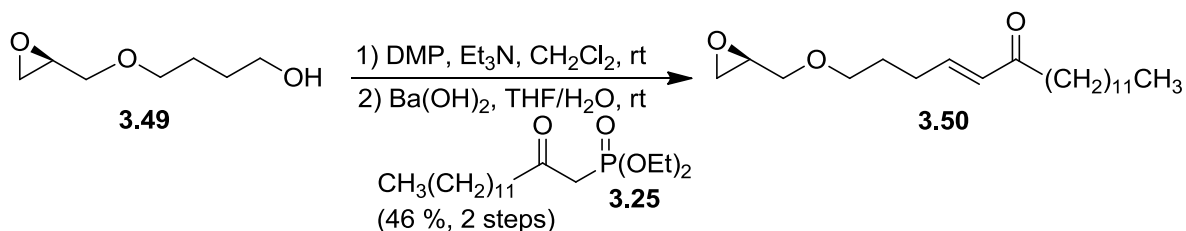


**Figure 3.35** <sup>1</sup>H and <sup>13</sup>C NMR spectra of **3.49** recorded in CDCl<sub>3</sub> at 400 MHz and 100 MHz respectively.

### Preparation of 3.50:



To Dess–Martin periodinane (638.2 mg, 1.50 mmol) was added 12 mL of methylene chloride, followed by triethylamine (553.7 mg, 5.47 mmol). To this reaction mixture was added alcohol **3.49** (200 mg, 1.36 mmol) dissolved on 1.0 mL of methylene chloride, and was stirred at room temperature for 1.5 h. The crude mixture was then concentrated using a rotary evaporator and filtered through a pad of silica (50 mL of 2:3 hexanes:ethyl acetate), and again concentrated using a rotary evaporator. This crude mixture dissolved in 6.0 mL of a tetrahydrofuran:water mixture (40:1) was then added to a solution of phosphonate **3.25** (300 mg, 0.86 mmol) in tetrahydrofuran (3 mL) and Ba(OH)<sub>2</sub> (215 mg) which had been stirring at room temperature for 30 min. After stirring for 2 h the reaction mixture was diluted with 100 mL of water and the aqueous phase was extracted three times with methylene chloride (350 mL). The organic extracts were dried with MgSO<sub>4</sub> and concentrated using a rotary evaporator. The crude mixture was purified using flash column chromatography (hexanes:ethyl acetate 5:1), to give **3.50** as a clear oil (211.7 mg, 0.62 mmol, 45.6 %). <sup>1</sup>H NMR (400 MHz, CDCl<sub>3</sub>) δ 6.84 (dt, J = 14.0, 6.8 Hz, 1H), 6.10 (d, J = 16.0 Hz, 1H), 3.73 (dd, J = 11.6, 2.8 Hz, 1H), 3.5 (m, 2H), 3.35 (dd, J = 11.6, 6.0 Hz, 1H), 3.14 (m, 1H), 2.80 (t, J = 4.4 Hz, 1H), 2.60 (dd, J = 5.2, 2.8 Hz, 1H), 2.51 (t, J = 7.2 Hz, 2H), 2.30 (q, J = 7.2 Hz, 2H), 1.77 (quin, J = 7.6 Hz, 2H), 1.59 (m, 2H), 1.25 (m, 18H), 0.87 (t, J = 6.8 Hz, 3H); <sup>13</sup>C NMR (100 MHz, CDCl<sub>3</sub>) δ 201.0, 146.4, 130.7, 71.7, 70.6, 50.9, 44.3, 40.4, 32.1,

29.8, 29.7, 29.7, 29.65, 29.60, 29.5, 29.5, 29.2, 28.3, 24.5, 22.8, 14.3. HRESIMS  $[M+H]^+$   
calcd for  $C_{21}H_{39}O_3$  339.2899, found 339.2896;  $[\alpha]_D^{24} = -6.49^\circ$  (*c* 0.04).

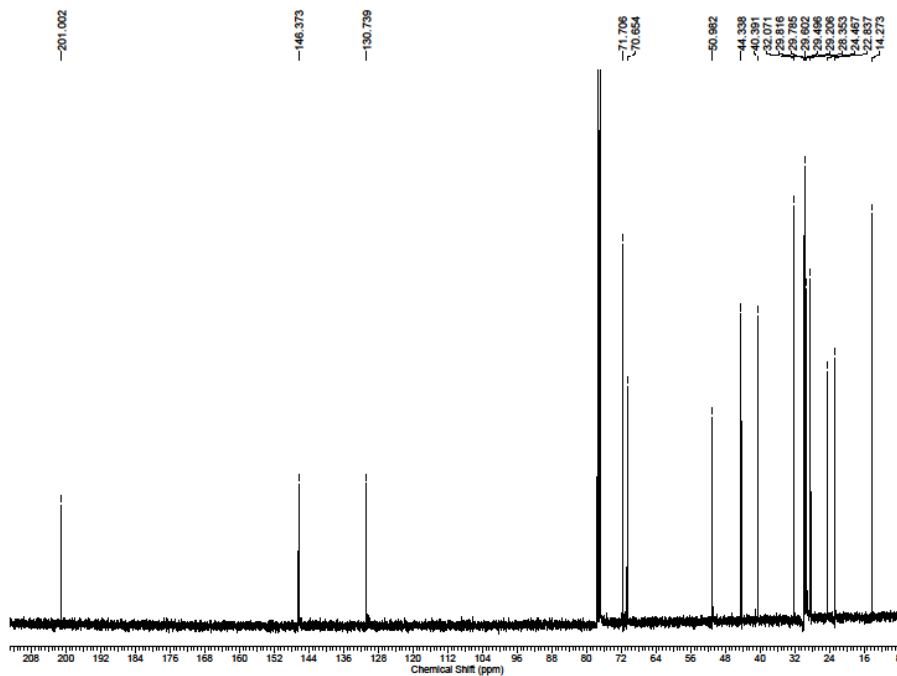
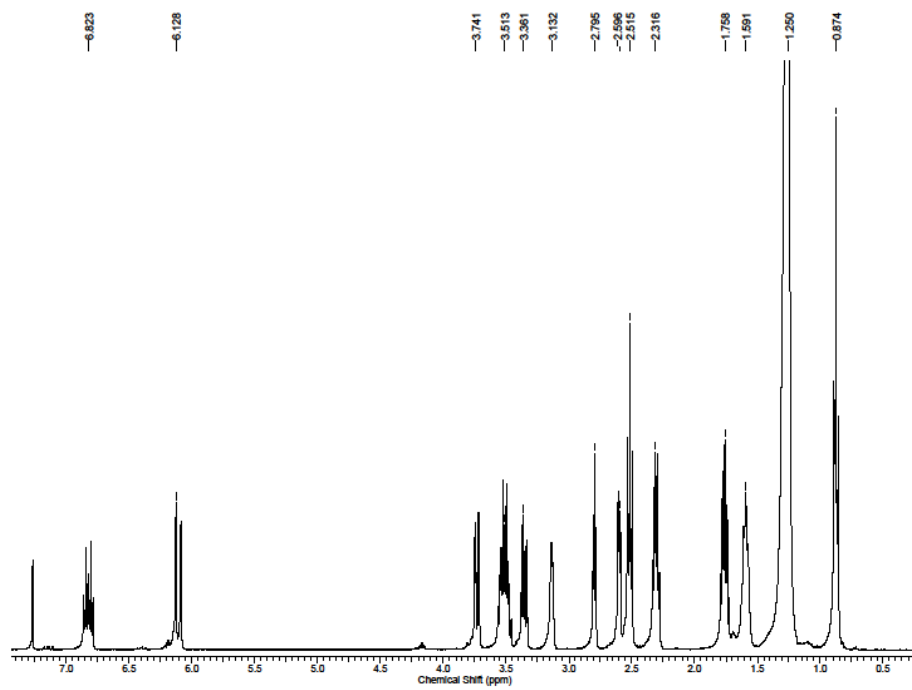
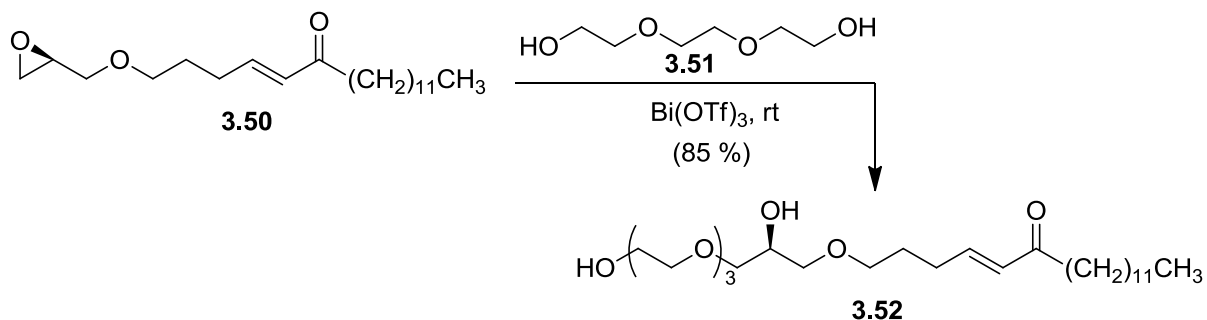


**Figure 3.36**  $^1\text{H}$  and  $^{13}\text{C}$  NMR spectra of **3.50** recorded in  $\text{CDCl}_3$  at 400 MHz and 100 MHz respectively.

### Preparation of 3.52:



To epoxide **3.50** (20.0 mg, 0.059 mmol) dissolved in 1 mL of triethylene glycol (**3.51**) (7.32 mmol) was added bismuth(III) trifluoromethanesulfonate (3.8 mg, 0.0059 mmol), and the mixture allowed to stir at room temperature. After stirring for 1.5 h the reaction mixture was diluted with 25 mL of water and the aqueous phase was extracted three times with methylene chloride (100 mL). The organic extracts were dried with MgSO<sub>4</sub>, and concentrated using a rotary evaporator. The crude mixture was purified using flash column chromatography (methylene chloride:methanol 95:5), to give **3.52** as a clear oil (24.7 mg, 0.050 mmol, 84.7 %). <sup>1</sup>H NMR (400 MHz, C<sub>6</sub>D<sub>6</sub>) δ 6.67 (dt, J = 14.0, 7.2 Hz, 1H), 6.04 (d, J = 16.0 Hz, 1H), 4.09 (m, 1H), 3.62 (m, 2H), 3.56-3.43 (m, 6H), 3.34 (m, 2H), 3.29 (m, 2H), 3.34 (m, 2H), 3.19 (m, 6H), 2.28 (t, J = 7.2 Hz, 2H), 1.97 (q, J = 7.2 Hz, 2H), 1.66 (m, 2H), 1.43 (quin, J = 7.6 Hz, 2H), 1.28 (m, 18H), 0.91 (t, J = 6.8 Hz, 3H); <sup>13</sup>C NMR (100 MHz, C<sub>6</sub>D<sub>6</sub>) δ 198.7, 145.6, 130.8, 74.0, 73.3, 72.1, 70.7, 70.6, 70.6, 70.6, 70.5, 70.0, 69.8, 61.7, 40.3, 32.3, 30.1, 30.1, 29.9, 29.9, 29.7, 29.7, 29.2, 28.5, 24.4, 23.0, 14.3. HRESIMS [M+Na]<sup>+</sup> calcd for C<sub>27</sub>H<sub>52</sub>O<sub>7</sub>Na 511.3611, found 511.3616; [α]<sub>D</sub><sup>24</sup> = -11.9° (c 0.007).

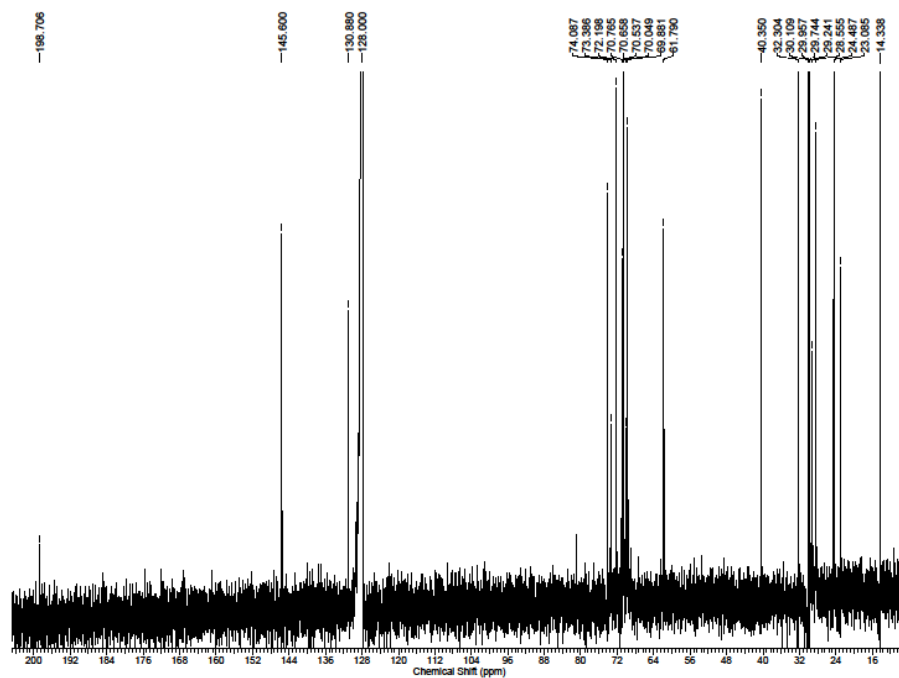
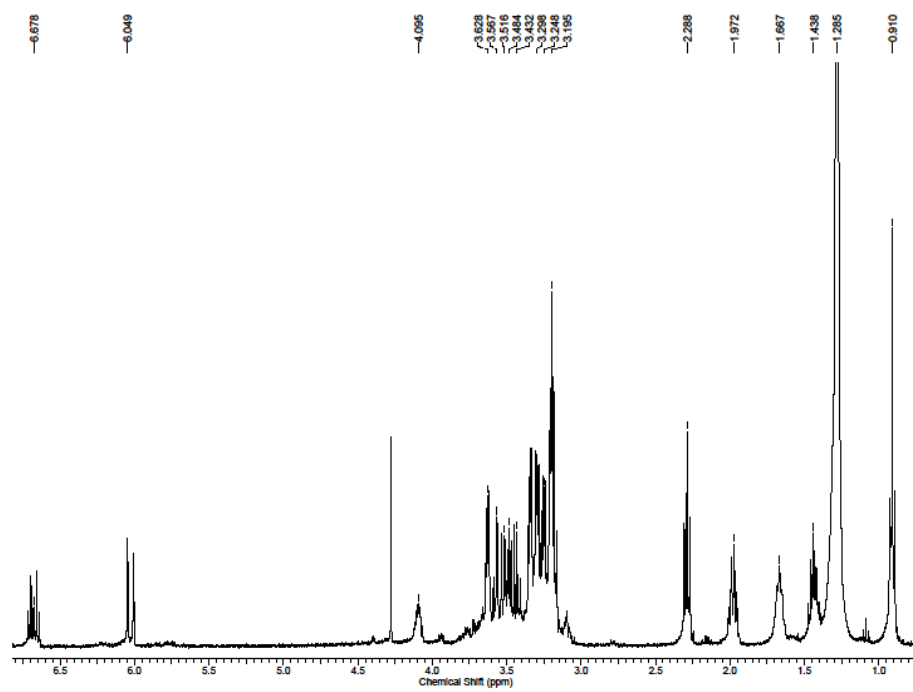
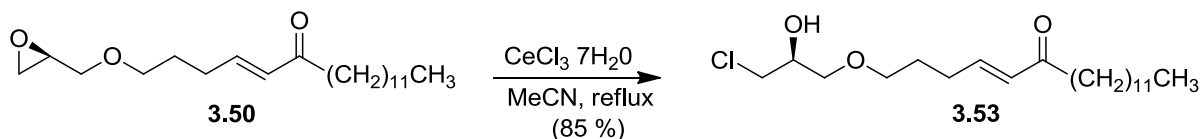


**Figure 3.37**  $^1\text{H}$  and  $^{13}\text{C}$  NMR spectra of **3.52** recorded in  $\text{C}_6\text{D}_6$  at 400 MHz and 100 MHz respectively.

### Preparation of **3.53**:



To epoxide **3.50** (23.4 mg, 0.069 mmol) dissolved in 1.5 mL of acetonitrile was added cerium(III) chloride heptahydrate (12.87 mg, 0.034 mmol) and heated at reflux for 4 h. The reaction mixture was then concentrated using a rotary evaporator and extracted three times with ethyl acetate (60 mL). The crude mixture was then concentrated using a rotary evaporator and purified using flash column chromatography (hexanes: ethylacetate gradient 6:1 - 4:1) to give chlorohydrin **3.53** as a clear oil (22.1 mg, 0.058 mmol, 85.3 %).  $^1\text{H}$  NMR (400 MHz,  $\text{CDCl}_3$ )  $\delta$  6.76 (dt,  $J = 14.0, 6.8$  Hz, 1H), 6.10 (d,  $J = 16.0$  Hz, 1H), 3.78 (bs, 1H), 3.42 (m, 2H), 3.29 (m, 1H), 3.24 (m, 1H), 3.10 (t,  $J = 6.4$  Hz, 2H), 2.39 (t,  $J = 7.2$  Hz, 2H), 2.23 (bs, 1H), 2.00 (q,  $J = 7.2$  Hz, 2H), 1.78 (m, 2H), 1.39 (m, 20H), 1.02 (t,  $J = 6.4$  Hz, 3H);  $^{13}\text{C}$  NMR (100 MHz,  $\text{CDCl}_3$ )  $\delta$  198.6, 145.1, 130.7, 71.5, 70.39, 70.33, 46.2, 40.5, 32.2, 30.0, 30.0, 30.0, 29.9, 29.9, 29.7, 29.6, 29.0, 28.2, 24.4, 23.0, 14.3. HRESIMS  $[\text{M}+\text{H}]^+$  calcd for  $\text{C}_{21}\text{H}_{40}\text{O}_3^{35}\text{Cl}$  375.2666, found 375.2676;  $[\alpha]_D^{24} = +7.61^\circ$  ( $c$  0.009).

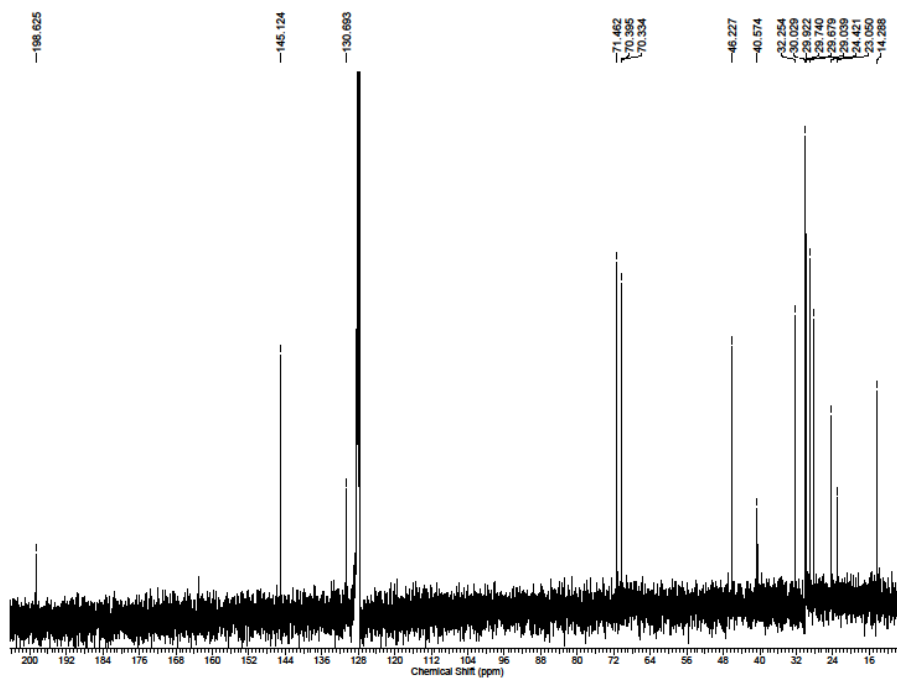
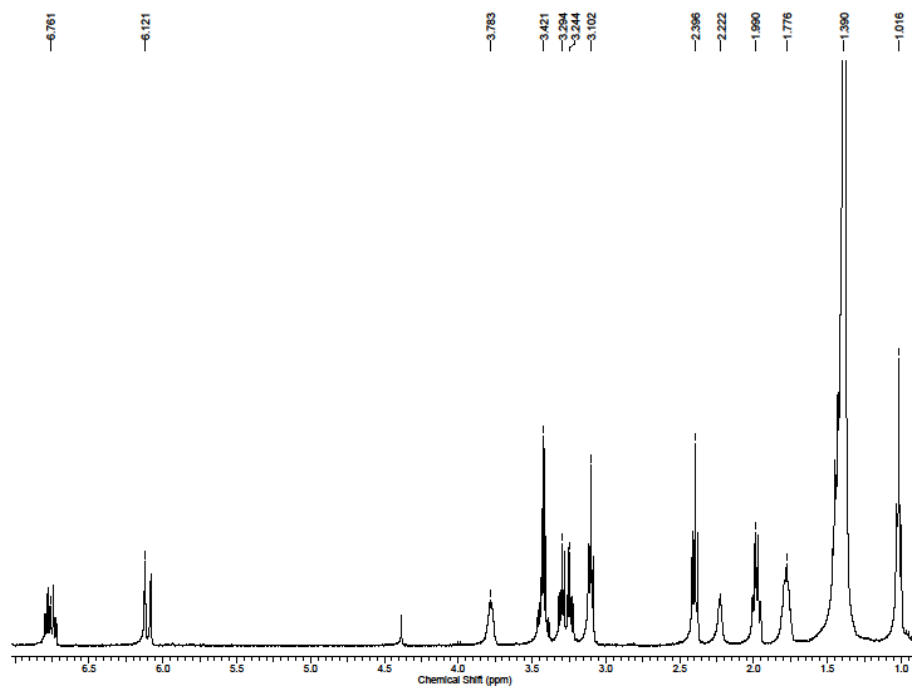
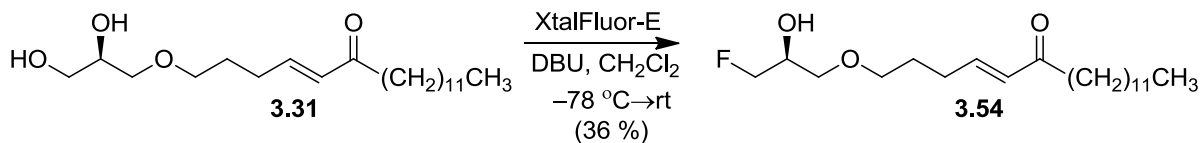


**Figure 3.38**  $^1\text{H}$  and  $^{13}\text{C}$  NMR spectra of **3.53** recorded in  $\text{CDCl}_3$  at 400 MHz and 100 MHz respectively.

### Preparation of 3.54:



To diol **3.31** (9.8 mg, 0.027 mmol) dissolved in 1 mL of methylene chloride at  $-78\text{ }^{\circ}\text{C}$  was added DBU (8.2 mg, 0.054 mmol), followed by XtalFluor-E (12.58 mg, 0.054 mmol), and the reaction allowed to stir for one hour. After stirring for one hour at  $-78\text{ }^{\circ}\text{C}$  the reaction mixture was allowed to warm to room temperature over 12 hours, after which it was concentrated under a stream of nitrogen and the crude reaction mixture was purified using flash column chromatography (hexanes:ethyl acetate 3:1 to ethyl acetate) to give fluorohydrin **3.54** (3.5 mg, 0.0097 mmol, 35.9 %).  $^1\text{H}$  NMR (600 MHz,  $\text{CD}_2\text{Cl}_2$ )  $\delta$  6.81 (dt,  $J = 13.8, 6.6$  Hz, 1H), 6.10 (d,  $J = 15.6$  Hz, 1H), 4.51-4.35 (m, 2H), 3.99 (m, 1H), 3.51-3.46 (m, 3H), 2.51 (t,  $J = 7.2$  Hz, 2 H), 2.30 (m, 2 H), 1.75 (quin,  $J = 6.6$  Hz, 2H), 1.56 (m, 8H), 1.27 (m, 14H), 0.89 (t,  $J = 6.6$  Hz, 3H);  $^{13}\text{C}$  NMR (150 MHz,  $\text{CD}_2\text{Cl}_2$ )  $\delta$  199.9, 145.4, 130.1, 81.0, 70.48, 70.2, 68.5, 39.6, 31.5, 29.2, 29.1, 29.1 29.0, 29.0, 28.9, 28.8, 28.4, 27.6, 23.7, 22.2, 13.4. HRESIMS  $[\text{M}+\text{Na}]^+$  calcd for  $\text{C}_{21}\text{H}_{39}\text{O}_3\text{FNa}$  381.2781, found 381.2783.

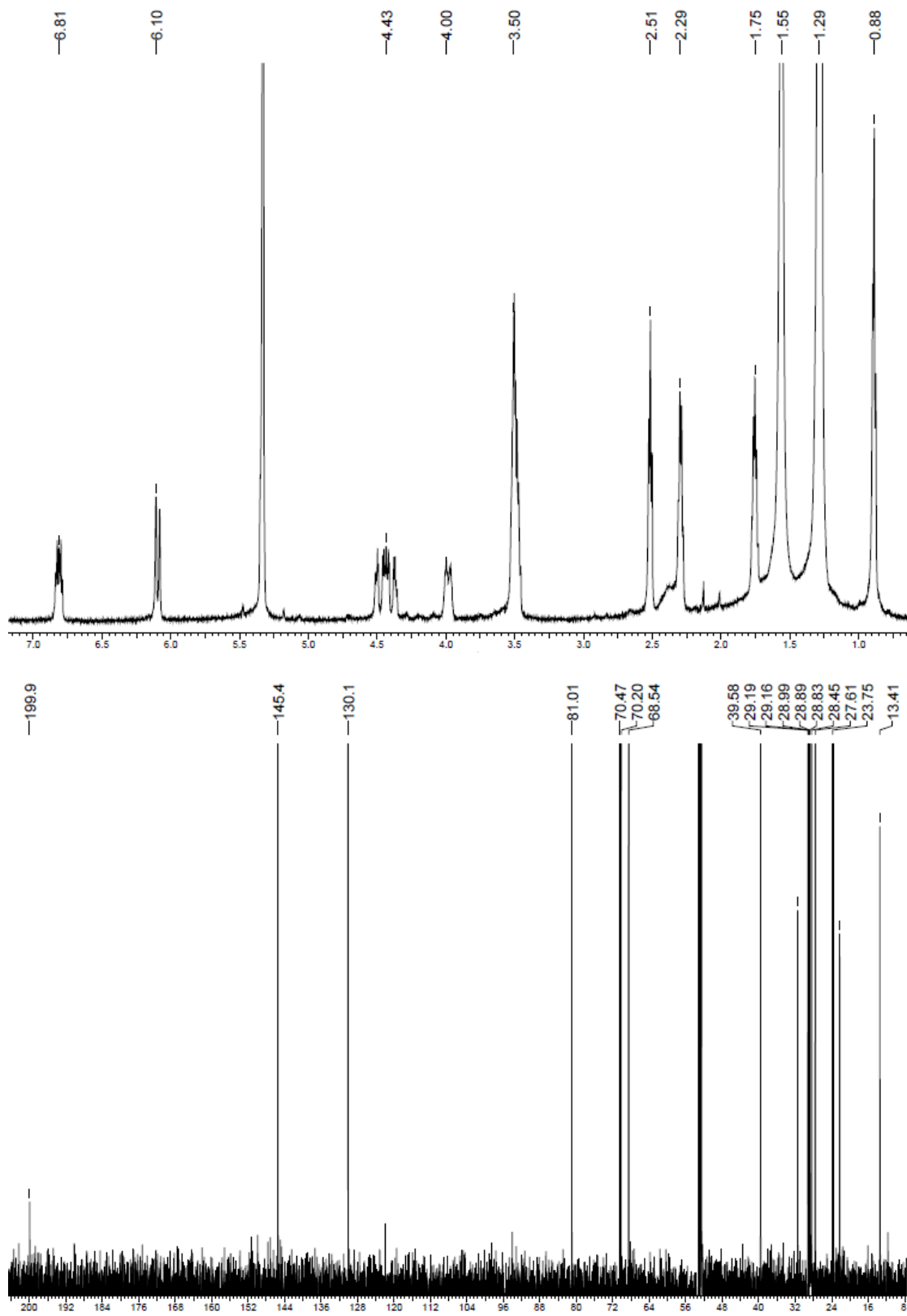
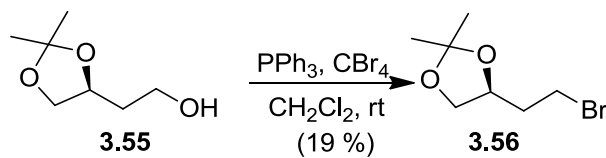


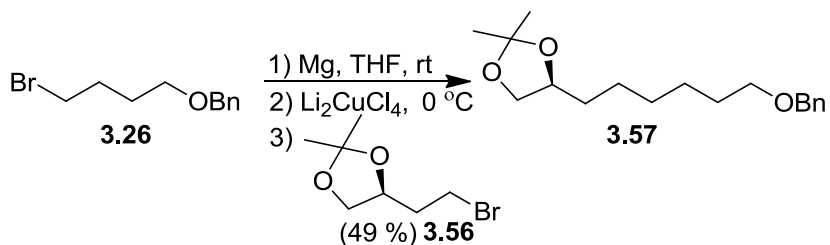
**Figure 3.39**  $^1\text{H}$  and  $^{13}\text{C}$  NMR spectra of **3.54** recorded in  $\text{CD}_2\text{Cl}_2$  at 600 MHz and 150 MHz respectively.

### Preparation of **3.56**:



To acetonide **3.55** (1.0 g, 6.25 mmol), dissolved in 15 mL of methylene chloride, was added triphenyl phosphine (1.80 g, 6.87 mmol), followed by carbon tetrabromide (2.28 g, 6.87 mmol) and allowed to stir at room temperature. After stirring for 5 h the reaction mixture was loaded on to a pad of silica and washed with 150 mL of hexanes:ethyl acetate (2:1). The organic extract was concentrated using a rotary evaporator and the crude mixture was purified using flash column chromatography (hexanes:ethyl acetate 15:1) to give known bromide **3.56** (259 mg, 1.23 mmol, 19.6 %).

### Preparation of **3.57**:



To bromide **3.26** (562 mg, 2.31 mmol), dissolved in 5 mL of tetrahydrofuran, was added sanded magnesium turnings (84.3 g, 6.87 mmol). After the reaction mixture cooled to room temperature (~ 1 h), it was transferred to an empty N<sub>2</sub> filled round bottom with a syringe. This was cooled to 0 °C and Li<sub>2</sub>CuCl<sub>4</sub> (0.1 M in tetrahydrofuran, 0.115 mmol, 1.115 mL) added, followed by bromide **3.56** (259 mg, 1.23 mmol) dissolved in 2.5 mL of tetrahydrofuran, and the reaction mixture was allowed to warm to room temperature. After 4 h, the reaction mixture was quenched with 0.5 mL of methanol, and loaded on to a pad of silica and washed with 200 mL of hexanes:ethyl acetate (4:1). The crude mixture was concentrated using a rotary evaporator and purified using flash column chromatography (hexanes:ethyl acetate 12:1) to give acetone **3.57** (177.7 mg, 0.607 mmol, 49.3 %). <sup>1</sup>H NMR (400 MHz, CDCl<sub>3</sub>) δ 7.33 (m, 4H), 7.27 (m, 1H), 4.49 (s, 2H), 4.06 (quin, J = 6.0 Hz, 1H), 4.00 (m, 1H), 3.46 (m, 3H), 1.62 (m, 2H), 1.52-1.29 (m, 8H), 1.41 (s, 3H), 1.35 (s, 3H); <sup>13</sup>C NMR (100 MHz, CDCl<sub>3</sub>) δ 138.9, 128.5, 127.7, 127.6, 108.7, 76.2, 73.0, 70.5, 69.6, 33.7, 29.8, 29.6, 27.1, 27.1, 26.3, 25.9. HRESIMS [M+Na]<sup>+</sup> calcd for C<sub>18</sub>H<sub>28</sub>O<sub>3</sub>Na 315.1936, found 315.1938; [α]<sub>D</sub><sup>24</sup> = +5.36° (c 0.04).

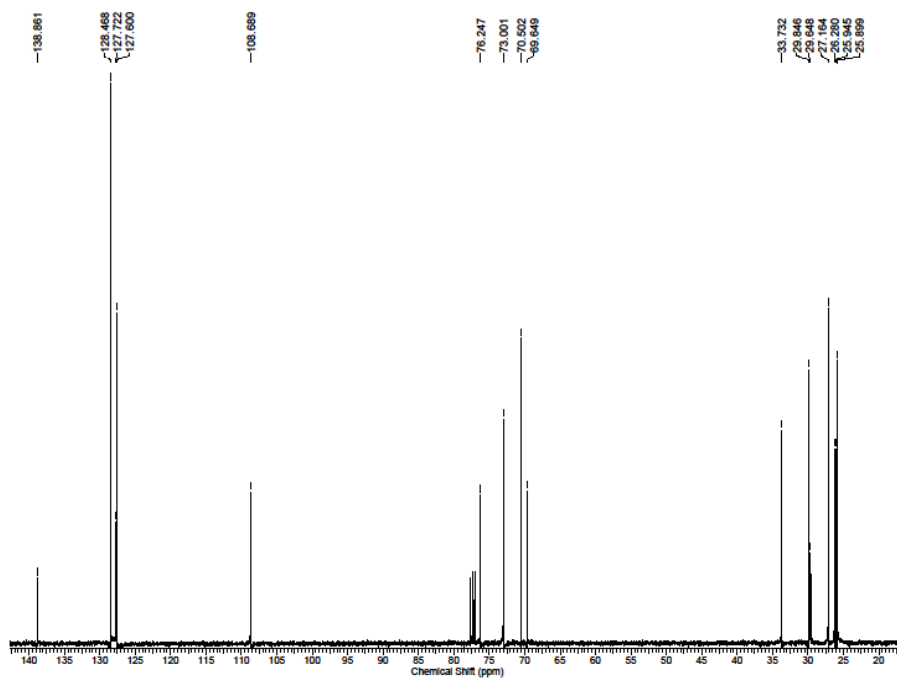
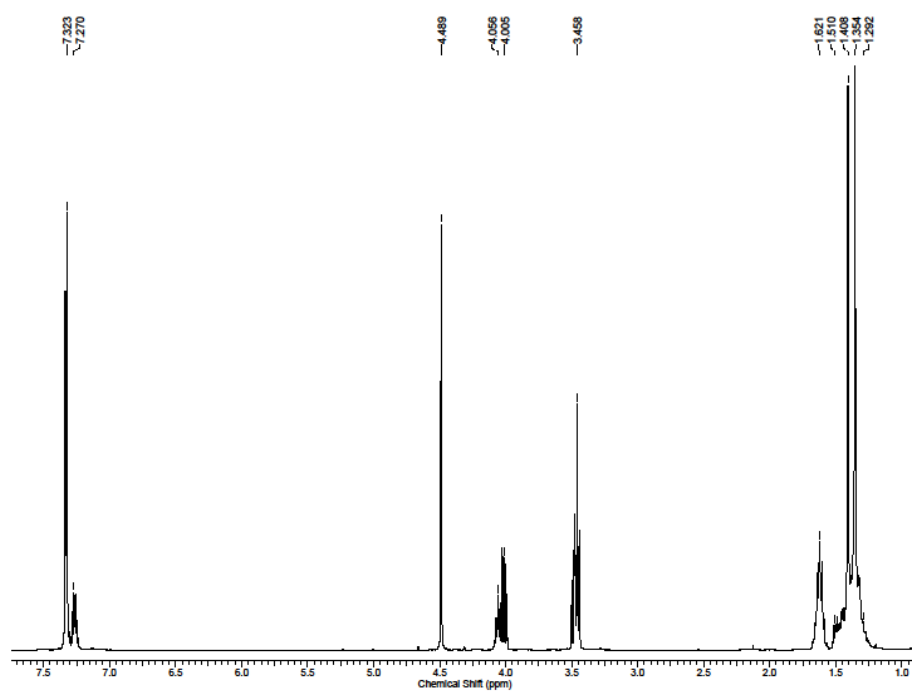
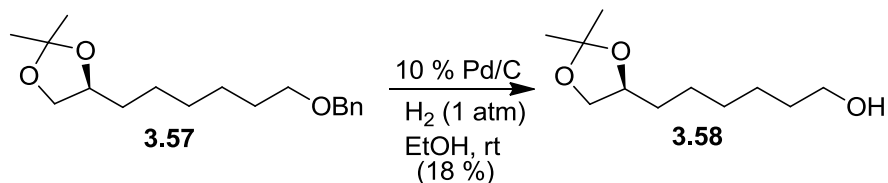


**Figure 3.40**  $^1\text{H}$  and  $^{13}\text{C}$  NMR spectra of **3.57** recorded in  $\text{CDCl}_3$  at 400 MHz and 100 MHz respectively.

### Preparation of 3.58:



To **3.57** (2.5 g, 8.54 mmol) dissolved in 10 mL of ethanol was added 200 mg 10 % Pd/C, and exposed to 1 atm of H<sub>2</sub> and allowed to stir at room temperature overnight. The mixture was then filtered through filter paper and concentrated using a rotary evaporator then purified using flash column chromatography (hexanes:ethyl acetate 2:1) to give alcohol **3.58** (315.1 mg, 1.55 mmol, 18.1 %). <sup>1</sup>H NMR (400 MHz, CDCl<sub>3</sub>) δ 3.98 (quin, J = 6.4 Hz, 1H), 3.93 (m, 1H), 3.50 (t, J = 6.4 Hz, 2H), 3.40 (t, J = 7.2 Hz, 1H), 2.71 (bs, 1H), 1.59-1.17 (m, 10H), 1.31 (s, 3H), 1.26 (s, 3H); <sup>13</sup>C NMR (150 MHz, CDCl<sub>3</sub>) δ 108.1, 75.6, 68.9, 62.1, 33.0, 33.0, 32.1, 28.9, 26.4, 25.2, 25.1. HRESIMS [M+Na]<sup>+</sup> calcd for C<sub>11</sub>H<sub>22</sub>O<sub>3</sub>Na 225.1467, found 225.1459; [α]<sub>D</sub><sup>24</sup> = +9.02° (c 0.04).

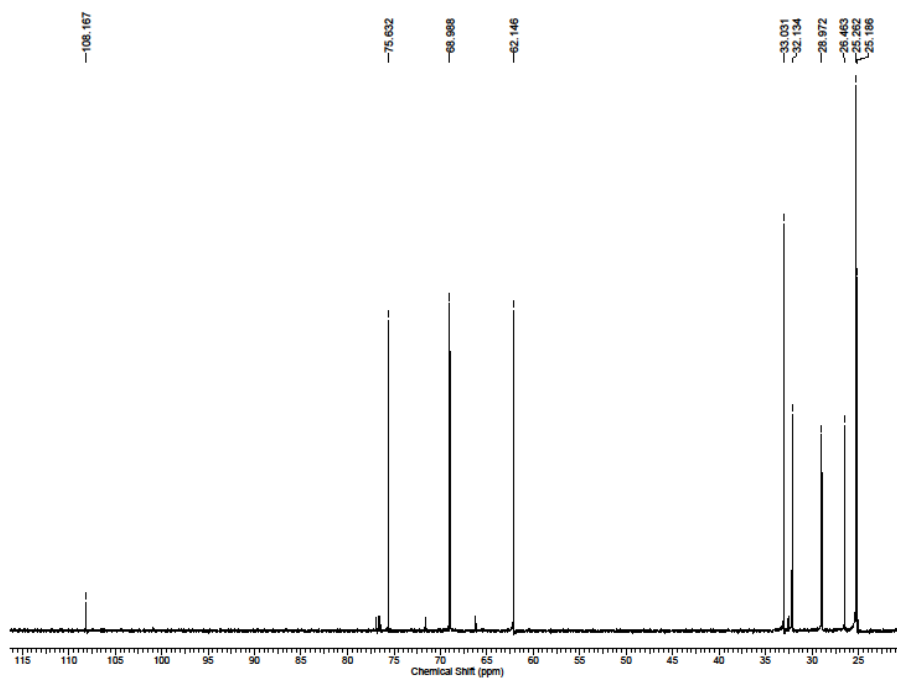
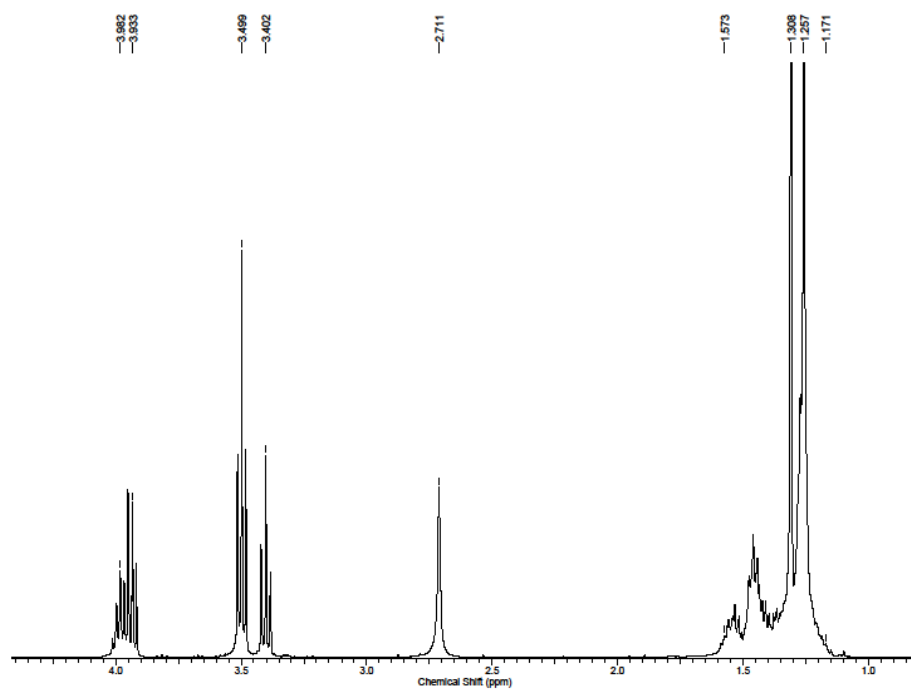
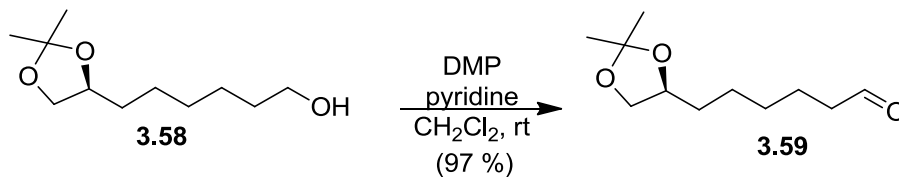


**Figure 3.41** <sup>1</sup>H and <sup>13</sup>C NMR spectra of **3.58** recorded in CDCl<sub>3</sub> at 400 MHz and 150 MHz respectively.

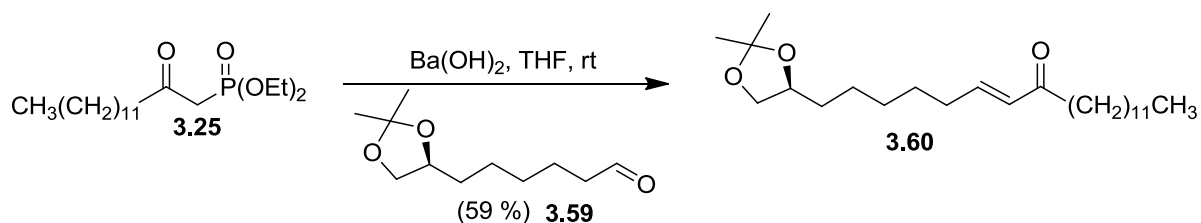
### Preparation of 3.59:



To alcohol **3.58** (150 mg, 0.741 mmol) dissolved in 7 mL of methylene chloride, was added pyridine (0.45 mL, 5.55 mmol), and Dess–Martin periodinane (471.0 mg, 1.11 mmol), and allowed to stir at room temperature for 30 min. The crude reaction mixture was concentrated using a rotary evaporator and purified using flash column chromatography (hexanes:ethyl acetate 5:1) to give aldehyde **3.59** (144.2 mg, 0.72 mmol, 97.1 %). <sup>1</sup>H NMR (600 MHz, CDCl<sub>3</sub>) δ 9.78 (s, 1H), 4.18 (m, 1H), 4.08 (t, J = 6.0 Hz, 1H), 4.04 (m, 1H), 3.5 (t, J = 6.6 Hz, 1H), 2.44 (t, J = 7.2 Hz, 2H), 1.66 (quin, J = 7.2 Hz, 4H), 1.54-1.37 (m, 3H), 1.41 (s, 3H), 1.36 (s, 3H); <sup>13</sup>C NMR (150 MHz, CDCl<sub>3</sub>) δ 202.2, 108.2, 75.5, 69.0, 43.3, 32.9, 28.7, 26.5, 25.3, 25.1, 21.5. HRESIMS [M+Na]<sup>+</sup> calcd for C<sub>11</sub>H<sub>20</sub>O<sub>3</sub>Na 223.1310, found 223.1315; [α]<sub>D</sub><sup>24</sup> = +7.94° (c 0.01).



### Preparation of 3.60:



To phosphonate **3.25** (191 mg, 0.55 mmol) in 2.5 mL of tetrahydrofuran, was treated with barium hydroxide (185.7 mg, 1.08 mmol) and allowed to stir at room temperature for 30 min. To this heterogeneous mixture was added aldehyde **3.59** (110.0 mg, 0.55 mmol) dissolved in 4.1 mL of a tetrahydrofuran:water mixture (40:1), and the reaction mixture was allowed to stir at room temperature overnight. The reaction mixture was then filtered through a pad of silica and washed with 100 mL of hexanes:ethyl acetate 3:1, and concentrated using a rotary evaporator. The crude mixture was purified using flash column chromatography (hexanes:ethyl acetate 9:1) to give acetonide **3.60** (129.9 mg, 0.329 mmol, 59.8 %).  $^1\text{H}$  NMR (600 MHz,  $\text{CDCl}_3$ )  $\delta$  6.83 (dt,  $J = 6.6, 16.2$  Hz, 1H), 6.10 (d,  $J = 16.2$  Hz, 1H), 4.08 (sep,  $J = 6.6$  Hz, 1H), 4.04 (dd,  $J = 6.0, 1.8$  Hz, 1H), 3.51 (t,  $J = 6.6$  Hz, 1H), 2.52 (t,  $J = 7.8$  Hz, 2H), 2.22 (m, 2H), 1.00 (m, 4H), 1.49 (m, 6H), 1.41 (s, 3H), 1.36 (s, 3H), 1.26 (m, 18H), 0.87 (t,  $J = 7.2$  Hz, 3H);  $^{13}\text{C}$  NMR (150 MHz,  $\text{CDCl}_3$ )  $\delta$  200.5, 146.5, 129.9, 108.2, 75.6, 69.0, 39.7, 33.0, 31.9, 31.5, 29.2, 29.2, 29.0, 29.0, 28.9, 28.9, 28.7, 28.7, 27.5, 26.5, 25.3, 25.1, 23.9, 22.2, 13.7. HRESIMS  $[\text{M}+\text{Na}]^+$  calcd for  $\text{C}_{25}\text{H}_{46}\text{O}_3\text{Na}$  417.3345, found 417.3351;  $[\alpha]_D^{24} = +4.56^\circ$  ( $c$  0.03).

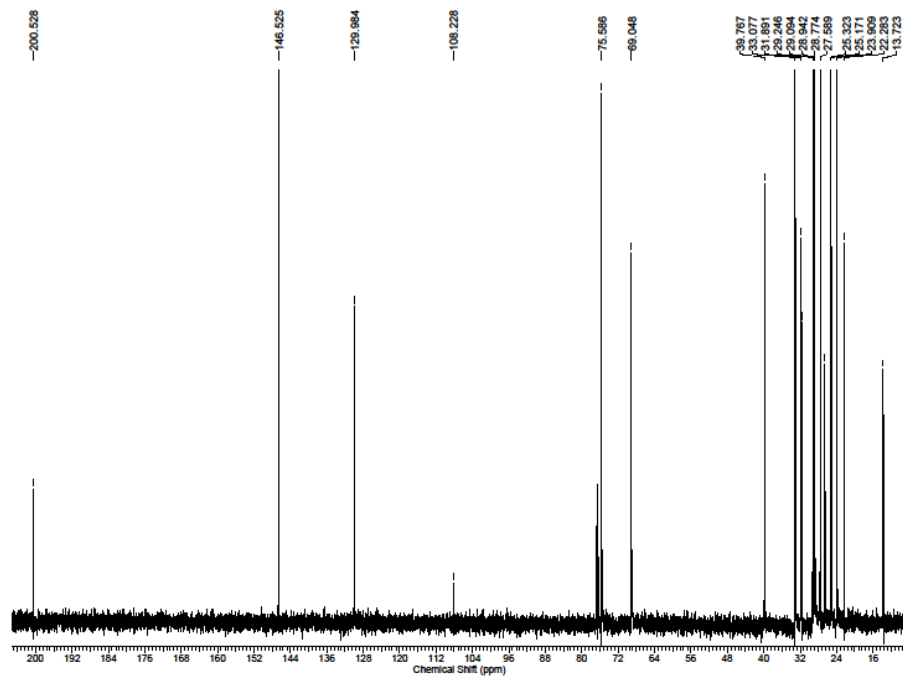
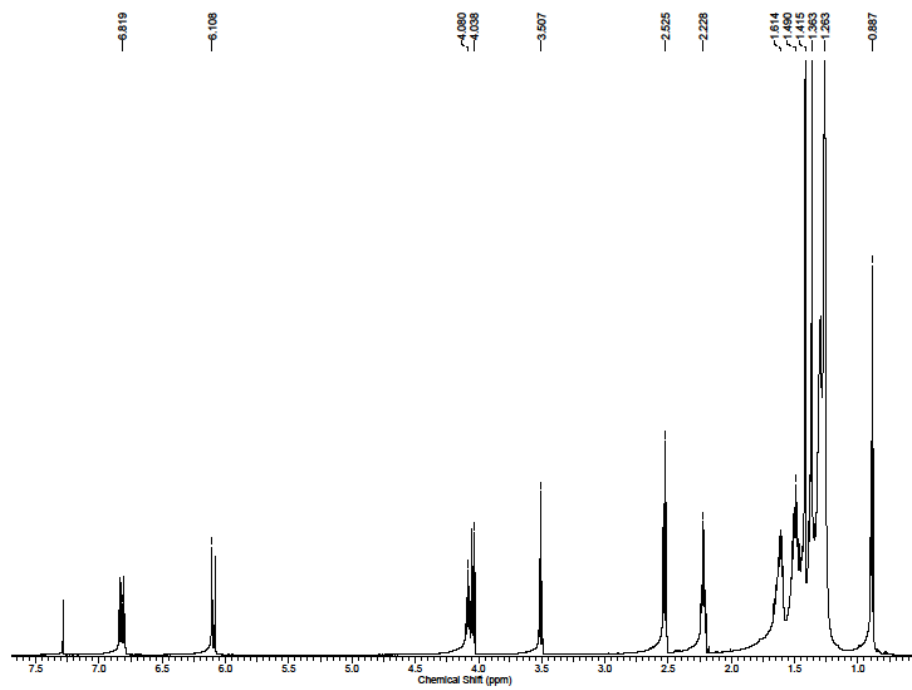
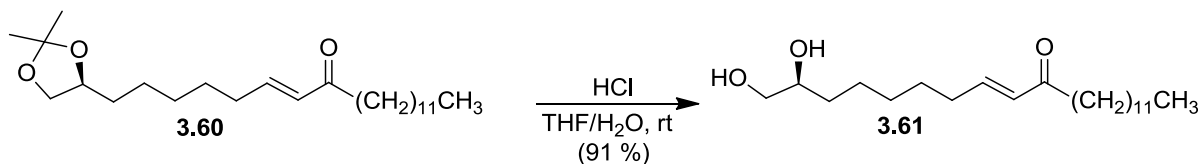


**Figure 3.43**  $^1\text{H}$  and  $^{13}\text{C}$  NMR spectra of **3.60** recorded in  $\text{CDCl}_3$  at 600 MHz and 150 MHz respectively.

### Preparation of 3.61:



To acetonide **3.60** (90.0 mg, 0.228 mmol) dissolved in 5 mL of a tetrahydrofuran:water mixture (5:1) was added 12.4 M HCl (0.91 mL, 11.28 mmol), and allowed to stir at room temperature for thirty minutes. The reaction mixture was then concentrated under a stream of nitrogen and purified using flash column chromatography (hexanes:ethyl acetate 2:3) to give diol **3.61** (73.8 mg, 0.208 mmol, 91.2 %). <sup>1</sup>H NMR (600 MHz, CDCl<sub>3</sub>) δ 6.83 (dt, J = 15.6, 7.2 Hz, 1H), 6.10 (d, J = 15.6 Hz, 1H), 3.7 (m, 1H), 3.66 (m, 1H), 3.45 (dd, J = 7.2, 3.6 Hz, 1H), 2.53 (t, J = 7.2 Hz, 2H), 2.48 (bs, 2H), 2.24 (q, J = 7.8 Hz, 2H), 1.60 (m, 2H), 1.51-1.44 (m, 4H), 1.37 (m, 4H), 1.26 (m, 18H), 0.89 (t, J = 6.6 Hz, 3H); <sup>13</sup>C NMR (150 MHz, CDCl<sub>3</sub>) δ 200.8, 146.7, 129.9, 71.7, 66.3, 39.7, 32.5, 31.9, 31.5, 29.2, 29.2, 29.2, 29.0, 29.0, 28.9, 28.9, 28.7, 27.5, 24.9, 23.9, 22.2, 13.7. HRESIMS [M+Na]<sup>+</sup> calcd for C<sub>22</sub>H<sub>42</sub>O<sub>3</sub>Na 377.3032, found 377.3030; [α]<sub>D</sub><sup>24</sup> = +3.69° (c 0.01).

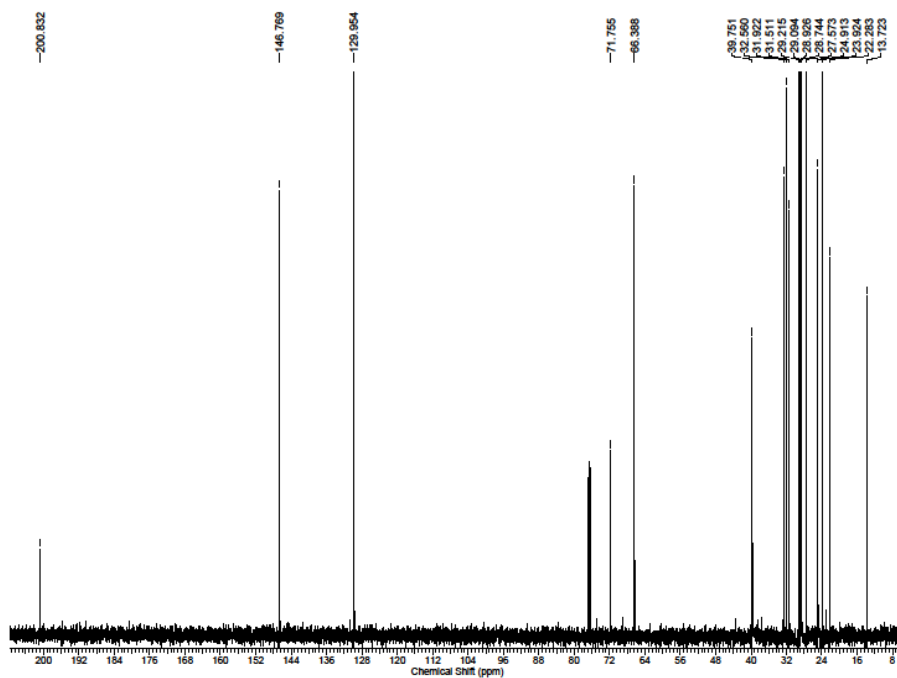
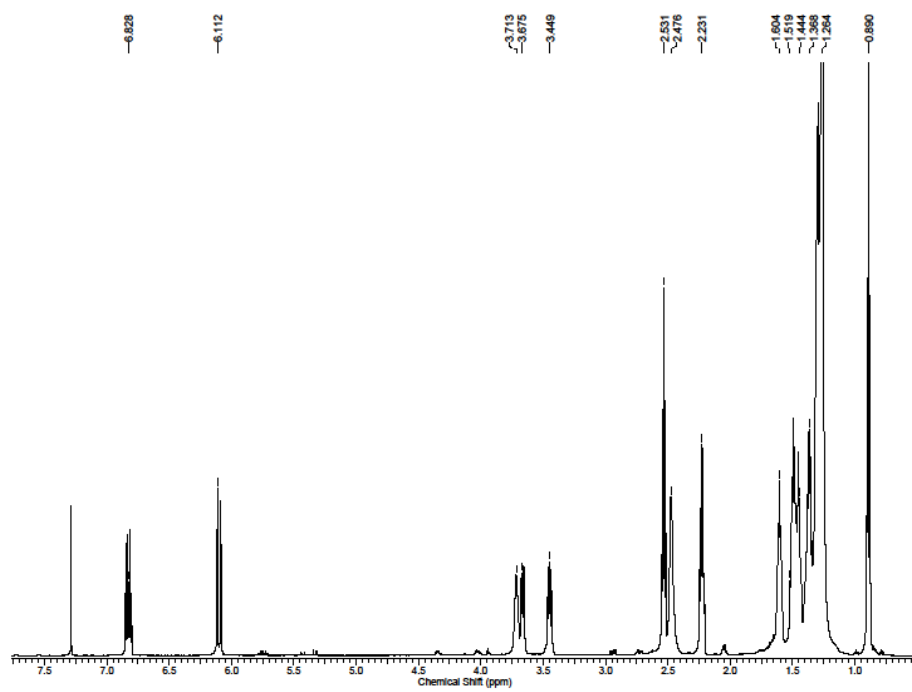
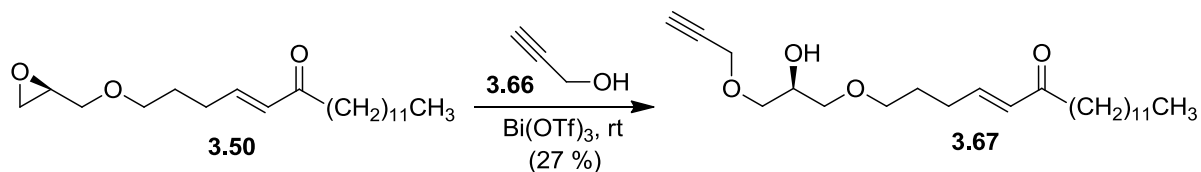


**Figure 3.44**  $^1\text{H}$  and  $^{13}\text{C}$  NMR spectra of **3.61** recorded in  $\text{CDCl}_3$  at 600 MHz and 150 MHz respectively.

### Preparation of 3.67:



To epoxide **3.50** (80.0 mg, 0.236 mmol) along with propargyl alcohol (13.2 mg, 0.236 mmol) was added bismuth(III) trifluoromethanesulfonate (14.77 mg, 0.0236 mmol), and the mixture allowed to stir at room temperature. After stirring for 30 min the reaction mixture was purified using flash column chromatography (hexanes:ethyl acetate gradient 3:1-2:1), to give **3.67** as a clear oil (25.4 mg, 0.064 mmol, 27.1 %).  $^1\text{H}$  NMR (600 MHz,  $\text{CDCl}_3$ )  $\delta$  6.76 (dt,  $J = 9.6, 4.8$  Hz, 1H), 6.09 (d,  $J = 10.4$  Hz, 1H), 4.00 (q,  $J = 4.0$  Hz, 1H), 3.92 (m, 2H), 3.57 (m, 2H), 3.39 (d,  $J = 3.6$  Hz, 2H), 3.18 (m, 2H), 2.38 (t,  $J = 5.2$  Hz, 2H), 2.11 (t,  $J = 1.6$  Hz, 1H), 2.02 (q,  $J = 4.8$  Hz, 2H), 1.76 (m, 2H), 1.47 (q,  $J = 4.8$  Hz, 3H), 1.38 (m, 18H), 1.00 (t,  $J = 4.4$  Hz, 3H);  $^{13}\text{C}$  NMR (150 MHz,  $\text{CDCl}_3$ )  $\delta$  198.0, 144.7, 130.1, 79.3, 74.1, 71.6, 70.8, 69.8, 68.9, 57.9, 31.7, 29.5, 29.5, 29.4, 29.4, 29.33, 29.30, 29.15, 29.09, 28.5, 27.8, 23.8, 22.5, 13.7. HRESIMS  $[\text{M}+\text{H}]^+$  calcd for  $\text{C}_{24}\text{H}_{43}\text{O}_4$  395.3161, found 395.3169;  $[\alpha]_D^{24} = -3.39^\circ$  ( $c$  0.01).

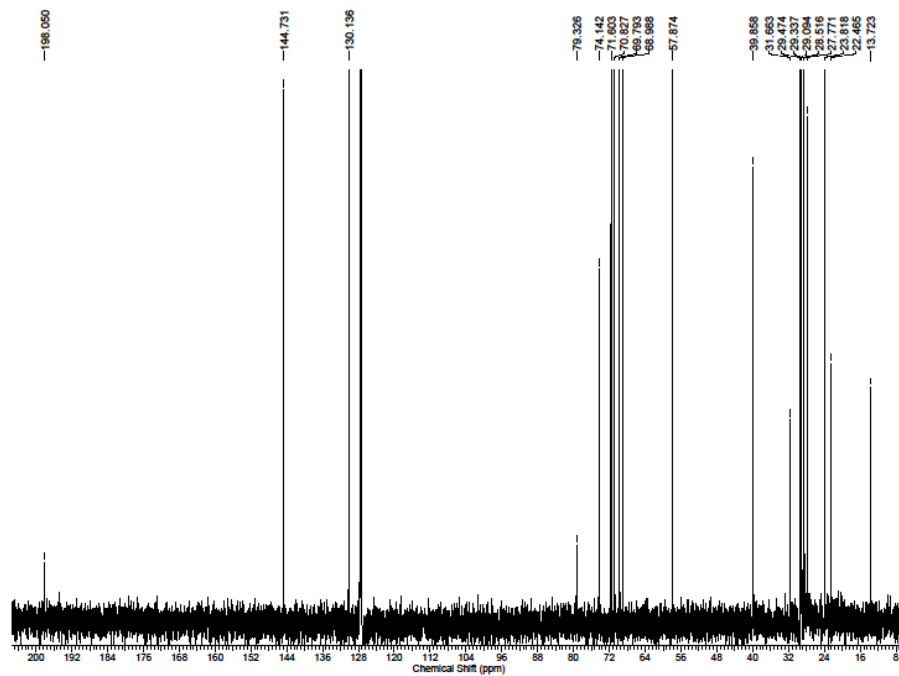
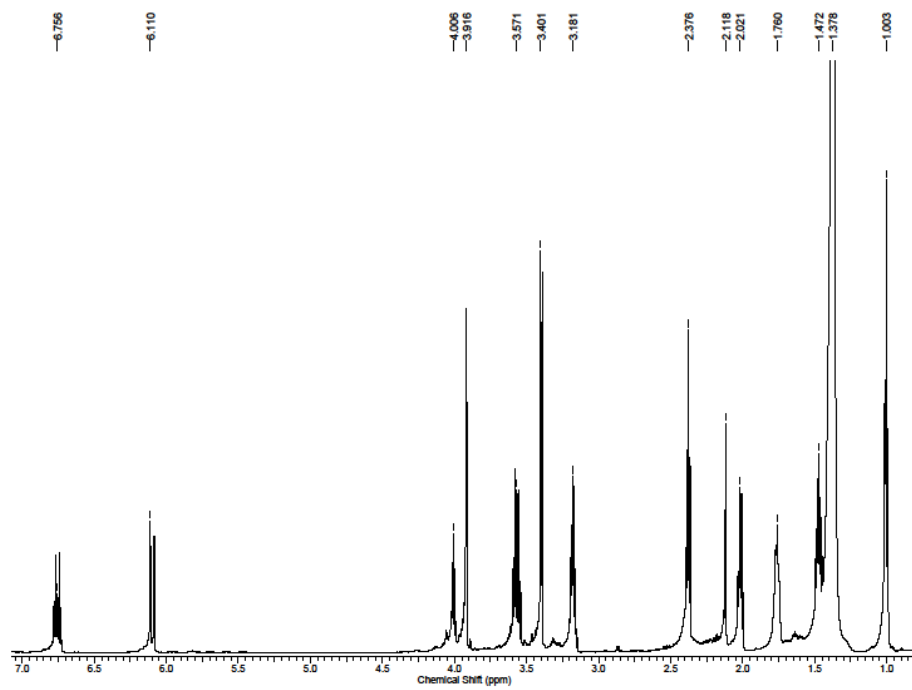
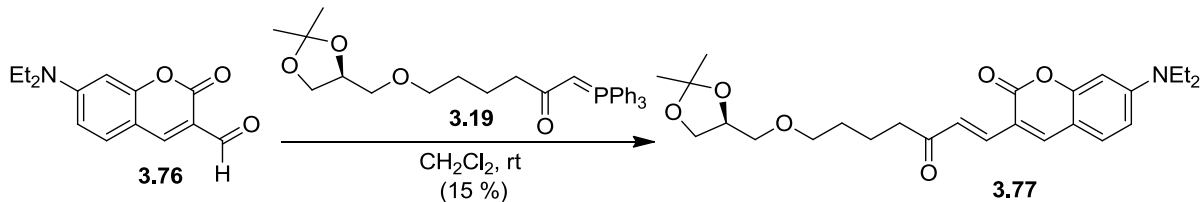


**Figure 3.45**  $^1\text{H}$  and  $^{13}\text{C}$  NMR spectra of **3.67** recorded in  $\text{CDCl}_3$  at 600 MHz and 150 MHz respectively.

### Preparation of **3.77**:



To phosphonate **3.19** (~0.79 mmol, crude) in 3 mL of methylene chloride was added aldehyde<sup>161</sup> **3.76** (106.4 mg, 0.43 mmol), and allowed to stir at room temperature overnight. The solvent was evaporated and the crude mixture was purified using flash column chromatography (hexanes:ethyl acetate 2:1-3:2) to give **3.77** (28.9 mg, 0.063 mmol, 14.6 %).  $^1\text{H}$  NMR (400 MHz,  $\text{CDCl}_3$ )  $\delta$  7.74 (s, 1H), 7.44 (d,  $J = 15.6$  Hz, 1H), 7.28 (t,  $J = 8.8$  Hz, 1H), 7.20 (d,  $J = 15.6$  Hz, 1H), 6.60 (dd,  $J = 8.8, 2.4$  Hz, 1H), 6.47 (s, 1H), 4.25 (q,  $J = 6.4$  Hz, 1H), 4.04 (t,  $J = 6.4$  Hz, 1H), 3.72 (t,  $J = 6.4$  Hz, 1H), 3.54-3.40 (m, 8H), 2.65 (t,  $J = 7.2$  Hz, 2H), 1.72 (m, 2H), 1.64 (m, 2H), 1.41 (s, 3H), 1.35 (m, 3H), 1.33 (t,  $J = 7.2$  Hz, 6H);  $^{13}\text{C}$  NMR (100 MHz,  $\text{CDCl}_3$ )  $\delta$  200.8, 160.6, 157.0, 151.9, 144.8, 137.2, 130.0, 126.6, 114.7, 109.6, 109.5, 108.9, 97.1, 74.9, 72.0, 71.5, 67.0, 45.1, 45.1, 41.5, 29.2, 26.9, 25.5, 21.0, 12.6, 12.6. HRESIMS  $[\text{M}+\text{H}]^+$  calcd for  $\text{C}_{26}\text{H}_{36}\text{NO}_6$  458.2543, found 458.2536.

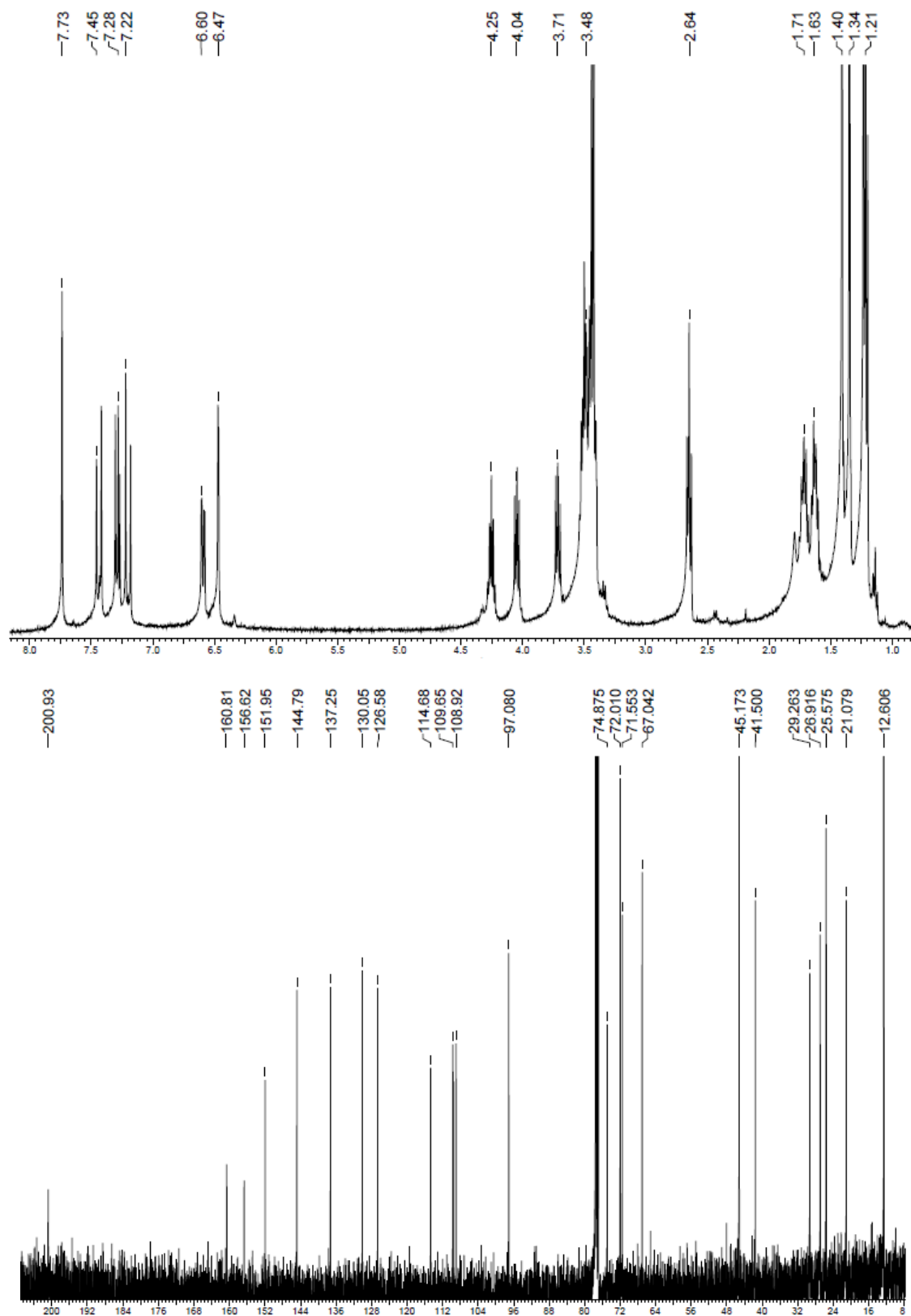
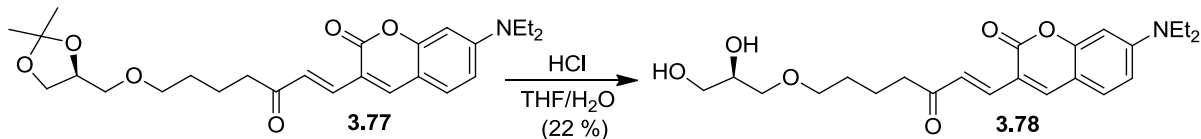


**Figure 3.46**  $^1\text{H}$  and  $^{13}\text{C}$  NMR spectra of **3.77** recorded in  $\text{CDCl}_3$  at 400 MHz and 100 MHz respectively.

### Preparation of **3.78**:



To **3.77** (20.0 mg, 0.043 mmol) in 1 mL of a tetrahydrofuran:water mixture (5:1) was added 12.4 M HCl (17.6  $\mu$ l, 0.22 mmol), and allowed to stir at room temperature for 2 hours. The crude reaction mixture was concentrated under a stream of nitrogen and purified using flash column chromatography (ethyl acetate) to give **3.78** (4.0 mg, 0.0095 mmol, 22.1 %).  $^1\text{H}$  NMR (600 MHz,  $\text{CD}_2\text{Cl}_2$ )  $\delta$  7.82 (s, 1H), 7.44 (d,  $J = 15.6$  Hz, 1H), 7.37 (d,  $J = 8.4$  Hz, 1H), 7.18 (d,  $J = 15.6$  Hz, 1H), 6.72 (d,  $J = 8.4$  Hz, 1H), 6.57 (s, 1H), 3.82 (m, 1H), 3.67 (dd,  $J = 11.4, 4.2$  Hz, 1H), 3.61 (dd,  $J = 11.4, 6.0$  Hz, 1H), 3.52-3.44 (m, 8H), 2.67 (t,  $J = 6$  Hz, 2H), 1.72 (m, 2H), 1.63 (m, 2H), 1.23 (t,  $J = 7.2$  Hz, 6H);  $^{13}\text{C}$  NMR (150 MHz,  $\text{CD}_2\text{Cl}_2$ )  $\delta$  199.8, 144.0, 136.4, 129.5, 129.5, 125.9, 109.6, 109.5, 96.9, 71.9, 70.7, 70.7, 70.0, 63.6, 44.9, 44.9, 40.5, 28.6, 20.4, 11.6, 11.6. HRESIMS  $[\text{M}+\text{Na}]^+$  calcd for  $\text{C}_{21}\text{H}_{31}\text{NO}_6\text{Na}$  440.2049, found 440.2055.

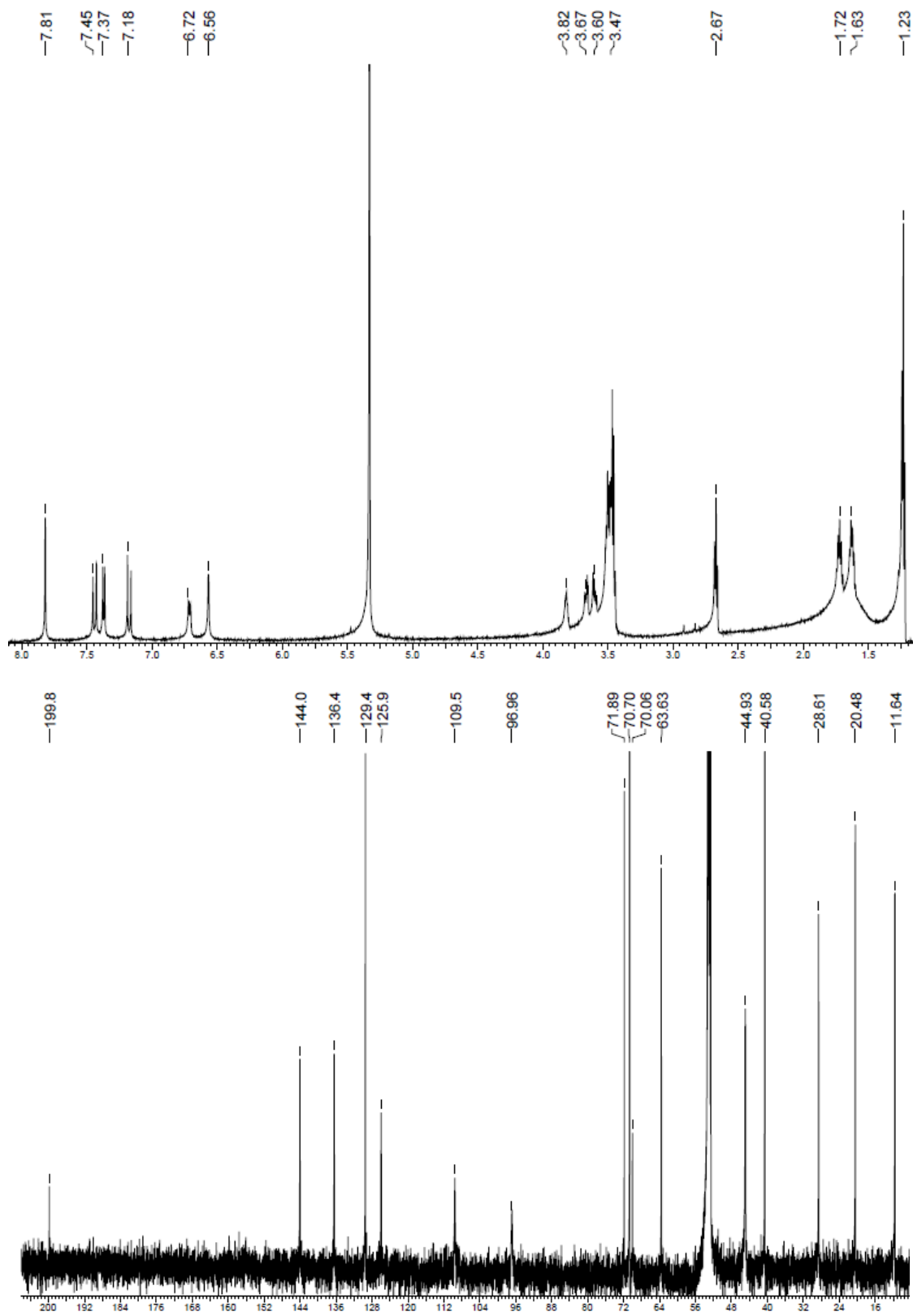


**Figure 3.47**  $^1\text{H}$  and  $^{13}\text{C}$  NMR spectra of **3.78** recorded in  $\text{CD}_2\text{Cl}_2$  at 600 MHz and 150 MHz respectively.

**AR Transcriptional Activity Assay:** AR transcriptional activity was measured using the PSA (6.1 kb)-luciferase reporter gene construct transiently transfected into LNCaP human prostate cancer cells which express functional AR. This reporter contains several well-characterized androgen response elements to which the AR specifically binds to increase luciferase activity in response to androgen such as R1881. LNCaP ( $2.5 \times 10^4$  cell/well) cells were seeded on 24-well plates overnight before transfection with PSA (6.1 kb)-luc, (0.5  $\mu\text{g/well}$ ) in serum-free, phenol red-free media using lipofectin (Invitrogen) according to published methods. For SAR analysis, LNCaP cells in 12-well plates were pre-treated 1 hr with (*S*)-niphatenone B (**3.35**), (*R*)-niphatenone B (**3.31**) or their SAR analogues (all added at 7  $\mu\text{M}$ , with the exception of **3.43**, which was tested at 3.5  $\mu\text{M}$  due to solubility limitations) prior to addition of 1 nM R1881 (Metribolone). After 48 h of exposure, cells were harvested, luciferase activity measured and normalized to protein concentration determined by the Bradford assay.

**Proliferation Assay:** Experiments using LNCaP human prostate cancer cells were done in phenol red-free RPMI 1640 medium with 0.5 % (v/v) fetal bovine serum, while for PC3 human prostate cancer cells, they were done in phenol red DMEM medium with 5 % (v/v) fetal bovine serum. Both media were supplemented with, 100 units/mL penicillin, and 100 mg/mL streptomycin. Cells were seeded in 96-well plates for 24 hrs before pre-treatment for 1 h with bicalutamide (10  $\mu\text{M}$ ), (*S*)-niphatenone B (**3.35**) and (*R*)-niphatenone B (**3.31**) (~14  $\mu\text{M}$ ) before treatment with 0.1 nM R1881 for LNCaP cells. LNCaP cells were incubated for 72 h with R1881, while the duration of the experiment was 24 h for PC3 cells. BrdU was added to the cells for an additional 2 h. Cells were fixed prior to incubation for 1.5 h with the

anti-BrdU-POD antibody (Roche). BrdU incorporation was measured at 570 nm via VersaMax ELISA Microplate Reader (Molecular Devices).

**Expression and Purification of Recombinant Protein:** AR AF1 recombinant protein was expressed and purified as described previously. The Ni<sup>2+</sup>-agarose affinity chromatography purified recombinant AR AF1 protein was further purified by size exclusion chromatography.

***In vitro* Binding Assay:** The binding reaction was carried out by incubating 10 mM AR AF1 protein with 20 mM of compound **3.67** containing an alkyne group or dimethyl sulfoxide on ice for 50 min. The binding reaction was diluted in half (i.e. 5 mM AR AF1 protein and 10 mM compound **3.67**) for fluorescein labeling on compound. Labeling was done by a Click chemistry reaction with 10 mM fluorescein azide, 0.1 mM ascorbic acid and 0.1 mM Copper(II)-TBTA complex (Lumiporbe) and incubated at room temperature for 30 – 40 min. Samples were separated on 12.5 % SDS-PAGE. Fluorescein was detected by an image analyzer (Fujifilm FLA-7000, GE Healthcare). The same gel was stained with Coomassie blue.

## Chapter 4: Synthetic Efforts Towards a Novel AR Antagonist (4.1)

### 4.1 Terpene AR Antagonist (4.1)

Small molecule antagonists<sup>130</sup> of the AR are used as a means to treat prostate cancer in patients suffering from the disease (Chapter 3, Section 3.1). In an ongoing effort to identify marine natural products that are AR antagonists, the Andersen natural product extract library was screened using Dr. Marianne Sadar's cell based transcriptional activity assay<sup>140</sup> at the BC Cancer Agency. The assay uses LNCaP prostate cancer cells containing an engineered PSA gene with a luciferase reporter. Stimulation of the cells with forskolin to stimulate protein kinase A (PKA) or interleukin 6 (IL6), activates the AR NTD leading to AR-dependent production of PSA-luciferase that generates light upon addition of luciferin.<sup>140</sup> Antagonists of the AR inhibit light production, providing a positive hit in the assay. Bioassay-guided fractionation of a marine sponge extract carried out by Gavin Carr in the Andersen group identified the terpene **4.1** as the active compound (Figure 4.1).

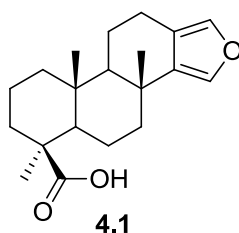


**Figure 4.1** AR antagonist lead compound **4.1**.

Prior to its discovery in the Andersen and Sadar laboratories terpene **4.1**<sup>162,163</sup> had no previously known biological activity. Lead compound **4.1** was found to inhibit the transcriptional activity of the AR *in vitro*. The carbon skeleton structure of **4.1** resembles that

of a steroid (Figure 4.2) and it was proposed that the mode of binding is through the LBD of the AR, which is the same as current antiandrogens (Chapter 3, Figure 3.2).

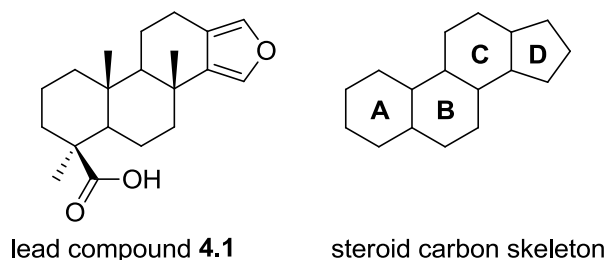
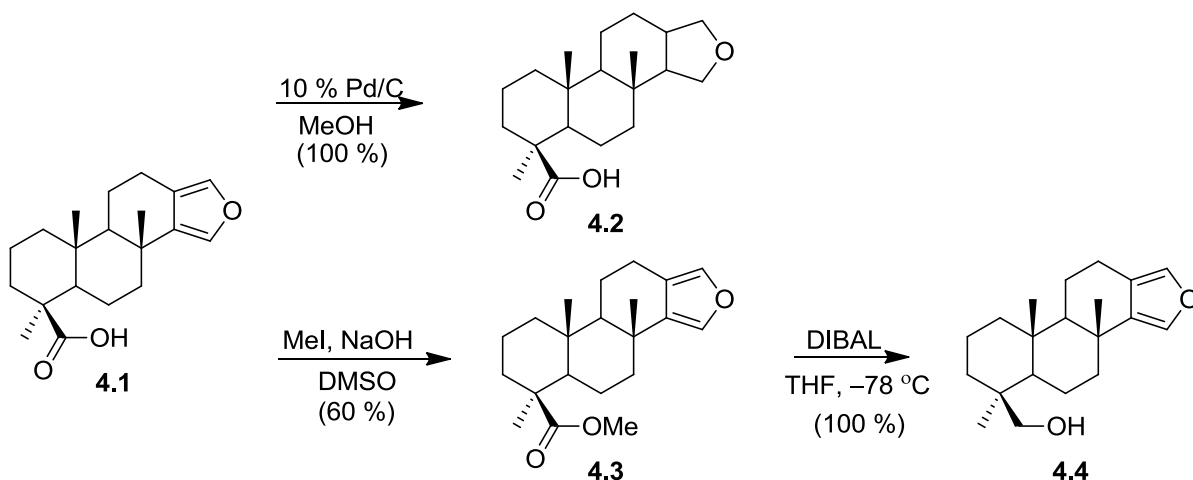


**Figure 4.2** Structural similarity between **4.1** and a steroid carbon skeleton.

The two functional groups of this natural product are a D-ring substituted furan and a neopentyl carboxylic acid moiety. Analogues of **4.1** were constructed by semisynthesis in a preliminary SAR study to address the role of these functional groups in the AR antagonist activity (Scheme 4.1).

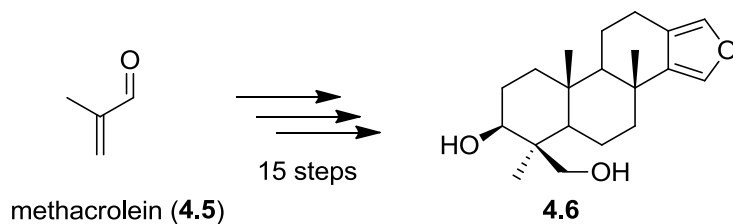
First, we desired to construct an analogue that would have a modified furan functional group. This was accomplished by hydrogenating<sup>164</sup> compound **4.1** (previously synthesized by Gavin Carr) to give the tetrahydrofuran analogue **4.2** (Scheme 4.1). Next, we attempted to reduce the carboxylic acid moiety in **4.1** directly to the primary alcohol with LiAlH<sub>4</sub>, however, this gave poor yields (15 %). Alternatively, **4.1** was converted to the methyl ester<sup>165</sup> (**4.3**) with sodium hydroxide and methyl iodide. Reduction of **4.3** with DIBAL at -78 °C gave alcohol **4.4** in a quantitative yield.



**Scheme 4.1** Semisynthesis of **4.1** analogues.

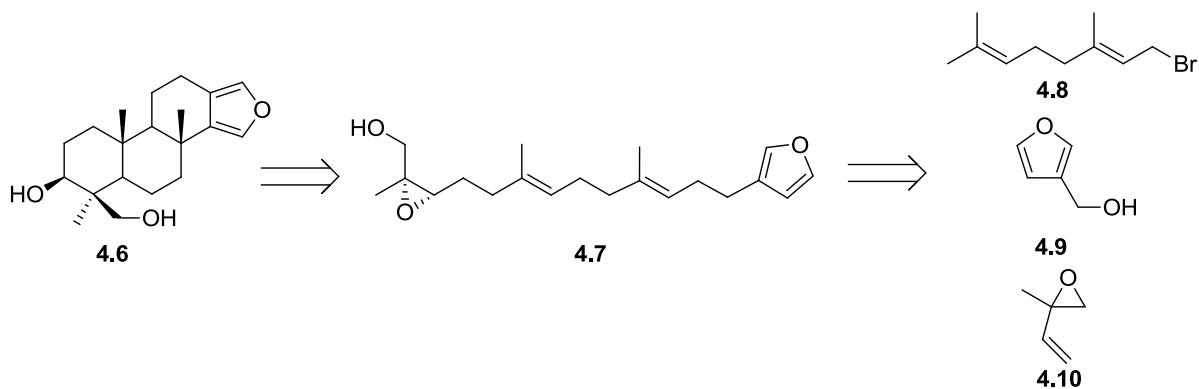
Analogue **4.4** is a known<sup>166</sup> marine natural product found to inhibit the lyase activity of DNA polymerase  $\beta$ . However, no AR antagonist properties have been previously reported. Analogues **4.4** and **4.2** in addition to the lead compound (**4.1**) were tested in Sadar's cell based transcriptional activity assay to determine how well they inhibit the transcriptional activity of the AR receptor. The biological data revealed that by reducing the natural product (**4.1**) to the tetrahydrofuran analogue (**4.2**), there was a drastic decrease in the activity. In addition, primary alcohol **4.4** was shown to be more active than the lead compound (**4.1**), and had *in vitro* activity similar to that of the known antiandrogen bicalutamide (**3.4**) (Chapter 3, Figure 3.2). With this promising biological activity, efforts towards constructing A-ring analogues of **4.4** were undertaken to probe the SAR. Furthermore, analogue **4.4** has limited solubility in water (CLogP = 5.88), therefore, water soluble analogues may potentially enhance the drug-like properties (Chapter 2, Section 2.4) of this novel AR antagonist pharmacophore. A-ring analogues of **4.4** have been previously synthesized<sup>167</sup> by Zoretic *et*

*al.* However, the synthesis is lengthy at fifteen linear steps starting from commercially available methacrolein<sup>168,169</sup> (**4.5**) (Scheme 4.2).



**Scheme 4.2** Zoretic's synthesis of an A-ring **4.4** analogue (**4.6**).

We envisioned an epoxide-initiated cationic cascade (Chapter 2, Section 2.4) to construct A-ring analogues of **4.4**. Retrosynthetic analysis of A-ring analogue **4.6** revealed the precursors needed. Analogue **4.6** could come from the epoxide-initiated cascade of **4.7**. Terminal epoxide **4.7** could come from geranyl bromide **4.8**, furan **4.9**, and epoxide **4.10** (Scheme 4.3).



**Scheme 4.3** Retrosynthesis of a **4.4** A-ring analogue **4.6**.

This synthetic route was devised with full recognition of the inherent reactivity of the furan ring system toward an electrophile. Furan ring systems are known to undergo preferential attack by the C-2 position (Figure 4.3) due to enhanced stabilization, through greater charge delocalization when compared with nucleophilic attack by the C-3 position. This results in a lower transition state energy for C-2 attack versus C-3 attack.

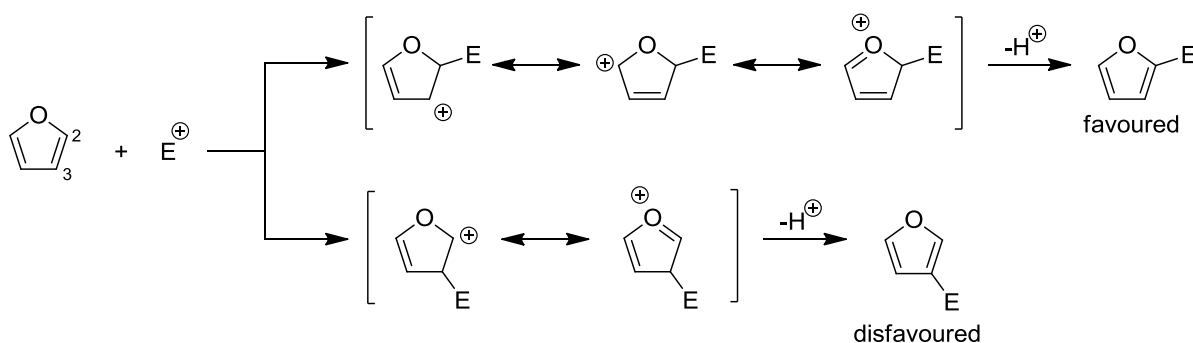


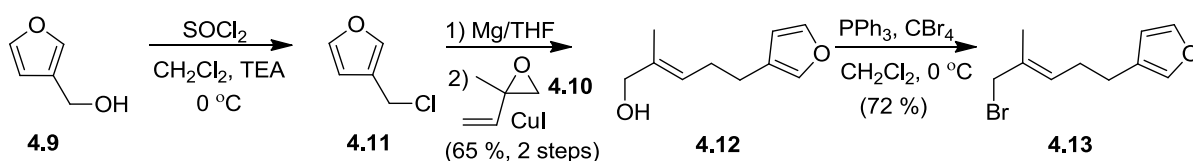
**Figure 4.3** Delocalization of charge in a furan ring system.

This preference in reactivity towards the C-2 position differs from what we desire in order to construct analogue **4.6**, which is reactivity at the C-3 position. It was hypothesized that the cyclization would yield at least a small amount of the disfavored C-3 regioisomer to provide us with the desired analogue **4.6**, while the C-2 regioisomer analogue would help broaden the SAR.

## 4.2 Epoxide-Initiated Cationic Cascade Towards AR Antagonist **4.6**

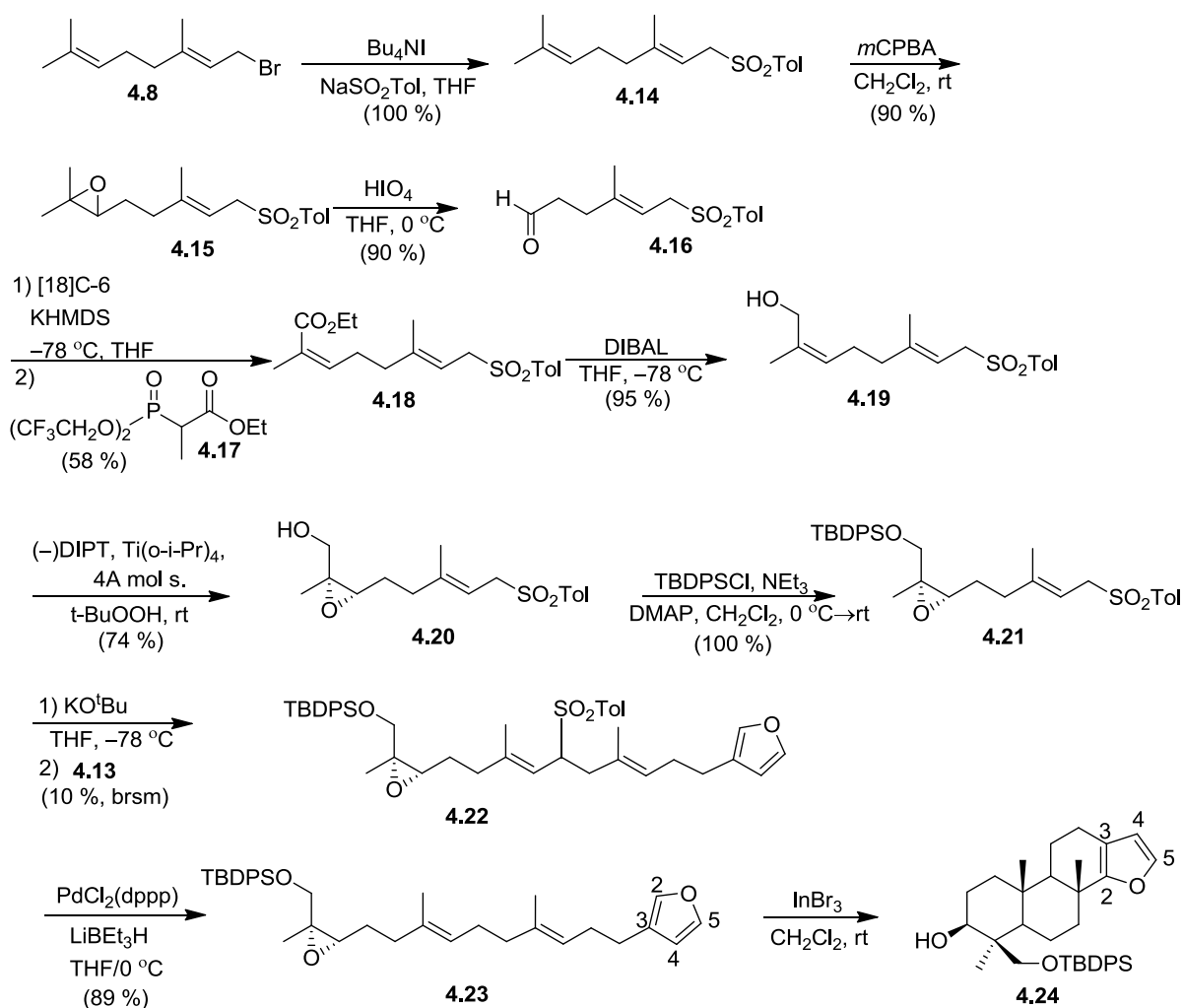
With the retrosynthesis in mind, construction of **4.6** began. The furanyl isoprene fragment (**4.13**) was synthesized first (Scheme 4.4). Compound **4.13** is known and was constructed using the literature protocol.<sup>170</sup> Commercially available 3-furan methanol **4.9** was

converted to chloride **4.11**, which was then exposed to sanded magnesium turnings in tetrahydrofuran to form the Grignard reagent *in situ* (Scheme 4.4). To the Grignard reagent was added copper iodide followed by vinyl epoxide **4.10** to give alcohol **4.12**. The published procedure to brominate **4.12** used  $\text{PBr}_3$ , however, it was found that this methodology gave low yields (< 30 %). Changing the bromination strategy to the Appel<sup>143</sup> reaction resulted in a higher yield for **4.13** (Scheme 4.4).



**Scheme 4.4** Synthesis of furanyl isoprene **4.13**.

The geranyl building block intermediate **4.21** (Scheme 4.5) was constructed next. Geranyl bromide **4.8** was converted to the allylic sulfone<sup>171</sup> **4.14** using *p*-toluenesulfinate and tetrabutylammonium iodide. Sulfone **4.14** was oxidized using *m*CPBA to give epoxide **4.15**, which had been previously synthesized by Matt Nodwell in the Andersen group.



**Scheme 4.5** Synthesis of regioisomer **4.24**.

Epoxide **4.15** was cleaved using periodic acid<sup>172</sup> to give aldehyde **4.16**. Phosphonate **4.17** was prepared following literature protocol<sup>173</sup> and was used in a Still–Gennari modified Horner–Wadsworth–Emmons olefination<sup>174</sup> with aldehyde **4.16** to give the *Z*-ethyl ester **4.18** in a moderate yield (Scheme 4.5). Attempts to reduce ester **4.18** with  $\text{LiAlH}_4$  were unsuccessful. However, using DIBAL to reduce ester **4.18** gave allylic alcohol **4.19** in a high yield. Alcohol **4.19** was then oxidized to chiral epoxide **4.20** using the Sharpless<sup>175</sup> asymmetric epoxidation method with (–)-diisopropyl tartrate (DIPT) serving as the chiral

ligand. Changing the chiral ligand from (-) to (+)-DIPT, would allow us to access the antipodal configuration of the natural product (**4.1**) for further SAR studies. At this stage of the synthesis, the primary alcohol of **4.20** was protected, in order to prevent any coordination to it by a Lewis acid in a future annulation step. A *tert*-butyldiphenylsilyl protecting group was chosen for its steric bulk, shielding the alcohol during the epoxide-initiated cascade step. Alcohol **4.20** was protected as the TBDPS-ether (**4.21**) in a quantitative yield (Scheme 4.5). Sulfone **4.21** was deprotonated with potassium *tert*-butoxide<sup>176</sup> at -78 °C and coupled to bromide **4.13** to give sulfone intermediate **4.22**. Palladium catalyzed reductive elimination<sup>177</sup> of the tosyl sulfone moiety in **4.22** gave the terminal epoxide intermediate (**4.23**).

With the terminal epoxide in hand, the epoxide-initiated cascade step was next. Indium tribromide served as the Lewis acid to initiate the cascade since it worked well for the construction of SHIP1 activators (Chapter 2, Section 2.4). The resultant crude annulation mixture contained a number of compounds. Using semisynthetic material **4.4** as a reference for comparing <sup>1</sup>H NMR spectra, there was no evidence of the desired regioisomer in the synthetic annulation reaction mixture. The two proton signals at the C-2 and C-5 positions (Figure 4.4) in semisynthetic analogue **4.4** are found at 7.11 and 7.05 ppm respectively in the <sup>1</sup>H NMR spectrum. However, all isolated synthetic compounds that showed annulation to the furan moiety had furan resonances at 7.17 and 6.10 ppm. The resonance at 6.10 ppm is indicative of the furan C-4 proton, suggesting the exclusive formation of regioisomer **4.24** (Figure 4.4).

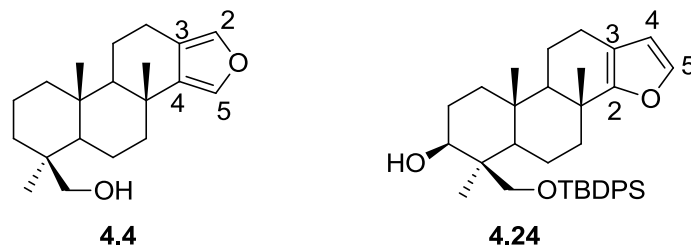


**Figure 4.4** Favored and disfavored regioisomers.

### 4.3 Furan Blocking Group as a Strategy to Construct Desired Regioisomer 4.24

Having failed to construct the desired A-ring analogue of AR antagonist **4.4**, we decided to modify the furan functionality by installing a blocking group at the C-2 position (Figure 4.5). Silyl functional groups were chosen as the best candidate to succeed for a number of reasons. Silyl groups come in a range of sizes from the large triisopropyl silyl (TIPS) to the small trimethyl silyl (TMS) group, and this allows for potential tuning of the steric component.

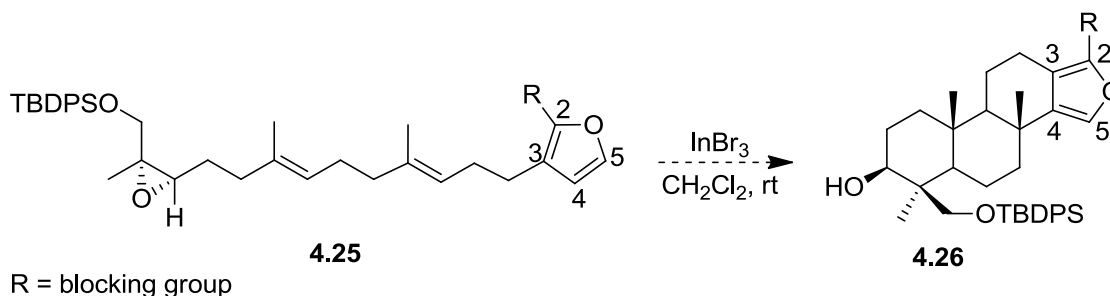
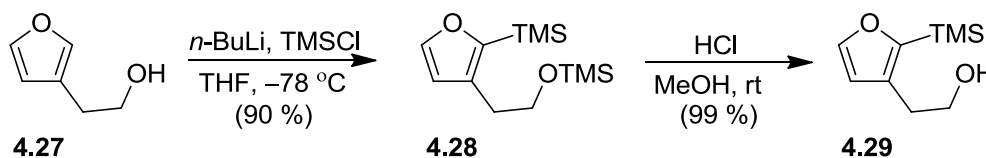


**Figure 4.5** Blocking group to construct A-ring analogues of **4.4**.

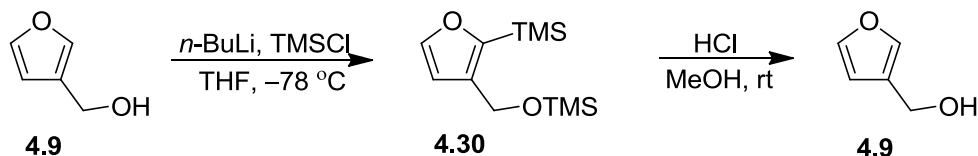
In addition, silicon is electropositive relative to carbon with an electronegativity of 1.90 versus 2.55 respectively (Pauling scale). This should result in an inductive effect, which

should increase the electron density of the furan ring, thus enhancing the nucleophilicity at the C-4 position. Goldsmith<sup>178</sup> *et al.* reported a directed ortho metalation (DOM) of 3-furan ethanol (**4.27**) and subsequent quenching with TMSCl to give the di-silylated intermediate **4.28**. Subsequent deprotection with HCl resulted in TMS removal from the O-silyl group, but left the C-silyl group intact (Scheme 4.6).



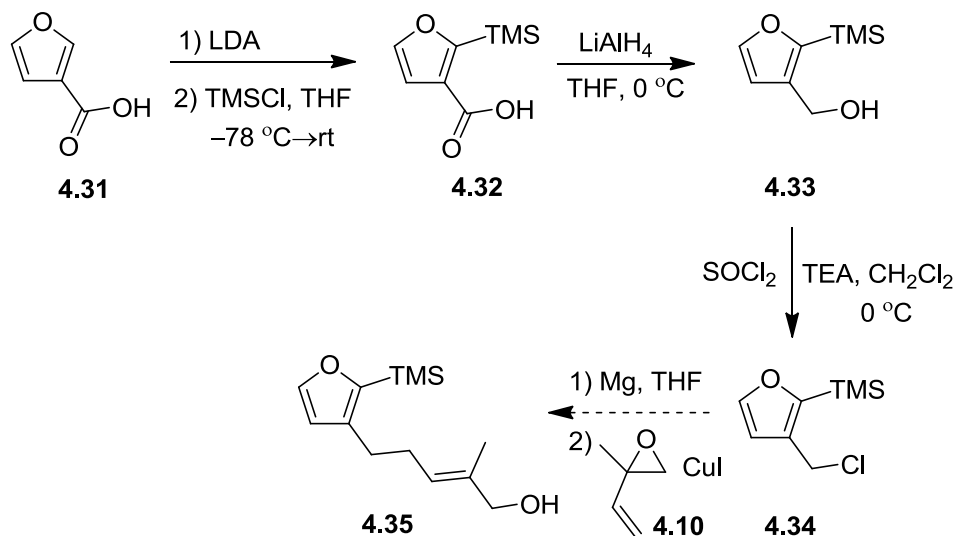
**Scheme 4.6** Goldsmith's furan C-2 silylation strategy.

This was used as an inspiration to construct a **4.13** C-2 silyl analogue (Scheme 4.7). 3-Furan methanol **4.9** was protected as the di-silyl intermediate **4.30**. Unfortunately, attempts to selectively deprotect the O-silyl ether as was shown by Goldsmith *et al.* proved unsuccessful and resulted in complete deprotection to yield starting material **4.9** (Scheme 4.7). Silylation of the furan ring by this route was abandoned.



**Scheme 4.7** Failed selective TMS deprotection.

An alternative strategy using 3-furoic acid (**4.31**) was employed (Scheme 4.8).<sup>179</sup> Deprotonation of 3-furoic acid (**4.31**) by LDA followed by quenching with TMSCl gave C-2 silyl intermediate **4.32**.



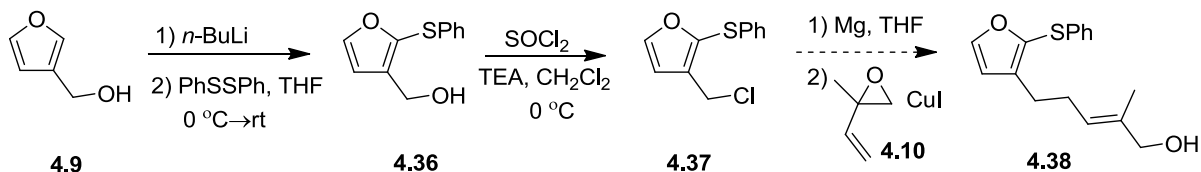
**Scheme 4.8** Synthetic attempt towards C-2 silylated intermediate **4.35**.

Reduction of the acid moiety in **4.32** to the primary alcohol by  $\text{LiAlH}_4$  gave intermediate **4.33**. Chlorination of **4.33** with thionyl chloride in the presence of triethylamine gave a complex mixture. The reactive nature of chlorinated furan analogues such as **4.34** warranted its immediate use without further purification.<sup>178</sup> Intermediate **4.34** was exposed to sanded magnesium turnings in tetrahydrofuran, after which epoxide **4.10** was added. Purification of the reaction mixture failed to provide any evidence of silylated compound **4.35**.

With the failed attempts of constructing C-2 silyl analogues of **4.12**, thiol based blocking groups were considered as an alternative to silyl groups. Sulfur with an electronegativity of 2.58 versus 2.55 (Pauling scale) of carbon is slightly more

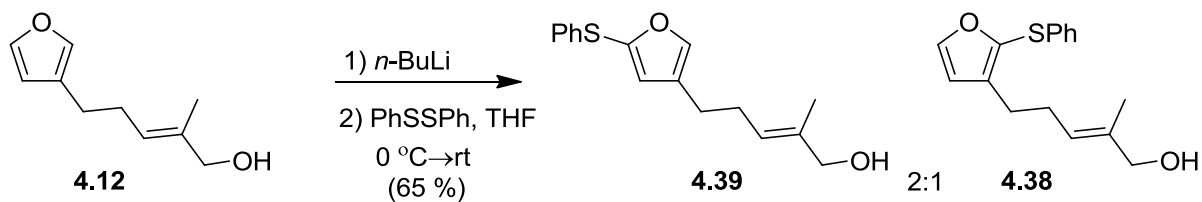
electronegative and, therefore, through-bond inductive effects to increase electron density in the ring as with silicon is unlikely. However, thiol groups were chosen to provide steric hindrance at the C-2 position. Furthermore, literature precedent in constructing thiol based analogues of furan<sup>178</sup> existed allowing for their rapid development.

The construction of thiolated furan analogues began in a similar fashion as to the silylated analogues. 3-Furan methanol (**4.9**) was treated with *n*-BuLi followed by quenching with phenyl disulfide to give thiol **4.36**<sup>178</sup> (Scheme 4.9). A reaction sequence analogous to the one shown in Scheme 4.8 was attempted to access the thiolated analogue **4.38** without success (Scheme 4.9).



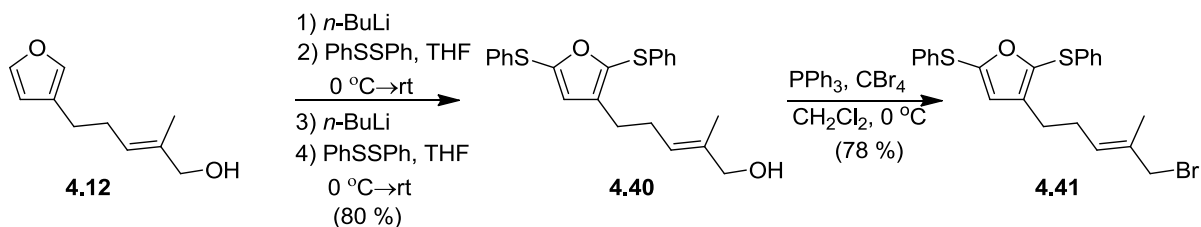
**Scheme 4.9** Attempt at constructing thiolated analogue **4.38**.

Without successfully constructing substituted furan analogues by DOM of 3-furan methanol (**4.9**) at an early stage of the synthesis, we turned our attention towards furan substitution at a later stage of the synthesis. Lithiation<sup>180</sup> of intermediate **4.12** gave a mixture of mono-thiolated compounds **4.39** and **4.38** at a 2:1 ratio respectively (Scheme 4.10).



**Scheme 4.10** Mono-thiolated analogues of **4.12**.

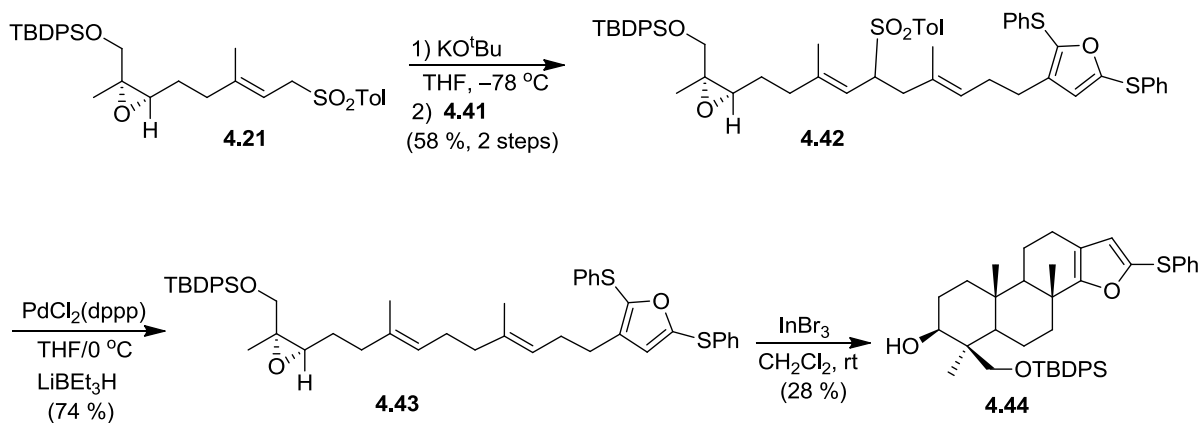
While this strategy was successful in generating thiol substituted furan analogues, the regioselectivity of the reaction was poor due to the absence of a directing group for lithiation. Furthermore, compounds **4.39** and **4.38** are inseparable by flash column chromatography, which complicates characterization and future steps. A variation of this route was completed in which successive lithiations gave the di-thiol substituted furan intermediate **4.41** (Scheme 4.11).



**Scheme 4.11** Di-thiolated analogues of **4.12**.

This provided a better overall yield along with no purification issues when compared to the mono-thiolated synthesis. Bromination of **4.40** with carbon tetrabromide and triphenyl phosphine gave **4.41** (Scheme 4.11). Having constructed a furan analogue that was substituted at both the C-2 and C-5 position with phenyl sulfide, we continued the synthesis.

Sulfone **4.21** was coupled with bromine **4.41** to give **4.42**, and subsequent de-sulfonylation provided key epoxide intermediate **4.43** (Scheme 4.12).



**Scheme 4.12** Epoxide-initiated cationic cascade using a thiol blocking group.

Cyclization with indium tribromide gave a complex reaction mixture, which was purified using flash column chromatography. None of the desired product was observed and the major annulation compound in the mixture was **4.44**, which had the undesired regiochemistry. The exclusive formation of **4.44** provided evidence that using a blocking group as the only means to prevent nucleophilic attack by the more reactive C-2 position in this furan ring system is not sufficient.

## 4.4 Biological Results

The semisynthetic analogues **4.2** and **4.4** were tested alongside the lead compound **4.1** in an androgen receptor competitive binding assay. Synthetic androgen R1881 (metribolone) and clinically approved antiandrogen bicalutamide (**3.4**) were used as positive controls. This assay utilizes the property of fluorescence polarization<sup>181</sup> to determine the affinity of a ligand to the AR. When fluorescent molecules in solution are excited with plane-polarized light, the light they emit is also in a fixed plane (polarized light). However, this only occurs if the fluorophore remains stationary during the excitation.

The assay consists of AR-LBD and an androgen ligand with a fluorescent tag (Fluormone<sup>TM</sup> AL Green) in the presence of a competitor ligand. The formation of the AL Green/AR-LBD complex results in the fluorophore being in a bound state. When excited with polarized light, the slow rotation of the peptide-bound fluorophore results in the emission of polarized light. A ligand with affinity to the AR-LBD causes the displacement of AL Green from its bound stationary state. This will result in a decrease in polarization of the emitted light due to the enhanced tumbling rate of the small molecule fluorophore in solution. The difference in net polarization in the presence of a test compound is used to determine the affinity for the AR-LBD. The binding curves of the cell-based assay are shown in Figure 4.7.

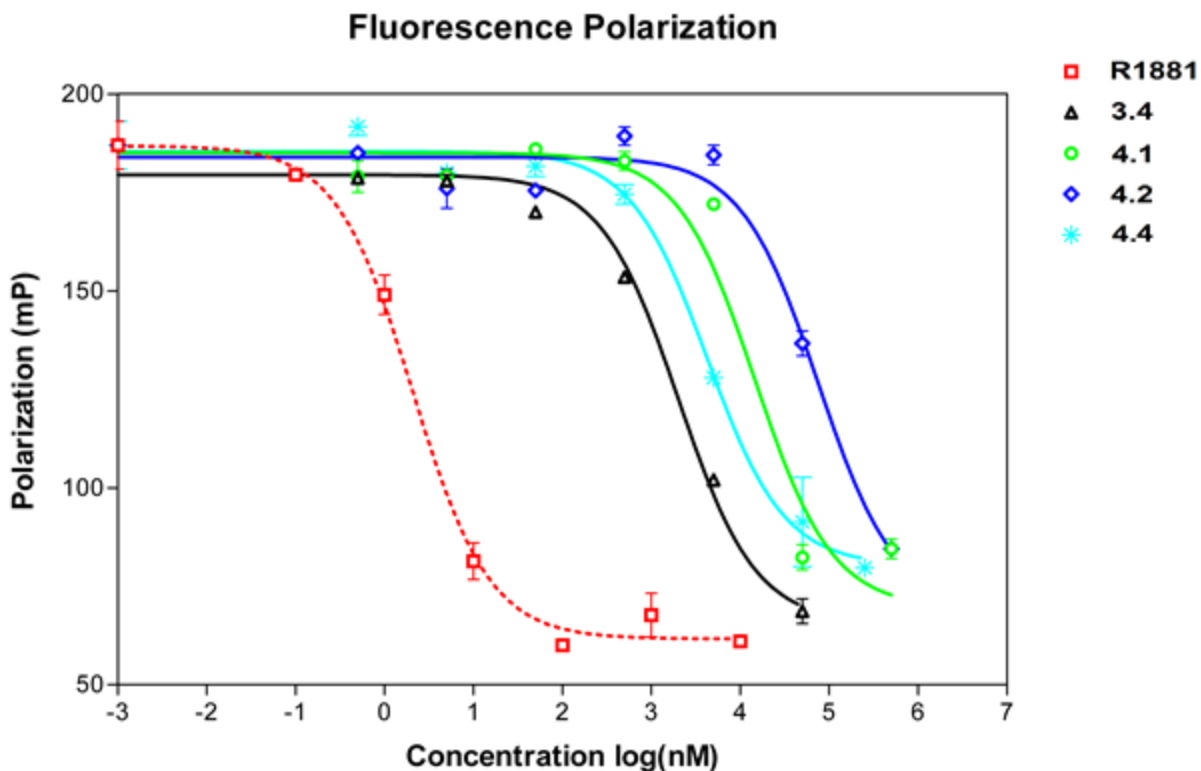


**Figure 4.6** AR competitor *in vitro* assay.

Half-maximal effective concentration (EC<sub>50</sub>) values were calculated for each compound from the binding curves. The values from a representative experiment are shown in Table 4.1. The biological results of the *in vitro* assay provide a clear SAR for the lead compound **4.1** and semisynthetic analogues **4.2** and **4.4**. There is an approximate fivefold increase in the EC<sub>50</sub> value between **4.1** and reduced analogue **4.2**. This suggests that the aromaticity of the furan moiety in **4.1** is necessary in order to maintain activity.

**Table 4.1** EC<sub>50</sub> values for tested compounds in an AR competitor *in vitro* assay.

Compound	EC <sub>50</sub> (nM)
<b>R1881</b>	2.09
<b>3.4</b>	2014
<b>4.1</b>	14718
<b>4.2</b>	75569
<b>4.4</b>	4249

There is an approximate 3.5 fold decrease in the EC<sub>50</sub> value when comparing the lead compound **4.1** to its semisynthetic analogue in alcohol **4.4**. This result indicates that there is enhanced potency in converting the neopentyl carboxylic acid to a neopentyl alcohol in the natural product (**4.1**). In fact, the affinity towards the AR of analogue **4.4** is comparable to the clinically approved antiandrogen drug bicalutamide (**3.4**) (Chapter 3, Figure 3.2), which is currently used as a treatment for prostate cancer.

Lead compound **4.1** in addition to analogues **4.2** and **4.4** were also tested in an *in vitro* assay to determine their effect on AR transcriptional activity. This assay is similar to the assay completed for the niphatenones (Chapter 3, Figure 3.11). It was found that tetrahydrofuran analogue **4.2** had no effect on inhibiting the transcriptional activity of the AR. This is further evidence that the furan moiety plays an important role in the biological activity. The data also suggested that both **4.1** and **4.4** inhibited AR transcriptional activity, however, analogue **4.4** was almost three times as potent. These results reinforce those of the *in vitro* AR affinity assay (Table 4.1). The detailed results of this experiment will be described elsewhere. The biological results of both *in vitro* assays are promising, and suggest a clear SAR for the natural product (**4.1**), and semisynthetic analogues **4.2** and **4.4**.

## 4.5 Conclusion

Small molecule antagonists<sup>130</sup> of the AR are currently used as a therapeutic treatment for prostate cancer in patients suffering from the disease. In an ongoing effort to identify marine natural products that are AR antagonists, the Andersen natural product extract library was screened using Dr. Marianne Sadar's cell based transcriptional assay at the BC Cancer Agency.

Bioassay-guided fractionation of the crude methanol extract of a marine sponge led to the identification of terpene **4.1** as an antagonist of the AR. Using compound **4.1**, a semisynthesis was completed to probe this novel AR pharmacophore. Two semisynthetic analogues were constructed providing reduced analogue **4.2** and alcohol **4.4**. An *in vitro* assay was completed to determine the binding affinity to the AR of lead compound **4.1** and analogues **4.2** and **4.4**. There were several conclusions that were made from this data: 1) the furan moiety is necessary in order to have affinity for the AR, 2) the carboxylic acid moiety found in the natural product is responsible for attenuated activity when compared to its primary alcohol analogue in **4.4**, and 3) analogue **4.4** is almost as active as the clinical drug bicalutamide (**3.4**) in its ability to displace a fluorescently-tagged androgen ligand bound to the AR.

Furthermore, an *in vitro* assay was completed to determine the ability of the natural product (**4.1**) and its analogues **4.2** and **4.4** at inhibiting AR transcriptional activity. The results of this assay mirror those of the *in vitro* AR affinity assay. The tetrahydrofuran analogue **4.2** had lost all activity while analogue **4.4** was more active than the lead compound (**4.1**). The results of both *in vitro* assays suggest a clear SAR for these novel AR pharmacophores.

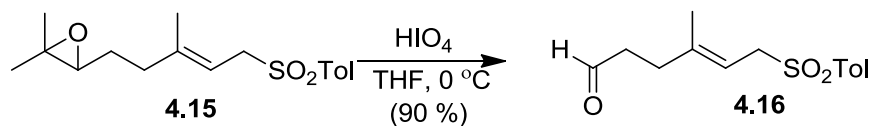
The focus of this chapter is dedicated towards the synthesis of **4.4** analogues to broaden the SAR, and to enhance the solubility of these compounds in water for enhanced drug-like effects. An epoxide-initiated cationic cascade was devised as a method to construct A-ring analogues of **4.4** (Scheme 4.3). Annulation of the key terminal epoxide intermediate **4.23** provided the undesired regioisomer **4.24** exclusively (Scheme 4.5). This was caused by the inherent reactivity of the furan C-2 center versus the C-4 center (Figure 4.3). To address the issue of furan reactivity, analogues of terminal epoxide **4.23** with a silyl group at the C-2 position was proposed (Figure 4.5). The purpose of this silylated analogue was to block attack by the reactive C-2 position, and increase the electron density of the ring, all in the hopes that the C-4 position would react. Unfortunately, our attempts to construct silylated analogues failed.

Alternatively, thiol groups were installed in the C-2 position of **4.23**, in order to attenuate the reactivity of the C-2 position by blocking nucleophilic attack. Epoxide-initiated cationic cascade of thiol-substituted furan **4.43**, gave exclusively the C-2 substituted analogue **4.44** with the undesired regiochemistry (Scheme 4.12). This outcome was a clear indication that steric factors alone are not sufficient to form the desired regioisomer. The synthesis of **4.4** analogues using an epoxide-initiated cascade is a continuing project in the Andersen lab. Lead compound **4.1** and semisynthetic analogue **4.4** represent promising drug leads in the development of small molecule antagonists of the AR.

## 4.6 Experimental

**General Methods:** All non-aqueous reactions were carried out in flame-dried glassware and under an Ar or N<sub>2</sub> atmosphere unless otherwise noted. Air and moisture sensitive liquid reagents were manipulated via a dry syringe. All solvents and reagents were used as obtained from commercial sources without further purification. <sup>1</sup>H and <sup>13</sup>C NMR spectra were obtained on Bruker Avance 400 direct, 300 direct, or Bruker Avance 600 CryoProbe spectrometers at room temperature. Flash column chromatography was performed using Silicycle Ultra-Pure silica gel (230-400 mesh). Analytical thin-layer chromatography (TLC) plates were aluminum-backed ultrapure silica gel 250 μm. Electrospray ionization mass spectrometry (ESI-MS) spectra were recorded on a Micromass LCT instrument.

### Preparation of 4.16:



To a solution of metaperiodic acid (918.5 mg, 4.78 mmol, 3.60 mL water) was added epoxide **4.15** (1.12 g, 3.63 mmol) dissolved in 7 mL of tetrahydrofuran at 0 °C and allowed to stir for half an hour. To this mixture was added brine (100 mL) and the aqueous layer was extracted three times with methylene chloride (350 mL). The combined organic extracts were dried with MgSO<sub>4</sub> and concentrated using a rotary evaporator. The crude mixture was purified using flash column chromatography (hexanes:ethyl acetate 2:1) to give **4.16** (869.8 mg, 3.26 mmol, 89.8 %). <sup>1</sup>H NMR (400 MHz, CDCl<sub>3</sub>) δ 9.68 (s, 1H), 7.65 (d, J = 8.0 Hz, 2H), 7.28 (d, J = 8.4 Hz, 2H), 5.15 (t, J = 8.0 Hz, 1H), 3.72 (d, J = 8.0 Hz, 2H), 2.45 (t, J = 7.6 Hz, 2H), 2.39 (s, 3H), 2.27 (t, J = 7.6 Hz, 2H), 1.31 (s, 3H); <sup>13</sup>C NMR (100 MHz, CDCl<sub>3</sub>) δ 201.5, 144.8, 144.3, 135.8, 129.8, 128.5, 111.6, 56.0, 41.6, 31.7, 21.7, 16.4. HRESIMS [M + H]<sup>+</sup> calcd for C<sub>14</sub>H<sub>19</sub>O<sub>3</sub><sup>32</sup>S 267.1055, found 267.1059.

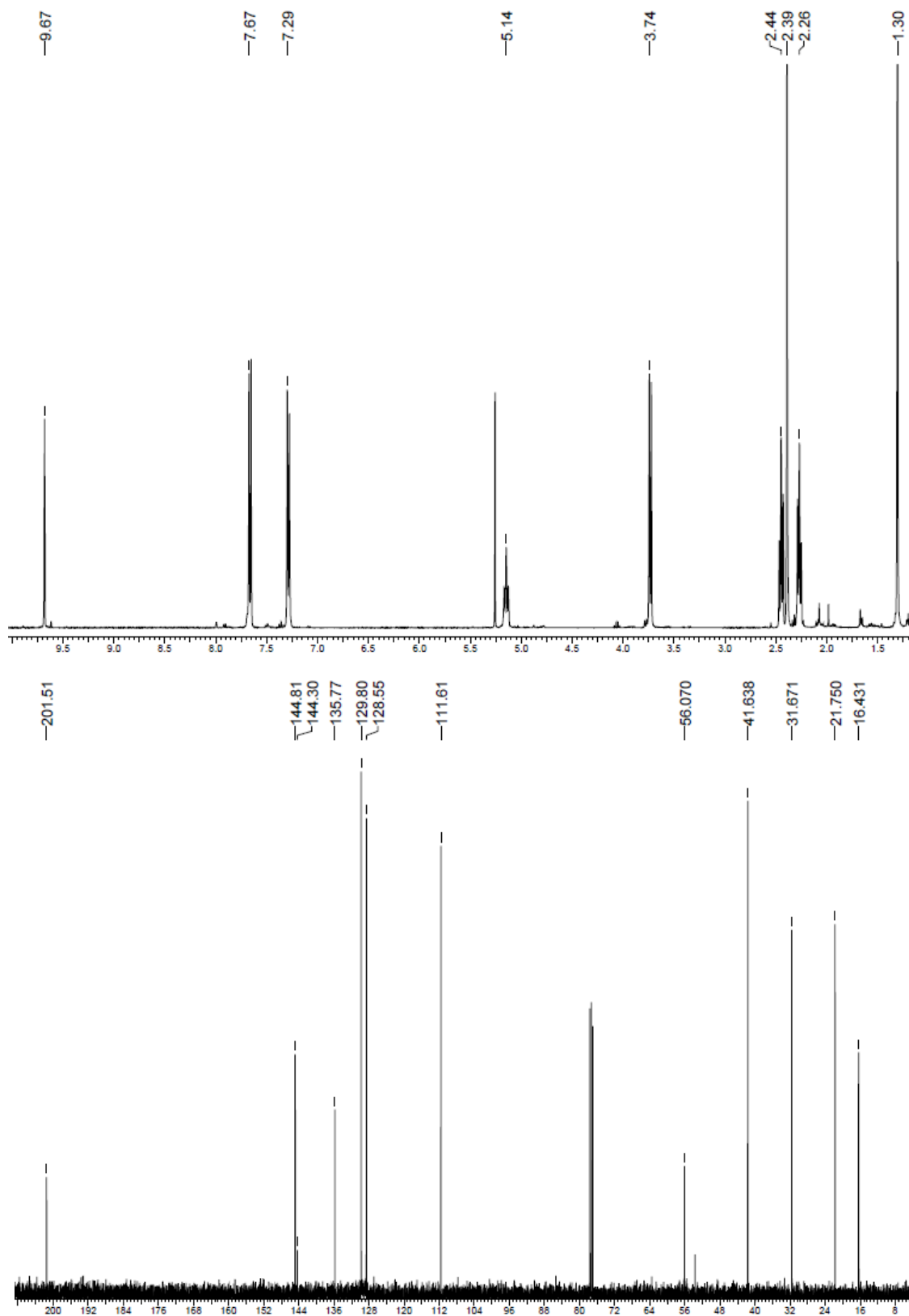
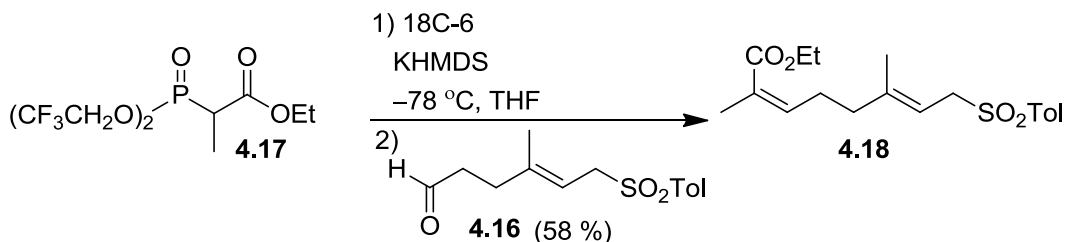


**Figure 4.7**  $^1\text{H}$  and  $^{13}\text{C}$  NMR spectra of **4.16** recorded in  $\text{CDCl}_3$  at 400 MHz and 100 MHz respectively.

### Preparation of 4.18:



To phosphonate **4.17** (440 mg, 1.27 mmol) dissolved in 1.88 mL tetrahydrofuran was added 18C-6 (1.00 g, 3.81 mmol) and the solution was cooled to  $-78\text{ }^{\circ}\text{C}$ . To this solution was added KHMDS (278.9 mg, 1.39 mmol) dissolved in 1.5 mL of toluene, and allowed to stir for thirty minutes, after which aldehyde **4.16** (320.4 mg, 1.27 mmol) dissolved in 2 mL of tetrahydrofuran was added dropwise using a syringe. After stirring at  $-78\text{ }^{\circ}\text{C}$  for one hour, the reaction mixture was quenched with saturated  $\text{NH}_4\text{Cl}_{(\text{aq})}$  (100 mL) and allowed to warm to room temperature. The aqueous layer was extracted three times with methylene chloride (350 mL). The combined organic extracts were dried with  $\text{MgSO}_4$  and concentrated using a rotary evaporator. The crude mixture was purified using flash column chromatography (hexanes:ethyl acetate 5:1) to give **4.18** (259.6 mg, 0.74 mmol, 58.2 %).  $^1\text{H}$  NMR (400 MHz,  $\text{CDCl}_3$ )  $\delta$  7.62 (d,  $J = 8.0$  Hz, 2H), 7.22 (d,  $J = 8.4$  Hz, 2H), 5.76 (t,  $J = 7.6$  Hz, 1H), 5.11 (t,  $J = 8.0$  Hz, 1H), 4.10 (q,  $J = 7.2$  Hz, 2H), 3.70 (d,  $J = 8.0$  Hz, 2H), 2.43 (q,  $J = 7.6$  Hz, 2H), 2.33 (s, 3H), 2.00 (t,  $J = 7.6$  Hz, 2H), 1.80 (s, 3H), 1.24 (s, 3H), 1.20 (t,  $J = 7.2$  Hz, 3H);  $^{13}\text{C}$  NMR (100 MHz,  $\text{CDCl}_3$ )  $\delta$  167.8, 145.5, 144.5, 141.6, 135.9, 129.7, 128.5, 127.8, 111.2, 60.1, 56.1, 39.2, 27.6, 21.6, 20.7, 16.1, 14.4. HRESIMS  $[\text{M} + \text{Na}]^+$  calcd for  $\text{C}_{19}\text{H}_{26}\text{O}_4\text{Na}^{32}\text{S}$  373.1450, found 373.1457.

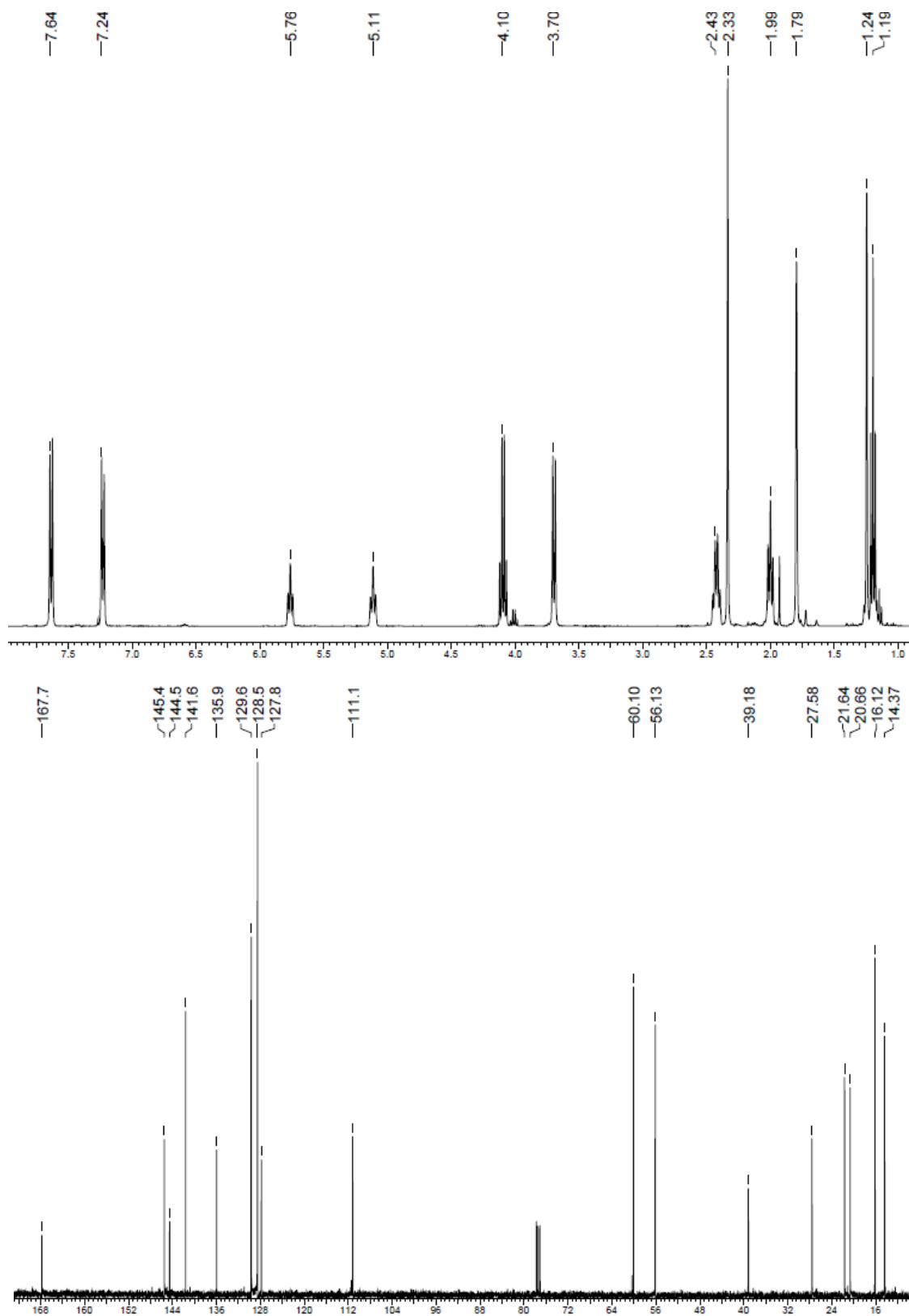
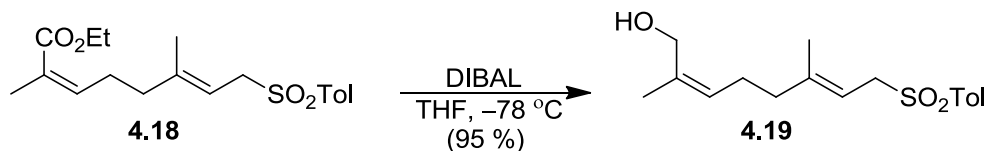


**Figure 4.8**  $^1\text{H}$  and  $^{13}\text{C}$  NMR spectra of **4.18** recorded in  $\text{CDCl}_3$  at 400 MHz and 100 MHz respectively.

### Preparation of 4.19:



To **4.18** (333 mg, 0.95 mmol) dissolved in 8 mL of tetrahydrofuran cooled to  $-78\text{ }^\circ\text{C}$  was added a 1.0 M solution of DIBAL (2.85 mL, 2.85 mmol) dropwise using a syringe. After stirring at  $-78\text{ }^\circ\text{C}$  for two hours, the reaction mixture was quenched with saturated  $\text{NH}_4\text{Cl}$  (aq) (100 mL) and allowed to warm to room temperature. The aqueous layer was extracted three times with methylene chloride (250 mL). The combined organic extracts were dried with  $\text{MgSO}_4$  and concentrated using a rotary evaporator. The crude mixture was purified using flash column chromatography (hexanes:ethyl acetate 3:2) to give **4.19** (277.5 mg, 0.89 mmol, 94.6 %).  $^1\text{H}$  NMR (300 MHz,  $\text{CDCl}_3$ )  $\delta$  7.72 (d,  $J = 8.4$  Hz, 2H), 7.32 (d,  $J = 7.8$  Hz, 2H), 5.18 (m, 2H), 4.12 (s, 2H), 3.80 (d,  $J = 7.8$  Hz, 2H), 2.45 (s, 3H), 2.13 (quin,  $J = 6.9$  Hz, 2H), 2.04 (m, 2H), 1.91 (bs, 1H), 1.81 (s, 3H), 1.40 (s, 3H);  $^{13}\text{C}$  NMR (75 MHz,  $\text{CDCl}_3$ )  $\delta$  145.9, 144.8, 135.9, 135.4, 129.8, 128.6, 127.2, 110.8, 61.6, 56.2, 39.8, 25.7, 21.8, 21.5, 16.5. HRESIMS  $[\text{M} + \text{Na}]^+$  calcd for  $\text{C}_{17}\text{H}_{24}\text{O}_3\text{Na}^{32}\text{S}$  331.1344, found 331.1349.

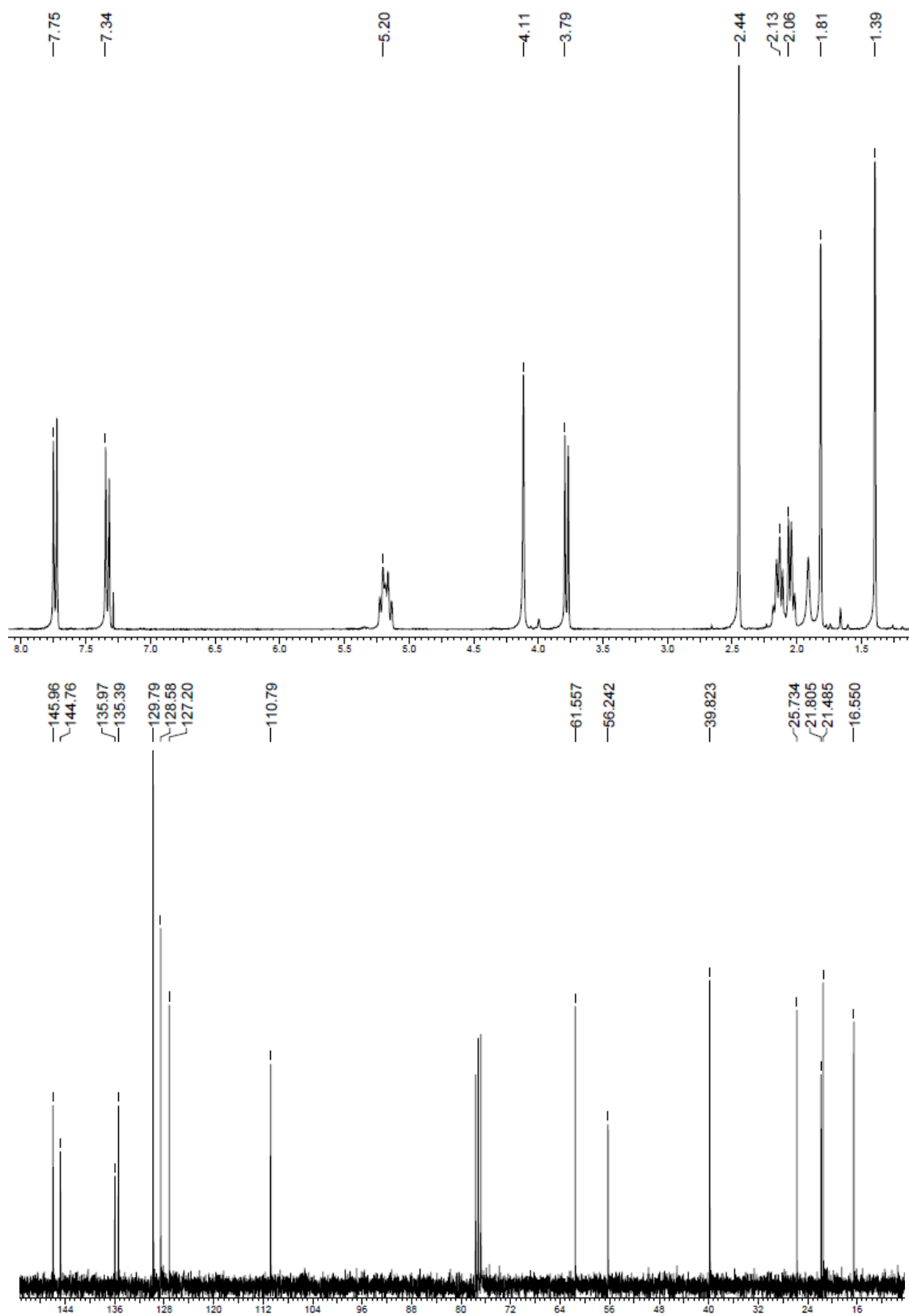
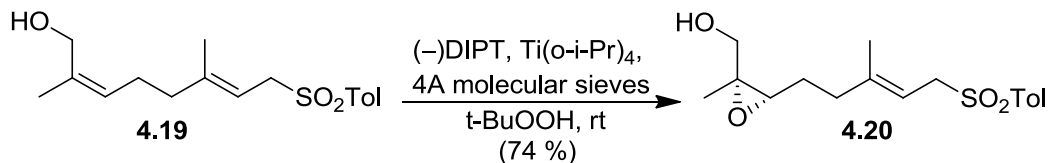


**Figure 4.9**  $^1\text{H}$  and  $^{13}\text{C}$  NMR spectra of **4.19** recorded in  $\text{CDCl}_3$  at 300 MHz and 75 MHz respectively.

### Preparation of 4.20:



To (-)-DIPT (0.115 mL, 0.549 mmol) and Ti(O-*i*-Pr)<sub>4</sub> (0.115 mL, 0.329 mmol) in 10 mL of methylene chloride was added crushed 4 Å molecular sieves (1.07 g) and allowed to stir for twenty minutes at -20 °C, after which was added a 5.5 M solution of *t*-BuOOH (1.44 mL, 7.9 mmol) in decane and the mixture allowed to stir for an additional twenty minutes. To this mixture was added alcohol **4.19** (1.21 g, 3.92 mmol) dissolved in 6.5 mL of methylene chloride. After stirring for 2.5 hours TLC indicated the presence of starting materials, and so (+)-DIPT (0.115 mL, 0.549 mmol), Ti(O-*i*-Pr)<sub>4</sub> (0.115 mL, 0.329 mmol), and *t*-BuOOH (0.75 mL, 4.1 mmol) was added to the reaction mixture and it was allowed to warm to room temperature overnight. The crude reaction mixture was then filtered through filter paper and to it added 100 mL of 2 M NaOH, and allowed to stir until two distinct layers were visible (5 hours). The aqueous layer was extracted three times with methylene chloride (400 mL). The combined organic extracts were dried with MgSO<sub>4</sub> and concentrated using a rotary evaporator. The crude mixture was purified using flash column chromatography (hexanes:ethyl acetate 3:2) to give **4.20** (935.5 mg, 2.88 mmol, 73.5 %). <sup>1</sup>H NMR (300 MHz, CDCl<sub>3</sub>) δ 7.66 (d, J = 8.1 Hz, 2H), 7.27 (d, J = 8.1 Hz, 2H), 5.17 (t, J = 6.6 Hz, 1H), 3.76 (d, J = 7.8 Hz, 2H), 3.59 (s, 2H), 2.73 (dd, J = 6.9, 5.4 Hz, 1H), 2.61 (bs, 1H), 2.39 (s, 3H), 2.10 (oct, J = 7.8 Hz, 2H), 1.69-1.49 (m, 2H), 1.34 (s, 3H), 1.33 (s, 3H); <sup>13</sup>C NMR (75 MHz, CDCl<sub>3</sub>) δ 145.4, 144.8, 135.8, 129.8, 128.5, 111.2, 64.1, 63.9, 61.2, 56.1, 36.6, 26.4, 21.7, 20.2, 16.4. HRESIMS [M + Na]<sup>+</sup> calcd for C<sub>17</sub>H<sub>24</sub>O<sub>4</sub>Na<sup>32</sup>S 347.1293, found 347.1299.

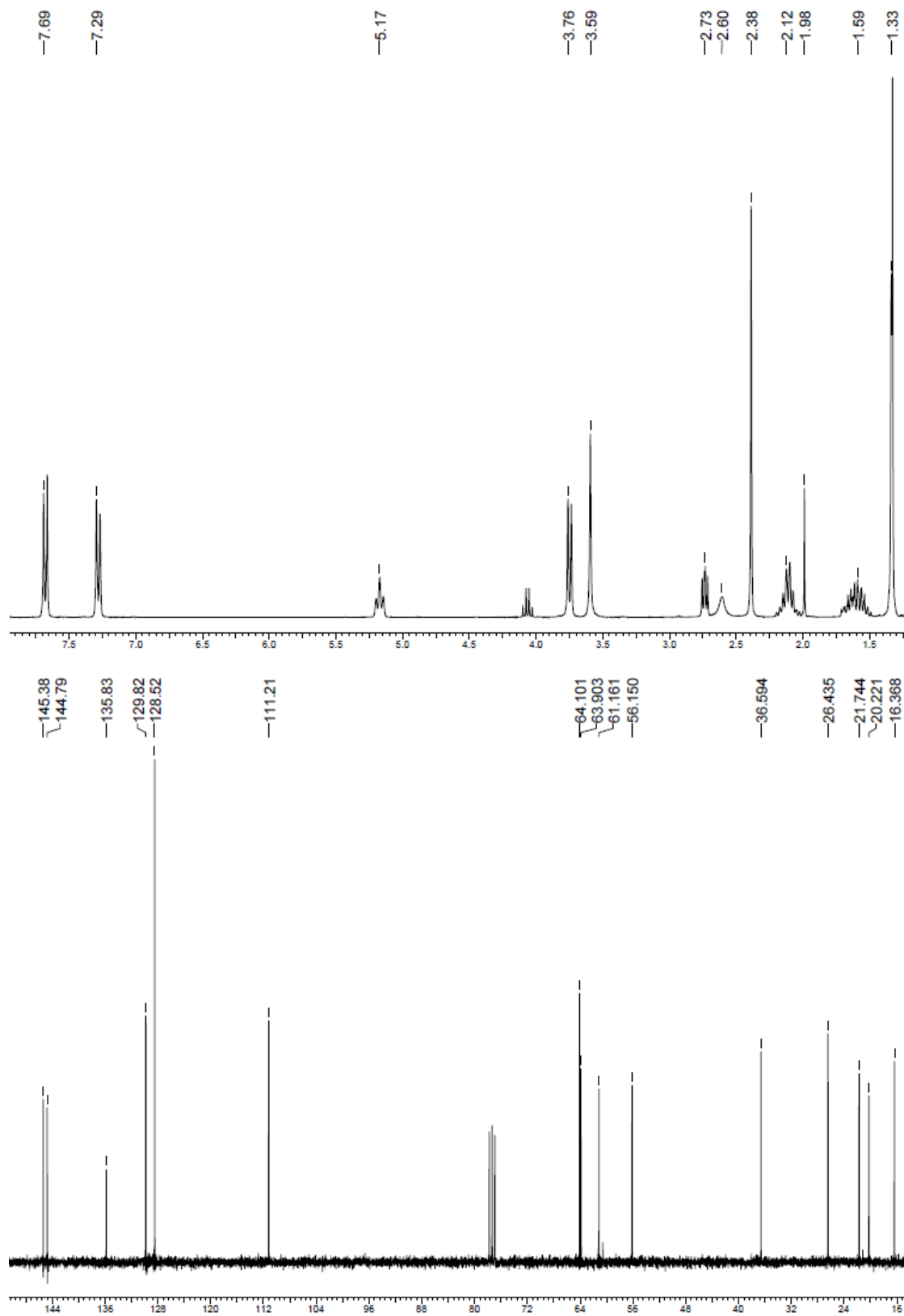
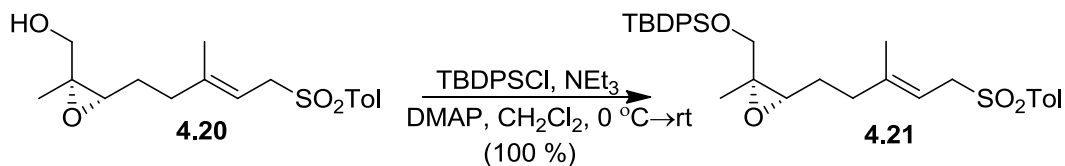


**Figure 4.10**  $^1\text{H}$  and  $^{13}\text{C}$  NMR spectra of **4.20** recorded in  $\text{CDCl}_3$  at 300 MHz and 75 MHz respectively.

### Preparation of 4.21:



To alcohol **4.20** (65 mg, 0.20 mmol) dissolved in 0.5 mL of methylene chloride was added DMAP (2.44 mg, 0.019 mmol) and triethylamine (0.033 mL, 0.24 mmol) and the reaction mixture was cooled to 0 °C, after which TBDPSCI (0.056 mL, 0.22 mmol) was added and allowed to warm to room temperature overnight. The crude reaction mixture was concentrated under a stream of nitrogen and was purified using flash column chromatography (hexanes:ethyl acetate 4:1) to give **4.21** (113 mg, 0.20 mmol, 100 %). <sup>1</sup>H NMR (400 MHz, CDCl<sub>3</sub>) δ 7.72-7.66 (m, 6H), 7.46-7.37 (m, 6H), 7.28 (d, J = 8.4 Hz, 2H), 5.17 (t, J = 6.8 Hz, 1H), 3.78 (d, J = 8.0 Hz, 2H), 3.70 (d, J = 10.8 Hz, 1H), 3.63 (d, J = 11.2 Hz, 1H), 2.39 (s, 3H), 2.14 (m, 2H), 1.56-1.49 (m, 1H), 1.42-1.38 (m, 1H), 1.44 (s, 3H), 1.32 (s, 3H), 1.26 (t, J = 7.2 Hz, 1H), 1.09 (s, 9H); <sup>13</sup>C NMR (100 MHz, CDCl<sub>3</sub>) δ 145.3, 144.7, 135.8, 135.7, 133.5, 133.1, 130.0, 128.6, 127.9, 111.3, 65.5, 63.6, 60.9, 56.1, 36.6, 26.9, 26.5, 20.5, 19.4, 16.3, 14.4. HRESIMS [M + Na]<sup>+</sup> calcd for C<sub>33</sub>H<sub>42</sub>O<sub>4</sub>Na<sup>28</sup>Si<sup>32</sup>S 585.2498, found 585.2485.

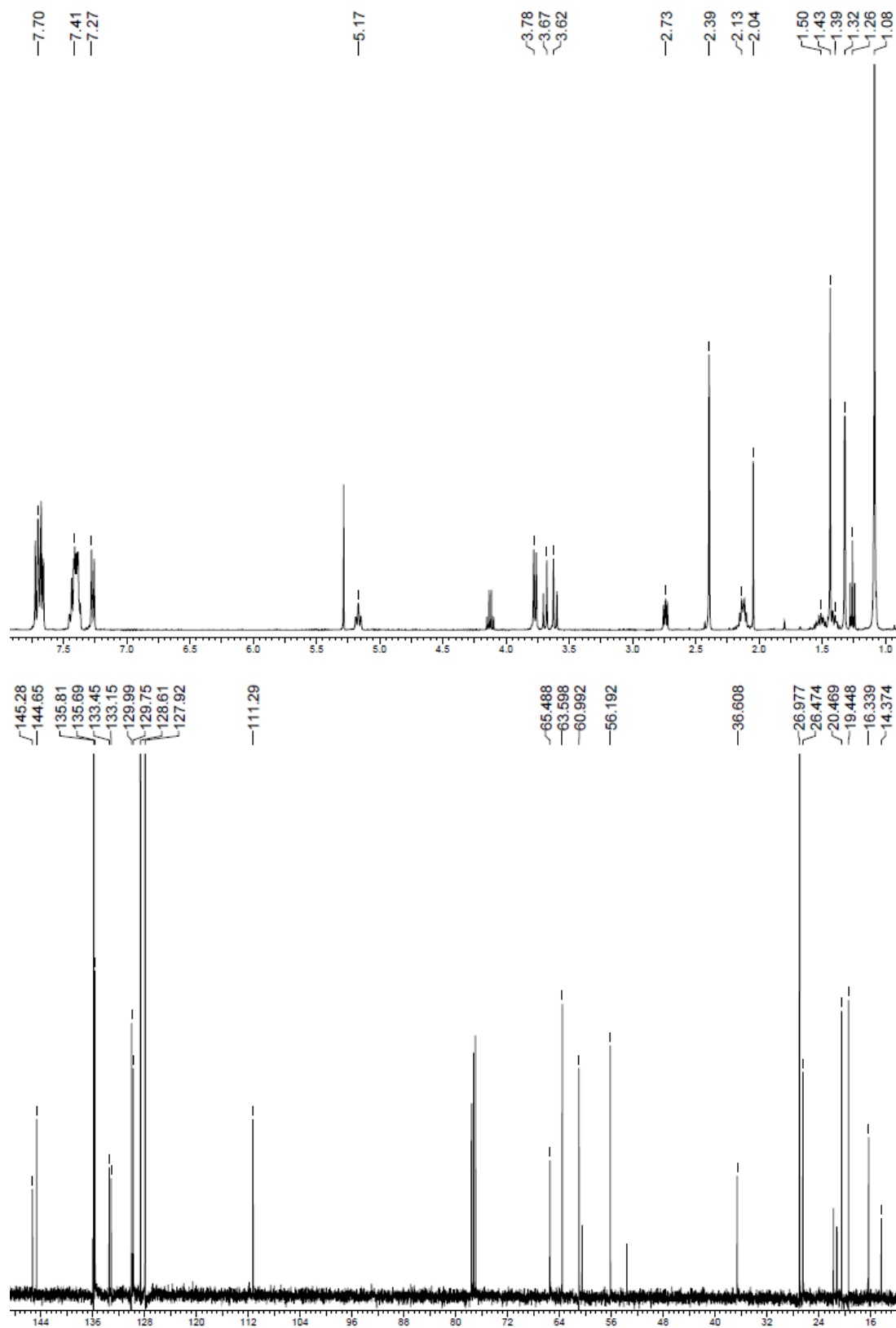
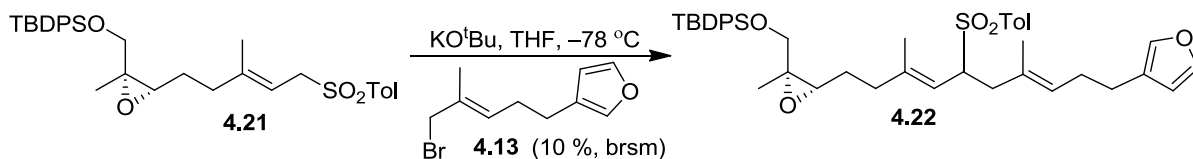


**Figure 4.11**  $^1\text{H}$  and  $^{13}\text{C}$  NMR spectra of **4.21** recorded in  $\text{CDCl}_3$  at 400 MHz and 100 MHz respectively.

### Preparation of 4.22:



To bromide **4.13** (55.0 mg, 0.238 mmol) and sulfone **4.21** (96 mg, 0.17 mmol), dissolved in 2 mL of tetrahydrofuran cooled to -78 °C was added KO<sup>t</sup>Bu (28.6 mg, 0.25 mmol), and the reaction mixture allowed to stir for three hours. The reaction was then quenched with the addition of 0.1 mL of methanol, and concentrated under a stream of nitrogen, and purified using flash column chromatography (hexanes:ethyl acetate 6:1) to give **4.22** (8.3 mg, 0.011 mmol, 9.5 % brsm). <sup>1</sup>H NMR (400 MHz, CDCl<sub>3</sub>) δ 7.68 (m, 6H), 7.46-7.37 (m, 6H), 7.30-7.21 (m, 3H), 7.12 (s, 1H), 6.20 (s, 1H), 5.13 (t, J = 6.8 Hz, 1H), 4.89 (d, J = 10.4 Hz, 1H), 3.89-3.83 (m, 1H), 3.69-3.60 (m, 2H), 2.87 (d, J = 13.2 Hz, 1H), 2.72 (m, 1H), 2.38 (s, 3H), 2.35 (m, 2H), 2.24 (m, 2H), 2.17 (m, 2H), 2.06 (m, 2H), 1.49 (s, 3H), 1.42 (s, 3H), 1.20 (m, 4H), 1.08 (s, 9H); <sup>13</sup>C NMR (100 MHz, CDCl<sub>3</sub>) δ 142.7, 138.9, 135.8, 135.7, 133.5, 133.2, 130.0, 129.5, 129.4, 129.3, 127.9, 127.9, 118.3, 118.3, 111.1, 65.5, 63.5, 63.5, 61.0, 36.6, 36.6, 28.5, 26.9, 26.5, 24.8, 21.7, 20.5, 19.5, 16.5, 16.2. HRESIMS [M + Na]<sup>+</sup> calcd for C<sub>43</sub>H<sub>54</sub>O<sub>5</sub>Na<sup>28</sup>Si<sup>32</sup>S 733.3359, found 733.3342.

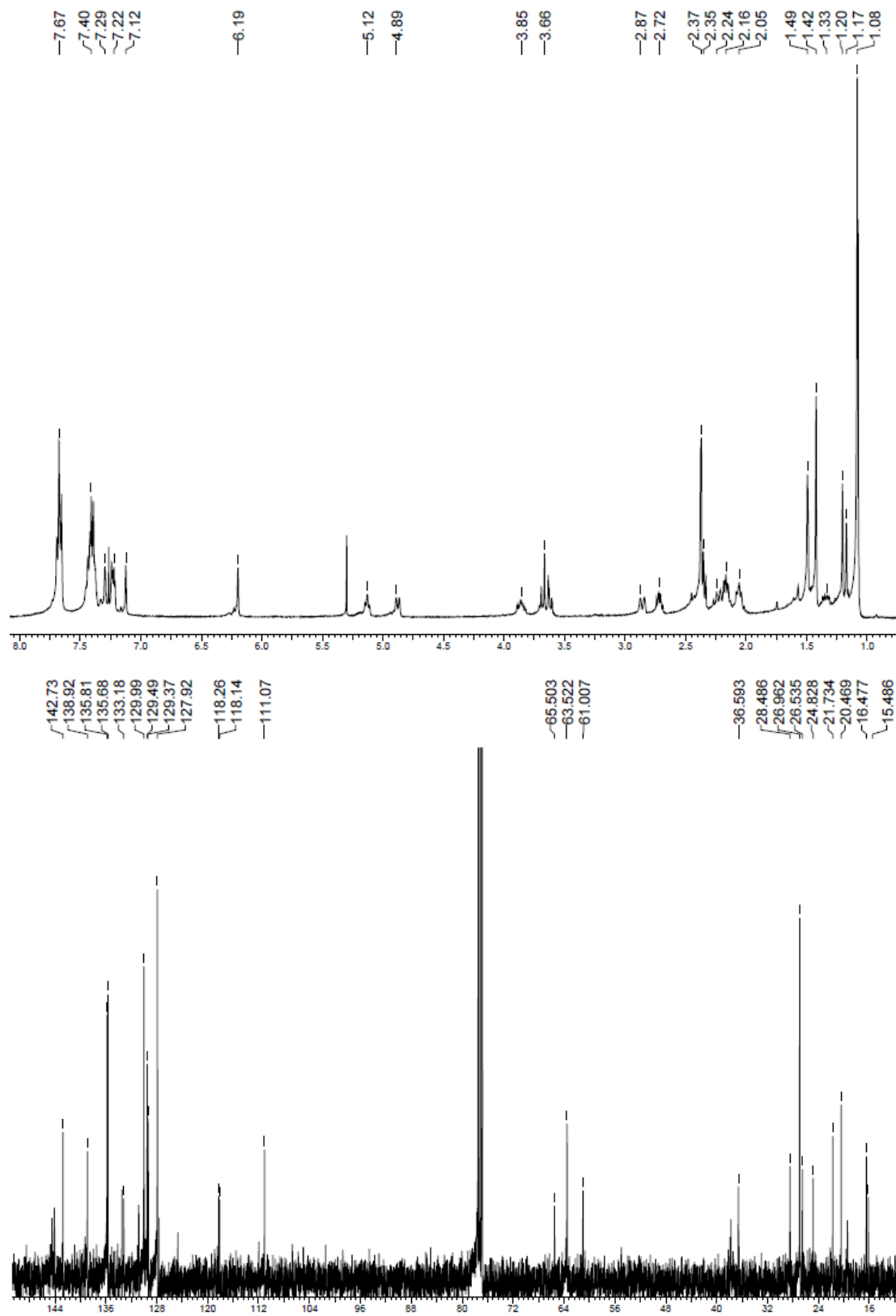
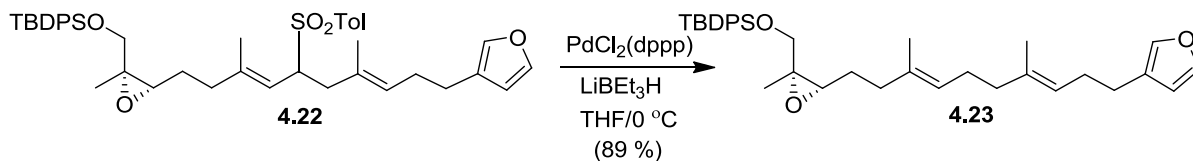


**Figure 4.12** <sup>1</sup>H and <sup>13</sup>C NMR spectra of **4.22** recorded in CDCl<sub>3</sub> at 400 MHz and 100 MHz respectively.

### Preparation of 4.23:



To sulfone **4.22** (46.6 mg, 0.065 mmol) dissolved in 1 mL of tetrahydrofuran was added PdCl<sub>2</sub>(dppp) (7.7 mg, 0.013 mmol) and cooled to 0 °C, to which a 1.0 M solution of LiBEt<sub>3</sub>H (0.13 mL, 0.13 mmol) was added dropwise using a syringe. After stirring for one hour, the reaction was quenched with 0.1 mL of methanol and was concentrated under a stream of nitrogen. The crude mixture was purified using flash column chromatography (hexanes:ethyl acetate 10:1), to give epoxide **4.23** (32.4 mg, 0.058 mmol, 88.5 %, yield includes small impurity). <sup>1</sup>H NMR (400 MHz, CDCl<sub>3</sub>) δ 7.70-7.66 (m, 5H), 7.46-7.34 (m, 5H), 7.34 (t, J = 1.6 Hz, 1H), 7.21 (s, 1H), 6.28 (s, 1H), 5.17 (t, J = 6.8 Hz, 1H), 5.11 (t, J = 6.8 Hz, 1H), 3.70 (d, J = 10.8 Hz, 1H), 3.64 (d, J = 10.8 Hz, 1H), 2.78 (t, J = 6.4 Hz, 1H), 2.45 (t, J = 7.2 Hz, 2H), 2.25 (m, 2H), 2.12-1.98 (m, 6H), 1.59 (s, 3H), 1.55 (s, 3H), 1.51 (m, 2H), 1.43 (s, 3H), 1.08 (s, 9H); <sup>13</sup>C NMR (100 MHz, CDCl<sub>3</sub>) δ 142.5, 138.8, 135.7, 135.5, 133.9, 133.4, 133.1, 129.7, 127.7, 125.0, 124.8, 123.8, 111.1, 65.4, 64.0, 60.7, 39.6, 36.4, 28.5, 26.8, 26.7, 26.6, 25.0, 20.3, 19.3, 16.1. HRESIMS [M + Na]<sup>+</sup> calcd for C<sub>36</sub>H<sub>48</sub>O<sub>3</sub>Na<sup>28</sup>Si 579.3270, found 579.3265.

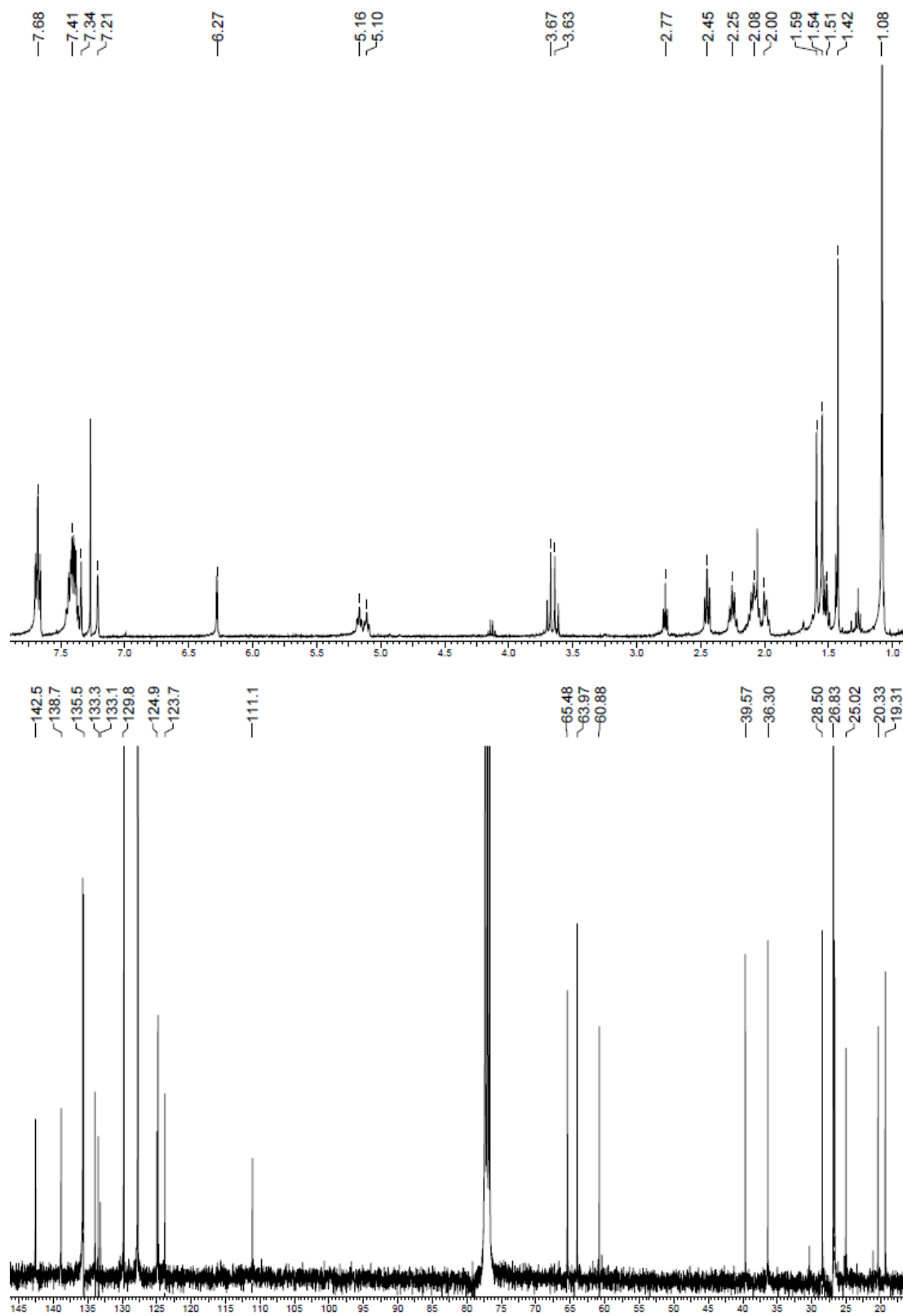
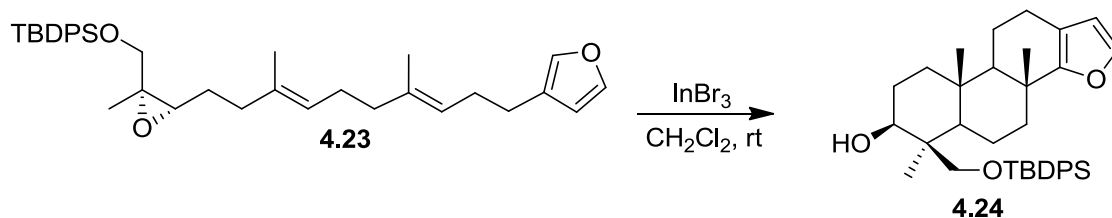


**Figure 4.13**  $^1\text{H}$  and  $^{13}\text{C}$  NMR spectra of **4.23** recorded in  $\text{CDCl}_3$  at 400 MHz and 100 MHz respectively.

**Preparation of 4.24:**



To epoxide **4.23** (32 mg, 0.057 mmol) dissolved in 1 mL of methylene chloride was added  $\text{InBr}_3$  (40.7 mg, 0.11 mmol), and allowed to stir at room temperature for forty minutes. The reaction was quenched with 4 drops of saturated  $\text{NaHCO}_3$  and concentrated under a stream of nitrogen. The mixture was purified using flash column chromatography (hexanes:ethyl acetate 12:1) to give a crude mixture of **4.24** and side products. A  $^1\text{H}$  NMR spectrum of a mixed fraction believed to contain **4.24** shows resonances at 7.17 and 6.10 indicative of protons at the C-5 and C-4 positions respectively. HRESIMS  $[\text{M} + \text{H}]^+$  calcd for  $\text{C}_{36}\text{H}_{49}\text{O}_3^{28}\text{Si}$  557.3451, found 557.3446.

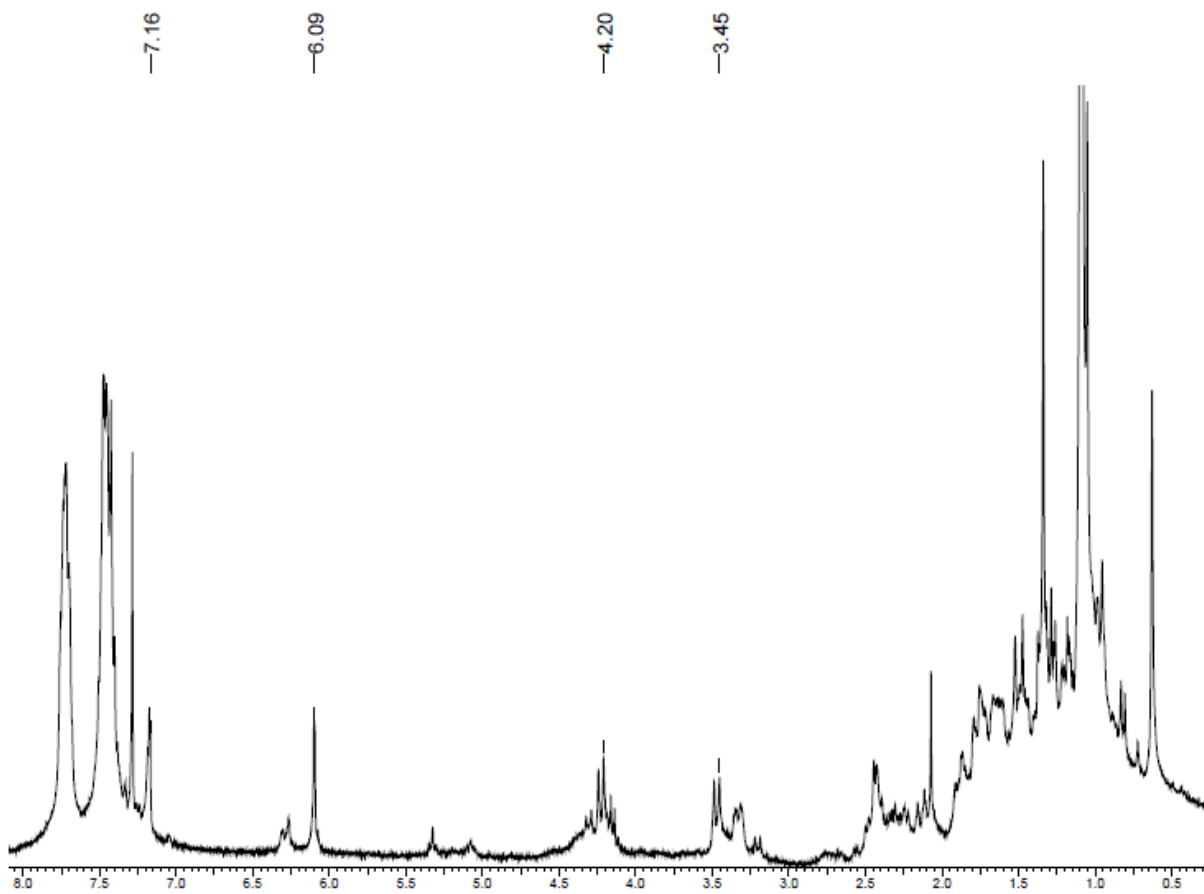
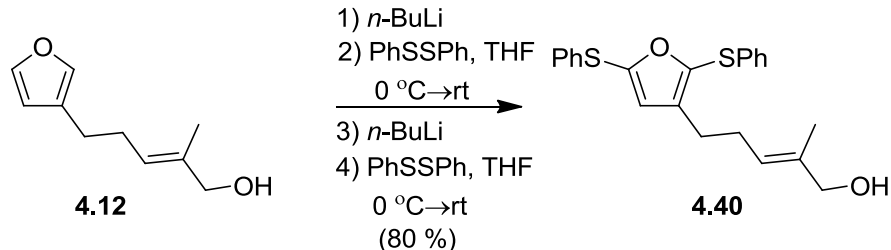


**Figure 4.14**  $^1\text{H}$  spectrum of **4.24** recorded in  $\text{CDCl}_3$  at 400 MHz.

### Preparation of 4.40:



To furan **4.12** (100 mg, 0.60 mmol) dissolved in 3 mL of tetrahydrofuran and cooled to  $-20\text{ }^{\circ}\text{C}$  was added a 1.6 M solution of *n*-BuLi (0.8 mL, 1.28 mmol) and cooled to  $-10\text{ }^{\circ}\text{C}$ . The mixture was allowed to stir for 30 minutes after which diphenyl disulfide (151 mg, 0.69 mmol) was added and the mixture stirred at  $-10\text{ }^{\circ}\text{C}$  for 30 minutes then room temperature for one hour. The mixture was then cooled to  $-20\text{ }^{\circ}\text{C}$  and to it was added a 1.6 M solution of *n*-BuLi (0.8 mL, 1.28 mmol) and cooled to  $-10\text{ }^{\circ}\text{C}$ . The mixture was allowed to stir for 30 minutes after which diphenyl disulfide (151 mg, 0.69 mmol) was added and the mixture was allowed to warm to room temperature overnight. The mixture was then quenched with the addition of 0.5 mL of methanol, concentrated using a rotary evaporator, and purified using flash column chromatography (hexanes:ethyl acetate 6:1 – 4:1) to give **4.40** (183.6 mg, 0.48 mmol, 80 %).  $^1\text{H}$  NMR (400 MHz,  $\text{CDCl}_3$ )  $\delta$  7.29-7.13 (m, 10H), 6.71 (s, 1H), 5.37 (t,  $J = 8.4\text{ Hz}$ , 1H), 3.92 (s, 2H), 2.61 (t,  $J = 7.2\text{ Hz}$ , 2H), 2.29 (q,  $J = 7.2\text{ Hz}$ , 2H), 1.58 (s, 3H), 1.38 (s, 1H);  $^{13}\text{C}$  NMR (100 MHz,  $\text{CDCl}_3$ )  $\delta$  146.8, 143.4, 136.4, 136.2, 135.5, 135.2, 129.3, 129.2, 128.5, 127.5, 126.9, 126.5, 124.5, 121.3, 68.8, 28.1, 25.7, 13.8. HRESIMS  $[\text{M} + \text{Na}]^+$  calcd for  $\text{C}_{22}\text{H}_{22}\text{O}_2\text{Na}^{32}\text{S}_2$  405.0959, found 405.0956.

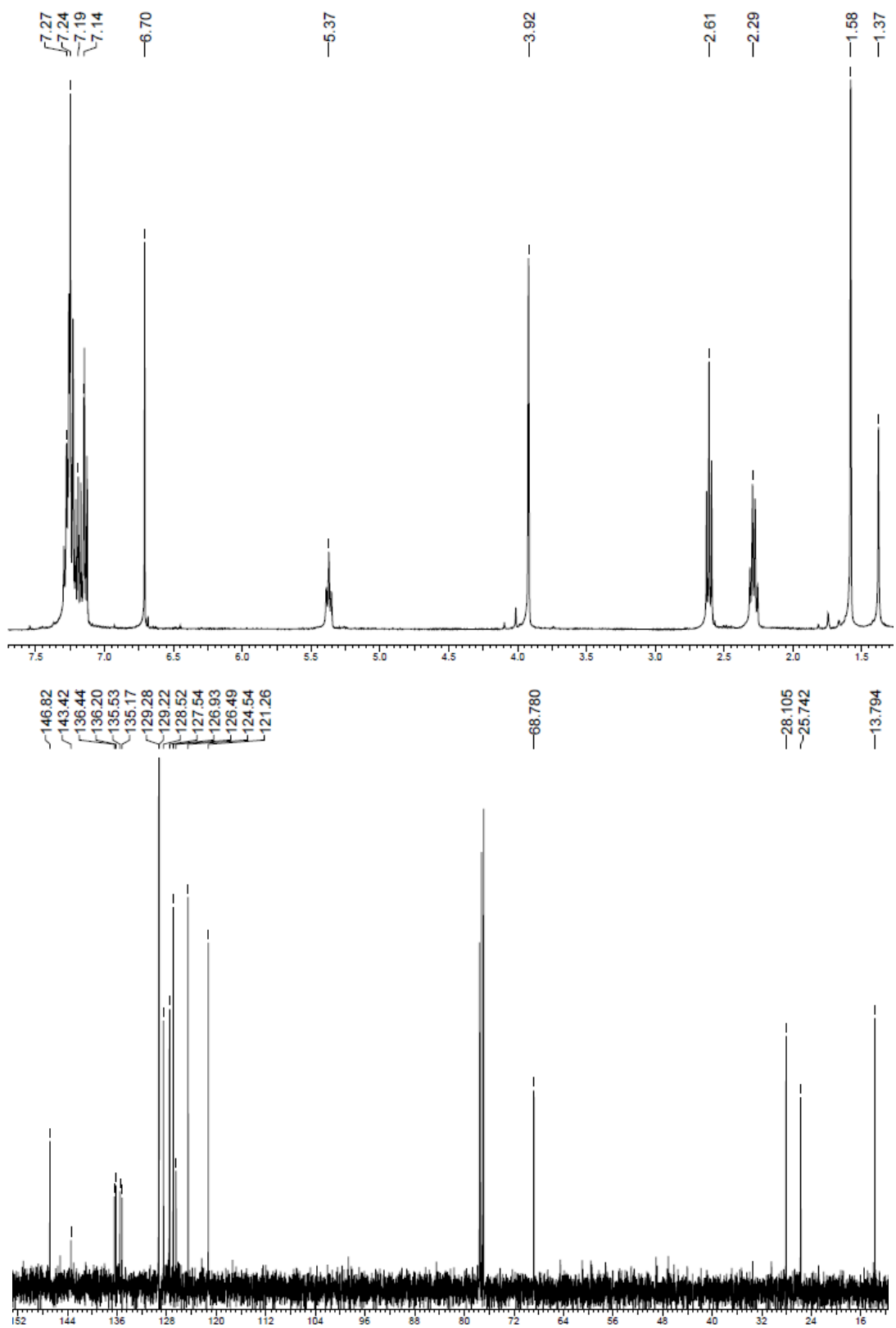
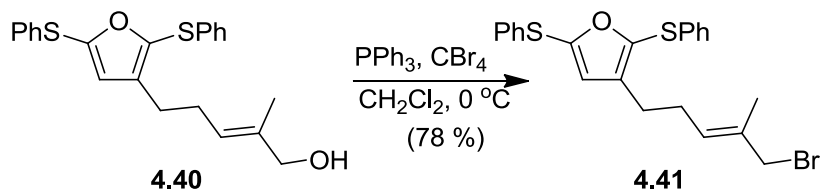


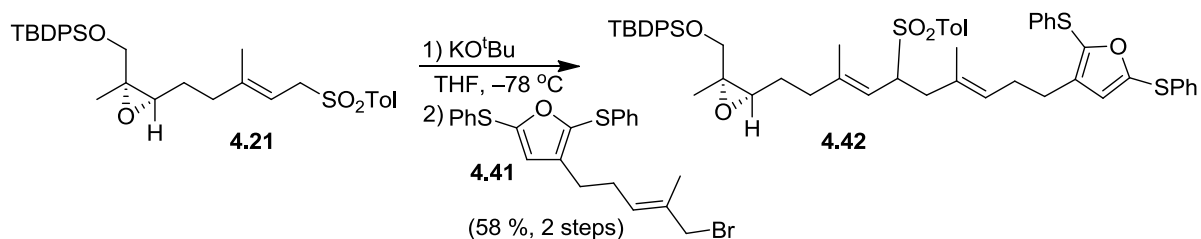
**Figure 4.15**  $^1\text{H}$  and  $^{13}\text{C}$  NMR spectra of **4.40** recorded in  $\text{CDCl}_3$  at 400 MHz and 100 MHz respectively.

### Preparation of 4.41:



To alcohol **4.40** (64.3 mg, 0.17 mmol) dissolved in 2 mL of methylene chloride was added triphenylphosphine (57.2 mg, 0.22 mmol) and cooled to 0 °C, after which carbon tetrabromide (72.3 mg, 0.22 mmol) was added and the reaction allowed to stir for 45 minutes at 0 °C. The crude reaction mixture was concentrated using a rotary evaporator and filter through a plug of silica (hexanes:ethyl acetate 4:1) to give **4.41** (59.0 mg, 0.13 mmol, 78 % estimated from crude material) and immediately used in the next step.

### Preparation of 4.42:



To sulfone **4.21** (900 mg, 1.74 mmol) and bromide **4.41** (895.3 mg, 2.0 mmol) dissolved in 18 mL of tetrahydrofuran and cooled to  $-78\text{ }^{\circ}\text{C}$  was added KO<sup>t</sup>Bu (234.3 mg, 2.08 mmol) and the reaction allowed to warm to room temperature overnight. The crude reaction mixture was quenched with 1 mL of methanol, concentrated under a stream of nitrogen and purified using flash column chromatography (hexanes:ethyl acetate 6:1-4:1) to give **4.42** (597.9 mg, 0.64 mmol, 58.2 %, brsm, 272.2 mg of **4.21**). <sup>1</sup>H NMR (400 MHz, CD<sub>2</sub>Cl<sub>2</sub>)  $\delta$  7.22-7.63 (m, 6H), 7.47-7.40 (m, 6H), 7.31-7.10 (m, 12H), 6.88 (s, 1H), 5.11 (t, J = 7.2 Hz, 1H), 4.88 (d, J = 10.8 Hz, 1H), 3.84 (m, 1H), 3.67 (d, J = 1.6 Hz, 2H), 2.80 (d, J = 12.8 Hz, 1H), 2.68 (q, J = 7.6 Hz, 1H), 2.48 (t, J = 7.6 Hz, 2H), 2.38 (s, 3H), 2.22-2.11 (m, 3H), 2.04 (t, J = 7.2 Hz, 2H), 1.56 (s, 1H), 1.45 (s, 3H), 1.41 (s, 3H), 1.36-1.30 (m, 1H), 1.17 (dd, J = 8, 1.2 Hz, 3H), 1.09 (s, 9H); <sup>13</sup>C NMR (100 MHz, CD<sub>2</sub>Cl<sub>2</sub>)  $\delta$  146.5, 144.62, 144.1, 143.8, 136.2, 135.7, 135.6, 135.4, 135.3, 133.6, 133.3, 133.3, 131.5, 129.9, 129.5, 129.3, 129.2, 129.2, 128.3, 127.9, 127.8, 127.4, 127.0, 127.0, 126.9, 126.5, 121.3, 118.1, 65.6, 63.3, 63.3, 60.7, 37.7, 37.7, 36.5, 36.5, 28.4, 26.7, 26.5, 25.6, 21.4, 20.2, 19.3, 16.1, 15.8. HRESIMS [M + Na]<sup>+</sup> calcd for C<sub>55</sub>H<sub>62</sub>O<sub>5</sub>Na<sup>28</sup>Si<sup>32</sup>S<sub>3</sub> 949.3426, found 949.3448.

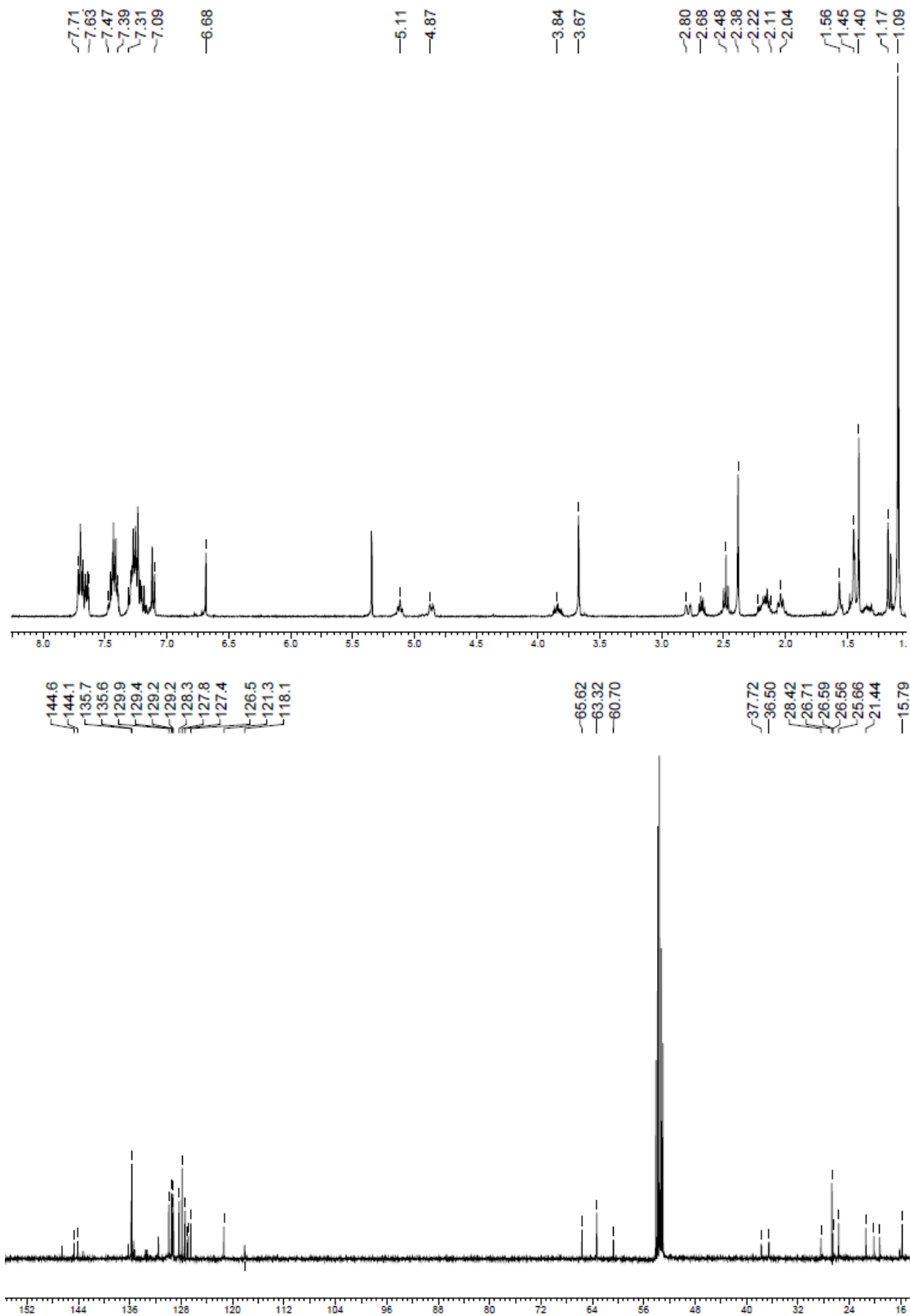
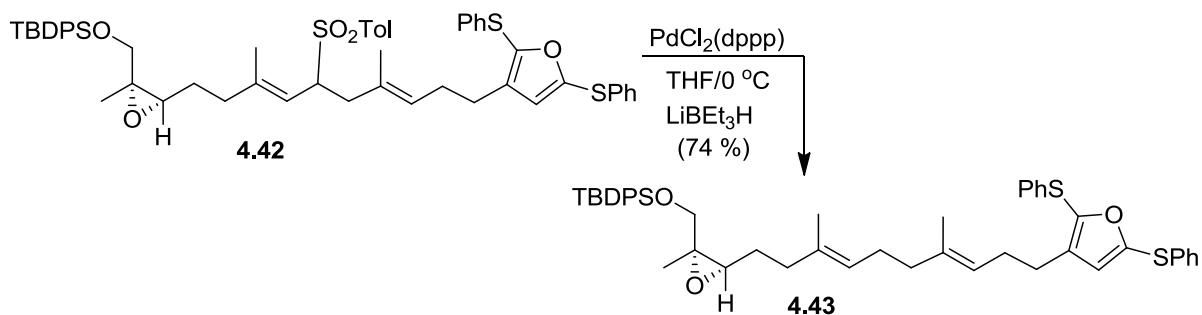


**Figure 4.16**  $^1\text{H}$  and  $^{13}\text{C}$  NMR spectra of **4.42** recorded in  $\text{CD}_2\text{Cl}_2$  at 400 MHz and 100 MHz respectively.

### Preparation of 4.43:



To sulfone **4.42** (600 mg, 0.65 mmol) and  $\text{PdCl}_2(\text{dppp})$  (76.5 mg, 0.13 mmol) in 16 mL of tetrahydrofuran cooled to 0 °C was added a 1 M solution of  $\text{LiBEt}_3\text{H}$  (1.3 mL, 1.3 mmol) dropwise using a syringe. After stirring for four hours, the mixture was quenched with saturated  $\text{NH}_4\text{Cl}$  (aq) (150 mL) and allowed to warm to room temperature. The aqueous layer was extracted three times with methylene chloride (400 mL). The combined organic extracts were dried with  $\text{MgSO}_4$  and concentrated using a rotary evaporator. The crude mixture was purified using flash column chromatography (hexanes:ethyl acetate 15:1) to give **4.43** (376.4 mg, 0.48 mmol, 73.8 %).  $^1\text{H}$  NMR (400 MHz,  $\text{CDCl}_3$ )  $\delta$  7.67 (t,  $J = 8.0$  Hz, 6H), 7.45-7.36 (m, 7H), 7.25-7.11 (m, 7H), 6.69 (s, 1H), 5.11 (q,  $J = 6.4$  Hz, 2H), 3.69 (d,  $J = 11.2$  Hz, 1H), 3.63 (d,  $J = 10.8$  Hz, 1H), 2.76 (t,  $J = 6.4$  Hz, 1H), 2.55 (t,  $J = 7.2$  Hz, 2H), 2.22 (q,  $J = 7.2$  Hz, 2H), 2.09 (q,  $J = 6.4$  Hz, 2H), 2.04-1.91 (m, 4H), 1.53 (m, 8H), 1.42 (s, 3H), 1.08 (s, 9H);  $^{13}\text{C}$  NMR (100 MHz,  $\text{CDCl}_3$ )  $\delta$  146.5, 136.5, 135.8, 135.7, 135.6, 133.3, 129.9, 129.2, 129.1, 128.4, 127.9, 127.8, 127.5, 126.8, 126.3, 124.9, 123.1, 121.5, 118.6, 111.8, 65.5, 64.1, 39.7, 36.5, 28.5, 27.0, 26.9, 26.8, 26.7, 26.0, 22.1, 20.5, 19.4, 16.2, 16.1. HRESIMS  $[\text{M} + \text{Na}]^+$  calcd for  $\text{C}_{48}\text{H}_{56}\text{O}_3\text{Na}^{28}\text{Si}^{32}\text{S}_2$  795.3338, found 795.3355.

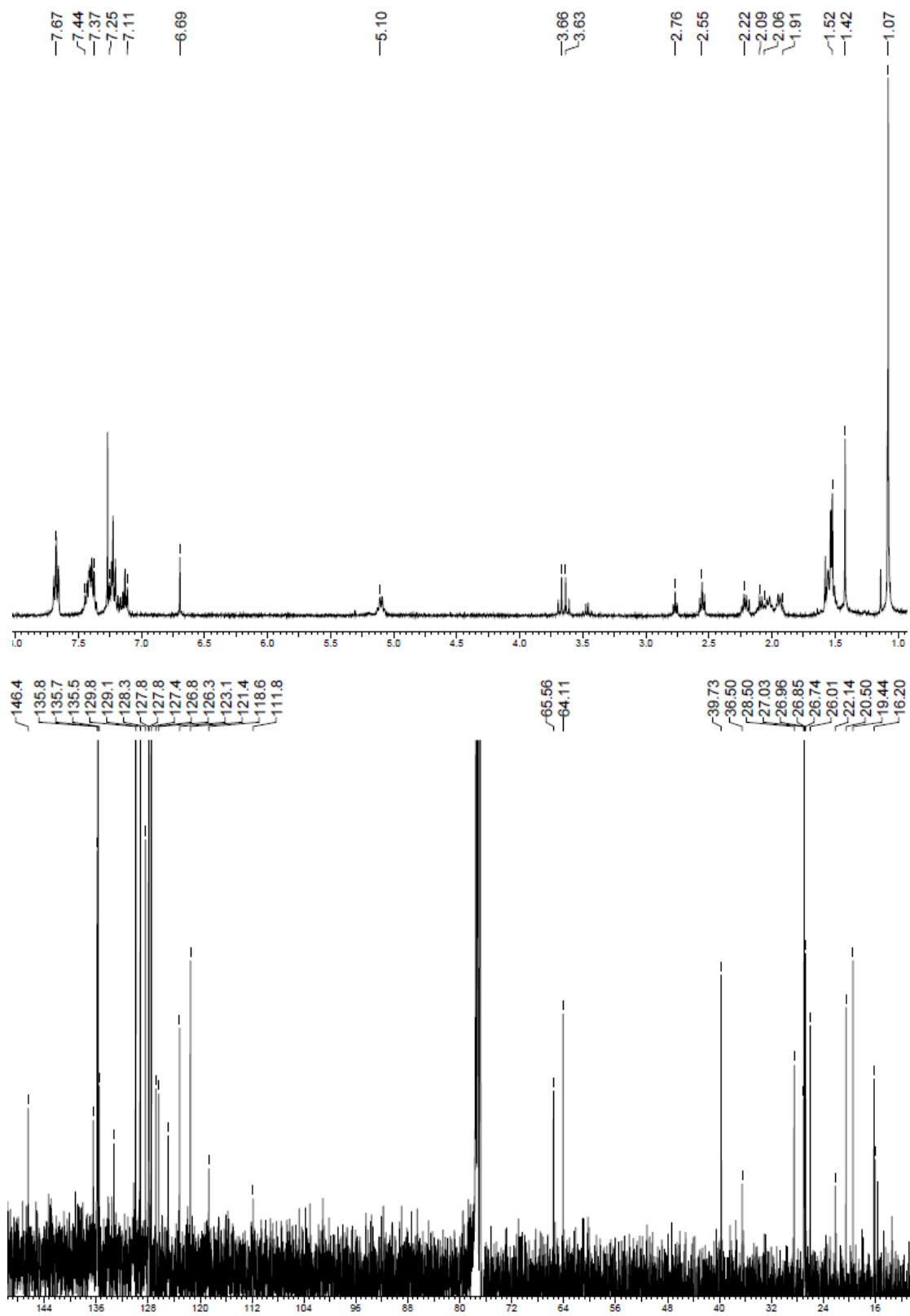
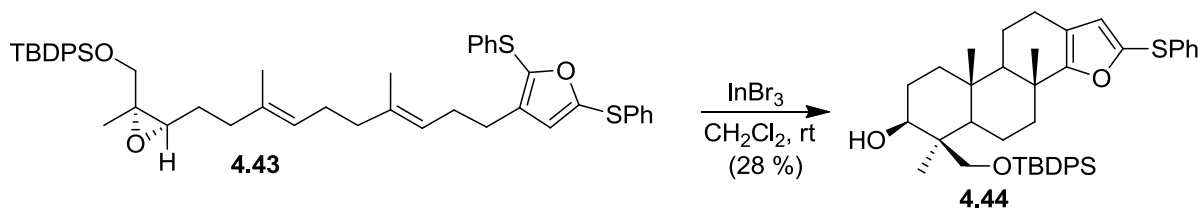


**Figure 4.17**  $^1\text{H}$  and  $^{13}\text{C}$  NMR spectra of **4.43** recorded in  $\text{CDCl}_3$  at 400 MHz and 100 MHz respectively.

### Preparation of 4.44:



To polyene **4.43** (300 mg, 0.38 mmol) dissolved in 10 mL of methylene chloride was added  $\text{InBr}_3$  (275 mg, 0.77 mmol) and allowed to stir at room temperature for one hour. The mixture was quenched with saturated  $\text{NaHCO}_3$  (100 mL) and the aqueous layer was extracted three times with methylene chloride (250 mL). The combined organic extracts were dried with  $\text{MgSO}_4$  and concentrated using a rotary evaporator. The crude mixture was purified using flash column chromatography (hexanes:ethyl acetate 15:1) to give **4.44** (71.3 mg, 0.10 mmol, 28.4 %, yield includes a small impurity).  $^1\text{H}$  NMR (600 MHz,  $\text{CDCl}_3$ )  $\delta$  7.72 (dd,  $J = 16.2, 7.2$  Hz, 4H), 7.49-7.45 (m, 5H), 7.24 (t,  $J = 4.8$  Hz, 2H), 7.13 (t,  $J = 5.2$  Hz, 2H), 7.09 (m, 2H), 6.47 (s, 1H), 4.20 (d,  $J = 10.2$  Hz, 1H), 3.47 (d,  $J = 10.2$  Hz, 1H), 3.32 (m, 1H), 2.49 (dd,  $J = 15.6, 5.4$  Hz, 1H), 2.32 (m, 1H), 2.17 (dt,  $J = 13.2, 3.0$  Hz, 1H), 1.90 (m, 1H), 1.78 (m, 2H), 1.70-1.61 (m, 3H), 1.47 (m, 1H), 1.39 (m, 2H), 1.34 (s, 6H), 1.30-1.18 (m, 2H), 1.08 (s, 9H), 0.99 (m, 1H), 0.62 (s, 3H);  $^{13}\text{C}$  NMR (150 MHz,  $\text{CDCl}_3$ )  $\delta$  163.6, 135.3, 135.2, 132.1, 131.7, 129.5, 128.5, 127.4, 126.0, 125.3, 120.3, 115.9, 80.0, 65.5, 55.9, 55.8, 47.5, 42.4, 37.7, 36.7, 35.3, 35.2, 27.5, 26.4, 22.5, 22.3, 21.8, 18.0, 17.6, 16.6. HRESIMS  $[\text{M} + \text{H}]^+$  calcd for  $\text{C}_{42}\text{H}_{53}\text{O}_3^{28}\text{Si}^{32}\text{S}$  665.3485, found 665.3474 .

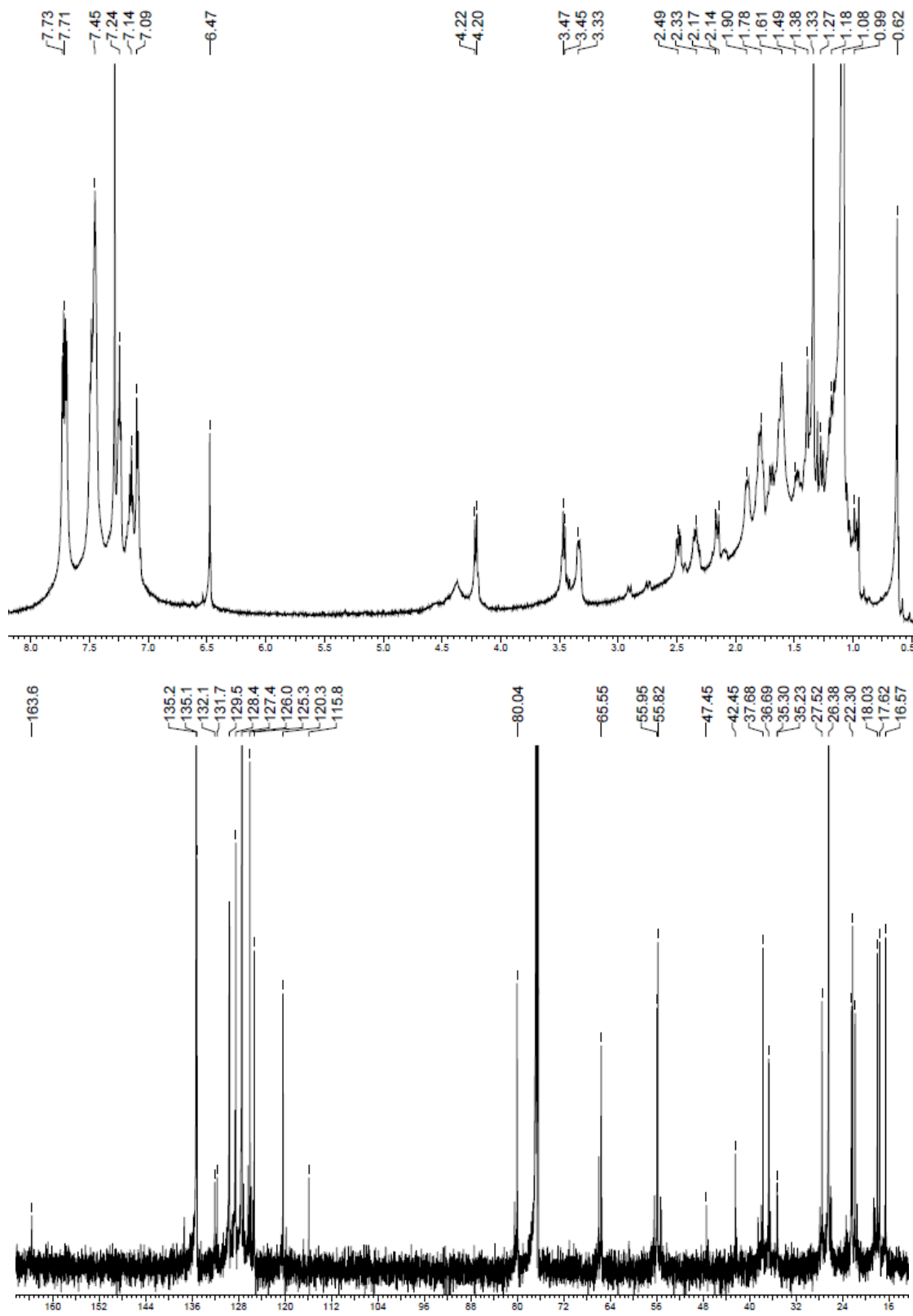


**Figure 4.18**  $^1\text{H}$  and  $^{13}\text{C}$  NMR spectra of **4.44** recorded in  $\text{CDCl}_3$  at 600 MHz and 150 MHz respectively.

**Ligand-Binding Affinities of Terpenes in AR:** Androgen Receptor Competitor Assay Kit (Invitrogen™) was employed for the *in vitro* binding assay. Recombinant AR-LBD and fluorescently labeled androgen ligand were used to test the binding affinities of semisynthetic analogues **4.1**, **4.2**, and **4.4** using synthetic androgen R1881 (metribolone) and clinically approved antiandrogen bicalutamide (**3.4**) as positive controls. Each testing compound underwent serial dilutions and was added in triplicates to a Greiner 384-well black clear bottom plate. At excitation wavelength of 470 nm and emission of 535 nm, fluorescence polarization was measured by Infinite M1000 (TECAN®). The graph was generated by plotting polarization value (mP) against concentration (Log(nM)) using Prism software (GraphPad Software) as nonlinear regression fit for One-site Competition curves. Representative data of a single experiment is plotted. Error bars represent the mean  $\pm$  SEM of technical triplicates for each data point measured.

## Chapter 5: Synthetic Efforts Towards Lichostatinal (5.4): A Potent Cathepsin K Inhibitor

### 5.1 Cysteine Protease Inhibitors

Proteases are ubiquitous in human physiology where they play important roles in apoptosis,<sup>182</sup> breakdown of intracellular proteins,<sup>183</sup> and clearance of organic particulates and microorganisms. Although a variety of proteases exists, many have a similar mechanism of action. A nucleophilic amino acid residue in the protease is responsible for amide bond cleavage, resulting in the hydrolysis of a peptide into smaller units (Figure 5.1).<sup>183</sup>

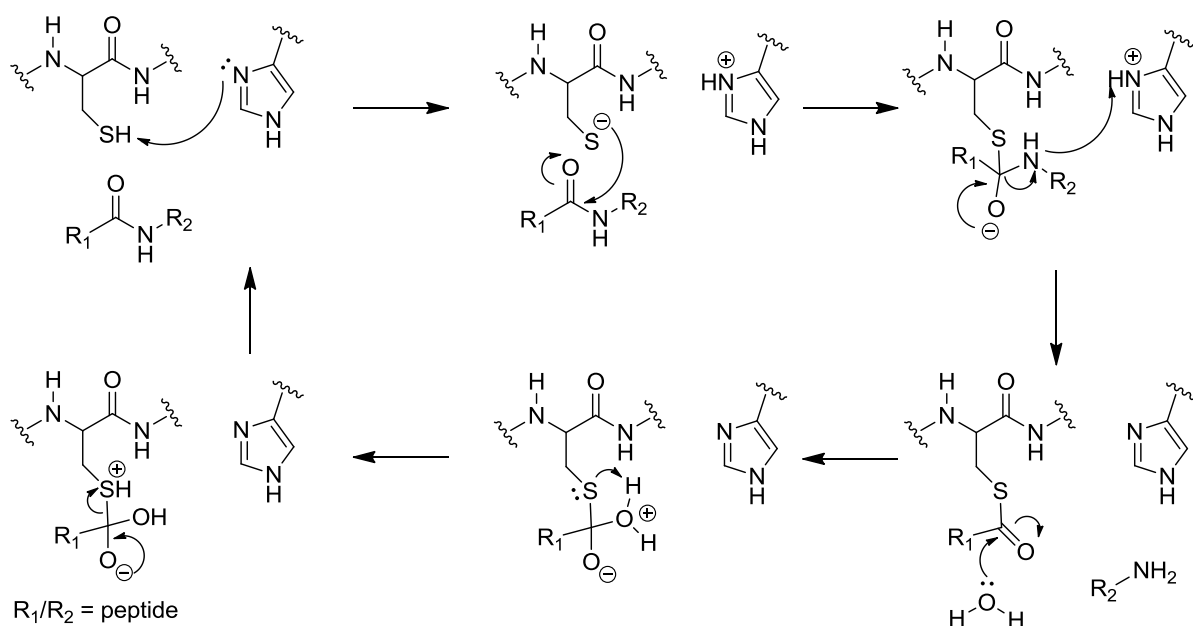


**Figure 5.1** Hydrolysis of a peptide by a cysteine protease.

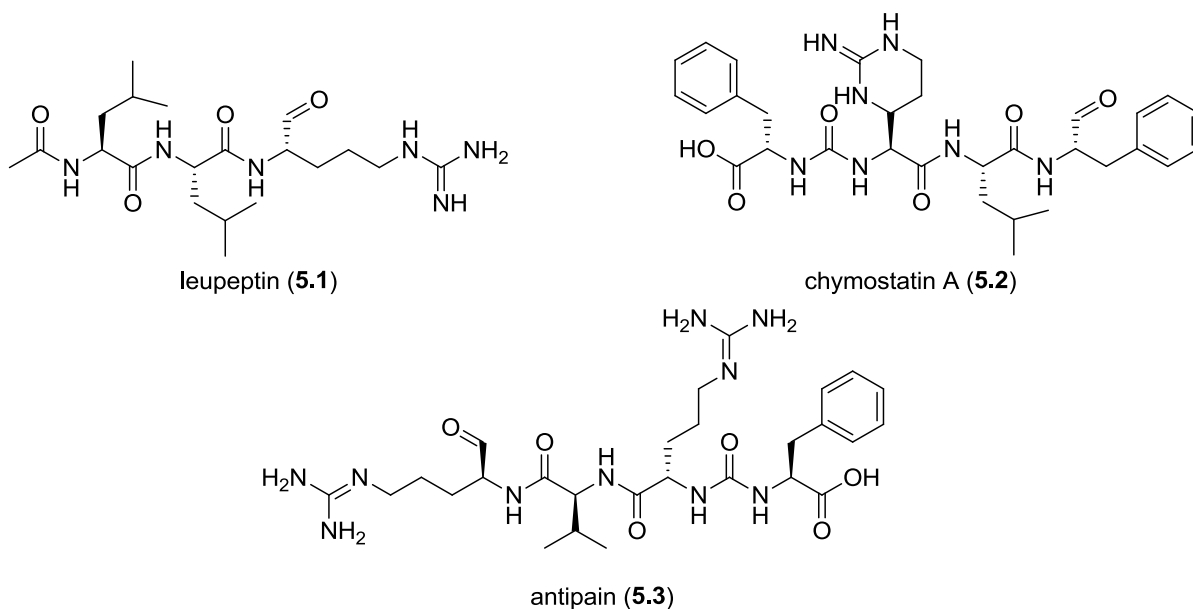
Proteases are classified as serine,<sup>184</sup> threonine, cysteine,<sup>185</sup> aspartate<sup>186</sup> and metalloproteases. The mechanism of proteolysis by cysteine proteases<sup>187,188</sup> is exemplified in

Figure 5.1. The first step entails deprotonation of the cysteine residue in the active site of the protease by a nearby basic moiety, typically a histidine residue (Figure 5.1). The next step is attack of the carbonyl carbon of the peptide substrate by the sulfide anion of cysteine, liberating a new *N*-terminus subunit. The resulting thioester intermediate is then hydrolyzed to regenerate the cysteine and histidine residues along with a carboxylic acid subunit (Figure 5.1).

Unlike many other reversible post-translational modifications that peptides typically undergo, such as phosphorylation,<sup>189</sup> proteolysis is irreversible. Once hydrolyzed, the only means available to regain the peptide is for mRNA translation to occur. Because of this irreversible effect on peptides, proteases are compartmentalized in the lysosome<sup>190</sup> and/or in the endosome<sup>191</sup> within the cell. However, low concentrations of proteases are found throughout the body. The activity of cysteine proteases is kept in check by endogenous cysteine protease inhibitors such as cystatins<sup>192</sup> and serpins.<sup>193</sup> These inhibitors are found in excess concentrations in the cytoplasm and extracellular space. An imbalance between cysteine proteases and their inhibitors can lead to human diseases such as muscular dystrophy,<sup>194</sup> arthritis,<sup>195</sup> bone resorption,<sup>196</sup> and Alzheimer's disease.<sup>197</sup>

Caspase<sup>198</sup> and cathepsin<sup>199</sup> proteases make up the two groups of cysteine proteases. Cathepsin K is expressed in osteoclasts<sup>200</sup> and has been implicated in bone resorption. The biological role of cathepsin K has led to the development of small molecule inhibitors as potential therapeutics to combat osteoporosis,<sup>201</sup> with natural products playing an important role in lead compound discovery. The first cysteine protease inhibitor to be discovered was leupeptin<sup>202</sup> (**5.1**), a peptide-aldehyde produced in culture by various *actinomycetes* bacteria.

Shortly afterwards, additional peptide-aldehyde natural product inhibitors of cathepsin such as chymostatin<sup>203</sup> (5.2) and antipain<sup>204</sup> (5.3) were also isolated (Figure 5.2).



**Figure 5.2** Peptide-aldehyde inhibitors of cysteine proteases.

While these peptide-aldehyde natural products are potent inhibitors of cathepsin K, they also show activity towards other cathepsins and serine proteases. In addition, these inhibitors bind cysteine proteases covalently. Typically, the thiol or alcohol side chain in a cysteine and/or serine will attack the electrophilic aldehyde moiety in the natural product as shown in Figure 5.3.

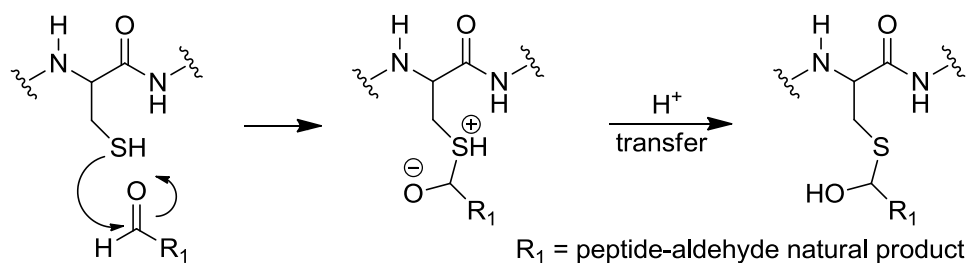


**Figure 5.3** Covalent binding mechanism between a peptide-aldehyde natural product and a cysteine protease.

This covalent binding mechanism along with the chronic nature of osteoporosis treatment leads to these peptide-aldehyde inhibitors as being unlikely drug candidates due to potential off-target effects.<sup>205</sup> However, these inhibitors often find use as chemical tools when an enzyme is being studied in an *in vitro* setting. In these studies the cell is lysed, which releases the once compartmentalized proteases. The addition of a small molecule protease inhibitor stops proteolysis of potential target enzymes allowing them to be studied.

## 5.2 Lichostatinal (5.4) a Novel Peptide-Aldehyde Inhibitor of Cathepsin K

Several cathepsin K inhibitors are currently in development and include balicatib<sup>206</sup> (Novartis), relacatib<sup>207</sup> (GlaxoSmithKline), and odanacatib<sup>208</sup> (Merck & Co.). However, there is currently no available therapeutic cathepsin K inhibitor for the treatment of osteoporosis.

The lack of available therapeutics led to a collaboration between the laboratories of Dr. Julian Davies and Dr. Dieter Bromme at the University of British Columbia. The laboratory of Dr. Davies has a collection of more than 2000 strains of *streptomyces*, and of those, 384 were screened in a cathepsin K inhibition assay by Vincent Paul Lavallée in Dr. Bromme's laboratory. Attempts to purify the most active extract by reversed phase HPLC purification failed. However, samples of enriched purity were isolated that showed activity in

the nM range in a cathepsin K enzyme inhibition assay. Co-crystallization of the ligand-substrate complex was successful by soaking the active fraction with cathepsin K. The crystal was analyzed by a beamline,<sup>209</sup> which is a light source of high-energy (X-rays) emitted from a synchrotron and often used for protein crystallography. The structure of the active metabolite was elucidated to be the novel peptide-aldehyde lichostatinal (**5.4**) (Figure 5.4). Lichostatinal (**5.4**) is the first example of a natural product to be isolated from a complex mixture by co-crystallization with its biological target.

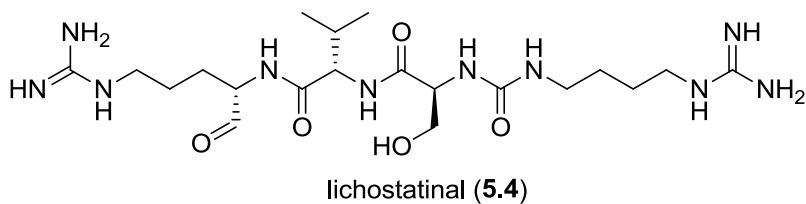
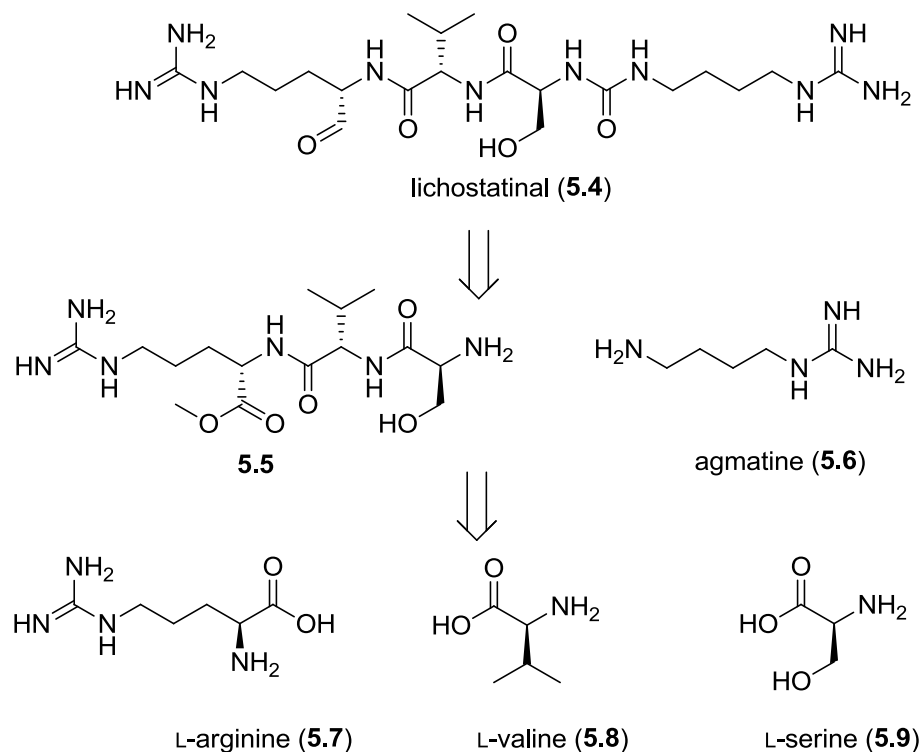


**Figure 5.4** Novel peptide-aldehyde lichostatinal (**5.4**).

Lichostatinal (**5.4**) is a peptide tetramer comprised of arginine, valine, serine, and arginine residues, with a urea linkage between serine and arginine. Peptide **5.4** is structurally similar to leupeptin (**5.1**) and antipain (**5.3**), in that the arginine residue bears the reactive aldehyde functionality that presumably covalently binds to cathepsin K. While the beamline data was successful in providing a structure for the active metabolite, additional spectroscopic data was required to further verify the structure of lichostatinal (**5.4**) and compare it with biological data gathered on the crude sample.

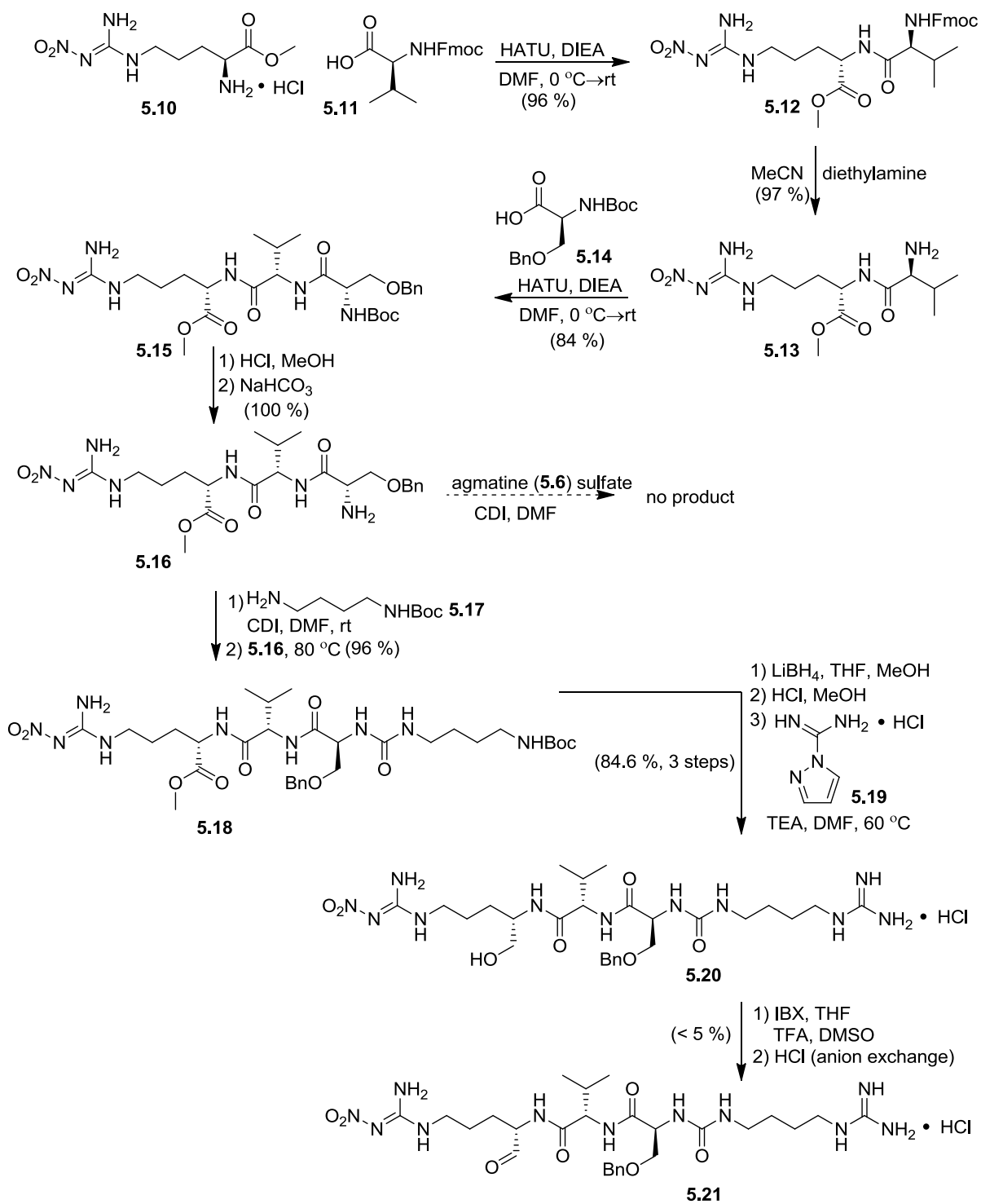
The role of the author was to construct synthetic lichostatinal (**5.4**) to verify the proposed structure through biological testing and co-crystallization with cathepsin K. The retrosynthetic analysis of lichostatinal (**5.4**) shows that it can be derived from linking

agmatine (**5.6**) and tripeptide **5.5** by a urea bond. Tripeptide **5.5** may be constructed from coupling the amino acids L-arginine (**5.7**), L-valine (**5.8**), and L-serine (**5.9**) (Scheme 5.1).



**Scheme 5.1** Retrosynthetic analysis of lichostatinal (**5.4**).

The first step in the synthesis was the coupling of **5.10** to L-valine-*N*-Fmoc (**5.11**), using standard coupling methodology (Scheme 5.2). Various peptide coupling reagents<sup>210</sup> exist, and are typically used in a 1:1 ratio to the corresponding amino acid. HATU<sup>211</sup> was used to couple nitro-protected arginine **5.10** with Fmoc protected L-valine (**5.11**) to construct **5.12**. Intermediate **5.12** was then deprotected<sup>212</sup> with diethylamine in acetonitrile to give amine **5.13**. HATU was again used to couple **5.13** to O-benzyl protected L-serine-*N*-Boc (**5.14**) to give intermediate **5.15**. The Boc-protecting group was removed with concentrated HCl to give amine **5.16**.

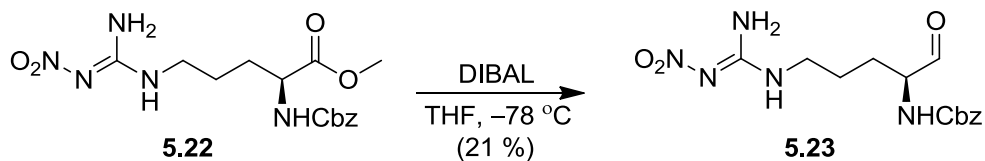


**Scheme 5.2** Synthesis toward lichostatinal (**5.4**).

At this point, coupling commercially available agmatine sulfate (**5.6**) to **5.16** with CDI<sup>213</sup> as the coupling reagent was thought to be the most expeditious route. Unfortunately, agmatine sulfate (**5.6**) is sparingly soluble in *N,N*-dimethylformamide, dimethyl sulfoxide, or tetrahydrofuran, which are classic CDI coupling solvents. Agmatine sulfate (**5.6**) and its corresponding freebase are only freely soluble in water, which decomposes CDI. Nevertheless, the coupling was attempted using the aforementioned solvents, to no avail (Scheme 5.2). Alternatively, mono-Boc protected putrescine<sup>214</sup> **5.17** was coupled with **5.16**. Varying the reaction conditions was done to optimize the yields for this step. This involved changing the order of amine addition to CDI. It was found that exposing CDI to tripeptide **5.16** for several hours, followed by addition of **5.17**, failed to yield product. However, exposing CDI to **5.17**, followed by addition of **5.16** resulted in product formation (**5.18**) (Scheme 5.2). Dimethyl sulfoxide and *N,N*-dimethylformamide were both tested as solvents for the reaction and provided similar yields. *N,N*-dimethylformamide was favored due to ease of handling when compared with dimethyl sulfoxide. An alternative method in forming the urea linkage was attempted using triphosgene,<sup>215</sup> however, this was unsuccessful in the hands of the author.

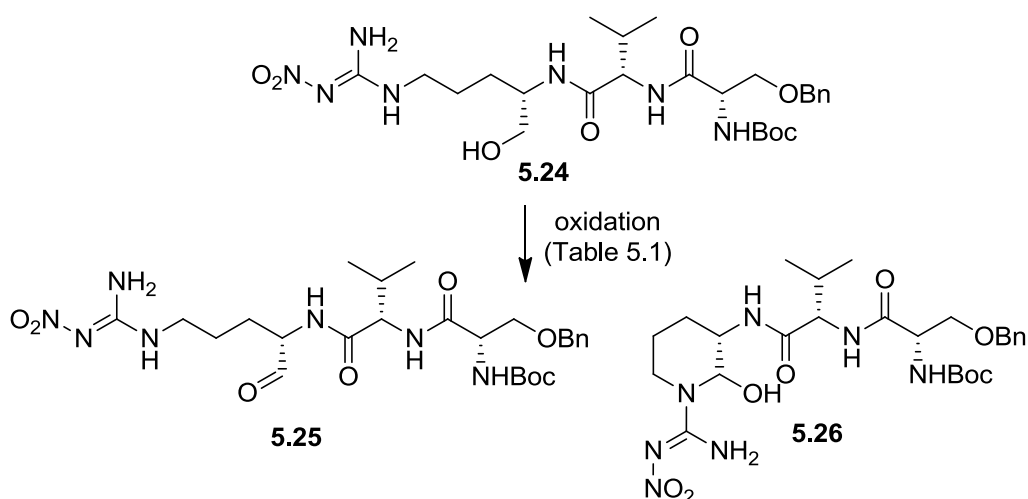
Next, methods of forming the aldehyde moiety were considered. One way to access an amino aldehyde is to reduce the ester with DIBAL at  $-78\text{ }^{\circ}\text{C}$  as shown by Ito<sup>216</sup> *et al.* (Scheme 5.3), however, their published results of a 21 % yield in reducing *N*-Cbz protected nitro arginol was not promising. Nevertheless, the DIBAL reduction of intermediate **5.15** was attempted and gave a complex reaction mixture. The crude <sup>1</sup>H NMR spectra showed trace amounts of reduction products (< 5 %). Alternatively, reducing the ester moiety to the

primary alcohol and oxidizing it back to the aldehyde at a later step was considered (Scheme 5.2).



**Scheme 5.3** Ito's reduction of Cbz protected arginine **5.22**.

The synthesis carried on with intermediate **5.18** being reduced with  $\text{LiBH}_4$ ,<sup>217</sup> followed by deprotection with HCl, and guanylation<sup>218</sup> with **5.19** to give intermediate **5.20** (Scheme 5.2). Amino alcohol oxidation of **5.20** with IBX<sup>219</sup> in dimethyl sulfoxide under acidic conditions was used to prepare the corresponding aldehyde. However, only trace amounts of benzyl-protected lichostatinal (**5.21**) were observed (< 5 %), and modifying the reaction conditions had no effect. To address this apparent inertness of our amino alcohol (**5.20**) towards oxidative conditions, the literature was examined for precedent in amino alcohol oxidation. In the original synthesis of leupeptin (**5.1**) by Shimizu<sup>220</sup> *et al.* it was shown that arginol oxidation to the corresponding aldehyde resulted in cyclization to give a mixture of a hemiaminal in addition to the expected aldehyde. Arginol oxidation was investigated in a model study by oxidizing **5.24** using a variety of conditions (Scheme 5.4).<sup>221,222,223,224,225</sup>



**Scheme 5.4** Oxidation of Arginol (**5.24**).

**Table 5.1** Results of arginol (**5.24**) oxidation model study.

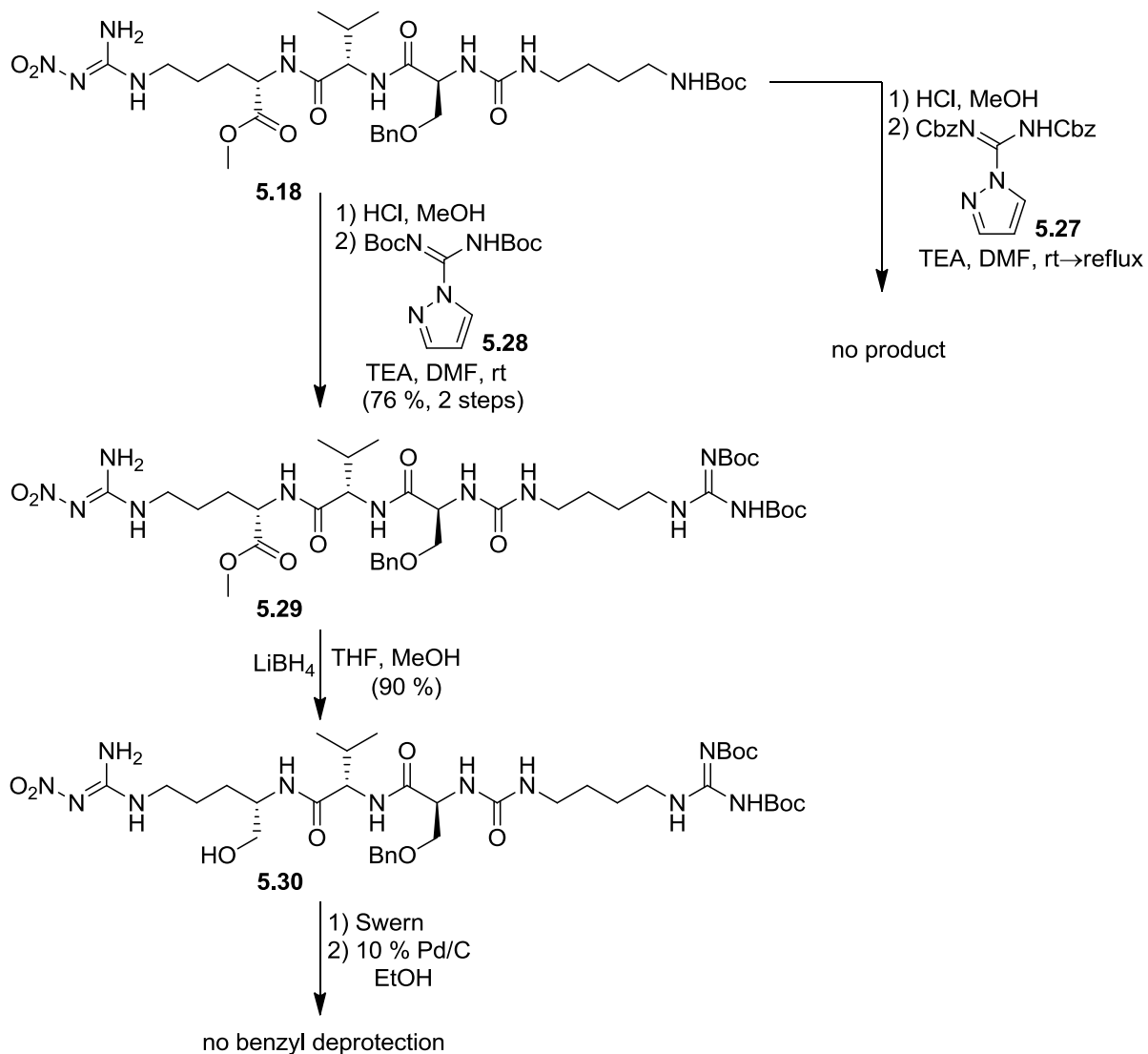
Reagents	Solvent	Temperature	Yield <sup>a</sup>
IBX	dimethyl sulfoxide	rt	< 5 %
IBX	acetone	reflux	no rxn
DMP, pyridine	methylene chloride	rt	~ 10 %
SO <sub>3</sub> pyr, dms, <i>i</i> -PrNEt	methylene chloride	rt	~ 20 %
oxalyl chloride, dms, NEt <sub>3</sub>	methylene chloride	-78 °C	~ 40 %
TEMPO, NaBr, NaOCl, NaHCO <sub>3</sub>	toluene, ethyl acetate water	rt	no reaction
TEMPO, TBACl, NaHCO <sub>3</sub> , K <sub>2</sub> CO <sub>3</sub> , NCS	methylene chloride	rt	no reaction
PCC	methylene chloride	rt	no reaction

<sup>a</sup> Based on the crude <sup>1</sup>H NMR spectra of **5.25/5.26** mixture.

The results of the model study are summarized in Table 5.1. Oxidation of **5.24** with IBX is low yielding. Oxidations using TEMPO and PCC as oxidants did not yield any product. Dess–Martin and Parikh–Doering oxidation conditions were more successful. Swern oxidation of **5.24** gave the highest yields, so it was selected as the favored oxidation method.

The synthesis continued by deprotecting **5.18** followed by guanylation<sup>226</sup> with di-Boc protected reagent **5.28** to give **5.29** (Scheme 5.5). Guanylation using di-Cbz protected **5.27**

was attempted in order to shorten future deprotection steps. The nitro functional group on the arginine moiety and the Cbz group on the guanidine can be removed by hydrogenation simultaneously. Unfortunately, even under reflux the guanylation of **5.18** with **5.27** was unsuccessful (Scheme 5.5).



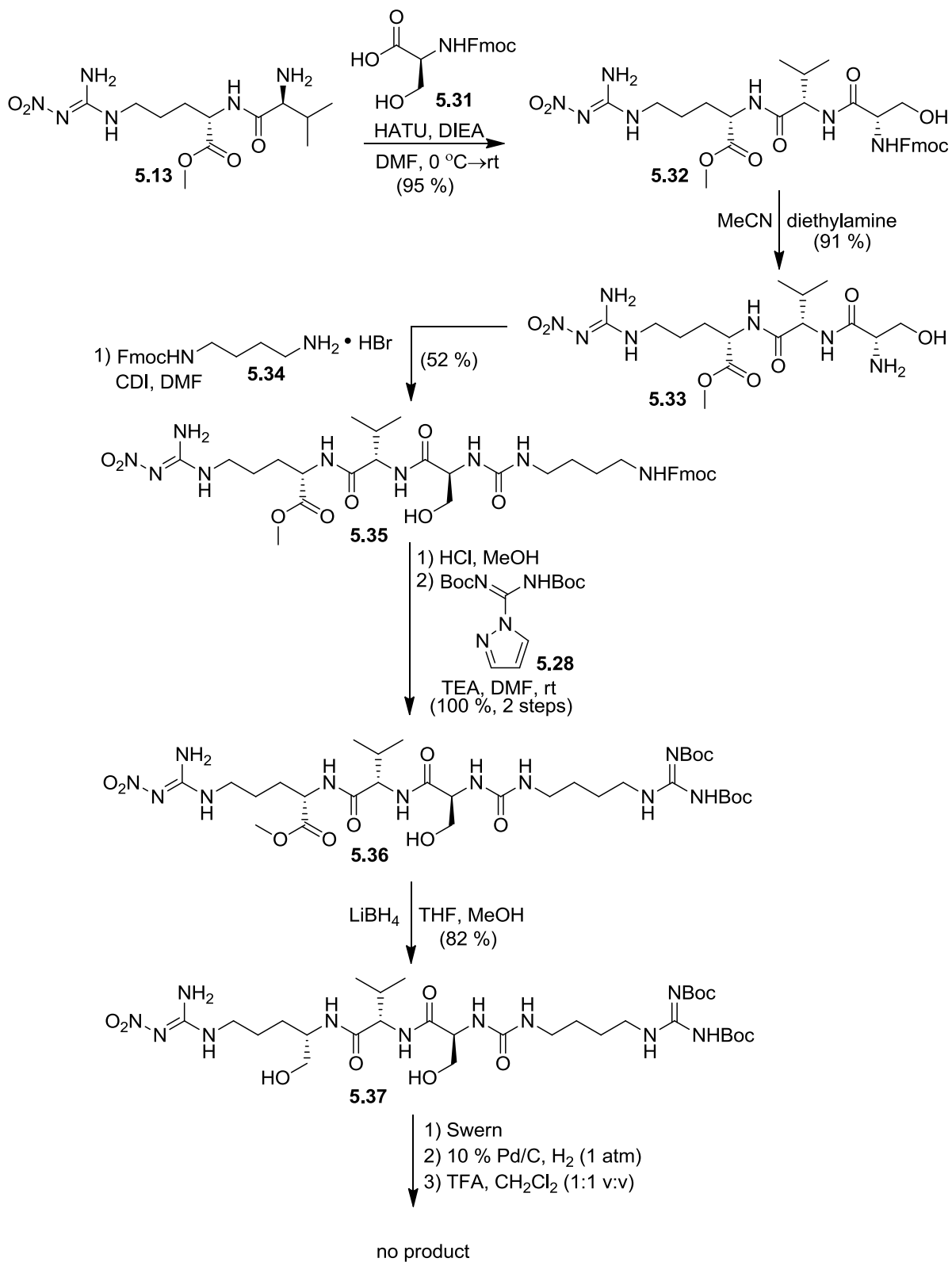
**Scheme 5.5** Synthesis towards lichostatinal (**5.4**).

The synthesis continued with intermediate **5.29** being reduced with LiBH<sub>4</sub> to give **5.30**, followed by Swern oxidation to afford the expected aldehyde/hemiaminal mixture. Attempted deprotection of the O-benzyl serine residue on this intermediate with 10 % palladium/charcoal under H<sub>2</sub> (1 atm) was unsuccessful. This was a surprising outcome, and a model study was undertaken in which intermediate **5.15** was exposed to different O-benzyl deprotection conditions (Table 5.2).<sup>227,228,229,230</sup>

**Table 5.2** Results of an O-benzyl deprotection model study of intermediate **5.15**.

Reagent	Solvent	Temperature/H <sub>2</sub>	Product Observed
10 % Pd/C	ethanol	rt/1 atm	none
10 % Pd/C	ethanol	reflux/1 atm	none
10 % Pd/C/TFA	ethanol	rt/1 atm	none
10 % Pd/C	ethanol	rt/15 atm	none
20 % Pd(OH) <sub>2</sub>	ethanol	rt/1 atm	none
20 % Pd(OH) <sub>2</sub>	ethanol	reflux/1 atm	none
NH <sub>4</sub> HCO <sub>2</sub> /Zn	methanol	rt	none
NH <sub>4</sub> HCO <sub>2</sub> , 10 % Pd/C	methanol/tetrahydrofuran	rt	none
Et <sub>3</sub> SiH, 10 % Pd/C	methanol	rt	none

Unfortunately, none of the conditions was successful in benzyl deprotection and this synthetic route was abandoned. However, a similar route in which the serine residue could be left unprotected was devised (Scheme 5.6). This synthesis does not have the problems associated with the benzyl deprotection, and may provide a regioisomer of lichostatinal (**5.4**) to broaden the SAR. The synthesis began with amine **5.13** being coupled to *N*-Fmoc-Serine **5.31** with HATU to give intermediate **5.32** in high yield. Intermediate **5.32** was deprotected with diethylamine to yield **5.33**, and subsequently coupled with CDI and mono Fmoc<sup>231</sup> protected putrescine **5.34** to provide **5.35** in a modest yield (Scheme 5.6).



**Scheme 5.6** Alternative route to lichostatinal (**5.4**).

Intermediate **5.35** was guanylated with **5.28** to give **5.36**, which was reduced with LiBH<sub>4</sub> to give **5.37**. Intermediate **5.37** was oxidized by a Swern oxidation. The crude material was carried through to the next step, which was deprotection of the nitro group with 10 % palladium/charcoal and hydrogen (1 atm). The Boc protecting groups were then removed with a 1:1 mixture of trifluoroacetic acid:methylene chloride to give a complex mixture (Scheme 5.6). A <sup>1</sup>H NMR resonance at approximately 5.5 ppm suggested that the aldehyde had cyclized to produce the hemiaminal as shown in Shimizu's synthesis of leupeptin<sup>220</sup> (**5.1**). However, absolute confirmation of the presence of lichostatinal (**5.4**) was not verified. Nevertheless, this complex mixture was given to Vincent Paul Lavallée in Dr. Bromme's lab for biological testing in a cathepsin K enzymatic assay. Unfortunately, the crude mixture showed activity in the μM range in contrast to the nM range found for the natural product (**5.4**). This suggested that we were unsuccessful in constructing lichostatinal (**5.4**). The synthesis of lichostatinal (**5.4**) is an on-going project in the Andersen lab.

### 5.3 Conclusion

Cathepsin K is a cysteine protease that has been implicated in bone resorption,<sup>196</sup> which has led to the development of small molecule inhibitors of cathepsin K. In a continued effort to identify natural product inhibitors of cathepsin K, the Davies' natural product extract library was screened using a cathepsin K enzymatic inhibition assay in the laboratory of Dr. Bromme. This led to the isolation and identification of lichostatinal (**5.4**), which is a novel peptide-aldehyde inhibitor of cathepsin K.

Lichostatinal (**5.4**) is the first natural product known to be isolated by co-crystallization with its biological target from a complex mixture. The crystal of the enzyme-

ligand complex was analyzed by a beamline, and the structure of lichostatinal (**5.4**) was elucidated. This chapter describes the synthetic effort towards constructing lichostatinal (**5.4**) in order to verify its structure by NMR.

Construction of the peptide utilized solution phase peptide chemistry to assemble the necessary amino acids to obtain intermediate **5.16** (Scheme 5.1). Initial attempts to couple **5.16** to agmatine sulfate (**5.6**) were unsuccessful. However, by modification of the synthesis by using amine building block **5.17**, it was possible to construct intermediate **5.18**. Oxidation of alcohol **5.20** with IBX gave low yields of the desired aldehyde. A corresponding model study was undertaken using compound **5.24** in order to examine the yields for oxidation based on known protocol.

Compound **5.24** was exposed to various oxidative conditions (Table 5.1). A number of known amino alcohol oxidation methods provided no product or gave only poor yields. However, Swern oxidation was found to give the highest and most reproducible yield. Having chosen an appropriate oxidative method, the synthesis moved forward (Scheme 5.5). Attempts to deprotect the benzyl group on the serine residue with known conditions were fruitless and a model study to examine benzyl deprotection was completed using intermediate **5.15** as a substrate (Scheme 5.2). None of the attempted literature protocols were successful in removing the benzyl functionality from **5.15**.

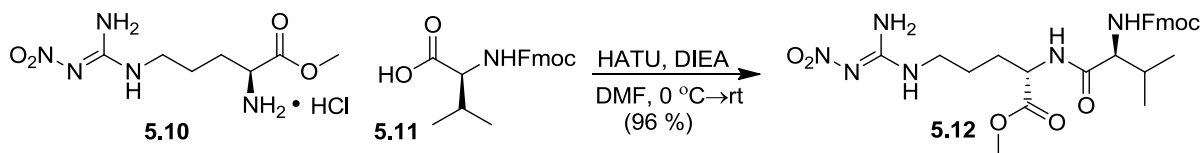
A benzyl protecting group free synthetic route to construct lichostatinal (**5.4**) and its regioisomer was pursued (Scheme 5.6). From a medicinal chemistry perspective, this is advantageous since it would broaden the SAR and potentially yield an analogue with enhanced or comparable potency. Unfortunately, biological testing of a complex reaction mixture thought to contain lichostatinal (**5.4**) and its regioisomer was less active than the

natural product (**5.4**) suggesting that the synthesis had failed to construct the natural product. Completion of the synthesis of the novel peptide-aldehyde lichostatinal (**5.4**) is currently ongoing in the Andersen lab.

## 5.4 Experimental

**General Methods:** All non-aqueous reactions were carried out in flame-dried glassware and under an Ar or N<sub>2</sub> atmosphere unless otherwise noted. Air and moisture sensitive liquid reagents were manipulated via a dry syringe. All solvents and reagents were used as obtained from commercial sources without further purification. <sup>1</sup>H and <sup>13</sup>C NMR spectra were obtained on Bruker Avance 400 direct, 300 direct, or Bruker Avance 600 CryoProbe spectrometers at room temperature. Flash column chromatography was performed using Silicycle Ultra-Pure silica gel (230-400 mesh). Analytical thin-layer chromatography (TLC) plates were aluminum-backed ultrapure silica gel 250 μm. Electrospray ionization mass spectrometry (ESI-MS) spectra were recorded on a Micromass LCT instrument.

### Preparation of 5.12:



To Fmoc-L-valine **5.11** (1.25 g, 3.70 mmol) dissolved in 5 mL of *N,N*-dimethylformamide was added HATU (1.48 g, 3.89 mmol) and *N,N*-diisopropylethylamine (1.29 mL, 7.41 mmol) at 0 °C. To this mixture was added ester **5.10** (1.0 g, 3.70 mmol) dissolved in 5 mL of *N,N*-dimethylformamide, and allowed to warm to room temperature overnight. To the crude mixture was added saturated NaHCO<sub>3</sub> (150 mL) and the aqueous layer extracted three times with methylene chloride (300 mL). The organic extracts were combined and washed three times with brine, then concentrated using a rotary evaporator, filtered through a pad of silica (methylene chloride:methanol 4:1), and concentrated again using a rotary evaporator. Upon the addition of methanol a precipitate formed. This was triturated with additional methanol (500 mL) and the solid was determined to be **5.12** (1.97 g, 3.55 mmol, 95.9 %). Alternatively **5.12** may be purified using flash column chromatography (methylene chloride:methanol 95:5). <sup>1</sup>H NMR (400 MHz, (CD<sub>3</sub>)<sub>2</sub>SO) δ 8.49 (bs, 1H), 8.34 (d, J = 7.2 Hz, 1H), 7.87 (d, J = 7.2 Hz, 2H), 7.72 (t, J = 6.8 Hz, 2H), 7.39 (t, J = 7.6 Hz, 2H), 7.30 (t, J = 7.2 Hz, 2H), 4.31-4.19 (m, 4H), 3.88 (t, J = 7.6 Hz, 1H), 3.59 (s, 3H), 3.14 (m, 2H), 1.96 (quin, J = 6.8 Hz, 1H), 1.73 (m, 1H), 1.62 (m, 1H), 1.5 (m, 2H), 0.89 (d, J = 6.8 Hz, 3H), 0.86 (d, J = 6.8 Hz, 3H); <sup>13</sup>C NMR (100 MHz, (CD<sub>3</sub>)<sub>2</sub>SO) δ 172.8, 172.2, 162.9, 156.7, 144.5, 144.3, 141.3, 128.3, 127.7, 125.9, 120.7, 66.3, 60.5, 52.4, 47.3, 40.7, 31.0, 28.3, 19.6, 18.9. HRESIMS [M + Na]<sup>+</sup> calcd for C<sub>27</sub>H<sub>34</sub>N<sub>6</sub>O<sub>7</sub>Na 577.2387, found 577.2373.

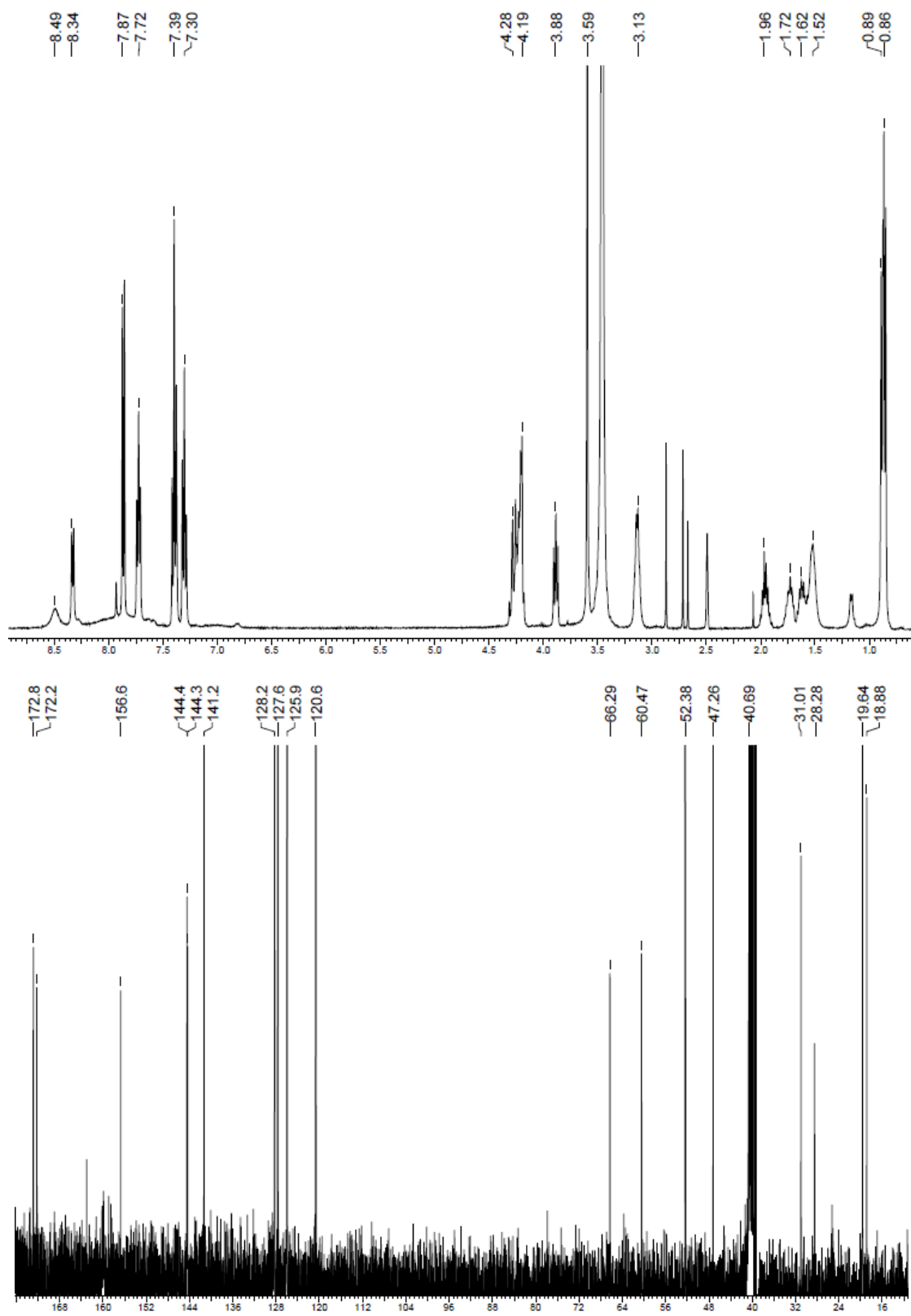
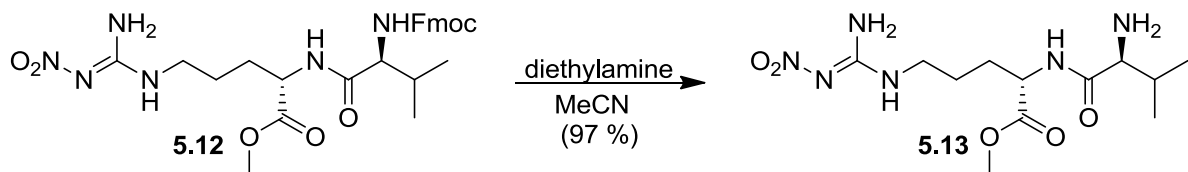


**Figure 5.5**  $^1\text{H}$  and  $^{13}\text{C}$  NMR spectra of **5.12** recorded in  $(\text{CD}_3)_2\text{SO}$  at 400 MHz and 100 MHz respectively.

### Preparation of 5.13:



To **5.12** (7.0 g, 12.6 mmol) dissolved in 400 mL of acetonitrile was added diethylamine (26.1 mL, 252.4 mmol) dropwise, and the mixture allowed to stir at room temperature for ninety minutes, after which the reaction mixture was filtered through a pad of silica and the acetonitrile eluent discarded, the pad of silica was then washed with 200 mL of methylene chloride:methanol (4:1), then concentrated using a rotary evaporator to give **5.13** (4.05 g, 12.2 mmol, 96.7 %).  $^1\text{H}$  NMR (400 MHz,  $\text{D}_2\text{O}$ )  $\delta$  4.36 (dd,  $J = 8.0$  Hz, 1H), 3.8 (d,  $J = 6.0$  Hz, 1H), 3.63 (s, 3H), 3.17 (m, 2H), 2.15 (quin,  $J = 6.4$  Hz, 1H), 1.80 (m, 1H), 1.71 (m, 1H), 1.58 (m, 2H), 0.94 (d,  $J = 6.8$  Hz, 6H);  $^{13}\text{C}$  NMR (100 MHz,  $\text{D}_2\text{O}$ )  $\delta$  173.5, 169.5, 158.7, 58.4, 53.1, 52.8, 40.6, 30.2, 27.6, 24.0, 17.6, 16.9. HRESIMS  $[\text{M} + \text{H}]^+$  calcd for  $\text{C}_{12}\text{H}_{25}\text{N}_6\text{O}_5$  333.1886, found 333.1884.

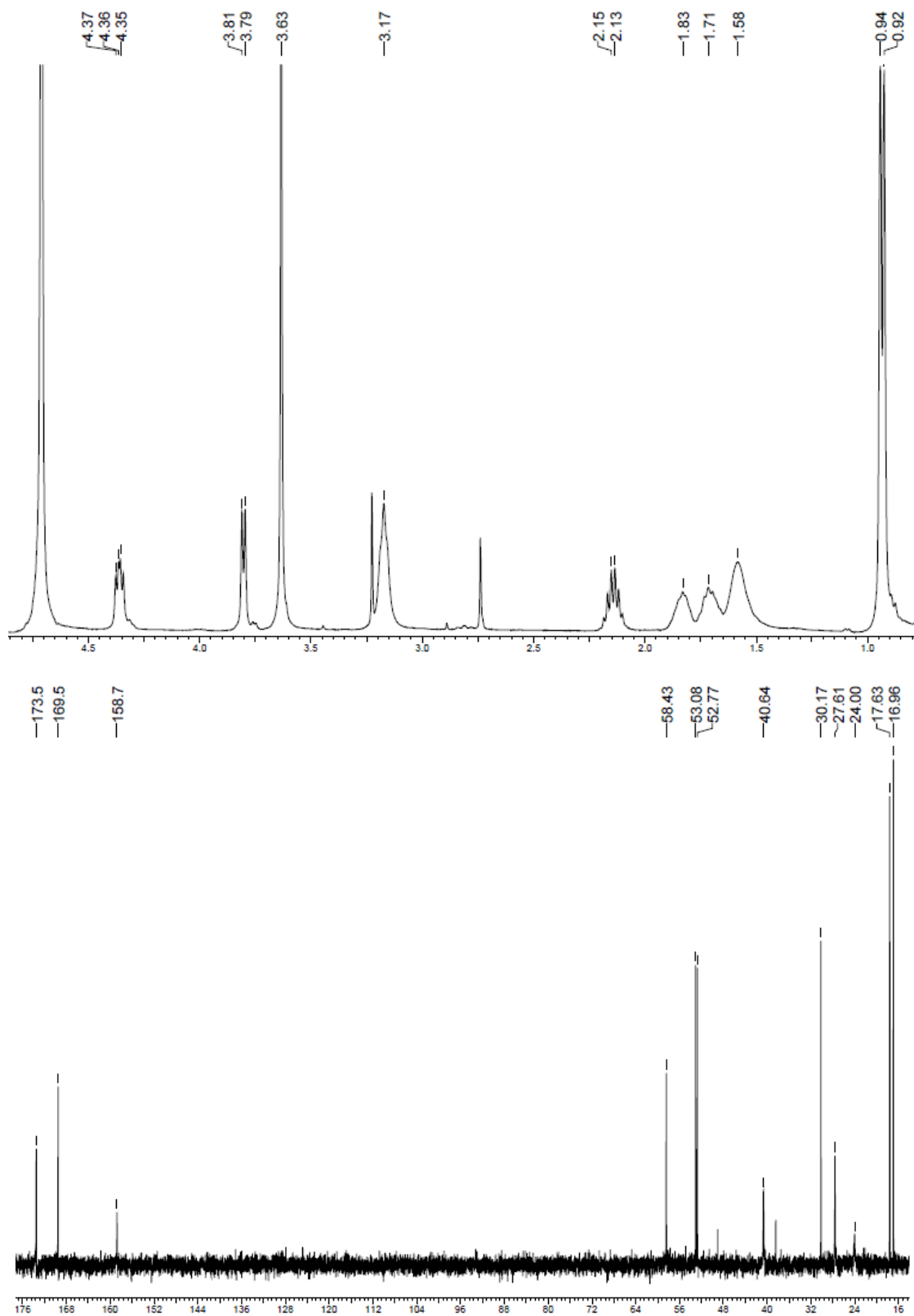
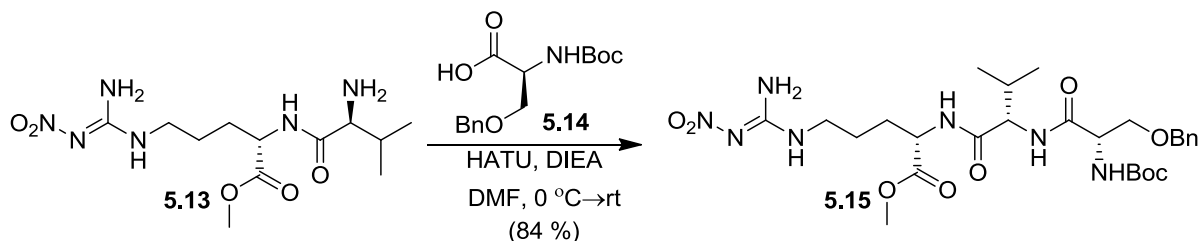


**Figure 5.6**  $^1\text{H}$  and  $^{13}\text{C}$  NMR spectra of **5.13** recorded in  $\text{D}_2\text{O}$  at 400 MHz and 100 MHz respectively.

### Preparation of 5.15:



To O-benzyl-Boc-L-serine **5.14** (888.6 mg, 3.0 mmol) and *N,N*-diisopropylethylamine (1.04 mL, 6.0 mmol) dissolved in 30 mL of *N,N*-dimethylformamide and cooled to 0 °C was added HATU (1.2 g, 3.15 mmol) followed by amine **5.13** (1.0 g, 3.0 mmol) and the reaction allowed to warm to room temperature overnight. The reaction mixture was diluted with methylene chloride (250 mL) and washed with saturated NaHCO<sub>3</sub> (150 mL) followed by brine (200 mL) and dried with MgSO<sub>4</sub> and concentrated using a rotary evaporator. The crude mixture was purified using flash column chromatography (methylene chloride:methanol 96:4) to give **5.15** (1.54 g, 2.53 mmol, 84.3 %). <sup>1</sup>H NMR (600 MHz, (CD<sub>3</sub>)<sub>2</sub>SO) δ 8.47 (bs, 1H), 8.39 (d, J = 7.2 Hz, 1H), 7.66 (d, J = 8.4 Hz, 1H), 7.28 (m, 5H), 7.24 (m, 1H), 7.09 (d, J = 9.0 Hz, 1H), 4.4 (s, 2H), 4.23 (t, J = 6.6 Hz, 2H), 4.17 (q, J = 7.8 Hz, 1H), 3.58 (s, 3H), 3.54 (m, 1H), 3.31 (s, 2H), 3.09 (m, 2H), 1.92 (quin, J = 7.2 Hz, 1H), 1.69 (m, 1H), 1.58 (m, 1H), 1.47 (m, 2H), 1.36 (s, 9H), 0.84 (d, J = 6.6 Hz, 3H), 0.80 (d, J = 6.6 Hz, 3H); <sup>13</sup>C NMR (150 MHz, CD<sub>2</sub>Cl<sub>2</sub>) δ 171.6, 171.4, 170.5, 158.9, 155.8, 137.2, 127.9, 127.3, 127.2, 79.9, 72.9, 69.3, 58.2, 54.5, 51.8, 50.9, 40.1, 30.4, 28.6, 27.6, 24.0, 18.5, 17.3. HRESIMS [M + Na]<sup>+</sup> calcd for C<sub>27</sub>H<sub>43</sub>N<sub>7</sub>O<sub>9</sub>Na 632.3020, found 632.3016.

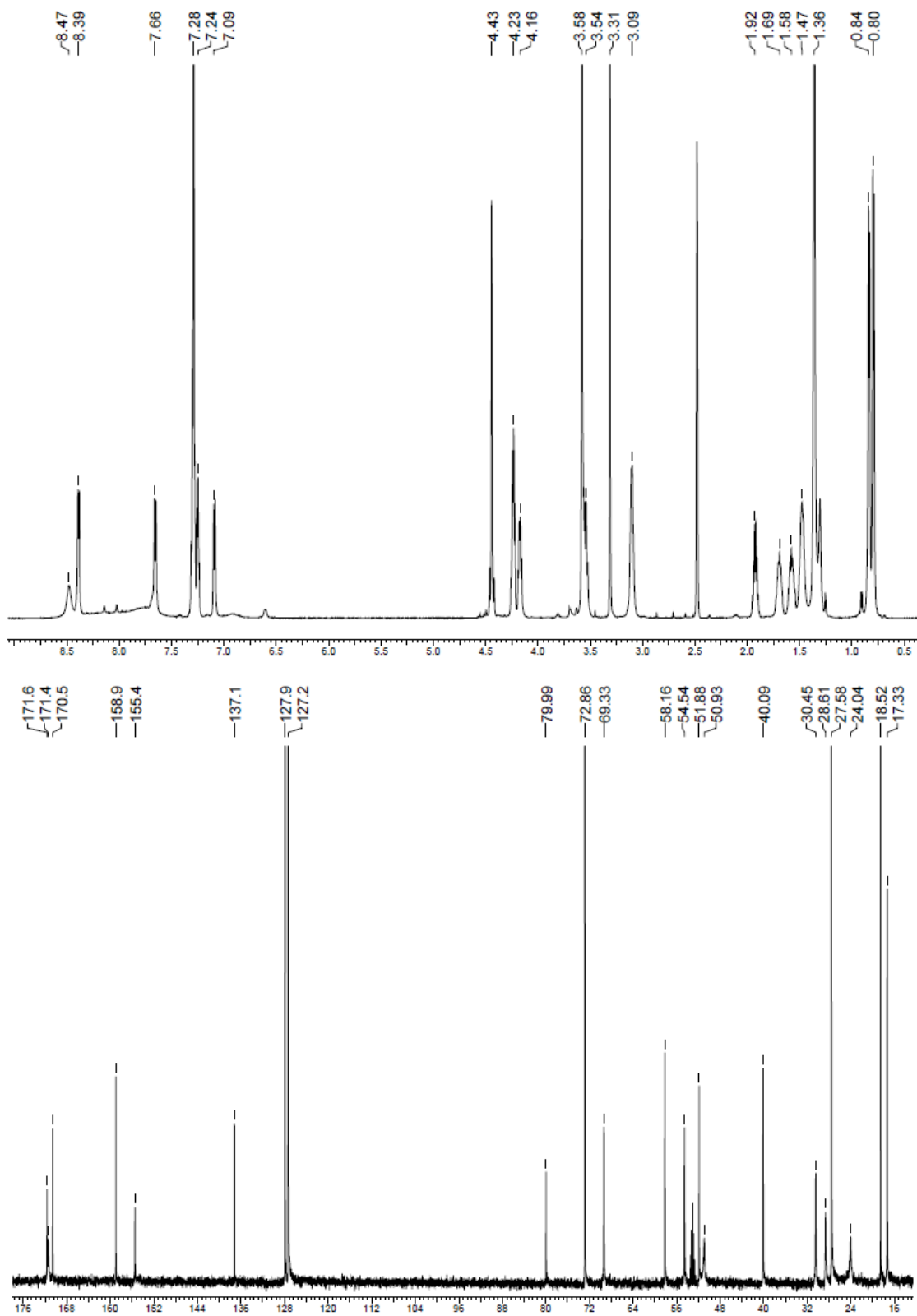
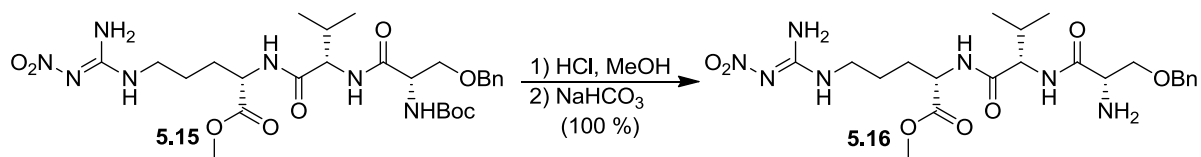


**Figure 5.7**  $^1\text{H}$  and  $^{13}\text{C}$  NMR spectra of **5.15** recorded in  $(\text{CD}_3)_2\text{SO}$  at 600 MHz and  $\text{CD}_2\text{Cl}_2$  at 150 MHz respectively.

### Preparation of 5.16:



To **5.15** (232.5 mg, 0.38 mmol) dissolved in 4 mL of methanol was added 12.4 M HCl (0.5 mL, 6.2 mmol) and the mixture allowed to stir at room temperature overnight. The reaction was then diluted with water (100 mL) and extracted three times with methylene chloride (200 mL), and the organic layers were discarded. To the acidic aqueous extract was added enough NaHCO<sub>3</sub> to basify and was extracted three times with methylene chloride (250 mL), dried with MgSO<sub>4</sub> and concentrated using a rotary evaporator to give **5.16** (193.4, 0.38 mmol, 100 %, yield includes small impurity). <sup>1</sup>H NMR (600 MHz, (CD<sub>3</sub>)<sub>2</sub>SO) δ 8.48 (bs, 1H), 8.44 (d, J = 6.6 Hz, 1H), 8.05 (d, J = 8.4 Hz, 1H), 7.29 (m, 5H), 7.25 (m, 1H), 4.45 (s, 2H), 4.23 (t, J = 7.2 Hz, 1H), 4.19 (q, J = 6.0 Hz, 1H), 3.58 (s, 3H), 3.52 (m, 2H), 3.41 (m, 1H), 3.1 (m, 2H), 2.86 (s, 1H), 2.70 (s, 1H), 2.2 (bs, 1H), 1.92 (quin, J = 6.6 Hz, 1H), 1.69 (m, 1H), 1.58 (m, 1H), 1.48 (m, 2H), 0.84 (d, J = 6.6 Hz, 3H), 0.78 (d, J = 6.6 Hz, 3H); <sup>13</sup>C NMR (150 MHz, (CD<sub>3</sub>)<sub>2</sub>SO) δ 172.2, 171.0, 171.0, 162.3, 138.3, 128.2, 127.4, 127.3, 72.5, 72.1, 56.5, 54.6, 51.8, 51.7, 40.1, 31.4, 27.8, 24.7, 19.0, 17.7. HRESIMS [M + H]<sup>+</sup> calcd for C<sub>22</sub>H<sub>36</sub>N<sub>7</sub>O<sub>7</sub> 510.2676, found 510.2675.

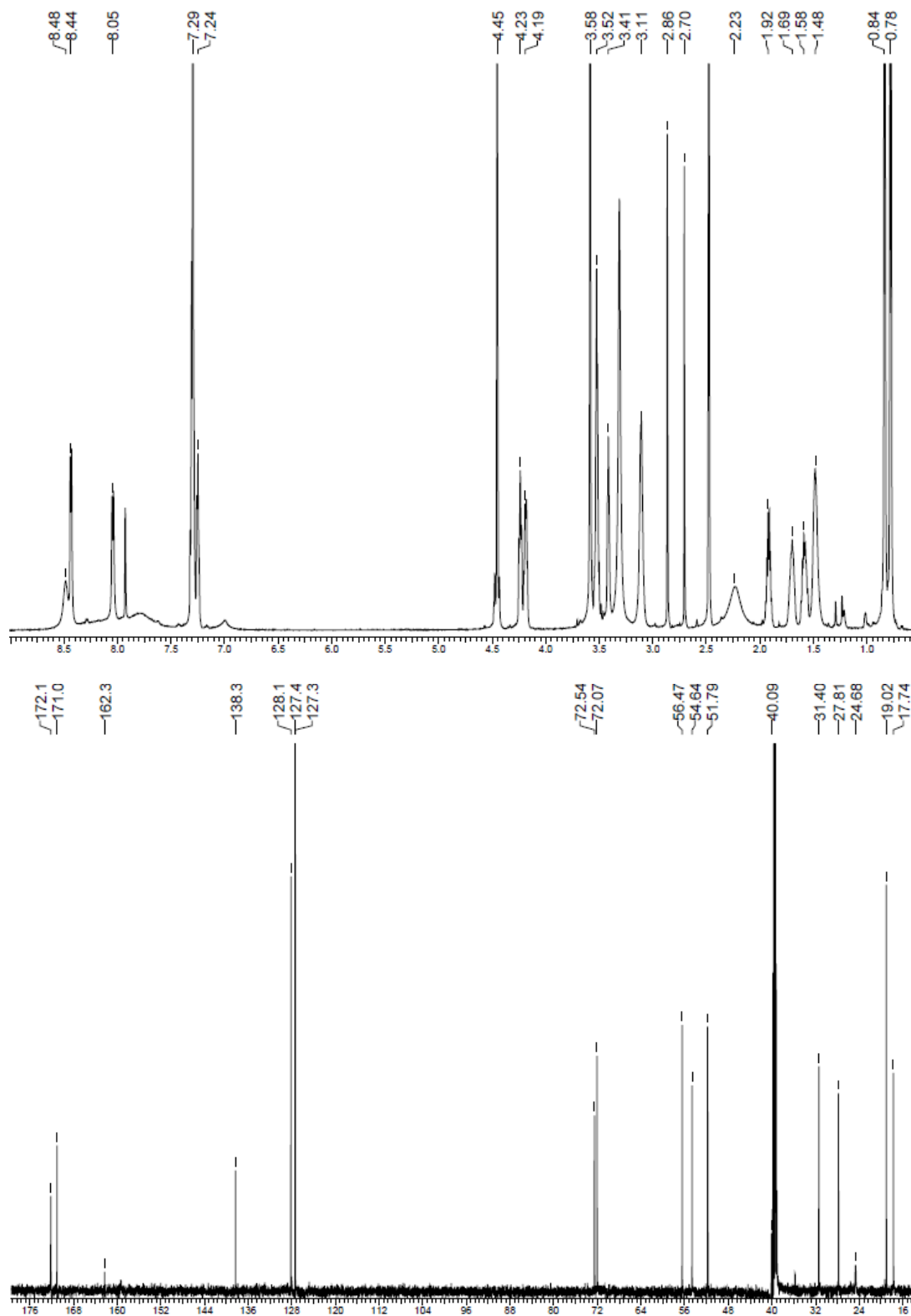
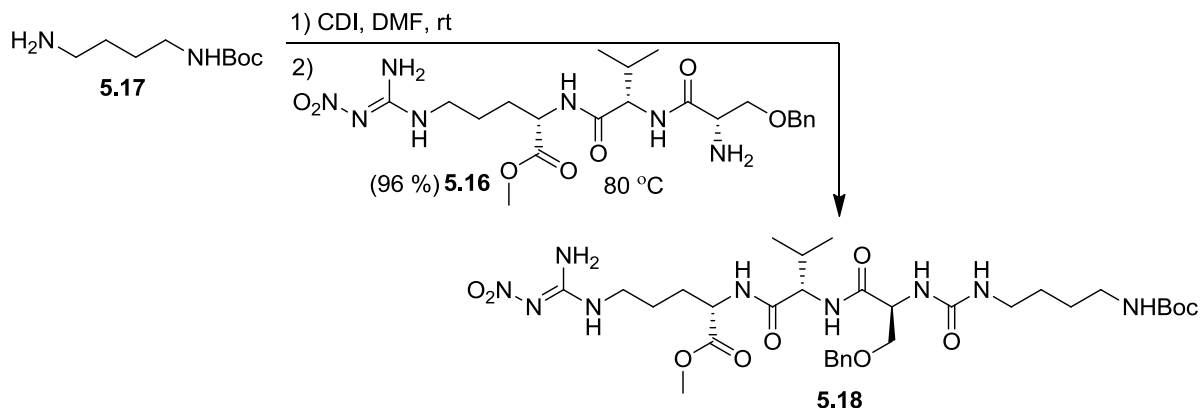


**Figure 5.8**  $^1\text{H}$  and  $^{13}\text{C}$  NMR spectra of **5.16** recorded in  $(\text{CD}_3)_2\text{SO}$  at 600 MHz and 150 MHz respectively.

### Preparation of 5.18:



Mono Boc protected putrescine freebase **5.17** (340.9 mg, 1.81 mmol) and CDI (293.4 mg, 1.81 mmol) dissolved in 8 mL of *N,N*-dimethylformamide were allowed to stir at room temperature for ten hours, after which amine **5.16** (307.4 mg, 0.60 mmol) dissolved in 3.0 L of *N,N*-dimethylformamide was added and the mixture allowed to stir overnight at room temperature. TLC indicated the presence of starting material so the mixture was heated at 80 °C overnight, after which the reaction was allowed to cool and the mixture evaporated using a lyophilizer. The crude mixture was purified using flash column chromatography (methylene chloride:methanol 96:4) to give **5.18** (416.2 mg, 0.57 mmol, 95.8 %). <sup>1</sup>H NMR (600 MHz, (CD<sub>3</sub>)<sub>2</sub>SO) δ 8.49 (bs, 1H), 8.38 (d, J = 7.2 Hz, 1H), 7.71 (d, J = 8.4 Hz, 1H), 7.29 (m, 5H), 6.77 (t, J = 4.8 Hz, 1H), 6.24 (t, J = 4.8 Hz, 1H), 6.20 (d, J = 8.4 Hz, 1H), 4.45 (m, 2H), 4.39 (m, 1H), 4.25 (t, J = 9.0 Hz, 1H), 4.19 (q, J = 7.8 Hz, 1H), 3.65 (dd, J = 9.6, 4.8 Hz, 1H), 3.59 (s, 3H), 3.51 (dd, J = 9.6, 4.8 Hz, 1H), 3.33 (s, 3H), 3.11 (m, 2H), 2.96 (m, 2H), 2.89 (m, 2H), 1.96 (quin, J = 6.6 Hz, 1H), 1.70 (m, 1H), 1.59 (m, 1H), 1.49 (m, 2H), 1.36 (s, 9H), 1.32 (bs, 3H), 0.87 (dd, J = 6.6 Hz, 3H), 0.82 (dd, J = 6.6 Hz, 3H); <sup>13</sup>C NMR (150 MHz, (CD<sub>3</sub>)<sub>2</sub>SO) δ 172.9, 171.8, 171.3, 160.1, 158.3, 156.4, 139.0, 128.9, 128.2, 128.1, 78.1, 72.9,

71.6, 57.8, 53.9, 52.6, 52.6, 40.9, 39.8, 31.9, 29.1, 28.6, 28.2, 28.2, 27.8, 25.4, 19.8, 18.6.

HRESIMS  $[M + Na]^+$  calcd for  $C_{32}H_{53}N_9O_{10}Na$  746.3812, found 746.3822.

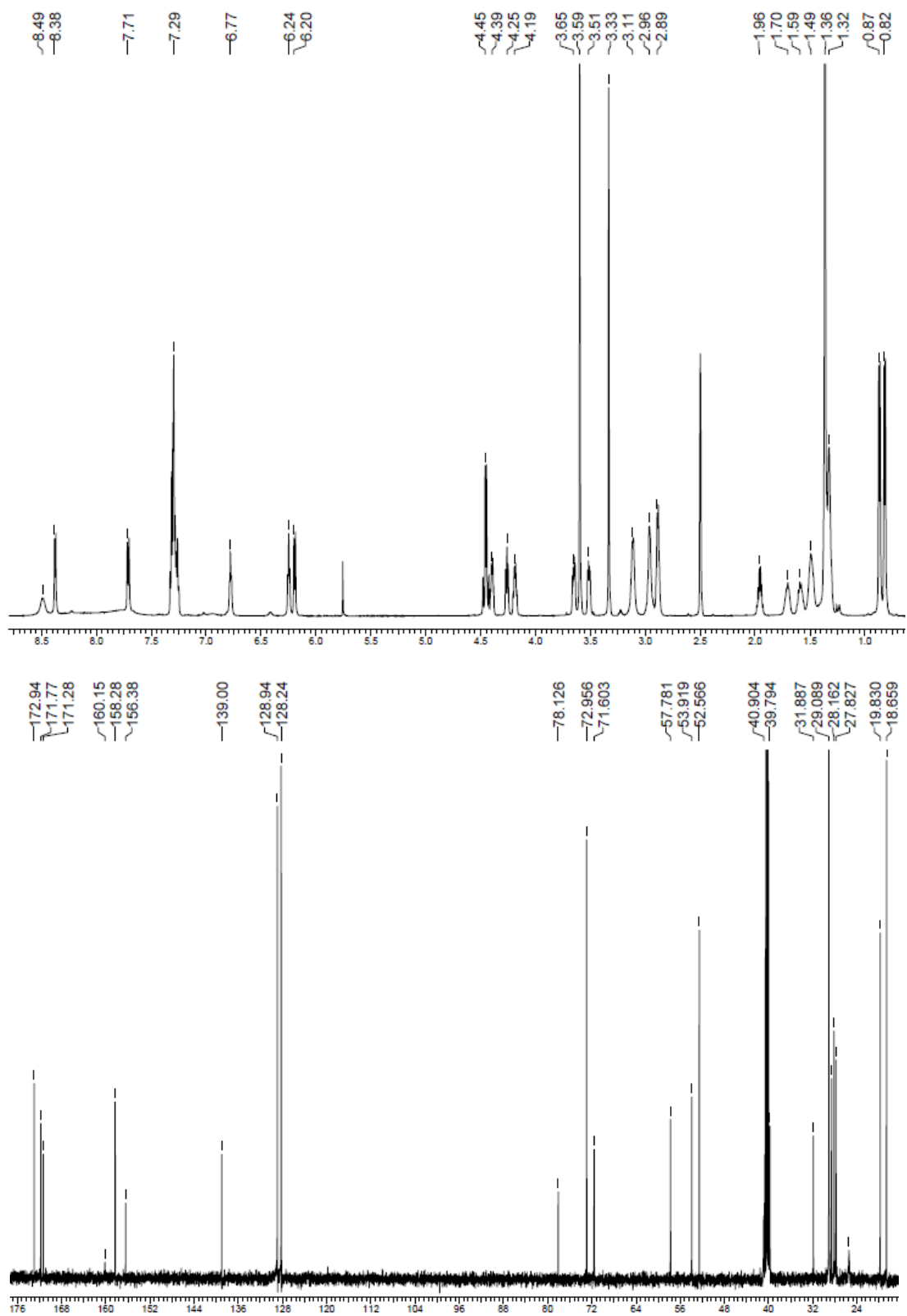
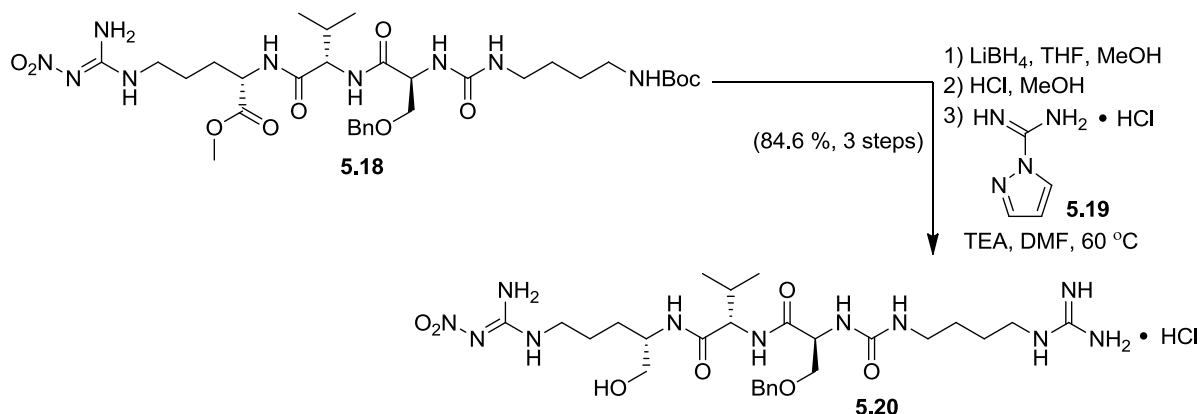


**Figure 5.9**  $^1\text{H}$  and  $^{13}\text{C}$  NMR spectra of **5.18** recorded in  $(\text{CD}_3)_2\text{SO}$  at 600 MHz and 150 MHz respectively.

### Preparation of 5.20:



To **5.18** (102.6 mg, 0.14 mmol) reduced in a similar fashion to **5.36**, was filtered through a plug of silica (methylene chloride:methanol 9:1) and used in the subsequent reaction without further purification, by dissolving it in 5 mL of methanol and addition of a 12.4 M solution of HCl (0.35 mL, 4.3 mmol) and allowing the mixture to stir at room temperature overnight. The mixture was concentrated under a stream of nitrogen and evaporated using a lyophilizer overnight. To this crude mixture dissolved in 1.5 mL of *N,N*-dimethylformamide was added triethylamine (0.041 mL, 0.30 mmol) and guanylyating reagent **5.19** (22.0 mg, 0.15 mmol) and heated to at 60 °C overnight, acidified with 1 M HCl, then concentrated using a lyophilizer. The crude mixture was purified using a 5 g  $\text{C}_{18}$  sep pak (water:methanol, 100 %, 9:1, 3:1, 3:2, 100% methanol) to give **5.20** (80.9 mg, 0.12 mmol, 84.6 %).  $^1\text{H}$  NMR (600 MHz,  $(\text{CD}_3)_2\text{SO}$ )  $\delta$  8.45 (bs, 1H), 7.79 (m, 1H), 7.74 (d,  $J = 9.0$  Hz, 1H), 7.42 (bs, 1H), 7.27 (m, 5H), 6.98 (bs, 1H), 5.22 (bs, 5H), 4.42 (m, 2H), 4.34 (t,  $J = 4.2$  Hz, 1H), 4.10 (t,  $J = 7.8$  Hz, 1H), 3.62 (m, 2H), 3.49 (dd,  $J = 9.0, 3.6$ , Hz, 1H), 3.29 (dd,  $J = 10.8, 4.8$  Hz, 1H), 3.18 (dd,  $J = 9.6, 6.0$  Hz, 1H), 3.06 (m, 4H), 2.96 (m, 2H), 1.92 (quin,  $J = 6.6$  Hz, 1H), 1.52 (m, 2H), 1.41 (m, 3H), 1.36 (m, 4H), 1.21 (bs, 1H), 0.80 (dd,  $J = 6.6$  Hz, 3H), 0.77 (dd,  $J = 6.6$  Hz, 3H);  $^{13}\text{C}$  NMR (150 MHz,  $(\text{CD}_3)_2\text{SO}$ )  $\delta$  170.6, 170.5, 138.1, 128.1,

127.5, 127.4, 72.2, 70.6, 63.1, 57.8, 53.3, 50.3, 40.6, 40.4, 38.6, 30.7, 27.8, 27.8, 27.1, 27.1,  
25.9, 25.9, 24.7, 19.1, 18.0. HRESIMS  $[M + H]^+$  calcd for  $C_{27}H_{48}N_{11}O_7$  638.3738, found  
638.3736.

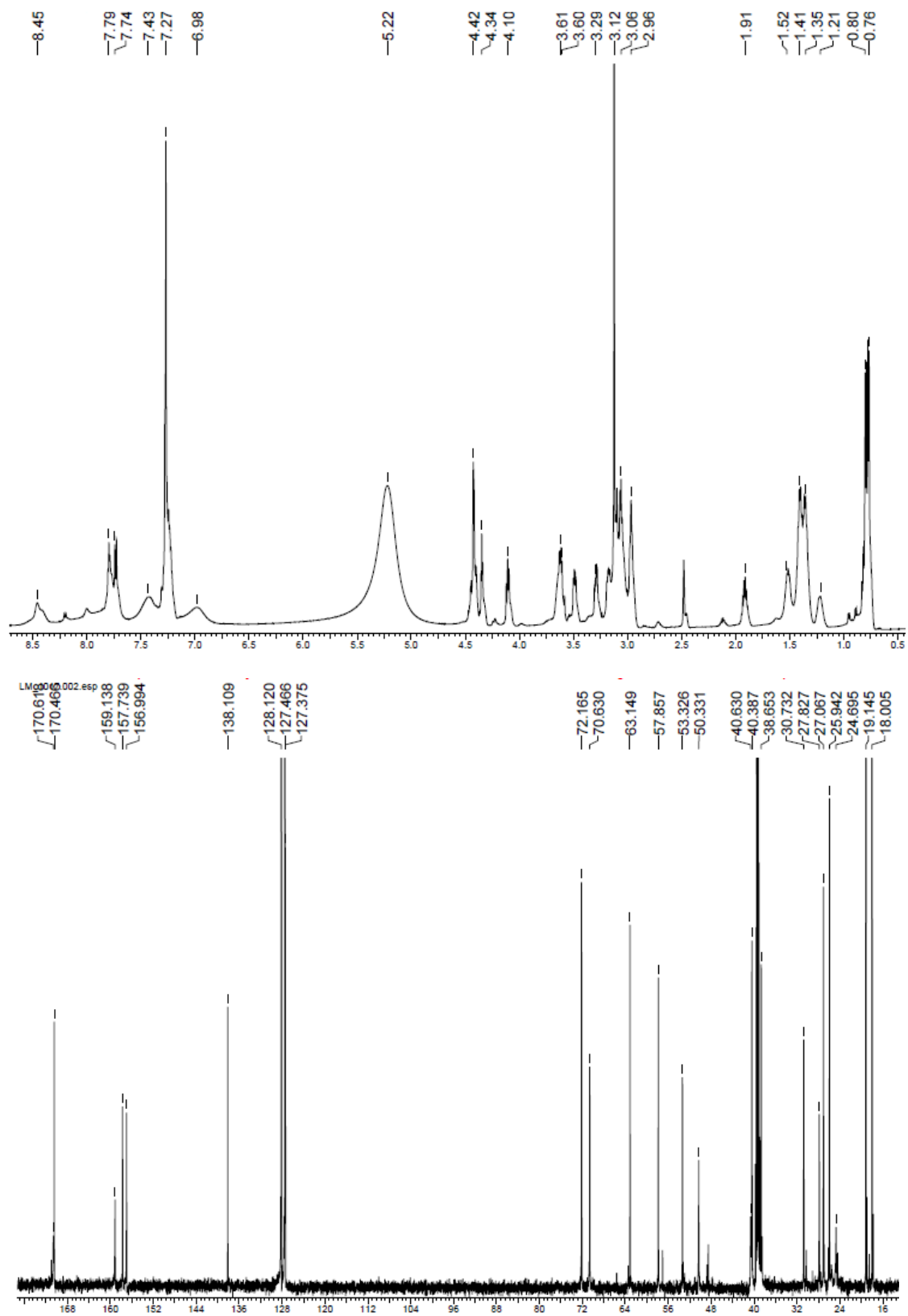
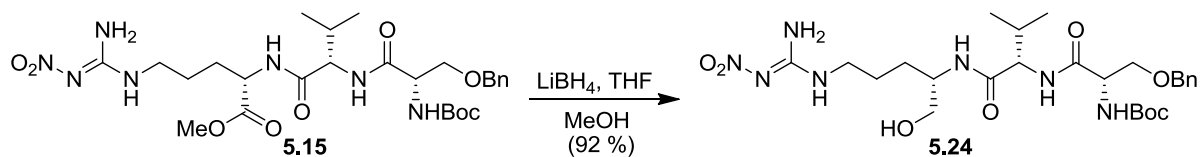


**Figure 5.10**  $^1\text{H}$  and  $^{13}\text{C}$  NMR spectra of **5.20** recorded in  $(\text{CD}_3)_2\text{SO}$  at 600 MHz and 150 MHz respectively.

### Preparation of 5.24:



To **5.15** (356.5 mg, 0.58 mmol) dissolved in 5 mL of tetrahydrofuran and 0.22 mL of methanol was added  $\text{LiBH}_4$  (44.5 mg, 2.0 mmol) dissolved in 10 mL of tetrahydrofuran and the reaction allowed to stir at room temperature for two hours after which the reaction was diluted with water (100 mL) and extracted three times with methylene chloride (250 mL), dried with  $\text{MgSO}_4$  and concentrated using a rotary evaporator. The crude mixture was purified using flash column chromatography (methylene chloride:methanol 10:0.5) to give **5.24** (313.6 mg, 0.54 mmol, 92.5 %).  $^1\text{H}$  NMR (600 MHz,  $(\text{CD}_3)_2\text{SO}$ )  $\delta$  8.47 (bs, 1H), 7.71 (m, 1H), 7.66 (d,  $J = 7.8$  Hz, 1H), 7.29 (m, 5H), 7.24 (m, 1H), 7.10 (d,  $J = 7.2$  Hz, 1H), 4.64, (m, 1H), 4.44 (s, 2H), 4.23 (m, 1H), 4.13 (t,  $J = 6.6$  Hz, 1H), 3.67 (m, 1H), 3.56 (m, 2H), 3.32 (m, 2H), 3.19 (t,  $J = 4.8$  Hz, 1H), 3.11 (m, 1H), 3.06 (t,  $J = 5.4$  Hz, 1H), 1.90 (quin,  $J = 6.0$  Hz, 1H), 1.54 (m, 1H), 1.44 (m, 1H), 1.36 (s, 9H), 1.30 (bs, 1H), 1.24 (m, 1H), 0.81 (d,  $J = 6.0$  Hz, 3H), 0.79 (d,  $J = 6.0$  Hz, 3H);  $^{13}\text{C}$  NMR (150 MHz,  $(\text{CD}_3)_2\text{SO}$ )  $\delta$  170.4, 169.6, 159.3, 155.3, 138.2, 128.1, 127.5, 127.4, 78.4, 71.9, 69.8, 63.2, 57.5, 54.5, 50.4, 40.6, 30.9, 28.1, 27.9, 24.8, 19.1, 17.9. HRESIMS  $[\text{M} + \text{Na}]^+$  calcd for  $\text{C}_{26}\text{H}_{43}\text{N}_7\text{O}_8\text{Na}$  604.3071, found 604.3063.

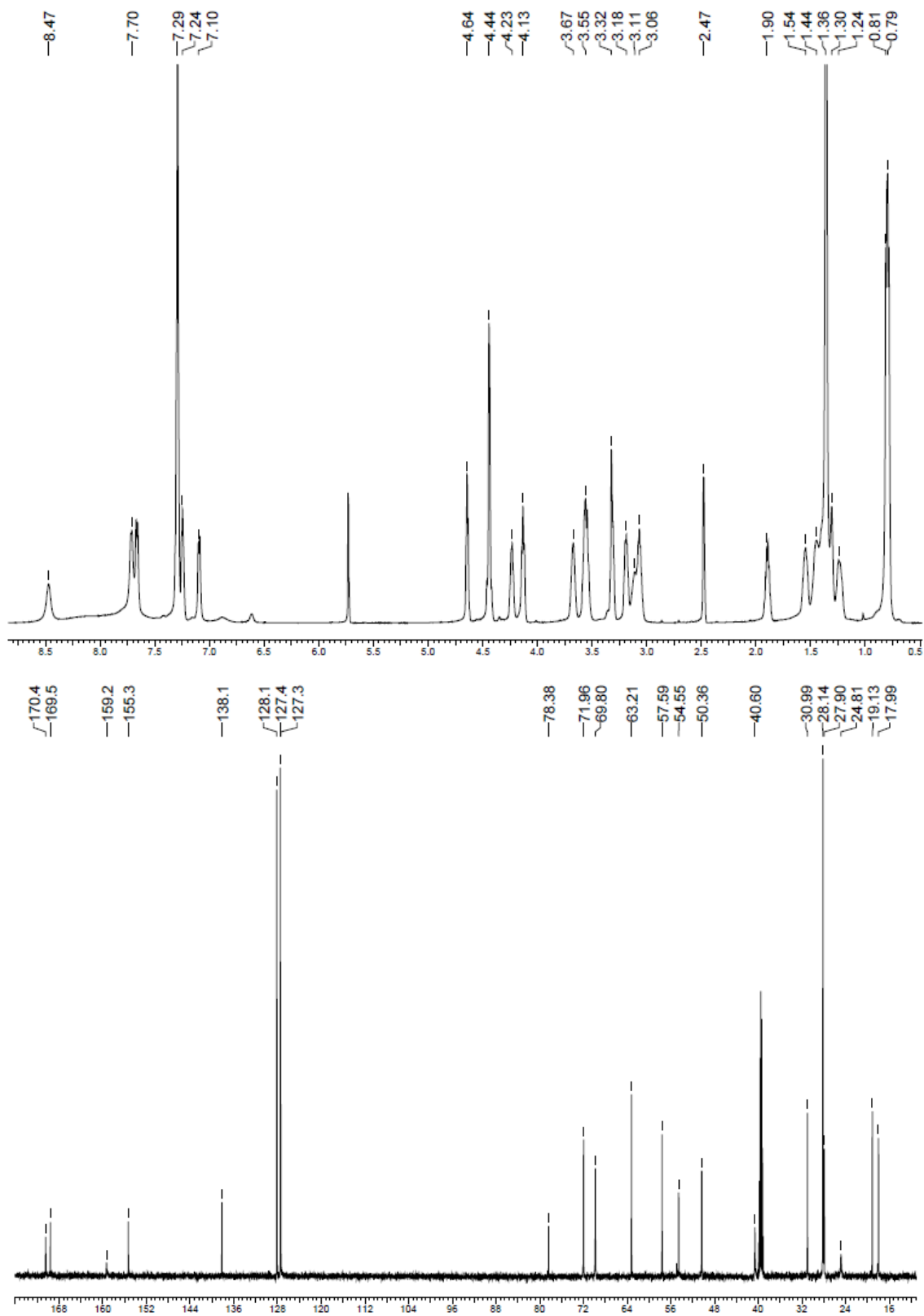
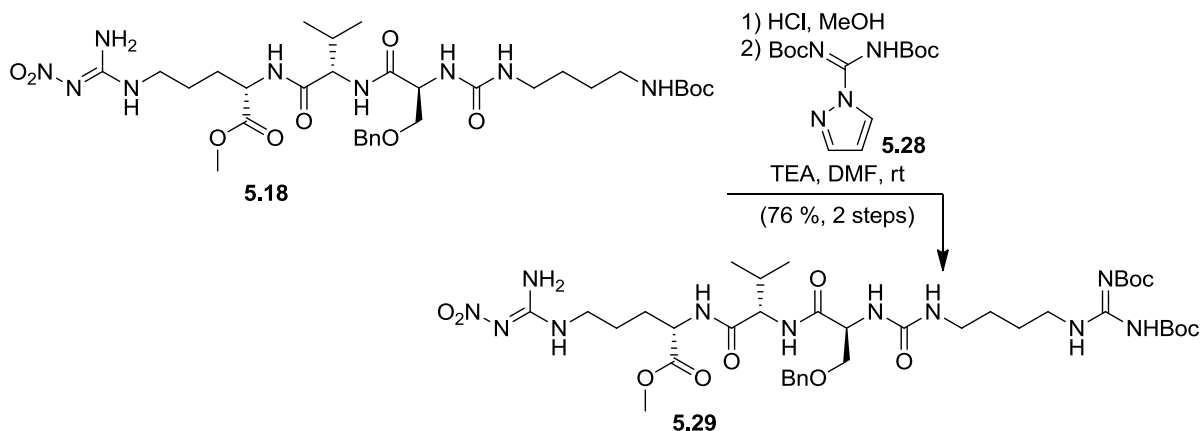


**Figure 5.11**  $^1\text{H}$  and  $^{13}\text{C}$  NMR spectra of **5.24** recorded in  $(\text{CD}_3)_2\text{SO}$  at 600 MHz and 150 MHz respectively.

### Preparation of 5.29:



To **5.18** (45.7 mg, 0.064mmol) deprotected in a similar fashion to **5.15** was dissolved in 2 mL of *N,N*-dimethylformamide was added triethylamine (0.01 mL, 0.074 mmol) followed by Boc protected guanylyating reagent **5.28** (20.9 mg, 0.067 mmol). The reaction mixture was allowed to stir at room temperature for 48 hours, after which the solvent was evaporated on a lyophilizer and the crude mixture purified using flash column chromatography (methylene chloride:methanol 5:1) to give **5.29** (37.3 mg, 0.048 mmol, 76 %).  $^1\text{H}$  NMR (600 MHz,  $\text{CD}_2\text{Cl}_2$ )  $\delta$  11.42 (s, 1H), 8.45 (s, 1H), 7.29 (m, 5H), 7.14 (s, 2H), 6.37 (s, 1H), 6.00 (s, 1H), 4.5 (m, 3H), 4.43 (s, 1H), 4.27 (t,  $J = 7.8$  Hz, 1H), 3.91 (s, 1H), 3.71 (s, 3H), 3.69 (dd,  $J = 9.6, 4.2$  Hz, 1H), 3.35 (m, 3H), 3.22 (m, 3H), 2.07 (s, 1H), 1.90 (m, 1H), 1.68 (s, 2H), 1.61 (m, 3H), 1.51 (m, 7H), 1.51 (s, 9H), 1.46 (s, 9H), 0.93 (d,  $J = 6.6$  Hz, 3H), 0.88 (d,  $J = 6.6$  Hz, 3H);  $^{13}\text{C}$  NMR (100 MHz,  $\text{CD}_2\text{Cl}_2$ )  $\delta$  172.2, 172.0, 172.0, 163.4, 162.5, 159.7, 158.8, 156.3, 153.2, 149.5, 137.9, 128.4, 127.8, 83.2, 79.2, 73.4, 70.4, 59.0, 55.0, 52.3, 51.4, 40.6, 40.2, 36.3, 31.2, 30.4, 29.1, 28.1, 27.9, 27.8, 26.8, 19.1, 18.0. HRESIMS  $[\text{M} + \text{H}]^+$  calcd for  $\text{C}_{38}\text{H}_{63}\text{N}_{11}\text{O}_{12}$  866.4736, found 866.4734.

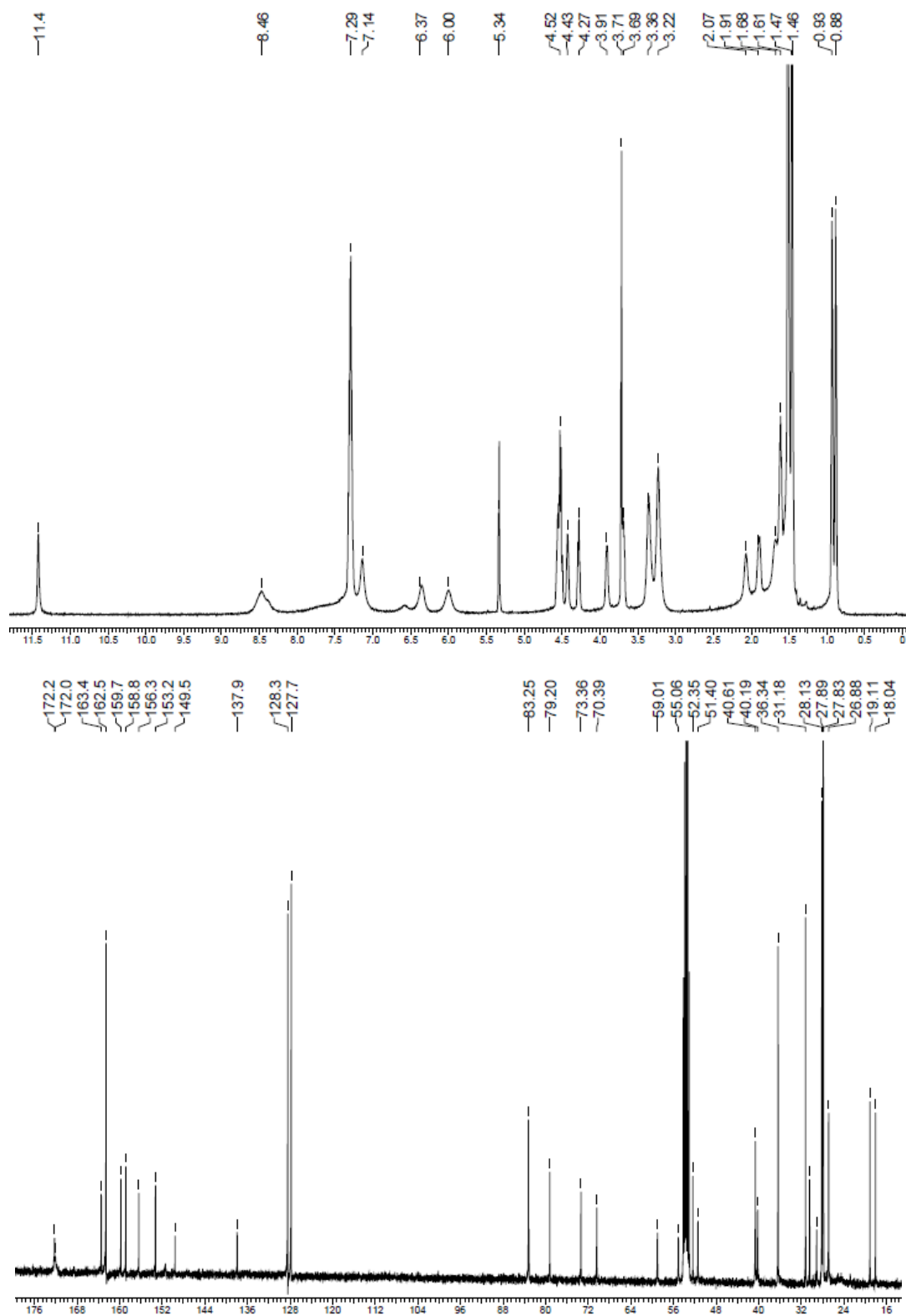
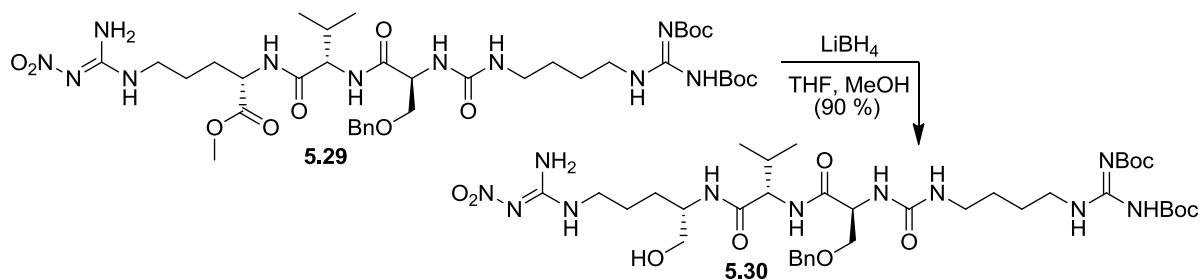


**Figure 5.12**  $^1\text{H}$  and  $^{13}\text{C}$  NMR spectra of **5.29** recorded in  $\text{CD}_2\text{Cl}_2$  at 600 MHz and 100 MHz respectively.

### Preparation of 5.30:



To **5.29** (42.8 mg, 0.049 mmol) dissolved in 1 mL of tetrahydrofuran was added 18  $\mu\text{L}$  methanol and the mixture cooled to 0  $^\circ\text{C}$ . To this was added  $\text{LiBH}_4$  (3.7 mg, 0.017 mmol) dissolved in 3 mL of tetrahydrofuran, and the reaction mixture allowed to stir for two hours. The reaction mixture was quenched with the addition of water (20 mL), and concentrated using a lyophilizer. The crude material was purified using flash column chromatography (methylene chloride:methanol 20:1) to give **5.30** (37.3 mg, 0.044 mmol, 89.7 %).  $^1\text{H}$  NMR (600 MHz,  $(\text{CD}_3)_2\text{CO}$ )  $\delta$  11.6 (s, 1H), 8.32 (s, 1H), 7.38 (d,  $J = 8.4$  Hz, 1H), 7.32 (m, 5H), 7.25 (t,  $J = 6.6$  Hz, 1H), 6.30 (t,  $J = 4.8$  Hz, 2H), 4.52 (m, 2H), 4.40 (m, 1H), 4.21 (t,  $J = 6.6$  Hz, 1H), 4.01 (s, 1H), 3.97 (s, 1H), 3.88 (dd,  $J = 9.0, 4.2$  Hz, 1H), 3.70 (dd,  $J = 9.6, 3.6$  Hz, 1H), 3.53 (s, 2H), 3.39 (quin,  $J = 6.0$  Hz, 2H), 3.22 (m, 3H), 2.85 (m, 2H), 2.14 (s, 1H), 1.61 (m, 6H), 1.52 (m, 4H), 1.49 (s, 9H), 1.42 (s, 9H), 0.92 (d,  $J = 6.6$  Hz, 3H), 0.88 (d,  $J = 6.6$  Hz, 3H);  $^{13}\text{C}$  NMR (150 MHz,  $(\text{CD}_3)_2\text{CO}$ )  $\delta$  171.2, 170.9, 163.2, 159.5, 158.1, 155.6, 152.4, 137.7, 127.7, 127.1, 127.0, 82.3, 77.7, 72.3, 69.7, 63.9, 58.5, 54.5, 50.0, 40.3, 39.8, 39.1, 28.9, 28.8, 28.6, 28.5, 28.4, 28.2, 27.9, 27.1, 26.8, 26.7, 26.0, 18.5, 17.0. HRESIMS  $[\text{M} + \text{H}]^+$  calcd for  $\text{C}_{37}\text{H}_{64}\text{N}_{11}\text{O}_{11}$  838.4787, found 838.4791.

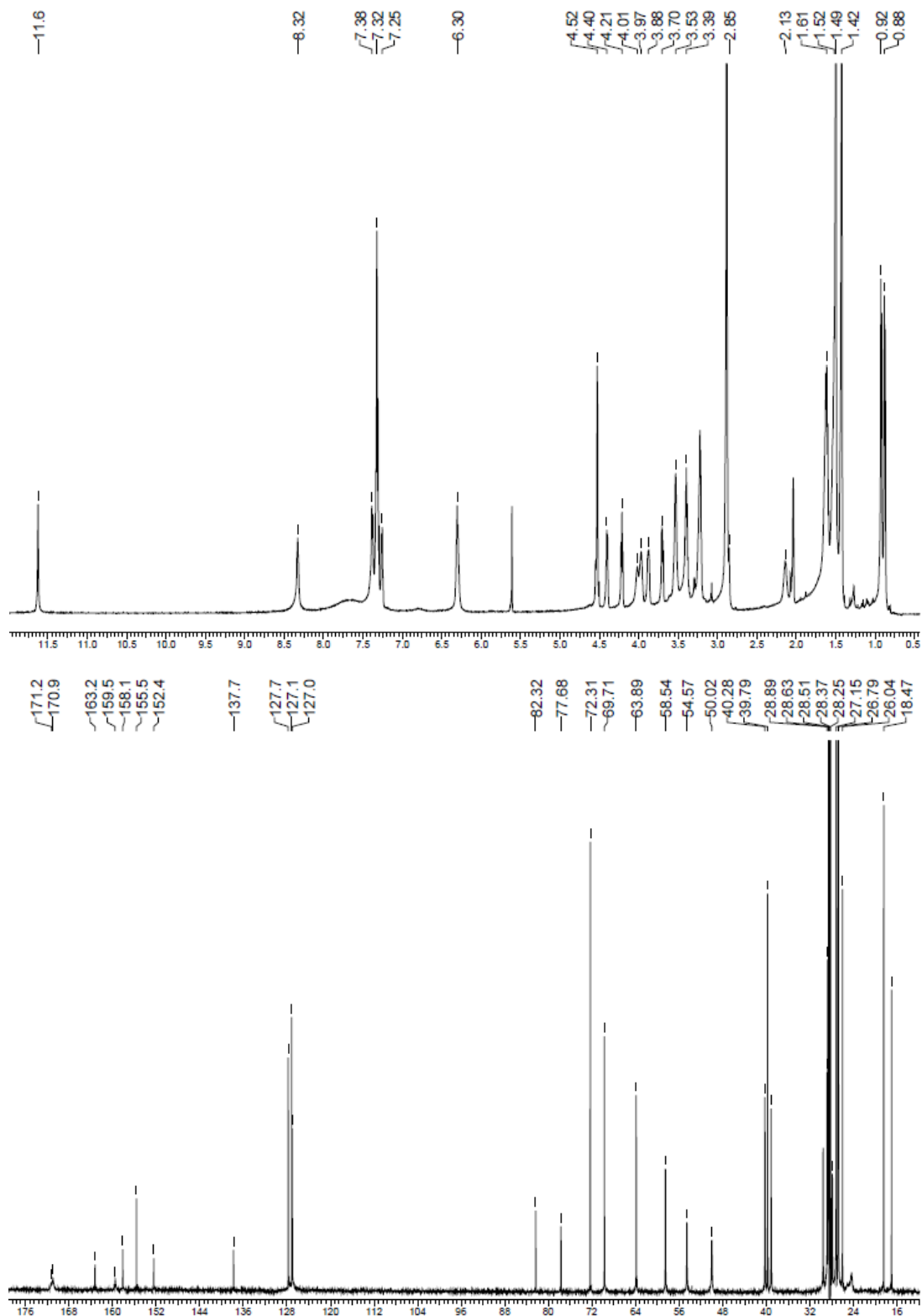
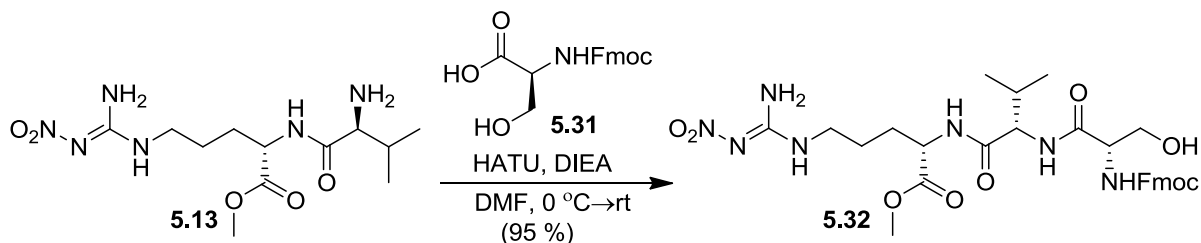


**Figure 5.13**  $^1\text{H}$  and  $^{13}\text{C}$  NMR spectra of **5.30** recorded in  $(\text{CD}_3)_2\text{SO}$  at 600 MHz and 150 MHz respectively.

### Preparation of 5.32:



To Fmoc-L-serine **5.31** (318.6 mg, 0.97 mmol) dissolved in 2 mL of *N,N*-dimethylformamide cooled to 0 °C was added HATU (388 mg, 1.02 mmol) and *N,N*-diisopropylethylamine (0.34 mL, 1.95 mmol) followed by **5.13** (323.4 mg, 0.97 mmol) dissolved in 2 mL of *N,N*-dimethylformamide and the mixture was allowed to warm to room temperature overnight. To the reaction was added saturated NaHCO<sub>3</sub> (100 mL) and the aqueous layer was washed three times with methylene chloride (250 mL). The organic extracts were combined and washed three times with brine and dried with MgSO<sub>4</sub> and concentrated using a rotary evaporator. The crude mixture was purified using flash column chromatography (methylene chloride:methanol 95:5) to give **5.32** (591.3 mg, 0.92 mmol, 94.8 %). <sup>1</sup>H NMR (600 MHz, (CD<sub>3</sub>)<sub>2</sub>SO) δ 8.49 (bs, 1H), 8.35 (d, J = 6.6 Hz, 1H), 7.87 (d, J = 7.2 Hz, 2H), 7.72 (t, J = 7.8 Hz, 3H), 7.41 (d, J = 4.2 Hz, 1H), 7.39 (d, J = 7.8 Hz, 2H), 7.30 (t, J = 7.2 Hz, 2H), 4.91 (t, J = 6.0 Hz, 1H), 4.27-4.13 (m, 7H), 3.58 (s, 3H), 3.56-3.51 (m, 2H), 3.12 (m, 2H), 2.0 (s, 1H), 1.97 (quin, J = 6.6 Hz, 1H), 1.70 (m, 1H), 1.60 (m, 1H), 1.50 (m, 2H), 0.86 (d, J = 7.2 Hz, 3H), 0.81 (d, J = 7.2 Hz, 3H); <sup>13</sup>C NMR (150 MHz, (CD<sub>3</sub>)<sub>2</sub>SO) δ 172.1, 171.1, 170.0, 159.3, 155.9, 143.8, 143.7, 140.7, 127.6, 127.1, 125.3, 125.2, 120.1, 65.7, 61.9, 57.1, 57.0, 54.9, 51.8, 51.7, 46.6, 40.1, 30.8, 27.8, 24.6, 19.0, 17.7. HRESIMS [M + H]<sup>+</sup> calcd for C<sub>30</sub>H<sub>40</sub>N<sub>7</sub>O<sub>9</sub> 642.2888, found 642.2829.

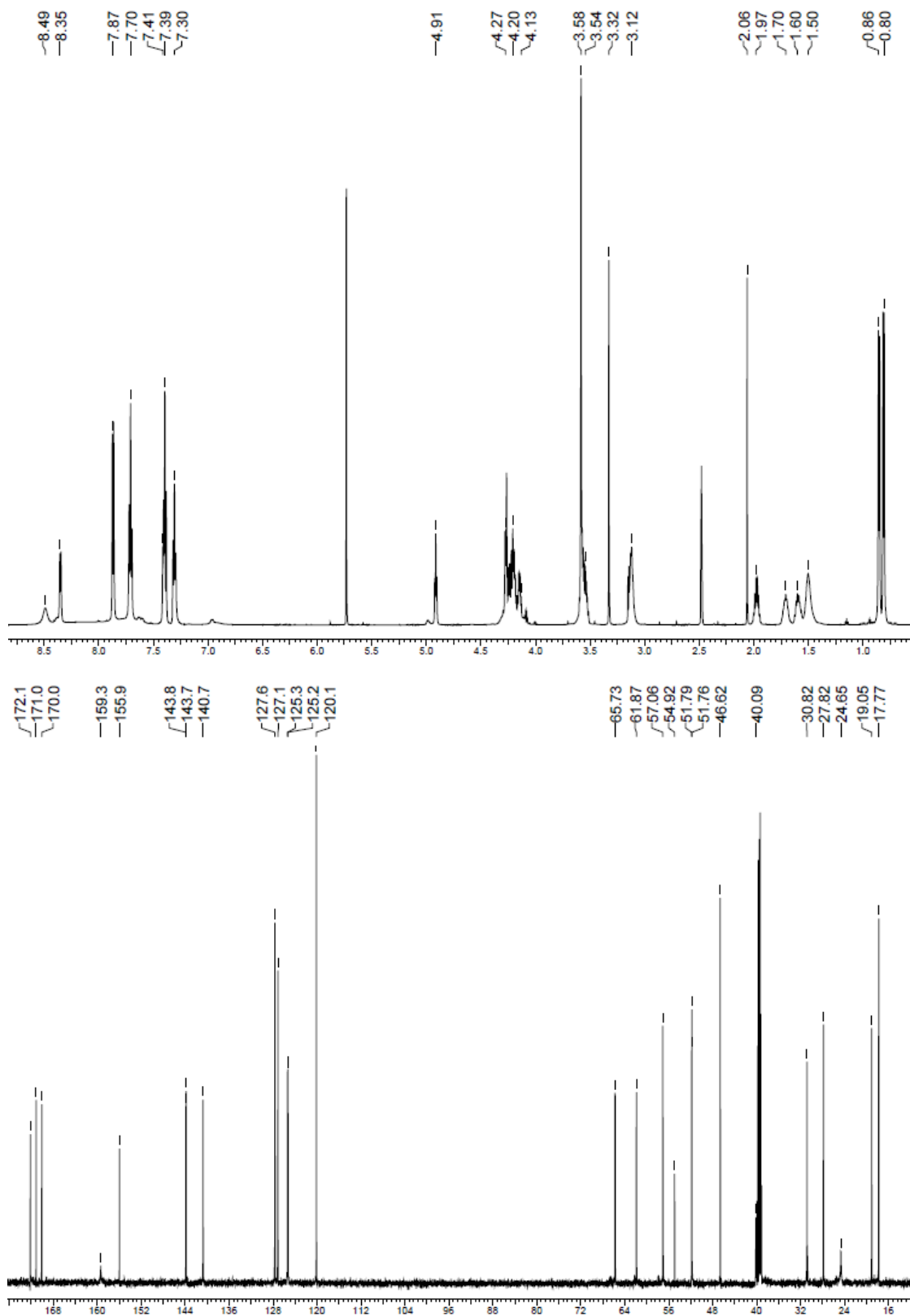
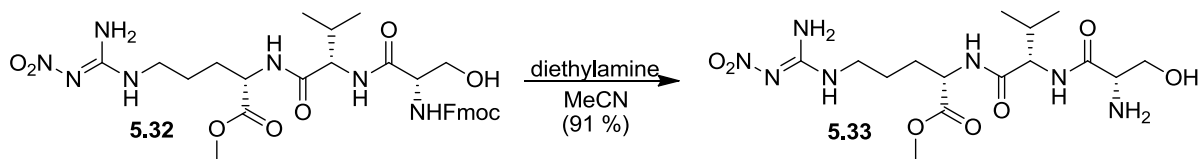


**Figure 5.14**  $^1\text{H}$  and  $^{13}\text{C}$  NMR spectra of **5.32** recorded in  $(\text{CD}_3)_2\text{SO}$  at 600 MHz and 150 MHz respectively.

### Preparation of 5.33:



**5.32** (591.3 mg, 0.92 mmol) was deprotected in a similar fashion to **5.12**. The crude freebase was purified using a 5 g  $\text{C}_{18}$  Sep-Pak (water:methanol 9:1) to give **5.33** (539.0 mg, 0.84 mmol, 91.3 %).  $^1\text{H}$  NMR (400 MHz,  $\text{D}_2\text{O}$ )  $\delta$  4.37 (dd,  $J = 8.4, 4.4$  Hz, 1H), 4.05 (m, 1H), 3.77-3.69 (m, 1H), 3.66 (m, 1H), 3.64 (s, 3H), 3.60 (q,  $J = 4.8$  Hz, 1H), 3.19 (t,  $J = 6.4$  Hz, 2H), 1.99 (sep,  $J = 6.8$  Hz, 1H), 1.83 (m, 1H), 1.70 (m, 1H), 1.58 (m, 2H), 0.86 (t,  $J = 6.8$  Hz, 6H);  $^{13}\text{C}$  NMR (100 MHz,  $(\text{CD}_3)_2\text{SO}$ )  $\delta$  172.7, 172.2, 171.1, 159.4, 64.1, 59.7, 56.4, 51.8, 51.7, 40.0, 31.3, 30.6, 27.8, 19.0, 17.7. HRESIMS  $[\text{M} + \text{H}]^+$  calcd for  $\text{C}_{15}\text{H}_{30}\text{N}_7\text{O}_7$  420.2207, found 420.2212.

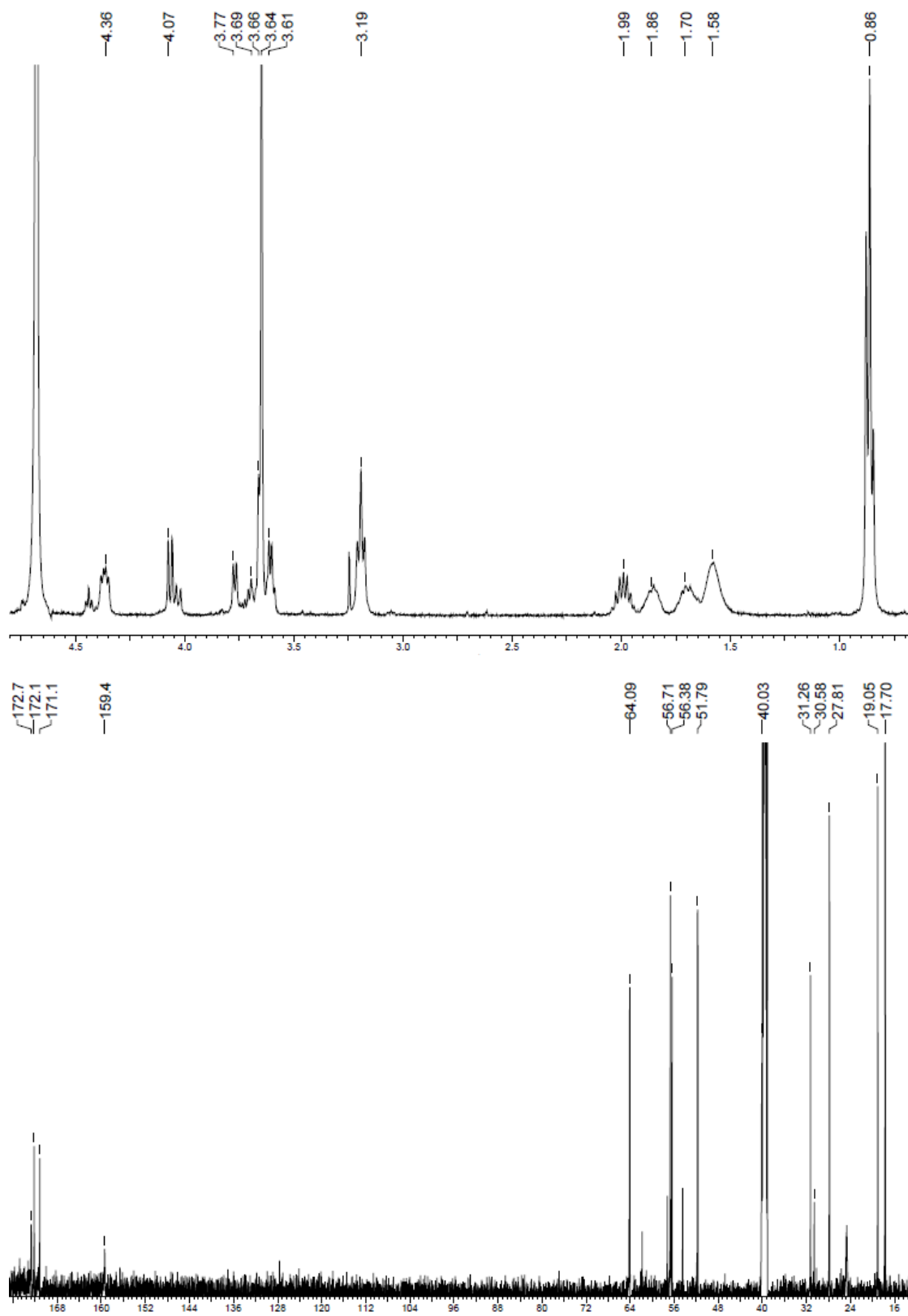
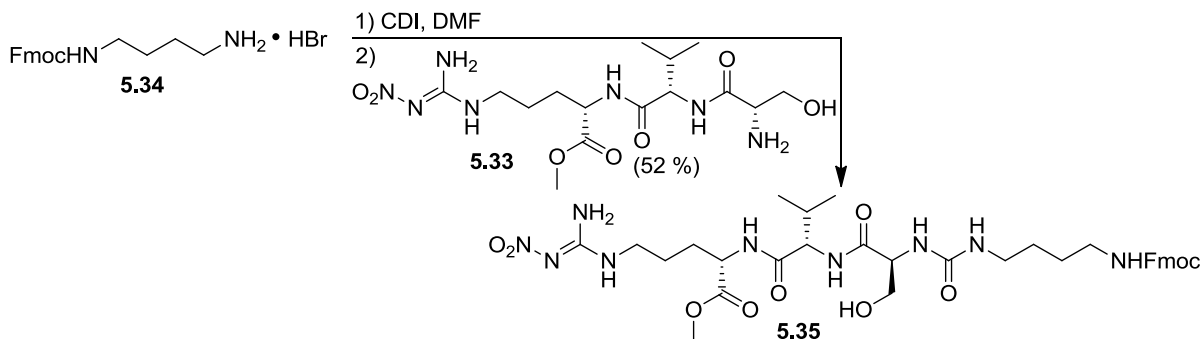


**Figure 5.15**  $^1\text{H}$  and  $^{13}\text{C}$  NMR spectra of **5.33** recorded in  $\text{D}_2\text{O}$  and  $(\text{CD}_3)_2\text{SO}$  at 400 MHz and 100 MHz respectively.

### Preparation of 5.35:



To the Fmoc protected putrescine HBr salt **5.34** (58.1 mg, 0.15 mmol) and CDI (28.1 mg, 0.18 mmol) dissolved in 1.25 mL of *N,N*-dimethylformamide was allowed to stir for three hours at room temperature, after which amine **5.33** (58.1 mg, 0.15 mmol) dissolved in 0.6 mL of *N,N*-dimethylformamide was added and the mixture was allowed to stir at room temperature overnight. The crude mixture was evaporated by a lyophilizer and purified using flash column chromatography (methylene chloride:methanol 10:1) to give **5.35** (58.9 mg, 0.078 mmol, 52.4 %). <sup>1</sup>H NMR (400 MHz, CD<sub>3</sub>OD) δ 7.80 (d, J = 7.6 Hz, 2H), 7.65 (d, J = 7.6 Hz, 2H), 7.39 (t, J = 7.2 Hz, 2H), 7.30 (t, J = 7.6 Hz, 2H), 4.50 (m, 1H), 4.33 (t, J = 6.8 Hz, 3H), 4.20 (t, J = 6.0 Hz, 2H), 3.83 (dd, J = 11.2, 5.2 Hz, 1H), 3.70-3.66 (m, 2H), 3.69 (s, 3H), 3.22 (t, J = 7.2 Hz, 2H), 3.12 (m, 4H), 2.11 (sep, J = 6.8 Hz, 1H), 1.9 (m, 1H), 1.65 (m, 3H), 1.5 (m, 3H), 0.98 (t, J = 6.8 Hz, 6H); <sup>13</sup>C NMR (150 MHz, (CD<sub>3</sub>)<sub>2</sub>SO) δ 172.1, 171.1, 171.0, 159.3, 157.6, 156.1, 143.9, 140.7, 127.6, 127.1, 125.1, 120.1, 65.2, 62.4, 59.7, 56.9, 54.9, 51.8, 46.7, 40.0, 39.9, 38.9, 30.7, 27.8, 27.3, 26.9, 19.1, 17.6, 14.1. HRESIMS [M + Na]<sup>+</sup> calcd for C<sub>35</sub>H<sub>49</sub>N<sub>9</sub>O<sub>10</sub>Na 778.3500, found 778.3502.

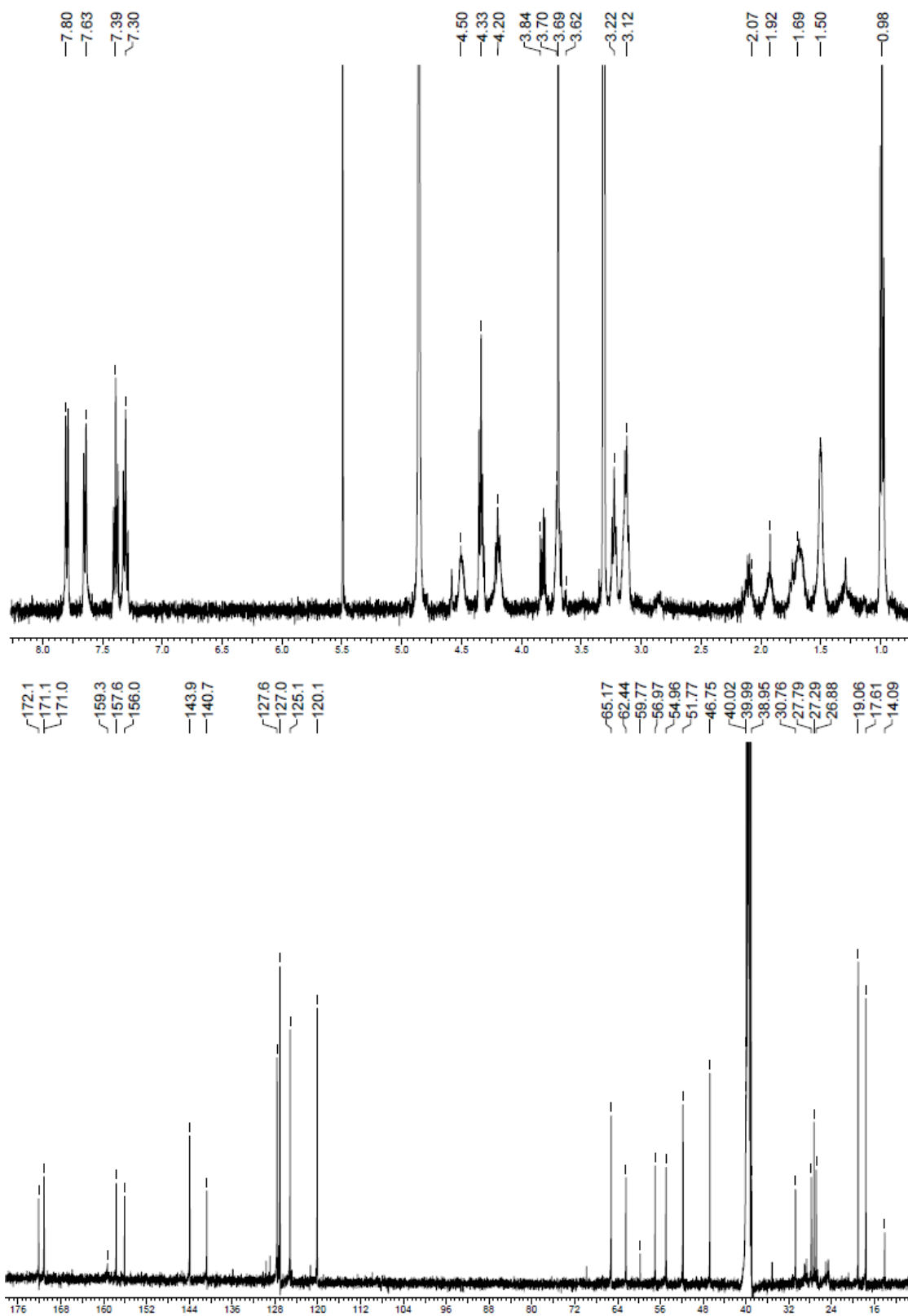
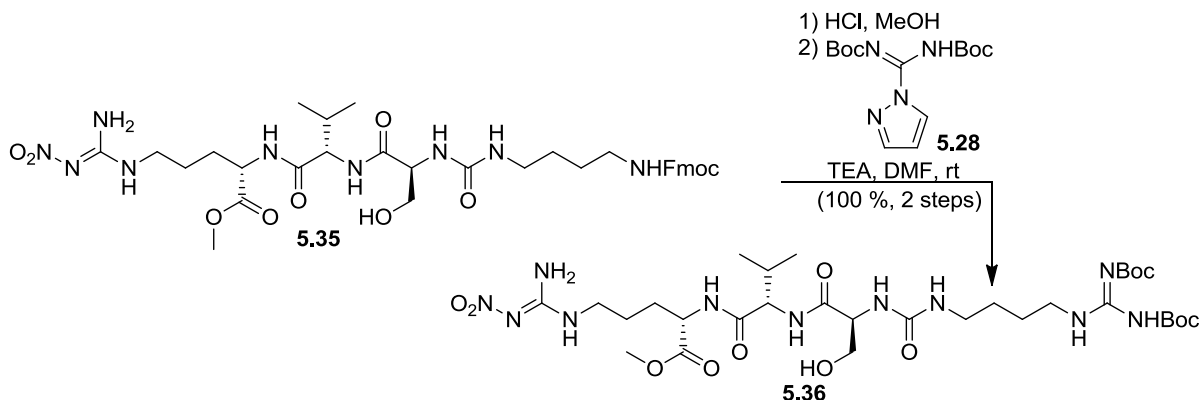


**Figure 5.16** <sup>1</sup>H and <sup>13</sup>C NMR spectra of **5.35** recorded in CD<sub>3</sub>OD at 400 MHz and (CD<sub>3</sub>)<sub>2</sub>SO at 150 MHz respectively.

### Preparation of 5.36:



Compound **5.35** (67.8 mg, 0.11 mmol) was deprotected in a similar fashion to **5.12** and purified in a similar manner. It was used in the following guanylation by dissolving it in 1 mL of *N,N*-dimethylformamide and adding guanylation agent **5.28** (40 mg, 0.13 mmol) and triethylamine (0.1 mL, 0.71 mmol) and the reaction allowed to stir at room temperature for 48 hours. The crude mixture was then concentrated using a lyophilizer and purified using flash column chromatography (methylene chloride:methanol 97:3) to give **5.36** (85.6 mg, 0.11 mmol, 100 %).  $^1\text{H}$  NMR (600 MHz,  $\text{CD}_3\text{OD}$ )  $\delta$  4.47 (s, 1H), 4.32 (t,  $J = 4.8$  Hz, 1H), 4.18 (s, 1H), 3.81 (dd,  $J = 10.8, 4.8$  Hz, 1H), 3.70 (s, 3H), 3.68 (m, 1H), 3.58 (t,  $J = 6.6$  Hz, 2H), 3.22 (t,  $J = 6.6$  Hz, 2H), 3.16 (t,  $J = 6.6$  Hz, 2H), 2.10 (quin,  $J = 6.6$  Hz, 1H), 1.93 (s, 1H), 1.67 (m, 3H), 1.61 (m, 2H), 1.53 (m, 2H), 1.51 (s, 9H), 1.46 (s, 9H), 0.99 (d,  $J = 6.6$  Hz, 3H), 0.97 (d,  $J = 6.6$  Hz, 3H);  $^{13}\text{C}$  NMR (150 MHz,  $\text{CD}_3\text{OD}$ )  $\delta$  172.1, 171.9, 171.6, 162.7, 159.1, 158.6, 155.7, 152.3, 82.5, 78.5, 61.9, 58.5, 55.0, 50.9, 39.7, 39.7, 38.8, 29.8, 27.6, 26.7, 26.6, 26.4, 25.8, 25.8, 23.8, 17.8, 16.8. HRESIMS  $[\text{M} + \text{H}]^+$  calcd for  $\text{C}_{31}\text{H}_{58}\text{N}_{11}\text{O}_{12}$  776.4263, found 776.4266.

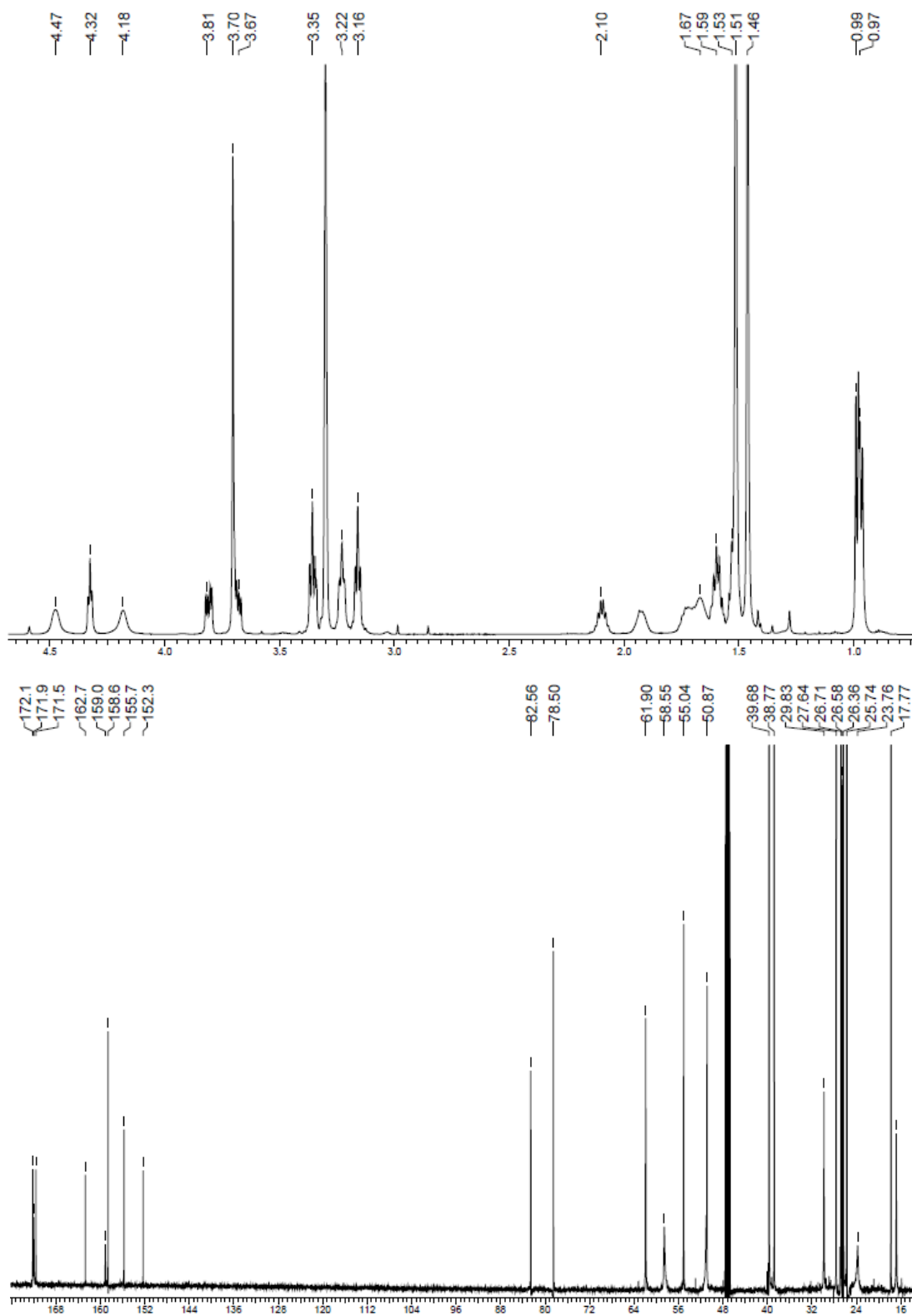
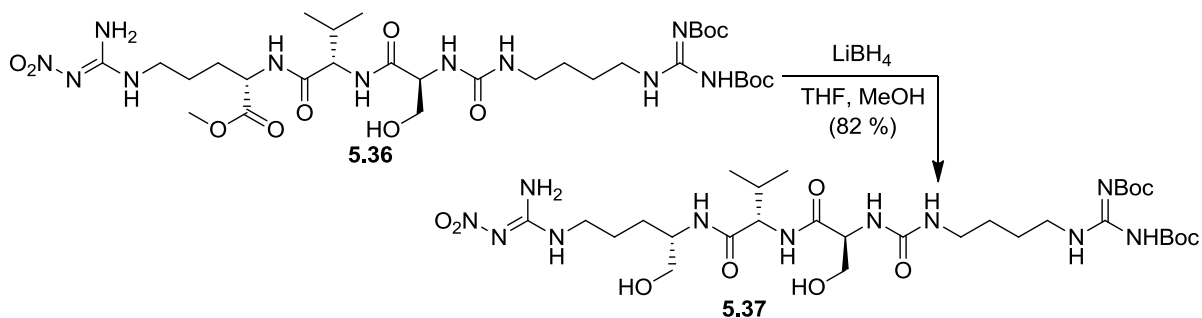


**Figure 5.17**  $^1\text{H}$  and  $^{13}\text{C}$  NMR spectra of **5.36** recorded in  $\text{CD}_3\text{OD}$  at 600 MHz and 150 MHz respectively.

### Preparation of **5.37**:



To **5.36** (13.7 mg, 0.017 mmol) dissolved in 0.5 mL of tetrahydrofuran was added methanol 5.8  $\mu\text{L}$  and the mixture cooled to 0  $^\circ\text{C}$ . To the cooled solution was added  $\text{LiBH}_4$  (1.3 mg, 0.061 mmol) dissolved in 1 mL of tetrahydrofuran, and allowed to stir for 1 hour, after which 0.1 mL of water was added and mixture concentrated on a lyophilizer. The crude was purified using flash column chromatography (methylene chloride:methanol 9:1) to give **5.37** (10.4 mg, 0.013 mmol, 81.8 %).  $^1\text{H}$  NMR (600 MHz,  $\text{CD}_3\text{OD}$ )  $\delta$  4.31 (t,  $J = 5.4$  Hz, 1H), 4.10 (s, 1H), 3.92 (s, 1H), 3.82 (dd,  $J = 10.8, 4.8$  Hz, 1H), 3.67 (dd,  $J = 10.8, 5.4$  Hz, 1H), 3.59 (dd,  $J = 13.2, 5.4$  Hz, 1H), 3.48 (dd,  $J = 9.0, 5.4$  Hz, 2H), 3.35 (t,  $J = 7.2$  Hz, 3H), 3.31 (m, 1H), 3.16 (t,  $J = 6.6$  Hz, 3H), 2.12 (quin,  $J = 6.6$  Hz, 1H), 1.66 (s, 2H), 1.59 (m, 3H), 1.53 (m, 1H), 1.51 (s, 9H), 1.46 (s, 9H), 0.97 (t,  $J = 7.2$  Hz, 6H);  $^{13}\text{C}$  NMR (150 MHz,  $\text{CD}_3\text{OD}$ )  $\delta$  172.3, 171.9, 162.7, 159.1, 158.6, 155.7, 152.3, 82.6, 78.5, 63.2, 61.9, 60.6, 59.1, 55.1, 52.5, 40.1, 39.7, 38.8, 29.4, 27.3, 26.6, 26.3, 25.7, 23.9, 17.9, 16.8. HRESIMS  $[\text{M} + \text{H}]^+$  calcd for  $\text{C}_{30}\text{H}_{58}\text{N}_{11}\text{O}_{11}$  748.4325, found 748.4317.

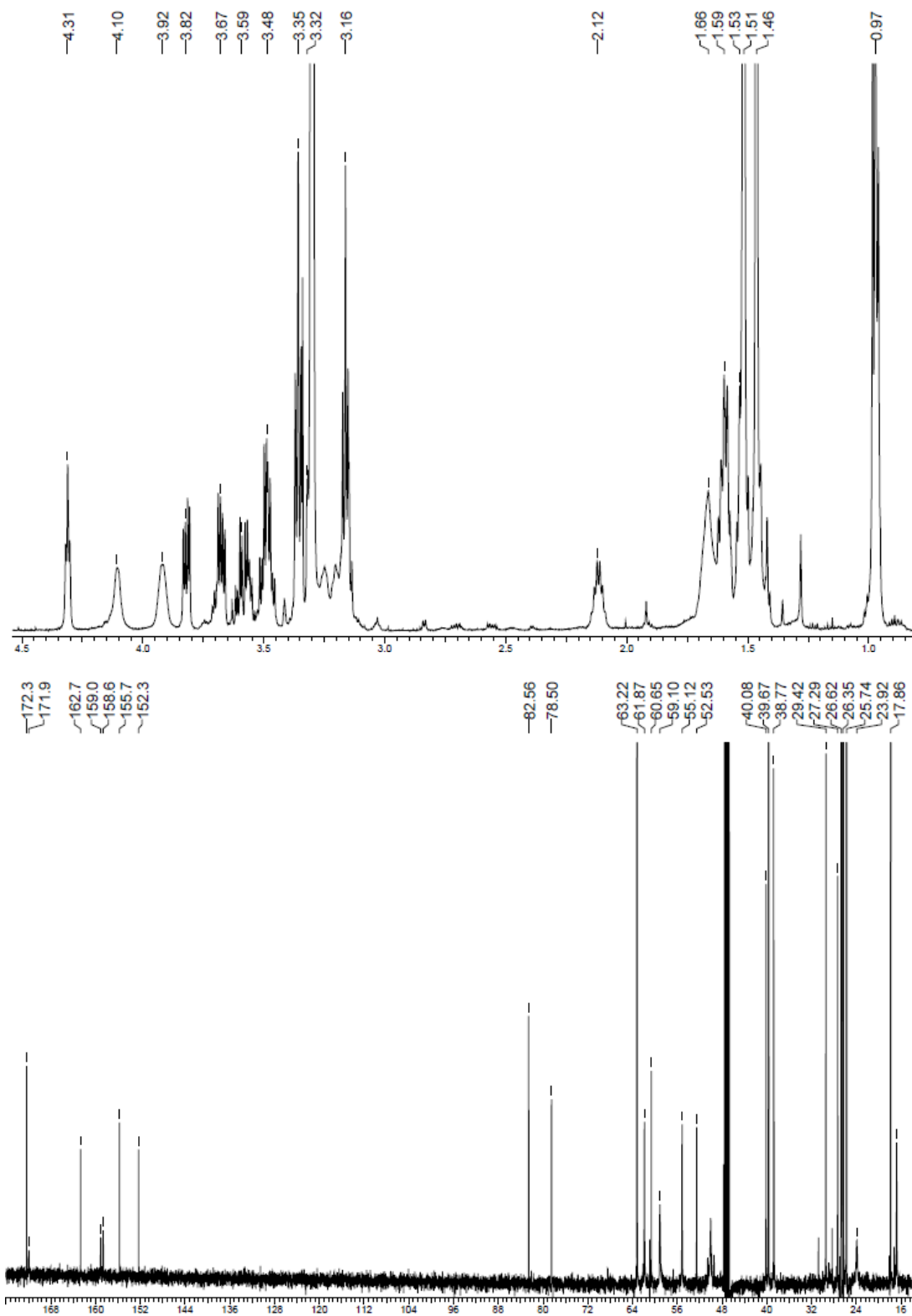
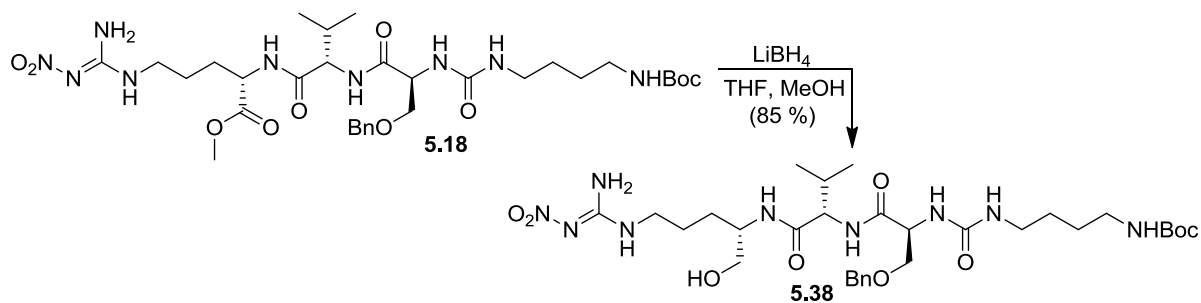


**Figure 5.18**  $^1\text{H}$  and  $^{13}\text{C}$  NMR spectra of **5.37** recorded in  $\text{CD}_3\text{OD}$  at 600 MHz and 150 MHz respectively.

### Preparation of **5.38**:



To **5.18** (100 mg, 0.14 mmol) dissolved in 2 mL of tetrahydrofuran and 0.06 mL methanol was added  $\text{LiBH}_4$  (14 mg, 0.64 mmol) dissolved in 3 mL of tetrahydrofuran and the reaction allowed to stir at room temperature for thirty minutes, after which the reaction was diluted with water (50 mL) and extracted three times with methylene chloride (150 mL), dried with  $\text{MgSO}_4$  and concentrated using a rotary evaporator. The crude was purified using flash column chromatography (methylene chloride:methanol 9:1) to give **5.38** (82.8 mg, 0.12 mmol, 85.5 %).  $^1\text{H}$  NMR (600 MHz,  $(\text{CD}_3)_2\text{SO}$ )  $\delta$  8.45 (bs, 1H), 7.67 (m, 2H), 7.28 (m, 5H), 6.75 (m, 1H), 6.24 (m, 1H), 6.19 (m, 1H), 4.63 (m, 1H), 4.43 (m, 2H), 4.36 (dd,  $J = 7.8, 4.8$  Hz, 1H), 4.12 (m, 1H), 4.08 (t,  $J = 4.8$  Hz, 1H), 3.67 (bs, 1H), 3.61 (dd,  $J = 8.4, 3.6$  Hz, 1H), 3.49 (dd,  $J = 9.6, 4.8$  Hz, 1H), 3.29 (m, 3H), 3.18 (m, 1H), 3.12 (t,  $J = 4.8$  Hz, 2H), 3.04 (m, 1H), 2.94 (m, 2H), 2.86 (m, 2H), 1.91 (m, 1H), 1.52 (m, 1H), 1.42 (m, 2H), 1.34 (s, 9H), 1.31 (m, 2H), 1.21 (m, 1H), 0.81 (d,  $J = 6.0$  Hz, 3H), 0.80 (d,  $J = 6.0$  Hz, 3H);  $^{13}\text{C}$  NMR (150 MHz,  $(\text{CD}_3)_2\text{SO}$ )  $\delta$  170.5, 170.5, 159.3, 157.5, 155.6, 138.1, 128.1, 127.4, 127.3, 77.3, 72.1, 70.7, 63.2, 57.7, 53.2, 50.3, 40.5, 38.9, 30.8, 28.3, 27.9, 27.3, 27.3, 27.0, 24.7, 19.1, 17.9. HRESIMS  $[\text{M} + \text{Na}]^+$  calcd for  $\text{C}_{31}\text{H}_{53}\text{N}_9\text{O}_9\text{Na}$  718.3864, found 718.3870.

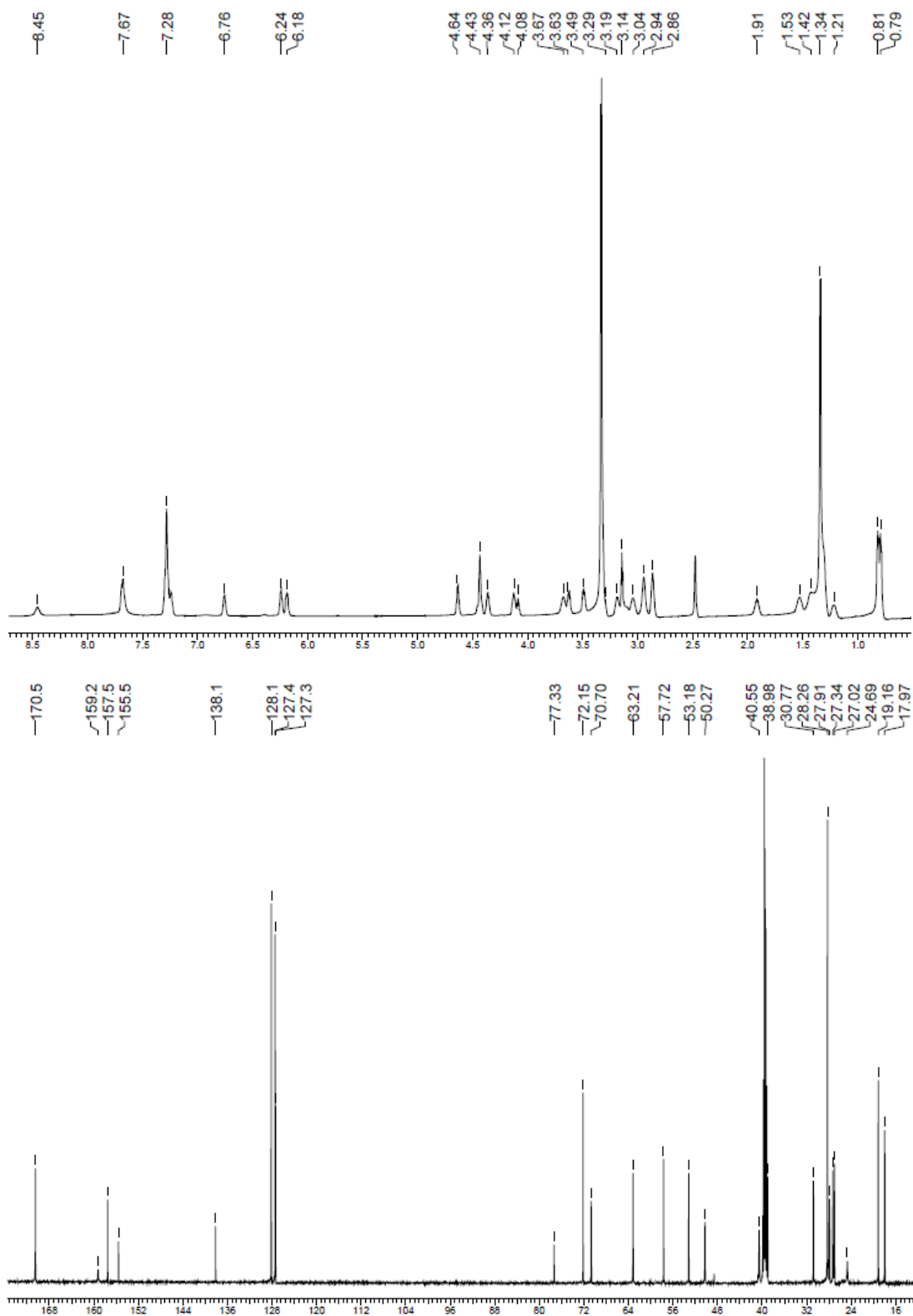
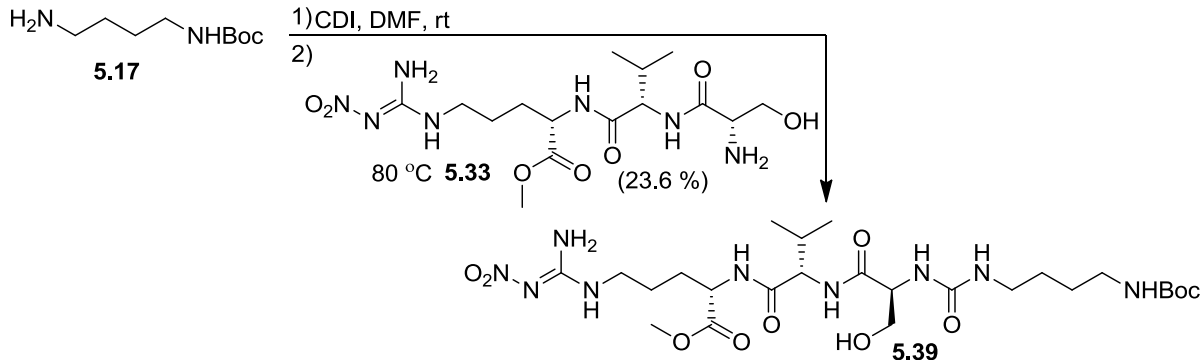


**Figure 5.19**  $^1\text{H}$  and  $^{13}\text{C}$  NMR spectra of **5.38** recorded in  $(\text{CD}_3)_2\text{SO}$  at 600 MHz and 150 MHz respectively.

### Preparation of **5.39**:



To Boc protected putrescine **5.17** (57.0 mg, 0.30 mmol) dissolved in 3 mL of *N,N*-dimethylformamide was added CDI (49.1 mg, 0.30 mmol), and the reaction mixture allowed to stir at room temperature for 8 hours. To this was added peptide **5.33** (84.8 mg, 0.20 mmol) dissolved 4 mL of *N,N*-dimethylformamide and the reaction was heated to 80 °C overnight. The crude was concentrated using a lyophilizer and purified using flash column chromatography (methylene chloride:methanol 23:2) to give **5.39** (46.6 mg, 0.071 mmol, 23.6 %). <sup>1</sup>H NMR (600 MHz, CD<sub>3</sub>OD) δ 4.59 (s, 1H), 4.48 (s, 1H), 4.31 (s, 1H), 4.16 (m, 1H), 3.81 (dd, J = 10.2, 4.8 Hz, 1H), 3.70 (s, 3H), 3.67 (m, 1H), 3.22 (t, J = 6.6 Hz, 2H), 3.12 (s, 2H), 3.03 (s, 2H), 2.09 (quin, J = 6.6 Hz, 1H), 1.92 (s, 1H), 1.67 (m, 3H), 1.47 (m, 5H), 1.41 (s, 9H), 0.98 (t, J = 7.8 Hz, 6H); <sup>13</sup>C NMR (150 MHz, CD<sub>3</sub>OD) δ 172.1, 172.0, 171.6, 159.1, 158.6, 156.7, 77.9, 61.9, 58.6, 55.0, 50.8, 39.6, 39.2, 38.8, 29.8, 29.8, 27.6, 26.9, 26.9, 26.6, 26.4, 23.7, 17.7, 16.8. HRESIMS [M + Na]<sup>+</sup> calcd for C<sub>25</sub>H<sub>47</sub>N<sub>9</sub>O<sub>10</sub>Na 656.3344, found 656.3351.

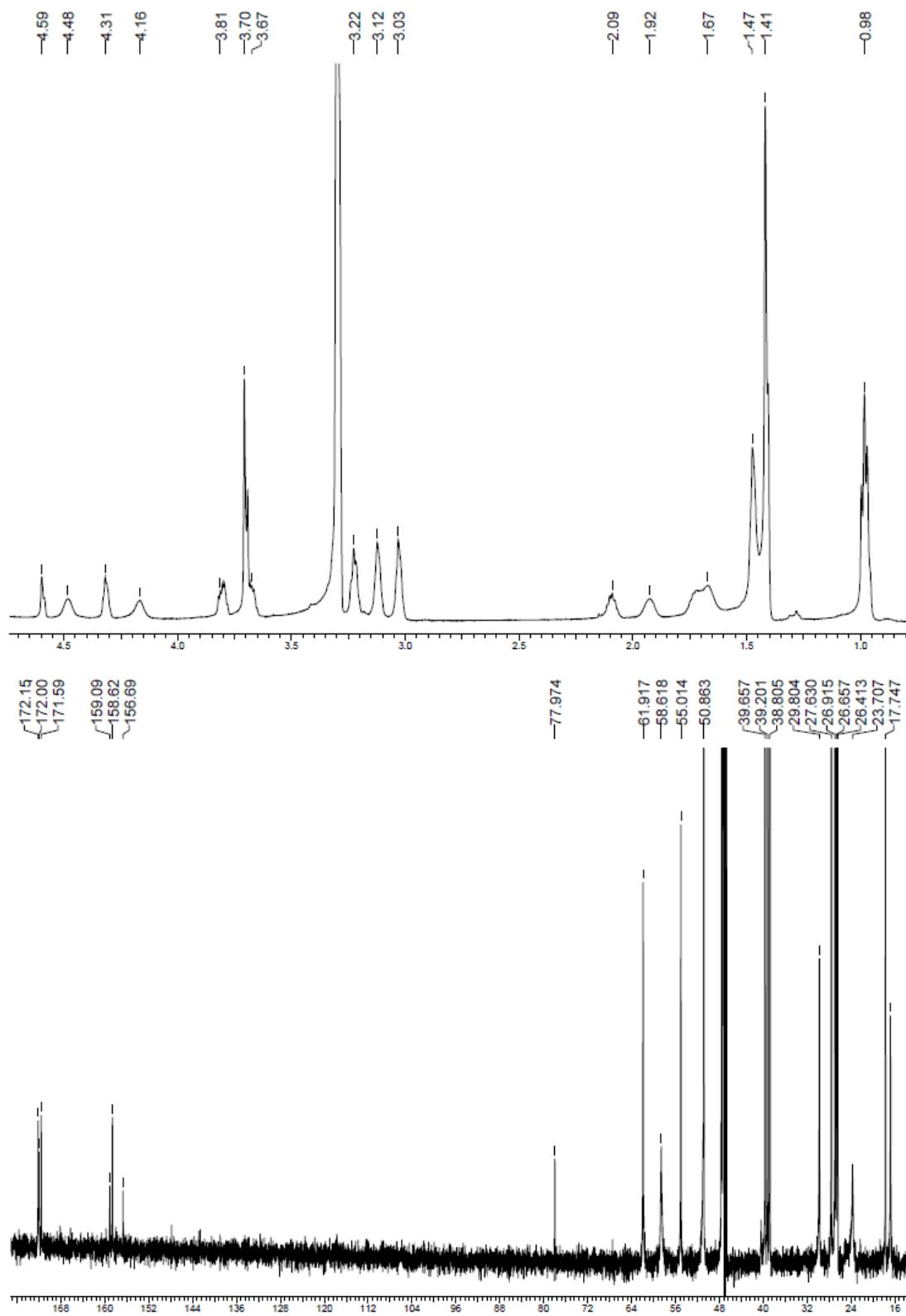
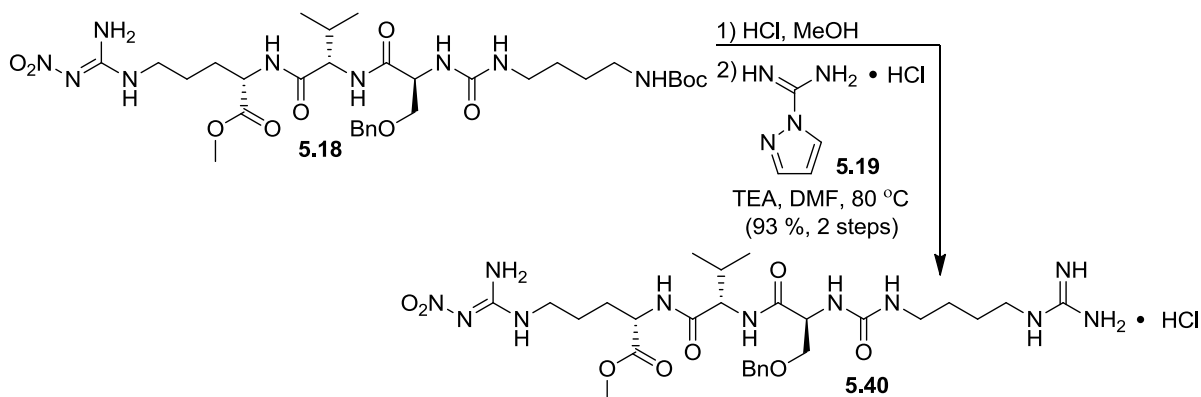


**Figure 5.20**  $^1\text{H}$  and  $^{13}\text{C}$  NMR spectra of **5.39** recorded in  $\text{CD}_3\text{OD}$  at 600 MHz and 150 MHz respectively.

### Preparation of 5.40:



To **5.18** (300 mg, 0.41 mmol) dissolved in 10 mL of methanol was added 12.4 M HCl (1.0 mL, 12.0 mmol) and the mixture allowed to stir at room temperature overnight. The mixture was concentrated under a stream of nitrogen and the crude evaporated overnight using a lyophilizer, and used in the subsequent guanylation without further purification. This primary amine HCl salt was dissolved in 3 mL of *N,N*-dimethylformamide followed by the addition of triethylamine (0.12 mL, 0.87 mmol) and guanylyating reagent **5.19** (63.7 mg, 0.43 mmol). The mixture was then heated at 80 °C overnight after which it was concentrated using a lyophilizer, and purified using a 5 g C<sub>18</sub> Sep-Pak (water:methanol 100 % water, 9:1, 3:2, 100 % methanol) to give **5.40** (269.6 mg, 0.38 mmol, 92.7 % 2 steps). <sup>1</sup>H NMR (600 MHz, (CD<sub>3</sub>)<sub>2</sub>SO) δ 8.47 (bs, 1H), 8.40 (d, J = 6.0 Hz, 1H), 7.71 (d, J = 9.0 Hz, 1H), 7.66 (m, 1H), 7.28 (m, 5H), 6.85 (bs, 1H), 6.35 (bs, 1H), 4.85 (bs, 5H), 4.43 (m, 2H), 4.37 (m, 1H), 4.24 (t, J = 6.6 Hz, 1H), 4.14 (m, 1H), 3.63 (m, 1H), 3.57 (s, 3H), 3.50 (m, 1H), 3.07 (m, 4H), 2.97 (m, 2H), 1.95 (quin, J = 6.0 Hz, 1H), 1.68 (m, 1H), 1.57 (m, 1H), 1.47 (m, 2H), 1.42 (m, 2H), 1.35 (m, 2H), 0.84 (d, J = 6.0 Hz, 3H), 0.80 (d, J = 6.0 Hz, 3H); <sup>13</sup>C NMR (150 MHz, (CD<sub>3</sub>)<sub>2</sub>SO) δ 172.1, 170.9, 170.4, 159.3, 157.6, 156.8, 138.2, 128.1, 127.4, 127.3, 72.2, 70.8, 56.9, 53.2, 51.8, 51.7, 40.4, 40.1, 38.6, 31.1, 27.8, 27.2, 25.9, 24.4, 19.0, 17.9. HRESIMS [M + H]<sup>+</sup> calcd for C<sub>28</sub>H<sub>48</sub>N<sub>11</sub>O<sub>8</sub> 666.3687, found 666.3695.

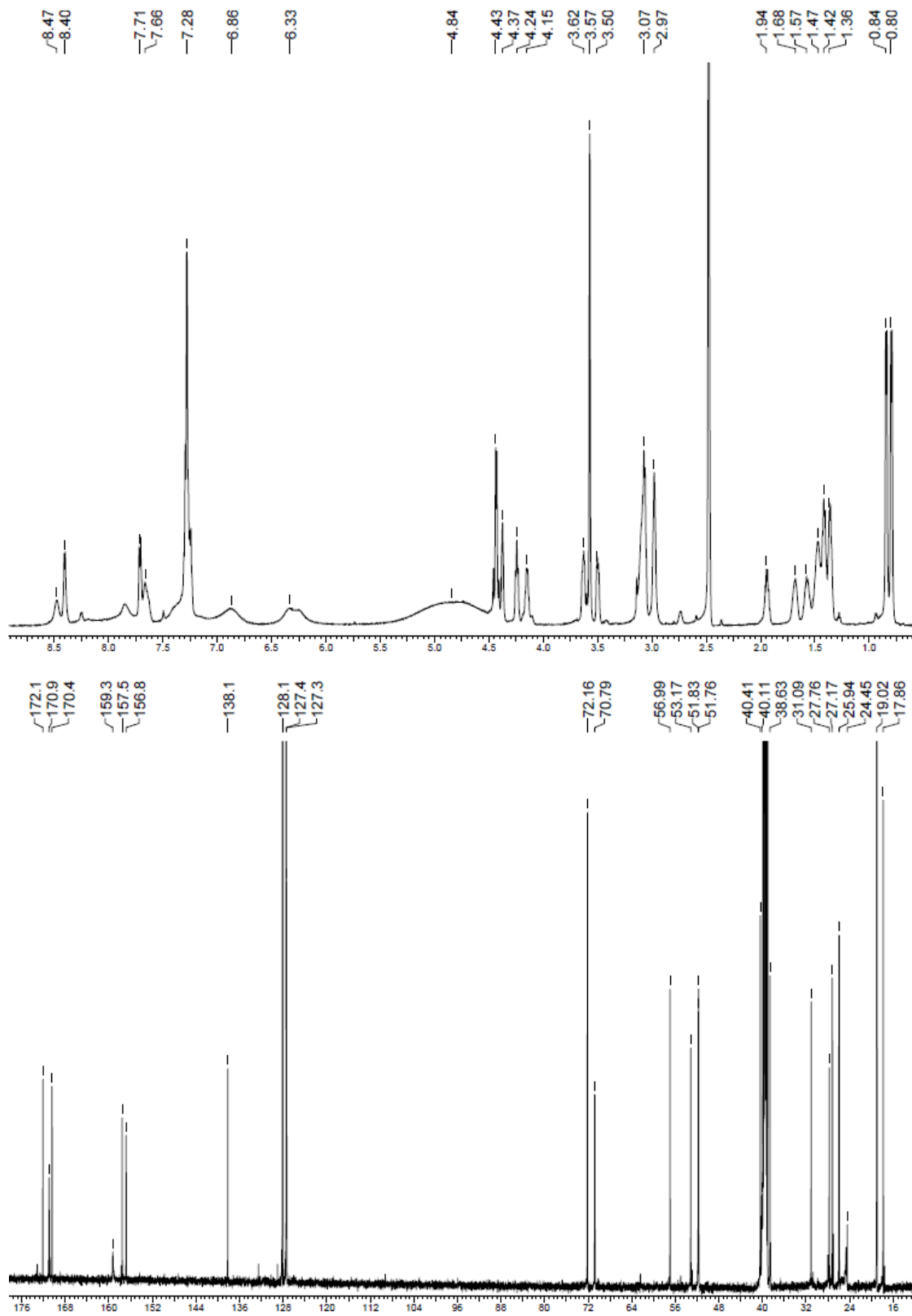


**Figure 5.21**  $^1\text{H}$  and  $^{13}\text{C}$  NMR spectra of **5.40** recorded in  $(\text{CD}_3)_2\text{SO}$  at 600 MHz and 150 MHz respectively.

## Chapter 6: Conclusion

### 6.1 Biological and Pharmacokinetic Evaluation for Water Soluble SHIP1 Activators

It has been proposed that small molecule activators of SHIP1<sup>49</sup> may be used as a novel therapy for hematopoietic malignancies as well as inflammatory disorders. Furthermore, activation of the SHIP1 enzymatic pathway may also provide an alternative to PI3K inhibition.<sup>47</sup> Chapter 2 describes the continuation of a comprehensive SAR study, which began with the lead compound pelorol<sup>51</sup> (**2.1**) (Figure 2.2), a marine natural product. The goal of the SAR study was to construct water-soluble analogues of compound **2.18** (Figure 2.10) for the purpose of enhancing its drug-like properties.<sup>16</sup> Compound **2.18** is an analogue of pelorol (**2.1**) and a SHIP1 activator.

Several objectives need to be completed to provide additional biological insight. Lead compounds **2.20** and **2.42** should be evaluated for their pharmacokinetic properties<sup>232</sup> in order to understand their absorption and distribution properties *in vivo*. This would further validate the concept of enhanced water solubility in providing enhanced drug-like effects in analogues **2.20** and **2.42**. Additional biological testing in animal models other than inflammation such as multiple myeloma, which has been implicated with SHIP1,<sup>233</sup> should be completed. Furthermore, analogues **2.40**, **2.44**, and **2.45** (Scheme 2.11) and their enantiomers should be evaluated in a SHIP1 enzymatic assay.<sup>51</sup> This would provide additional information as to the role of configuration in the activity of these analogues.

Additional STDD NOE NMR<sup>92</sup> experiments of analogues **2.20** and **2.42** (Figure 2.19) should be completed. The future experiment should be performed so that each analogue is evaluated in a separate sample, rather than testing each analogue sequentially in the same

NMR tube. This may provide more accurate evidence for binding of these analogues to SHIP1, since potential intermolecular interactions between **2.20** and **2.42**, which may affect the experiment, would be eliminated. Finally, the benzophenone photoaffinity probe<sup>101</sup> **2.53** (Scheme 2.14), found to be active in a SHIP1 enzymatic assay, should be used to identify the SHIP1 amino acid residue(s) responsible for binding, and for additional proof of interaction *in vivo*.

## 6.2 Additional Biological Evaluations of the Niphatenones and their Analogues

It has been proposed<sup>140</sup> that small molecule antagonists of the NTD of the AR are an appealing avenue of exploration for treating CRPC, an advanced form of prostate cancer resistant to current therapies. Chapter 3 describes the total syntheses of the marine natural products niphatenone A (**3.8**) and B (**3.9**) (Figure 3.5). These marine metabolites represent a novel NTD-AR antagonist pharmacophore. The purpose of the total syntheses was to aid in structure determination. In consequence, the (*S*) configuration was assigned to the natural products. An SAR study was completed, and it was shown that the unnatural (*R*) configuration of niphatenone B in **3.31** (Figure 3.11) was the most active compound.

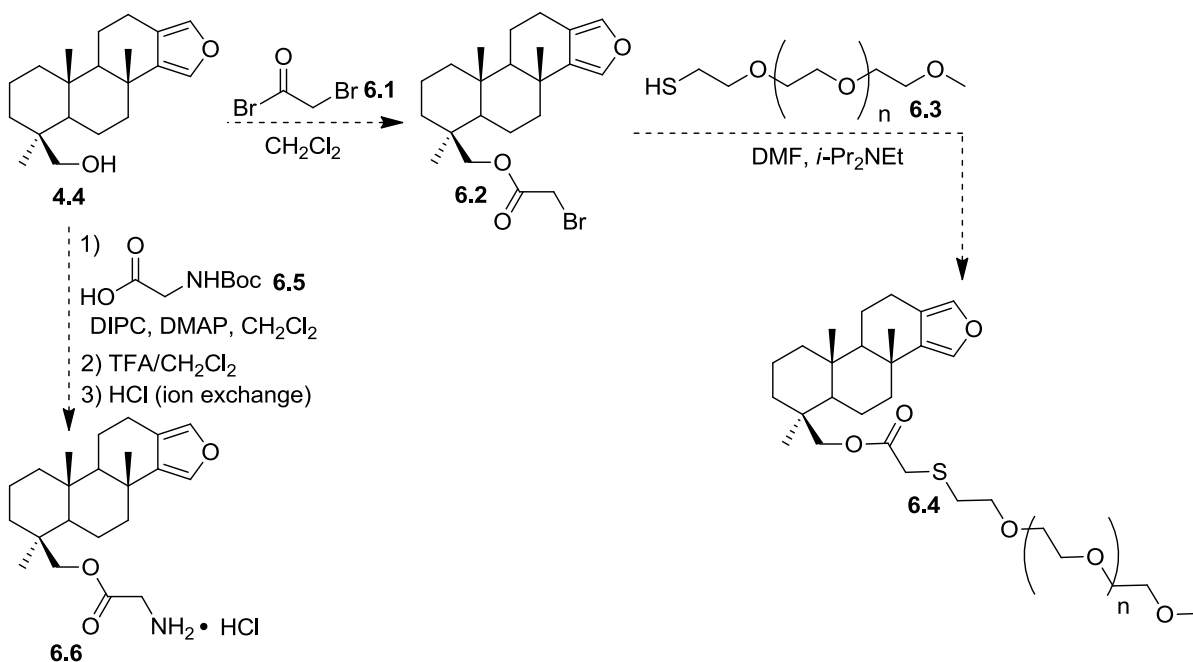
A few areas in the project remain to be completed. Fluorinated analogue **3.54** (Scheme 3.9) should be tested in an *in vitro* AR transcriptional activity assay.<sup>140</sup> Potential fluorescent<sup>155</sup> probe **3.78** (Scheme 3.14) should be tested *in vitro* to determine if it is an NTD-AR antagonist. If found to be active, it may be determined through fluorescence imaging if the photochemical properties of the ligand (**3.78**) change due to covalent binding to the NTD-AR, for use as a fluorescent imaging agent.<sup>160</sup> Furthermore, *in vivo* studies using

either niphatenone A (**3.8**) and/or B (**3.9**), or a suitable analogue, should be completed to properly evaluate if these AR antagonists have any effect on prostate tissue growth.

### **6.3 Future Synthetic Strategies Towards Terpene 4.4: An LBD AR Antagonist**

Small molecule AR antagonists are currently used as a therapeutic treatment for prostate cancer.<sup>130</sup> Chapter 4 describes the semisynthesis of analogues based on the marine natural product lead compound **4.1**, which was discovered to be an AR antagonist (Figure 4.1). The semisynthetic analogue **4.4** has enhanced activity compared to the lead compound **4.1** in both an *in vitro* AR transcriptional activity assay as well as an *in vitro* AR affinity assay (Figure 4.7).

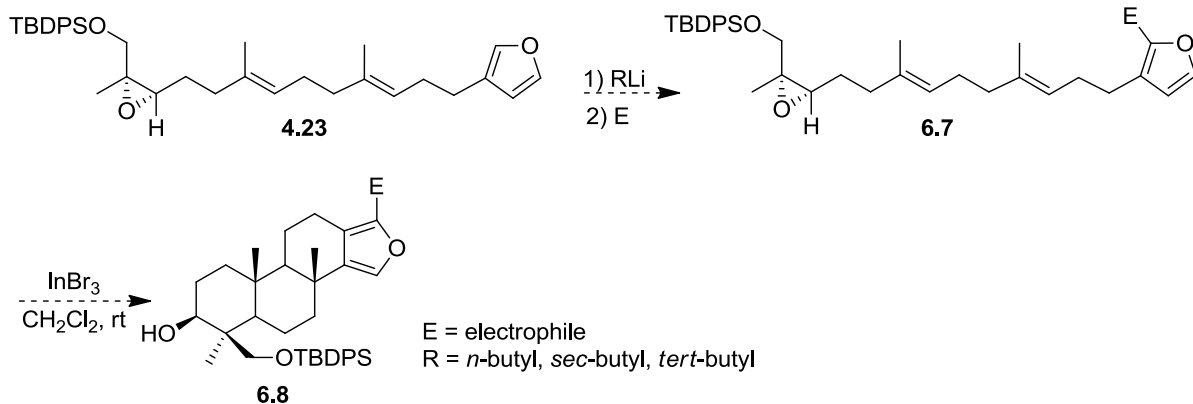
A number of questions remain in order to elucidate the biological effect of this novel LBD-AR antagonist (**4.4**). Analogue **4.4** should be tested *in vivo* to observe its effects on prostate tumor tissue. Furthermore, prodrugs<sup>68</sup> of **4.4** could be constructed using semisynthetic material (**4.4**) in order to decrease the CLogP of analogue **4.4**.<sup>16</sup>



**Scheme 6.1** Syntheses towards polar analogues of **4.4**.

One potential prodrug of analogue **4.4** would be a PEG analogue<sup>152</sup> (Scheme 6.1). Compound **4.4** could be esterified using bromoacetyl bromide (**6.1**) to give intermediate **6.2**. Bromide **6.2** may be reacted with PEG thiol **6.3** to afford the highly water soluble pegylated analogue **6.4**. Alternatively, the amine-derivatized prodrug **6.6** could be constructed. Esterification of analogue **4.4** with Boc-protected glycine **6.5** followed by a deprotection and ion exchange should yield prodrug **6.6** as the hydrochloride salt (Scheme 6.1).

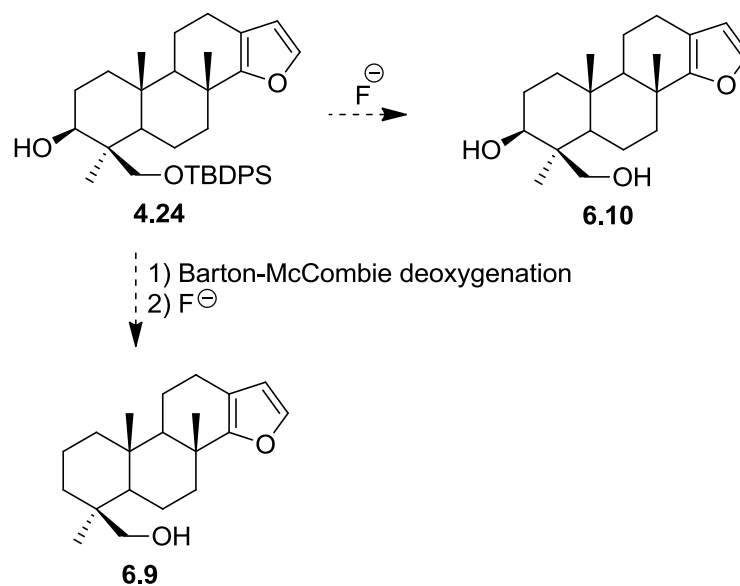
The method of accessing A-ring analogues of **4.4**, by an epoxide-initiated cationic cascade<sup>69</sup> should be pursued. One avenue of exploration would be to lithiate the terminal epoxide intermediate **4.23** (Scheme 6.2). Lithiation of **4.23** may be accomplished by using a variety of bases such as *n*-BuLi, *sec*-BuLi, and *tert*-BuLi. By quenching the resultant alkyl lithium with  $\text{D}_2\text{O}$ ,<sup>234</sup> one should be able to observe deuterium incorporation in the furan ring system by  $^1\text{H}$  NMR and establish ideal deprotonation conditions.



**Scheme 6.2** Lithiation strategy to construct A-ring analogues of **4.4**.

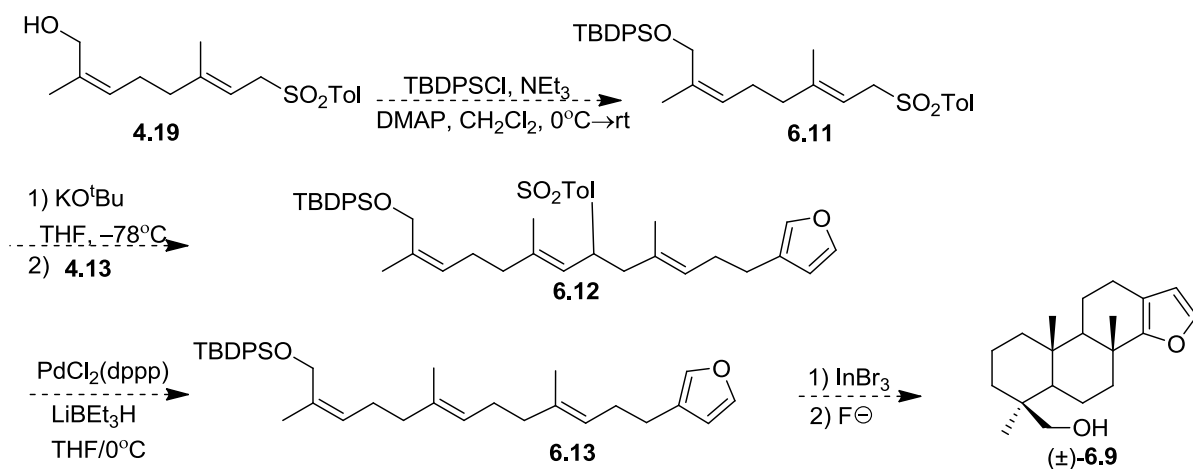
Once the conditions have been identified, quenching with various electrophiles should be attempted. Initial focus should be on the aforementioned silyl electrophiles (Section 4.3). This would allow for rapid construction of several functionalized intermediates, which could then be cyclized. The resulting reaction mixtures can then be analyzed for the desired product regioselectivity.

Furthermore, previously synthesized intermediate **4.24** (Scheme 4.5) should be deprotected to yield analogue **6.10** for biological testing (Scheme 6.3). The regioisomer **6.9** should be readily accessible due to the inherent reactivity of the furan ring system (Section 4.1). Compound **6.9** could be synthesized by a Barton-McCombie deoxygenation<sup>88</sup> followed by a TBDPS deprotection (Scheme 6.3).



**Scheme 6.3** Deprotection of regioisomer **4.24**.

Another interesting compound would be analogue ( $\pm$ )-**6.9**. A synthetic route for constructing regioisomer ( $\pm$ )-**6.9** is shown in Scheme 6.4. By using previously synthesized intermediates (**4.19**) and a similar route (Scheme 4.5) the construction of ( $\pm$ )-**6.9** should be readily accessible. Polyene<sup>55</sup> **6.13** could be cyclized with indium tribromide,<sup>78</sup> then deprotected to give ( $\pm$ )-**6.9**. This synthetic route also has the advantage of providing the antipodal configuration to the lead compound (**4.1**) which would help broaden the SAR.



**Scheme 6.4** Alternative synthesis of regioisomer (±)-6.9.

#### 6.4 Alternative Synthetic Strategy Towards Lichostatinal (5.4)

The biological role of cathepsin K in bone resorption<sup>196</sup> has led to the development of inhibitors of cathepsin K as potential therapeutics to combat osteoporosis.<sup>201</sup> However, there are currently no available cathepsin K inhibitors for the treatment of osteoporosis. The lack of available cathepsin K inhibitors led to a collaboration between the laboratories of Dr. Julian Davies and Dr. Dieter Bromme at the University of British Columbia. This culminated in the discovery of lichostatinal (**5.4**), a peptide-aldehyde natural product isolated from cultures of a terrestrial *actinomycete*. Lichostatinal (**5.4**) is the first natural product to be isolated by co-crystallization with its biological target from a complex mixture.

Chapter 5 details the synthetic efforts towards lichostatinal (**5.4**), in order to verify its structure and to provide additional material for biological testing. A reasonable alternative to the syntheses presented in Chapter 5 is to utilize the chemistry developed for the construction of leupeptin<sup>220</sup> (**5.1**), the first natural product cathepsin K inhibitor. In Shimizu's synthesis of leupeptin (**5.1**), the aldehyde/hemiaminal mixture that results from arginol oxidation was

converted entirely to the semicarbazone with semicarbazide. This simplifies the mixture to give only a single compound (**6.14**), which should be easily purified by flash column chromatography (Figure 6.1). This alternative may prove useful if a benzyl-protected serine is utilized (Figure 6.1). Since the aldehyde/hemiaminal mixture is protected as the semicarbazone, it would allow for exploration of alternative benzyl deprotection strategies without having a labile aldehyde moiety present in the molecule.

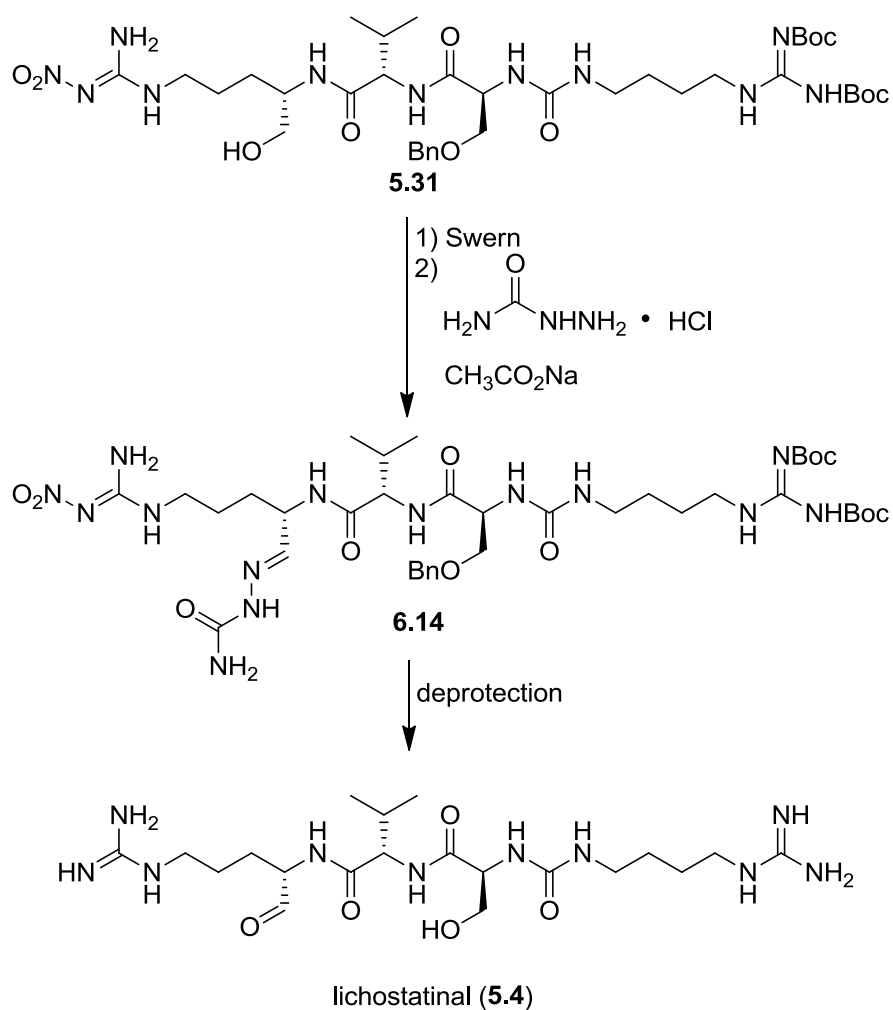


**Figure 6.1** Alternative route to lichostatinal (**5.4**).

## References

- (1) McGovern, P. E.; Mirzoian, A.; Hall, G. R. *Proc. Natl. Acad. Sci. U.S.A.* **2009**, *106*, 7361–7366.
- (2) Móró, L.; Simon, K.; Bárd, I.; Rácz, J. *J. Psychoact. Drugs* **2011**, *43*, 188–198.
- (3) Mahdi, J. G.; Mahdi, a J.; Bowen, I. D. *Cell prolif.* **2006**, *39*, 147–155.
- (4) Mahdi, J. G.; Mahdi, a J.; Bowen, I. D. *Phytochem.* **2005**, *66*, 1399–1406.
- (5) Eisenreich, W.; Schwarz, M.; Zenk, M. H.; Bacherl, A.; Cartayrade, A.; Arigoni, D. *Chem. Biol.* **1998**, *5*, 221–233.
- (6) Facchini, P. J. *Annu. Rev. Plant Physiol. Plant Mol. Biol.* **2001**, *52*, 29–66.
- (7) Staunton, J.; Weissman, K. J. *Nat. Prod. Rep.* **2001**, *18*, 380–416.
- (8) Kleinkauf, H.; Von Doehren, H. *Eur. J. Biochem.* **1990**, *192*, 1–15.
- (9) Zhu, C.; Jiang, L.; Chen, T. *Eur. J. Med. Chem.* **2002**, *37*, 399–407.
- (10) Hann, M. M.; Oprea, T. I. *Curr. Opin. Chem. Biol.* **2004**, *8*, 255–263.
- (11) Agresti, J. J.; Antipov, E.; Abate, A. R.; Ahn, K.; Rowat, A. C.; Baret, J.-C.; Marquez, M.; Klibanov, A. M.; Griffiths, A. D.; Weitz, D. *Proc. Natl. Acad. Sci. U.S.A* **2010**, *107*, 4004–4009.
- (12) Schwarz, H.; Karreman, M.; Agronskaia, A. *Curr. Biol.* **1994**, *4*, 564–567.
- (13) Ortholand, J.-Y.; Ganesan, A. *Curr. Opin. Chem. Biol.* **2004**, *8*, 271–280.
- (14) Montaser, R.; Luesch, H. *Future Med. Chem.* **2011**, *3*, 1475–1489.
- (15) Lee, M. L.; Schneider, G. *J. Comb. Chem.* **2001**, *3*, 284–289.
- (16) Lipinski, C.; Lombardo, F.; Dominy, B. W.; Feeney, P. J. *Adv. Drug Delivery Rev.* **2001**, *46*, 3–26.
- (17) Oprea, T. I. *Curr. Opin. Chem. Biol.* **2002**, *6*, 384–389.

- (18) Feling, R. H.; Buchanan, G. O.; Mincer, T. J.; Kauffman, C. A.; Jensen, P. R.; Fenical, W.; John, D. *Angew. Chem. Int. Ed.* **2003**, *42*, 355–357.
- (19) Groll, M.; Ditzel, L.; Lowe, J.; Stock, D.; Bochtler, M.; Bartunik, H. *Nature* **1997**, *386*, 463–471.
- (20) Groll, M.; Huber, R.; Potts, B. C. M. *J. Am. Chem. Soc.* **2006**, *128*, 5136–5141.
- (21) Kong, D.-X.; Jiang, Y.-Y.; Zhang, H.-Y. *Drug Discov. Today* **2010**, *15*, 884–886.
- (22) Munro, M. H.; Blunt, J. W.; Dumdei, E. J.; Hickford, S. J.; Lill, R. E.; Li, S.; Battershill, C. N.; Duckworth, R. *J. Biotechnol.* **1999**, *70*, 15–25.
- (23) Mayer, A. M. S.; Glaser, K. B.; Cuevas, C.; Jacobs, R. S.; Kem, W.; Little, R. D.; McIntosh, J. M.; Newman, D. J.; Potts, B. C.; Shuster, D. E. *Trends Pharmacol. Sci.* **2010**, *31*, 255–265.
- (24) Searle, P.; Molinski, T. F. *J. Am. Chem. Soc.* **1995**, *117*, 8126–8131.
- (25) Macmillan, J. B.; Xiong-zhou, G.; Skepper, C. K.; Molinski, T. F. *J. Org. Chem.* **2008**, *73*, 3699–3706.
- (26) Dalisay, D. S.; Morinaka, B. I.; Skepper, C. K.; Molinski, T. F. *J. Am. Chem. Soc.* **2009**, *131*, 7552–7553.
- (27) Kinnel, R. B.; Gehrken, H.-peter; Scheuer, P. J. *J. Am. Chem. Soc.* **1993**, *115*, 3376–3377.
- (28) Cipres, A.; Li, K.; Finlay, D.; Baran, P. S.; Vuori, K. *ACS. Chem. Biol.* **2010**, *5*, 195–202.
- (29) Holt, T. O. M. G.; Fregeau, N. L.; Jr, T. J.; Sam, R. *J. Nat. Prod.* **1990**, *53*, 771–792.
- (30) Buchanan, M. S.; Carroll, A. R.; Addepalli, R.; Avery, V. M.; Hooper, J. N. A.; Quinn, R. J. *J. Org. Chem.* **2007**, *72*, 2309–2317.

- (31) Seiple, I. B.; Su, S.; Young, I. S.; Lewis, C.; Yamaguchi, J.; Baran, P. S. *Angew. Chem. Int. Ed.* **2010**, *49*, 1095–1098.
- (32) Schreiber, S. L. *Proc. Natl. Acad. Sci. U.S.A.* **2011**, *108*, 6699–6702.
- (33) Bai, R.; Cichacz, Z.; Herald, C. L.; Pettit, G. R.; Hamel, E. *Mol. Pharmacol.* **1993**, *44*, 757–766.
- (34) Schyschka, L.; Rudy, A.; Jeremias, I.; Barth, N.; Pettit, G. R.; Vollmar, a M. *Leukemia* **2008**, *22*, 1737–1745.
- (35) Smith, A. B.; Tomioka, T.; Risatti, C.; Sperry, J. B.; Sfougataki, C. *Org. Lett.* **2008**, *10*, 4359–4362.
- (36) Ball, M.; Gaunt, M. J.; Hook, D. F.; Jessiman, A. S.; Kawahara, S.; Orsini, P.; Scolaro, A.; Talbot, A. C.; Tanner, H. R.; Yamanoi, S.; Ley, S. V. *Angew. Chem. Int. Ed.* **2005**, *44*, 5433–5438.
- (37) Towle, M. J.; Salvato, K. A.; Budrow, J.; Wels, B. F.; Kuznetsov, G.; Aalfs, K. K.; Welsh, S.; Zheng, W.; Seletsky, B. M.; Palme, M. H.; Habgood, G. J.; Singer, L. A.; Dipietro, L. V.; Wang, Y.; Chen, J. J.; Quincy, D. A.; Davis, A.; Yoshimatsu, K.; Kishi, Y.; Yu, M. J.; Littlefield, B. A. *Cancer Res.* **2001**, *61*, 1013–1021.
- (38) Smith, A. B.; Risatti, C.; Atasoylu, O.; Bennett, C. S.; Liu, J.; Cheng, H.; TenDyke, K.; Xu, Q. *J. Am. Chem. Soc.* **2011**, *133*, 14042–14053.
- (39) Schumacher, M.; Kelkel, M.; Dicato, M.; Diederich, M. *Molecules* **2011**, *16*, 5629–5646.
- (40) Miljanich, G. P. *Curr. Med. Chem.* **2004**, *11*, 3029–3040.
- (41) Mcgivern, J. G. *Acute Pain.* **2006**, *11*, 245–253.

- (42) Sasaki, T.; Takasuga, S.; Sasaki, J.; Kofuji, S.; Eguchi, S.; Yamazaki, M.; Suzuki, A. *Prog. Lipid Res.* **2009**, *48*, 307–343.
- (43) Bunney, T. D.; Katan, M. *Nat. Rev. Cancer* **2010**, *10*, 342–352.
- (44) Martelli, A. M.; Evangelisti, C.; Chiarini, F.; Grimaldi, C.; Manzoli, L.; McCubrey, J. *Expert Opin. Invest. Drugs* **2009**, *18*, 1333–1349.
- (45) Harris, S. J.; Parry, R. V.; Westwick, J.; Ward, S. G. *J. Biol. Chem.* **2008**, *283*, 2465–2469.
- (46) Ware, M. D.; Rosten, P.; Damen, J. E.; Liu, L.; Humphries, R. K.; Krystal, G. *Blood* **1996**, *88*, 2833–2840.
- (47) Jänne, P.; Gray, N.; Settleman, J. *Nat. Rev. Drug Discovery* **2009**, *8*, 709–723.
- (48) Vivanco, I.; Sawyers, C. L. *Nat. Rev. Cancer* **2002**, *2*, 489–501.
- (49) Ong, C. J.; Ming-Lum, A.; Nodwell, M.; Ghanipour, A.; Yang, L.; Williams, D. E.; Kim, J.; Demirjian, L.; Qasimi, P.; Ruschmann, J.; Cao, L.-P.; Ma, K.; Chung, S. W.; Duronio, V.; Andersen, R. J.; Krystal, G.; Mui, A. L.-F. *Blood* **2007**, *110*, 1942–1949.
- (50) Damen, J. E.; Liu, L.; Rosten, P.; Humphries, R. K.; Jefferson, A. B.; Majerus, P. W.; Krystal, G. *Proc. Natl. Acad. Sci. U.S.A.* **1996**, *93*, 1689–1693.
- (51) Yang, L.; Williams, D. E.; Mui, A.; Ong, C.; Krystal, G.; van Soest, R.; Andersen, R. *J. Org. Lett.* **2005**, *7*, 1073–1076.
- (52) Goclik, E.; König, G. M.; Wright, a D.; Kaminsky, R. *J. Nat. Prod.* **2000**, *63*, 1150–1152.
- (53) Kwak, J. H.; Schmitz, F. J.; Kelly, M. *J. Nat. Prod.* **2000**, *63*, 1153–1156.
- (54) Cavalieri, E. L.; Li, K.-ming; Balu, N.; Saeed, M.; Devanesan, P.; Higginbotham, S.; Zhao, J.; Gross, M. L.; Rogan, E. G. *Carcinogenesis* **2002**, *23*, 1071–1077.

- (55) Woodward, R.; Bloch, K. *J. Am. Chem. Soc.* **1953**, *75*, 2023–2024.
- (56) Surendra, K.; Corey, E. J. *J. Am. Chem. Soc.* **2008**, *130*, 8865–8869.
- (57) Johnson, W. S.; Gravestock, M. B.; McCarry, B. E. *J. Am. Chem. Soc.* **1971**, *93*, 4332–4334.
- (58) Johnson, W. S.; Crandall, J. K. *J. Org. Chem.* **1965**, *30*, 1785–1790.
- (59) Johnson, W. S.; Kinnel, R. B. *J. Am. Chem. Soc.* **1966**, *88*, 3861–3862.
- (60) Johnson, W. S.; Semmelhack, M. F.; Sultanbawa, M.; Dolak, L. A. *J. Am. Chem. Soc.* **1968**, *90*, 2994–2996.
- (61) Dijkink, J.; Speckamp, W. *Tetrahedron Lett.* **1977**, *18*, 935–938.
- (62) Johnson, W. S.; Daub, G. W.; Lyle, T. A.; Niwa, M. *J. Am. Chem. Soc.* **1980**, *102*, 7800–7802.
- (63) Johnson, W. S.; Hughes, L. R.; Carlson, J. L. *J. Am. Chem. Soc.* **1979**, *101*, 1281–1282.
- (64) Bartlett, P. A.; Johnson, W. S. *J. Am. Chem. Soc.* **1973**, *95*, 7501–7502.
- (65) Tanis, S. P.; Herrinton, P. M. *J. Org. Chem.* **1983**, *48*, 4572–4580.
- (66) Linares-Palomino, P. J.; Salido, S.; Altarejos, J.; Sánchez, A. *Tetrahedron Lett.* **2003**, *44*, 6651–6655.
- (67) Leo, A.; Hansch, C.; Elkins, D. *Chem. Rev.* **1971**, *71*, 525–616.
- (68) Rautio, J.; Kumpulainen, H.; Heimbach, T.; Oliyai, R.; Oh, D.; Järvinen, T.; Savolainen, J. *Nat. Rev. Drug Discovery* **2008**, *7*, 255–270.
- (69) Yoder, R.; Johnston, J. N. *Chem. Rev.* **2005**, *105*, 4730–4756.
- (70) Vilotijevic, I.; Jamison, T. F. *Angew. Chem. Int. Ed.* **2009**, *48*, 5250–5281.
- (71) Xiong, Z.; Busch, R.; Corey, E. *Org. Lett.* **2010**, *12*, 1512–1514.

- (72) Nunomoto, S.; Kawakami, Y.; Yamashita, Y. *J. Org. Chem.* **1983**, *48*, 1912–1914.
- (73) Zhang, W.; Loebach, J. L.; Wilson, S. R.; Jacobsen, E. N. *J. Am. Chem. Soc.* **1990**, *112*, 2801–2803.
- (74) Wang, Z. X.; Tu, Y.; Frohn, M.; Zhang, J. R.; Shi, Y. *J. Am. Chem. Soc.* **1997**, *119*, 11224–11235.
- (75) Van Tamelen, E.; Seiler, M.; Wierenga, W. *J. Am. Chem. Soc.* **1972**, *94*, 8229–8231.
- (76) Corey, E.; Wood Jr, H. B. *J. Am. Chem. Soc.* **1996**, *118*, 11982–11983.
- (77) Bogenstätter, M.; Limberg, A.; Overman, L. E.; Tomasi, A. L. *J. Am. Chem. Soc.* **1999**, *121*, 12206–12207.
- (78) Zhao, J.-F.; Zhao, Y.-J.; Loh, T.-P. *Chem. Commun.* **2008**, *1*, 1353–1355.
- (79) Dale, J. A.; Dull, D. L.; Mosher, H. S. *J. Org. Chem.* **1969**, *34*, 2543–2549.
- (80) Mukherjee, R.; Jaggi, M.; Rajendran, P.; Srivastava, S. K.; Siddiqui, M. J.; Vardhan, A.; Burman, A. C. *Bioorg. Med. Chem. Lett.* **2004**, *14*, 3169–3172.
- (81) Scribner, A.; Moore, J.; Ouvry, G.; Fisher, M.; Wyvratt, M.; Leavitt, P.; Liberator, P.; Gurnett, A.; Brown, C.; Mathew, J.; Thompson, D.; Schmatz, D.; Biftu, T. *Bioorg. Med. Chem. Lett.* **2009**, *19*, 1517–1521.
- (82) Borsch, R.-F.; Bernstein, M.-D.; Durst, H.-D. *J. Am. Chem. Soc.* **1971**, *93*, 2897–2904.
- (83) Zhao, M.-X.; Shi, Y. *J. Org. Chem.* **2006**, *71*, 5377–5379.
- (84) Mori, K. *Tetrahedron Asymm.* **2011**, *22*, 1006–1010.
- (85) Qian, K.; Yu, D.; Chen, C.-H.; Huang, L.; Morris-Natschke, S. L.; Nitz, T. J.; Salzwedel, K.; Reddick, M.; Allaway, G. P.; Lee, K.-H. *J. Med. Chem.* **2009**, *52*, 3248–3258.

- (86) Parra-Delgado, H.; Compadre, C. M.; Ramírez-Apan, T.; Muñoz-Fambuena, M. J.; Compadre, R. L.; Ostrosky-Wegman, P.; Martínez-Vázquez, M. *Bioorg. Med. Chem.* **2006**, *14*, 1889–1901.
- (87) Holland, H. *Tetrahedron Lett.* **1979**, 3395–3396.
- (88) Barton, D. H. R.; McCombie, S. W. *J. Chem. Soc., Perkin Trans. I.* **1975**, 1574–1585.
- (89) Witschel, M. C.; Höffken, H. W.; Seet, M.; Parra, L.; Mietzner, T.; Thater, F.; Niggeweg, R.; Röhl, F.; Illarionov, B.; Rohdich, F.; Kaiser, J.; Fischer, M.; Bacher, A.; Diederich, F. *Angew. Chem. Int. Ed.* **2011**, *50*, 7931–7935.
- (90) Takatsuka, Y.; Chen, C.; Nikaido, H. *Proc. Natl. Acad. Sci. U.S.A.* **2010**, *107*, 6559–6565.
- (91) Dror, R. O.; Arlow, D. H.; Borhani, D. W.; Jensen, M. Ø.; Piana, S.; Shaw, D. E. *Proc. Natl. Acad. Sci. U.S.A.* **2009**, *106*, 4689–4694.
- (92) Mayer, M.; Meyer, B. *Angew. Chem. Int. Ed.* **1999**, *38*, 1784–1788.
- (93) Siriwardena, A. H.; Tian, F.; Noble, S.; Prestegard, J. H. *Angew. Chem. Int. Ed.* **2002**, *41*, 3454–3457.
- (94) Shuker, S. B.; Hajduk, P. J.; Meadows, R. P.; Fesik, S. W. *Science* **1996**, *274*, 1531–1534.
- (95) Meyer, B.; Weimar, T.; Peters, T. *Eur. J. Biochem.* **1997**, *246*, 705–709.
- (96) Chen, A.; Shapiro, M. J. *J. Am. Chem. Soc.* **1998**, *120*, 10258–10259.
- (97) Mayer, M.; Meyer, B. *J. Am. Chem. Soc.* **2001**, *123*, 6108–6117.
- (98) Claasen, B.; Axmann, M.; Meinecke, R.; Meyer, B. *J. Am. Chem. Soc.* **2005**, *127*, 916–919.

- (99) Ong, C. J.; Ming-Lum, A.; Nodwell, M.; Ghanipour, A.; Yang, L.; Williams, D. E.; Kim, J.; Demirjian, L.; Qasimi, P.; Ruschmann, J.; Cao, L.-P.; Ma, K.; Chung, S. W.; Duronio, V.; Andersen, R. J.; Krystal, G.; Mui, A. L.-F. *Blood* **2007**, *110*, 1942–1949.
- (100) Hernández Daranas, A.; Koteich Khatib, S.; Lysek, R.; Vogel, P.; Gavín, J. *Chemistry Open* **2012**, *1*, 13–16.
- (101) Cravatt, B. F.; Wright, A. T.; Kozarich, J. W. *Annu. Rev. Biochem.* **2008**, *77*, 383–414.
- (102) Liu, Y.; Patricelli, M. P.; Cravatt, B. F. *Proc. Natl. Acad. Sci. U.S.A.* **1999**, *96*, 14694–14699.
- (103) Pan, Z.; Jeffery, D.; Chehade, K.; Beltman, J.; Clark, J. M.; Grothaus, P.; Bogyo, M.; Baruch, A. *Bioorg. Med. Chem. Lett.* **2006**, *16*, 2882–2885.
- (104) Faleiro, L.; Kobayashi, R.; Fearnhead, H.; Lazebnik, Y. *EMBO. J.* **1997**, *16*, 2271–2281.
- (105) Das, J. *Chem. Rev.* **2011**, *111*, 4405–4417.
- (106) Saghatelian, A.; Jessani, N.; Joseph, A.; Humphrey, M.; Cravatt, B. F. *Proc. Natl. Acad. Sci. U.S.A.* **2004**, *101*, 10000–10005.
- (107) MacKinnon, A. L.; Garrison, J. L.; Hegde, R. S.; Taunton, J. *J. Am. Chem. Soc.* **2007**, *129*, 14560–14561.
- (108) Greenbaum, D.; Medzihradszky, K. F.; Burlingame, A.; Bogyo, M. *Chem. Biol.* **2000**, *7*, 569–581.
- (109) Vocadlo, D. J.; Bertozzi, C. R. *Angew. Chem. Int. Ed.* **2004**, *43*, 5338–5342.
- (110) Alexander, J. P.; Cravatt, B. F. *Chem. Biol.* **2005**, *12*, 1179–1187.
- (111) Kolb, H. C.; Sharpless, K. B. *Drug Discov. Today* **2003**, *8*, 1128–1137.

- (112) Bi, X.; Schmitz, A.; Hayallah, A. M.; Song, J.-N.; Famulok, M. *Angew. Chem. Int. Ed.* **2008**, *47*, 9565–9568.
- (113) Desantis, G.; Jones, J. B. *Bioorg. Med. Chem.* **2000**, *8*, 563–570.
- (114) Okerberg, E. S.; Wu, J.; Zhang, B.; Samii, B.; Blackford, K.; Winn, D. T.; Shreder, K. R.; Burbaum, J. J.; Patricelli, M. P. *Proc. Natl. Acad. Sci. U.S.A.* **2005**, *102*, 4996–5001.
- (115) Finn, F. M.; Titus, G.; Horstman, D.; Hofmann, K. *Proc. Natl. Acad. Sci. U.S.A.* **1984**, *81*, 7328–7332.
- (116) Greenbaum, D. *Mol. Cell. Proteomics* **2001**, *1*, 60–68.
- (117) Tisserand, S.; Baati, R.; Nicolas, M.; Mioskowski, C. *J. Org. Chem.* **2004**, *69*, 8982–8983.
- (118) Norell, J. R. *J. Org. Chem.* **1973**, *38*, 1924–1928.
- (119) Chen, X.; Tordeux, M.; Desmurs, J.-R.; Wakselman, C. *J. Fluorine Chem.* **2003**, *123*, 51–56.
- (120) Boyer, J.; Krum, J.; Myers, M.; Fazal, A.; Wigal, C. *J. Org. Chem.* **2000**, *65*, 4712–4714.
- (121) Rozenberg, V.; Danilova, T.; Sergeeva, E.; Vorontsov, E.; Starikova, Z.; Lysenko, K.; Belokon, Y. *Eur. J. Org. Chem.* **2000**, *2000*, 3295–3303.
- (122) Cullinane, N.; Woolhouse, R.; Edwards, B. *J. Chem. Soc.* **1961**, 3842–3845.
- (123) Halpern, B. N.; Neveu, T.; Spector, S. *Br. J. Pharmacol.* **1963**, *20*, 389–398.
- (124) Burnstein, K. L. *J. Cell. Biochem.* **2005**, *95*, 657–669.
- (125) Joseph, I. B.; Nelson, J. B.; Denmeade, S. R.; Isaacs, J. T. *Clin. Cancer Res.* **1997**, *3*, 2507–2511.

- (126) Tang, D. G.; Porter, a T. *Prostate* **1997**, *32*, 284–293.
- (127) Sadar, M. D. *Cancer Res.* **2011**, *71*, 1208–1213.
- (128) O'Donnell, A.; Judson, I.; Dowsett, M.; Raynaud, F.; Dearnaley, D.; Mason, M.; Harland, S.; Robbins, A.; Halbert, G.; Nutley, B.; Jarman, M. *Br. J. Cancer* **2004**, *90*, 2317–2325.
- (129) Attard, G.; Belldegrun, A. S.; de Bono, J. S. *BJU. Int.* **2005**, *96*, 1241–1246.
- (130) Singh, S. M.; Gauthier, S.; Labrie, F. *Curr. Med. Chem.* **2000**, *7*, 211–247.
- (131) Fradet, Y. *Expert Rev. Anticancer Ther.* **2004**, *4*, 37–48.
- (132) Jung, M. E.; Ouk, S.; Yoo, D.; Sawyers, C. L.; Chen, C.; Tran, C.; Wongvipat, J. *J. Med. Chem.* **2010**, *53*, 2779–2796.
- (133) Scher, H. I.; Sawyers, C. L. *J. Clin. Oncol.* **2005**, *23*, 8253–8261.
- (134) Montgomery, R. B.; Mostaghel, E.; Vessella, R.; Hess, D. L.; Kalhorn, T. F.; Higano, C. S.; True, L. D.; Nelson, P. S. *Cancer Res.* **2008**, *68*, 4447–4454.
- (135) Chen, Y.; Clegg, N. J.; Scher, H. I. *Lancet. Oncol.* **2009**, *10*, 981-991.
- (136) Taplin, M. E.; Bublely, G. J.; Shuster, T. D.; Frantz, M. E.; Spooner, A. E.; Ogata, G. K.; Keer, H. N.; Balk, S. P. *N. Engl. J. Med.* **1995**, *332*, 1393–1398.
- (137) Jenster, G. *J. Pathol.* **2000**, *191*, 227–228.
- (138) Guo, Z.; Yang, X.; Sun, F.; Jiang, R.; Linn, D. E.; Chen, H.; Chen, H.; Kong, X.; Melamed, J.; Tepper, C. G.; Kung, H.-J.; Brodie, A. M. H.; Edwards, J.; Qiu, Y. *Cancer Res.* **2009**, *69*, 2305–2313.
- (139) Shaffer, P. L.; Jivan, A.; Dollins, D. E.; Claessens, F.; Gewirth, D. T. *Proc. Natl. Acad. Sci. U.S.A.* **2004**, *101*, 4758–4763.

- (140) Sadar, M. D.; Williams, D. E.; Mawji, N. R.; Patrick, B. O.; Wikanta, T.; Chasanah, E.; Irianto, H. E.; Soest, R. V.; Andersen, R. J. *Org. Lett.* **2008**, *10*, 4947–4950.
- (141) Andersen, R. J.; Mawji, N. R.; Wang, J.; Wang, G.; Haile, S.; Myung, J.-K.; Watt, K.; Tam, T.; Yang, Y. C.; Bañuelos, C.; Williams, D. E.; McEwan, I. J.; Wang, Y.; Sadar, M. D. *Cancer Cell* **2010**, *17*, 535–546.
- (142) Versteegen, R. M.; van Beek, D. J. M.; Sijbesma, R. P.; Vlassopoulos, D.; Fytas, G.; Meijer, E. W. *J. Am. Chem. Soc.* **2005**, *127*, 13862–13868.
- (143) Appel, R. *Angew. Chem. Int. Ed.* **1975**, *14*, 801–811.
- (144) Shearman, G. C.; Yahioğlu, G.; Kirstein, J.; Milgrom, L. R.; Seddon, J. M. *J. Mater. Chem.* **2009**, *19*, 598–604.
- (145) Mehta, G.; Mohanrao, R.; Katukojvala, S.; Landais, Y.; Sen, S. *Tetrahedron Lett.* **2011**, *52*, 2893–2897.
- (146) Wadsworth, W. S.; Emmons, W. D. *J. Am. Chem. Soc.* **1961**, *83*, 1733–1738.
- (147) Garg, N. K.; Hiebert, S.; Overman, L. E. *Angew. Chem. Int. Ed.* **2006**, *45*, 2912–1215.
- (148) Sabitha, G.; Satheesh Babu, R.; Rajkumar, M.; Reddy, C. S.; Yadav, J. *Tetrahedron Lett.* **2001**, *42*, 3955–3958.
- (149) Bulger, P. G.; Moloney, M. G.; Trippier, P. C. *Org. Biomol. Chem.* **2003**, *1*, 3726–3737.
- (150) Zhu, W.; Jimenez, M.; Jung, W. H.; Camarco, D. P.; Balachandran, R.; Vogt, A.; Day, B. W.; Curran, D. P. *J. Am. Chem. Soc.* **2010**, *132*, 9175–9187.
- (151) Akiyama, T.; Ueoka, R.; van Soest, R. W. M.; Matsunaga, S. *J. Nat. Prod.* **2009**, *72*, 1552–1554.
- (152) Veronese, F. M.; Pasut, G. *Drug Discov. Today* **2005**, *10*, 1451–1458.

- (153) Filler, R.; Saha, R. *Future Med. Chem.* **2009**, *1*, 777–791.
- (154) Beaulieu, F.; Beaugard, L.-P.; Courchesne, G.; Couturier, M.; LaFlamme, F.; L'Heureux, A. *Org. Lett.* **2009**, *11*, 5050–5053.
- (155) Rao, J.; Dragulescu-Andrasi, A.; Yao, H. *Curr. Opin. Biotechnol.* **2007**, *18*, 17–25.
- (156) Ntziachristos, V.; Yodh, a G.; Schnall, M.; Chance, B. *Proc. Natl. Acad. Sci. U.S.A* **2000**, *97*, 2767–2772.
- (157) Bilski, P. J.; Risek, B.; Chignell, C. F.; Schrader, W. T. *Photochem. Photobiol.* **2009**, *85*, 1225–1232.
- (158) Gierlich, J.; Burley, G.; Gramlich, P. M. E.; Hammond, D. M.; Carell, T. *Org. Lett.* **2006**, *8*, 3639–3642.
- (159) Kim, G.-J.; Lee, K.; Kwon, H.; Kim, H.-J. *Org. Lett.* **2011**, *13*, 2799–2801.
- (160) Sakai, H.; Hirano, T.; Mori, S.; Fujii, S.; Masuno, H.; Kinoshita, M.; Kagechika, H.; Tanatani, A. *J. Med. Chem.* **2011**, *54*, 7055–7065.
- (161) Wu, J.-S.; Liu, W.-M.; Zhuang, X.-Q.; Wang, F.; Wang, P.-F.; Tao, S.-L.; Zhang, X.-H.; Wu, S.-K.; Lee, S.-T. *Org. Lett.* **2007**, *9*, 33–36.
- (162) Li, C. J.; Schmitz, F. J.; Kelly-Borges, M. *J. Nat. Prod.* **1999**, *62*, 287–290.
- (163) Hyosu, M.; Kimura, J. *J. Nat. Prod.* **2000**, *63*, 422–423.
- (164) Takadoi, M.; Katoh, T.; Ishiwata, A.; Terashima, S. *Tetrahedron* **2002**, *58*, 9903–9923.
- (165) San-miguelc, N. S. A. M. A.; Taranc, M.; Delmond, B. *Tetrahedron* **1991**, *47*, 9187–9194.
- (166) Chaturvedula, V. S. P.; Gao, Z.; Thomas, S. H.; Hecht, S. M.; Kingston, D. G. I. *Tetrahedron* **2004**, *60*, 9991–9995.

- (167) Zoretic, P.; Wang, M.; Zhang, Y.; Shen, Z.; Ribeiro, A. *J. Org. Chem.* **1996**, *61*, 1806–1813.
- (168) McGrath, N.; Lee, C.; Araki, H.; Brichacek, M.; Njardarson, J. T. *Angew. Chem. Int. Ed.* **2008**, *47*, 9450–9453.
- (169) Zoretic, P. A.; Weng, X.; Caspar, M. L.; Davis, D. G. *Tetrahedron Lett.* **1991**, *32*, 4819–4822.
- (170) Snider, B. *Synth. Commun.* **2001**, *31*, 3753–3758.
- (171) Tong, R.; Valentine, J. C.; McDonald, F. E.; Cao, R.; Fang, X.; Hardcastle, K. I. *J. Am. Chem. Soc.* **2007**, *129*, 1050–1051.
- (172) Mori, K. *Tetrahed. Asym.* **2011**, *22*, 1006–1010.
- (173) Seifert, A.; Vomund, S.; Grohmann, K.; Kriening, S.; Urlacher, V. B.; Laschat, S.; Pleiss, J. *Chem. Bio. Chem.* **2009**, *10*, 853–861.
- (174) Malerich, J. P.; Trauner, D. *J. Am. Chem. Soc.* **2003**, *125*, 9554–9555.
- (175) Rossiter, B. E.; Katsuki, T.; Sharpless, K. B. *J. Am. Chem. Soc.* **1981**, *103*, 464–465.
- (176) Kuk, J.; Kim, B. S.; Jung, H.; Choi, S.; Park, J.-Y.; Koo, S. *J. Org. Chem.* **2008**, *73*, 1991–1994.
- (177) Hutchins, R. O.; Learn, K. *J. Org. Chem.* **1982**, *47*, 4380–4382.
- (178) Goldsmith, D.; Liotta, D.; Saindane, M.; Waykole, L.; Bowen, P. *Tetrahed. Asym.* **1983**, *24*, 5835–5838.
- (179) Dong, J.-Q.; Wong, H. N. C. *Angew. Chem. Int. Ed.* **2009**, *48*, 2351–2354.
- (180) Tofi, M.; Georgiou, T.; Montagnon, T.; Vassilikogiannakis, G. *Org. Lett.* **2005**, *7*, 3347–3350.
- (181) Moerke, N. *Curr. Protoc. Chem Biol.* **2009**, *1*, 1–15.

- (182) Patel, T.; Gores, G. J.; Kaufmann, S. H. *FASEB. J.* **1996**, *10*, 587–597.
- (183) Ciechanover, A. *Biochim. Biophys. Acta.* **2005**, *44*, 5944–5967.
- (184) Hedstrom, L. *Chem. Rev.* **2002**, *102*, 4501–4524.
- (185) Chapman, H.; Riese, R. J.; Shi, G. P. *Annu. Rev. Physiol.* **1997**, *59*, 63–88.
- (186) Seelmeier, S.; Schmidt, H.; Turk, V.; von der Helm, K. *Proc. Natl. Acad. Sci. U.S.A.* **1988**, *85*, 6612–6616.
- (187) Turk, B.; Turk, D.; Turk, V. *Biochim. Biophys. Acta.* **2000**, *1477*, 98–111.
- (188) McGrath, M. E. *Annu. Rev. Bioph. Biom.* **1999**, *28*, 181–204.
- (189) Barford, D.; Das, K.; Egloff, M. P. *Annu. Rev. Bioph. Biom.* **1998**, *27*, 133–164.
- (190) Turk, V.; Turk, B. *EMBO. J.* **2001**, *20*, 4629–4633.
- (191) Fineschi, B.; Jim, M. *Trends Biochem. Sci.* **1997**, *22*, 377–382.
- (192) Barrett, A. J. *Trends Biochem. Sci.* **1987**, *12*, 193–196.
- (193) Gettins, P. *Chem. Rev.* **2002**, *102*, 4751–4804.
- (194) Katunuma, N.; Kominami, E. *Rev. Physiol. Bioch. P.* **1987**, *108*, 1–20.
- (195) Jørgensen, I.; Kos, J.; Krašovec, M.; Troelsen, L.; Klarlund, M.; Jensen, T. W.; Hansen, M. S.; Jacobsen, S. *Clin. Rheumatol.* **2011**, *30*, 633–638.
- (196) Bone, L.; Everts, V.; Korper, W.; Hoeben, K. A.; Jansen, I. D. C.; Bromme, D.; Cleutjens, K. B. J. M.; Heeneman, S.; Peters, C.; Reinheckel, T.; Saftig, P.; Beertsen, W. *J. Bone Miner. Res.* **2006**, *21*, 1399–1408.
- (197) Lemere, C. A.; Munger, J. S.; Shi, G. P.; Natkin, L.; Haass, C.; Chapman, H. A.; Selkoe, D. J. *Am. J. Pathol.* **1995**, *146*, 848–860.
- (198) Lamkanfi, M.; Festjens, N.; Declercq, W.; Vanden Berghe, T.; Vandenabeele, P. *Cell Death Differ.* **2007**, *14*, 44–55.

- (199) Mohamed, M. M.; Sloane, B. F. *Nat. Rev. Cancer* **2006**, *6*, 764–775.
- (200) Identification, S.; Bossard, M. J.; Tomaszek, T. A.; Thompson, S. K.; Amegadzie, B. Y.; Hanning, C. R.; Jones, C.; Kurdyla, J. T.; McNulty, D. E.; Drake, F. H.; Gowen, M.; Levy, M. A.; Chem, M. J. B. *Biochemistry* **1996**, *271*, 12517–12524.
- (201) Stoch, S.; Wagner, J. a *Pharmacol. Ther. Part C*. **2008**, *83*, 172–176.
- (202) Hozumi, M.; Ogawa, M.; Sugimura, T.; Takeuchi, T.; Umezawa, H. *Cancer Res.* **1972**, *32*, 1725–1728.
- (203) Umezawa, H.; Aoyagi, T.; Morishima, H.; Kunimoto, S.; Matsuzaki, M. *J. Antibiot.* **1970**, *23*, 425–427.
- (204) Umezawa, S.; Tatsuta, K.; Fujimoto, K.; Tsuchiya, T.; Umezawa, H. *J. Antibiot.* **1972**, *25*, 267–270.
- (205) Brömme, D.; Lecaille, F. *Expet. Opin. Investig. Drugs* **2009**, *18*, 585–600.
- (206) Jerome, C.; Missbach, M.; Gamse, R. *Osteoporosis Int.* **2012**, *23*, 339–349.
- (207) Kumar, S.; Dare, L.; Vasko-Moser, J.; James, I. E.; Blake, S. M.; Rickard, D. J.; Hwang, S.-M.; Tomaszek, T.; Yamashita, D. S.; Marquis, R. W.; Oh, H.; Jeong, J. U.; Veber, D. F.; Gowen, M.; Lark, M. W.; Stroup, G. *Bone* **2007**, *40*, 122–131.
- (208) Eisman, J.; Bone, H. G.; Hosking, D. J.; McClung, M. R.; Reid, I. R.; Rizzoli, R.; Resch, H.; Verbruggen, N.; Hustad, C. M.; DaSilva, C.; Petrovic, R.; Santora, A. C.; Ince, B. A.; Lombardi, A. *J. Bone Miner. Res.* **2011**, *26*, 242–251.
- (209) Arzt, S.; Beteva, A.; Cipriani, F.; Delageniere, S.; Felisaz, F.; Förstner, G.; Gordon, E.; Launer, L.; Lavault, B.; Leonard, G.; Mairs, T.; McCarthy, A.; McCarthy, J.; McSweeney, S.; Meyer, J.; Mitchell, E.; Monaco, S.; Nurizzo, D.; Ravelli, R.; Rey,

- V.; Shepard, W.; Spruce, D.; Svensson, O.; Theveneau, P. *Prog. Biophys. Mol. Biol.* **2005**, *89*, 124–152.
- (210) Valeur, E.; Bradley, M. *Chem. Soc. Rev.* **2009**, *38*, 606–631.
- (211) Carpino, L. A.; El-Faham, A.; Albericio, F. *J. Org. Chem.* **1995**, *60*, 3561–3564.
- (212) Lee, J. T.; Chen, D. Y.; Yang, Z.; Ramos, A. D.; Hsieh, J. J.-D.; Bogoy, M. *Bioorg. Med. Chem. Lett.* **2009**, *19*, 5086–5090.
- (213) Zheng, C.; Combs, A. P. *J. Comb. Chem.* **2002**, *4*, 38–43.
- (214) Singh, P.; Samor, C.; Toma, F. M.; Bussy, C.; Nunes, A.; Al-Jamal, K. T.; Ménard-Moyon, C.; Prato, M.; Kostarelos, K.; Bianco, A. *J. Mater. Chem.* **2011**, *21*, 4850–4860.
- (215) Majer, P.; Randad, R. S. *J. Org. Chem.* **1994**, *59*, 1937–1938.
- (216) Ito, A.; Takahashi, R.; Baba, Y. *Chem. Pharm. Bull.* **1975**, *23*, 3081–3087.
- (217) Brown, H.; Narasimhan, S.; Choi, Y. M. *J. Org. Chem.* **1982**, *47*, 4702–4708.
- (218) Coffey, D. S.; Overman, L. E.; Stappenbeck, F. *J. Am. Chem. Soc.* **2000**, *122*, 4904–4914.
- (219) Frigerio, M.; Santagostino, M.; Sputore, S.; Palmisano, G. *J. Org. Chem.* **1995**, *60*, 7272–7276.
- (220) Shimizu, B.; Saito, A.; Ito, A.; Tokawa, K. *J. Antibiot.* **1972**, *25*, 515–523.
- (221) Leanna, M. R.; Sowin, T.; Morton, H. E. *Tetrahedron Lett.* **1992**, *33*, 5029–5032.
- (222) Einhorn, J.; Einhorn, C.; Ratajczak, F.; Pierre, J.-L. *J. Org. Chem.* **1996**, *61*, 7452–7454.
- (223) Yasuma, T.; Oi, S.; Choh, N.; Nomura, T.; Furuyama, N.; Nishimura, A.; Fujisawa, Y.; Sohda, T. *J. Med. Chem.* **1998**, *41*, 4301–4308.

- (224) Shimokawa, J.; Ishiwata, T.; Shirai, K.; Koshino, H.; Tanatani, A.; Nakata, T.; Hashimoto, Y.; Nagasawa, K. *Chem. Eur. J.* **2005**, *11*, 6878–6888.
- (225) Myers, A. G.; Zhong, B.; Movassaghi, M.; Kung, D. W.; Lanman, B. A.; Kwon, S. *Tetrahedron Lett.* **2000**, *41*, 1359–1362.
- (226) Bernatowicz, M. S.; Wu, Y.; Matsueda, G. R. *Tetrahedron Lett.* **1993**, *34*, 3389–3392.
- (227) Mandal, P. K.; McMurray, J. S. *J. Org. Chem.* **2007**, *72*, 6599–6601.
- (228) Srinivasa, G. R.; Narendra Babu, S. N.; Lakshmi, C.; Gowda, D. C. *Synth. Commun.* **2004**, *34*, 1831–1837.
- (229) Lemke, A.; Büschleb, M.; Ducho, C. *Tetrahedron* **2010**, *66*, 208–214.
- (230) Yu, X.; Dai, Y.; Yang, T.; Gagné, M. R.; Gong, H. *Tetrahedron* **2011**, *67*, 144–151.
- (231) Adamo, I.; Ballico, M.; Campaner, P.; Drioli, S.; Bonora, G. M. *Eur. J. Org. Chem.* **2004**, 2603–2609.
- (232) Undevia, S. D.; Gomez-Abuin, G.; Ratain, M. J. *Nat. Rev. Cancer* **2005**, *5*, 447–548.
- (233) Fuhler, G. M.; Brooks, R.; Toms, B.; Iyer, S.; Gengo, E.; Park, M.-Y.; Gumbleton, M.; Viernes, D. R.; Chisholm, J. D.; Kerr, W. G. *Mol. Med.* **2012**, *18*, 65–75.
- (234) Cho, I.; Meimetis, L.; Britton, R. *Org. Lett.* **2009**, *11*, 1903–1906.

## Appendix A : X-Ray Structure Reports

### A.1 Compound 2.30

#### Data Collection:

A colorless plate crystal of  $C_{23}H_{34}O_3$  having approximate dimensions of 0.15 x 0.40 x 0.40 mm was mounted on a glass fiber. All measurements were made on a Bruker APEX II diffractometer with graphite monochromated Mo-K $\alpha$  radiation. The data were collected at a temperature of  $-170.0 \pm 0.1$  °C to a maximum  $2\theta$  value of  $56.0^\circ$ . Data were collected in a series of  $\phi$  and  $\omega$  scans in  $0.50^\circ$  oscillations with 10.0-second exposures. The crystal-to-detector distance was 40.00 mm.

#### Data Reduction:

Of the 25982 reflections that were collected, 4780 were unique ( $R_{int} = 0.033$ ); equivalent reflections were merged. Data were collected and integrated using the Bruker SAINT software package. The linear absorption coefficient,  $\mu$ , for Mo-K $\alpha$  radiation is  $0.78 \text{ cm}^{-1}$ . Data were corrected for absorption effects using the multi-scan technique (SADABS), with minimum and maximum transmission coefficients of 0.913 and 0.988, respectively. The data were corrected for Lorentz and polarization effects.

#### Structure Solution and Refinement:

The structure was solved by direct methods. All non-hydrogen atoms were refined anisotropically. Hydrogen H3O was located in a difference map and refined isotropically. All other hydrogen atoms were placed in calculated positions. The absolute configuration was determined on the basis of Bijvoet-pair intensity differences. The results suggest that if the sample is enantiopure there is a 93 % probability the configuration has been properly assigned.

**Crystal Data:**

Empirical Formula	$C_{23}H_{34}O_3n$
Formula Weight	358.50
Crystal Color, Habit	colorless, plate
Crystal Dimensions	0.15 X 0.40 X 0.40 mm
Crystal System	orthorhombic
Lattice Type	primitive
Lattice Parameters	$a = 7.0872(3) \text{ \AA}$ $b = 10.9264(6) \text{ \AA}$ $c = 25.447(2) \text{ \AA}$ $\alpha = 90^\circ$ $\beta = 90^\circ$ $\gamma = 90^\circ$ $V = 10269.2(6) \text{ \AA}^3$
Space Group	$P 2_12_12_1$ (#19)
Z value	4
$D_{\text{calc}}$	$1.208 \text{ g/cm}^3$
F000	784.00
$\mu$ (MoK $\alpha$ )	$0.78 \text{ cm}^{-1}$

### Intensity Measurements:

Diffractometer	Bruker X8 APEX II
Radiation	MoK $\alpha$ ( $\lambda = 0.71073 \text{ \AA}$ ) graphite monochromated
Data Images	1535 exposures @ 10.0 seconds
Detector Position	40.00 mm
$2\theta_{\max}$	56.0 $^{\circ}$
No. of Reflections Measured	Total: 25982
Corrections	Unique: 4780 ( $R_{\text{int}} = 0.033$ ) Absorption ( $T_{\text{min}} = 0.913$ , $T_{\text{max}} = 0.988$ ) Lorentz-polarization

## Structure Solution and Refinement:

Structure Solution	Direct Methods (SIR97)
Refinement	Full-matrix least-squares on $F^2$
Function Minimized	$\Sigma w (F_o^2 - F_c^2)^2$
Least Squares Weights	$w=1/(\sigma^2(F_o^2)+(0.0513P)^2+ 0.3340P)$
Anomalous Dispersion	All non-hydrogen atoms
No. Observations ( $I > 0.00\sigma(I)$ )	4780
No. Variables	245
Reflection/Parameter Ratio	19.51
Residuals (refined on $F^2$ , all data): R1; wR2	0.041; 0.090
Goodness of Fit Indicator	1.03
No. Observations ( $I > 2.00\sigma(I)$ )	4366
Residuals (refined on F): R1; wR2	0.035; 0.086
Max Shift/Error in Final Cycle	0.00
Maximum peak in Final Diff. Map	0.26 e <sup>-</sup> /Å <sup>3</sup>
Minimum peak in Final Diff. Map	-0.21 e <sup>-</sup> /Å <sup>3</sup>

## A.2 Compound 2.32

### Data Collection:

A colorless plate crystal of  $C_{33}H_{41}F_3O_5$  having approximate dimensions of 0.02 x 0.12 x 0.41 mm was mounted on a glass fiber. All measurements were made on a Bruker APEX II diffractometer with graphite monochromator and a  $CuK_{\alpha}$   $I\mu S$  MX microsource ( $\lambda = 1.54178$  Å). The data were collected at a temperature of  $-173.1 \pm 0.1$  °C to a maximum  $2\theta$  value of  $136.2^\circ$ . Data were collected in a series of  $\phi$  and  $\omega$  scans in  $0.50^\circ$  oscillations with 10.0-second exposures. The crystal-to-detector distance was 49.88 mm.

### Data Reduction:

Of the 10010 reflections that were collected, 4408 were unique ( $R_{int} = 0.025$ ; Friedels not merged); equivalent reflections were merged. Data were collected and integrated using the Bruker SAINT software package. The linear absorption coefficient,  $\mu$ , for  $Cu-K_{\alpha}$  radiation is  $8.49\text{ cm}^{-1}$ . Data were corrected for absorption effects using the multi-scan technique (SADABS), with minimum and maximum transmission coefficients of 0.847 and 0.983, respectively. The data were corrected for Lorentz and polarization effects.

### Structure Solution and Refinement:

The structure was solved by direct methods. All non-hydrogen atoms were refined anisotropically. All C-H hydrogen atoms were placed in calculated positions with only isotropic displacement parameters refined. The absolute configuration was determined based on the refined Flack parameter.

**Crystal Data:**

Empirical Formula	$C_{33}H_{41}F_3O_5$
Formula Weight	574.66
Crystal Color, Habit	colorless, plate
Crystal Dimensions	0.02 X 0.12 X 0.41 mm
Crystal System	monoclinic
Lattice Type	C-centered
Lattice Parameters	$a = 13.3572(6) \text{ \AA}$ $b = 6.8023(3) \text{ \AA}$ $c = 31.3214(14) \text{ \AA}$ $\alpha = 90^\circ$ $\beta = 95.788(2)^\circ$ $\gamma = 90^\circ$ $V = 2831.3(2) \text{ \AA}^3$
Space Group	$C 2$ (#5)
Z value	4
$D_{\text{calc}}$	$1.348 \text{ g/cm}^3$
F000	1224.00
$\mu(\text{CuK}\alpha)$	$8.49 \text{ cm}^{-1}$

### Intensity Measurements:

Diffractometer	Bruker X8 APEX II
Radiation	MoK $\alpha$ ( $\lambda = 0.71073 \text{ \AA}$ ) graphite monochromated
Data Images	6821 exposures @ 10.0 seconds
Detector Position	49.88 mm
$2\theta_{\max}$	136.2 $^{\circ}$
No. of Reflections Measured	Total: 10010
	Unique: 4408 ( $R_{\text{int}} = 0.025$ ; Friedels not merged)
Corrections	Absorption ( $T_{\min} = 0.847$ , $T_{\max} = 0.983$ ) Lorentz-polarization

**Structure Solution and Refinement:**

Structure Solution	Direct Methods (SIR97)
Refinement	Full-matrix least-squares on $F^2$
Function Minimized	$\Sigma w (F_o^2 - F_c^2)^2$
Least Squares Weights	$w=1/(\sigma^2(F_o^2)+(0.0289P)^2+ 1.3029P)$
Anomalous Dispersion	All non-hydrogen atoms
No. Observations ( $I>0.00\sigma(I)$ )	4408
No. Variables	419
Reflection/Parameter Ratio	10.52
Residuals (refined on $F^2$ , all data): R1; wR2	0.029; 0.068
Goodness of Fit Indicator	1.03
No. Observations ( $I>2.00\sigma(I)$ )	4218
Residuals (refined on F): R1; wR2	0.028; 0.067
Max Shift/Error in Final Cycle	0.00
Maximum peak in Final Diff. Map	0.20 e <sup>-</sup> /Å <sup>3</sup>
Minimum peak in Final Diff. Map	-0.15 e <sup>-</sup> /Å <sup>3</sup>

### A.3 Compound 2.42

#### Data Collection:

A colorless plate crystal of  $C_{23}H_{39}NO_4 \cdot HCl$  having approximate dimensions of 0.10 x 0.12 x 0.29 mm was mounted on a glass fiber. All measurements were made on a Bruker APEX DUO diffractometer with graphite monochromated Mo-K $\alpha$  radiation. The data were collected at a temperature of  $-183.0 \pm 0.1$  °C to a maximum  $2\theta$  value of  $60.2^\circ$ . Data were collected in a series of  $\phi$  and  $\omega$  scans in  $0.5^\circ$  oscillations using 3.0-second exposures. The crystal-to-detector distance was 59.84 mm.

#### Data Reduction:

The material crystallizes as a two-component twin with components one and two related by a  $179.3^\circ$  rotation about the (1 0 0) real axis. Data were integrated for both twin components, including both overlapped and non-overlapped reflections. In total 49944 reflections were integrated (13488 from component one only, 12668 from component two only, 23788 overlapped). Data were collected and integrated using the Bruker SAINT software packages. The linear absorption coefficient,  $\mu$ , for Mo-K $\alpha$  radiation is  $1.97 \text{ cm}^{-1}$ . Data were corrected for absorption effects using the multi-scan technique (TWINABS<sup>2</sup>), with minimum and maximum transmission coefficients of 0.740 and 0.980, respectively. The data were corrected for Lorentz and polarization effects.

#### Structure Solution and Refinement:

The structure was solved by direct methods using non-overlapped data from the major twin component. The material crystallizes with two molecules of methanol in the asymmetric unit. Subsequent refinements were carried out using an HKLF 5 format data set containing complete data from component one and overlapped reflections from component two. All

non-hydrogen atoms were refined anisotropically. All hydrogen atoms were placed in calculated positions.

**Crystal Data:**

Empirical Formula	C <sub>23</sub> H <sub>40</sub> NO <sub>4</sub> Cl
Formula Weight	430.01
Crystal Color, Habit	colorless, plate
Crystal Dimensions	0.10 x 0.12 x 0.29 mm
Crystal System	monoclinic
Lattice Type	C-centered
Lattice Parameters	a = 29.741(3) Å b = 7.3000(7) Å c = 21.452(2) Å α = 90° β = 102.638(2)° γ = 90° V = 4544.7(7) Å <sup>3</sup>
Space Group	C 2/c (#15)
Z value	8
D <sub>calc</sub>	1.257 g/cm <sup>3</sup>
F <sub>000</sub>	1872.00
μ(Mo-Kα)	1.97 cm <sup>-1</sup>

### Intensity Measurements:

Diffractometer	Bruker APEX DUO
Radiation	Mo-K $\alpha$ ( $\lambda = 0.71073 \text{ \AA}$ )
Data Images	2243 exposures @ 3.0 seconds
Detector Position	59.84 mm
$2\theta_{\text{max}}$	60.2 $^{\circ}$
No. of Reflections Measured	Total: 49944
Corrections	Unique: 6679 ( $R_{\text{int}} = 0.045$ ) Absorption ( $T_{\text{min}} = 0.740$ , $T_{\text{max}} = 0.980$ ) Lorentz-polarization

## Structure Solution and Refinement:

Structure Solution	Direct Methods (SIR97)
Refinement	Full-matrix least-squares on $F^2$
Function Minimized	$\Sigma w (F_o^2 - F_c^2)^2$
Least Squares Weights	$w=1/(\sigma^2(F_o^2)+(0.0580P)^2+ 9.3161P)$
Anomalous Dispersion	All non-hydrogen atoms
No. Observations ( $I>0.00\sigma(I)$ )	6679
No. Variables	297
Reflection/Parameter Ratio	22.49
Residuals (refined on $F^2$ , all data): R1; wR2	0.064; 0.146
Goodness of Fit Indicator	1.12
No. Observations ( $I>2.00\sigma(I)$ )	5968
Residuals (refined on F): R1; wR2	0.055; 0.142
Max Shift/Error in Final Cycle	0.00
Maximum peak in Final Diff. Map	0.43 e <sup>-</sup> /Å <sup>3</sup>
Minimum peak in Final Diff. Map	-0.52 e <sup>-</sup> /Å <sup>3</sup>